January 2008

Analysis of Coastal Erosion on Martha's Vineyard, Massachusetts: a Paraglacial Island

Denise M. Brouillette-jacobson
University of Massachusetts Amherst

ANALYSIS OF COASTAL EROSION ON MARTHA'S VINEYARD, MASSACHUSETTS: A PARAGLACIAL ISLAND

A Thesis Presented
by

DENISE BROUILLETTE-JACOBSON

Submitted to the Graduate School of the
University of Massachusetts Amherst in partial fulfillment
of the requirements for the degree of

MASTER OF SCIENCE
September 2008

Natural Resources Conservation

ANALYSIS OF COASTAL EROSION ON MARTHA'S VINEYARD, MASSACHUSETTS: A PARAGLACIAL ISLAND

A Thesis Presented

by

DENISE BROUILLETTE-JACOBSON

Approved as to style and content by:

____
John T. Finn, Chair

____
Robin Harrington, Member

____
John Gerber, Member

____
Paul Fisette, Department Head,
Department of Natural Resources Conservation

DEDICATION

All I can think about as I write this dedication to my loved ones is the song by The Shirelles called “Dedicated to the One I Love.” Only in this case there is more than one love. First, I’d like to acknowledge a few good friends who have waited patiently for me to finish my thesis and without whose emotional support this work would have been difficult. They constantly rooted for me and kept me going.

I am thankful to my family members, in particular to my brother, Butch, and his wonderful daughters, Brandy and Niki, for allowing me to be an absentee sister and aunt, yet they continued to offer words of encouragement throughout the years. In addition, I wish that my parents were here to see this moment because they always knew my persistence usually worked in my favor. They would have been proud to see their first family member receive a graduate degree.

As a mother, you think of yourself as a role model for your children, but little did Seth, Michael, and Jaclyn know that they were my role models. Their faith in me inspired me to continue this thesis to completion. I raised them to never give up on something while they were in the middle of it and to finish what they started. Those words came back to me from my children more than I can count. My children were selfless on many, many occasions when I felt that I was needed, yet they imparted their own inner strengths and pushed me to continue my work, allowing me to keep my dream alive. I’d like to thank my dear daughter-in-law, Joyce, who was always there with her smiling face and constantly cheer me on. Now as new parents, Seth and Joyce have a son, Zachary, who I hope to inspire one day to become a steward of the environment.

When I began my thesis, we had one fish (Fluffy), two birds (Mine and Yours), two cats (Percy and Cookie), and three dogs (Calvin, Lillie, and Lucy). As I finished my thesis, only one cat and three dogs remained. I want to acknowledge the pets that could not hang in for me to finish, but especially to our fluffy kitty, Percy, who died two months ago. He provided never-ending companionship while he sat on my lap as I did my research and wrote my thesis, keeping constant vigilance on my comings and goings. Next, to Calvin, Lillie, Lucy, and Cookie who followed me around every day as if we were in a parade. Even though I was quite boring, all of them were by my side, day in and day out, not asking for anything but an occasional pat or treat. They were the consummate friends.

In spite of support from colleagues, friends, children, and pets, I would never have even started this thesis without the understanding and generosity from my loving husband, Allan. Besides being an established scientist, he was always inspirational, supportive, funny, an excellent cook, a fantastic editor and a true friend. Not only did he see the value of my work for my own personal growth, but he understands what this research means to the scientific community and to the people who will be affected by global sea level rise in the near future. I dedicate my thesis to Allan because he always believed in me and never let me down.

ACKNOWLEDGMENTS

This thesis could not have been completed without the help of numerous individuals who played crucial inspirational and supporting roles. My first inspiration came from Donna Williams during our years together as members of the League of Women Voters. Her passion and professionalism for protecting and enhancing the environment is a model which all of us should live by. Her husband, Ted Williams, an environmental writer who challenges all of us to think critically, was always on the other end of cyber space to offer words of encouragement and to provide an endless supply of jokes, when needed.

When I went back to college in 2001, Dr. John Gerber was my sponsor, my professor, and an advocate for my education. He has continued his support by willingly accepting my request to become a member of my thesis committee. He has provided stability for me during my ups and downs at the University of Massachusetts. Dr. Robin Harrington was not only a member of my committee, but she became a friend and a mentor for me throughout my graduate school years. I will always be grateful to her for excellent lectures, her open door policy, and her warm hugs when either one of us needed one. She was truly an inspiration to me, particularly as a woman scientist. Last, but certainly not least, my thesis advisor, Dr. Jack Finn, took me on as his graduate student in 2005, without even a moment of hesitation on his part. Jack is a very humble person, but the wealth of knowledge he has about the oceans, coastal areas, ecology, spatial data modeling, and more specifically, mathematics, always astounded me. Between his knowledge, working style, views on life, sense of humor, and devotion to the

sciences, I never wanted to finish. If it wasn't for deadlines set by the University, I would still be working away.

I am also indebted to several researchers and organizations for their investigative work and historical data collections. Data from "The Massachusetts Shoreline Change Projected," led by Dr. Robert Thieler of the United States Geological Survey (USGS), was invaluable to me and established the underlying structure of my thesis. All this data was made readily available to me by the Massachusetts Office of Coastal Zone Management (MA CZM). The work of a USGS geologist, Robert N. Oldale, whose book I purchased in the mid-1990s (*Cape Cod and the Islands, the Geologic Story*) led me to become when of his favorite followers. The Office of Geographic and Environmental Information (MassGIS), the USGS, the National Oceanic and Atmospheric Administration (NOAA), the Permanent Service for Mean Sea Level (PSMSL) in the United Kingdom, the United States Department of Agriculture (USDA), and the Natural Resources Conservation Service (NRCS) all provided data relevant to my research.

ABSTRACT

ANALYSIS OF COASTAL EROSION ON MARTHA'S VINEYARD, MASSACHUSETTS: A PARAGLACIAL ISLAND

SEPTEMBER 2008

DENISE BROUILLETTE-JACOBSON, B.A.,

UNIVERSITY OF MASSACHUSETTS AMHERST

M.S., UNIVERSITY OF MASSACHUSETTS AMHERST

Directed by: Professor John T. Finn

As the sea rises in response to global climate changes, small islands will lose a significant portion of their land through ensuing erosion processes. The particular vulnerability of small island systems led me to choose Martha's Vineyard (MV), a 248 km^2 paraglacial island, 8 km off the south shore of Cape Cod, Massachusetts, as a model system with which to analyze the interrelated problems of sea level rise (SLR) and coastal erosion. Historical data documented ongoing SLR (~3mm/yr) in the vicinity of MV. Three study sites differing in geomorphological and climatological properties, on the island's south (SS), northwest (NW), and northeastern (NE) coasts, were selected for further study. Mathematical models and spatial data analysis, as well as data on shoreline erosion from almost 1500 transects, were employed to evaluate the roles of geology, surficial geology, wetlands, land use, soils, percent of sand, slope, erodible land, wind, waves, and compass direction in the erosion processes at each site. These analyses indicated that: 1) the three sites manifested different rates of erosion and accretion, from a loss of approximately 0.1 m/yr at the NE and NW sites to over 1.7 m/yr at the SS site; 2) the NE and NW sites fit the ratio predicted by Bruun for the rate of erosion vs. SLR,

but the SS site exceeded that ratio more than fivefold; 3) the shoreline erosion patterns for all three sites are dominated by short-range effects, not long-range stable effects; 4) geological components play key roles in erosion on MV, a possibility consistent with the island's paraglacial nature; and 5) the south side of MV is the segment of the coastline that is particularly vulnerable to significant erosion over the next 100 years. These conclusions were not evident from simple statistical analyses. Rather, the recognition that multiple factors besides sea level positions contribute to the progressive change in coastal landscapes only emerged from more complex analyses, including fractal dimension analysis, multivariate statistics, and spatial data analysis. This suggests that analyses of coastal erosion that are limited to only one or two variables may not fully unravel the underlying processes.

TABLE OF CONTENTS

Page

ACKNOWLEDGMENTS vi

ABSTRACT... viii

LIST OF TABLES……………………………...……………………………..xvii

LIST OF FIGURES xx

ABBREVIATIONS xxvi

CHAPTER

1. LITERATURE REVIEW 1

Introduction.. 1
Coastal Geology.. 3
Coastal Geomorphology 8
Coastal Erosion 10
Soils/Sediments... 12
Climate 18

Climate Background 18
Climate Research 20
Intergovernmental Panel on Climate Change 23
Climate Data 23
Climate Projections.. 26
Global Warming Skeptics 31

Sea Level Overview... 34

Sea Level Historical Data 35
Sea Level Projections.. 39

Weather 43

Precipitation 43
Hurricanes 45
Winter Storms (Nor’easters) 48

Coastal Zone 52

Beaches and Barrier Beaches 53
Coastal Sand Dunes 55
Sea Level Position and Tides 56
Coastline Length 56

Coastal Population 57
Coastal Tourism 59

Coastal Economics 60
Human Dimensions 63

2. MARTHA'S VINEYARD AND THE STUDY SITES 68

Introduction 68
Historical Overview 69
Coastal Geomorphology 71

Coastal Evolution and Surficial Geology 71
Bedrock and Surficial Sediments 76
Soils 78
Continental Shelf and Depth of Closure 79

Sea Level 81

Tides 82
Sediment Transport and Currents 83

Coastal Erosion 85
Climate 86

Climate Change 87

Weather 88

Hurricanes 88
Northeasters 91

Population 91
Tourism and Coastal Economy 93
Descriptions of the Study Sites 95

SS Study Site 97
NE Study Site 100
NW Study Site 101

3. METHODS 103

Geographic and sea level data 103
Classic statistics, geostatistics, and software 103
Derivation of sea levels 105
Identification of historic shoreline change 107
Mean shoreline change/year 108
Shoreline rate of change/year (least squares linear regression) 108
Anderson-Darling test 109
Methods to test the Bruun model 110
Area of land lost or gained 114
Soil taxonomy, texture, ternary diagram, and hydrologic groups 114

Geophysical characteristics of the transects 116
Distinction between geology, surficial geology, and soils 117
Geology 117
Surficial geology 117
Soils 118
Percent of sand, silt, clay, and hydrologic group 118
Slope 118
HEL water 118
Wetland. 120
Land Use. 120
Compass direction 120
Wind and waves. 121

Intersection of transects and attributes 122
Linear, quadratic, cubic, and multiple regression 124
Transect means/attribute (> 25%) 126
Akaike Information Criterion (AIC) 127
Spatial autocorrelation (Moran's I Index and Z-score) 130
Inverse distance weighting and kriging 132
Fractal dimension analysis 135
Principal component analysis (PCA) 136
Geomorphological risk assessment 143

4. RESULTS 147

Introduction 147
Shoreline Erosion 148

Historical Changes to the Shoreline of Martha's Vineyard 148

MV ERA 01 150
MV ERA 02 155
MV ERA03. 157
MV ERA04. 159
MV ERA01-04 Cumulative Data 161

Historical Changes to the Shorelines of the Study Sites 165

SS Historic Erosion. 166
NE Historic Erosion. 172
NW Historic Erosion 177
Summary of the Study Sites 181

Sea Level Change 182

Historical and Projected Sea Level Changes in the Proximity of Martha's Vineyard 182

Depth of Closure (for Bruun's Rule) 190
Coastal Retreat Based on the Bruun Rule 193
GIS Layers for Candidate Predictor Variables 196

Soil Taxonomy, Texture, and Ternary Diagram 196

Entisols 196
Inceptisols 197
Histosols 198
Spodosols 198
Utisols 199

Geophysical Features Within 800 m of the Martha's Vineyard Shoreline 205

Geology 205
Surficial Geology 207
Soil and Percent of Sand at the Study Sites 209

SS Site 209
NE Site 215
NW Site 223

Slope 227

SS Site 227
NE Site 229
NW Site 229

Highly Erodible Land 230
Wetlands 232

SS Site 232
NE Site 234
NW Site 235

Land Use 236
Compass Direction 239

SS Site 239
NE Site 240
NW Site 240

Wind and Waves 245

Wind 245
Waves 250

Spatial Analysis of Shoreline Erosion 254

Spatial Autocorrelation (Moran's *I* Index and Z-score).. 254
Fractal Dimension Analysis 255

SS Fractal Dimension Analysis 258
NE Site Fractal Dimension Analysis 260
NW Site Fractal Dimension Analysis 263

Predicting Erosion from GIS Layers.. 268

Linear, Quadratic, Cubic, and Multiple Linear Regression 268

SS Regression Results.. 268

Geology 268
Surficial Geology. 268
Soil…. 268
Average Percentage of Sand. 269
Soil and Average Percentage of Sand. 269
Slope... 269
Average Slope 269
Slope and Average Slope 270
Erodible Soil Features 270
Wetland. 270
Land Use 270
Compass Direction 271
Winter and Summer Wind Speed by Percentage of Direction. 271
Winter and Summer Wave by Percentage of Direction......................... 271
Winter Wind Speed and Winter Waves by Percentage of Direction 272

NE Regression Results.. 274

Geology. 274
Surficial Geology. 274
Soil…. 275
Average Percentage of Sand. 275
Soil and Average Percentage of Sand. 275
Slope… 276
Average Slope 276
Slope and Average Slope 276
Erodible Soil Features 276
Wetland. 276
Land Use 277
Compass Direction 277

Winter and Summer Wind Speed by Percentage of Direction 277
Winter and Summer Wave by Percentage of Direction 278
Winter Wind Speed and Winter Waves by Percentage of Direction 278

NW Regression Results 281

Geology. 281
Surficial Geology. 281
Soil…. 281
Average Percentage of Sand. 281
Soil and Average Percentage of Sand. 282
Slope... 282
Average Slope. 282
Slope and Average Slope. 282
Erodible Soil Features. 282
Wetland 283
Land Use. 283
Compass Direction 283
Winter and Summer Wind Speed by Percentage of Direction 284
Winter and Summer Wave by Percentage of Direction 284
Winter Wind Speed and Winter Waves by Percentage of Direction 284

Transect Means/Attribute (> 25%) 287
Akaike Information Criterion (AIC) 291

SS Site 291
NE Site 292
NW Site 292

Principal Component Analysis (PCA) 297

PCA Results for the SS Site 298

Correlation Matrix 298
PCA Interpretations 298

PCA Results for the NE Site 302

Correlation Matrix 302
PCA Interpretations 302

PCA Results for the NW Site 306

Correlation Matrix 306
PCA Interpretations 306
Communality 307

PCA analyses of MV identify two significant variables: geology and surficial geology 310

Geomorphological Risk Assessment 312

Risk Assessment for the SS Site 314
Risk Assessment for the NE Site 319
Risk Assessment for the NW Site 323

5. DISCUSSION 331

Sea level rise in the vicinity of Martha's Vineyard 331

Erosion of the Martha's Vineyard coastline 333
Factors affecting erosion: testing for the applicability of Bruun's rule 334

Addressing erosion one attribute at a time 335
Single variables vs. erosion 336
Analyses of single attributes at the SS site 337
Analyses of single attributes at the NE Site 338
Analyses of single attributes at the NW Site 340
Single variable summary 344
Multiple factors vs. erosion: the application of PCA 345
Risk assessment: the identification of specific MV areas that may be particularly vulnerable to coastal erosion in the next 100 years. 348
Technical difficulties 349
Conclusions and perspectives. 351

APPENDICES

A. SUPPLEMENTAL FIGURES AND TABLES 355

B. VARIABLE AND ATTRIBUTE DESCRIPTIONS 372

BIBLIOGRAPHY 392

LIST OF TABLES

Table Page

1. Hurricane direct hits on New England from 1851-2004, classified according to the Saffir/Simpson Scale. 89
2. Population of the towns of Martha's Vineyard. 91
3. Population densities on Martha's Vineyard. 92
4. Condensed wetland codes used for MV classification. 119
5. Condensed land use classifications. 120
6. Formulas used to calculate the AIC. 129
7. Significance of PCA components. 141
8. Risk assignments based on rates of shoreline change. 143
9. MV transect data during four time periods. 149
10. MV transect statistics by distance changed in meters/year and by shoreline erosion rates of change in meters/year. 150
11. MV shoreline change by towns for eras 01-04 153
12. SS site linear regression rates of shoreline change. 167
13. NE site linear regression rates of shoreline change. 173
14. NW site linear regression rates of shoreline change. 180
15. Summary of historical shoreline rate of change for each study site, from mid-1800's to 1994. 181
16. Historical and projected sea level rise in meters. 189
17. Results for each study site based upon Bruun's ratio. 194
18. Projected shoreline erosion based upon three scenarios for sea level rise. 195
19. Summary table of soil taxonomic classifications on Martha's Vineyard. 199
20. Soil taxonomy on Martha's Vineyard. 200
21. Percentage of surficial geology attributes by study sites. 208

22. Percentage of surficial geology areas by study sites. 209

23. SS study site soil summary and percent of sand, silt, and clay. 210

24. NE study site soil summary and percent of sand, silt, and clay. 217

25. NW study site soil summary and percent of sand, silt, and clay. 224

26. Percentage of slope by study sites. 227

27. Percentage of land by erodible characteristics for each study site. 230

28. Wetland classifications by acreage and percentage on the SS study site. 232

29. Wetland classifications by percentage for SS, NE, and NW study sites. 233

30. Wetland classifications by acreage and percentage on the NE study site. 235

31. Wetland classifications by acreage and percentage on the NE study site. 236

32. Summary percentage of land use characteristics for each study sites. 236

33. Land use classified by MassGIS and the percent of area for each study site. 237

34. SS study site percentage of compass directions for transects. 239

35. NE and NW study sites percentage of compass directions for transects. 240

36. Mean summer and winter wsp (m/sec) and percent of direction. 247

37. Percent of mean wave direction by seasons, 1980-1999. 250

38. Percent of wave direction by month, 1980-1999. 251

39. Spatial autocorrelation results for the SS, NE, and NW study sites. 255

40. SS site regression results for every attribute and variable. 274

41. NE site regression results for every attribute and variable. 280

42. NW site regression results for every attribute and variable. 286

43. Mean SS site attributes that are > 25% on the transects. 288

44. Mean NE site attributes that are > 25% on the transects. 289

45. Mean NW site attributes that are > 25% on the transects. 290

46. SS, NE, and NW sites Akaike Information Criterion major variables results. 293

47. SS site Akaike Information Criterion attributes results. 294

48. NE site Akaike Information Criterion attributes results. 295

49. NW site Akaike Information Criterion attributes results. 296

50. SS site correlation matrix and principal component analysis, significant components highlighted. 301

51. NE site correlation matrix and principal component analysis, significant components highlighted. 304

52. NW site correlation matrix and principal component analysis, significant components highlighted. 308

53. Summary of significant principal components for each study site. 311

54. Summary of communality results for each study site. 311

55. Summary of communality results by variable. 312

56. SS site risk assessment by major variables. 314

57. NE site risk assessment by major variables. 319

58. NW site risk assessment by major variables. 323

LIST OF FIGURES

Figure Page

1. The geologic time scale. 4

2. The USDA soil texture triangle. 14

3. Keeling Curve of CO^2 Concentration.. 19

4. Global Temperature and CO_2 Concentrations. 20

5. History of atmospheric CO_2 back 420K years ago as recorded by the gas content in the Vostock ice core from Antarctica. 22

6. U.S. Temperatures from 1895-2005. 24

7. Global mean temperature... 25

8. Global mean warming 29

9. Global surface warming: actual from 1900 to 2000 and projected from 2000 to 2100. 30

10. Thermohaline circulation pathways... 32

11. Global Mean Sea Level from 1870 to 2003, reconstructed from sea level fields; tide gauge measurements since 1950; and satellite altimetry since 1992. Units are in mm relative to the average for 1961 to 1999. 37

12. Projected sea level rise in meters at 2090-2099 relative to 1980-1999. Model-based range excluding rapid dynamical changes in ice flow. 40

13. Correlation between sea surface temperature and annual intensity of cyclones....... 47

14. U.S. hurricane season.. 49

15. Frequency of intense winter storms in the northern hemisphere from 1900-2000... 51

16. Tidal ranges along the northeastern seaboard of North America. 57

17. Map of Martha’s Vineyard, Massachusetts. 69

18. Diagram of a glacial ice margin... 73

19. Surficial geology of the northeastern U.S. The glacial limit line is depicted by the black dashed line.. 75

20. Major storm tracks across the North American continent and their convergence near New England. 76

21. Continental shelf in the vicinity of Martha's Vineyard 80

22. Longshore sediment along the coastline of the northeastern U.S. 84

23. Aerial photo of the coastline south of Oak Bluffs Harbor, showing littoral drift movement towards the southeast. 84

24. Classification of barrier coastlines according to Hayes' (1979) scheme 86

25. Atlantic hurricanes in the vicinity of Martha's Vineyard (MV). (A) Atlantic hurricane tracks from 1851 to 2004. (B) Hurricanes within 300 km of MV. (C) Hurricanes within 50 km of MV 90

26. Population of the towns of Martha's Vineyard. 92

27. Location of the three study sites on MV. 95

28. IPCC Projected SLR by end of 2100 in meters. High and low values are depicted by several different models 107

29. Diagram of Bruun's Rule depicting equilibrium profile 111

30. Location of WIS Model #74 off the shores of Martha's Vineyard. 121

31. Calculation of the average distance using spatial statistics. 131

32. The PCA geomorphical index process used to derive correlation matrices and risk assessment. 138

33. MV transects in Era 01: shoreline distance changed by m/yr. 151

34. MV summary statistics for era 01: distance in m/yr. 154

35. MV transects in era 02: distance changed in the shoreline by m/yr. 156

36. MV summary statistics for era 02: distance in m/yr. 157

37. MV transects by era 03: distance changed in the shoreline by m/yr. 158

38. MV summary statistics for era 03: distance in m/yr. 159

39. MV transects by era 04: distance changed in the shoreline by m/yr. 160

40. MV summary statistics for era 04: distance in m/yr. 161

41. MV cumulative distance and mean distance by era (regression rate). 162

42. MV summary statistics for era 01-04: distance in m/yr. 163

43. MV shoreline change for era 01-04 in m/yr. 164

44. SS, NE, and NW study sites and linear shoreline rates of change. 164

45. SS site summary statistics for linear regression rates. 166

46. Shoreline change patterns near Lucy Vincent Beach. 168

47. Erratic shoreline change patterns along the south side of Martha's Vineyard, near Jobs Ponds and Jacobs Pond. 169

48. SS, NE, NE sites summary statistics of the percentage of transects that are either eroding, accreting, or in equilibrium. 170

49. SS, NE, NW sites summary by shoreline change and era, LR rate of change. 171

50. NE site summary statistics for linear regression rates. 172

51. Significant erosion east of Farm Pond in Oak Bluffs. 174

52. Accretion on Joseph Sylvia State Beach, Oak Bluffs and Edgartown. 175

53. Shoreline changes at the entrance of Edgartown Harbor (A) 2001; (B) 1890s. 176

54. NW site summary statistics for linear regression rates. 178

55. Accretion (A) and Erosion (B) at the NW study site. 179

56. Scatterplot of sea level rise from 1930-2003 (Woods Hole [WH], Nantucket [ACK], Buzzards Bay [BB], and the Cape Cod Canal [CC]). 183

57. Sea level trend analysis plot (A) and regression analysis (B) near Woods Hole (1933-2003). 185

58. Rate of sea level rise from 1933-1964 (A) and from 1966-2003 (B) near Woods Hole. 186

59. Trend analysis of the rate of sea level rise (A) and linear regression (B) near Nantucket from 1965-2003. 187

60. Trend analysis plot for scenarios #1 and #2. 189

61. Trend analysis plot for scenarios #3 and #4. 190

62. Bathymetry and estimated depth of closure for Martha's Vineyard. 191

63. Continental shelf off the coast of Martha's Vineyard. 192

64. Soil taxonomy map of Martha's Vineyard. 201

65. Ternary diagram showing the percentages of clay, silt, and sand on Martha's Vineyard. 202

66. Map of soils not classified on ternary diagram. 204

67. Map of geologic characteristics on Martha's Vineyard. 206

68. Map of surficial geology on Martha's Vineyard. 207

69. Percentage of sand at the study sites. 211

70. SS study site soil types within 800 m of shoreline. 213

71. Map of nonbedrock escarpment locations in Chilmark and Aquinnah. 214

72. Percentage of sand at the NE study site. 216

73. Barrier beaches at the SS, NE, and NW study sites. 218

74. NE study site soil types within 800 m of shoreline. 220

75. NE study site nonbedrock escarpment and short, steep slopes. 221

76. Nonbedrock escarpment and short, steep slopes in Oak Bluffs. 222

77. NW study site soil types within 800 m of shoreline. 225

78. Map of slope on Martha's Vineyard. 228

79. Map of erodible land classifications for the study sites. 231

80. Map of the wetlands at the SS, NE, and NW study sites. 233

81. Land use characteristics at SS, NE, and NW study sites. 238

82. Map of SS transect compass directions. 239

83. Map of the northern NE study site compass direction transects. 241

84. Map of the southern NE study site compass direction transects. 242

85. Map of the northern NW study site compass direction transects. 243

86. Map of the southern NW study site compass direction transects. 244

87. Histogram of monthly mean wind speed m/sec. 247

88. Compass rose indicating percent of winter and summer wind direction (A), and compass rose with summer, winter and mean directional wind speed m/sec (B). 248

89. Percent of wind speed (m/sec) for all months........ 249

90. Histogram of mean wind speed data per year from 1980 to 1999, by summer and winter seasons. 249

91. Wave direction by quarter for years 1980-1999. 252

92. Summer and winter percent of mean wave direction (1980-1999)........ 252

93. Pie chart of the percentage of wave direction vs. time. 253

94. SS site trend analysis of shoreline change behavior based on historical linear regression rates........ 256

95. NE site trend analysis of shoreline change behavior based on historical linear regression rates........ 257

96. NW site trend analysis of shoreline change behavior based on historical linear regression rates........ 257

97. Cross validation predicted errors from the SS site point data based on historical linear regression results........ 258

98. SS study site semivariogram for point data based upon the linear regression rate for 487 transects. 259

99. SS study site semivariogram fitted line plot - shoreline change m/yr vs distance in meters. 260

100. Cross validation predicted errors from the NE site point data based on historical linear regression results........ 261

101. NE study site semivariogram for point data based upon the linear regression rate for 487 transects. 261

102. NE study site semivariogram for point data based upon the linear regression rate for 487 transects. 263

103. Cross validation predicted errors from the NW site point data based on historical linear regression results........ 264

104. NW study site semivariogram for point data based upon the linear regression rate for 487 transects. 265

105. NW study site semivariogram for point data based upon the linear regression rate for 487 transects. 265

106. Map of SS, NE, and NW study site ordinary prediction kriging results based on historical shoreline changes. 267

107. PCA surface, scree, and loading plots of the SS study site. 300

108. PCA surface, scree, and loading plots of the NE study site. 305

109. PCA surface, scree, and loading plots of the NW study site. 309

110. SS site mean risk assessment for each major variables. 316

111. Mean risk assessment results for the SS study site, with and without wetlands in the analysis. 317

112. Inverse Distance Weighting (IDW) for the SS site based upon risk assessment. ... 318

113. NE site mean risk assessment for each major variables. 320

114. Mean risk assessment results for the NE study site, with and without wetlands in the analysis. 321

115. Inverse Distance Weighting (IDW) for the NE site based upon risk assessment. .. 322

116. NW site mean risk assessment for each major variables. 325

117. Risk assessment results for the NW study site, with and without wetlands in the analysis. 326

118. Inverse Distance Weighting (IDW) for the NW site based upon risk assessment. 327

119. IDW Risk assessment for Martha's Vineyard 328

120. Kriging predictions for geomorphological risk assessment for MV 329

121. Kriging prediction standard error map based upon geomorphological risk assessment for Martha's Vineyard. 330

122. Example of technical difficulties with transects in the water. 350

ABBREVIATIONS

Abbreviation	Description
ACK	Nantucket
AD	Anderson-Darling Test Statistic
AIC	Akaike Information Criterion
AQ	Aquinnah
AR4	Fourth IPCC Assessment Report
BB	Buzzards Bay
CC	Cape Cod Canal
CH	Chilmark
Chappy	Chappaquiddick
CI	Confidence Interval
CZM	Coastal Zone Management
CZMA	Coastal Zone Management Act
DOC	Depth of Closure
DSAS	Digital Shoreline Analysis System
ED	Edgartown
EPA	Environmental Protection Agency
EPICA	European Project for Ice Coring in Antarctica
ERA	Measure of Time Period for Shoreline Change Data
ESO	Escarpment
FAR	First IPCC Assessment Report
FEMA	Federal Emergency Management Agency
GEO	Geology
GIA	Glacial Isostatic Adjustments
GIS	Geographical Information System
HEL	Highly Erodible Land
IDW	Inverse Distance Weighting
IPCC	Intergovernmental Panel on Climate Change
LR	Linear Regression (Historical Rate of Shoreline Change)
LUS	Land Use
MA CZM	Massachusetts Coastal Zone Management
MassGIS	Massachusetts Geographical Information System
MEMA	Massachusetts Emergency Management Agency
MOC	Meridional Overturning Circulation
MSL	Mean Sea Level
MV	Martha's Vineyard
NE	Northeast Study Site
NESIS	Northeast Snowfall Impact Scale

Abbreviation	Description
NOAA	National Oceanic and Atmospheric Administration
NRCS	Natural Resources Conservation Survey
NW	Northwest Study Site
OK	Oak Bluffs
OLS	Ordinary Least Squares
PCA	Principal Components Analysis
PSMSL	Permanent Service for Mean Sea Level
RLR	Revised Local Reference
RSL	Relative Sea Level
RUSLE2	Revised Universal Soil Loss Equation
SAR	Second IPCC Assessment Report
SG	Surficial Geology
SLR	Sea Level Rise
SRES	Special Report on Emission Scenarios
SS	South Side Study Site
SST	Sea Surface Temperature
SSURGO	Soil Survey Geographic Database
STATSGO	State Soil Geographic Database
TAR	Third IPCC Assessment Report
UNEP	United Nations Environment Programme
USDA	United States Department of Agriculture
USGS	United States Geological Survey
VIF	Variance Inflation Factors
WCED	World Commission on Environment and Development
WET	Wetland
WGI	IPCC Working Group I
WH	Woods Hole
WHOI	Woods Hole Oceanographic Institution
WIS	Wave Information Studies
WMO	World Meterological Organization
WSP	Wind Speed
WT	West Tisbury

CHAPTER 1

LITERATURE REVIEW

Introduction

The coastline is one of the first systems to feel the effects of sea level rise caused by warming of the Earth's atmosphere and ocean. Coastal environments are in a dynamic relationship with the sea, with their sand and soil constantly shifting, creating new shorelines or eroding others. Sea level rise exacerbates erosion, and human activities, such as construction of buildings, roads, and seawalls, block the natural landward migration of marshes and dunes. As a result, shorelines erode, increasing the threat to coastal development and infrastructure (Briguglio, 2004). Continued sea level rise, as predicted by the Intergovernmental Panel on Climate Change (IPCC), will only exacerbate these problems.

A confluence of problems ensures that islands are the environment most sensitive to global climate change and sea level rise (Field *et al.*, 2001). Simply because of physical geography, islands and low-lying coastal areas are the most vulnerable to sea level rise. Small islands are particularly vulnerable to the effects of global warming, including sea level rise, because of their size, insularity, remoteness (in some cases), and susceptibility to natural disasters (Briguglio, 2004). They have limited resources, existing environmental concerns attributable to water shortages, waste disposal, pollution, loss of biodiversity, and increases in tourism, and their economies are generally vulnerable to forces outside their control (Oldale, 1992).

Small islands, in many cases, will lose a significant portion of their land to the sea as it rises. Many islands also face overdevelopment and rapid population growth.

Population growth increases development pressure on islands, and sea level rise forces barrier islands and beach/dune systems to back up against already developed land. In addition, land use changes and potential increases in storm frequency and/or severity have the potential to increase shoreline erosion, accelerating land loss and overwhelming the mechanisms by which barrier islands and salt marshes have remained above sea level since the last glacial period.

Predictions indicate that as temperatures increase, on land and in the sea, glaciers will melt and seas will rise at a faster rate than previously witnessed (IPCC WGI, 2007). In the past, there have been many cycles of glaciation and deglaciation and with each, the landscape changed. The effects of these glaciation cycles have had a pivotal role in the current New England landscape. In Massachusetts, the islands of Martha's Vineyard (MV) and Nantucket were formed as a direct result of the last glacial period, approximately 30,000 to 18,000 years ago (Balco *et al.*, 2002; Lambeck *et al.*, 2002; Oldale, 1992; Upham, 1879). Essentially, glacial debris is the major component of these islands, which fundamentally is unstable, as long as the drift material remains easily accessible for fluvial erosion and transportation (Church & Ryder, 1972). These islands are considered to be paraglacial in nature (Fitzgerald & Van Heteren, 1999) because they were formerly ice-covered terrain, created from glacial sediments that have a recognizable influence on the character and evolution of the coast and nearshore deposits (Forbes & Syvitski, 1997).

Martha's Vineyard is located 8 km (~5 miles) off the south shore of Cape Cod, Massachusetts. Cape Cod and the islands (Martha's Vineyard and Nantucket) depend heavily on tourism and therefore, desirable environmental conditions are critical to supporting the economy of Massachusetts (Massachusetts Ocean Management Task Force, 2004). Because of its economic value to the state, its small size, geology, and perceived value as a prime vacation spot, Martha's Vineyard provides an excellent model system for this thesis. Year-round and seasonal residents are relatively pro-active in both land-use policies and tactics to preserve the island's natural resources, especially when compared to the residents of many island nations around the world. Armed with a better understanding of coastal erosion patterns, residents will be able to plan for their future. When seas rise, the coastline responds, either through simple inundation, or by a variety of complicated landward retreat patterns. Ultimately, I argue that a coastal island can never be a sustainable level in perpetuity, because of all the natural and manmade forces acting upon it. The best that can be hoped for is that, with long term planning, the inhabitants of Martha's Vineyard will safely retreat from the island, rather than attempt to guard themselves against the forces of the ocean.

This thesis examines the glacial history of New England, coastal geomorphology, climate, weather, sea level, and the primary factors that influence shoreline erosion patterns on the Vineyard. To understand the fundamental processes driving coastal erosion on this paraglacial island, data on shoreline erosion at 2000[2] transects (MA CZM, 2001) over the last 150 years was used. Mathematical models and spatial data analysis were employed to discover the underlying processes affecting erosion on these transects.

Coastal Geology

Ancient geological events shaped coastal regions around the globe, from eons, eras, periods, to the most recent Epoch, the Holocene (Figure 1). The time scale of most importance for this thesis began during the Quaternary Period (between 1.8 million – 2.6

million years ago) and continues into the present. This period is divided into two epochs: the Pleistocene (1.8 million to ~ 10,000 years ago), which resulted in both glacial deposition and erosion of New England (NOAA, 2003c; Oldale, 1992), and the Holocene, which began ~ 10,000 years ago, is still ongoing, and comprises the period of time since the last major ice age and the rise of civilizations.

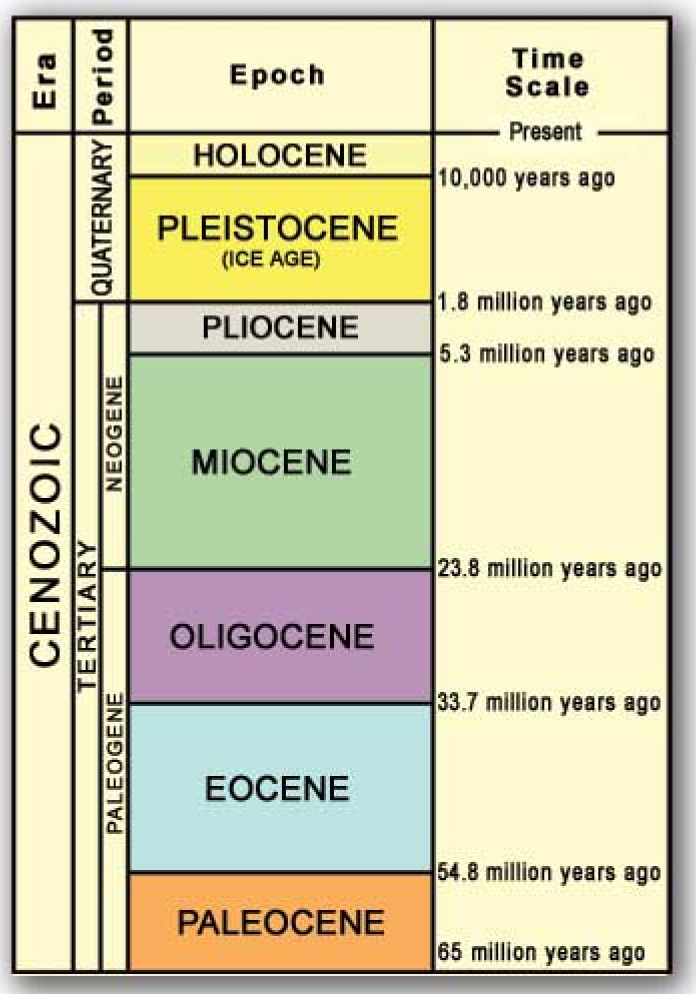

Figure 1. The geologic time scale.
From http://www.dep.state.fl.us/geology/geologictopics/rocks/time_scale.htm

The Pleistocene Epoch witnessed dramatic climatic fluctuations in the Northern Hemisphere, marked by the modern Ice Age. The effects of its glaciers played a pivotal role in establishing the current New England landscape. As the glaciers began to recede, the oceans began to receive all the land-based, locked up water, and sea levels began to rise, covering the Atlantic Continental Shelf to the current shorelines.

The Atlantic Ocean Basin formed when North America, Africa, and Europe began to move apart during the late Triassic and early Jurassic (200-180 million years ago) (Emery & Uchupi, 1972; Schlee *et al.*, 1976). As the three continental plates began to move apart, the Atlantic Basin began to fill, and it continued to widen during the Cenozoic (Poag, 1978). Subsidence along the U.S. Atlantic Coastal Margin occurred, along with eustatic sea level changes, and activity of the Gulf Stream (Poag, 1978). During the Paleocene, Eocene, and Oligocene, warm tropic to subtropical environments accompanied the Gulf Stream (Poag, 1978). However, during the Miocene, the Gulf Stream shifted southward and the northern sediments became increasingly clastic (Poag, 1978). During the Peistocene and Holocene, most clastic sediments were deposited on the continental slope and this process was accentuated during glacial sea levels when the shoreline moved close the present continental shelf break (Poag, 1978).

At present, most of eastern North America is considered to be relatively stable tectonically (Brett & Caudill, 2004; Sykes, 1978; Zoback & Zoback, 1981). While tectonics have been a major factor in shaping the Vineyard over millions of years, it is not the primary variable of shoreline change within the last 150 years, nor is it likely to be an influential factor within the next 100 years. Therefore, tectonics will not be considered further in this thesis, and will only serve as background information.

The Earth has gone through many cycles of glaciation and deglaciation, and with each, the landscape has changed. During each of these cycles, sediment was formed by two methods: through glacial abrasion, which is the mechanical scraping of a rock surface by friction, and/or by plucking, which is the process when a glacier erodes chunks of bedrock that are then carried along by ice and dropped either at the most forward position of the glacier, or along the way. The sediments that reside in glacial till and moraines may then be strewn in fluvial outwash and eolian loess deposits (Anderson, 2007).

Landscapes affected by glaciation are described as paraglacial (Forbes & Syvitski, 1997). The term "paraglacial" was first coined by Church and Ryder (1972) to describe alluvial deposits in south-central British Columbia and east-central Baffin Island, Northwest Territory. Later, Forbes and Syvitski (1997) broadened the definition to include paraglacial coasts "to be those on or adjacent to formerly ice-covered terrain, where glacially excavated landforms or glaciogenic sediments have a recognizable influence on the character and evolution of the coast and nearshore deposits." Their definition excludes the effects of glacio-isostatic rebound because it is an indirect tectonic response and not a direct response to glaciations (Ballantyne, 2002b; Forbes & Syvitski, 1997).

In a 2002 review about paraglacial morphology, Ballantyne defined paraglacial as "nonglacial earth-surface processes, sediment accumulation, landforms, landsystems and landscapes that are directly conditioned by glaciations and deglaciation" (Ballantyne, 2002b). The reworking of glacigenic sediments within the coastal zone equilibrates to non-glacial conditions over differing time scales (Ballantyne, 2002a). It may take several tens of thousands of years for the paraglacial landscape to become non-glaciated because the glacigenic sediments along coastlines still dominate sediment budgets (Ballantyne, 2002a). This reworking of "glacially conditioned sediment release" (Ballantyne, 2002a) results "in exposure of unstable or metastable sediment sources" over a wide range of timescales (Ballantyne, 2002a).

Ballantyne defines 'paraglacial processes' as "the timescale over which a glacially conditioned sediment source either becomes exhausted or attains stability in relation to particular reworking processes. Once this has occurred, sediment release may be envisaged as having relaxed to an 'equilibrium' or 'non-glacial state, indistinguishable from that which would result from primary denudation of the land surface" (Ballantyne, 2002a). A 'paraglacial period' is, therefore, the period of readjustment, or relaxation, from a glacial to a nonglacial condition (Ballantyne, 2002b; Benn & Evans, 1998). Large fluvial systems may continue to rework glacigenic sediment for more than 10,000 years before they achieve stability (Ballantyne, 2002b). Temporal patterns of sediment delivery and/or availability are largely determined by the disposition of glacigenic deposits relative to the coastline and by changes in relative sea levels (Forbes & Syvitski, 1997).

According to Orford, *et al*., (2002), the fundamental controls on the initiation and development of beaches and barriers on paraglacial coasts are particle size and shape, sediment supply, storm wave activity (primarily runup), relative sea-level (RSL) change, and terrestrial basement structure.

Morphodynamic responses of paraglacial coasts are distinctly different from those associated with sand-dominated coasts (Carter & Orford, 1993; Forbes & Taylor, 1987; Orford *et al*., 2002). These differences depend upon morphosedimentary memory and dynamic feedback process, leading to self-organization and potentially chaotic evolution of barrier form and stability (Forbes *et al*., 1995).

Coastal Geomorphology

Coastal geomorphology implies the progressive change in the shape of the coastal landscape induced by perturbations in geomorphic processes or environmental changes (Coastal Landform, 2008a). The coastal geologic setting controls surficial geomorphology, sediment type and availability, and overall gradient (Morang & Parson, 2006; USACE, 1995). The most critical lithologic parameters responsible for a rock's susceptibility to erosion are the mineral composition and the degree of consolidation (Morang & Parson, 2006; USACE, 1995). There is a difference between coasts underlain by consolidated rock and those by unconsolidated material (e.g., Maine's coastline vs. that of Martha's Vineyard).

Consolidated coasts consists of firm and coherent material and the degree of consolidation greatly influences the ability of a rocky coastline to resist weathering and erosion (Morang & Parson, 2006; USACE, 1995). Resistance to weathering depends on the hardness and solubility of minerals and cementation, nature and density of voids, and climatic conditions (Morang & Parson, 2006; USACE, 1995). Deposition and erosional processes dominate unconsolidated coasts because of large amounts of sediment that are usually available, and morphological changes occur rapidly (Morang & Parson, 2006; USACE, 1995).

Presently, sea level rise caused by global warming comprises a major perturbation (Smith, 2004). As seas rise, the coastline responds, either through simple inundation, or by a variety of complicated landward retreat patterns. Coastal environments are in a dynamic relationship with the sea, with shorelines constantly shifting. The coastline may evolve yet remain close to its original equilibrium state, which is considered stable, or the coastline may move further away from the original state and become unstable.

Other factors, besides sea level positions, that contribute to the progressive change in coastal landscapes include: time scale, tectonic setting, geological structure, sediment type and availability, coastline length, wave and current processes, and the adjacent terrestrial and oceanic environments (Carter & Woodroffe, 1997). Ideally, all of these factors need to be considered when studying the coastal environment because they work together as a system. To limit analyses to only one or two variables may not fully unravel the interactions between all of them.

In contrast to geologic time, storms play a major role in short term shoreline change along the eastern seaboard of the U.S. (Forbes *et al.*, 2004; Hill *et al.*, 2004; Ogden, 1974; Uchupi *et al.*, 2005; USGS, 2005). The effects of storms tend to be short-lived and coastlines typically return to their pre-storm position. Under storm conditions, coastal erosion is increased by the type of tides, wave energy, and the duration of the event (Zhang *et al.*, 2001). Storms often cause short-term flooding and erosion, but the coastline rebounds over a period of time.

However, the combination of sea level rise and the increased frequency of storm surges, caused by global warming, results in increased coastal erosion, coastal flooding, and loss of coastal wetlands (IPCC, 2002). This is particularly noticeable in Louisiana, Florida, and other parts of the U.S. Atlantic coast (IPCC, 2002). With sea level rise, it is estimated that approximately 50% of North American coastal wetlands could be inundated (IPCC, 2002).

Coastal Erosion

Erosion is the gradual physical wearing of surface materials, either by water or wind. Along the coastline, this is exacerbated by currents, wave action and/or tides. There is a delicate balance at the coastline between the forces that erode the beach by carrying away the sand and the forces that tend to move sand onto the beach from other areas, a process known as accretion (Caldwell, 1949).

Wave conditions and currents help shape the coastline by greatly influencing sand transport, thereby serving as major causes of erosion and accretion (Beatley *et al.*, 2002; Sea Grant Woods Hole, 2003). As waves approach the shoreline, they become unstable and break, varying as a function of the slope of the bottom and wavelength (Denny, 1987, 1988; Sea Grant Woods Hole, 2003). The steeper the beach profile, the more wave energy increases and the greater the sediment disturbance (Beatley *et al.*, 2002). Other factors influencing erosion include: exposure to high-energy storm waves, sediment size, composition of eroding coastal landforms feeding adjacent beaches, alongshore variations in wave energy and sediment transport rates, and relative sea level rise. Humans help to accelerate these processes by using coastal defense mechanisms that interfere with sediment supply (e.g., groins and jetties) and by incorrect beach nourishing (Sea Grant Woods Hole, 2003).

There is a difference between coastal erosion and inundation. Inundation occurs when the high water line migrates landward, resulting in severe flooding, especially if there is a low coastal slope. Under global warming conditions, this landward movement of water is permanent (as contrasted to the typical short-term effects of storms). Erosion of sandy beaches, commonly occurring from coastal storms, involves a temporary increase in sea levels, and a redistribution of sand from the beach face to offshore (Zhang *et al.*, 2004). Usually, the sand eroded in storms moves back towards the shore when normal conditions resume (Zhang *et al.*, 2004).

In 1997, approximately 11% of the Massachusetts shoreline was seriously eroding (Bernd-Cohen & Gordon, 1999). More recent estimates by Massachusetts Coastal Zone Management suggest that approximately 65% to 70% of the coastline is eroding (MA CZM, 2006b). Not all erosion is detrimental to the coastline. Shifting sediment can provide material for beaches, dunes, barrier beaches, and estuaries.

A report published by the USGS in 1999 ranked the eastern coastline of the United States according to coastal vulnerability to sea level rise (Thieler & Hammar-Klose, 1999). The coastline of northern New England, particularly Maine, shows a relatively low vulnerability to future sea level rise because of steep coastal slopes and rocky shorelines characteristic of the region, as well as the large tidal range (Thieler & Hammar-Klose, 1999). In contrast, southern New England, Cape Cod, Nantucket, and Martha's Vineyard have the highest coastal vulnerability because of their high-energy coastlines, the low coastal slope, and the existence of barrier islands as the major landform type (Thieler & Hammar-Klose, 1999).

Over the next 60 years, erosion may claim one out of four houses within 152 m (500 ft) of the U.S. shoreline (The Heinz Center, 2000). Most of the damage from erosion over the next 60 years will occur in low-lying areas subject to flooding. Additional damage will also occur along eroding coastal bluffs (The Heinz Center, 2000). Massachusetts is already eroding: approximately 68% (826 km/513 miles) of Massachusetts' ocean-facing shore exhibits a long-term erosional trend; 30% (364 km/226 miles) shows a long-term trend of accretion; and 2% shows no net change (Sea Grant Woods Hole, 2003).

Soils/Sediments

River inputs of sediment are virtually non-existent on coastlines such as that of Martha's Vineyard, thereby increasing the importance of sea level rise to release additional sediments further inland. When these sediments slide into the sea, in theory, an equilibrium profile should be re-established, according to the Bruun Rule (to be discussed below). Ballantyne suggests that on paraglacial coasts, where the main source of sediment is composed of reworked in situ glacigenic deposits, additional sediment supplies may be prolonged by rising sea levels (Ballantyne, 2002b).

There are three categories of rocks: igneous, sedimentary, and metamorphic. Igneous rocks result from the cooling of hot molten rock; sedimentary rocks form from the laying down of layers of loose sediment and the transformation of loose sediment into rock through time and pressure; and metamorphic rocks result from pre-existing sedimentary, igneous and metamorphic rocks that are exposed to increases in temperature and pressure (Ansley, 2000; Soil Survey Division Staff, 1993; Tarbuck & Lutgens, 2000). Soil, a combination of minerals, organic matter, water and air, is formed from weathering processes (Tarbuck & Lutgens, 2000). Soils must be capable of supporting plants and areas that do not support plant growth are not considered soil (Turenne, 2007). Therefore, beaches, active gravel pits, urban land, deepwater habitats, bedrock outcrops, and glaciers are not classified as soil, but are mapped as miscellaneous areas in soil survey reports (Turenne, 2007).

Soil taxonomy is a hierarchial system, determined by the U.S. Department of Agriculture's (USDA's) Global Soil Regions data set (Palm *et al.*, 2007). Soil taxonomy is classified into 12 orders, Alfisols, Andisolds, Aridisols, Entisols, Gelisols, Histosols, Inceptisols, Mollisols, Oxisols, Spodosols, Utisols, and Vertisols (Palm *et al.*, 2007; Soil Survey Staff, 2006). It is not my intent to review all 12 of these orders. However, Martha's Vineyard contains 5 of these 12 which will be summarized in the soils section under "Martha's Vineyard Literature Review" and "Results."

The U.S. Department of Agriculture (USDA) and the Natural Resources Conservation Survey (NRCS) define soil as: "a natural body comprised of solids (minerals and organic matter), liquid, and gases that occurs on the land surface, occupies space, and is characterized by one or both of the following: horizons, or layers, that are distinguishable from the initial material as a result of additions, losses, transfers, and transformations of energy and matter or the ability to support rooted plants in a natural environment (Soil Survey Staff, 2006)." The lower boundary of soil has been arbitrarily set at 200 cm (~6.5 ft) by the USDA. Little biological activity occurs in the "non-soil" beyond 200 cm (Soil Survey Staff, 2006).

Soil texture determines the surface area, soil bulk density, total soil porosity, and pore size distribution, and these combined properties affect the movement of water in the soil (Flanagan *et al.*, 1999). To classify sediments, Shepard (1954) divided a ternary diagram into ten classes: 1) clay; 2) silty clay; 3) clayey silt; 4) sand, silt, clay; 5) silt; 6) sandy silt; 7) silty sand; 8) sand; 9) clayey sand; and 10) sandy clay (Figure 2).

The USDA uses the basic principles of Shepard's classification to describe the texture of soils by the percent of sand, silt, and clay (Soil Survey Division Staff, 1993).

The USDA's texture triangle includes the following 12 categories: clay, silty clay, silty clay loam, silt loam, silt, loam, sandy loam, loamy sand, sand, sandy clay loam, sandy clay, and clay loam (USDA, 2007a).

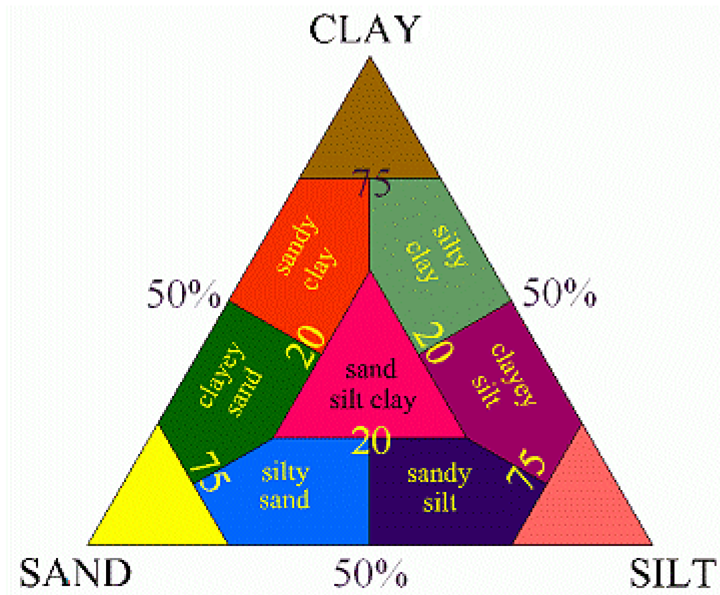

Figure 2. The USDA soil texture triangle (USDA, 2007a).

The following are soil texture definitions for sand, silt, and clay, published by the USDA: 1) sand (coarse texture) - more than 85% sand, the percentage of silt plus 1.5 times the percentage of clay is less than 15; 2) silt (medium textured) - 80% or more silt and less than 12% clay; and 3) clay (fine textured) - 40% or more clay, 45% of less sand, and less than 40% silt (Soil Survey Division Staff, 1993).

Organic material is not included in Shepard's ternary diagram, but is considered a form of soil. Within the organic materials there are three classifications: 1) peat; 2) muck; and 3) mucky peat. Organic material accumulates in wet places where it is deposited more rapidly than it decomposes (Soil Survey Division Staff, 1993). This is the formation of peat (fibric) which may in turn become parent material for soils (Soil Survey Division

Staff, 1993). If all the organic remains are sufficiently fresh and intact to permit identification of plant forms, then the organic matter is called peat (Soil Survey Division Staff, 1993). Mucky peat (hemic) occurs when a significant part of the material can be recognized and a significant part cannot (Soil Survey Division Staff, 1993). If virtually all of the plant material has undergone sufficient decomposition and has limited recognition, this is considered muck (sapric) (Soil Survey Division Staff, 1993).

Particle sizes, from < 2 mm to > 76 mm, are classified as follows (Soil Survey Division Staff, 1993):

- Fine: < 2 mm
- Medium: 2 - 5 mm
- Coarse: 5 - 20 mm
- Very coarse: 20 - 76 mm
- Extremely coarse: > 76 mm

The USDA uses the following size classifications for the <2 mm mineral material (Soil Survey Division Staff, 1993):

- Very coarse sand: 2.0-1.0 mm
- Coarse sand: 1.0-0.5 mm
- Medium sand: 0.5-0.25 mm
- Fine sand: 0.25-0.10 mm
- Very fine sand: 0.10-0.05 mm
- Silt: 0.05-0.002 mm
- Clay: < 0.002 mm

In 1955, Musgrave assigned soils to a hydrologic group based on measured rainfall, runoff, and infiltrometer data (Musgrave, 1955). Since then, assignments of soils have been based on the judgment of soil scientists (Mockus *et al.*, 2007). Some factors that are considered when classifying hydrologic soils depend upon climatic regions, transmission rate of water, texture, structure, and degree of swelling when saturated (Mockus *et al.*, 2007). Other factors include the intake and transmission of water under the conditions of maximum yearly wetness; soil not frozen; bare soil surface; and maximum swelling of expansive clays (Mockus *et al.*, 2007). Interestingly, the slope of the surface is not considered when assigning hydrologic soil groups (Mockus *et al.*, 2007). The definition of hydrologic group is "a group of soils having similar runoff potential under similar storm and cover conditions" (Mockus *et al.*, 2007). Changes in soil properties caused by land management or climate changes can cause the hydrologic soil group to change (Mockus *et al.*, 2007).

Hydrologic groups are classified into four groups A, B, C, and D, and three dual classes A/D, B/D, and C/D, according to soil properties that influence runoff potential under similar storm and cover conditions (Turenne, 2007; USDA, 2007b). Definitions for each of these classes are:

- A: Soils with low runoff potential. Soils having high infiltration rates even when thoroughly wetted and consisting chiefly of deep, well drained to excessively well-drained sands or gravels. This group typically has 90% sand or gravel, and has gravel or sand textures. Some soils may have loamy sand, sandy loam, loam or silt loam textures as well (Mockus *et al.*, 2007).

- B: Soils having moderate infiltration rates even when thoroughly wetted and consisting chiefly of moderately deep to deep, moderately well drained to well drained soils with moderately fine to moderately coarse textures. Group B soils typically have between 10-20% clay and 50-90% sand, and have loamy sand or sandy loam textures (Mockus *et al.*, 2007).
- C: Soils having slow infiltration rates even when thoroughly wetted and consisting chiefly of soils with a layer that impedes downward movement of water, or soils with moderately fine to fine textures. These soils have between 20-40% clay and less than 50% sand and have loam, silt loam, sandy clay loam, clay loam, and silty clay loam textures (Mockus *et al.*, 2007)
- D: Soils with high runoff potential. Soils having very slow infiltration rates even when thoroughly wetted and consisting chiefly of clay soils with a high swelling potential, soils with a permanent high water table, soils with a claypan or clay layer at or near the surface, and shallow soils over nearly impervious material. Group D soils typically have greater than 40% clay, less than 50% sand, and have clayey textures (Mockus *et al.*, 2007).
- Dual hydrologic soil groups A/D, B/D, and C/D: Soils are classified as D soils based on the presence of a water table within 60 cm (24 in) of the surface even though the saturated hydraulic conductivity may be favorable for water transmission (Mockus *et al.*, 2007). Therefore, if these soils can be adequately drained, then they are classified in the dual hydrologic soil groups. The first letter applies to the drained condition and the second letter applies to the undrained condition (Mockus *et al.*, 2007).

Climate

Climate can be defined by the long-term statistics of temperature, precipitation, wind, and other aspects of the climate system (NOAA, 2006f).

Climate Background

Life on Earth depends on the hospitability of its climate. Any change in the Earth's climate will have an impact on humankind, on biodiversity, on the health and services delivered by ecosystems around the globe, and on the ability of the earth to support socio-economic development (Wang & Schimel, 2003). Modern humans have occupied the Earth for approximately 130,000 years. During this time, climate changes occurred naturally with little human influence. Since the Industrial Revolution, from the late 1700s to the mid-1800s, agricultural and industrial practices changed, altering the climate and environment at an unprecedented pace (EPA, 2006; Houghton, 2004; NRC, 2001; UCS, 2006).

Toward the end of the 19^{th} century, Nobel Laureate Svante August Arrhenius hypothesized that the increasing amounts of carbon dioxide (CO_2) emitted by factories of the Industrial Revolution were causing an increase in the atmospheric concentration of greenhouse gases, which could result in global climatic changes (Philander, 2000). The first person to confirm the rise of atmospheric carbon dioxide was Charles D. Keeling (Scripps Institution of Oceanography, 2005). He measured "pristine air" at Mauna Loa, Hawaii, and other locations from 1958 until 2004 (Keeling & Whorf, 2004). His time-series data set of CO_2 concentrations is important for the study of global change. Figure 3 shows the monthly average CO_2 concentration in parts per million at the Mauna Loa Observatory in Hawaii.

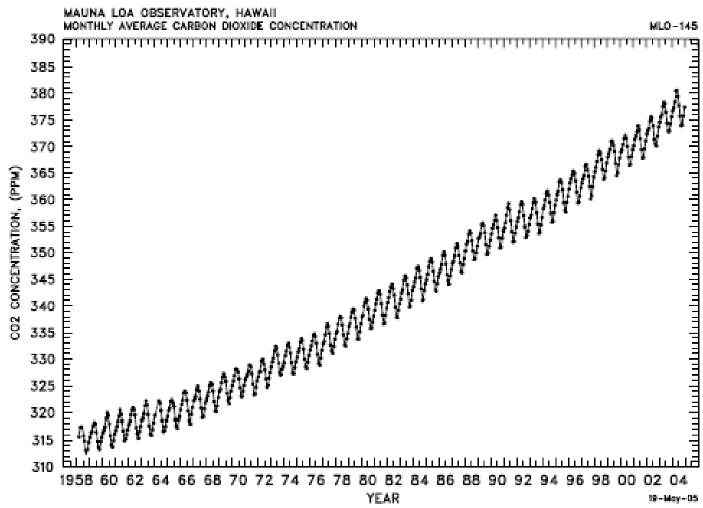

Figure 3. Keeling Curve of CO^2 Concentration (Keeling and Whorf, 2004).

Overlaying Keeling's CO_2 measurements on top of global temperatures for the same time period (Figure 4) shows that the time-dependent changes in global average surface heating parallel the CO_2 increases (Karl & Trenberth, 2003). While there are many factors that may alter global temperatures, data suggest that CO_2 may be one of them. The IPCC reports that carbon dioxide is the most important anthropogenic greenhouse gas (IPCC WGI, 2007). Greenhouse gases trap Earth's outgoing radiation in the lower atmosphere (Karl & Trenberth, 2003), thereby raising temperatures. To some degree, the "greenhouse effect" is important because it helps to moderate the climate on Earth. In its absence, the average temperature of the planet would be approximately -18 C (-0.40°F) instead of 14°C (57°F) (NOAA, 2006b).

The naturally occurring greenhouse gases include CO_2, as well as methane (CH_4), nitrous oxide (N_2O), water vapor, (H_2O), ozone (O_3), and the chloroflurocarbons (EPA, 2006; NRC, 2001). These greenhouse gases, in particular carbon dioxide, are increasing unnaturally. Atmospheric concentrations of carbon dioxide (CO_2) have increased by 31%

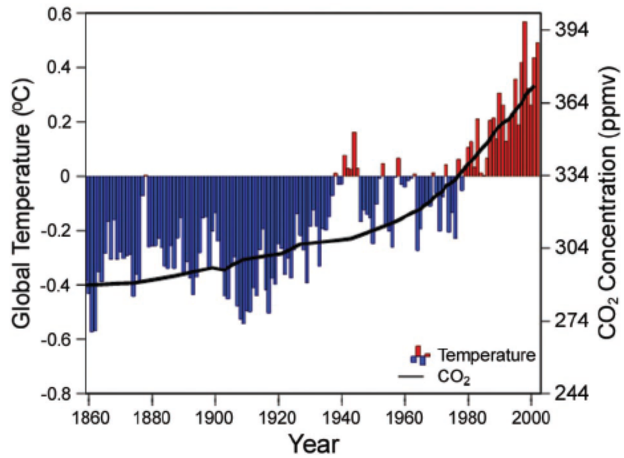

Figure 4. Global Temperature and CO_2 Concentrations (Karl and Trenberth, 2003).

since 1750 (IPCC, 2001a). The current rate of increase is unprecedented during at least the past 20,000 years (IPCC, 2001a). About three-fourths of the anthropogenic emissions of CO_2 to the atmosphere during the past 20 years are due to the burning of fossil fuel and the rest is predominantly due to land-use change, especially deforestation (IPCC, 2001a). It is thought that CO_2 is the major greenhouse gas of concern (Houghton, 2004), yet one that could be managed because humans are spewing it into the atmosphere at an accelerated pace.

Climate Research

In the Northern Hemisphere, large sheets of continental ice have grown and retreated many times in the past. Glacial/interglacial variations occur approximately every 100,000 years (Lambeck *et al.*, 2002; Petit *et al.*, 1999; Sigman & Boyle, 2000) and these changes are thought to occur because of the Earth's precession (rotation on its axis), obliquity (tilt of the Earth's axis relative to the orbit), and eccentricity (Earth's elliptical orbit) (Berger, 1978; Imbrie *et al.*, 1992; Petit *et al.*, 1999). Climate studies underway are investigating whether the Earth is presently in one of these periods. Methods employed in the study of climate examine paleoclimate evidence from ice cores, tree rings, and other natural recorders that document large changes in climate, such as in temperature and precipitation (NOAA, 2006f).

A significant climate study from Lake Vostok (Priscu *et al.*, 1999), the largest and deepest glacial lake identified beneath the Antarctic ice, has produced ice cores two kilometers long that carry a 150,000 year climate record (Barnola *et al.*, 1987; Weart, 2003). Analyses of these cores showed a correlation between the levels of atmospheric CO_2 and the rise and fall of temperatures (Lorius *et al.*, 1985).

Since the initial drilling in the mid-1980s, Petit, *et al*. (1999) and the European Project for Ice Coring in Antarctica (EPICA) team drilled deeper into the surface and retrieved cores that date back approximately 420,000 and 740,000 years, respectively (Augustin *et al.*, 2004). Paleoclimatology of ice cores reveals detailed information about local temperature and precipitation rates, moisture source conditions, wind strength and aerosol fluxes of marine, volcanic, terrestrial, cosmogenic, and anthropogenic origin (Augustin *et al.*, 2004; Petit *et al.*, 1999). Figure 5 illustrates the findings of atmospheric CO_2 and the ratio of deuterium to hydrogen (δD) in ice from 420,000 years ago, recorded by the gas content in the Vostok ice core (Petit *et al.*, 1999; Sigman & Boyle, 2000). During peak glacial periods, atmospheric CO_2 is 80-100 parts per million by volume (ppmv) lower than during peak interglacial periods, with upper and lower limits that are reproduced in each of the 100,000 year cycles (Sigman & Boyle, 2000).

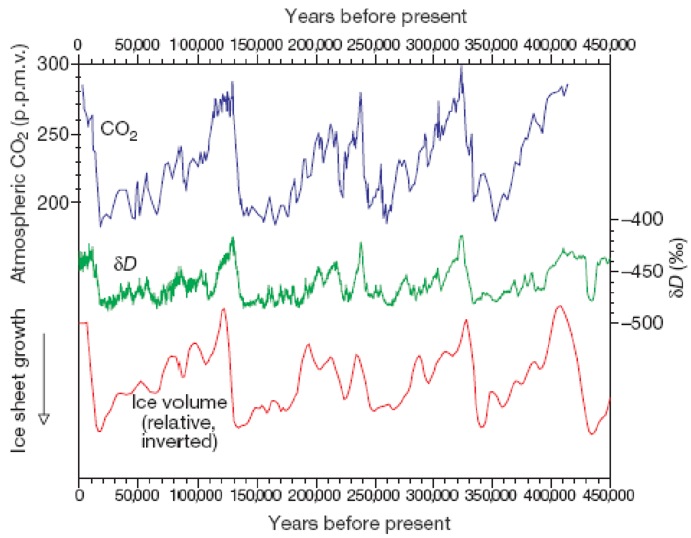

Figure 5. History of atmospheric CO_2 back 420K years ago as recorded by the gas content in the Vostock ice core from Antarctica (Petit et al., 1999; Sigman and Boyle, 2000).

For the first time in Earth's detectable history, this excess amount of anthropogenic CO_2 is an anomaly, as opposed to a natural phenomenon cycling approximately every 100,000 years. At no time in at least the past 10 million years, has the atmospheric concentration of CO_2 exceeded the present value of 380 ppmv (Kennedy & Hanson, 2006). In fact, the amount of carbon dioxide in the atmosphere in 2005 far exceeded the natural range over the last 650,000 years (180 to 300 ppmv) (IPCC WGI, 2007).

Experts are still not clear on the exact causes of interglacial/glacial periods, and many hypotheses have been put forth. What is known is that this is the first time that anthropogenic forces have been in the forefront of climate change. Consequently, we have an excess of anthropogenic greenhouse gases in the "commons" that is believed to cause global warming. As biologist Garrett Hardin (1968) noted, with considerable circumspect, "Ruin is the destination toward which all men rush, each pursuing his own best interest in society that believes in the freedom of the commons. Freedom in a commons brings ruin to all."

Intergovernmental Panel on Climate Change

The Intergovernmental Panel on Climate Change was established by the World Meteorological Organization (WMO) and the United Nations Environment Programme (UNEP) in 1988 (IPCC, 2001b). Its primary goal is to provide an assessment of all aspects of climate change, including how human activities can cause such changes and be impacted by them (IPCC, 2001b). This organization does not carry out research, nor monitor climate related data; rather, it bases its reports mainly on peer reviewed and published scientific/technical literature (IPCC, 2006). The First IPCC Assessment Report (FAR) was published in 1990; in 1995 the Second Assessment Report: Climate Change (SAR), was published. The Third Assessment Report: Climate Change (TAR) was published in 2001. In 2007, the IPCC completed its Fourth Assessment Report (AR4), called "Climate Change 2007" (IPCC, 2006). All these reports have become the gold standard reference for climatological research and, in 2007, the IPCC won the Nobel Peace Prize (along with Albert Arnold (Al) Gore Jr.) "for their efforts to build up and disseminate greater knowledge about man-made climate change, and to lay the foundations for the measures that are needed to counteract such change" (IPCC, 2007).

Climate Data

The global average surface temperature has increased since 1860 (IPCC, 2001b; IPCC WGI, 2007; NOAA, 2006a) and the temperature increase of approximately 0.6°C since the last century (IPCC, 2001b; NOAA, 2006a) is likely to have been the largest temperature increase of any century during the past 1,000 years (IPCC, 2001a). In the last 25 to 30 years, this trend has increased to a rate of 1.8° C/century (NOAA, 2006a). It should be noted, however, that some parts of the Southern Hemisphere oceans and parts of Antarctica have not warmed in recent decades (IPCC, 2001a).

In the Fourth Assessment Report published by the IPCC, the last 11 of 12 years (1995-2006) ranked among the 12 warmest years in the instrumental record of global surface temperature since 1850 (IPCC WGI, 2007). In the U.S., NOAA reports that 2005 was the 13th warmest year on record (NOAA, 2006a) and 0.7°C above the 1895-2004 mean. The last five 5-year periods (2001-2005, 2000-2004, 1999-2003, 1998-2002, 1997-2001) were the warmest in the last 111 years of national records (Figure 6) (NOAA, 2006a).

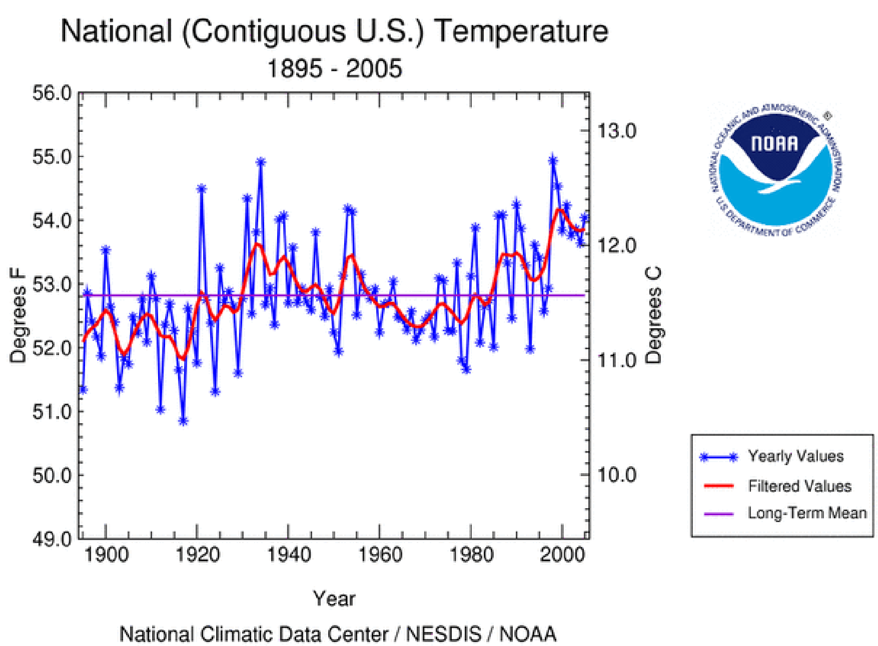

Figure 6. U.S. Temperatures from 1895-2005 (NOAA, 2006).

Temperatures have risen during the past four decades in the lowest 8 km of the atmosphere (IPCC, 2001a; NOAA, 2006a). Data collected by NOAA's TIROS-N polar-orbiting satellites indicate that temperatures over the U.S. in the lower half of the atmosphere (8 km) were warmer than the 20-year (1979-1998) average for the 8th consecutive year (NOAA, 2006a). Factors thought to influence these temperatures are ozone depletion, atmospheric aerosols, and the El Niño phenomenon (IPCC, 2001a).

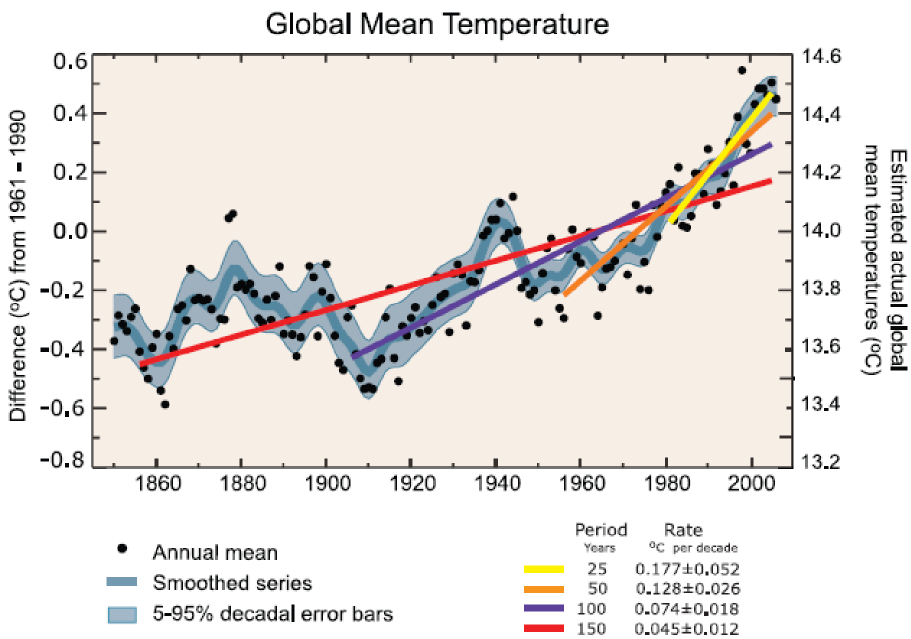

Figure 7. Global mean temperature (IPCC WGI, 2007).

Figure 7, published by the IPCC, Working Group I, addresses the "understanding of human and natural drivers of climate change, observed climate change, climate processes and attribution, and estimates of projected future climate change" (IPCC WGI, 2007). This analysis considers the annual global mean observed temperatures (black dots), along with simple fits to the data. The left hand axis depicts average differences (°C) from 1961 to 1990 and the right hand axis shows the estimated actual global mean temperatures (°C). Linear trend fits for the last 25 years (1981 to 2005 - yellow), 50 years (1956 to 2005 - orange), 100 years (1906 to 2005 - purple) and 150 years (1856 to 2005-red) are shown. Note that for shorter recent periods, the slope is greater, indicating accelerated rates of warming. The blue curve is a smoothed depiction intended to capture the decadal variations, with decadal 5% to 95% (light blue) error ranges about that line shown to provide an assessment of whether the fluctuations are meaningful (accordingly, annual values do exceed those limits). Results from climate models driven by estimated radiative forcings for the 20th century suggest that there was little change prior to about 1915, and that a substantial fraction of the early 20th century change was contributed by naturally occurring influences including solar radiation changes, volcanism, and natural variability. Following World War II, from the 1940s to the 1970s, as industrialization increased, pollution increased in the Northern Hemisphere. Initially, this contributed to cooling, increases in carbon dioxide, and other greenhouse gases, but after the mid-1970s, observed warming began to dominate (IPCC WGI, 2007).

In summary, the global average surface temperature increased in the latter half of the 20th century (IPCC WGI, 2007), and the rate of warming averaged over the last 50 years is nearly twice that for the last 100 years (IPCC WGI, 2007). The years 2005 and 1998 were the warmest two years in the instrumental global surface air temperature recorded since 1850 (IPCC WGI, 2007).

Climate Projections

Beginning with its first report in 1990, and continuing in its most recent report in 2007, the IPCC has predicted further growth of greenhouse gas emissions and consequent significant increases in the average global surface temperature that exceed the natural variation of the past several millennia (IPCC, 2001b; 2007).

Using simulation models with a range of scenarios of future greenhouse gas abundance, a set of possible responses of the climate system was proposed. The six scenarios, called the "Special Report on Emission Scenarios" (SRES) and designated A1B, A1F1, A1T, A2, B1, B2, did not include any additional climate initiatives that may occur in the future (IPCC WGI, 2007).

The A1B, A1F1, A1T models describe a future world of very rapid economic growth, global population that peaks in mid-century and declines thereafter, the rapid introduction of new and more efficient technologies, and a substantial reduction in regional differences in per capita income that imply greater homogeneity. The technological emphasis of A1F1 is fossil intensive and that of A1T is non-fossil oriented. Scenario A1B models a balance across all sources and does not rely heavily on any one energy source (IPCC WGI, 2007).

The A2 scenario is more heterogeneous and depends on self reliance and preservation of local identities. In this model, population growth continues to increase, economic development is primarily regionally oriented, and per capita economic growth and technological change are more fragmented than in the other scenarios (IPCC WGI, 2007).

The B1 scenario is similar to the A1 models in that the global population is projected to peak in mid-century and decline thereafter. However, this scenario differs from the others in projecting rapid change in economic structures toward a service and information economy, with a reduction in material intensity and the introduction of lean and resource efficient technologies. Here, the emphasis is on global solutions to economic, social, and environmental sustainability (IPCC WGI, 2007).

Emphasis on local solutions to economic, social and environmental sustainability is the focus of the B2 scenario. In this model, global population continues to grow at a rate lower than A2, economic development is also more moderate, and there are fewer technological changes than in the other scenarios. B2 is more focused on environmental protection and social equity, but at local and regional levels (IPCC WGI, 2007).

Future emission scenarios, predicted by the IPCC TAR, suggest that globally averaged surface temperature will increase by 1.4°C to 5.8°C over the period 1990 to 2100, for the full range of SRES models (IPCC, 2001b, 2002). Land areas are projected to warm more than the oceans, and the high latitudes to warm more than the tropics (IPCC, 2002). The IPCC also projects a warming of about 0.2°C per decade for the next two decades (IPCC WGI, 2007). If greenhouse gases held constant at year 2000 levels, a further warming of about 0.1°C would be expected, with a best estimate of 0.6°C (IPCC WGI, 2007). Under the six SRES scenarios, estimates range from a minimum of 1.1°C to a maximum of 6.4°C, and the best estimates range from 1.8°C to 4.0°C (IPCC WGI, 2007).

Figure 8, generated by the IPCC in 2007, compares observed warming with previous projections, thereby increasing the confidence in short-term projections. Observed temperature anomalies are shown as annual (black dots) and decadal average values (black line). Projected trends and their ranges from the IPCC First (FAR) and Second (SAR) Assessment Reports are shown in green and purple solid lines and shaded areas, and the projected range from the Third Assessment Report (TAR) is shown by vertical blue bars. For this graph, the IPCC projections were adjusted to start at the observed decadal average value in 1990. Newer model mean projections are shown for the period 2000 to 2025 as blue, green, and red curves, with uncertainty ranges indicated against the right-hand axis. The orange curve shows model projections of warming if greenhouse gases and aerosol concentrations were held constant from the year 2000 (IPCC WGI, 2007).

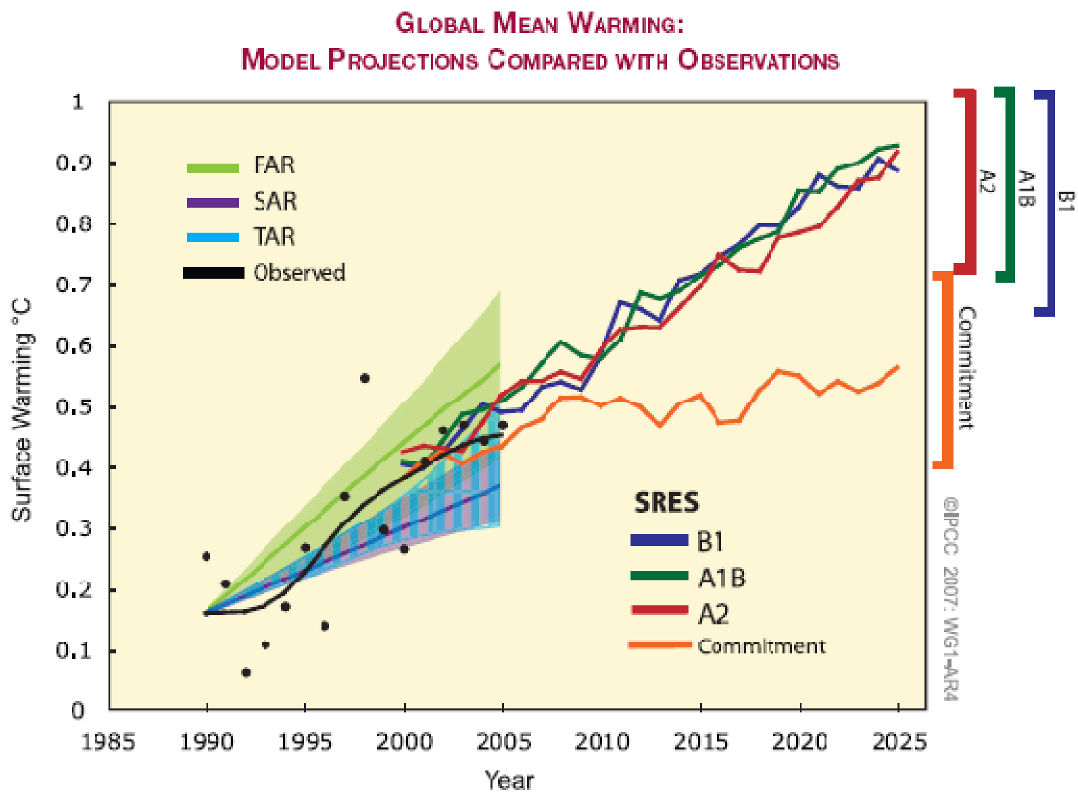

Figure 8. Global mean warming (IPCC WGI, 2007).

Longer term projections by the IPCC are shown in Figure 9, a graph depicting a greater range of variability amongst models. The solid lines are multi-model global averages of surface warming (relative to 1980-1999) for the scenarios A2, A1B, and B1, shown as continuations of the 20th century simulations. Shading denotes the ± standard deviation range of individual model annual averages and the orange line represents the experiment where concentrations were held constant at 2000 values. The grey bars at right indicate the best estimate (solid line within each bar) and the likely range assessed for the six SRES marker scenarios (IPCC WGI, 2007).

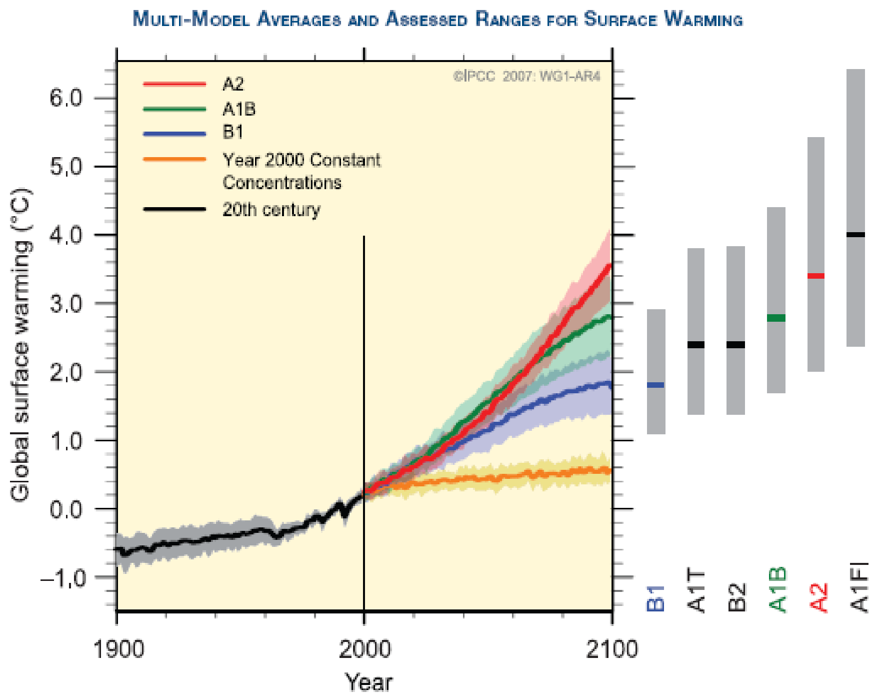

Figure 9. Global surface warming: actual from 1900 to 2000 and projected from 2000 to 2100 (IPCC WGI, 2007).

Models with high climate sensitivity indicate that temperatures could rise even more than thought previously (Kerr, 2005; Stainforth *et al.*, 2005). Climate modelers suggest that when greenhouse gases are doubled, warming could approach 2°C to 4°C (Kerr, 2005; Stainforth *et al.*, 2005). Ranges in the Stainforth *et al*. model demonstrate a wide range of climate sensitivities from 1.9 to 11.5K (Kelvin) (Stainforth *et al.*, 2005). The range of sensitivities across different versions of the same model is more than twice that reported in the IPCC Third Assessment Report published in 2001 (Stainforth *et al.*, 2005).

Researchers from the Woods Hole Oceanographic Institution (WHOI) have found evidence that tropical Atlantic Ocean temperatures may have once reached 42°C (107°F), about 14°C (25°F) higher than ocean temperatures today (WHOI, 2006). These temperatures occurred millions of years ago when CO_2 levels in the Earth's atmosphere were also high, a correlation suggesting that greenhouse gases could heat the oceans of the future much more than currently anticipated (WHOI, 2006).

Assuming that greenhouse gases continue to increase at or above current rates, further warming is expected to continue and to induce many changes in the global climate system during the 21st century. These changes would "very likely" (> 90%) be larger than those observed during the 20^{th} century (IPCC WGI, 2007).

Meehl *et al*. (2005) note that, even if greenhouse gases stabilized in 2000, global warming would continue, with temperatures rising by about another 0.5 °C before leveling off. Hence, even when greenhouse gases are stabilized, there will still be a commitment to future climate changes that will be greater than those currently observed (Meehl *et al.*, 2005).

Global Warming Skeptics

Some scientists dispute predictions of increased temperature and present models indicating that temperatures will decrease (Giles, 2005; Vellinga & Wood, 2002). Others believe that the temperature increases are related to solar activity (sun spots) (Bashkirtsev & Mashnich, 2003) and that they will be followed by temperature decreases by 2040 (Bashkirtsev & Mashnich, 2003; Giles, 2005).

Additional skeptics suggest that the temperature variations are part of a natural cycle (Gray, 2006) or that there may be a temporary collapse of the Atlantic Ocean thermohaline circulation (also known as the Atlantic Ocean Meridional Overturning Circulation [MOC]). (For an excellent review of MOC, see Church (2007)). The MOC, a major factor controlling the ocean's vertical movements and layered circulation (Figure 10), is governed to a large extent by water temperature and salinity (Marotzke, 2000; The Maury Project, 1998). In theory, when the strength of the haline forcing increases due to excess precipitation, runoff, or ice melt, the thermohaline circulation will weaken and shut down (Clark *et al.*, 2002; Marotzke, 2000; UNEP, 2000).

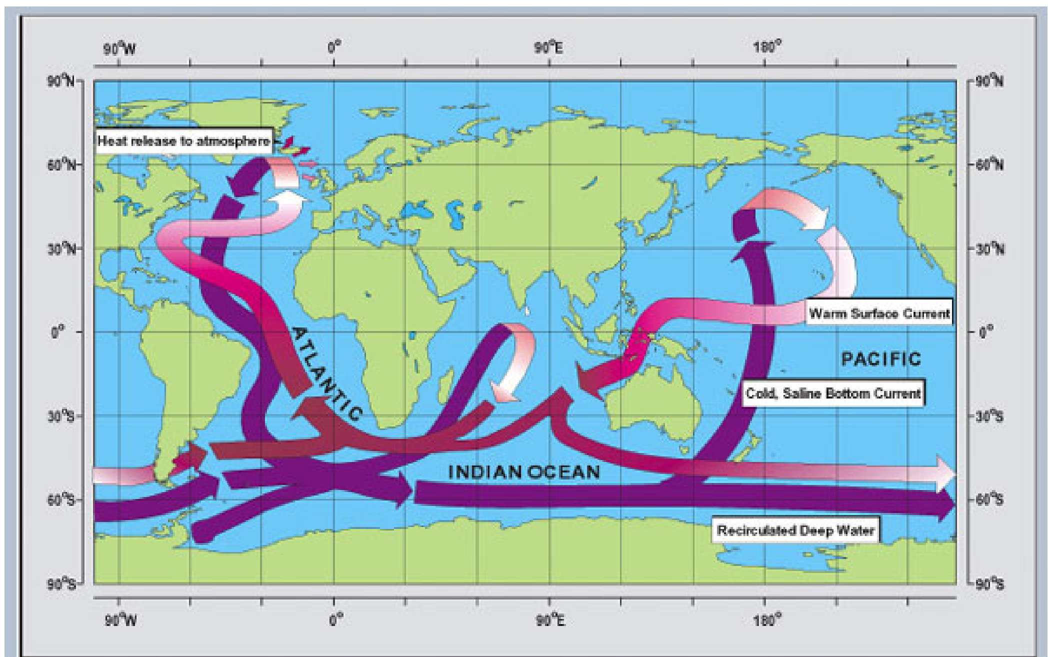

Schematic diagram of the global ocean circulation pathways, the 'conveyer' belt (after W. Broecker, modified by E. Maier-Reimer).

Figure 10. Thermohaline circulation pathways (NOAA, 2005).

A model put forth by Vellinga and Wood (2002) shows that a temporary collapse of the MOC could lower the temperature for much of the Northern Hemisphere (locally up to 8° C; 1-2° C on average) and generate a weak warming of the Southern Hemisphere (locally up to 1° C; 0.2° C on average), for the first 50 years. The same model predicts that precipitation will be reduced over large parts of the Northern Hemisphere and increase in South America and Africa (Vellinga & Wood, 2002). Colder and drier temperatures in the Northern Hemisphere would reduce soil moisture and net primary productivity of the terrestrial vegetation, phenomena compensated for in the Southern Hemisphere (Vellinga & Wood, 2002). After about 100 years, the model suggests that thermohaline circulation would largely recover, leading to the disappearance of most climatic anomalies (Vellinga & Wood, 2002).

An alternative version of the previous theory suggests that greenhouse-induced warming would increase the delivery of precipitation and river runoff to the North Atlantic and that this excess fresh water could weaken or even disrupt the global thermohaline circulation causing the conveyor to sag and, in the extreme, shut down, as suggested by Vellinga and Wood (Alley *et al.*, 2005; Broecker, 2003; Broecker, 2004; Johannessen *et al.*, 2005; Vellinga & Wood, 2002). However, the time required for this scenario is more likely a century, not a decade (Broecker, 2004; Marotzke, 2000).

A possible shutdown of the MOC does not necessarily neutralize projections of possible global warming. The 2007 report from the IPCC considers it “very likely” (>90% probability) that the MOC will slow down during the course of the 21st century. Nevertheless, most models suggest that there will still be a warming of surface temperatures around the Atlantic region as a result of an increase of greenhouse gases (IPCC WGI, 2007). None of the IPCC models shows a collapse of the MOC by the year 2100, suggesting instead that it is “very unlikely” (<10% probability) that the MOC will undergo a large abrupt transition during the course of the 21st century (IPCC WGI, 2007).

Current research by Cunningham *et al*. (2007) and Kanzow *et al*. (2007) suggests that the lack of long-term data on the MOC limits an understanding of its natural variations. It should be noted, however, that these researchers have already shown that the daily variability of the system is large. Clearly, a better understanding will be critical for more reliable projections of climate change (Church, 2007).

The U.S. government has recruited global warming skeptics in order to promote funding for overseas energy projects (Kintisch, 2005). Prominent scientists disagree with the U.S. government's arguments because there is a general consensus among the scientific community about both the causes and possible consequences of global warming (Kintisch, 2005).

While there are a variety of scenarios about the future of the Earth's climate, including significant disagreements as to whether temperatures will rise or fall, in this thesis I will assume that temperatures will continue to increase as suggested by the latest projections from the IPCC in 2007. I will also use historical regional data to build my model.

Sea Level Overview

One of the major consequences of global warming is a rise in sea level (Smith, 2004), a change attributable to two processes: first, there is an increase of the mass of water in the oceans (the eustatic component), derived largely from the melting of ice on land (Cazenave & Nerem, 2003) and variations in salinity (Meier & Wahr, 2002); second, there is an increase of the volume of the ocean without change in mass (the steric component), largely caused by the thermal expansion of ocean water (Meier & Wahr, 2002). Neither of these components are fully understood, and observations are not developed sufficiently to give a precise assessment of the causes of present-day sea level rise, let alone a projection of future rise (Meier & Wahr, 2002). In fact many of the analyses produce conflicting results (Meier & Wahr, 2002) .

The definition of sea level rise differs between sea level, "mean sea level" (MSL), and "relative sea level" (RSL). Generally, sea level is the height that the sea surface would assume if it were undisturbed by waves, tides, or winds (Bascom, 1964), but this is not what is measured in most situations. Mean sea level (MSL) is the average of all possible sea levels. This is the number generally used when referring to the height of the sea. In the United States, the mean sea level, defined by NOAA, is the average mean of hourly heights of the sea, over a 19 year National Tidal Datum Epoch (NOAA, 2003d). Relative sea level (RSL) is the position and height of the sea *relative* to land, which determines the location of the shoreline. RSL does not always give a true indication of sea level because of a variety of vertical displacements caused, for example, by geoid changes, thermo-isostatic and volcano-isostatic deformation, glacioisostatic and hydro-isostatic deformation, collision zones, etc. (Pirazzoli, 1997).

Sea Level Historical Data

Sea levels have risen more than 100 m (328 ft) since the last glacial maximum (18,000 years ago) (Douglas *et al.*, 2001), and the IPCC provides evidence that global MSL has risen by approximately 120 m (393.70 ft) during the several millennia that followed the end of the last ice age (~ 21,000 years ago), stabilizing between 3,000 and 2,000 years ago (IPCC WGI, 2007).

Even though sea levels have essentially leveled off since the last glacial maximum, they continue to change moderately around the globe and to exhibit variability in height (Peltier, 1999). It should be noted the rates of change are not equivalent in different parts of the planet because of regional differences in temperature, salinity, ocean circulation (IPCC WGI, 2007), meterological effects, and glacial isostatic adjustments (GIA) (Douglas *et al.*, 2001).

The IPCC TAR reports that average global sea level rose between 0.1 m (0.33 ft) and 0.2 m (0.66 ft) during the 20th century, or 1.0 to 2.0 mm/yr (0.04 to 0.08 in), with a central value of 1.5 mm/yr (0.06 in/yr) (IPCC, 2001b). These estimates were based on the Permanent Service for Mean Sea Level (PSMSL) data set.

Thermal water expansion contributed 0.5 ± 0.2 mm (0.2 ± 0.008 in) in steric change to this rise (IPCC, 2001b; Munk, 2003) and the rest came from the addition of water to the oceans (eustatic change), due mostly to melting of land ice (IPCC, 2001b). Since the 1950s (the period for which adequate observations of sub-surface ocean temperatures have been available) global ocean heat content rose (Munk, 2003). Satellite altimetry (Cazenave & Nerem, 2003) now indicates a rate of rise approaching 3 mm/year (0.1 in/yr) since the early 1990s (IPCC, 2001b, 2002).

The 2007 IPCC report from WGI estimates the total 20th century rise to be 0.17 m ± 0.05 m (0.56 ft ± 0.16 ft) and the 20th century rates for global average sea level rise to be 1.7 mm/year (~0.07 in/year) (IPCC WGI, 2007). From 1961 to 2003, the global MSL estimated from tide gauge data was 1.8 ± 0.5 mm/yr (0.07 ± 0.2 in/yr), and the global average rate of sea level rise measured by satellite altimetry during 1993 to 2003 was 3.1 ± 0.7 mm /yr (0.1 ± 0.03 in/yr) (Figure 11**)** (IPCC WGI, 2007). The average thermal expansion (steric) contribution to sea level rise from 1961 to 2003 was 0.4 mm ± 0.1 mm /yr (0.02 ± 0.004 in/yr). However, the period from 1993 to 2003 saw an increase from thermal expansion of 1.6 ± 0.5 mm/yr (0.06 ± 0.2 in/yr) (IPCC WGI, 2007).

Satellite observations and tide gauges used since the early 1990s indicate that global MSLs have been rising at a rate around 3 mm/year (0.1 in) (IPCC WGI, 2007). Another method to determine current sea levels comes from recent advances with offshore seismic stratigraphy and bottom profiling, geomorphic features and biological indicators providing the clearest evidence of historic changes in sea level. By using boreholes, vibracores, and seismic data, Uchupi and Mulligan (2006) provided a

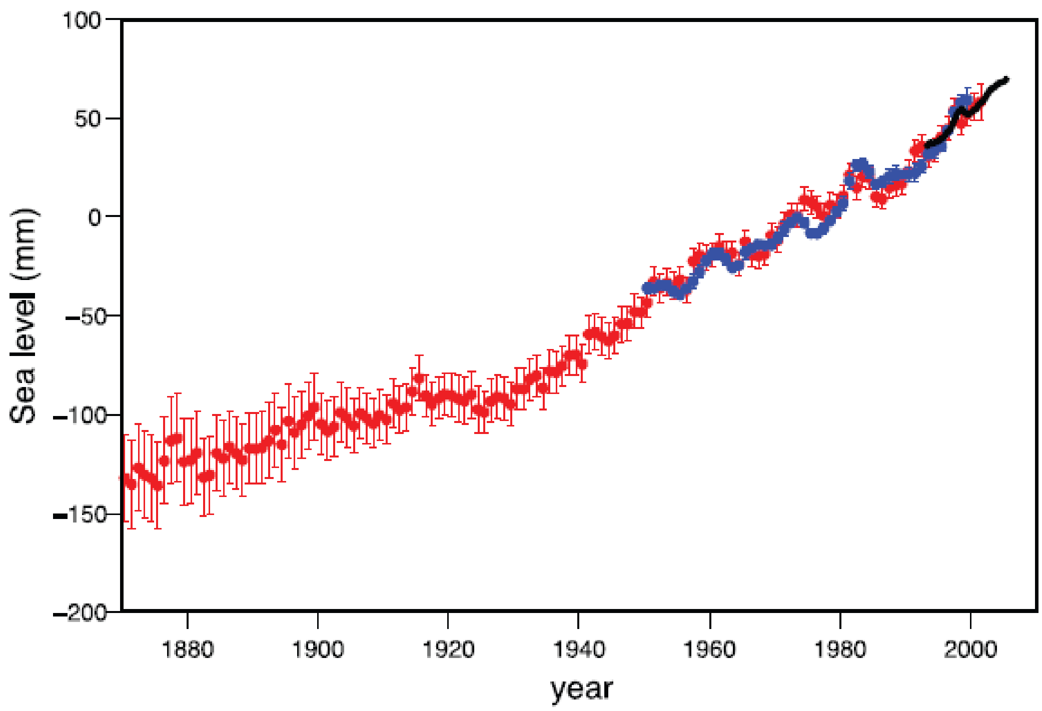

Figure 11. Global Mean Sea Level from 1870 to 2003, reconstructed from sea level fields (red) (Church and White, 2006); tide gauge measurements since 1950 (blue) (Holgate and Woodworth, 2004); and satellite altimetry since 1992 (black) (Leuliette et al., 2004). Units are in mm relative to the average for 1961 to 1999. Error bars are 90% confidence intervals (IPCC WGI, 2007).

comprehensive review and analysis of the late Pleistocene stratigraphic record for Cape Cod and Nantucket Sound. They determined that the sea level was at least 120 m (394 ft) below its present level and that the shoreline was located along the upper continental slope. Their results are in agreement with those of the IPCC.

Analyses of salt marsh foraminifera stratigraphy in coastal Maine, Connecticut, and Nova Scotia (Edwards *et al.*, 2004; Gehrels *et al.*, 2002; Gehrels *et al.*, 2005), show that sea levels from these areas were relatively stable between the years 800 to 1300, and reached a lowstand around 1800 (Gehrels *et al.*, 2002). Since 1800, sea levels in the Gulf of Maine have risen by 0.3-0.4 m (1-1.3 ft) (Gehrels *et al.*, 2002). In Nova Scotia, the 19th century sea level rose at a mean rate of 1.6 mm/yr (0.06 in); between 1900-1920, sea levels rose at a mean rate of 3.2 mm/yr (0.1 in), accelerating to the approximate modern mean rate of 3 mm/yr (0.1 in) (Gehrels *et al.*, 2002; Gehrels *et al.*, 2005). These studies suggest that the rapid onset of sea level rise corresponds with regional climatic warming and could be interpreted as thermal expansion of the Gulf of Maine and the North Atlantic sea surface, corresponding in time with global temperature rise (Gehrels *et al.*, 2002; Gehrels *et al.*, 2005). Indeed, the 20th century rates are unprecedented in the last millennium and correspond with hemispheric warming (Gehrels *et al.*, 2002; Gehrels *et al.*, 2005).

GIA is a physical process caused by the intense cycles of glaciation and deglaciation, occurring approximately every 100,000 years for the last 900,000 years (Peltier, 1999). During each glaciation cycle, the sea level has fallen an average of 120 m (394 ft) as freshwater is produced by evaporation from the oceans and then deposited as snow at higher latitudes (Peltier, 1999). The snow is transformed into ice under its own weight, until it reaches a thickness of approximately 4 km (2.49 miles) at which point the deglaciation cycle begins and sea levels rise again by approximately 120 m (394 ft) (Peltier, 1999).

With global climate changes occurring quickly, the affect of sea level rise only considers the eustatic component (Giese, 1997). If the relative sea-level rise rate doubled, from 3 mm/yr to 6 mm/yr (0.1 in/yr to 0.2 in/yr), eustatic sea level must triple (increasing from 1.5 mm/yr to 4.5 mm /yr) (0.06 in/yr to 0.2 in/yr) (Giese, 1997). Giese reports that the ratio of future rates of submergence to present rates would approximately equal the ratio of future sea level rise rates to present relative sea level rise rates (Giese, 1997). It should be noted that land subsidence does not alter the volume of ocean water (IPCC WGI, 2007).

Sea Level Projections

The IPCC TAR global MSL was projected to rise by 0.09 m (3.54 in) to 0.88 m (2.9 ft) between 1990 and 2100 (IPCC, 2001b). But, by the time the 2007 IPCC report was published, the projected sea level rise range narrowed to 0.18 m (7.09 in) to 0.59 m (1.9 ft) (Figure 12). This change is due to an improvement of methods to evaluate ocean heat uptake and thermal expansion. All the IPCC scenarios, except B1, very likely exceed the 1961-2003 average rate (1.8 mm ± 0.5 mm /yr) (0.07 ± 0.02 in/yr) (IPCC WGI, 2007). These SRES ranges do not include uncertainties in carbon-cycle feedbacks or ice flow processes because of a lack of data at the time of the IPCC 2007 publishing.

Using the six SRES emission scenarios by the IPCC, projections for sea level rise to 2100 range from 0.18 m to 0.59 m (7 in to 2 ft) (IPCC WGI, 2007). The mid-point of these ranges is within 10% of the TAR model average for 2090-2099, narrower than the previous report because of improved information about some uncertainties in the projected contributions. None of these models include the full effects of changes in ice sheet flow because there is a lack of published literature (IPCC WGI, 2007). These projections do take into account the rate of increased ice flow from Greenland and Antarctica from 1993 to 2003, but these rates can either increase or decrease in the future (IPCC WGI, 2007).

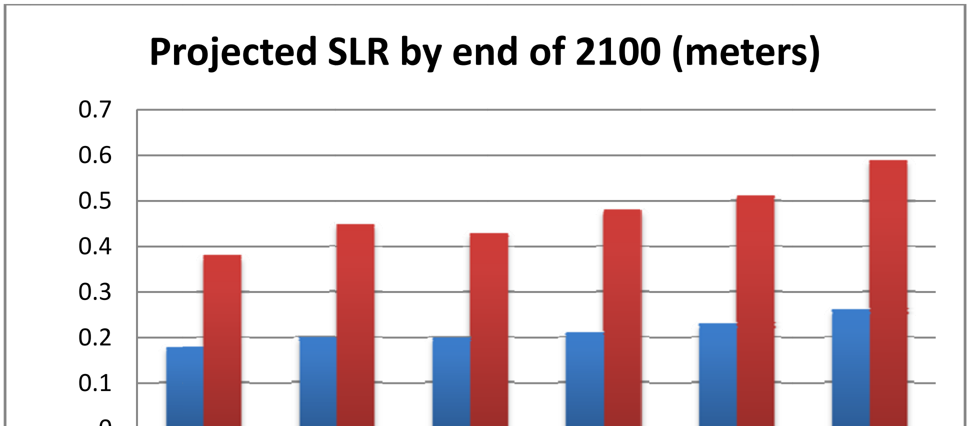

	B1	A1T	B2	A1B	A2	A1F1
Low	0.18	0.2	0.2	0.21	0.23	0.26
High	0.38	0.45	0.43	0.48	0.51	0.59

Figure 12. Projected sea level rise in meters at 2090-2099 relative to 1980-1999. Model-based range excluding rapid dynamical changes in ice flow. Adapted from IPCC WGI (2007).

Timescales associated with climate processes and feedbacks continue for years. Therefore, even if temperatures had stabilized by the year 2000, after 100 years, models show that sea level would continue to rise unabated with proportionately much greater increases compared to temperature (Meehl *et al.*, 2005). It is projected that sea level would rise by an additional 320% due to thermal expansion by the end of the 21st century (Meehl *et al.*, 2005). Recent articles contend that current models used to project the contribution to sea level from the Greenland Ice Sheet in a changing climate do not account for the physical effects of glacier dynamics (Rignot & Kanagaratnam, 2006). Because of this, they only provide lower limits to the potential contribution of Greenland to sea level rise (Dowdeswell, 2006). This is of concern because the flow of several large glaciers is accelerating, suggesting that existing estimates of future sea level rise are too low (Rignot & Kanagaratnam, 2006). Therefore, as more glaciers accelerate their melting, the mass loss from Greenland will continue to increase well above predictions (Johannessen *et al.*, 2005). If just the Greenland Ice Sheet melted completely, it would raise global sea level by about 7 m (23 ft), taking as long as a millennium to only a few thousand years (Velicogna & Wahr, 2006).

Other scientists have noted a change in ice sheets. Velicogna and Wahr (2006) took measurements from satellites and determined that the Antarctic sheet decreased significantly during 2002-2005. This loss translates into the equivalent of 0.4 ± 0.2 mm/yr (0.02 ± 0.008 in/yr) of global sea level rise (Abdalati, 2001; Abdalati *et al.*, 2001; Johannessen *et al.*, 2005; Steffen, 2004). Most of this melting and thinning of the Greenland Ice Sheet comes from melting and thinning in the coastal marginal areas (Meehl *et al.*, 2005).

James Hansen, the head of the climate science program at the National Aeronautics and Space Administration’s Goddard Institute for Space Studies, was a contributing author to the 2007 IPCC report (Chapter 10: Global Climate Projections). Soon after this report was published, a new article by Hansen, *et al*., (2007) claimed that sea level projections were too low based on a temperature increase of ~3° C. This increase is well within the range of the 6 SRES scenarios: estimates range from a minimum of 1.1°C to a maximum of 6.4°C, and the best estimates range from 1.8°C to

4.0°C (IPCC WGI, 2007).The IPCC analysis does not take into account the nonlinear behavior of ice sheet behavior and continues to assume a linear response to climate forcings (Hansen *et al.*, 2007). During the middle Pleioscene, temperatures were not more than 2-3°C warmer than they are now and sea level, at that time, was ~ 25 m ± 10 m higher (82 ft ± 33 ft) (Dowsett *et al.*, 1994). Hansen *et al*., (2007) suggest that it is "difficult to predict time of collapse (of ice sheets) in such a nonlinear problem, but we find no evidence of millennial lags between forcing and ice sheet response in palaeoclimate data" and "we cannot rule out large changes on decadal time scales once wide-scale surface melt is underway."

Oppenheimer, also a contributing author to the 2007 IPCC report, believes that the time scale of the ice sheet melting should not be measured by millennia, but by centuries (Kerr, 2006a). The CO_2 being pumped into the atmosphere could melt the glacial ice sheets much faster than anticipated, raising the sea levels by 5 m to 10 m (16.4 ft to 33 ft) (Kerr, 2006a) and putting many coastal areas under water. As Oppenheimer says, "this is not an experiment you get to run twice" (Kerr, 2006a).

Rahmstorf *et al*., (2007), contributing authors to the 2007 IPCC report, compared recent climate observations to projections from the IPCC and suggest that in some respects the IPCC may have underestimated projection in sea level change. By reconstructing primarily tide gauge data and satellite altimeter data (both corrected for GIA), sea level has been rising faster than the rise projected by models. "The rate of rise for the past 20 years of the reconstructed sea level is 25% faster than the rate of rise in any 20-year period in the preceding 115 years" (Rahmstorf *et al.*, 2007). The compiled satellite data show a linear trend of 3.3 mm ± 0.4 mm /year (0.13 in ± 0.02 in/yr) from

1993 to 2006 whereas the IPCC projected a best-estimate rise of less than 2 mm/year (Rahmstorf *et al.*, 2007).

Noted scientist Richard Peltier (2007) agrees that the IPCC estimates are conservative, but doesn't think that the ice caps will melt as quickly as Hansen suggest (Hansen, 2007).

According to Hansen, the 2007 IPCC report lacks information on more rapid rates of rise because the IPCC has a cumbersome review process which led to the exclusion of all recent data, making them "very handicapped" (Peltier, 2007).

Weather

Weather describes the constantly changing atmospheric circulation, including storms and hurricanes (NOAA, 2006f). While atmospheric processes are responsible for daily changes in the weather, other interactive components of the Earth contribute to climate changes. The sea surface forms the lower boundary condition for 71% of the atmosphere and its temperature is partly controlled by oceanic processes. The ocean interacts with the atmosphere on timescales from months to hundreds of years, and is therefore considered a coupled system (Institute for Geophysics, 2005).

Precipitation

Measuring temperature is easy compared to measuring global and regional precipitation (IPCC WGI, 2007). Most precipitation samples are taken from land, leaving the majority of the global surface under sampled. Further complicating matters, these samples can be affected by the wind, particularly when there is light snow or rain (IPCC WGI, 2007). Moreover, as temperatures increase, the moisture-holding capacity of the atmosphere increases at a rate of about 7% per °C (IPCC WGI, 2007). Estimates for precipitation amounts are compounded by aerosols because they block the sun, thereby reducing surface heat. Aerosol influences tend to be regional, and the net expected effect on precipitation is unclear (IPCC WGI, 2007).

In spite of these difficulties, data available for the IPCC TAR report indicated that precipitation had increased by 5-10% in the 20th century over most mid- and high latitudes of the Northern Hemisphere continents (IPCC, 2001b, 2002). Over the latter half of the 20th century, there was also a 2 to 4% increase in the frequency of heavy precipitation events (IPCC, 2001b, 2002).

The AR4 Report observed that the average atmospheric water vapor content has increased over land and oceans since "at least" the 1980s (IPCC WGI, 2007). From 1900 to 2005, long-term precipitation trends have been observed over many large regions, including a significant increase in the eastern parts of North America (IPCC WGI, 2007). Consistent with the observed increase of atmospheric water vapor, the frequency of heavy precipitation events have also increased over most land areas (IPCC WGI, 2007).

It is likely that precipitation will increase over high-latitude regions in both summer and winter and decrease in the subtropics, with an increase in heavy precipitation events (IPCC, 2002; IPCC WGI, 2007). Globally averaged annual precipitation is projected to increase during the 21st century, although, at regional scales, both increases and decreases of typically 5 to 20% are projected (IPCC, 2001a). In summary, there is a 90-99% likelihood that the annual mean precipitation will increase in the northeast portion of the United States (IPCC WGI, 2007)

Increased precipitation may advance the rate of erosion along the coast because of additional overland runoff and groundwater seepage. For this thesis, however, precipitation will not be considered a significant factor in the model because of the relatively flat terrain of Martha's Vineyard and the lack of major rivers that would alter the landscape under extreme precipitation events. Additionally, the composition of the glacial outwash plains and barrier beaches readily soak up precipitation. The more significant issues of coastal erosion on Martha's Vineyard are exacerbated by sea level rise and the physical composition of the island.

Hurricanes

Hurricanes are rated on the Saffir-Simpson scale, range from 1 to 5, based on the instantaneous intensity of the storm. These ratings provide an estimate of the potential for property damage and flooding along a coast anticipating a hurricane landfall. Wind speed is the determining factor in the scale, as storm surge values are highly dependent on the slope of the continental shelf and the shape of the coastline in the landfall region (NOAA, 2005c). The U.S. hurricane season lasts from June 1 through November 30, with the Massachusetts hurricane season peaking during August and September (MA CZM, 2002).

It has been postulated that current warming scenarios could lead to changes in the geographic range, frequency, timing, and intensity of hurricanes, as well as in the duration of their season (Broccoli & Manabe, 1990; Emanuel, 1987; Haarsma *et al.*, 1993; Mitchell *et al.*, 1990), and that these phenomena would vary significantly by region (Michener *et al.*, 1997). However, in April 2006, prominent researchers gathered for the 27th Conference on Hurricanes and Tropical Meteorology (AMS, 2006) and failed to come to a consensus as to whether there is indeed an increase in hurricanes (Kerr, 2006b) or even if global warming was caused by human activity (Gray, 2006).

Gray has presented evidence that global warming is primarily a result of natural global climate variability resulting from a salinity induced slow-down of the Atlantic thermohaline circulation (Gray, 2006). He suggests that there is no correlation between Atlantic hurricane frequency and strength since 1995, that these events are consequences of the large increase in the Atlantic thermohaline circulation, and that the large U.S. hurricane destruction of the last two seasons is due primarily to onshore upper-air steering currents (Gray, 2006).

Webster *et al*. (2005) examined the number of tropical cyclones, days, and intensity over the past 35 years and reported a large increase in the number and proportion of hurricanes that reached categories 4 and 5. In a model designed to understand the global hurricane intensity from 1970 to 2004 Hoyos, *et al*. (2006) proposed that the increase in category 4 and 5 hurricanes correlated directly with sea-surface temperature (SST) and other aspects of the tropical environment. However, even though these factors were thought to influence short-term variations in hurricane intensity, they were not thought to contribute substantially to the observed global trend. The results of Hoyos *et al.* (2006) underscore the findings of Webster *et al*. (Webster *et al.*, 2005) and indicate that there has been a small decline in extratropical systems over the past 50-100 years, but an increase in the frequency of very powerful storms, especially at higher latitudes (Emanuel, 2006; Keim *et al.*, 2004; Kerr, 2006b).

The intensity of hurricanes over the past half-century has risen along with temperature, matching both ups and downs (Figure 13). Kerry Emanuel (2005; 2006) has claimed that hurricanes in the Atlantic Ocean, north of the equator, are “spectacularly well correlated with sea surface temperature.” Nolan *et al*. (2006) presented a model with preliminary results that indicate if sea-surface temperatures (SST) are high enough, cyclones can form spontaneously. Saunders' (2006) findings indicate that the current and future impact of global warming on Atlantic hurricane activity may be higher than previously thought. Favorable conditions for hurricane development correlate with record high SSTs in the tropical North Atlantic region in 2005 (IPCC WGI, 2007).

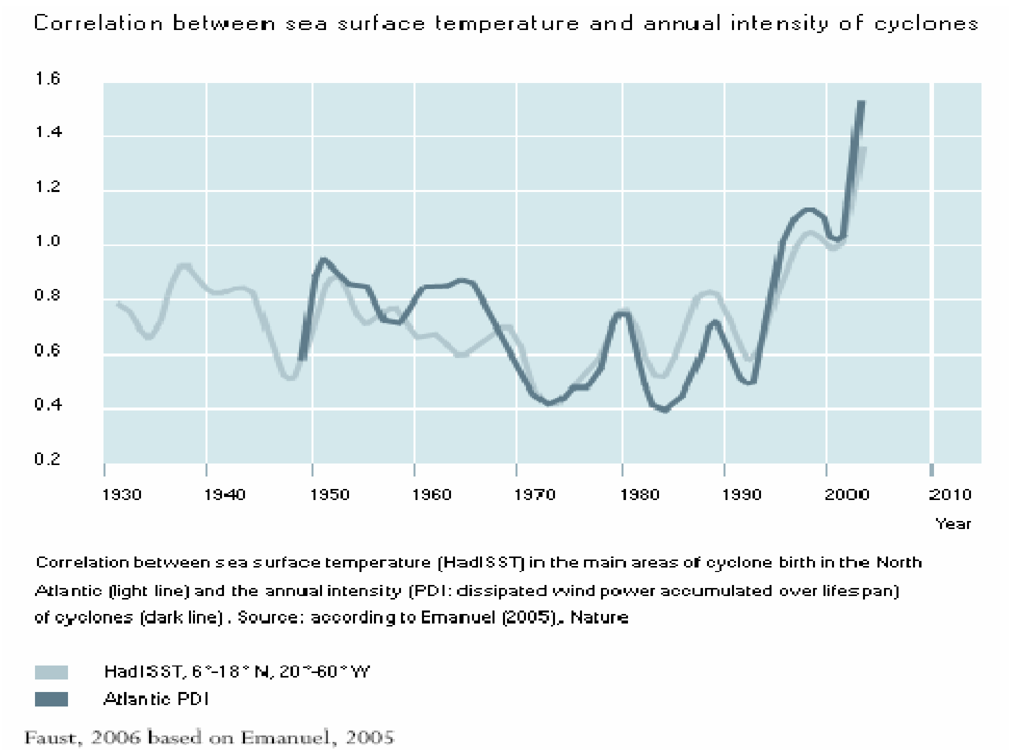

Figure 13. Correlation between sea surface temperature and annual intensity of cyclones (SPARC, 2006).

Hurricane records for the North Atlantic date back to 1851. After 1950, the use of reconnaissance aircraft improved the reliability of the records. Additional technological improvements after the early 1970s made records even more reliable (IPCC WGI, 2007). Since 1995, all but two Atlantic hurricane seasons have been above normal, contrasting sharply with generally below-normal seasons observed during the previous 25-year period (1970-1994) (IPCC WGI, 2007). From 1995-2004, hurricane seasons averaged 13.6 tropical storms, 7.8 hurricanes and 3.8 major hurricanes (IPCC WGI, 2007). The 2005 hurricane season broke all records; it featured the largest number of named storms, the only time the Greek alphabet had to be used, and the only time there have been four category 5 storms (IPCC WGI, 2007).

Storm predictions from Perrie *et al*. (2006) indicate that storm tracks will be nearer to the coastal areas of the North Atlantic and will tend to propagate approximately 10% faster. In their storm simulations, the net impact of the climate change scenario is to cause an increase of approximately 5% in the number of storms.

NOAA's tropical storm and hurricane data, compiled from the National Hurricane Center's North Atlantic Hurricane Database, indicates that the 5-year moving average of hurricanes has increased from 21% in 1915 to 30% by 2005 (NOAA, 2006f). Figure 14 is a compilation of the data on storms that crossed over contiguous U.S. land; in this compilation multiple landfalls from tropical systems are considered valid, i.e., they are scored as many times as they hit land.

Winter Storms (Nor'easters)

Northeasters (Nor'easters), or winter extra-tropical storms, are dominant along the U.S. east coast. They have counter-clockwise winds, coming from the east or northeast, from which they derive their name. These storms are sometimes called "bombs" because of their rapid intensification rates (DGS, 1998). The Northeasters affecting Massachusetts usually occur from October through April, and can persist for several days to a week (MA CZM, 2002; USGS, 2005).

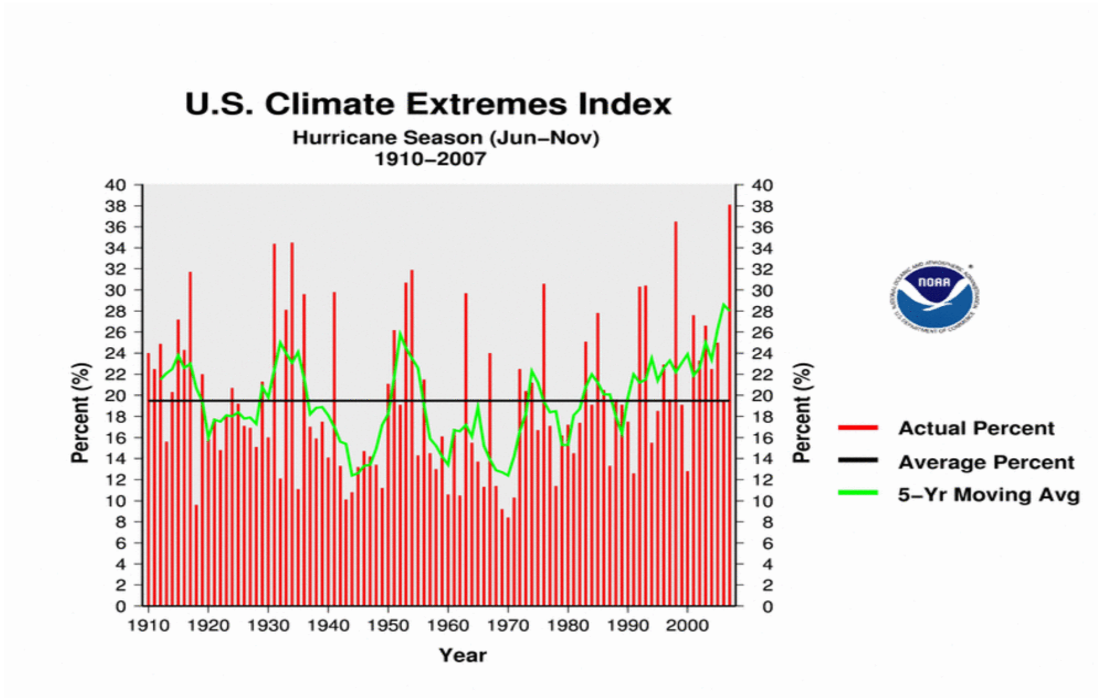

Figure 14. U.S. hurricane season (NOAA, 2006).

Northeasters have strong coastal impacts (USGS, 2005; Zhang *et al.*, 2000) because they generate large waves and enhance storm surge (MA CZM, 2002; USGS, 2005). When these storms move up the Atlantic coast, the winds blow from offshore to onshore and may actually accentuate incoming tides because they push the water in the same direction that the tide normally flows (DGS, 1998; MA CZM, 2002). As the tides recede, the winds can be sufficiently forceful to keep them from flowing away from the shore, creating a problem with the subsequent high tide. As a consequence of these events, when a Northeaster pounds the coast the storm surge increases during each tidal cycle, thereby increasing the flooding and erosion of beaches and dunes (DGS, 1998).

There was no method to rate these winter extra-tropical storm events until 2004, when Kocin and Uccellini (2004) developed a winter storm ranking system, called the

Northeast Snowfall Impact Scale (NESIS) (NOAA, 2006d). Similar to a tornado F-scale, this ranking system has five categories: Extreme, Crippling, Major, Significant, and Notable (NOAA, 2006c). Beginning in 2006, NOAA adopted this scale and now uses it to rate storms after they occur (NOAA, 2006d). The uniqueness of the NESIS indexing system is that it includes population information in addition to meteorological measurements (NOAA, 2006d) The NESIS value is determined by the area affected by the snowstorm, the amount of snow, and the number of people living in the path of the storm (NOAA, 2006d).

Little research data has been published on winter extra-tropical storms, and the bulk of it addresses hurricanes. Two independent studies found a higher frequency of extreme storms in the North Atlantic. Bouws *et al*. (1996) found a higher frequency of extreme winter storms since 1988/1989 than at any time since 1880 and Bruce *et al*. (1999) showed there has been a marked increase since the 1970s of intense winter storms in the Northern Hemisphere (Figure 15). In eastern North America, seven of the eight most intense storms that developed in the past 50 years occurred in the most recent 25 year period. However, determining changes in frequency and severity of storms in the North Atlantic is very difficult because of the many variables involved, (e.g., central atmospheric pressure, strongest winds, heavy rains, etc.) (Bruce *et al*., 1999).

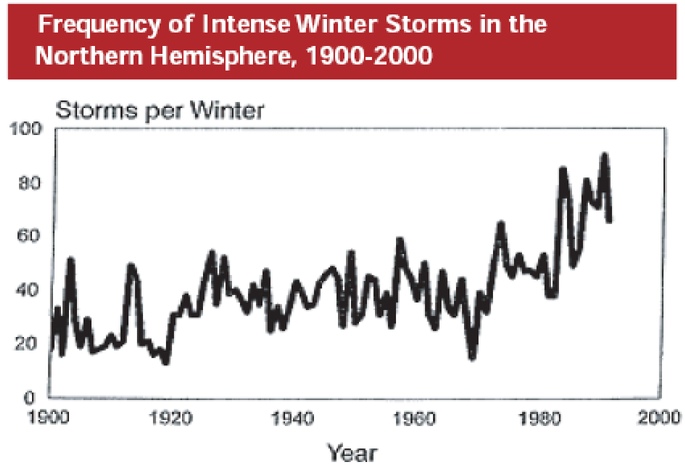

Figure 15. Frequency of intense winter storms in the northern hemisphere from 1900-2000 (UNEP/USGS).

There is evidence to suggest that Northern Hemisphere cyclonic storm tracks have shifted poleward during the months of January, February, and March over the past half century (Simmonds & Keay, 2002; Wang *et al.*, 2006). From 1958 to 1998, there was an increase of winter cyclone activity over the northern North Atlantic, exhibiting a significant intensifying trend along with a decadal timescale oscillation (Geng & Sugi, 2001). However, the mid-latitude North Atlantic indicates a decrease in strong cyclone activity (Wang *et al.*, 2006).

Not being able to come to a consensus on data from actual events makes it even more unlikely that researchers could come to an agreement on hurricane and winter storm projections. In fact, future trends in hurricane frequency and intensity remain very uncertain (IPCC WGI, 2007). Therefore, for this thesis, I will use the Precautionary Approach (UNEP, 1992) and assume that there will likely be an increase of storm activity, coupled with an increase in sea surface temperature.

Coastal Zone

Classifying the coastal zone has been problematic for years (Finkl, 2004). No single classification has been agreed upon, largely because of the complexities of mixing spatial and temporal timescales (Finkl, 2004). For example, the United States EPA defines the coastal zone as the lands and waters adjacent to the coast that exert an influence on the uses of the sea and its ecology, or whose uses and ecology are affected by the sea (EPA, 2005). Coastal Zone Management (CZM) (1996) defines the coastal zone as the coastal waters (including the lands therein and thereunder) and the adjacent shorelands (including the waters therein and thereunder), that are strongly influenced by each other and in proximity to the shorelines of beaches. Mann (2000) includes within the coastal zone the intertidal and subtidal areas above the continental shelf (to a depth of 200 m (656 ft)) and adjacent land area up to 100 km (62.14 miles) inland. Morang and Parson (2002) divide the coastal zone into four subzones: coast, shore, shoreface, and the continental shelf.

Within all these definitions of coastal zones, there exists a range of ecosystem types, both terrestrial and aquatic. These include coral reefs, mangrove forests, tidal wetlands, seagrass beds, salt marshes, sandplain grasslands, dunes, barrier islands, estuaries, and peat swamps. These ecosystems are both very productive and very vulnerable to environmental changes.

Within the global coastal zone, the impact of sea level rise on the coastal ecosystems will vary regionally and will depend on erosion processes from the sea and depositional processes from land (IPCC, 2002). It is estimated that, by the year 2080, about 20% of global coastal wetlands could be lost to sea level rise (Townsend *et al.*, 2004).

To protect the U.S. coastal zone and its fragile ecosystems, Congress, in 1972, enacted the Coastal Zone Management Act (CZMA). Since then it has been amended several times, but the primary purpose of the Act continues to be the encouragement of states to preserve, protect, develop, and, where possible, restore or enhance valuable natural coastal resources such as wetlands, floodplains, estuaries, beaches, dunes, barrier islands, and coral reefs, as well as the fish and wildlife using those habitats, for future generations (CZMA, 1996; DOE, 2006). State participation is voluntary, but the Act does makes federal financial assistance available to any coastal state or territory (DOE, 2006).

Massachusetts instituted its own Coastal Zone Management (MA CZM) Program in 1978 (MA CZM, 2002, 2006b). The mission of the Program is to balance the impact of human activities with the protection of coastal and marine resources (MA CZM, 2002). In early 2006, a Massachusetts Coastal Hazards Commission was formed to assess coastal hazards and vulnerabilities (including coastal storms, erosion, sea level rise, storm surge, etc.) (MA CZM, 2006a). In November 2007, the Commission initiated a Coastal Infrastructure and Protection Plan for Massachusetts coastal areas, including the islands of Martha's Vineyard and Nantucket (MA CZM, 2006a).

Beaches and Barrier Beaches

Beaches encompass the zone above the water line, marked by an accumulation of sand, stone, or gravel that has been deposited by the tide or waves. The shore extends from the low-water line to the normal landward limit of storm wave effect (i.e., the coastline) (Morang & Parson, 2002). Where beaches occur, the shore can be divided into two zones: backshore and foreshore (Morang & Parson, 2002). The backshore is horizontal and usually dry, being reached by only the highest tides (Ellis, 1978), while the foreshore slopes seaward, lying between the high and low water mark at ordinary tide (Ellis, 1978). The berm is the nearly horizontal position of the beach, or backshore, having an abrupt fall and formed by wave deposition of material and marking the limit of ordinary high tide (Ellis, 1978). The shoreface is the seaward-dipping zone that extends from the low-water line offshore to a gradual change to a flatter slope denoting the beginning of the continental shelf. The nearshore environment extends from the outer limit of the longshore bars that are usually present to the low-tide line (Coastal Landform, 2008b). This is the area where waves steepen and break, and then re-form in the passage to the beach, where they break for the last time and surge up the foreshore (Coastal Landform, 2008b). This nearshore zone is where much of the sediment is transported, both along the shore and perpendicular to it (Coastal Landform, 2008b).

Barrier coasts are an accumulation of nearshore sediments resulting in beaches, baymouth bars, spits and barrier islands (Ballantyne, 2002b). Many of the barrier beaches in New England were formed by spit accretion (Hoel, 1986). The sand was furnished by glacial deposits or by reworking of the glacial moraines, producing extensive beaches and barrier islands along Cape Cod, Martha's Vineyard, and Nantucket (NOAA, 2003c). Ocean longshore currents sweep the eastern seaboard of the U.S., running from north to south, depositing sand necessary to maintain beaches. Behind a barrier beach, a sound is formed creating opportunities for extensive salt marshes to develop (Hoel, 1986).

Barrier beaches are on the seaward side of shores, providing protection to coastal regions and absorbing the brunt of waves from storms and floods. They adapt to these forces by migrating inland, essentially rolling over themselves, including the shoreface, beach, dunes, and the marshes in the rear. The sand is moved by waves, wind, and storms, creating an overwash of sand behind the dunes. Eventually new dunes develop on the overwash, and the main dune is breached. This process continues over time; beach becomes dune, dune becomes beach.

Human induced activities, from development and infrastructure, change the ability of barrier beaches to adapt and migrate inland. Sediment supplies that feed the beaches are reduced when dams or other impoundments reduce the flow of sediment to the coast. Coastal armoring, groins, and jetties, starve the downward beaches. In the southern New England region, there are very few new sources of sediments from the land (Townsend & Pethick, 2002).

Beaches are rugged and adapt to environmental extremes, maintaining a dynamic equilibrium, as long as they have time to adapt to changes. However, with the increasing impact of humans on coastlines, combined with the projected rapid increase in sea levels over the next century, these environments will have great difficulty providing protection to local ecosystems, including people and their property.

Coastal Sand Dunes

Smith (1954) classified dunes into the following categories: 1) foredunes, 2) parabolic dunes, 3) barchan dunes, 4) transverse dune ridges, 5) longitudinal (seif) dunes, 6) blowouts, and 7) attached dunes. Within these categories, dunes may be divided into two categories: active and quiescent (Sanford, 1915). Active dunes are still growing, fed by supplies of windblown sand and sediment. Quiescent dunes are not growing (e.g., those along the Atlantic coast), are covered by vegetation, and furnish positive evidence of a rise in sea level (Sanford, 1915).

Coastal dunes develop when there is an abundant supply of sediment. Onshore winds move the sediment towards the shore, bouncing small particles of sand and rolling larger particles over the surface, called saltation (Pethick, 1984). This accounts for 75% of sand movement, leading to dune formation (Pethick, 1984). Dunes begin to form when this movement of sand is obstructed by wrack, plant debris, or other solid objects. These embryo dunes form just above the high tide line, migrate landward under the influence of saltation, and are stabilized when they are colonized by plants (Bertness, 1998).

Sea Level Position and Tides

Tides rise and fall along all shorelines with some heights larger than others. They are predictable and are semi-diurnal, with the timing of low and high water shifting forward every day by 50 minutes. When there are wide continental margins, bays, and estuaries, the amplitude of tides can be magnified (Bascom, 1964) (Figure 16).

Coastline Length

Estimates of the total length of shorelines worldwide vary from 855,038 km (531,296 miles) (Finkl, 2004) to 1.6 million km (994,194 miles) (PBS, 2000-2001). The U.S. accounts for 2.4% of the total coastlines in the world, of which the 30 coastal states contain a total of 673 coastal counties (NOAA, 2005b). Massachusetts has 2,445 km (1,519 miles) of coastline (MA CZM, 2006b) and Martha's Vineyard has approximately 200 km (124 miles) of coastline, with 8,777 acres of estuaries (Mass.Gov, 2003).

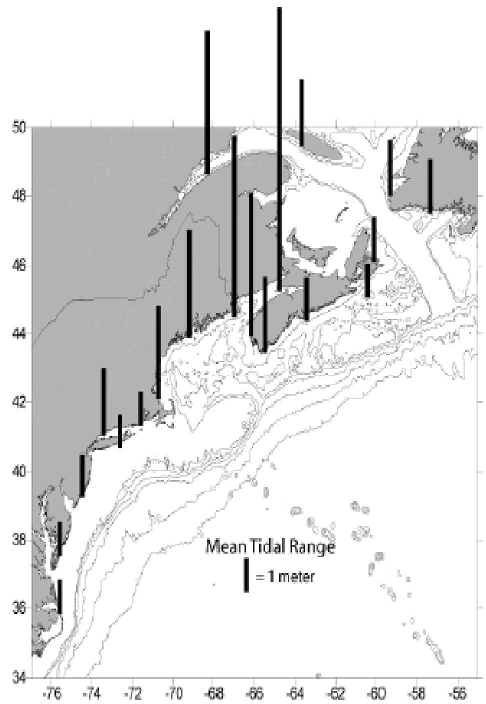

Figure 16. Tidal ranges along the northeastern seaboard of North America (Townsend *et al.*, 2004).

Coastal Population

Approximately 18.7% of the total land area of the world lies within 100 km (62 miles) of the coast (Dao, 1998), a zone that, as recently as 1997, was home to nearly 37% of the world's population (Cohen *et al.*, 1997). Today, almost half of the world's population resides there and, by 2025, it will be the home for an estimated 6.3 billion people (UN, 1998). The average population density in coastal areas is about 80 persons per square kilometer, twice the global average (UN, 2003). The actual population pressure on the coast in habitable areas must, however, be considerably higher because the averages include data on sparsely populated or uninhabited coastlines such as those of Antarctica and the far North (UN, 2003).

In the United States, coastal watershed counties comprise approximately 17% of the land area, but are home, as of 2003, to more than 53% of the total population (NOAA, 2005a). Simply put, about half of this country's population lives within an hour's drive of the Atlantic or Pacific Oceans, the Gulf of Mexico, or the Great Lakes (US Commission on Ocean Policy, 2004). Consistent with this distribution of the populace, almost half of all construction in the U.S. from the 1970s to the 1980s took place in coastal areas (Benchley & Gradwohl, 1995). Likewise, the number of building permits issued for homes in coastal counties between 1999 and 2003 totaled 2.8 million for single-family housing units (43% of the U.S. total) and 1 million for multi-family units (51% of the U.S. total) (NOAA, 2005a). This pattern is likely to continue, with population trends predicting an average of 3,600 people per day moving to coastal counties, reaching a population of 165 million by 2015 (Culliton, 1998).

While the coastal rate of growth is not different from that of other places in the U.S. (NOAA, 2004), the population density within the relatively small fixed coastal zone is creating pressure on its resources. The total population of coastal watersheds in 2000 was approximately 127 million people or 45% of the national population. This represented a growth of 24 million people since 1980 (NOAA, 2005a, b). The Northeast has the greatest regional distribution of coastal population at 34%, followed by the Pacific at 26%, the Great Lakes at 18%, the Gulf of Mexico at 13%, and the Southeast at 9% (NOAA, 2005a). Since it has been estimated that, within 30 years, a billion more people will be living along the coasts than are alive today (Benchley & Gradwohl, 1995), we can anticipate an ongoing conflict between the popular and political demand for coastal resources and competing efforts to sustain the natural coastal environment.

Coastal Tourism

Coastal tourism is a big business; it is an important source of income and foreign exchange for many islands (Jones & Mangun, 2001). It is the fastest growing sector of the global economy (WRI, 2001), and in the United States, coastal tourism and recreation constitute the fastest growing sector of the ocean economy (NOAA, 2004). Annually, an estimated 180 million tourists visit the U.S. coast (Marlowe, 1999). This industry has become highly competitive and continuously seeks to increase the number of visitors to U.S. beaches (Klein *et al.*, 2004).

Coastal communities offer a wealth of resources for people to enjoy, from natural beauty to economic opportunities. Although visiting the coast for a vacation has been a tradition for centuries, the last 35 years have seen these activities increase to the point that there has been a shift in these regions from traditional maritime activities to a more service-oriented and tourism-dependent economy (Jones & Mangun, 2001). Activities that drive this economy include swimming, sunbathing, bird watching, recreational boating, and fishing. Other sectors that follow are the hotel and resort industries and complementary retail businesses.

Clean, broad, sandy beaches are an important factor in attracting tourists (Finkl, 1996; Houston, 1996; Stronge, 2001), and the number of beach visitors shows a direct relationship to beach width (Jones & Mangun, 2001). Since the size of beaches decreases as they erode, many communities have resorted to nourishing beaches with sand. This enhances the recreational and aesthetic quality of the beach, helps to strengthen the economic value of the area, and, if done correctly, provides protection from storms (Douglass, 2002).

Ironically, while tourism supports coastal communities, the influx of visitors to coastal areas promotes the decline of their natural beauty. If not managed properly, population increases and the amenities added to support them lead to a degradation of critical habitats and biodiversity. The confluence of these events is likely to be exacerbated by the consequences of global warming, sea level rise, and adapting ecosystems.

Little research has been done about tourism and climate change (El-Raey *et al.*, 1999; Kent *et al.*, 2002; Scott, 2003; Scott *et al.*, 2003). What little research does exist deals with tourists' vulnerability and adaptation to climate change (IPCC, 2001a), with a high confidence level that tourism on islands will face severe disruption as sea levels rise (Jones & Mangun, 2001).

Coastal Economics

Coastal areas are home to a wealth of natural and economic resources and they are the most developed areas in the nation (Crosset *et al.*, 2004). The oceans and coastal areas provide unparalleled economic opportunities and revenues (Field *et al.*, 2001). One estimate suggests that as many as one out of every six jobs in the United States is marine-related (NOAA, 2004). In 2000, U.S. ocean-related activities directly contributed more than $117 billion to the economy and, if all coastal activities were included, more than $1 trillion (NOAA, 2004).

A service-oriented and tourist-dependent economy is an important driver of development in many U.S. coastal areas (Cicin-Sain & Knecht, 1999). Beach quality has a major impact on the value of the coastal zone, both for residents and tourists, seen in high property values, commercial and residential development, tourism, employment and tax revenues (Klein *et al.*, 2004). Sustainable development of coastal tourism depends on good coastal management, clean air and water, healthy ecosystems, a safe and secure recreational environment, and clean and functional beaches (YOTO, 1998).

In light of the importance of beaches and tourism, it is critical that coastal economies maintain stability by monitoring both environmental changes and human needs. However, coastal zones are the most sensitive to storms, environmental changes, and landuse patterns. Populations that inhabit small islands and/or low lying coastal areas are at particular risk of severe social and economic effects from sea level rise and storm surges (Field *et al.*, 2001). Resources critical to island and coastal populations such as beaches, and natural resources would also be at risk (Field *et al.*, 2001).

Roughly 1,500 homes and the land on which they are built are lost to erosion each year, with annual costs to coastal property owners expected to average $530 million over the next several decades (The Heinz Center, 2000). In 2004, it was estimated that 10 million people experience coastal flooding each year due to storm surges and landfall typhoons, and 50 million could be at risk by 2080 because of climate change and increasing population densities (Adger *et al.*, 2005; Nicholls, 2004). The IPCC reports that the number of people that would be flooded by coastal storms can reach 75 to 200 million people, depending on adaptive responses, for mid-range scenarios of 40 cm sea level rise by the 2080s, relative to scenarios with no sea level rise (IPCC, 2001a). In short, the number of people potentially affected by sea level rise is staggering.

There is a direct link between the increase of population and coastal hazards. As more and more people migrate to the coastlines, they, and the economic value of capital, are exposed to increased risks of flooding from sea level rise, storms, and flooding (SPARC, 2006). The rising socio-economic costs related to weather damage and to regional variations in climate suggest an increasing vulnerability to climate change (IPCC, 2001a). A comparison of U.S. population, natural catastrophes, and financial losses for 5-year periods between 1949 and 1994 indicates that the increasing costs of catastrophe losses since 1950 are strongly correlated to population, or changing vulnerability to storms (Changnon *et al.*, 1997). It should be noted that these numbers do not include hurricane-produced events (Changnon *et al.*, 1997). Since 1987, the property insurance industry has seen a rise in claims due to population increases, a higher standard of living, a greater concentration of people and goods in highly exposed areas, an increase in insurance density, and a change in environmental regulations (Berz, 1993; Changnon *et al.*, 1997). There has also been a rise in hurricane related damages and a decline in the number of deaths in recent years (Hebert *et al.*, 1996; Pielke, 1997). Interestingly, the increase in hurricane damages took place during an extended period of decreasing hurricane frequencies and intensities (Hebert *et al.*, 1996). While the debate continues as to whether hurricane activity is increasing or not, the fact remains that economic losses due to storm damages increase as the population increases, particularly in coastal zones.

There are direct (market-based) and indirect (non-market effects) costs related to natural disasters. Direct costs are associated with physical destruction of buildings, crops, and natural resources, while indirect costs typically represent temporary unemployment and business interruption, as consequences from the disaster (NAP, 1999). Being able to identify these socio-economic losses, through risk assessment, and determining their probabilities, helps to prevent, eliminate, or minimize the vulnerability of the population.

Human Dimensions

Basic survival for early inhabitants of the planet demanded awareness of their immediate surroundings. Their major concerns were for safety, shelter, food, water, and warmth, not entertainment. E.O. Wilson (1984) has analyzed the link between people and the environment and believes that picking a place to live is essential for the basic survival of various species and that the shelters people select are needed to protect them from prey. Given a choice, people and other organisms choose safe surroundings because the unsafe choices increase the likelihood of death.

Once fundamental survival issues were addressed, then the aesthetics of habitat became important. For almost two million years, people survived by living on the savannahs of Africa, vast, park-like grasslands, avoiding the equatorial rain forests on one side, and the deserts on the other (Orians, 1986; Wilson, 1984). Ancient survival instincts drove basic needs for safety, food, and shelter, as well as water. Oceans, lakes, and rivers provided food and water to drink and shorelines were a natural perimeter of defense (Wilson, 1984). During Medieval times, moats were put around castles for protection. Today, people enjoy sweeping water views and, even in cities, people would rather live or work on the top floors of buildings that offer grand views. “Those who exercise the greatest degree of free choice, the rich and powerful, congregate on high land above lakes, rivers, and along ocean bluffs (Wilson, 1984).”

Islands have had a tenacious hold on the human imagination throughout civilization (Tuan, 1990). They symbolize a place of bliss and a place to withdraw from high-pressured living on the mainland (Tuan, 1990). People flock to the coastline, whether to live there or to vacation, and coastal tourism creates an important source of income and foreign exchange for many islands (Jones & Mangun, 2001).

In "The Tragedy of the Commons," biologist Garrett Hardin (1968) saw the dangers of people withdrawing too much from common resources and/or the reverse, putting too much back into the commons, such as CO_2. Now we have a conundrum. Excess CO_2 in the atmosphere, believed to cause global warming (IPCC, 2001b; IPCC WGI, 2007), could thus also lead to sea level rise (IPCC, 2001b; IPCC WGI, 2007; Meier & Wahr, 2002). At the same time, the coastal population is increasing at a rapid rate, with almost half of the world's population residing there (UN, 2003). Flood insurance claims are rising in coastal areas from increases in the frequency and intensity of storm events, yet the coastal march is on.

Reaching a sustainable environment under these conditions is difficult, primarily because there isn't a general agreement as to the definition of sustainability. The concept of sustainability has broad social appeal, but has little specificity. The combination of development, environment, and equity has been used as a set of adjectives to describe it, but there are no indicator sets that are universally accepted (Parris & Kates, 2003).

The roots of "sustainability" came from a report made by the World Commission on Environment and Development (WCED) in 1987. The report was entitled "Our Common Future," but quickly became known as the "Brundtland Report," after the chairperson of the commission, Mrs. Gro Harlem Brundtland, then the Prime Minister of

Norway. The General Assembly of the United Nations had called upon the WCED to formulate "a global agenda for change" (WCED, 1987) and the ensuing report proposed global long-term environmental strategies for achieving sustainable development, through cooperation between countries, and the consideration of methods that international community's could use to effectively communicate environmental concerns, guided by shared perceptions of long-term environmental goals (WCED, 1987). The WCED report defined sustainable development as "development that meets the needs of the present without compromising the ability of future generations to meet their own needs" (WCED, 1987).

The question then becomes, what is the definition of sustainability for Martha's Vineyard, and what time frame is realistic to consider. The Martha's Vineyard Commission set out to define sustainability for the island and published a report in 2005 that defined sustainability as "relating to, or being a method of harvesting or using resources so that the resource is not depleted or permanently damaged" (MVC, 2005).

So, why is a coastal study of Martha's Vineyard important if they are already planning for a sustainable community? In 2001 and 2002, the various committees proposed 37 indicators, but did not succeed in identifying a process to use the indicators to promote better, broad-based decision-making in the community (MVC, 2005). Identifying a process and a method to accomplish this is a common thread in the literature. The nature of sustainability must encompass the interaction of global processes (e.g., air pollution), with ecological (e.g., coastal systems) and social characteristics (e.g., policies and human nature), focused on a particular place and sector (e.g., Martha's Vineyard) (Kates *et al.*, 2001). An understanding of these human/environment dynamics helps to give rise to changes in land use. This requires the integration of social, natural, and geographical information systems (GIS) (Rindfuss *et al.*, 2004).

Because they have legal voting power, the residents of Martha's Vineyard will have decisions to make regarding land use, such as caps on development, retreating from the coastline, and shifting prime businesses and support services inland (hospitals, fire, police). It should be noted that the residents make up approximately 20% of the inhabitants and that the majority of the population (80%) is comprised of tourists and second home owners, who are the driving economic force on the island. In spite of these facts, the year-round residents have become the stewards of the land. This situation is not necessarily surprising, because visitors and natives focus on different aspects of the environment (Tuan, 1990).

A significant aspect missing from the "Measures of Sustainability" Report was the issue of sea level rise and coastal erosion. It is not uncommon to perceive this type of risk as something that may happen sometime in the distant future. Shlyakhter and Wilson (1997) studied the concept of acceptable risk and found that public polls suggest that many people are unconcerned about a 5% chance of a climate-related catastrophe within their lifetime. But, they are concerned about a 1% chance of a nuclear accident during that same time period. If the nature of the uncertainties that underlie problems such as global warming and sea level rise are not expressed in a cogent manner, then the level of risk seems inconsequential. This is underscored by the fact that scientists do not agree about the future of the climate. Notwithstanding, the Precautionary Principle (UNEP, 1992) should be applied in this situation, i.e., "Where there are threats of serious or irreversible damage, lack of full scientific certainty shall not be used as a reason for postponing cost-effective measures to prevent environmental degradation."

CHAPTER 2

MARTHA'S VINEYARD AND THE STUDY SITES

Introduction

The paraglacial island of Martha's Vineyard (MV; "the Vineyard") is located 8 km (~5 miles) from the south shore of Cape Cod, Massachusetts, at a latitude and longitude of 41.416N and 70.616W (Figure 17). The 248 km^2 (61,253 acres) island is bounded by the open Atlantic Ocean on the south, Vineyard Sound on the northwest, and by Muskeget Channel and Nantucket Sound on the east/northeast. The Vineyard comprises most of Dukes County (with the remainder consisting of Cuttyhunk and the Elizabeth Islands) and encompasses six towns: Aquinnah (previously known as Gay Head), Chilmark, West Tisbury, Tisbury, Oak Bluffs, and Edgartown. It also includes 13 named streams, 62 lakes and ponds, approximately 200 km (124 miles) of coastline (including the bays), and 35 km^2 (8,777 acres) of estuaries (Mass.Gov, 2003). The island has a circumference of approximately 96 km (60 miles) and its eastern and southern shores are fringed with barrier beaches and dunes. The south shore has several large ponds that exert a major influence on MV's physical, natural, and socioeconomic infrastructure and activities (U.S. FWS, 1991b).

Elevation on the Vineyard begins at sea level and reaches 95 m (312 ft) at Peaked Hill, located on the southwestern portion in Chilmark. The southern portion is relatively flat, with elevations ranging from sea level to approximately 10.5 m (34 ft). The eastern portion is not as flat as the south coast; elevations in this locale range from sea level to 32 m (105 ft). The western portion of MV has the highest elevation, with most of it ranging from 21-95 m (69-312 ft).

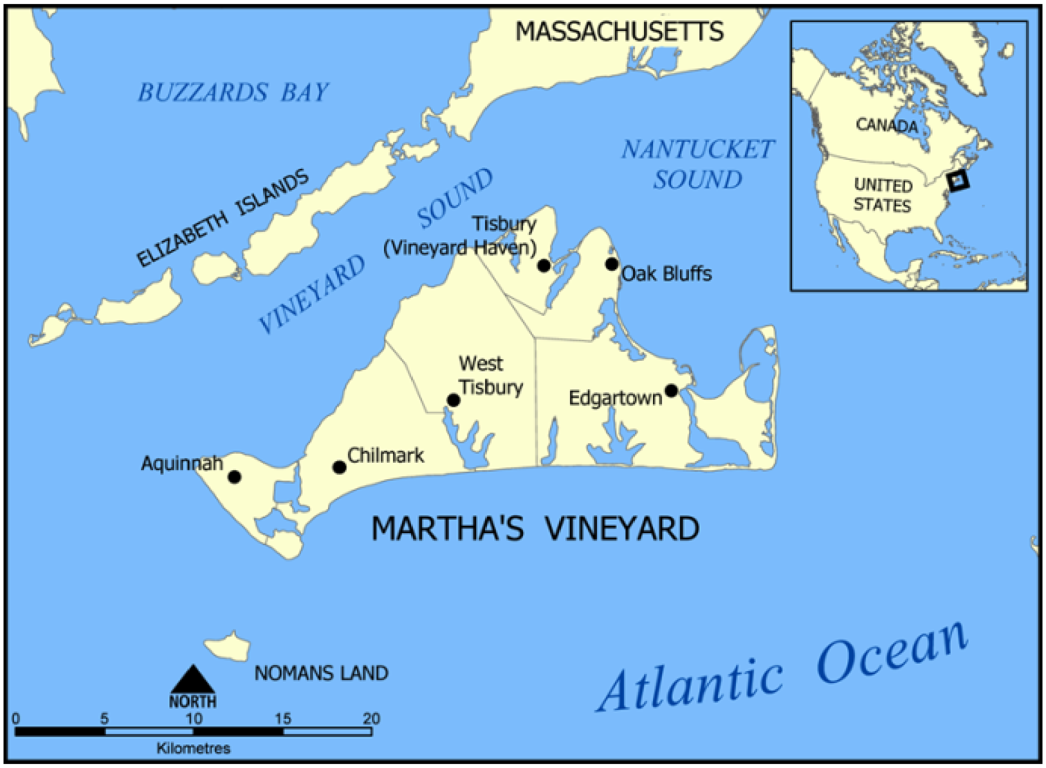

Figure 17. Map of Martha's Vineyard, Massachusetts. From Wikipedia.com (2006).

With the western side having the highest elevation, it is not surprising that the steepest slopes are located here, with ranges from 8-25%. Central MV and most of the southern portion are very slight sloped, ranging from 0-3%, and the eastern portion has slopes that range from 3-15%. Due to the presence of coastal dunes and sea cliffs most of the coastlines around the Vineyard have slopes of 8-15%.

Historical Overview

Bartholomew Gosnold, an explorer, named the island in 1602 after his first born daughter, Martha (Gookin, 1949). "Vineyard" was added to its name because of the island's abundance of wild grapes (Mood, 1933), but there was also an underlying motive. To influence English public opinion about the value of coastal New England, the notion of a “Vineyard” was intended to convince the British populace that the island would eventually supply sufficient wine to allow England to become independent of its European rivals (Mood, 1933).

The first permanent MV settlement was in Edgartown in 1641. At that time, much of the island was deforested, except a large center of the outwash plain (Foster *et al.*, 2002), and most of the population lived along the coastline. Extensive pastures were developed on the western moraine, south shore, and Chappaquiddick (Foster *et al.*, 2002). Early colonists learned the whaling trade from the Wampanoags and turned this skill into a profitable industry. As the population and industries grew (e.g., brickworks and whale oil factories), the wood supply became limiting (Foster *et al.*, 2002). By 1683, an Edgartown ordinance restricted the taking of firewood on common ground (Foster *et al.*, 2002). Interestingly, by 1762, the island was described as holding as many inhabitants as the land could comfortably support (Banks, 1911; Foster *et al.*, 2002).

For a long time the Vineyard was a wealthy, prosperous community. During its golden age of 1830 to 1845 sea captains built grand homes that still stand today. Tourism began on the island in 1844 with the development of the Methodist Camp Meeting in Oak Bluffs (Robbins, 1994) and eventually replaced the whaling industry as the island’s prime economic source (Dodge, 1935). During the latter part of the 1800s the forests began to grow back and, by 1950, 70% of the Vineyard was forested again (Foster *et al.*, 2002). When tourism began to boom in the 20th century, there was a major growth in house construction and, once again, the forest cover was reduced (to 55% of the island) (Foster *et al.*, 2002). Today, conservation land covers approximately 18% of the island and forests occur in patches between the towns and developments (Foster *et al.*, 2002). The only extensive open-land habitat is mainly restricted to the southern shore, barrier beaches, edges of coastal ponds, agricultural land, and airfields (Foster *et al.*, 2002)

Coastal Geomorphology

Coastal Evolution and Surficial Geology. Subsequent to its formation, the northeast portion of North America endured several periods of glaciation and deglaciation. The last glacial cycle, an event that took place during the Pleistocene Epoch (1.8 million to ~ 10,000 years ago), covered New England with extensive ice sheets, resulting in both glacial deposition and erosion (NOAA, 2003c; Oldale, 1992). Cretaceous sediments and thick areas of Quaternary glacial sediments were deposited in southern coastal areas (Robinson Jr. & Kapo, 2003). This deposition predominantly comprised elongate terminal moraines, typically containing large volumes of sand and gravel. Along Cape Cod, Martha's Vineyard, Nantucket, and Long Island, reworking of these moraines produced extensive beaches and barrier islands (NOAA, 2003c). In contrast, most of the northern New England coastline was stripped of sediments and is thus dominated today by irregular, rocky shorelines with only local pocket beaches, many of which are composed of gravel (NOAA, 2003c).

The glacial moraine and outwash plains of Martha's Vineyard sit upon bedrock that lies deep beneath the surface (Fullerton *et al.*, 2004). This bedrock is part of the Avalon Belt, located in eastern Massachusetts, Rhode Island, and coastal Connecticut (Robinson Jr. & Kapo, 2003). About 600 million years ago, the Avalon Belt was not connected to North America; rather, it was a microcontinent, originating from the African plate in the south and part of a chain of mountains and islands in the Iapetus Ocean

(Ansley, 2000; Warner, 1999). As the continental plates moved closer together, volcanoes erupted and the ocean floor sank beneath the new islands, giving rise to some of the granite formations that exist today (Warner, 1999). About 300 million years ago, when North America and the African continent collided, the Avalon Belt was "crushed" into the American continent and has remained attached ever since (Ansley, 2000; Warner, 1999).

During the last glacial period (sometime between 30,000 and 18,000 years ago), the Wisconsinan Laurentide glacier covered most of New England, including Martha's Vineyard (Balco *et al.*, 2002; Lambeck *et al.*, 2002; Oldale, 1992; Upham, 1879). When glaciers originally advanced across the landscape they carried eroded underlying material consisting of soft unconsolidated sediments and hard consolidated rock (Oldale, 1992). As the Buzzards Bay and Cape Cod Bay glacial lobes retreated, MV was formed as a continental island from the sediments left behind (Oldale, 1992; Upham, 1879). Whereas the Earth's crust had initially been depressed beneath the glacial ice (Fullerton *et al.*, 2004), there was an uplift, or rebound, as the ice disappeared. As the rate of uplift increased relative to the rate of sea level rise, the land emerged, leaving behind glaciomarine deposits of the late Wisconsin age (Fullerton *et al.*, 2004) that ultimately overlayed the bedrock (Oldale, 1992). At the time that the glaciers began to recede, global sea level was about 120 m (~394 ft) lower than today and the shoreline was approximately 121 km (75 miles) south of MV (Oldale, 1992; Peltier, 1999; Rohling *et al.*, 1998).

Water from melting glaciers generally moves toward the glacial margin, carrying along eroded till and sediment, emerging into meltwater streams and onto outwash plains

(Oldale, 1992). The latter are relatively flat, slope gently away from the position of the former glacier, and are underlain by stratified drift, mostly gravelly sand (Oldale, 1992). Unsorted glacial debris can be as large as boulder size to as small as microscopic clay-sized fragments (Oldale, 1992). End moraines, also refered to as kame or terminal moraines, are linear or arcuate, ridgelike accumulations of ice-contacted deposits (Fullerton *et al.*, 2004). These complex deposits are found in mounds, knobs, hummocks, or in irregular imbricated or overlapping ridges in belts of any of the latter landforms (Fullerton *et al.*, 2004) at or near stagnating glacial ice margins (Fullerton *et al.*, 2004) (Figure 18). The most southerly coastal end moraines run through Long Island, N.Y., portions of Connecticut and Rhode Island, and southeastern Massachusetts, and specifically along the NW and NE sides of Martha's Vineyard. The latter are designated

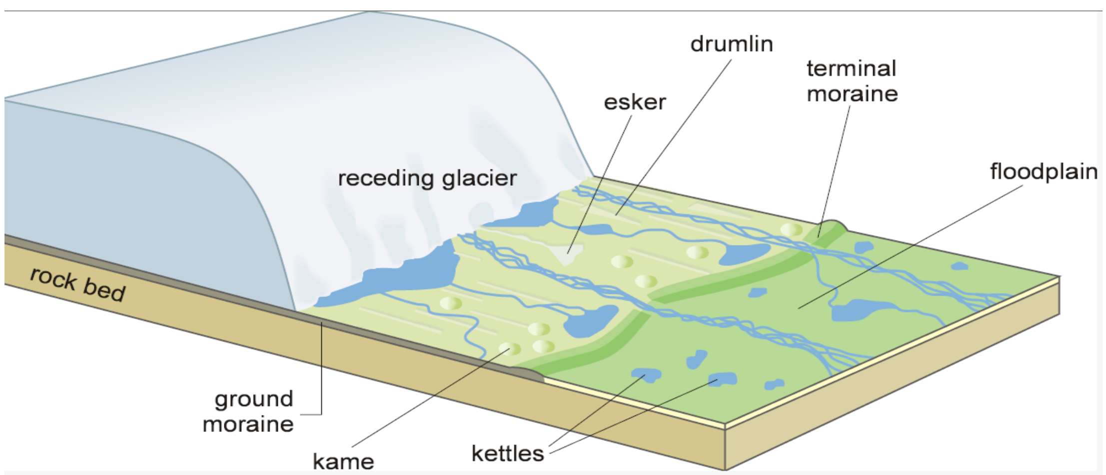

Figure 18. Diagram of a glacial ice margin.
From: http://upload.wikimedia.org/wikipedia/commons/d/da/Receding_glacier-en.svg

the Martha's Vineyard moraine deposit and the Gay Head moraine deposit. In some places, kame end moraine deposits grade laterally into, or are abruptly replaced by, till end moraine deposits . The thickness of these deposits generally ranges from 5-30 m (16-

98 ft), with a maximum thickness >80 m (262 ft) (Fullerton *et al.*, 2004). On Martha's Vineyard, the end moraines are underlain by a seaward-thickening wedge of unconsolidated sediment that, in turn, is underlain by much older consolidated rocks (Oldale, 1992).

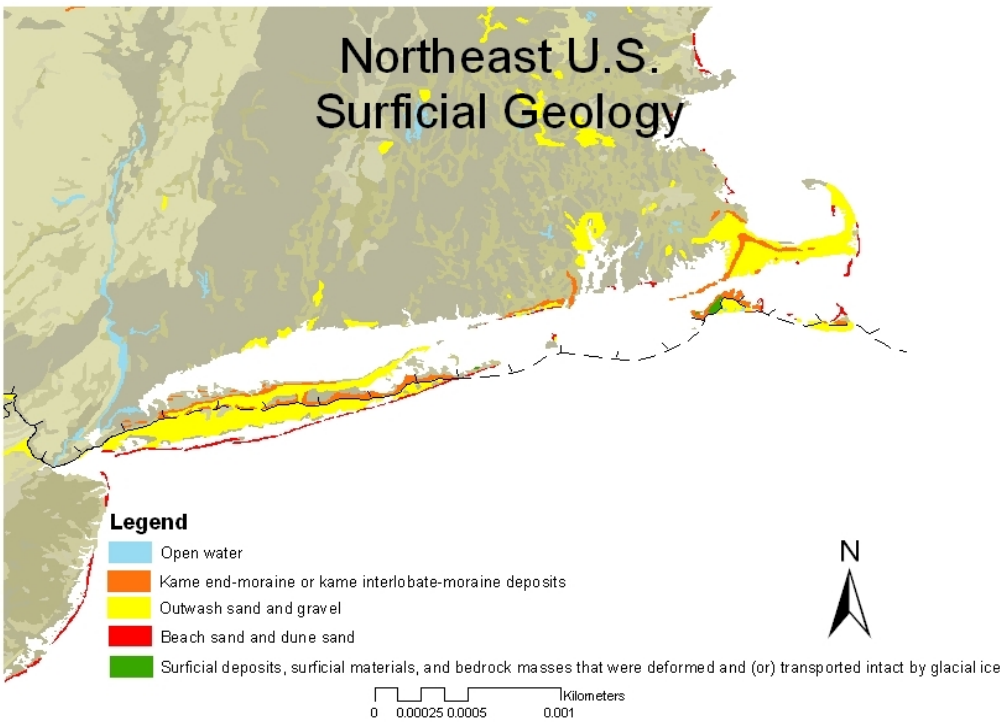

Figure 19. Surficial geology of the northeastern U.S. The glacial limit line is depicted by the black dashed line. Data from Fullerton et al. (2004).

The outwash sand and gravel present on the south side of Martha's Vineyard are called glaciofluvial deposits and consist of stratified gravel, sand, and silt. These sediments were deposited by melt-water streams from the glaciers. its open shelf, although a deep area approximately 110 km south (68 miles) of Martha's Vineyard is appropriately called the Mud Patch (Chang & Dickey, 2001; Dickey & A.J. Williams III, 2001; Townsend *et al.*, 2004). The sediment in the Mud Patch is illustrates the glacial limit line showing the position of maximum glacial advance in the northern U.S. and the surficial deposits and materials across the eastern U.S. that accumulated in the last two million years. The surfaces of these deposits are generally smooth, undulating, or gently rolling. On Martha's Vineyard these deposits mainly cover steeply tilted bedrock blocks overlain with till and/or stratified sediments. The thickness of the deposits range from 2 m to > 100 m (7-328 ft). In some areas, the outwash areas are overlain by thin till, or the outwash may have been further eroded, reworked, or redeposited by waves, currents, or wind. The thickness of the glaciofluvial deposits are ~ 1-25 m (3-82 ft); with the maximum thickness > 100 m (328 ft) (Fullerton *et al.*, 2004).

Martha's Vineyard is part of the Atlantic Coastal Plain, a physiographic province that lies between uplands and the sea (see picture) (Oldale, 1992). This nearly flat platform, composed largely of glacial outwash (Oldale, 1992), stretches from Cape Cod, Massachusetts, to beyond the Mexican border (United States, 2008). Sands dominate on its open shelf, although a deep area approximately 110 km south (68 miles) of Martha's Vineyard is appropriately called the Mud Patch (Chang & Dickey, 2001; Dickey & A.J. Williams III, 2001; Townsend *et al.*, 2004). The sediment in the Mud Patch is approximately 3 to 14 m (10-46 ft) thick, covers an area of approximately 100 km by 200 km (62 by 124 miles), and is composed of relatively uniform fine-grained material that overlies coarser sand-size sediment (Souza *et al.*, 2001; Twichell *et al.*, 1987). Typically this mud is carried away by coastal currents, whereas the coarser material tends to stay where the glaciers deposited it, and the sand is mobilized into mainland beaches (NOAA, 2003a).

The shelf waters of MV are located in a region of abrupt changes in water temperatures, with the confluence of the Gulf Stream flowing north and the Labrador

Current flowing south (Townsend *et al.*, 2004). Mid-latitude cyclones frequently track across North America and converge on this region (Figure 20) (Townsend *et al.*, 2004). The barrier coastline of Martha's Vineyard is defined as paraglacial and is divided into two classifications: Type 2 "clustered headland-separated" and Type 3a "wave-dominated mainland-segmented" (Fitzgerald & Van Heteren, 1999). The shoreline changes on a yearly cycle. Beaches erode more in the winter and accrete during the summer, a shift attributable to a change of wave action during the different seasons (see below). During the winter months, waves are typically larger and cut the beach berm back and, during the summer months, the smaller waves replace the sand (Bascom, 1964).

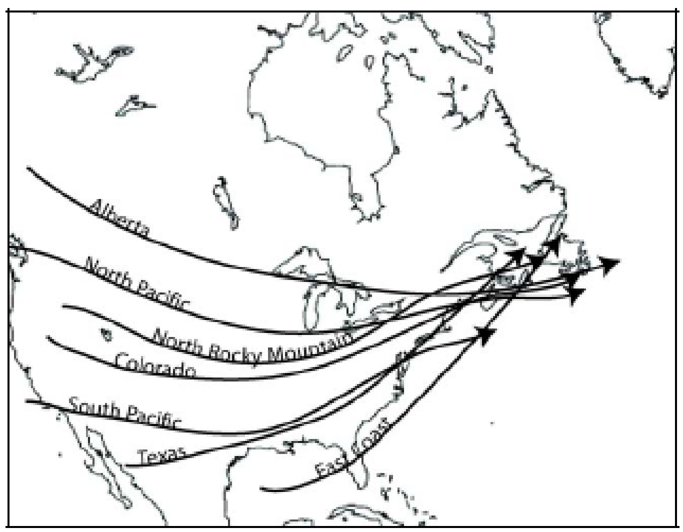

Figure 20. Major storm tracks across the North American continent and their convergence near New England (Townsend *et al.*, 2004).

Bedrock and Surficial Sediments. The type of bedrock that the MV glacial debris sits on is principally Precambian Z granite, granitic gneiss, and metasedimentary rocks of Precambian Z, Ordovician, and Devonian granites (Robinson Jr. & Kapo, 2003), as well as metabasalts, gneisses, schists, amphiobolites and metasediments (Oldale, 1992; Uchupi & Mulligan, 2006; USGS, 2007). Analyses derived from boreholes and marine seismic profiling indicates that the bedrock surface depth on Martha's Vineyard is approximately 183 m (600 feet) on the northern portions, sloping to 274 m (900 feet) on the southern sections (Oldale, 1992). It should be noted, however, that when boreholes were drilled on MV, bedrock was not reached, but it was assumed that it was very close (Oldale, 1992). The average lithology for the Vineyard reveals an upper sandy unit composed primarily of medium to very coarse sand with scattered layers of gravel, to approximately 122 m (400 feet), a clayey middle unit, from 122-213 m (400-700 feet), and a lower sandy unit with layers of variegated clay that rests on bedrock (Oldale, 1992).

Glacial deposits are unstable as long the drift material remains easily accessible for fluvial erosion and transportation (Church & Ryder, 1972). Hence, the combination of subsurface glacial deposits and irregular bedrock have exerted a major control on evolution of the New England coastline (NOAA, 2003b), producing coastlines that range from straight to deeply embayed, 360° shoreline orientations, and a variety of sediment sources and quantities of sand and gravel (FitzGerald *et al.*, 1994; Fitzgerald & Van Heteren, 1999; Johnson, 1925; Shepard & Wanless, 1971).

Two U.S. Geological Survey core holes were taken from Martha's Vineyard and Nantucket and produced Cretaceous sediments, with a maximum thickness of 350 m (1,148 ft) beneath Nantucket (Poag, 1978). These sediments are principally unconsolidated, fine-to-coarse clayey sand, interbedded with silty, and sandy clay of terrestrial origin. Paleocene rocks on Martha's Vineyard are composed of clayey silt containing a few planktic and benthic Foraminifera of outer shelf origin. Beneath the Vineyard, Eocene rocks are sparsely fossiliferous clayey and greensand, no more than 20 m thick. Surficial sediments of this region are largely sand, gravel, and boulders of glacial origin winnowed during the last post-glacial rise in sea level (Poag, 1978).

Reworking of Holocene glacial debris is the main source of surficial sediments in the region, with very little modern delivery of sediment from the land (Poag, 1978; Townsend *et al.*, 2004). This reworking has produced large volumes of sand and gravel, creating coastal sand dunes along the shores of Martha's Vineyard.

Soils. Once the glaciers retreated, soil began to develop on top of the MV moraines and outwash planes and its development, over time, was influenced by weather, climate, parent material, biota, and surface relief (Oldale, 1992). The onset of organic sedimentation probably began on MV between 18,000 (Oldale, 1992) to 10,000 years ago (Balco *et al.*, 2002). Soil formation is a lengthy process and, on Cape Cod and the islands, parent material and slope are two of the most important factors in the formation of mineral soils on glacial drift and outwash (Oldale, 1992).

Beach and dune sand deposits are the result of eroded glacial drift that was transported offshore and along the shore (Oldale, 1992). Winter storms remove the beach and dune sand, exposing the underlying pavements, till, or bedrock; beach sand and dune sand are then redeposited during the summer (Fullerton *et al.*, 2004). Dunes provide extensive protection to the shorelines, by serving as barriers to severe storms and waves (Carter, 1991). Dune sand commonly forms a narrow strip of fore-island dunes or back-island dunes adjacent to, and immediately inland from, the beach sand (Fullerton *et al.*, 2004). Beach sand and dune sand are transported nearly continuously by waves and wind.

On a decadal time scale, some of the landforms (for example, beaches, barriers, and dunes) shift geographically inland and (or) seaward hundreds of meters. Some barriers and dunes were virtually destroyed by hurricanes and storms (see below) and they were fully replaced by waves and wind in only a few years (Fullerton *et al.*, 2004).

Sea cliffs are formed wherever the glacial deposits face the open ocean and are unprotected from wave attack (Oldale, 1992). They are underlain by incohesive sandy deposits that are periodically attacked by storm waves causing slope failure (Oldale, 1992). The sea cliffs on MV are located along the NW and NE study sites and are composed of accumulations of ice-contacted deposits, designated as end moraines.

Continental Shelf and Depth of Closure. The continental shelf along the eastern seaboard of the U.S. is part of the Atlantic Coastal Plain and it is often referred to as the submerged Coastal Plain (Oldale, 1992). It is characterized by a surface of low relief and by altitudes near sea level (Oldale, 1992), particularly around Martha's Vineyard (Figure 21). The continental shelf is the shallow seafloor that begins at the toe of the shoreface all the way to the steep shelf break (Morang & Parson, 2002). Along the eastern seaboard of North America the continental shelf is wide and shallow. The continental shelf between Georges Bank, off the coast of Massachusetts, and Cape Hatteras, North Carolina, forms a comma shape that tapers in width and curves a full 90° in orientation from east-west off southern New England to north-south at Cape Hatteras (Townsend *et al.*, 2004). The Nantucket Shoals are relatively shallow (< 50 m, 164 ft) and the depth of Long Island Sound averages approximately 20 m (66 ft). The continental shelf from Georges Bank to Cape Hatteras has a gentle slope running from the coast to the shelf edge.

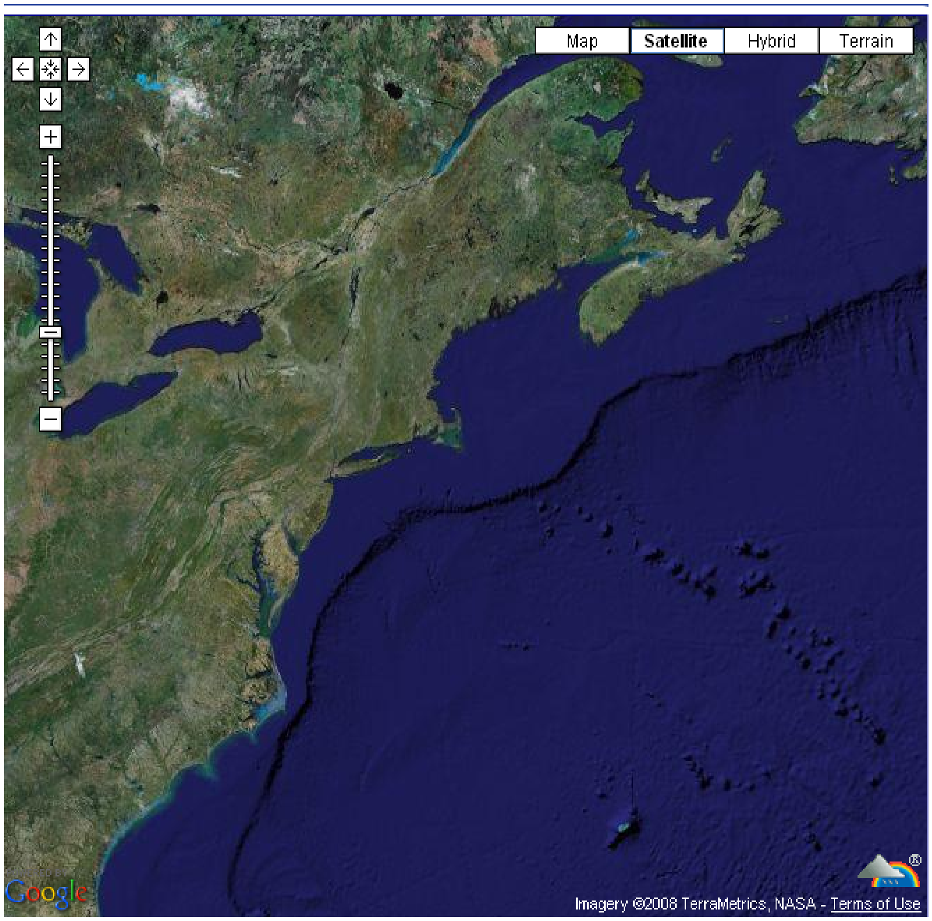

Figure 21 Continental shelf in the vicinity of Martha's Vineyard. From wunderground.com

Depth of closure (DOC) is the seaward limit of significant profile change, i.e., the depth of water at which there is no appreciable movement of sediments by wave action. Estimates for the DOC include: -5.5 m (18 ft) (Phillips & Williams, 2007), -7 m (23 ft) (Dalrymple, 1997), -8 m (26 ft) (Nicholls *et al.*, 1998), -9 to 12 m (30-39 ft) (near Long Island, New York) (Kana, 1995), and -18 m (-60 ft) (Bruun, 1962). The latter estimate considered the DOC at the -18 m contour line to represent the depth that differed between the "nearshore" and "deep-sea littoral drift phenomenon" (Bruun, 1962), i.e., that, generally, the short-term exchange of shore material (fluctuations of nature) and offshore bottom takes place up to this depth, but usually not beyond (Bruun, 1962). Generally, the movement of sediment, from the shore to the offshore area, is a slow process, varying with the different types of currents (Bruun, 1962). In contrast, the long-range effects of sediment movement are related more to geological adjustment processes (Bruun, 1962).

Sea Level

Two major factors influence sea level for the northeastern U.S.: 1) ocean volume change from steric and eustatic processes, and 2) land subsidence related to isostatic response of the crust and mantle caused by the loading and unloading of the Laurentide Ice Sheet (GIA) (Brown University, 2006; Casey, 1911; Fairchild, 1926; Giese *et al.*, 1987; Johnson, 1910; Johnson & Stolfus, 1924; Marsh, 1898; Ogden, 1974; Peltier, 1999, 2002; Redfield, 1967; Townsend, 1911). The present relative rate of sea level rise in Massachusetts is approximately 3 mm/yr (0.1 in/yr), the global average (Giese, 1997). Approximately half of that rate, or 1.5 mm/yr (0.06 in/yr) is the result of eustatic sea-level rise, and the other half is a result of crustal subsidence (Giese, 1997). It should be noted that land subsidence does not alter the volume of ocean water (IPCC WGI, 2007).

Historically, local sea level changes have been substantial and some Massachusetts islands have already disappeared due to sea level rise (Oldale, 1992). For example, Billingsgate Island, near the coast of Wellfleet (on Cape Cod), completely vanished in 1942 (O'Brien, 1995; Oldale, 1992; Rico & Rico, 1998). At one time this 60 acre island had 30 homes, a school, and a lighthouse (O'Brien, 1995). At very low tide, the remains of the island can be seen, along with the remnants of the lighthouse. Other land submerged in the area includes Stellwagen Bank, north of Cape Cod, and Georges Bank, east of Nantucket (Oldale, 1992). About 12,000 years ago, Stellwagen Bank stood well above sea level and may have even been connected to Cape Cod (Oldale, 1993/1994). Humans arrived at this location 11,000 years ago and their descendants may have witnessed its disappearance 1,000 years later as the Laurentide Ice Sheet retreated and the local sea level rose (Oldale, 1993/1994). The land between Martha's Vineyard, Nantucket, and Cape Cod was above sea level until marine waters respectively flooded Vineyard Sound and Nantucket Sound ~7,500 and ~6,000 years ago (Oldale, 1992). About 2,000 years ago, Cape Cod and the Islands began to look something like they do today, with the shoreline probably a half a mile to several miles farther seaward (Oldale, 1992).

Tides

Woods Hole (41°3 2' N, -70° 40' W) and Nantucket (41°1 7' N, -70° 06' W), two Massachusetts communities close to Martha's Vineyard, have active water level stations. The active tidal benchmark in Woods Hole has been in operation since 1932 (NOAA, 2005d). Its mean tidal range (the difference between mean high water and mean low water) is 0.545 m (1.79 ft) and the diurnal range (the difference in height between mean higher high water and mean lower low water) is 0.674 m (2.21 ft) (NOAA, 2005d). The tidal benchmark on Nantucket Island was established in 1963 and the mean tidal range on Nantucket is 0.92 m (3.03 ft) and the diurnal range is 1.01 m (3.57 ft) (NOAA, 2006e). Factors that influence tides include coastal configurations, local wind, weather patterns, and barometric pressure (Bascom, 1964; Bertness, 1998).

Sediment Transport and Currents

Longshore sediment movement to the vicinity of Martha's Vineyard originates from the coastal waters of Connecticut and Rhode Island and moves northeast, splitting its path when it reaches the waters near Aquinnah (van Gaalen, 2004). The shorelines of the SS site (see below) are fed with this sediment while some of it continues to move northeasterly, along the NW study site, to the south shore of Cape Cod (Figure 22) (van Gaalen, 2004). While van Gaalen does not show any sediment movement along the NE study site, examination of aerial photos and current speeds suggests some sediment movement southwest, towards Edgartown and along the NE site coastline (Figure 23).

The current in Vineyard Sound, near West Chop, follows a northeasterly (059°) direction with an average flood speed of 2.7 knots. At ebb, it decreases to 1.4 knots and moves southwest to west (241°). Approximately 1.6 km (1 mile) north of East Chop, the average flood speed current moves at 2.2 knots and heads east to southeast (116°). The ebb speed is the same (2.2 knots), but the current's direction changes to southwest to west (241°) (NOAA, 2007b).

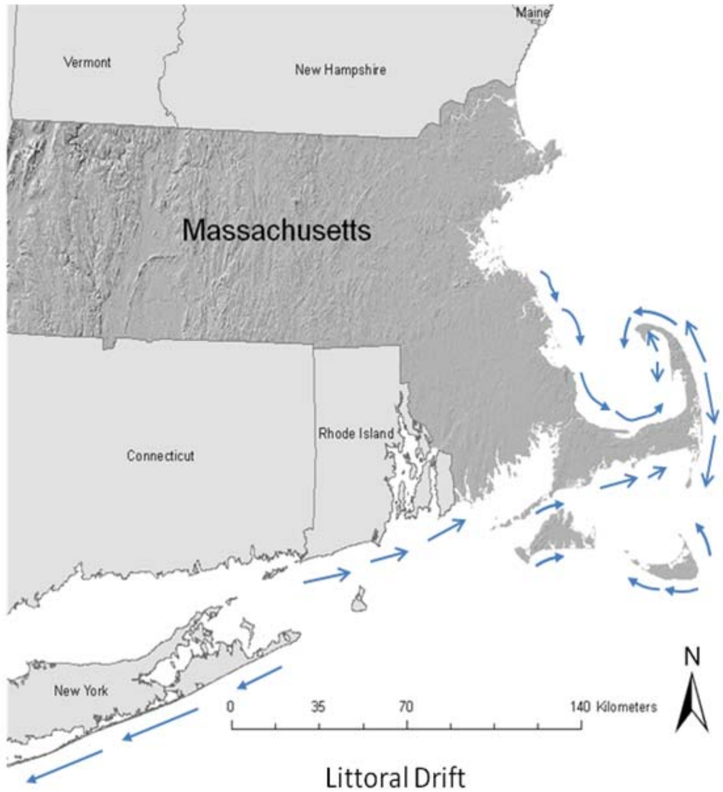

Figure 22. Longshore sediment along the coastline of the northeastern U.S. Modified from Joseph F. van Gaalen, 2004

Figure 23. Aerial photo of the coastline south of Oak Bluffs Harbor, showing littoral drift movement towards the southeast.

Coastal Erosion

Approximately 75% of the United States coastline is eroding (The Heinz Center, 2000). Within Massachusetts, approximately 68% of ocean-facing shoreline exhibits a long-term erosional trend, 30% shows a long-term accretion, and 2% shows no net change (Sea Grant Woods Hole, 2003). Data on the shorelines of Martha's Vineyard indicate that approximately 78% are eroding, 20.5% are accreting, and the remaining 1.5% shows no net change (Sea Grant Woods Hole, 2003).

Massachusetts shorelines tend to change seasonally, accreting slowly during the summer months when sediments are deposited by relatively low energy waves and eroding dramatically during the winter when sediments are moved offshore by high energy storm waves, such as those generated by Northeasters (MA CZM, 2006b). Besides long-term bluff retreat, these changes include beach and dune erosion, breaching and landward migration of sandy barriers, and longshore redistribution of sand (Buynevich & Evans, 2003). The wave-dominated northern and southern coastlines of Martha's Vineyard are respectively subject to mean offshore wave heights of 1.0 –1.5 m (3-5 ft) and 1.5-2.0 m (3-6.5 ft) (Figure 24) (Fitzgerald & Van Heteren, 1999).

Under storm conditions, coastal erosion is increased by the type of tides, wave energy, and the duration of the event (Zhang *et al.*, 2001). Storms often cause short-term flooding and erosion, but the coastline rebounds over a period of time. The short-term impact of storm-induced alterations to shorelines has been reviewed recently (Austin *et al.*, 2000; Buynevich & Evans, 2003; Fein, 2007; FitzGerald *et al.*, 2002; Ogden, 1974; Plum Vineyard, 2007; Seccombe, 2007; Sigelman, 2007; The Trustees of Reservations, 2007).

On Martha’s Vineyard, the Norton Point barrier beach between Katama Bay and the Atlantic Ocean, just to the east of the SS study site, has repeatedly been breached because of strong storms. Just as regularly, the barrier beach has returned within 10-15 years of the storm that breached it. Documents indicate that such openings occurred in 1886 after a strong winter gale, in 1938 after a hurricane, during the fall of 1954 after a succession of major hurricanes (Carol and Edna), and another one in 1969 (Ogden, 1974). More recent breaks at Norton Point occurred during the spring of 2007 (Fein, 2007) and in the spring of 2008 (MV Times, 2008).

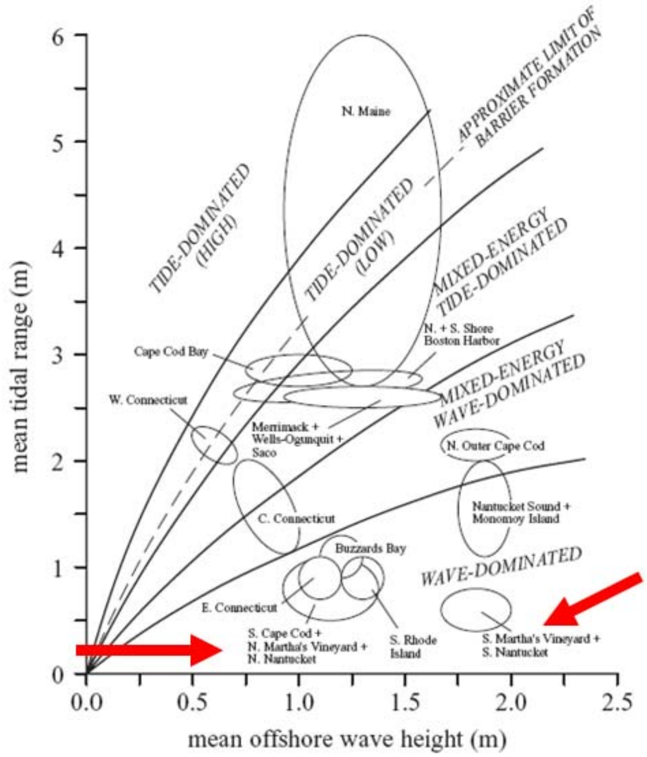

Figure 24. Classification of barrier coastlines according to Hayes’ (1979) scheme (Fitzgerald and Van Heteren, 1999).

Climate

Martha’s Vineyard has a moderate coastal climate, being milder in the winter and cooler in the summers than the Massachusetts mainland. The Vineyard is often sunny, although rain or fog can be unpredictable and somewhat changeable during the summer months. Average summer temperatures peak in July at approximately 25°C (77°F) and, at times, the island can be quite hot and humid. Winter temperatures are mild due to the proximity of the Gulf Stream along the southern New England coast. Average lowest winter temperatures (occurring in January) are -6°C (21° F). The Massachusetts annual temperature trend, from 1895-2005, is an increase of 0.10° F/decade, with inland temperatures (e.g., Bluehill) trending even higher (NOAA, 2006f, 2007a).

Prevailing winds average 14 kph (9 mph) from the west or southwest in the summer, turning to the west or northwest during the winter (NOAA, 1998). Martha's Vineyard is slightly protected from the strong winds of Northeasters because it is leeward of Cape Cod, which is to the north, northeast.

Climate Change

Recent analyses have shown that average global and northern hemisphere temperatures increased by approximately 0.6°C in the 20th century (IPCC, 2001a). In contrast, between 1895 and 1999, the average temperature of the northeastern part of the U.S. increased by 0.7°F (NECC, 2003; NERA, 2002). The below average temperatures of the northeast are thought to be accounted for by major differences in topography, proximity to the ocean, and large cities within the area (NERA, 2002). During the same period south coastal New England's temperature increased by approximately 2.1°F, double the national and global average. The warmest years in Massachusetts occurred at the end of the 20th century (EPA, 1997) and projections indicate an increase in regional annual minimum temperature between 6°F and 10°F (NECC, 2003).

Projections through 2090 for the northeast estimate an increase in precipitation of 10-30%, should present trends continue (NECC, 2003). Predictions for Massachusetts indicate that precipitation will increase: 10% during the spring and summer, 15% in the fall, and by 20-60% in the winter (NECC, 2003).

Weather

The average annual rainfall/precipitation in Martha's Vineyard and Massachusetts are, respectively, 1.15 m (45.3 in) and 1.09 m (43.37 in) (MVC, 2004; NOAA, 2007a). The annual trend for MV from 1895-2006 is an increase of 3 cm/decade (1.18 in/decade) (NOAA, 2007a). Statewide, precipitation is increasing by 2.9 cm/decade (1.15 in/decade) (NOAA, 2006f), whereas average precipitation in the northeast, from 1895 to 1999, increased by 4%. By comparison, the annual weighted coastal precipitation increased by 16.76% (NERA, 2002).

Hurricanes

In the U.S., hurricane season extends from June 1 through November 30. In Massachusetts, hurricane season peaks during August and September (MA CZM, 2002). Cape Cod and the Islands are particularly vulnerable because the land sticks out into the Atlantic Ocean, and Buzzard's Bay becomes a funnel, with the wind and water piling up at its end. Slightly cooler waters reduce the chances for Category 4 or 5 hurricanes in the area.

Table 1 shows that New England had 37 direct hits from hurricanes during the 153 year period from 1851 to 2004, with the south coastal states receiving most of the direct hits (Blake *et al.*, 2005). Massachusetts had 10 hurricanes, three of which were major, rated as Category 3. Most of the hurricanes to hit New England and Massachusetts were rated as Category 1 (NOAA, 2005c). Cape Cod has the highest average frequency of hurricane force winds, averaging one occurrence every 14 years (Mayewski *et al.*, 1998). The year with the highest number of storms making land fall in the region was 1888, which had three (Mayewski *et al.*, 1998).

STATE	Category 1	Category 2	Category 3	Category 4	Category 5	STATE TOTAL	MAJOR HURRICANES
CONNECTICUT	4	3	3	0	0	10	3
RHODE ISLAND	3	2	4	0	0	9	4
MASSACHUSETTS	**5**	**2**	**3**	**0**	**0**	**10**	**3**
NEW HAMPSHIRE	1	1	0	0	0	2	0
MAINE	5	1	0	0	0	6	0
TOTALS	**18**	**9**	**10**	**0**	**0**	**37**	**10**

Table 1. Hurricane direct hits on New England from 1851-2004, classified according to the Saffir/Simpson Scale. Modified from (Blake *et al.*, 2005).

Table 1 is somewhat deceiving because it suggests that, over a 153 year period, Massachusetts had only 10 major storms. However, the Atlantic Basin is very active and many more hurricanes pass near Massachusetts without making landfall, and are, therefore, not counted (Figure 25A). Nevertheless, the Martha’s Vineyard shoreline still feels the effects of all this storm activity, usually through increased surf, waves, and erosion. Figure 25B and C give a better view of hurricane tracks within 300 km of MV and even closer, at 50 km (31 miles). These data show that Martha’s Vineyard took five direct hits, three of which were a Category 1, one was downgraded from a Category 2 to Category 1 just off the shore of MV, and one was a Category 2. Within a 50 km (31 miles) radius, there were an additional four hurricanes, two Category 1 storms, one Category 2, and one Category 3, making a total of nine hurricanes within 50 km (31 miles) of Martha’s Vineyard.

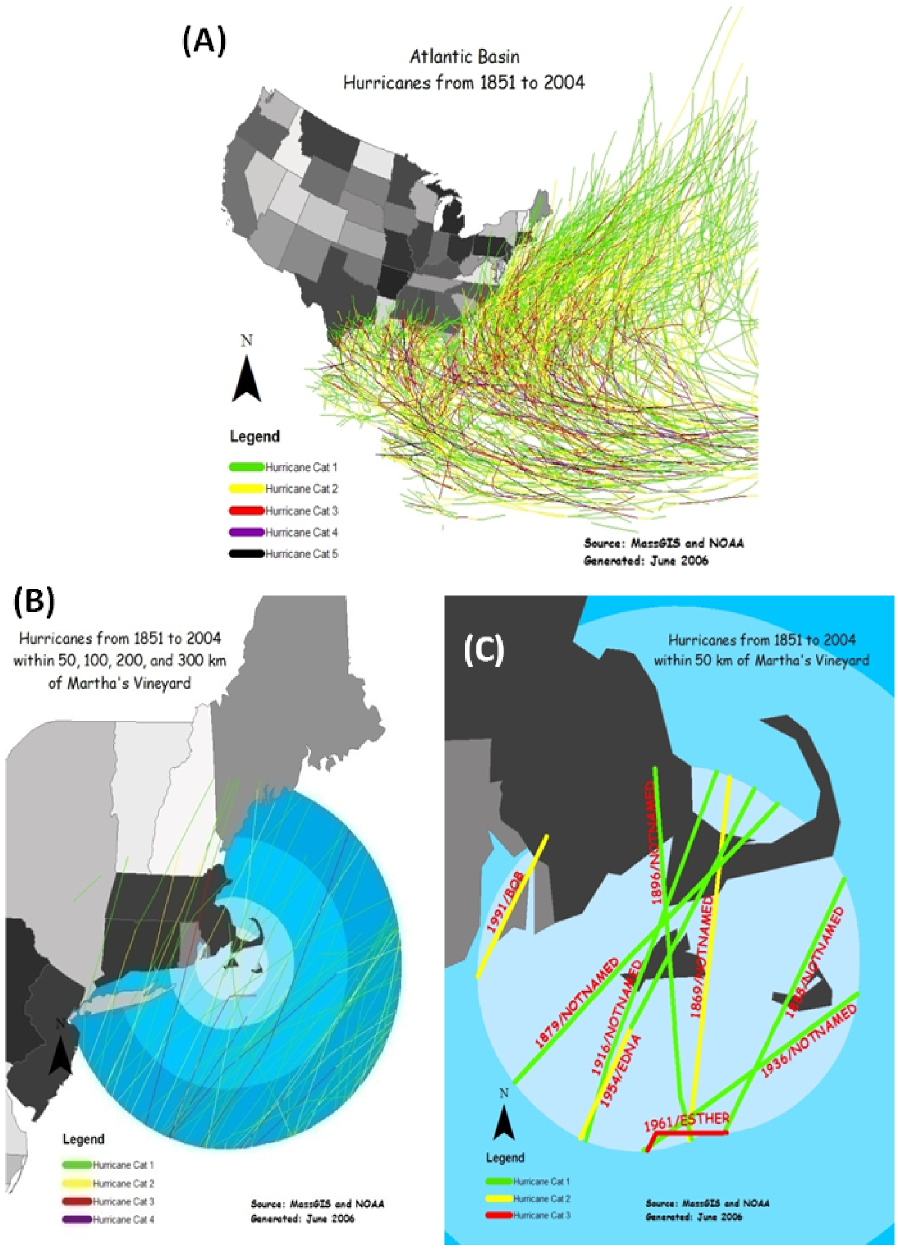

Figure 25.Atlantic hurricanes in the vicinity of Martha's Vineyard (MV). (A) Atlantic hurricane tracks from 1851 to 2004. (B) Hurricanes within 300 km of MV. (C) Hurricanes within 50 km of MV. From MassGIS and NOAA.

Northeasters

Extra-tropical Northeasters usually occur in Massachusetts from October through April. The counter-clockwise east or northeasterly winds of these storms can cause extensive damage, particularly along coastlines, because the wind removes and transports sand from beaches and dunes (DGS, 1998). Although the winds of Northeasters are not as strong as hurricanes, their destructive power is derived from their long duration (USGS, 2005). The potential for coastal erosion from severe northeasters is more dependent on storm tide than wave energy and duration (Zhang *et al.*, 2001).

Population

Population data from the U.S. Census Bureau (2008) indicate that the MV year-round population has recently grown from 10,005 in 1980 to 15,430 in 2006. The largest numerical increase in population occurred in Oak Bluffs (1,547), followed by West Tisbury (1,461), and Edgartown (1,285) whereas the largest percentage increase in growth occurred in Tisbury (84%), Edgartown (67%), and Chilmark (61%) (Table 2 and Figure 26).

TOWN	POP1980	POP1990	POP2000	POP2006
AQUINNAH	184	201	344	354
CHILMARK	583	650	843	953
EDGARTOWN	2,633	3,062	3,779	3,918
OAK BLUFFS	2,214	2,804	3,713	3,761
TISBURY	3,209	3,120	3,755	3,801
WEST TISBURY	1,182	1,704	2,467	2,643
TOTALS	**10,005**	**11,541**	**14,901**	**15,430**

Table 2. Population of the towns of Martha's Vineyard.

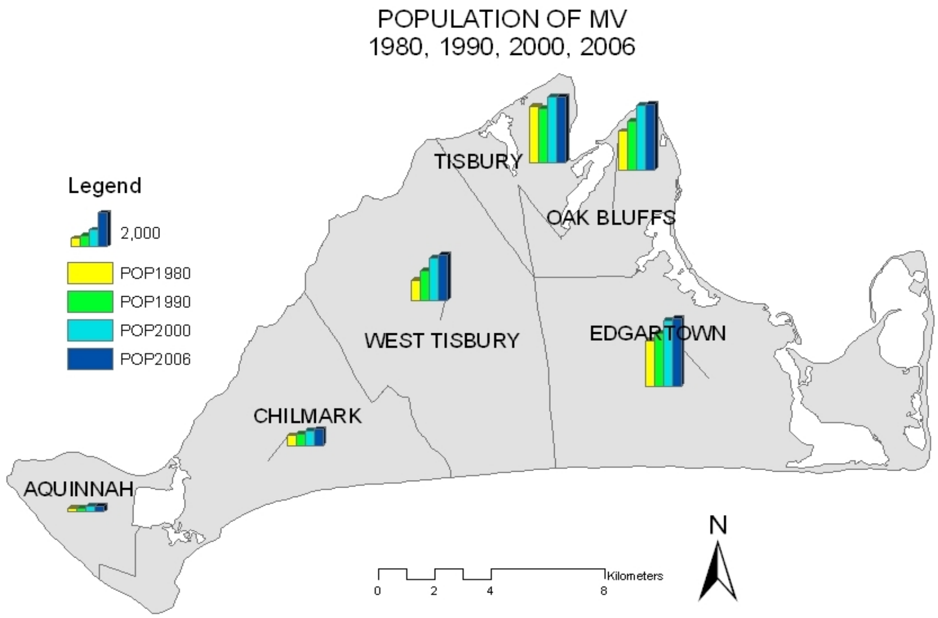

Figure 26. Population of the towns of Martha's Vineyard.

As of 2006, there were, on average, 161 people/sq. mile or 0.25 people/acre on Martha's Vineyard. Tisbury has the most people/sq. mile (578), followed by Oak Bluffs (503), then Edgartown (135); Chilmark has the fewest people/sq. mile (46) (Table 3**)**.

TOWN	CHG 1980-2006	% POP CHG	ACRES	PEOPLE/ ACRE	SQ MILES	PEOPLE/ SQ MILE
AQUINNAH	170	52%	3,693	0.10	5.77	61
CHILMARK	370	61%	13,139	0.07	20.53	46
EDGARTOWN	1,285	67%	18,552	0.21	28.99	135
OAK BLUFFS	1,547	59%	4,781	0.79	7.47	503
TISBURY	592	84%	4,211	0.90	6.58	578
WEST TISBURY	1,461	45%	16,880	0.16	26.37	100
TOTALS	**5,425**	**65%**	**61,256**	**0.25**	**95.71**	**161**

Table 3. Population densities on Martha's Vineyard.

During the summer months, the MV population grows to 75,000+ residents, not including guests and visitors (MVC, 2004, 2006). The island's proximity to the mainland ensures that more than 25,000 additional summer visitors come and go on ferries every day. Many of the summer tourists visit the beaches along the northeast and south side of the island which happen to have the highest rate of erosion and shoreline change in the northeast (Buynevich & Evans, 2003), making these areas extremely vulnerable to coastal hazards from global warming, sea level rise, and significant changes in ecosystem habitats. The growth in both year-round residents and tourists has brought an increased demand for greater public access to natural areas and beaches for the pursuit of recreational activities. Degradation of these areas from increased development and use, in addition to global climate change, threatens the resources and long-term survival of Martha's Vineyard.

Tourism and Coastal Economy

Cape Cod and the Islands host 4.7 million domestic visitors per year, or approximately 19% of all tourist visits to Massachusetts (Massachusetts Ocean Management Task Force, 2004). In 1997, tourists to Massachusetts spent $10.8 billion and, of this amount, $6.3 billion was spent in coastal counties (MA CZM, 2002).

Cape Cod and the Islands depend heavily on tourism and environmental conditions are, therefore, critical to supporting this economy (Massachusetts Ocean Management Task Force, 2004). Visitors and second-home owners thus comprise "the driving force of the island's economic base" (MVC, 2006).

The focus on tourism notwithstanding, the coast of Martha's Vineyard also encompasses significant industrial activities, including fuel transport and storage (Massachusetts Ocean Management Task Force, 2004). In part, these activities address the cruise ships and year-round ferry services that call upon the island's ports (Massachusetts Ocean Management Task Force, 2004).

Coastal real estate, tourism and fishing could all be affected by sea level rise and other effects of global warming. The south-facing coasts of Massachusetts and Rhode Island appear to be especially susceptible to the loss of land due to sea level rise; it is estimated that about 33 acres of land on Cape Cod are lost each year (NECC, 2003). Preserving coastal beaches and property could become a major economic drain (NECC, 2003). For example, the cumulative cost of sand replenishment on the Massachusetts coast from a 20-inch sea level rise by 2100 is estimated at between $490 million and $2.6 billion (EPA, 1997).

Commercial fishing, including fresh and frozen fish processing, and supporting transportation and marketing services, is a $4 billion industry in Massachusetts (MA CZM, 2002). The decline of estuarine habitat due to sea level rise and other factors could also have significant impacts on the commercial fishing industry in the region, already reeling from decades of over-fishing (NECC, 2003).

As temperatures slowly increase, and before sea level rises to the point of creating significant coastal disturbances, Martha's Vineyard's tourist season will probably be extended by several months, due to earlier warming in the spring and warmer temperatures lasting well into the fall. Rising sea surface temperatures will help f*uel* the warmer temperatures along the south coast of Massachusetts.

Descriptions of the Study Sites

Three sites on Martha's Vineyard were chosen for an analysis of the coastal response to sea level rise (Figure 27). Several considerations influenced the choice of these sites: geology, surficial geology, wetlands, soils, land use, shoreline orientation to wind, waves, and sea levels. The primary objective was to select sites that were representative of three different aspects of the Martha's Vineyard coast. These sites are located on the south side (SS), the northeast side (NE), and the northwest (NW) side of Martha's Vineyard. Each location is unique in its geomorphology. All three sites have 487 transects, perpendicular to the beach, with erosion rates grouped into four eras.

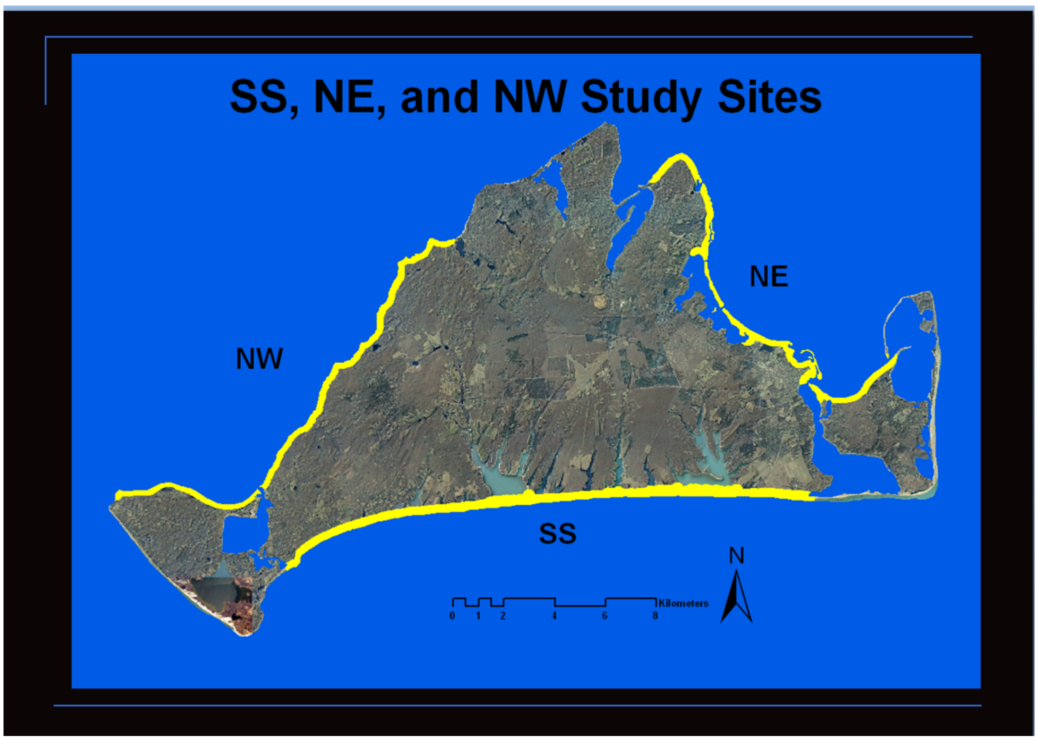

Figure 27. Location of the three study sites on MV. From: MassGIS 2006.

The three major geomorphological regions of the triangular island of Martha's Vineyard currently include: 1) the western end (NW study site), 2) the northeastern end (NE study site), and 3) the central, eastern, and southern coasts (SS study site). The western end consists of a series of moraines that form irregular and subparallel ridges and hills from 40 m (131 ft) (Foster *et al.*, 2002) to 95 m (312 ft) in elevation, including the highest point on MV, Peaked Hill, in Chilmark (Oldale, 1992). The moraines are composed of poorly-and-well-sorted sand, silt, and clay that were transported in the glacial ice and left behind when the ice retreated (USGS, 2004). The textural composition of the moraines generally varies more over short distances than does the textural composition of outwash deposits (USGS, 2004). The high cliffs of the Gay Head Moraine on MV consist largely of clay and silt with some sand and lignite (USGS, 2004). The northeastern end is composed of sandy glacial outwash which overlays the moraine, forming a region of low rolling hills and shallow depressions (Foster *et al.*, 2002). The central, eastern, and southern coasts are part of an extensive outwash plain that stretches across this part of the island and slopes gently from 30 m (98 ft) elevation in the north to < 3 m (9.8 ft) towards the southern coast where it is dissected by a series of north-south trending valleys that terminate in coastal ponds (Foster *et al.*, 2002). These broad outwash plains are mainly composed of sand and gravel, which, in places, are mixed with till and ice-contact deposits, silt and clay (USGS, 2004). All areas, except the southwest corner of the island, are underlain by >100 m (328 ft) of Quaternary and coastal plain sediments (Fletcher & Roffinoli, 1986; Foster *et al.*, 2002).

SS Study Site

Study site SS includes a large segment of the south-facing coastline from Chilmark, through West Tisbury, to Edgartown, approximately 21 km (13 miles) long. The transects begin at the edge of Stone Wall Beach and Wequobsque Cliffs (elevation = 15 m [50 ft]), on the western side of the south shore, and continue to Katama in Edgartown, ending at Mattakeset/Katama Bay. Zoning within the SS site includes mostly residential and agricultural land. The Katama Plains Airpark and Conservation area is one of Massachusetts' most significant ecosystems, and is protected from development.

Major water bodies within 800 m (0.5 miles) of the coastline include Chilmark Pond, Quenames Cove, Black Point Pond, Tisbury Great Pond, Homer Pond, Watcha Pond, Oyster Pond, Paqua Pond (Faqua Pond), Job Neck Pond, and Jacobs Pond (Herring Pond). Beaches include Lucy Vincent, both at the ocean and pond, Chilmark Pond Preserve, Great Pond at Long Point, Ocean at Long Point, Sepiessa Point, and South Beach (right fork and middle).

Properties that the Martha's Vineyard Land Bank own along the SS study site include: Allen Farm (91,054 m^2 or 22.5 acres); Chilmark Pond Preserve, with 61 m (200 feet) of beach front (33,588 m^2 or 8.3 acres); Tisbury Great Pond Beach (7,689 m^2 or 1.9 acres); and Edgartown Great Pond Beach (29,947 m^2 or 7.4 acres) (Martha's Vineyard Land Bank Commission, 2008).

The soil in this area is composed of sand and gravel deposits (Martha's Vineyard moraine outwash) and the coastline consists primarily of barrier and coastal beaches and coastal dunes.

This region is exposed to the Atlantic Ocean, and to all types of weather conditions, including hurricanes. The south facing beaches are wave dominated, with mean offshore wave heights of approximately 2 m (6.56 ft) (Fitzgerald & Van Heteren, 1999). 'Type 3a' barriers on Martha's Vineyard are found on the Atlantic south-facing section from Wasque Point to Squibnocket (Fitzgerald & Van Heteren, 1999). Type 3a' coasts are moderately long, with a range of 2 km to 12 km (1.2 ft to 7.5 ft), are composed primarily of sand, and are retrograding (Fitzgerald & Van Heteren, 1999).

Updrift moraines are the main sediment source of these barrier beaches, carried by longshore transport and storm processes (Fitzgerald & Van Heteren, 1999). Baymouth barriers (anchored to the mainland on both sides) are characteristic of 'Type 3' coasts and are fronted by shallow lagoons of limited extent (Fitzgerald & Van Heteren, 1999). The wave-exposed setting of the baymouth barriers makes them susceptible to overwash and breaching, which cause significant morphological and sedimentological changes in both barrier and back-barrier environments (Fitzgerald & Van Heteren, 1999).

The salt ponds in West Tisbury provide 10,000 bushels of oysters (over half of MV's annual harvest) and over 100 native plants line the shores (The Trustees of Reservations, 2006a). River Otters can be found here, along with over thirty species of fish. Rare habitats such as Scrub Oak shrublands, sandplain grasslands, and coastal heathlands are located in this area (The Trustees of Reservations, 2006a).

Sepiessa Point Reservation and Long Point Wildlife Refuge on Tisbury Great Pond are included in this area. Sepiessa Point Reservation has more than 2.23 km (7,300 feet) of shorefront, and contains 665,303 m² (164.4 acres). This area is predominantly wooded, but also includes grasslands and a savanna, restored by the Martha's Vineyard

Landbank as part of a plan to increase foraging habitat for owls and hawks (MV Landbank Commission). Long Point Wildlife Refuge contains 2,561,660 m² (633 acres) of coastal salt ponds, sandy beaches, sand barren ecosystems, and many rare species of plants and animals. Vegetation communities include Scrub Oak shrublands, sandplain grasslands, coastal heathlands, and pitch pine barrens (The Trustees of Reservations, 2006b).

The sandplains area extends from Chilmark Pond to the eastern shores of Edgartown Great Pond. The beach complex is sparsely vegetated, with foredunes dominated by American beach grass (*Ammophila breviligulata*) and seaside goldenrod (*Solidago sempervirens*) (U.S. FWS, 1991a). Behind the dunes, the slope decreases to 0-3%. Vegetation here consists of bayberry, saltspray rose (*Rosa rugosa*), poison ivy (*Toxicodendron radicans*) and winged sumac (*Rhus copallina*) (U.S. FWS, 1991b).

The large ponds and embayments, such as Great Tisbury Pond, Edgartown Great Pond, and Katama Bay are rich in biodiversity. They contain salt marshes and wooded marshes (scrub swamps), and are important as wintering grounds for waterfowl, particularly Bald eagles (*Haliaeetus leucocephalus*), a U.S. endangered species (U.S. FWS, 1991a). During the fall and spring migrations, Peregrine falcons (*Falco peregrinus*), also a U.S. endangered species is common in this area (U.S. FWS, 1991a). Commercially and recreationally, this area provides important shellfish beds, and within the coastal zone the waters are rich in bluefish (*Pomatomus saltatrix*), winter flounder (*Psedopleuronectes americanus*), striped bass (*Morone saxatilis*), Atlantic cod (*Gadus morhua*), and Atlantic bonito (*Sarda sarda*) (U.S. FWS, 1991a).

NE Study Site

The length of the NE site is 17.3 km (10.75 miles). This study site spans the coast between two towns, Oak Bluffs and Edgartown, containing the largest percentage of the population on Martha's Vineyard. Transects in Oak Bluffs cover approximately 8 km (4.97 miles) of shoreline and, on the northern shores of Edgartown, the study site shoreline is 9.3 km (5.78 miles) long. The NE transects begin in Eastville (Oak Bluffs), near Eastville Ave and end in Chappaquiddick, just before Cape Pogue Bay.

Major water bodies within 800 m (0.5 miles) of the shoreline include: Crystal Lake, Meadow Pond (Oak Bluffs Harbor), Farm Pond, Sengekontacket Pond, Trapps Pond, Eel Pond, and Edgartown Harbor/Katama Bay. Heading southeast of East Chop Light there are numerous beaches, including: Yacht Club Beach, Pay Beach, Joseph Syliva State Beach, Bend in the Road Beach, Fuller Beach, Chappy Point Beach, and East Chappy Beach.

The Martha's Vineyard Land Bank Commission owns properties along the NE study site. These include Farm Pond Preserve (110,075 m^2 or 27.2 acres), Chappy Point Beach, which includes 700 feet of beach front (11,736 m^2 or 2.9 acres), and North Neck Highlands Preserve between Cape Pogue Pond and Nantucket Sound (18,616 m^2 or 4.6 acres) (Martha's Vineyard Land Bank Commission, 2008).

This site faces northeast onto Nantucket Sound, exposing it to Northeasters. Because it is leeward of Cape Cod, by approximately 8 km (5 miles), it is somewhat protected. The northern coastlines of Martha's Vineyard are subject to mean offshore wave heights of 1–1.5 m (3 to 5 ft) (Fitzgerald & Van Heteren, 1999).

‘Type 3a’ barriers on Martha’s Vineyard are found on the northeast side, from East Chop to Wasque Point (on Chappaquiddick Island), are composed primarily of sand, and are retrograding (Fitzgerald & Van Heteren, 1999). From East Chop to Wasque Point, the main source of sediment for these barrier beaches is from updrift moraines carried by longshore transport and storm processes (Fitzgerald & Van Heteren, 1999).

NW Study Site

The NW study site is approximately 20 km (12.5 miles) long, on the northwestern side of the Vineyard, facing Vineyard Sound and the Elizabeth Island chain. Transects encompass the towns of Aquinnah (from the edge of Gay Head Cliffs in Aquinnah [formerly called Gay Head]), through Chilmark, and ending at Lambert’s Cove in West Tisbury. Large water bodies within 800 m (0.5 mile) of the shoreline include Menemsha Pond, where Menemsha Harbor is located. Menemsha is a classic New England fishing village within the town of Chilmark. Menemsha Pond connects to Nashaquita Pond, which borders Stone Wall Beach on the south side. There are two smaller ponds along the NW shoreline called Herlock Pond (51,852 m^2 or 13 acres) and Doggets Pond (44,143 m^2 or 11 acres).

The northern coastlines of Martha’s Vineyard are subject to mean offshore wave heights of 1–1.5 m (3 to 5 ft) (Fitzgerald & Van Heteren, 1999). ‘Type 2’ coastlines are found along the NW study site, from Squibnocket to East Chop (Fitzgerald & Van Heteren, 1999). They are built across embayments that were formed upon marine submergence of an irregularly shaped, bedrock-dominated landscape (Fitzgerald & Van Heteren, 1999). Their sediment was originally derived from updrift and onshore sources of glacial origin; current sources are from newly eroded or recycled glacial material

(Fitzgerald & Van Heteren, 1999). Type 2 coastlines are anchored to headlands that may provide protection from incoming waves, have a relatively small bay size, and limited tidal range (Fitzgerald & Van Heteren, 1999). On MV, these inlets are typically kept open by jetties and by periodic dredging (Fitzgerald & Van Heteren, 1999). Breaching of these barriers by catastrophic events has led to only limited long-term impacts (Fitzgerald & Van Heteren, 1999).

Lobsterville Beach, located in Aquinnah, has 930,777 m^2 (230 acres) of fragile bogs, dunes, and a barrier beach. This area used to be a fishing village until the 1938 hurricane (Wampanoag Tribe of Gay Head, 2006). Menemsha Public Beach is next to Menemsha Harbor. Wampanoag tribal lands are contained within this study site and governing conflicts arise sometimes between the tribe and the town.

Cedar Tree Neck Sanctuary is within 800 m (0.5 miles) of the coastline on the NW side and its current size is 1,262,619 m^2 (312 acres). This sanctuary consists of multiple habitats which include freshwater ponds, streams, sandy beaches, rocky cliffs, and woodland areas with oaks, maples, and beech groves (Sheriff's Meadow Foundation, 2005). Great Rock Bight Preserve is owned by the Martha’s Vineyard Land Bank Commission. Located northeast of Menemsha, it covers 396 m (1300 ft) of shoreline on Vineyard Sound and includes 115,335 m^2 (28.5 acres) (Martha's Vineyard Land Bank Commission, 2008). Gay Head Moraine is another MV Land Bank property, consisting of 202,342 m^2 (50 acres) southwest of Menemsha Pond. This segment of land is dotted with wetlands, including a sphagnum bog isolated near the center of the property (Martha's Vineyard Land Bank Commission, 2008).

CHAPTER 3

METHODS

Geographic and sea level data

The dynamic variables that influence the coastline of Martha's Vineyard have not been previously modeled or integrated. In this thesis, I examine a diverse array of natural mechanisms involved in coastal zones using state-of-the-art modeling software. The backbone of the geographic information data was obtained from MassGIS (the Commonwealth of Massachusetts Office of Geographic and Environmental Information) and the historical shoreline information was generously made available by the Massachusetts Coastal Zone Management (MA CZM).

To determine the sea level for Martha's Vineyard, data from the Permanent Service for Mean Sea Level (PSMSL) in the United Kingdom was compiled. This database contains monthly and annual mean sea levels from almost 2000 tide gauge stations around the world (PSMSL, 2006). Since 1933, the PSMSL has been responsible for the collection, publication, analysis, and interpretation of sea level data from the global network of tide gauges (PSMSL, 2006).

Classic statistics, geostatistics, and software

There are two main types of statistics used in this thesis: classic statistics and geostatistics. Classic statistical procedures were used to summarize and describe important characteristics of Martha's Vineyard and employed both univariate and multivariate approaches. Univariate statistical methods were employed to evaluate one attribute at a time. The statistical measures obtained by these methods included: mean, median, trimmed mean, range, standard deviation, variance, skewness, kurtosis, Anderson-Darling test for normality, and linear regression rates. Multivariate statistical methods were employed for the analysis of multiple attributes and variables at the same time. This approach is necessary in environmental studies because numerous variables typically interact with each other, often in unforeseen ways. The multivariate statistical methods used in this thesis include: multiple regression, Akaike Information Criterion (AIC), and Principal Component Analysis (PCA).

The geostatistical methods employed here treat geographic attributes as mathematical variables that depend on their positions on or above the earth's surface (Oliver *et al.*, 1989). Geostatistics assumes that all values in the study area are the result of a random processes with dependence (Johnston *et al.*, 2003). The goals of geostatistics are to uncover the dependency rules and to make predictions (Johnston *et al.*, 2003). Frequently within this thesis, geostatistical data was derived from digital data layers manipulated within *ESRI® ArcGIS® Desktop*, version 9.2, and exported into statistical packages such as *Minitab 15™* (Minitab, Inc.), *Microsoft® Office Excel®* 2007, or *Microsoft® Office Access*™ 2007. In other cases, geostatistics were performed within *ArcGIS®* v9.2 and no further analyses were done. Most often, data was continually transferred between the traditional software packages and *ESRI® ArcGIS®* in order to be analyzed. Processes unique to *ArcGIS®* included the dissection of features and attributes along transects, spatial autocorrelation, fractal dimension analysis, and geomorphological risk indexing of the MV shoreline.

To investigate the patterns of coastal erosion on Martha's Vineyard, classic statistics and geostatistics were used to analyze historic shorelines and erosion patterns, geology, surficial geology, soil components, slope of land, erodibility of the landscape, wetlands, land use, compass directions, wind, wave, and sea levels. Each of these processes is explained below. It should be noted that, in this thesis, the term "attribute" describes a sub-category within a major "variable." For example, a main *variable* is "Wetland" and some of its *attributes* include Barrier Beach, Coastal Beach, Rocky Intertidal Shore, Marsh, and Shrub Swamp. A major problem in this thesis is to convert class variables (such as wetland classes) into continuous variables (such as proportion of transect that is Marsh or Shrub Swamp, etc.).

Derivation of sea levels

Monthly and annual sea level means are reduced by the PSMSL to a common datum, called the Revised Local Reference (RLR). This datum is defined to be approximately 7000 mm (~23 ft) below mean sea level, a decision that was arbitrarily made many years ago (PSMSL, 2006). To work with the data in lower number values, I subtracted 7000 from each tidal gauge measurement, yielding values that ranged from -157 mm/yr (-6.81 in/yr) to 116 mm/yr (4.57 in/yr).

Using land-based data from the PSMSL, sea levels were obtained from 1932 to 2003 for Woods Hole (WH); 1965 to 2003 for Nantucket; 1955 to 1976 for Buzzards Bay (BB); and from 1955 to 1977 for the entrance to the Cape Cod Canal (CC). The Woods Hole Station (#960/165) is located in Falmouth, Massachusetts on the Woods Hole Oceanographic Institution property, latitude 41° 32' N and longitude -70° 40' W. The Nantucket station (#960/166) is located at latitude 41° 17' N and longitude -70° 06' W and has data from 1965 to 2006. The Buzzards Bay PSMSL station (#960/163) is located at latitude 41° 44' N and longitude -70° 37' W and was in operation for 22 years, from 1955 to 1976. The Cape Cod Canal Entrance PSMSL station (#960/168), located at latitude 41° 46’ N and longitude -70° 30’ W, was operational for 23 years (from 1955 to 1977).

The Glacial Isostatic Adjustments (GIA) process is often a significant factor in determining the rate of sea level change. Tide gauge data must be filtered so as to eliminate the GIA related bias from these estimates (Peltier, 2002). Using data from the Peltier Data Set (VM2), the rate of relative sea level rise in mm/yr for Woods Hole is 1.89 mm/yr (0.07 in/yr). Nantucket’s rate is 2.09 mm/yr (0.08 in/yr) and the mean value for the US east coast is 1.84 mm/yr (Peltier, 2002). This indicates that Woods Hole is subsiding by 0.7 mm/yr and that Nantucket is subsiding by 0.91 mm/yr. Based on these data, it is safe to assume that Martha’s Vineyard must be subsiding as well. While the GIA process is important, this is not a primary focus of this thesis, and therefore, for the remainder of this thesis, I used the land-based bench mark data from PSMSL (and NOAA) for mean sea level, rather than try to determine the difference between the effects of subsidence and eustatic sea level rise on Martha’s Vineyard. Either way, the sea is encroaching landward. More specifically, I used the sea level rise rate of 2.6 mm/yr for the NE and NW study sites because they are closer in proximity to Woods Hole waters. For the SS study site, I used 3 mm/yr sea level rise rate because it has a similar exposure as Nantucket. These numbers reflect sea level data through 2003, whereas the numbers reported from PSMSL/NOAA reflect sea level trends through 1999.

To estimate future sea level rise near Martha’s Vineyard in 25, 50, 75, and 100 years, I used four scenarios based upon both current measurements of SLR and the IPCC’s projections (Figure 28).

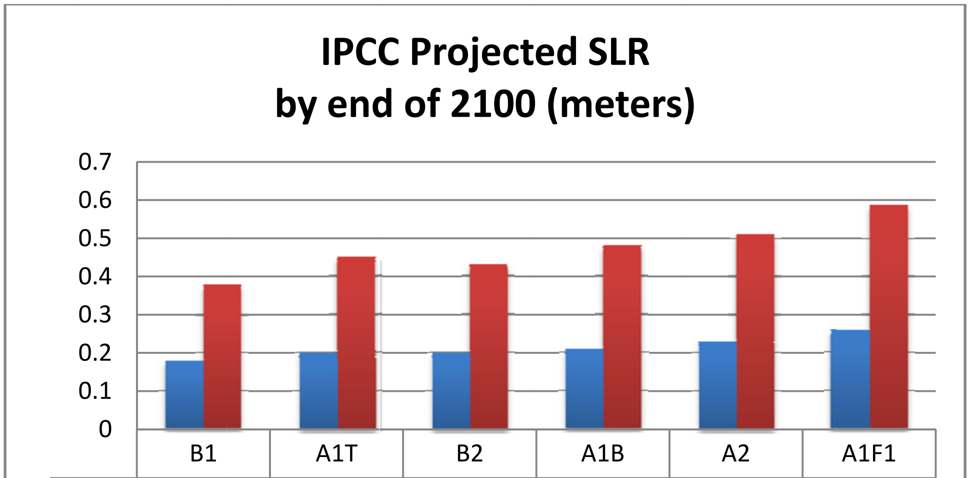

	B1	A1T	B2	A1B	A2	A1F1
Low	0.18	0.2	0.2	0.21	0.23	0.26
High	0.38	0.45	0.43	0.48	0.51	0.59

Figure 28. IPCC Projected SLR by end of 2100 in meters. High and low values are depicted by several different models (IPCC, 2007).

Identification of historic shoreline change

To identify historic shorelines on Martha's Vineyard, I used shoreline and transect data obtained from the Massachusetts Historic Shoreline Change Project (MA CZM, 2001), Massachusetts Geographic Information System (MassGIS, 2008), that was compiled by Thieler *et al.* (2001). Data that the authors used to identify shoreline change included: NOAA/NOS topographic maps, hydrographic maps, FEMA topographic maps, orthophotos, ground surveys, and aerial photos. The shorelines identified depict eight historic MV shorelines for 1845, 1846, 1888, 1897, 1955, 1978, 1979, and 1994. Generally, shorelines were delineated by using the high-tide wrack line. This is created when the high tide deposits seaweed and debris on the upper beach (MA CZM, 2001). Uniquely numbered transects were then cast by computer software (DSAS) at 40 m (131 ft) intervals (Thieler *et al.*, 2001).

Shoreline change maps were created by MA CZM at a scale of 1:10,000 and show the relative position of historic shorelines, including transects. Individual shoreline positions are generally accurate to within ±8.5 m (28 ft) (Thieler *et al.*, 2001). The rates of shoreline change, the focus of the project by Thieler *et al*., have a resolution of ± 0.12 m/yr (0.4 ft/year) (Thieler *et al.*, 2001). Transects generated by DSAS intersect with these historic shorelines, thereby generating data for shoreline movement and rate of change.

Mean shoreline change/year

To review historical shoreline changes for Martha's Vineyard, the mean shoreline change was calculated in meters/year for each transect and for each time period. The sum of the distance between each measured shoreline, along a transect, was determined and divided by the number of years during that period, resulting in the mean shoreline change. The value derived per transect gives the average overall change of shoreline position per year.

Shoreline rate of change/year (least squares linear regression)

To determine the rate of shoreline change, which differs from the mean change per year, linear regression was used by fitting a least squares regression line to all shoreline points for each transect. This method is viewed as the best available tool for computing long-term rates of shoreline change (Crowell & Leatherman, 1999; Leatherman *et al.*, 1998).

Linear regression was used to model the relationship between two variables using the formula:

$$y = \beta_0 + \beta_1 x + e$$

where y (distance of erosion) is the dependent or response variable and x (year) is the independent or predictor variable. β_0 is the intercept and β_1 is the slope, which measures the change in y per unit change in x. β_1 measures the strength of the relationship between y and x. The random variable, ε, is the error term in the model. The rate of shoreline change is determined by the measurement of the slope of the best fit, regression line.

For the purposes of this thesis, I determined that transects that had a rate of change value of < -0.5 m (~ -1.5 ft) were considered as eroding, > 0.5 m (~1.5 ft) were accreting, and the values between were considered to be stable. These assessments were based on the fact that shorelines typically move slightly every day and that the individual shoreline positions, provided by Thieler *et al*. (2001), are generally accurate to within ±8.5 m (28 ft).

Anderson-Darling test

For the SS, NE, and NW study sites, I converted the linear regression rate into a z-score, with $\mu = 0$ and $\sigma = 1$. This was done to test for a normal distribution of the site specific shoreline rate of change. Within *Minitab 15™*, I used the Calc function to standardize the observations. The mean is subtracted and then divided by the standard deviation. The purpose is to measure how far an observation lies from its mean, in units of standard deviation.

A standard normal distribution is described by two parameters, μ (mean) = 0 and σ (standard deviation) = 1. These values can be seen when the data to be analyzed is standardized to z-scores ($z = (x - \mu)/ \sigma$), which measure the distance the plot points fall from the mean, in units of standard deviation. The Anderson-Darling test statistic (A^2) is a measure of how far these plot points fall from the fitted line in a probability plot.

The A^2 test uses the actual observations, without grouping, and is sensitive to discrepancies at the tails of the distribution (Anderson & Darling, 1952, 1954), weighting the squared distance from the plot points to the fitted line, with larger weights in the tails of the distribution. The better the distribution fits the data, the smaller the A^2 statistic will be (Minitab 15™, 2006). The test statistic, A^2, does not indicate if the data is normally distributed. *Minitab 15*™ calculates the probability of each occurrence, for each observation, and uses the log of the calculated probabilities as the y-value (Minitab 15™, 2006). The assumed null hypothesis is that the data is normally distributed, but if the p-value is smaller than the chosen α, (for this study I used 0.05), then the null hypothesis can be rejected in favor of the alternate hypothesis, i.e., a conclusion that the data have a non-normal distribution (Minitab 15™, 2006).

Methods to test the Bruun model

Bruun's model predicts that beaches will erode by 50-100 times the rate of increase of sea level, a value much larger than that resulting from the coastline simply being inundated. For example, if the sea level rises by 3 mm /yr (0.12 in), then one might assume that the shoreline would move inland about 3 mm or 0.12 inches (assuming a 45° slope). This amount alone is not threatening. Over a 25 year period this would mean that the shoreline would change by 75 mm (3 in.), again not a substantial distance. However, according to the Bruun Rule, the shoreline would move inland by 3.75 m to 7.5 m (~12 ft to 25 ft) over a 25 year period, and this distance is considerably more significant.

Bruun's formula states that the elevation of the shore (*e*) and the depth of closure (*d*) are added together, then multiplied by shoreline recession/year (*x*) A model of the equilibrium profile is shown in Figure 29. This number equals sea level rise/year (*a*) times distance from the shoreline to the edge of the continental shelf (*b*):

$$x\ (e + d) = a\ b$$

Depth of closure (*d*) (DOC) is the seaward limit of significant profile change; it is the depth of water at which there is no appreciable movement of sediments by wave action. According to Bruun, the -18 m (-60 ft) contour line signifies the DOC, the difference between the "nearshore" and "deep-sea littoral drift phenomenon" (Bruun, 1962). [Other estimates for the DOC range from -5.5 m (18 ft) (Phillips & Williams, 2007), -7 m (23 ft) (Dalrymple, 1997), -8 m (26 ft) (Nicholls *et al.*, 1998), and -9 to 12 m (30-39 ft) near Long Island, New York (Kana, 1995)]. Application of these concepts implies that, in general, the short-term exchange of shore material (fluctuations of nature)

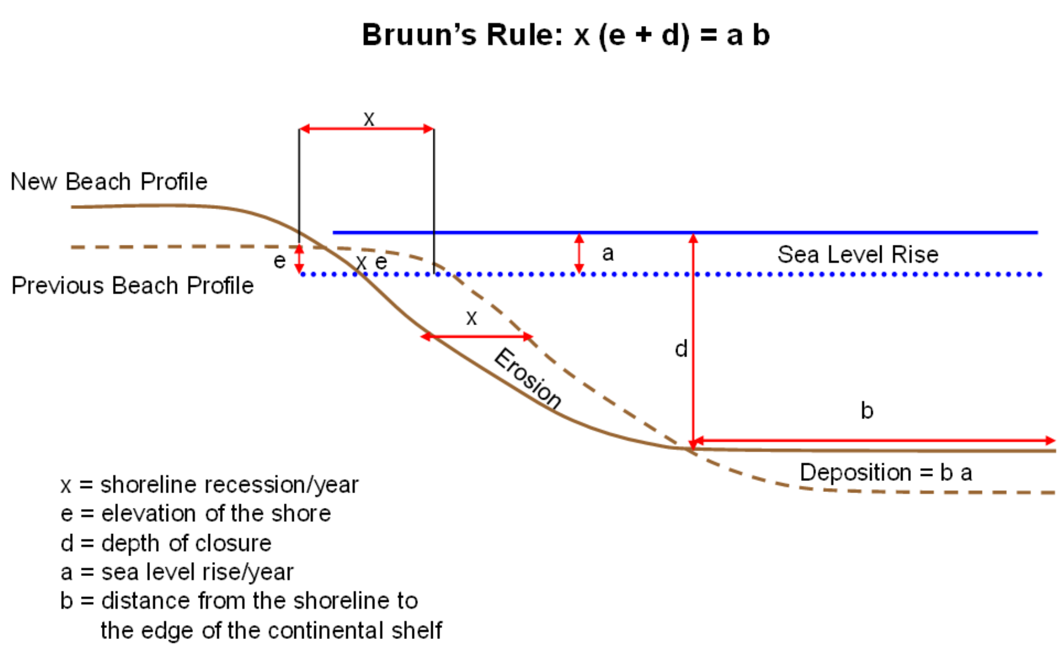

Figure 29. Diagram of Bruun's Rule depicting equilibrium profile.

and offshore bottom takes place up to the DOC, and usually not beyond (Bruun, 1962). Generally, the movement of sediment, from the shore to the offshore area, is a slow process, varying with the different types of currents (Bruun, 1962). Unlike the short-term effects, the long-range effects of sediment movement are related more to geological adjustment processes (Bruun, 1962). More importantly, the Bruun equation produces a ratio of x/a = 50 to 100, commonly referred to, or used, as a "rule of thumb" to estimate shoreline retreat due to sea level rise (Zhang *et al.*, 2004).

Bruun's model has been tested on seaward facing coastlines, but not on landward facing coastlines of islands. The distance from the shoreline to the edge of the continental shelf obviously does not apply to landward facing coastlines, such as the NE and NW study sites of Martha's Vineyard. Calculations for this thesis were determined by the x/a ratio for all sites, due to the geographical location of Martha's Vineyard. Moreover, for this thesis, I used the original model developed by Bruun that does not account for longshore drift and the 20 m contour line, provided by MassGIS.

The sea level rise for each site on MV and the shoreline recession rates (per year) from Thieler *et al*., (2001) were the primary data for calculating Bruun's Rule. Once the historical information was completed, I used Bruun's Rule to analyze the effects on the shoreline as sea levels continue to rise, based upon projections from the IPCC, Working Group I (2007).

To determine the DOC, I used ESRI® ArcGIS® v9.2 with GIS bathymetry and land data from MassGIS. I calculated the distance between the shoreline of MV and the 20 m contour line by overlaying the Massachusetts state outline on the bathymetry of the Gulf of Maine from December 1999. The bathymetry polygon represents seafloor topography all the way to the Continental Shelf. The contour lines are measured in meters below sea level, from -5, -10, -15, -20, -30, up to -4000 m.

Using the measurement tool in ArcGIS®, I took 10 measurements along the shoreline of each study site, and determined the mean distance to the 20 m contour line. To measure the distance from the southern shore of MV to the edge of the continental shelf, the same method was applied.

To determine the bathymetry slope, I converted the polygon into a raster, with a 100 m cell size, using ArcGIS®. Using *Spatial Analyst*®, the slope was calculated using degrees, again at a cell size of 100; therefore the output slope raster is in degree of slope. The Slope tool calculates the maximum rate of change between each cell and its neighbors and every cell in the output raster has a slope value. The lower the slope value, the flatter the terrain; the higher the slope value, the steeper the terrain (McCoy *et al.*, 2002).

Based on the four scenarios of sea level rise in Chapter 4, Results, I calculated the amount of shoreline lost at each study site. The formula I used to determine the amount of shoreline retreat is:

$$A = B(x*t)$$

A is shoreline retreat, B is the Bruun ratio determined from historical data from the previous analysis, x is the historical rate of erosion, and t is the time unit to be studied (i.e., 25, 50, 75, and 100 years), or simply put *Coastal Retreat = Ratio*(SLR * time unit).*

Assuming that wave action remains the same, there are no major alterations to the study site shorelines, and that the rate of sea level remained constant during the next 100 years, I calculated how much shoreline would be lost to maintain an equilibrium profile.

In order to project future shoreline retreat through 2100, I incorporated the new ratio, based upon the results derived from the three study sites on Martha's Vineyard. Three scenarios were considered for the 100 year period based upon SLR projections in Results**.** Scenario 1 assumes a linear trend of SLR near MV at 0.003 m/yr on the south side and 0.0026 on the NE and NW sides. The second scenario combines two models based upon the expectations that sea levels will rise exponentially near MV, and the IPCC projections. Scenario 2 begins at 0.003 m/yr, rather than 0.18 m/yr, and ends at 0.59 m/yr. Scenario 3 considers an exponential growth of SLR based upon the IPCC projections. For simplicity, all shoreline retreat projections are based upon a SLR base line of 0.003 m/yr for all three Martha's Vineyard study sites.

Area of land lost or gained

To determine the amount of land that was lost or gained during all four time periods, the changes in each time period were totaled to determine the sum of the meters changed, $\sum x_i$, and divided by the total number of transects, *T,* (487), resulting in the average distance changed, $\bar{x}$. This was multiplied by the total length (*d*) of the study area (determined from ArcGIS®) to determine the amount of area, *A*, either lost or gained, as shown below:

$$\left(\frac{\sum x_i}{T}\right) = \bar{x}$$

$$\bar{x} * d = A$$

Soil taxonomy, texture, ternary diagram, and hydrologic groups

The taxonomic classification of soils found on MV were obtained from three key sources: 1) the NEsoil.com website, an invaluable source of soil information for New England (Turenne, 2007) that draws heavily on Fletcher and Roffinoli's *Soil Survey of*

Dukes County Massachusetts (Fletcher & Roffinoli, 1986), 2) the MassGIS (2008), and 3) the USDA/NRCS website (*Soil Data Mart for Dukes County Massachusetts)*(USDA, 2007b). The latter database includes the U.S. General Soil Map (STATSGO) (Soil Survey Staff, 2007) and is the national SSURGO Template Database for Microsoft® Access™ 2002/2003 format (USDA, 2007b, c).

Developed by the National Cooperative Soil Survey, the digital soil dataset from the *Soil Data Mart* provides an inventory of soils and nonsoil areas that normally occur in a repeatable pattern on the landscape (USDA, 2007c). The primary reports that were used in this thesis included: Engineering Properties; Physical Soil Properties; Revised Universal Soil Loss Equation (RUSLE2) Related Attributes; Water Features; and Map Unit Names.

Descriptions of the taxonomic classifications were obtained from the 1999, second edition, *Soil Taxonomy: A Basic System of Soil Classification for Making and Interpreting Soil Survey* (Soil Survey Staff, 1999); from the tenth edition of *Keys to Soil Taxonomy* (Soil Survey Staff, 2006); and again from the *Soil Survey Data for New England States* (Turenne, 2007) and *Soil Survey of Dukes County, Massachusetts* (Fletcher & Roffinoli, 1986).

"Texture" is given in the standard terms used by the U.S. Department of Agriculture (USDA, 2007b). These terms are defined according to percentages of sand, silt, and clay in the fraction of the soil that is less than 2 mm in diameter (USDA, 2007b). "Loam," for example, is soil that is 7 to 27 percent clay, 28 to 50 percent silt, and less than 52 percent sand (USDA, 2007b). If the content of particles coarser than sand is 15 percent or more, an appropriate modifier is added, for example, "gravelly" (USDA, 2007b).

Based upon the percentage of sand, silt, and clay, Shepard (1954) divided a ternary diagram into these three main classes. The USDA's modified version of this diagram includes the following 12 categories: clay, silty clay, silty clay loam, silt loam, silt, loam, sandy loam, loamy sand, sand, sandy clay loam, sandy clay, and clay loam (USDA, 2007a). For Martha's Vineyard, I used the *RUSLE2 Related Attribute* report, generated by the *Soil Data Mart* (USDA, 2007b), to determine the representative percentage value of sand, silt, and clay. This information was then applied to a ternary diagram in the same manner as Shepard's and the USDA's. The attributes within this report include soil property data for each map unit component including hydrologic soil group, and erosion factors for the surface horizon. The silt and clay components were not used in the multivariate statistical analysis because the original focus was on sandy beaches. Therefore, only the percentage of sand for each soil type was analyzed.

The runoff potentials based on Hydrologic Groups were obtained from the *Soil Data Mart* (USDA, 2007a). The soils in the U.S. are placed into four groups, A, B, C, and D, and three dual classes, A/D, B/D, and C/D. These soil types are described in the Literature Review (Chapter 1). This information was not used in the multivariate statistical analysis, and is presented for informational purposes only.

Geophysical characteristics of the transects

To determine specific geophysical characteristics, I limited each study site to the area within 800 m (0.5 miles) of the coastline. Based on this criterion, the study site was buffered by clipping the GIS data for Dukes County, MA, mostly obtained from

MassGIS, unless otherwise noted below. This method was used to identify the type of geology, surficial geology, soil and percent of sand, slope, highly erodible land, wetland, land use, compass direction, wind, and waves. These characteristics were intersected with each transect in order to specifically determine the percentage of attributes located along each transect, for all study sites. A brief description of each GIS feature and attribute, followed by general methods for analysis, follows below. For some non-routine features that have not been considered previously as factors in coastal erosion I have provided a more detailed description of the process.

Distinction between geology, surficial geology, and soils. For the purpose of this thesis, geology refers to the glacial material overlaying the bedrock that makes up the foundation of Martha's Vineyard and which includes the following: Martha's Vineyard and Gay Head moraine deposits; Martha's Vineyard outwash deposits; and a combination of these materials. Surficial geology refers to the surface layers on top of this geologic material, including end moraines, till, and sand deposits. Soils are considered surficial geology, as well, and have been classified separately.

Geology. Geology refers to the moraine deposits, moraine outwash, and beach deposits. The geospatial vector digital data layers, published and distributed by the USGS, represent the geologic map of Cape Cod and the Islands (Cross, 2004). The source map, from Oldale and Barlow (1986), is called the "Geologic Map of Cape Cod and the Islands, Massachusetts."

Surficial geology. The surficial geology data layer, provided by MassGIS in 1999, shows the location of sand and gravel deposits, end moraines, and floodplain alluviums at 1:125,000 scale. MassGIS uses the surficial geology data only to produce volume or area measurements over a large region, and it is not accurate for site specific analysis (MassGIS, 2008).

Soils. The soil data (Soil Survey Geographic [SSURGO]) data base is published by the U.S. Department of Agriculture (USDA), Natural Resource Conservation Service (NRCS). The data set consists of georeferenced digital map data and computerized attribute data, compiled from 2001 to 2005. The inventory consists of soils and nonsoil areas that normally occur in a repeatable pattern on the landscape and that can be cartographically shown at the scale mapped (USDA, 2007c). There are 60 classifications of soil on Martha's Vineyard, including the miscellaneous categories: beaches, urban land, pits, sand and gravel, and three types of water: water, water ocean, and water saline. To reduce the number of variables, the remaining 54 soil classifications were condensed into 18, by major soil type.

Percent of sand, silt, clay, and hydrologic group. The percentage of sand, silt, and clay in the surface horizon, as well as the hydrologic soil group is published by the USDA Soil Data Mart. This report is summarized according to The Revised Universal Soil Loss Equation Version 2 (RUSLE2) (Soil Survey Staff, 2007).

Slope. Slope is the inclination of the surface of the soil, measured between two points and is expressed as a percentage of the distance between those two points (Soil Survey Staff, 2007). Slope is delineated according the six categories: *0-3%; 3-8%; 8-15%; 15-25%; 25-35%;* and *no slope* which includes water and/or urban land.

HEL water. This classification is based on an evaluation of water erosion hazard of the components within the map unit and is distributed in the Soil Survey Geographic (SSURGO) database (USDA, 2007c). If all components of a single class apply, then that unit is assigned the appropriate category, such as *Highly Erodible Land* or *Not Highly Erodible Land*. If there are multiple classes within a soil map unit, then *Potentially Highly Erodible* was assigned. All these classifications were obtained from the USDA and NRCS (Soil Survey Staff, 2007), except for the *Erodible Land* category, which I added for the beach classification. The justification was that beaches do erode. If no class was assigned by the USDA, except for beaches, I labeled it *Not Applicable*.

WETLAND - CONDENSED	WETLAND - ORIGINAL
BARRIER BEACH	BARRIER BEACH - COASTAL BEACH BARRIER BEACH SYSTEM
BARRIER BEACH - COASTAL DUNE	BARRIER BEACH - COASTAL DUNE
COASTAL BANK BLUFF OR SEA CLIFF	COASTAL BANK BLUFF OR SEA CLIFF
COASTAL BEACH	COASTAL BEACH
COASTAL DUNE	COASTAL DUNE
ROCKY INTERTIDAL SHORE	ROCKY INTERTIDAL SHORE
SALT MARSH	SHALLOW MARSH, MEADOW, OR FEN DEEP MARSH BARRIER BEACH - MARSH BARRIER BEACH - SALT MARSH
TIDAL FLATS	TIDAL FLATS
SHRUB SWAMP	SHRUB SWAMP WOOD SWAMP BARRIER BEACH - SHRUB SWAMP BARRIER BEACH - WOODED SWAMP CONIFEROUS BARRIER BEACH - WOODED SWAMP DECIDUOUS BARRIER BEACH 0 WOODED SWAMP MIXED TREES WOODED SWAMP DECIDUOUS WOODED SWAMP MIXED TREES BOG CRANBERRY BOG
OPEN WATER	OPEN WATER BARRIER BEACH - OPEN WATER

Table 4. Condensed wetland codes used for MV classification.

Wetland. The DEP Wetlands datalayer is distributed by MassGIS at a scale of 1:12,000 (MassGIS, 2008). The layer for MV includes 24 wetland codes, which I consolidated into 10 in order to minimize the variables under study (Table 4).

Land Use. The land use datalayer (LUS) is classified into 21 categories, interpreted from 1:25,000 aerial photography by MassGIS (MassGIS, 2008). These categories were reduced to five main types of land use: beach, developed land, salt marsh, upland, and water (Table 5).

LUS - CONDENSED	LUS - ORIGINAL
BEACH	WATER BASED RECREATION
DEVELOPED LAND	MEDIUM DENSITY RESIDENTIAL
	HIGH DENSITY RESIDENTIAL
	MULTI-FAMILY RESIDENTIAL
	COMMERCIAL
	INDUSTRIAL
	TRANSPORTATION
	WASTE DISPOSAL
SALT MARSH	WETLAND
	SALT MARSH
UPLAND	CROPLAND
	PASTURE
	FOREST
	OPEN LAND
	PARTICIPATION RECREATION
	LOW DENSITY RESIDENTIAL
	URBAN OPEN
	WOODY PERENNIAL
WATER	WATER

Table 5. Condensed land use classifications.

Compass direction. To identify the compass direction (general mean) for the transect lines at each study site, I used the *Linear Directional Mean* tool in ESRI® ArcGIS® v9.2. This tool calculates the trend of line features by measuring the average angle by direction or orientation and creates a new feature class. Attributes that are created include: *Compass Angle* (clockwise from due North); (counterclockwise from due East); *Circular Variance* (an indication of how much directions or orientations deviate from directional mean); *Mean Center X and Y Coordinates*; and *Mean Length* (ESRI®, 2006). Based on the results from *Compass Angle*, I categorized the transects according to compass direction (**see Appendix B**).

Wind and waves. Wind and wave information was consolidated from the Coastal Hydraulics Laboratory, Wave Information Studies (WIS), WIS Model #074, longitude -71.00024, latitude 41.24976, located southwest of Aquinnah (Figure 30). Data from this WIS model was collected every hour for nineteen years, from 1980-1999, for a total of 175,294 occurrences (see the Appendix A (Appendix 1 - Appendix 4) for details by month and direction).

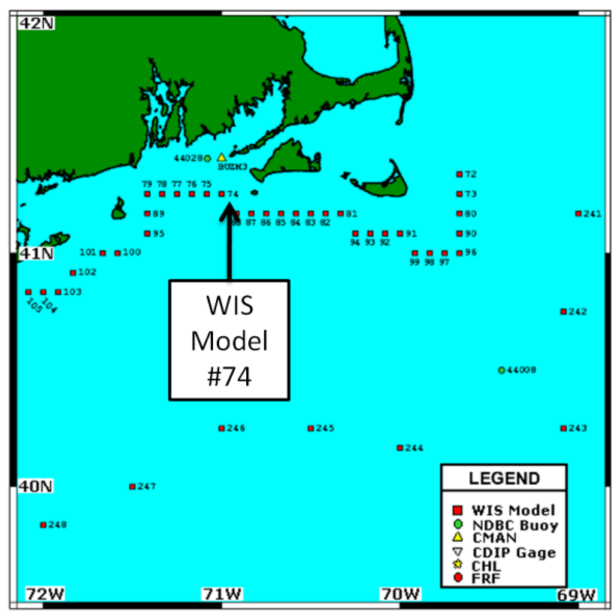

Figure 30. Location of WIS Model #74 off the shores of Martha's Vineyard.

The percentages of compass direction for winter and summer wind and waves were derived based upon 12 months. The wind speed, in meters/second, reflects the percentage of time that it blows from that compass direction. The winter months range from October through March and the summer months range from April through September. For example, the winter wind months were analyzed as follows. To normalize the data, I totaled the *winter percent direction* and then divided each direction by its sum. I multiplied the *mean winter wind speed* times the *normalized winter percent of direction* in order to weight the length of time the wind came from a certain direction and at specific speeds. Rather than work with small fractions, I multiplied this number by 100. A similar process was used for summer wind.

For winter and summer wave conditions, the methods involved determining the *percent of direction* and for each month, then determining the mean per quarter, then per season.

Intersection of transects and attributes

"Intersect" is a method in ArcGIS® that computes a geometric intersection between two or more features which overlap one another. The output feature class contains a portion of the features that are common to all. In this study, every major feature was "intersected" with a transect for that particular study site. The primary features that were intersected with the transects were: geology, surficial geology, soil and percent of sand, slope, highly erodible land, wetland, land use, compass direction, wind, and waves.

To ascertain the part of the transect that intersected with each of the attributes, *ESRI® ArcGIS®* v9.2, *Microsoft® Office Excel®* 2007, *Microsoft® Office Access*™ 2007, and *Minitab 15™* were used as follows:

1. Within *ESRI® ArcGIS®* v9.2, the toolbox option was chosen and the *Analysis Tools*, *Overlay*, and *Intersect* option was selected.
    a. The *Input Features* consists of the transects for the study site and one of the main features mentioned previously.
    b. The *Output Feature Class* creates a shape file for the new intersected features.
    c. All the attributes were joined and no specific *XY Tolerance* was selected. The *Output Type* chosen was *Line*.

d. The new feature class is added to the project.

2. Within the toolbox again, select *Conversion*, then *Coverage*, and *Feature Class* to *Coverage*. This method creates a single ArcInfo coverage from the input feature class.

    a. The *Input Feature Class* is the new feature that was just intersected in #1d.

    b. Output Coverage is the designated name of the new coverage file.

    c. No *XY Tolerance* was chosen and the *Double Precision* box checked. This is the default option.

    d. A new coverage file is created in the designated folder in #2b.

3. Add the coverage file to the data layers in the project. This is not done automatically.

4. Repeat the method described in #1; this time the intersecting features include the coverage layer from #1d and #2d. A new shape file is created and added to the project.

5. Right click the new #4 shape file, open attribute table to confirm that the intersect occurred. Click *Options* and the *Export* the database file to a designated folder, giving it an appropriate name (ex. *MV_Results*). Add the table to the current map. Close attribute table.

6. Open the *MV_Results* folder and open the new coverage file table (.dbf) and save it as a *Microsoft® Office Excel™ 2007* file (.xlsx).

7. Open *Microsoft® Office Access™ 2007* and create a new database.

    a. On the toolbar, chose *External Data* tab and *Excel®*.

        - Specify the location of the new *Excel®* file created in #6 and *Import the source data into a new table in the current database*. Assign an appropriate name to the new *Access™* file.

        - Under *Tables*, click on the new file that was imported.

    b. On the toolbar, chose *Create* tab.

        - Then under *Other*, click *Query Wizard*, and *Crosstab Query Wizard*.

- Select the table of choice (view Table)

- In the *Available Fields*, select the *transect number* attribute. Continue to add fields that are to be sorted. In this case, the feature descriptions were selected, then the *Field* to be calculated was the *Length* of the transect, and function is *Sum.*

- Name the query, view the results, and *save*.

c. A new file exists in the *Access*™ database displays the calculated length of each attribute within the feature class by transect. For example, the SS Geology transect number, 20007, is 293.78 m long: 145.98 m consists of beach deposits and 147.80 m consists of Martha's Vineyard moraine outwash.

d. Export the #7b results into *Excel*®, then copy and paste the file into *Minitab 15*™ to begin statistical analyses.

Linear, quadratic, cubic, and multiple regression

A linear regression analysis was performed on every attribute within each variable for the purpose of investigating the relationship between the response variable (historical rate of shoreline change - LR) and the predictor variable (the percentage of a transect that intersects with the attribute). The goal was to determine how the historical linear regression rates of change vary based upon the multitudinous attributes for each study site. To analyze the relationship between all the predictor attributes within each variable, multiple linear regression analysis was performed. The main purpose was to explain a proportion of the variance in the shoreline change rate, based upon its response to each attribute. Some attributes within the variables did not resemble a linear response. Therefore, quadratic and cubic models were used depending upon the fit of the line.

The α-level used throughout this analysis is 0.05. For this section, the adjusted R^2 is reported, even though it is more conservative than R^2, because it adjusts for the number of explanatory terms in the model, the degrees of freedom.

Standard statistical methods were applied to the results from the previous method to determine the percentage of specific attributes located on the transects. By determining the percentage for each attribute and feature, the data is normalized for each transect. Statistical analyses were completed in *Minitab 15™* for 161 attributes distributed as follows: 53 for the SS site, 60 for the NE site, and 48 for the NW site.

For each of these attributes, ordinary least squares (OLS) linear regression was performed. In OLS linear regression, the dependent response (Y) variable was the linear regression rate derived from Thieler *et al*., (2001) based upon historical shoreline movement. The independent predictor (X) variable was the attribute within each feature, determined by the percentage on each transect.

With some attributes, the data did not resemble a linear response, thus quadratic and cubic models were tested to reflect the trend in the data, as needed. Whereas, linear models show a steady rate of increase or decrease, a quadratic model accounts for a single curve in the data, and a cubic model describes two curves and a valley. The quadratic equation is: $Y = \beta_o + \beta_1 x + \beta_2 x^2 + \varepsilon$; and the cubic equation is: $Y = \beta_o + \beta_1 x + \beta_2 x^2 + \beta_3 x^3 + \varepsilon$. A listing of each of these attributes was assembled for each corresponding variable, which indicated the rate of erosion, the corresponding p-values, the adjusted R^2 values, and linear regression rate of shoreline change.

To learn more about the relationship between the predictor attributes within each feature, multiple regression analysis was performed. This was done to in order to explain a larger proportion of the variance in the dependent variable (shoreline change rate), at a significant R^2 level.

When multiple regression analysis was done on a feature with many attributes that consisted of polynomials, the variance inflation factors (VIF) were elevated, indicating multicollinearity. It should be noted that within a feature, the attributes are independent of each other; therefore in theory there is no multicollinearity, only induced correlations. When this occurs, the induced correlations make it appear as if there is a lot of uncertainty in the individual coefficients, but this does not translate into a lot of uncertainty in the estimates of the points on a regression line (Buonaccorsi, 2008). Because I created an induced collinearity situation within some features, I chose to ignore the elevated VIF's. However, this was not done when multiple regression models were run for different features.

Transect means/attribute (> 25%)

Using results from the above method, *Intersection of Transects and Attributes*, generated with Microsoft® Office Access™, I was able to identify which transects encompassed more than 25% of a particular attribute. This data was moved into *Microsoft® Office Excel*™ and every attribute that met this criterion was highlighted with a single color, and then sorted by transect number. By visually scanning the data for highlighted attributes, the intent was to identify a pattern of erosion (≤ -0.5 m/yr), equilibrium (-0.5 to 0.5 m/yr), or accretion (≥ 0.5 m/yr). The logic was to determine if any of these attributes always gave rise to accretion, for example.

As a second method, all the transects for each study site were divided into three categories, erosion, equilibrium, and accretion, based upon their linear regression results, and I calculated the percentage mean for each of these attributes. If the mean for that particular attribute was greater than 25%, then they were listed in a summary table to see if any pattern arose. The summary data does not include the following attributes: *Average Percent of Sand; Average Slope*; and *Winter and Summer Wind and Wave* data. While a summary did prove useful, it still didn't adequately explain shoreline change patterns.

Akaike Information Criterion (AIC)

Another method widely used to evaluate the "best" model is Akaike Information Criterion (AIC). This method measures the goodness of fit of an estimated statistical model. The "best" model is the one with the smallest ranked AIC score, which most likely influences shoreline erosion patterns on Martha's Vineyard.

In 1974, Hirotsugu Akaike introduced "a new estimate minimum information theoretical criterion (AIC) estimate which is designed for the purpose of statistical identification" (Akaike, 1974). This model measures the goodness of fit of an estimated statistical model and is defined as:

$$A = (-2)log_e\,(\ell(\hat{\theta}|data) + 2K$$

where the natural log, $log_e(\ell(\hat{\theta}|data)$, is the value of the maximize log-likelihood over the unknown parameters (θ), given the data and the model, and K is the number of parameters estimated in that approximating model (Anderson *et al.*, 2000). When using least squares models, the AIC is calculated in the following way:

$$AIC = n * log_e(\hat{\sigma}^2) + 2K$$

where n is sample size and $(\hat{\sigma}^2) = RSS/n$ (Anderson *et al.*, 2000). The residual sum of squares (RSS) is known after performing regression analysis of the model. The Akaike weights are the relative likelihood of the model, given the data. These are normalized to sum to 1, and are interpreted as probabilities (Burnham & Anderson, 1998).

I used AIC in three different ways for each study site to rank models by the following: 1) using the ten major variables (*Geology, Surficial Geology, Soil, Average % of Sand, Slope, Erodible Land, Wetland, Land Use, Compass Direction, and Winter Wind and Winter Waves*) based upon multiple regression results; 2) the individual attributes that had more than 25% of the attribute along the transect; and 3) combinations of attributes. The actual formula used in *Minitab 15*™ to calculate AIC is:

*'Number of Data Points' * LOGE(('Regression Sum of Squares (SSE)'/ 'Number of Data Points'))+(2 * K)*

where the "*Number of Data Points*" in this thesis is 487, based on the number of transects within the study site, "*LOGE*" calculates the natural logarithms to the base *e,* "*Regression Sum of Squares*" is the ANOVA residual error, and "*K*" is the number of parameters, plus 1. Table 6 provides the formulas I used within *Minitab 15*™ to calculate the AIC. Everything in italics is the actual formula; otherwise, the information was manually provided as a result of multiple regression for each featured variable. While I calculated the *corrected AIC,* this was not used in the thesis because it is typically used for small samples (<40) (Burnham & Anderson, 1998).

Model	Feature Variables
p-value	Multiple Regression p-value
R^2 adjusted	Multiple Regression R^2 adjusted
Number of Data Points	Number of Data Points (487 is number of transects/study site)
Number of Parameters Fitted	*'Number of Parameters Fitted'* (df + 1 (constant))
K	*# of Parameters + 1*
Regression Sum of Squares (SSE)	Regression SSE (ANOVA Residual Error)
AIC	*'Number of Data Points' * LOGE(('Regression Sum of Squares (SSE)' / 'Number of Data Points'))+(2 * K)*
AIC Corrected	*AIC + ((2*K * (K + 1)))/('Number of Data Points' - K-1)*
Rank	*RANK(AIC)*
Delta	*AIC-MIN(AIC)*
exp(-delta/2)	*EXP(-Delta / 2)*
Akaike Weights	*'exp(-delta/2)' / 'Weight Sum'*
Weight Sum	*SUM('exp(-delta/2)')*

Table 6. Formulas used to calculate the AIC.

It should be noted that by combining various attributes within each study site, it quickly became apparent that the probability of finding the right combination was low because the SS site had 52 attributes, the NE had 58 attributes, and the NW had 46 attributes. Attributes included in this count that were not included in the section Transect Means/Attribute >25%, are the following: *Average Percent of Sand, Average Percent of Slope, Winter Wind,* and *Winter Waves*. Linear regression results for *Summer Wind and Summer Waves* were not significant for any of the three study sites and this attribute was therefore eliminated from this study.

While the AIC method was used, it became a minor component of the overall analysis; therefore an extensive review of AIC methods is beyond the scope of this thesis. For a more thorough understanding of AIC, consult Burnham and Anderson's (1998) book called "Model selection and inference: a practical information-theoretic approach" and/or the journal article by Anderson, Burnham, and Thompson (2000), called "Null Hypothesis Testing: Problems, Prevalence, and an Alternative" in the Journal of Wildlife Management.

Spatial autocorrelation (Moran's I Index and Z-score)

In geography, on average, values of variables that are closer to one another tend to be more similar than those that are farther away (Tobler, 1970). Geostatistics assumes that all values of the variables in the study area are the result of random processes with dependence (Johnston *et al.*, 2003). This dependence relationship is known as spatial autocorrelation, a measure of spatial dependence between values of random variables over geographic locations. Positive spatial autocorrelation has similar values together, while negative spatial autocorrelation has dissimilar values appearing in close proximity.

As a beginning step in evaluating coastal erosion, it is important to determine whether there are any spatial patterns within the study site. The results determine whether there is a positive or negative spatially autocorrelated pattern. If there is no spatial clustering of erosion, then the null hypothesis can be rejected. Moran's I Index is based upon neighborhood similarities or dissimilarities.

Moran's I Index is a method to calculate the significance of clustering with the values of the variables (Moran, 1948). It measures the spatial autocorrelation (similarities) of these variables by spatial location and feature values. A Moran's Index value of +1 indicates spatial autocorrelation (clustering). The reverse is true for a Moran's Index of -1, which indicates negative spatial autocorrelation (dispersion). A zero (0) indicates no spatial autocorrelation (random) (Johnston *et al.*, 2003).

Z-scores are a measurement of distance between an observation and the mean, measured in units of standard deviation (e.g., ±2.5, ±1.96) (Mendenhall *et al.*, 2003). The z-score is calculated as follows: z-score = $(x-\bar{x})/s$. When using a 95% confidence interval, a z-score between ±1.96 indicates that the null hypothesis cannot be rejected because the pattern exhibited could be one of random chance (Johnston *et al.*, 2003). Very high or very low z-scores (±2.5) are found in the tails of the normal distribution, indicating that the probability is very unlikely to be a random spatial pattern. If the z-score falls outside the range ±2.5, then the pattern is probably too unusual to be considered a version of random chance and the alternative hypothesis can be accepted (Johnston *et al.*, 2003).

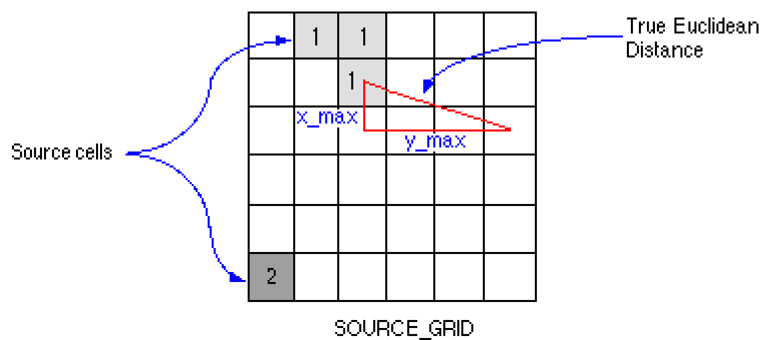

Figure 31. Calculation of the average distance using spatial statistics.

By using spatial statistics in ArcGIS® v9.2, I calculated the average distance band from neighbors, using Euclidean measurements (think of it "as the crow flies") (ESRI®, 2006). This distance is calculated to each source cell by calculating the hypotenuse, with the x-max and y-max as the other two legs of the triangle (Figure 31). First, ArcGIS® internally converts the feature class into a raster, then calculations are derived by using the center of the cell to measure the distance to other center of cells.

To determine if there were any patterns within the study sites, two calculations were done to evaluate neighboring transects for each study site. The first test performed included five neighbors and the second included 400 neighbors. An expectation would be, based on regional variable theory, that it would be highly likely that five neighbors would be more spatially autocorrelated than 400. By testing both extremes, I should get a more accurate depiction of spatial autocorrelation for each study site.

Once the average distance in meters for 5 and 400 neighbors was calculated, the spatial pattern was analyzed with Moran's I Index, using ArcGIS® v9.2. The toolbox in "Spatial Statistical Tools" is called "Analyzing Patterns." The input feature class is the transect layers containing the linear regression shoreline rate of change. Inverse distance was chosen as the conceptualization of spatial relationships because the impact of one feature on another decreases with distance. Again, the measurement method used was Euclidean distance, no spatial weights were applied, and the threshold distances that were used were derived from calculating average neighborhood distance bands.

Inverse distance weighting and kriging

Kriging is a geostatistical technique, based on statistical models that include autocorrelation (statistical relationships among the measured points that are positively related), used to interpolate and create surfaces from measured points (Johnston *et al.*, 2003). As noted earlier, in geography, on average, places close to one another tend to be more similar in value than those farther apart. The value of kriging is the ability to estimate and predict environmental values in between sampled points because it is unreasonable to measure every location in the environment. The use of geostatistics enables scientists to study the continuity of the environment. Interpretation of the predictions between sampled data points facilitates the management of the study area.

Regionalized variable theory describes spatial variation in phenomena over the earth's surface (Matheron, 1971; Oliver *et al.*, 1989). This theory provides quantitative tools for estimation and interpolation of surfaces that are unknown (Oliver *et al.*, 1989). Kriging is a statistical tool based on this theory. Regionalized variable theory assumes that the spatial variation in the phenomenon represented by the z-values is statistically homogeneous throughout the surface (Johnston *et al.*, 2003). This pattern of spatial homogeneity, the same pattern of variation observed at all locations on the surface, is fundamental to regionalized variable theory (Johnston *et al.*, 2003).

Ordinary kriging assumes the following model:

$$Z(x) = \mu + \varepsilon(x)$$

where x = (X,Y) is a location, and the value of $Z(x)$ is the value of that location, μ is constant mean for the data (no trend), and $\varepsilon(x)$ is a random component drawn from a distribution with mean zero and a covariance function (autocorrelated errors) (Johnston *et al.*, 2003; Webster & Oliver, 2001). Ordinary kriging uses a local average of the scatter points in the kriging subset for a particular interpolation point.

Kriging is divided into two distinct tasks: 1) quantifying the spatial structure (variography) of the data and 2) producing a prediction of the surface area between points (Johnston *et al.*, 2003). In spatial modeling of the structure of the measured points the initial step is the generation of a graph of the empirical semivariogram, computed as:

$$\textit{Semivariogram (distance H)} = 0.5 * \textit{average} \, [Z(x_i) - Z(x_j)]^2$$

for all pairs of locations separated by distance h (half of the distance squared) (Johnston *et al.*, 2003). This procedure calculates the difference squared between the values of the paired locations within a dataset and plots them as a function of the distance between two locations (Johnston *et al.*, 2003; Webster & Oliver, 2001).

Instead of plotting each pair, the pairs are grouped into lag bins based on their common distance from one another (Johnston *et al.*, 2003). Each bin (a specified range of distances) contains the squared differences from the values for all pairs of locations that are linked, and these are then averaged and multiplied by 0.5, resulting in one empirical semivariogram value per bin (Johnston *et al.*, 2003). To determine the lag size, a useful starting point is to use the average separation between nearest neighbors as the interval (Johnston *et al.*, 2003). Another method that is considered "a rule of thumb" is to multiply the lag size by the number of lags (or bins), which should be about "half the largest distance among all points" (Johnston *et al.*, 2003).

In this study, the autocorrelation between linear regression rates of erosion at each transect against the function of distance were examined. As in geography, as the distances between each transect increases, autocorrelation should decrease. The measured location data is weighted more heavily at closer intervals, than those farther away. The null hypothesis, however, is that there would be no correlation between transects with distance, because all linear regression rates at each transect are assumed to be independent.

Using ESRI® ArcGIS® v9.2, variograms and covariance graphs were generated for each study site by estimating autocorrelation values for linear regression rates at each transect. From this, predictions of the unknown values were generated. The variogram is considered "the cornerstone of practical geostatistics" (Webster & Oliver, 2001) and, therefore, was a primary method for study.

Fractal dimension analysis

Fractal dimension analysis was used to analyze the patterns in shoreline changes at each study site, not the actual shoreline. Fractal dimensions are used in geomorphology primarily as a means of descriptive parameterization of patterns and landscape topography (Baas, 2002). The historical linear regression rates for each transect were used as a means to identify whether shoreline changes were gradually changing over a significantly long time frame, or whether the stresses of rising seas is causing the shorelines to change more rapidly

An isotropic spherical ordinary kriging model was used, with No Transformation and No Trend of the data selected for all three study sites. The neighborhood search consisted of five neighbors, with a minimum of two, with the neighborhood divided into four sectors and a 45° offset, ensuring to get values from all directions. The number of lags was 10 and the lag size was 100 for the SS and NE sites. A lag size of 300 was used for the NW study site. These parameters were chosen for the 487 samples because this configuration resulted in the lowest root-mean-square and average standard error, compared to multiple experiments resulting in higher numbers (data not shown).

Fractal dimension calculations were derived from the following formula (Burrough, 2002; Phillips, 1986):

$$d = (4-m)/2$$

where m is the slope of the semivariogram and d is the fractal dimension.

Principal component analysis (PCA)

Univariate statistics is a powerful and useful tool when investigating one attribute. However, when analyzing coastal erosion, multivariate statistics becomes necessary to uncover patterns in data of high dimension. Unlike multiple regression, PCA transforms correlated attributes into a smaller number of uncorrelated variables, thereby reducing a complex data set to a lower dimension in order to possibly reveal the underlying phenomenon. PCA seeks a linear combination of variables such that the maximum variance is explained with the fewest number of principal components.

By using PCA, multicollinearity in regression is avoided. Multicollinearity was even more pronounced when certain features were combined with each other because many of the features are related at some level. For example, the compass direction of wind and waves, and the compass direction of the transects are very similar, as is soil composition and percentage of sand, or slope, or erodible land characteristics. Because of very high multicollinearity, I had to abandon the idea of using multiple regression across numerous correlated features. Therefore, PCA is an excellent tool in this situation because, "in theory, there is no redundancy in the principal components; they are completely independent and complementary" (McGarigal *et al.*, 2000).

I used the correlation matrix to calculate the principal components because the component analysis gives equal weight to all the variables. A correlation matrix describes correlation among the variables. This is important because, in this study, it is not clear which variable should be weighed more heavily than the other.

An advantage to using the correlation matrix is that it provides the Pearson correlation coefficient for the relationships, typically denoted by *r*, when calculated for a sample. It measures the strength and direction between two variables, *X* and *Y*. A strong positive linear relationship results is a positive number, close to 1, and a strong negative linear relationship is close to -1. Numbers that are mid-range and close to zero have weak linear relationships (or may actually be nonlinear). A value of -1.0 is a perfect negative (inverse) correlation, 0.0 indicates no correlation, and +1.0 is a perfect positive correlation. It should be noted that correlation does not necessarily imply causation (Minitab 15™, 2006). It merely suggests a degree of parallelism or association between the variables; the cause of which may be unknown.

In this analysis, there are eight variables under consideration: Geology, Surficial Geology, Wetland, Soil, Slope, Sand, Erodible Land, and Land Use. These variables result in twenty eight unique correlations, calculated by the following formula (Trochim, 2006):

$$\frac{N * (N - 1)}{2}$$

The correlation matrix was computed for each study site with ArcGIS® v9.2, using *ArcToolbox®*: *Model Builder®; Spatial Analyst® Tools; Multivariate*; and the *Principal Components* tools. Because of the multiple study sites and numerous attributes, there are several steps involved in this process. For this reason, I used *Model Builder®,* within ArcGIS®, to automate the process (Figure 32). First, I recycled the polygons that were previously clipped to within 800 m of the shoreline (Step 1). Land use polygons for each town were combined by using the *Mosaic®* function (Step 1a). This is a useful tool when a set of adjacent rasters need to be merged into one entity. Subsequently, the eight major features were converted into rasters (Step 2).

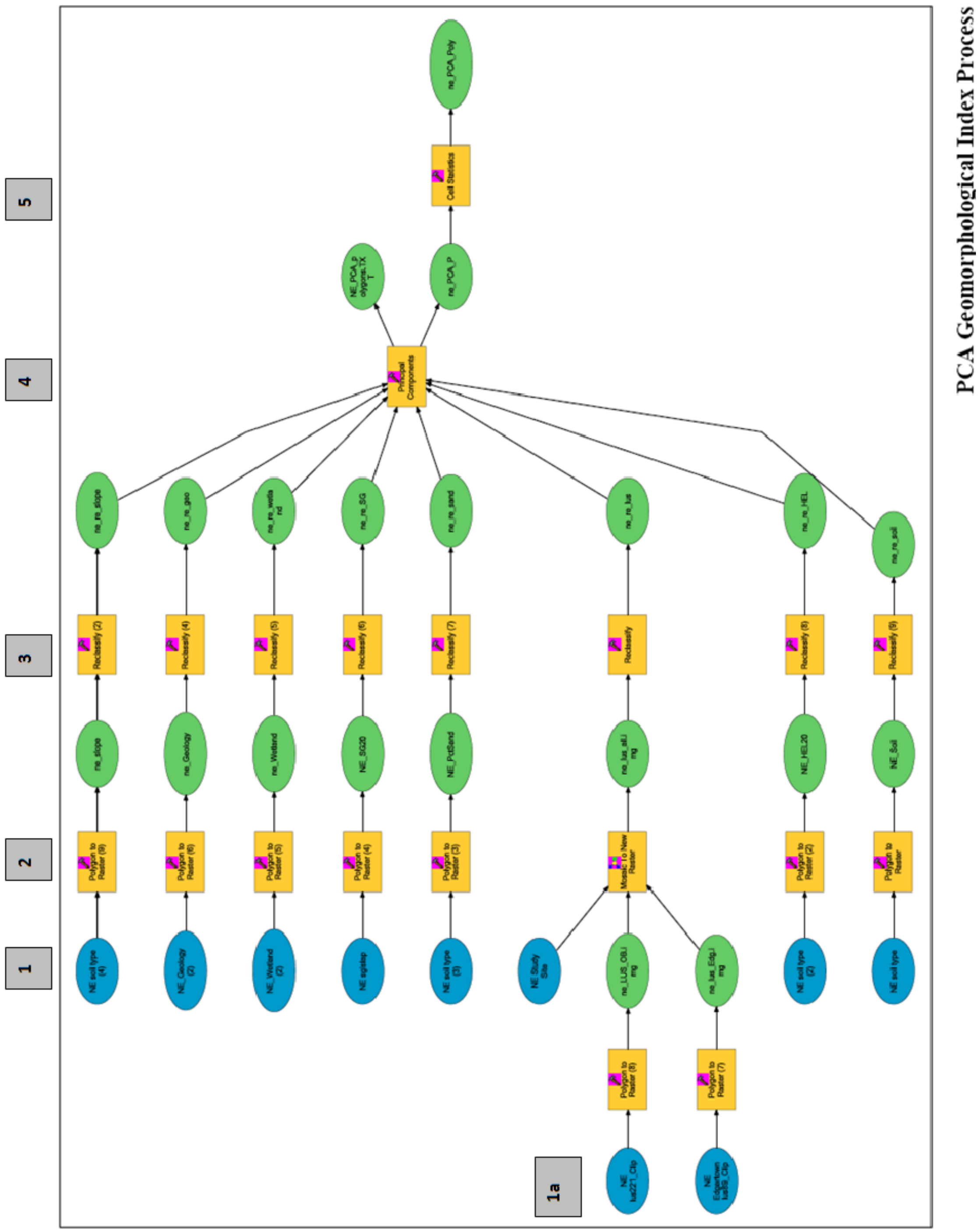

Figure 32. The PCA geomorphical index process used to derive correlation matrices and risk assessment. Individual steps are highlighted in grey boxes.

Next, every attribute within the raster was reclassified based upon the linear regression rate of shoreline change (Step 3) (see Appendix A (Appendix 5) for reclassifications for each attribute). These ratings ranged from 1 to 5 based upon the following criteria (see below):

- 1 = significant accretion (> 1 m/yr)
- 2 = accretion (0.05 to 1 m/yr)
- 3 = equilibrium (0.5 to -0.5 m/yr)
- 4 = erosion (-0.5 to -1 m/yr)
- 5 = significant erosion (> - 1 m/yr).

The reclassified feature raster bands were used to perform principal component analysis (Step 4). PCA, within ArcGIS®, transforms the data into several rasters per multiband raster, from the input multivariate attribute space to a new multivariate attribute space whose axes are rotated with respect to the original space. This eliminates redundancy and helps to make the data more interpretable (ESRI®, 2006). Once PCA was completed, a new multiband raster was created based upon the criteria listed above. These results were used to determine PCA and the Geomorphological Risk Assessment (Step 5), to be discussed further.

ArcGIS® first calculates the covariance matrix, followed by the correlation matrix. The following formula is used to determine the covariance between raster layers *i* and *j* (ESRI®, 2006):

$$Cov_{ij} = \frac{\sum_{k=1}^{N}(Z_{ik} - \mu_i)(Z_{jk} - \mu_j)}{N - 1}$$

where, Z – value of a cell, i, j – are layers of a stack, μ - is the mean of a layer, N – is the number of cells, and k – denotes a particular cell.

The covariance of two layers is the intersection of the appropriate row and column. The values of the covariance matrix are dependent on the value units, while the correlation matrix is not (ESRI®, 2006).

The correlation matrix shows the values of the Pearson correlation coefficient that depict the relationship between two datasets. The correlation matrix presents the cell values from one layer as they relate to the cell values of another layer. The correlation between two layers is a measure of dependency between the layers. It is the ratio of the covariance between the two layers divided by the product of their standard deviations. Because it is a ratio of *(units^2/unit^2*), it is a unitless number. The equation used to calculate the correlation is (ESRI®, 2006):

$$Corr_{ij} = \frac{Cov_{ij}}{\delta_i \, \delta_j}$$

The resulting correlation matrix was loaded into *Minitab 15*™ in order to calculate the principal component eigenvectors, eigenvalues, the percent of variance, the cumulative percent of variance, the associated scree graphs and loading plots for the first two components, and communality.

The eigenvalue for a given feature measures the variance in all the variables which are accounted for by that feature. The eigenvalue is not the percent of variance explained, but rather a measure of amount of variance in relation to total variance (Garson, 2008). Eigenvalues are calculated by the following matrix equation:

$$|R - \lambda I| = 0$$

where R is the correlation (or covariance) matrix, λ is the vector of eigenvalue solutions, and I is the identity matrix, and each eigenvalue is associated with one principal component (McGarigal *et al.*, 2000).

Eigenvectors define the coefficients of the original variables in the linear equations that define the new axes that maximize some objective criterion (McGarigal *et al.*, 2000). Eigenvectors are determined by the following:

$$[R - \lambda_i I]v_i = 0$$

where R is the correlation (or covariance) matrix, λ_i is the eigenvalue corresponding to the i^{th} principal component, I is the identity matrix, and v_i is the eigenvector associated with the i^{th} eigenvalue (McGarigal *et al.*, 2000). Eigenvectors are also known as principal component loadings or weights.

A PCA Scree Plot plots the eigenvalue associated with a principal component versus the number of the component. The purpose of this graph is to judge the relative magnitude of eigenvalues. A PCA Loading Plot displays the loadings for the second principal component (y-axis) versus the loadings for the first principal component (x-axis). A line is drawn from each loading to the (0,0) point. The PCA surface plot evaluates the relationships between the first three components at once. These graphs were generated in *Minitab 15™*.

Hair *et al.* (1987) put forth several rules to guide interpretations of which PCA components are worth considering. One of these subjective rules suggests that principal components with loadings greater than 0.30 or less than -.30 are considered significant;

PC Eigenvectors	Significance
> 0.30 or < -0.30	Significant
> 0.40 or < -0.40	More Significant
> 0.50 or < -0.50	Very Significant

Table 7. Significance of PCA components (from Hair et al., 1987).

loadings greater than 0.40 or less than -0.40 are considered more significant; while loadings greater than 0.50 or less than -0.50 are considered very significant (Table 6). This rule is useful when the sample size is greater than or equal to 50 (McGarigal *et al.*, 2000). This method is often used as a rule of thumb by researchers (McGarigal *et al.*, 2000) and is used in this thesis.

Communality, in PCA, refers to the proportion of a variable's variance that is accounted for by the retained principal components. Variance represents the spread of observations around the expected value (mean) of a probability distribution. It is equal to the sum of the squared multiple correlations from the retained principal components, as follows:

$$c_j = \sum_{i=1}^{P} S_{ij}^2$$

where C_j is the communality of the j th variable and S_{ij} is the loading (or correlation) between the i th principal component and the j th variable (McGarigal *et al.*, 2000). On the SS and NW sites, three principal components were retained; four principal components were retained on the NE site. The "final communality estimates indicate how well the original variables are accounted for by the retained principal components" (McGarigal *et al.*, 2000). Another way to look at this is that R^2 is the percent of variance explained. Since the factors are uncorrelated in PCA, the squared loadings of each principal component may be added to get the total variance explained. This was accomplished in *Minitab 15™* with the following formula: *(PC1**2) + (PC2**2) + (PC3**2).* In summary, to measure communality, square the correlation coefficient and multiply by 100, to obtain the percentage of variance accounted for (Minitab 15™, 2006).

Geomorphological risk assessment

The EPA defines risk as “the chance of harmful effects to human health or to ecological systems resulting from exposure to an environmental stressor” (EPA, 2008). In this study, the environmental stressor is an increase in sea level around Martha’s Vineyard, probably caused by global warming. Here, I undertook a risk assessment of the three study sites by evaluating the risk of erosion based upon statistical analyses. To assess the risk of coastal erosion due to the effects of sea level rise, risk ratings were determined by the historic linear regression rate of erosion for each attribute, at each study site. A rating of “1” indicates a low risk of shoreline erosion, based on shorelines accreting at the rate of more than 1 m/yr, and a “5” indicates a high risk of shoreline erosion, with shorelines eroding more than 1 m/yr (Table 6). These ratings ranged from 1 to 5 based upon the following criteria:

Assessment	Level	Shoreline Change Rate
Low Risk	1	(> 1 m/yr)
Low-Medium Risk	2	(0.05 to 1 m/yr)
Medium	3	(0.5 to -0.5 m/yr)
Medium-High Risk	4	(-0.5 to -1 m/yr)
High Risk	5	(> - 1 m/yr)

Table 8. Risk assignments based on rates of shoreline change.

Appendix A **-** Appendix 5 lists all the features and attributes by risk level for each study site. It should be noted that some of the same attributes have different risk levels assigned by site because the linear response rate to sea level rise varies from transect to transect.

Step 5 of the PCA geomorphical index process (Figure 32**)** calculated the *mean* per cell from the study site rasters, based upon the retained principal components for each study site. For the SS and NW study sites, three principal components were retained; four principal components were retained from the NE study site. Eight major features were included in this analysis (Geology, Surficial Geology, Soil, Percent of Sand, Erodible Land, Slope, Wetland, and Land Use). Winter Waves and Winter Wind were eliminated from the analysis because the results of the correlation matrix resulted in zeros for all study sites (data not shown). Compass Direction was removed in the next series of analyses because the communality results were less than 1%, for all study sites (data not shown).

Using *Spatial Analyst*® *Tools* in *ArcGIS*® v9.2 (*Local toolbox* > *Cell Statistics*), the mean for each raster cell, size 20 m x 20 m, was calculated based upon the retained principal components. The output raster map displayed the geomorphological risk assessment for each study site. When the raster bands were calculated, the Wetlands raster did not have a common intersection with each of them; therefore, no output was created. Because of this dilemma, two results are presented for each study site, rather than one. The first results were based upon the full suite of retained principal components, and the second results were recalculated without *Wetlands* as a variable.

To gain further insight into the risk assessment for the Vineyard, I interpolated data to create a new surface. Interpolation creates a surface grid based on the principals of spatial autocorrelation, which measures the degree of relationship/dependence between near and distant points. To do this, both raster data sets for each study site were *joined*, with and without wetlands, and then the joined rasters were converted to point features. These points are positioned at the center of the cells, which represent the mean value.

The Inverse Distance Weighting (IDW) method was applied for each study site using *Geostatistical Analysis*. This is a quick deterministic interpolator that is exact, with minimal model parameters, based on the extent of similarity of cells, and it can be a good technique to look at an interpolated surface. Fifteen neighbors (points) were included, with a minimum of ten, and a power size of 2. This power size gives more influence to the points that are further away, resulting in a smoother surface (ESRI®, 2006).

After each study site was analyzed independently of each other, the next process was to combine this data into one analysis. By merging the multiple rasters through the *Data Management Tools*, within *ArcGIS®* v9.2, a new raster dataset was created through the *Mosaic* function. The input rasters included the all the retained principal components, and the principal components that were calculated without the variable, *Wetlands*. The *Mosaic* method chosen to calculate the data set was *Mean*; the mean is calculated for any overlapping cells. *Mosaic Tolerance* was set to zero. This is a unit of tolerance for a pixel and a tolerance of zero guaranties resampling if there is a misalignment in pixels (ESRI®, 2006). By synthesizing this data, a new raster dataset was generated, thereby allowing me to convert this information into points.

To culminate this analysis, the geostatistical technique kriging was used within *ArcGIS®* v9.2; this method does not require the data to have a normal distribution (Johnston *et al.*, 2003). Kriging assumes that the distance or direction between points reflects a spatial correlation that can be used to explain variation in the surface. Essentially, it is the statistical relationship among the measured points, by weighing the sum of the data. The primary purpose of kriging is to predict the variable values at unsampled locations (McCoy *et al.*, 2002). Besides predicting cell values at unsampled locations, kriging uses statistical models to generate probability and prediction standard error maps. Please refer to the section on *Fractal Dimension* for more details on kriging.

Specifically for the risk assessment analysis, the cell size was 40 m x 40 m, for a total of 402,360 points. The kriging type used was *Ordinary*, which means that the weight of the data depends on the fitted model to the measured points, the distance to the prediction location, and the spatial relationships among the measured values around the prediction location (McCoy *et al.*, 2002). A *Prediction* model was chosen as output type, and *no trend type* was designated. Five neighbors were chosen, with a minimum of two. There were 12 lags, nugget size of 0.15, model type was spherical, range was ~ 8528, no anisotropy, and partial sill was ~ 0.7. (A *spherical model* shows a progressive decrease of spatial autocorrelation, until at some distance, the autocorrelation becomes zero). A prediction model was determined from the kriging weights for the measured values which calculates a prediction for the location with the unknown value. Kriging uses geostatistics which makes it possible to calculate a statistical measure of uncertainty for the prediction, called the kriging standard error.

CHAPTER 4

RESULTS

Introduction

In the sections that follow I first consider whether the coastline of Martha's Vineyard has changed in recent time by using transects perpendicular to the coast all along the island. Then, I examine whether sea level has also varied during approximately the same period. Having obtained evidence in support of both recent coastal erosion and sea level rise, I then examine whether one or more specific geophysical or ecological properties (viz. geology, surficial geology, wetlands, soils, land use, and shoreline orientation to wind or waves) played a significant role in the observed shoreline change. GIS layers for each of these categories were assembled and analyzed, where possible. While some of these properties were evaluated for the entire island, to simplify the study, three distinct Martha's Vineyard sites were chosen for detailed analysis. These sites each had unique morphology and were located on the south side (SS), the northeast side (NE), and the northwest (NW) side of Martha's Vineyard. The properties as represented by GIS layers are then related to the coastal erosion transects by overlaying and examining the proportion of each value or type on each transect. Then these proportions are related to the erosion at each transect using a variety of univariate and multivariate regression, including PCA regression. Finally, a risk assessment is performed for the Martha's Vineyard coastline, using three sea level rise scenarios and predicted shoreline erosion.

Shoreline Erosion

Historical Changes to the Shoreline of Martha's Vineyard

Using ESRI® ArcGIS® v9.2 and data compiled by Thieler, *et al*. (2001), generously provided by the Massachusetts Office of Coastal Zone Management, 2810 transects were identified along the coastline of Martha's Vineyard. Besides providing historic shoreline movement information, the data of Thieler, *et al*. (2001) also provided ordinary least squares regression analysis of shoreline movement.

The data from these transects spans 149 years and was reorganized as four eras according to approximate year-ending dates (1897, 1955, 1979, and 1994) (Table 9). In this section I describe results derived from the analysis of shoreline change for all of Martha's Vineyard. A later section addresses the data from a subset of the transects, i.e., from the individual study sites. Analyses for each era include the number of transects per time period, the mean distance the shoreline eroded at each transect, the least squares linear regression rate of change, and the proximity of eroded areas to specific geographic features or MV towns.

ERA 01	Count	Percent	ERA 02	Count	Percent
07/1845-07/1888	690	77.97	07/1845-07/1955	1	0.04
07/1845-07/1897	3	0.34	07/1846-07/1955	98	3.84
07/1846-07/1897	192	21.69	07/1846-07/1994	1	0.04
N=	885		07/1888-07/1955	730	28.64
=	1925		07/1897-07/1955	1719	67.44
			N=	2549	
			=	261	
ERA 03	**Count**	**Percent**	**ERA 04**	**Count**	**Percent**
07/1888-07/1979	2	0.09	07/1955-07/1994	443	15.84
07/1897-07/1978	1	0.04	07/1978-07/1994	1435	51.3
07/1955-07/1978	1367	59.77	07/1979-07/1994	919	32.86
07/1955-07/1979	917	40.1	N=	2797	
N=	2287		=	13	
=	523				

Table 9. MV transect data during four time periods.

<u>MV ERA 01</u>. This era has a range of 52 years (1845-1897) and includes data from only 885 of the possible 2810 transects (31%) (Table 9). Of these 885 transects, 78% span 43 years, 21.7% span 51 years, and 0.3% (3 transects) range the full 52 years. These transects are primarily located around the northeast quadrant of MV, near Oak Bluffs, and the south, southwest side of Aquinnah and Chilmark (Figure 33).

During the 52 year period, the mean distance eroded for these transects was -3.53 m (Table 10). The trimmed mean for this data equaled -2.68 m, thereby reducing the overall significance of erosion by 24%. (The trimmed mean is less sensitive to extreme values than is the mean because the smallest and largest 5% of the observations are dropped.) The amount of shoreline movement in ERA01 varied greatly, from 120.1 m of erosion to 94.4 m in accretion (Table 10).

VARIABLE	MEAN	TrMEAN	StDEV	VAR	MIN	MAX
ERA01 M DIS/YR	-3.53	-2.68	26.78	717.24	-120.08	94.36
ERA02 M DIS/YR	-21.28	-18.56	47.57	2262.90	-218.39	251.27
ERA03 M DIS/YR	-10.90	-9.73	26.58	706.72	-198.07	187.05
ERA04 M DIS/YR	-11.40	-11.36	16.22	263.04	-193.11	90.61
ERA01-04 M DIS/YR	-40.63	-36.73	67.06	4497.02	-277.98	274.79

VARIABLE	MEAN	TrMEAN	StDEV	VAR	MIN	MAX
ERA01 M/YR	-0.087	-0.066	0.615	0.379	-2.79	2.19
ERA02 M/YR	-0.350	-0.300	0.807	0.650	-3.77	4.33
ERA03 M/YR	-0.459	-0.410	1.13	1.28	-8.61	8.13
ERA04 M/YR	-0.673	-0.650	0.988	0.976	-12.07	5.37
ERA01-04 M/YR	-0.491	-0.436	0.720	0.518	-5.45	2.14

Table 10. MV transect statistics by distance changed in meters/year and by shoreline erosion rates of change in meters/year.

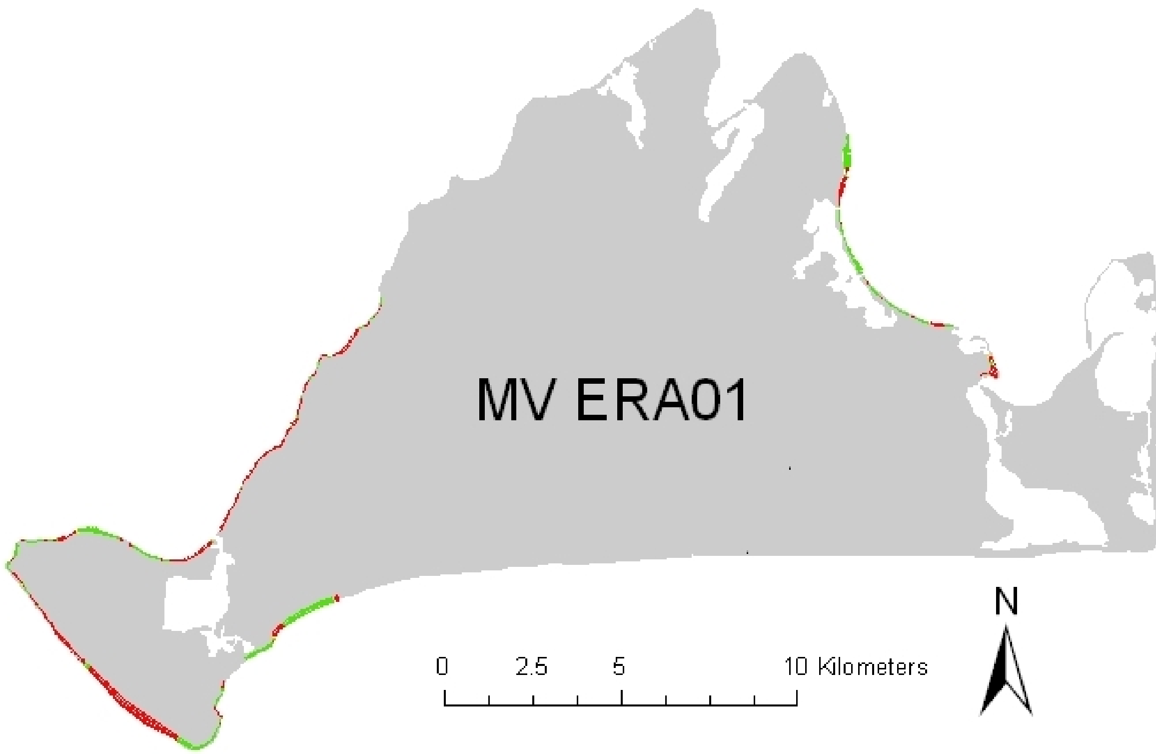

Figure 33. MV transects in Era 01: shoreline distance changed by m/yr.

The changes to the MV coastline during ERA01 are summarized by colors in the map of Figure 33. In this figure, red depicts erosion of -0.5 m or more, a property characteristic of 471 (53%) transects. Accretion of greater than 0.5 m (shown in green) occurred at 395 (45%) transects. The remaining 19 transects, in yellow, (2%), are in equilibrium, with shorelines fluctuating 0.5 m or less in each direction. Most of the erosion occurred along the northwest coast of Chilmark and Aquinnah, particularly the Gay Head Cliffs (Table 11). Most of the accretion occurred along a thin strip of beach, Joseph Silvia State Beach, in Oak Bluffs. Chilmark had the most erosion, with a mean distance of -8.08 m, followed by Aquinnah, with -3.78 m. West Tisbury, Edgartown, and Oak Bluffs had mean accretions of 4.02 m, 5.2 m, and 6.89 m, respectively (Table 11).

The overall shoreline change rate for ERA01, as assessed by least squares linear regression, was -0.087 m/yr, indicating erosion. Chilmark and Aquinnah eroded at rates of -0.19 m/yr and -0.09 m/yr and Edgartown (0.10 m/yr), Oak Bluffs (0.14 m/yr), and West Tisbury (0.09 m/yr) all showed accretion (Table 11).

Exploratory analysis for a normal distribution of transects, using the Anderson-Darling (AD) test, indicate that the distance data are not normally distributed for all the transects in ERA01 (AD score =18.84; p-value <0.005), a result that is not particularly surprising in light of the various forces acting on each location (Figure 34). Closer examination shows that each town has a low AD score, ranging from 1.89 to 0.31, suggesting a normal distribution (data not shown).

TOWN	VARIABLE	MEAN DIS/YR	VARIABLE	MEAN M/YR
CHILMARK	ERA01 M DIS/YR	-8.08	ERA01 M/YR	-0.19
EDGARTOWN		5.20		0.10
AQUINNAH		-3.78		-0.09
OAK BLUFFS		6.89		0.14
TISBURY		No Data		No Data
WEST TISBURY		4.02		0.09
CHILMARK	ERA02 M DIS/YR	-51.07	ERA02 M/YR	-0.83
EDGARTOWN		-2.63		-0.04
AQUINNAH		-11.09		-0.17
OAK BLUFFS		-21.41		-0.35
TISBURY		-1.13		-0.02
WEST TISBURY		-46.41		-0.80
CHILMARK	ERA03 M DIS/YR	-24.84	ERA03 M/YR	-1.04
EDGARTOWN		-6.70		-0.29
AQUINNAH		-6.97		-0.29
OAK BLUFFS		2.18		0.09
TISBURY		-1.87		-0.08
WEST TISBURY		-29.75		-1.24
CHILMARK	ERA04 M DIS/YR	-15.40	ERA04 M/YR	-0.98
EDGARTOWN		-11.13		-0.67
AQUINNAH		-1.69		-0.11
OAK BLUFFS		-6.50		-0.42
TISBURY		-10.53		-0.66
WEST TISBURY		-19.00		-0.86
CHILMARK	ERA01- 04 M DIS/YR	-95.09	ERA01-04 M/YR	-0.84
EDGARTOWN		-18.58		-0.45
AQUINNAH		-23.42		-0.17
OAK BLUFFS		-19.55		-0.20
TISBURY		-13.45		-0.25
WEST TISBURY		-74.57		-0.73

Table 11. MV shoreline change by towns for eras 01-04

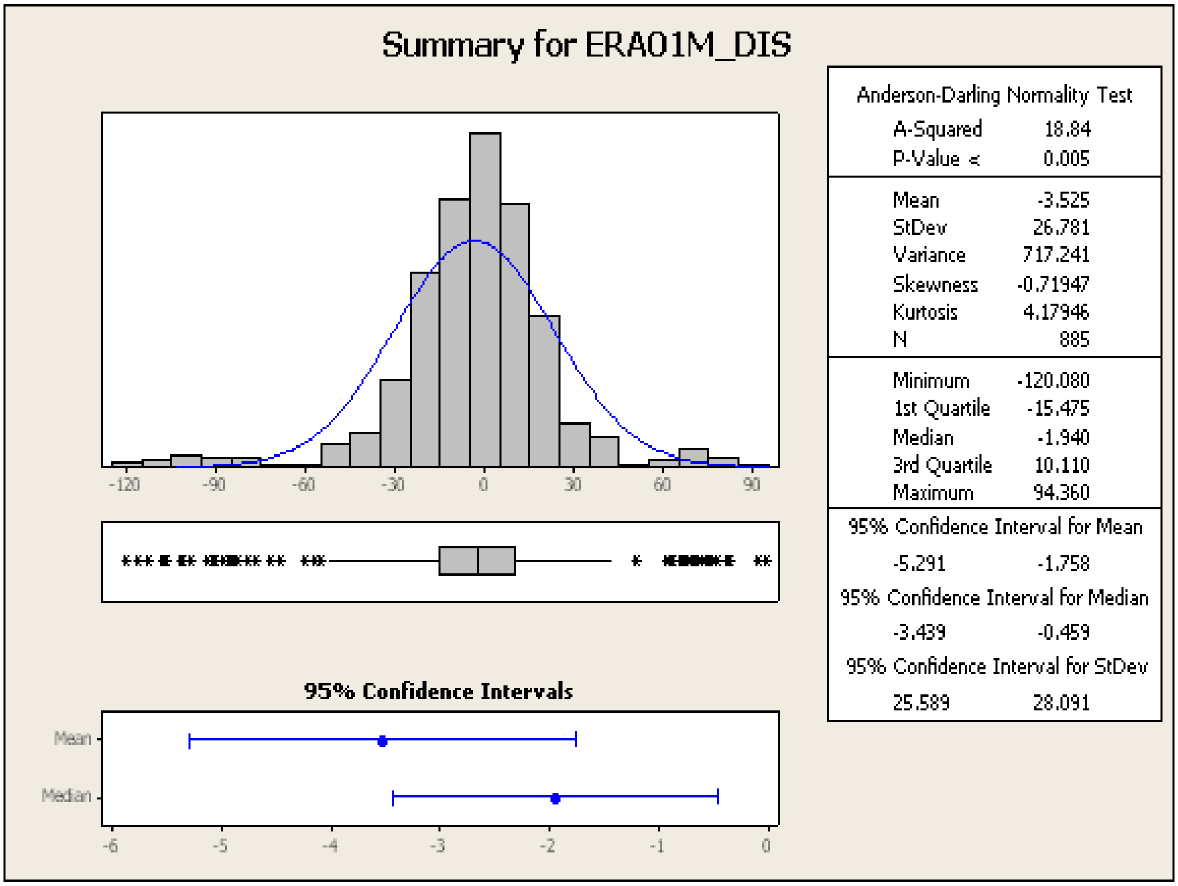

Figure 34. MV summary statistics for era 01: distance in m/yr.

MV ERA 02. The second period, ERA02, ranges from 1845-1994 (149 years), and includes 2549 (91%) of the possible transects (Table 9). The majority of these transects (1719; 67%) cover a 58 year window from 1897-1955. An additional 730 transects (29%) range from 1888-1955 (67 years). One transect (0.04%) extended from 1846 to 1994 (148 years), one transect (0.04%) ranged from 1845-1955 (110 years), and 98 (3.84%) transects ranged from 1846-1955 (109 years). The transects of ERA02 cover most of Martha's Vineyard except the southern shore of Edgartown (Figure 35).

During ERA02, 96% of which occurs during a 58-67 year time period, the mean erosion was -21.28 m, and the trimmed mean was -18.56 m (Table 10). The amount of shoreline movement varied greatly, from -218.39 m of erosion to 251.27 m in accretion, with a range of 469.66 m. Using the same color-based scoring as the previous figure, Figure 35 summarizes the coastline distances changed during ERA02 and depicts 1740 (68%) transects that eroded 0.5 m or more (red), 753 (30%) transects that accreted (green), and 56 (2%) transects in equilibrium (yellow), i.e., with shorelines fluctuating 0.5 m or less each way. Most of the erosion occurred in Chilmark, with a mean of -51.07 m, followed by West Tisbury, with a mean of -46.41 m (Table 11). Overall, every town appeared to manifest erosion, with insufficient accretion to compensate for the loss of shorefront.

The mean shoreline linear regression rate of change for ERA02 was -0.35 m/yr (Table 10). All towns eroded during this time period, with Chilmark (-0.83 m/yr) and Oak Bluffs (-0.35 m/yr) the fastest, and Tisbury (-0.02 m/yr) and Edgartown (-0.04 m/yr) the slowest (Table 11).

Exploratory analyses of the data included testing for a normal distribution (Figure 36). Results from the AD test indicate that the data is not normally distributed: the AD score for ERA02 is 138.82, with a p-value <0.005. The data for the individual towns all have p-values of <0.005 and their AD values range from 42.13 (West Tisbury) to 2.59 (Aquinnah) (data not shown).

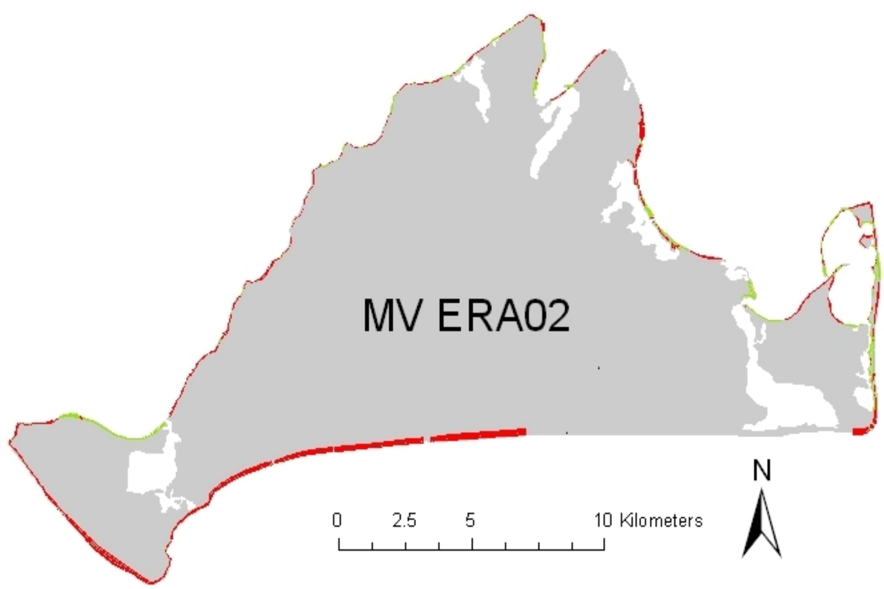

Figure 35. MV transects in era 02: distance changed in the shoreline by m/yr.

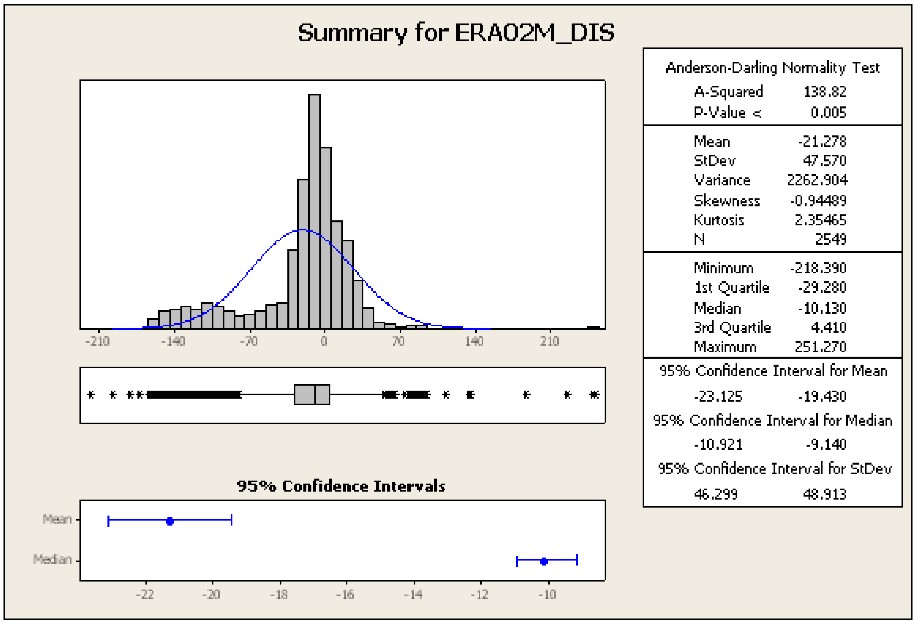

Figure 36. MV summary statistics for era 02: distance in m/yr.

<u>MV ERA03.</u> ERA03 ranged from 1888-1979 (91 years), but more than 99% of its measurements fell within a 23-24 year window (1955-1979) (Table 9). Eighty-one percent of the possible transects have data reported in ERA03.

The mean distance eroded from 1955-1979 was -10.9 m and the trimmed mean was -9.73 m (Table 10). The highest distance eroded was -198.07 m and the most accretion was 187.05 m, with a range of 385 m. West Tisbury had the highest mean of erosion, -29.75 m, followed by Chilmark at -24.84 m (Table 11). Oak Bluffs was the only town that indicated accretion (2.18 m). Most of the south shore, and the Gay Head Cliffs eroded, but the eastern end of Chappaquiddick and the area near Menemsha Harbor accreted (Figure 37).

The linear regression rate indicated that the mean rate of change during this time period was -0.459 m/year (Table 10). West Tisbury, at -1.24 m/yr, had the highest rate of shoreline change, followed by Chilmark, at -1.04 m/yr (Table 11). The remaining towns appeared to be in a state of equilibrium with rates of change ranging from -0.29 to 0.09 m/yr.

Exploratory analysis of the data included testing for a normal distribution. Results from the AD test indicate that the data is not normally distributed: the score for ERA03 is 57.98, with a p-value <0.005 (Figure 38).

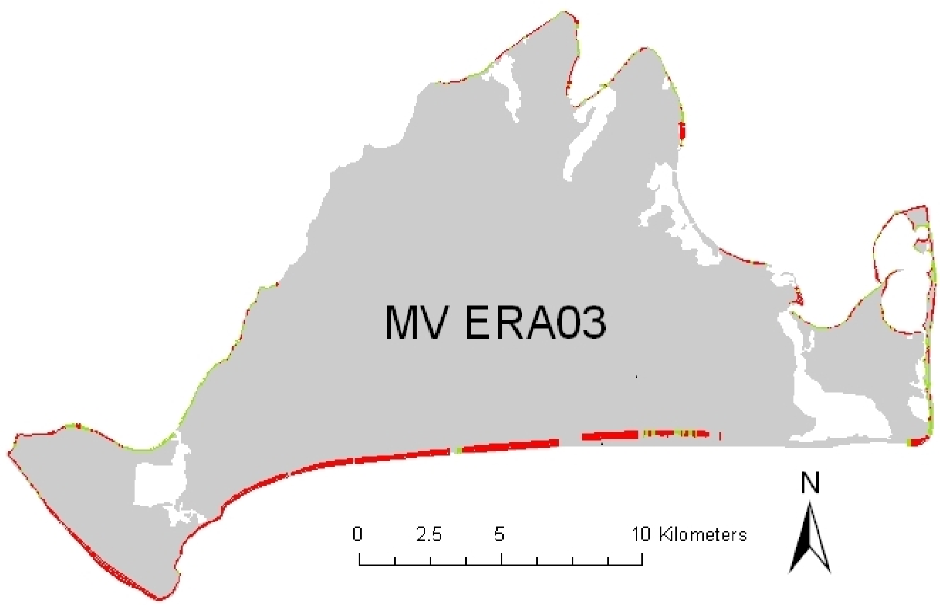

Figure 37. MV transects by era 03: distance changed in the shoreline by m/yr.

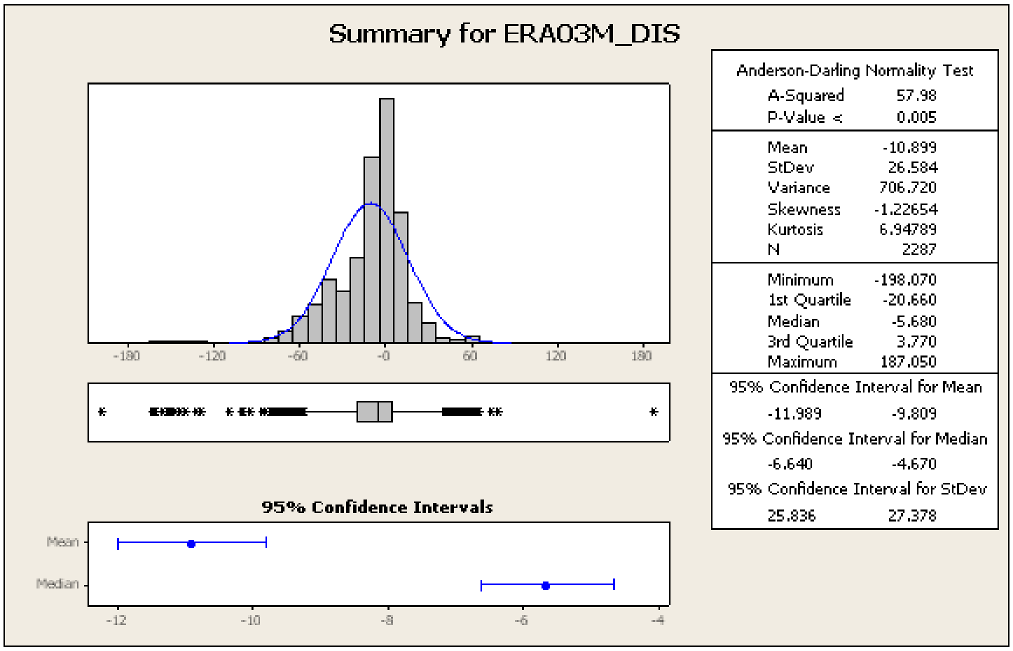

Figure 38. MV summary statistics for era 03: distance in m/yr.

<u>MV ERA04.</u> The last time period, ERA04, ranged from 1955-1994 (39 years) (**Table 9**). Approximately 16% of the transects fell within this window, while the other 84% ranged from 1978(9)-1994 (15-16 years). ERA04 had a mean distance of erosion of -11.40 m and a range of shoreline change from -193.11 m of erosion to accretion as high as 90.61 m (Table 10). West Tisbury had the highest mean distance eroded, -19 m, followed by Chilmark, with -15.4 m. Every town experienced erosion (Table 11).

Chilmark had the highest rate of change (-0.84 m/yr), followed by West Tisbury (-0.73 m/yr) (Table 11). The other towns had mean erosion rates within the range of equilibrium (-0.45 to -0.17 m/yr). During ERA04, Martha's Vineyard experienced a mean rate of erosion of -0.49 m/yr (Table 10). This time period had more erosion on the east side of Chappaquiddick, areas around Menemsha, and less at the Gay Head Cliffs (Figure 39).

The AD score for this time period was 42.67, with a p value <0.005. Once again, this data was not normally distributed (Figure 40).

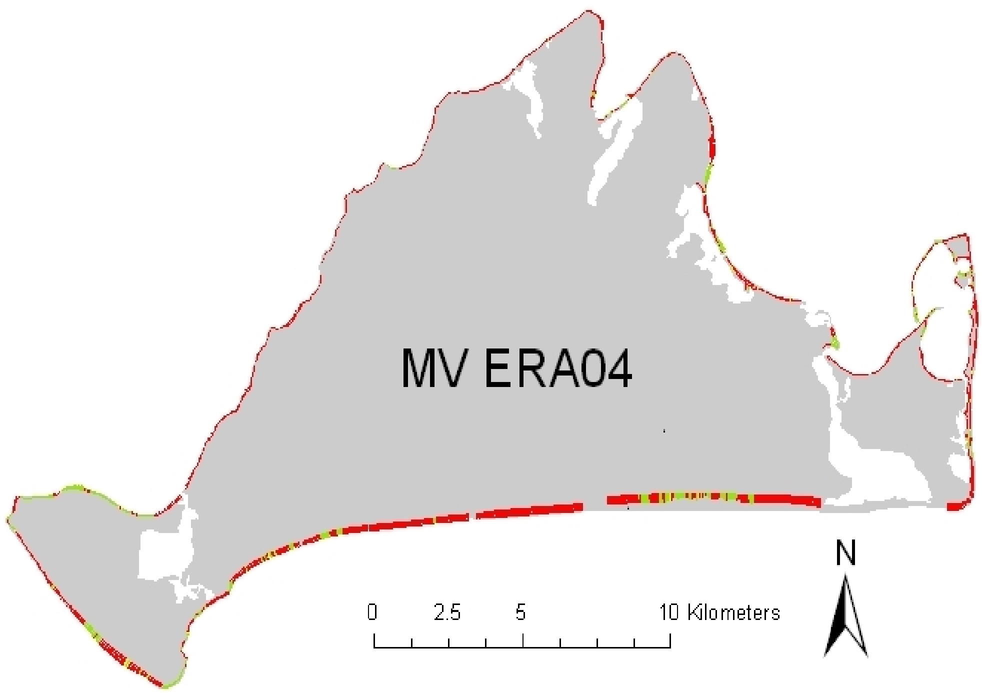

Figure 39. MV transects by era 04: distance changed in the shoreline by m/yr.

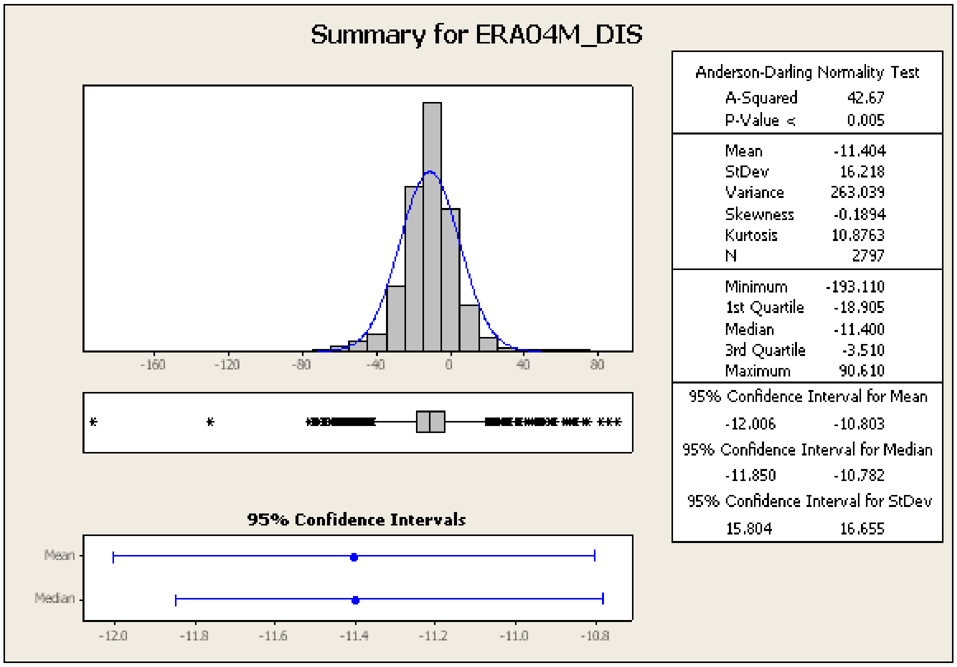

Figure 40. MV summary statistics for era 04: distance in m/yr.

MV ERA01-04 Cumulative Data. The mean total shoreline distance changed for all 2810 transects during the 149 year time frame of all four eras indicates a cumulative shoreline erosion of -46.38 meters (~152 ft) (Figure 41), and a mean recession of shoreline of -40.63 meters (~133 feet) (Table 10). The 95% confidence interval for the mean is -43.11 m to -38.15 m, the standard deviation is 67.06, the variance is 4497.02, the skewness is -1.107, and the kurtosis is 1.624 (Figure 42). The range of shoreline change ranges from -278 m to 275 m (Table 10), the Anderson-Darling test score is 156.63, and the p-value for that test is <0.005 (Figure 42), indicating that the distribution is not normal. Chilmark had the highest mean distance changed of -95.09 m, followed by West Tisbury at -74.57 m, Aquinnah at -23.42 m, Oak Bluffs at -19.55 m, Edgartown at -18.58 m, and Tisbury, with the least distance lost at -13.45 m (Table 11). Collectively, these data lead to a mean shoreline recession of -0.49 m/year for Martha's Vineyard over 149 years (Table 10).

Overall, ERA04 represented the best transect coverage (99.5%). ERA02 (91%) was second, ERA03 (81%) was third, and ERA01 (31%) was last. Even though there was some overlap in time for each period, there was no overlap of time for any transect.

In summary, from 1851-1994, the shoreline change rate indicates that 74% (2076 transects) of the shoreline were in "equilibrium," ranging from 0.5 m/yr to – 0.5 m/yr, 24% (689 transects) were eroding, with erosion rates exceeding -0.5 m/yr, and 2% (45 transects) were accreting more than 0.5 m/yr. See Figure 43 for locations.

Another way to report the results suggests that 85% (2399) of the transects are eroding because the shoreline change rate is < 0, 14% (404) of the transects are accreting because the rate of change is > 0. The remaining 1% of the transects (7) have a mean m/yr change rate of zero.

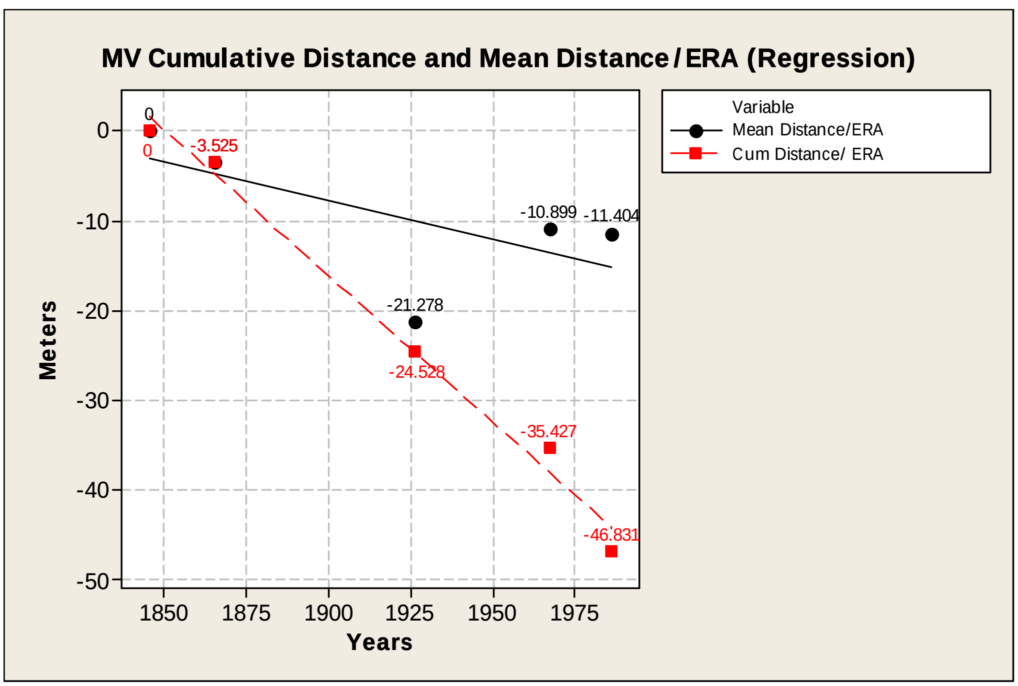

Figure 41. MV cumulative distance and mean distance by era (regression rate).

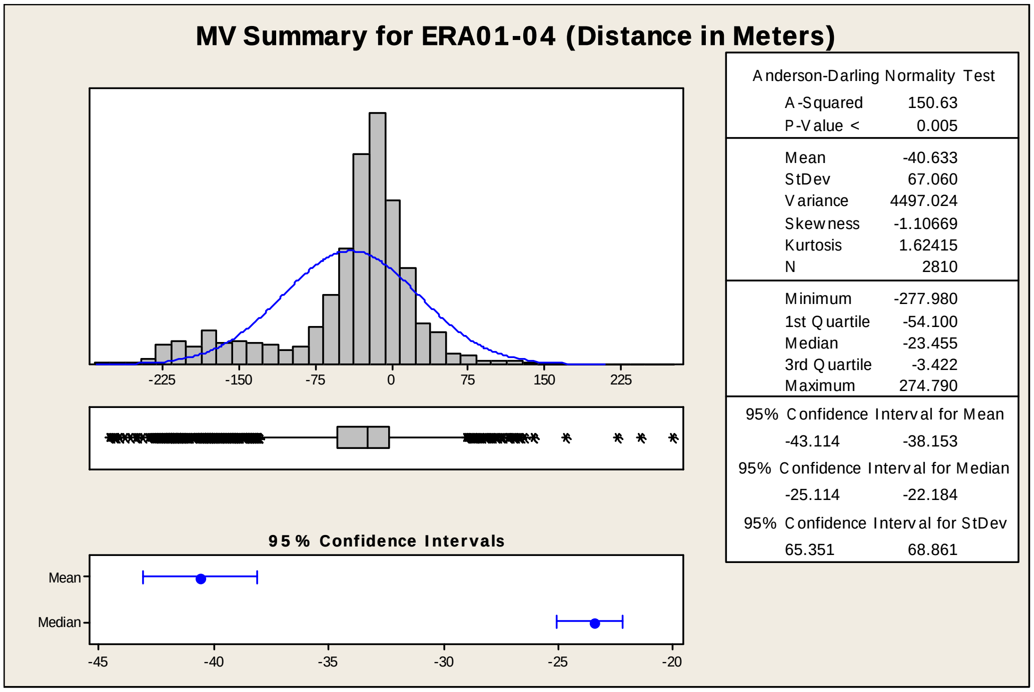

Figure 42. MV summary statistics for era 01-04: distance in m/yr.

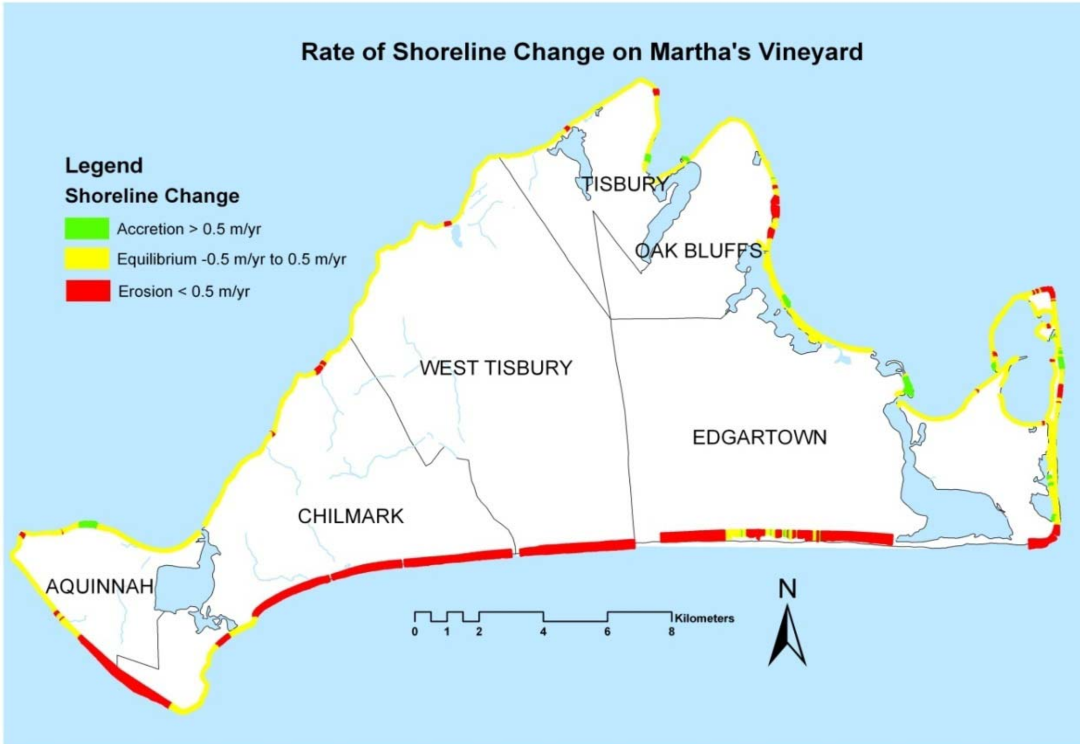

Figure 43. MV shoreline change for era 01-04 in m/yr.

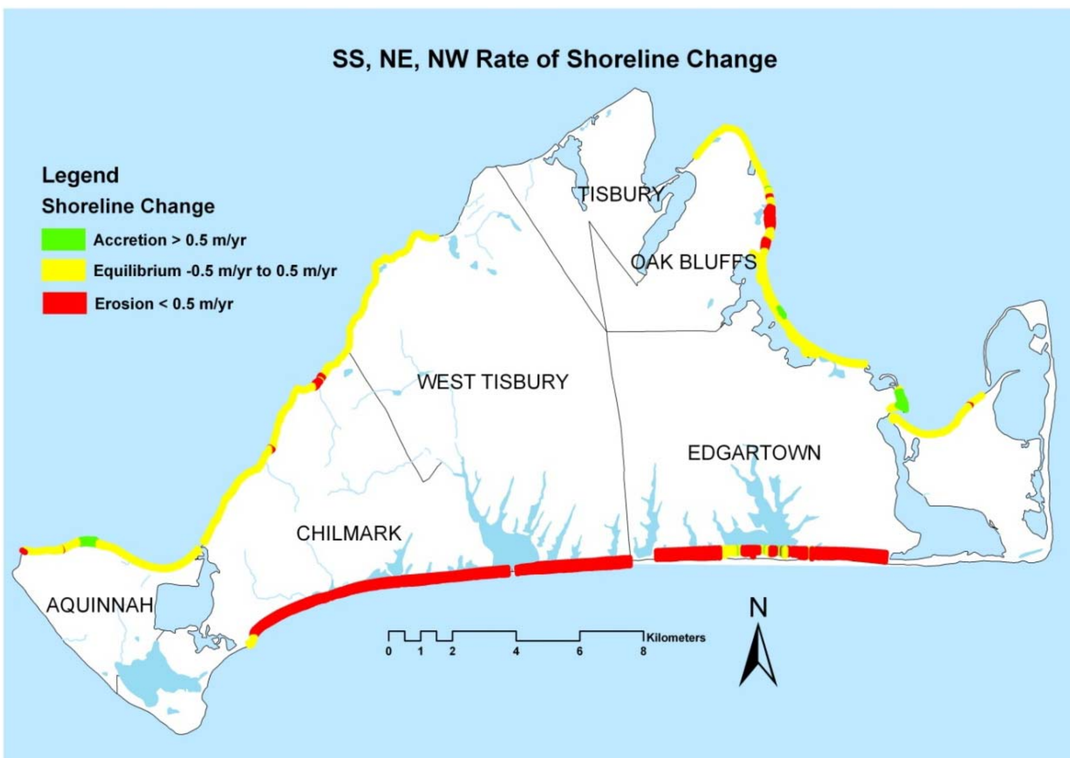

Figure 44. SS, NE, and NW study sites and linear shoreline rates of change.

Historical Changes to the Shorelines of the Study Sites

The complexity inherent in studying all of Martha's Vineyard led me to reduce the number of transects to 1461, thereby allowing a comprehensive analysis and comparison of limited segments of the coastline. The transects were divided equally between three sites differing in paraglacial aspects that were located on the south shore (SS), the northeast shore (NE), and the northwest shore (NW) of Martha's Vineyard (Figure 44). The 487 transects of each site were grouped into the four time periods used for analyzing the entire island (ERA01:1845-1897, 52 years; ERA02: 1846-1955, 109 years; ERA03: 1888-1979, 91 years; and ERA04: 1955-1994, 39 years). Unlike the analyses of the entire island, the study site analyses focused primarily on the shoreline rate of change (m/yr), rather than the distance changed. All subsequent analyses were based upon the linear regression (LR) rates of change derived from these studies.

SS Historic Erosion. Of the 487 transects in the SS study site, data was available for 13% (62) in ERA01 (1845-1897), 63% (306) in ERA02 (1845-1955; 80% of these transects fell within 58 years), 85% (416) in ERA03 (1955-1979), and 100% (487) in ERA04 (1955-1994) (data not shown).To test for a normal distribution of the SS shoreline rate of change, I converted the LR rate to a z-score, with $\mu = 0$, and $\sigma = 1$. Applying the Anderson-Darling test, $A^2 = 12.44$, with a p-value < 0.005 (Figure 45). The

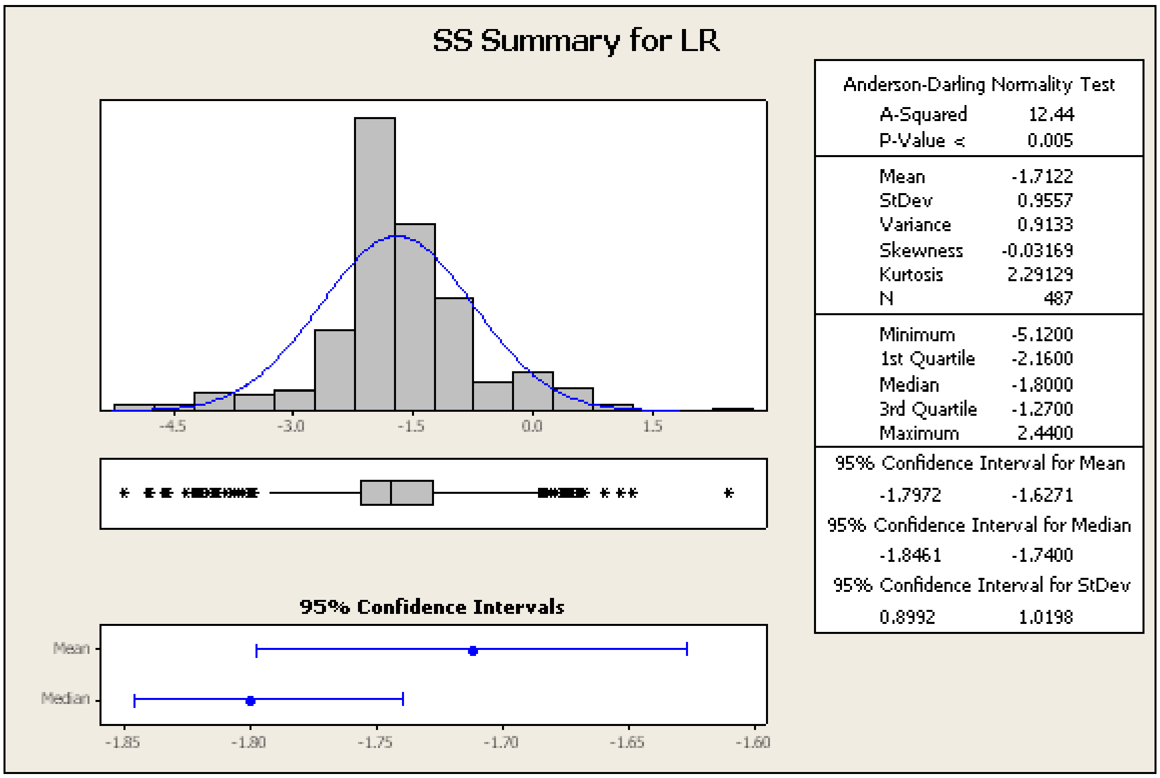

Figure 45. SS site summary statistics for linear regression rates.

95% confidence interval (CI) for the mean is -1.7972 to -1.6271. The chosen α was 0.05. Therefore, the null hypothesis was rejected in favor of the alternate hypothesis, i.e., that the linear regression rate of shoreline change data for the SS site are not normally distributed.

Using linear regression, the mean rate of shoreline change for this study site is -1.71 m/yr (-5.62 ft/yr). Within the SS site, West Tisbury has the highest rate of shoreline change at -2.15 m/yr (-7.05 ft/yr), followed by Edgartown at -1.75 m/yr (-5.74 ft/yr), and Chilmark at -1.5 m/yr (-4.92 ft/yr). Interestingly, since 1955 (ERA03), erosion has decreased in Chilmark by 47% (Table 12).

Location	ERA01 m/yr	ERA02 m/yr	ERA03 m/yr	ERA04 m/yr	ERA01-04 m/yr	LR m/yr	ERA01-04 mean Dist.
SS	0.05	-1.21	-1.51	-1.21	-1.57	-1.71	-123.80
Chilmark	0.11	-1.68	-1.79	-0.87	-1.33	-1.50	-151.63
Edgartown	0.00	-0.01	-1.26	-1.24	-1.65	-1.75	-49.70
W. Tisbury	0.00	-2.51	-1.35	-1.99	-1.95	-2.15	-207.81

Table 12. SS site linear regression rates of shoreline change.

The far western transects, near Lucy Vincent Beach, indicate equilibrium, while the remaining beach areas, to the east, indicate erosion, based on linear regression results (Figure 46). Coastal areas fronting Jobs Neck Ponds, Jacobs Pond, and Crackatuxet Pond, in Edgartown, indicate a mix of erosion, equilibrium, and accretion. This is the only stretch along the SS shoreline that has any accretion (Figure 44, Figure 47).

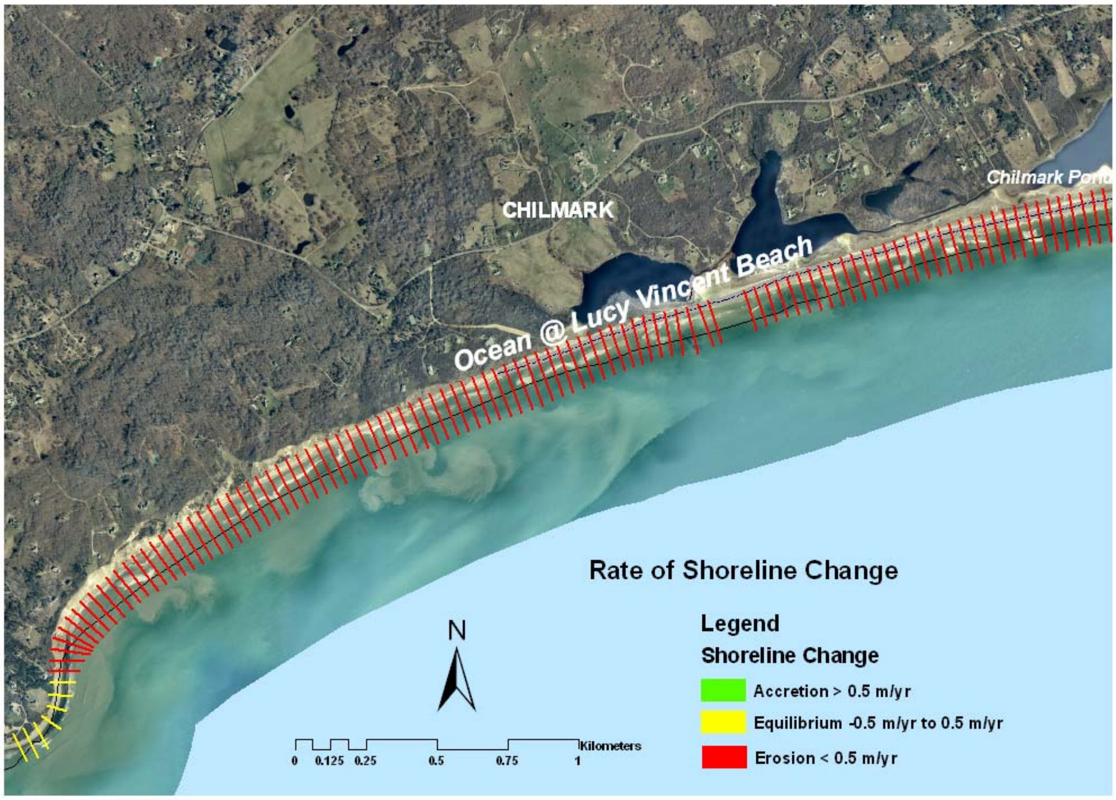

Figure 46. Shoreline change patterns near Lucy Vincent Beach.

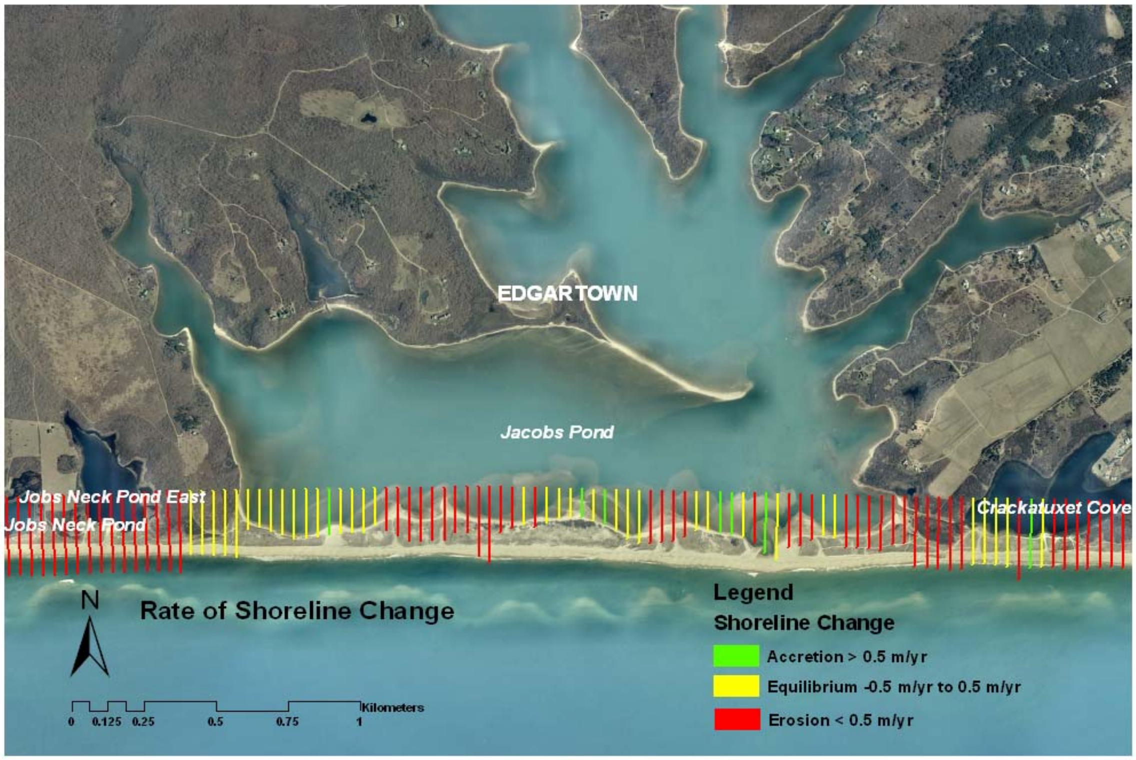

Figure 47. Erratic shoreline change patterns along the south side of Martha's Vineyard, near Jobs Ponds and Jacobs Pond.

Based on shoreline linear regression rates of change, 90% of the SS transects (439) are eroding an average of -1.92 m/yr (-6.3 ft/yr), 8.5% (41) are in equilibrium at 0.004 m/yr (0.16 in/yr), and 1.5 % (7) are accreting at 1.06 m/yr (3.48 ft/yr) (Figure 48; data not shown).

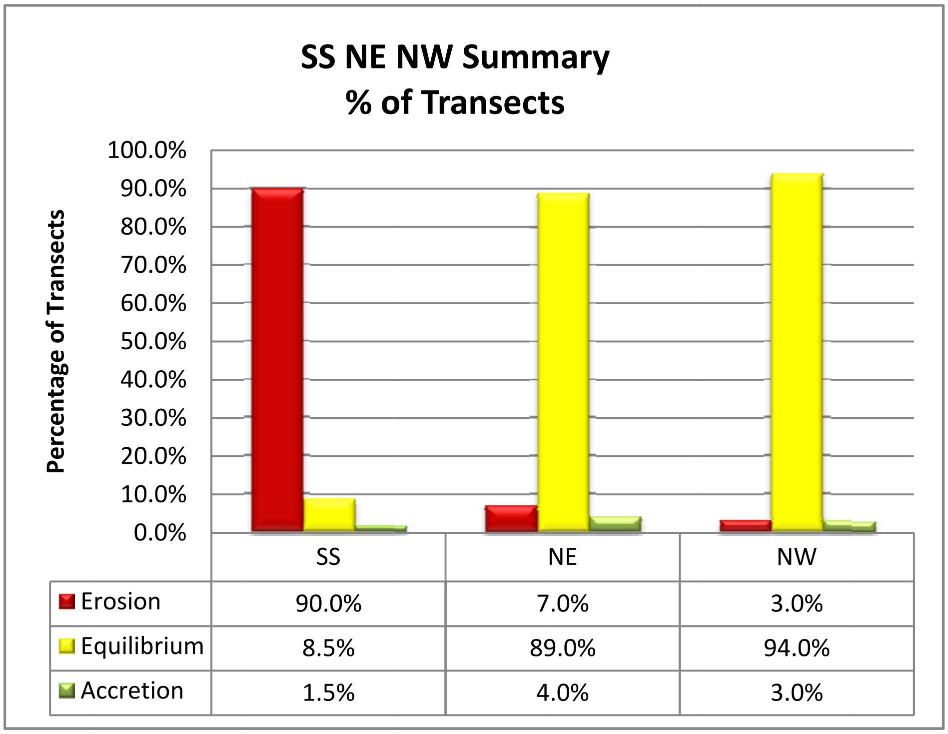

Figure 48. SS, NE, NE sites summary statistics of the percentage of transects that are either eroding, accreting, or in equilibrium.

The SS study site eroded for all 4 time periods, for a total shoreline loss of 60.29 km (37.46 miles), with a mean transect loss of -123.8 m (-406 ft) (Figure 49). This translates to 2.6 km^2 (1.04 miles^2) of land lost, calculated as follows:

$$\left(\frac{-60.29\ km}{487}\right) = -0.124\ km * 21\ km = -2.6\ km^2$$

$$\left(\frac{-37.46\ miles}{487}\right) = -0.08\ miles * 13\ miles = -1.04\ miles^2$$

During the first time period, Era 01, accreted at a rate of 0.05 m/yr. After that, the shoreline eroded in all time periods. During Era 03, the south side of Martha's Vineyard had the highest rate of erosion, -1.51 m/yr, while the rate of erosion remained the same in Era 02 and Era 04 (-1.21 m/yr) (Figure 49).

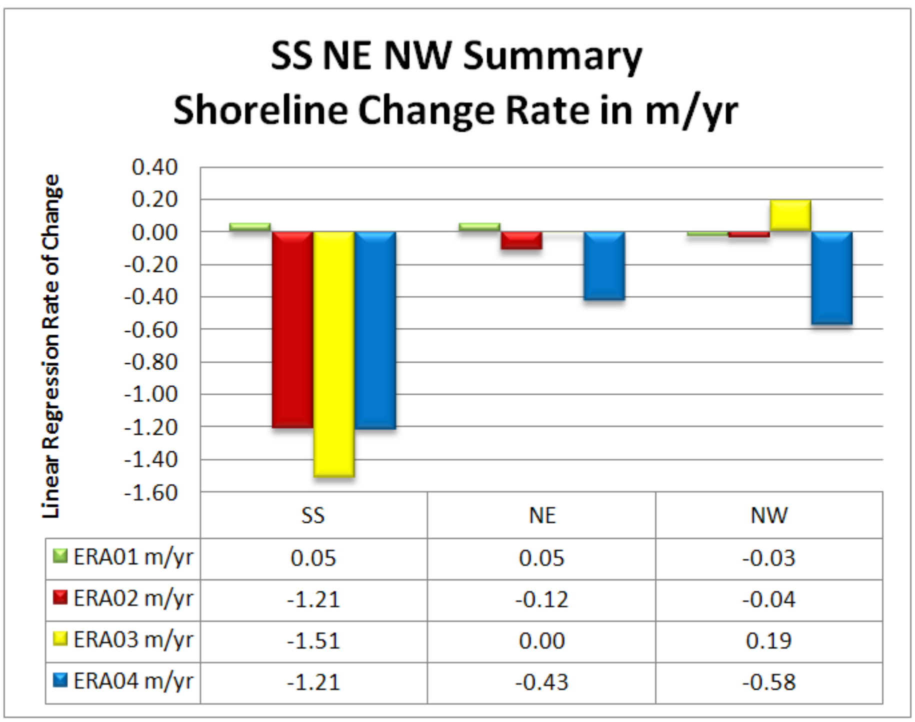

Figure 49. SS, NE, NW sites summary by shoreline change and era, LR rate of change.

NE Historic Erosion. Of the 487 transects in the NE study site, data was available for 39% (192) in ERA01 (1846-1897), 87% (424) in ERA02 (1846-1955; 77% of these transects fell within 58 years), 59% (287) in ERA03 (1955-1978), and 98% (477) in ERA04 (1955-1994) (data not shown).

As above, to test for a normal distribution of the shoreline rate of change, I converted the LR rate to a z-score, with $\mu = 0$, and $\sigma = 1$. Using the Anderson-Darling test, $A^2 = 15.05$, with a p-value < 0.005 and the 95% confidence interval (CI) for the mean is -0.13883 to -0.07152 (Figure 50). The chosen α was 0.05 and the null hypothesis was, therefore, rejected in favor of the alternate hypothesis, i.e., that the NE linear regression rate of shoreline change data are not normally distributed.

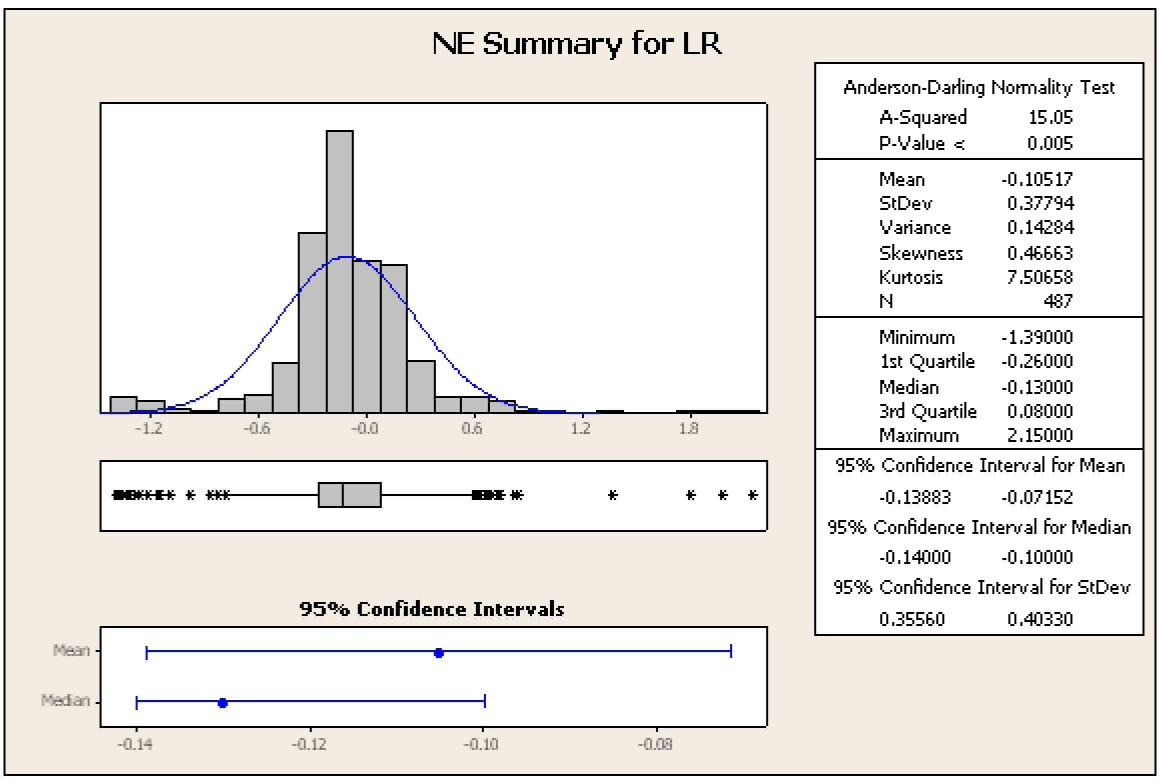

Figure 50. NE site summary statistics for linear regression rates.

Using linear regression, the rate of shoreline change for the NE study site is -0.11 m/yr (4.3 in) (Table 13), with a standard deviation of 0.37794 (Figure 50). Within this site, Oak Bluffs has the highest shoreline erosion rate at -0.19 m/yr (2 ft) and Edgartown has -0.01 m/yr (~1 in) (Table 13).

Location	ERA01 m/yr	ERA02 m/yr	ERA03 m/yr	ERA04 m/yr	ERA01-04 m/yr	LR m/yr	ERA01-04 mean Dist.
NE	0.05	-0.12	0.00	-0.43	-0.12	-0.11	-12.84
Edgartown	0.04	0.10	-0.07	-0.42	-0.09	-0.01	-3.52
Oak Bluffs	0.05	-0.31	0.06	-0.43	-0.16	-0.19	-21.38

Table 13. NE site linear regression rates of shoreline change.

A significant area of erosion at the NE study site is located east of Farm Pond, in Oak Bluffs (Figure 51). Transects that are eroding are indicated in red, transects that are in equilibrium are in yellow, and transects that are accreting are in green. The transects in yellow are located near jetties, while the areas in red are located south of the jetties (Figure 51). The coastal sediment moves from north to south along this portion of the coastline, thereby trapping the sand at the jetties, while starving the beaches downdrift.

Within the NE site, there two beaches accreting. The first is along Joseph Sylvia State Beach, in Oak Bluffs, at the entrance of Sengekontacket Pond (Figure 52A). A close up view (Figure 52B) clearly shows a large jetty that is holding the sand at this beach. The other is located at Fuller Street Beach and the entrance of Edgartown Harbor (Figure 53A). It is interesting to note the accretion of beach area around Edgartown Harbor Light, as shown in Figure 53B. In the late 1800's to early 1900's, Edgartown Harbor Light was in the water at the entrance to the harbor. The historical map images were obtained by MA CZM from the Harvard Map Collection (MassGIS, 2008).

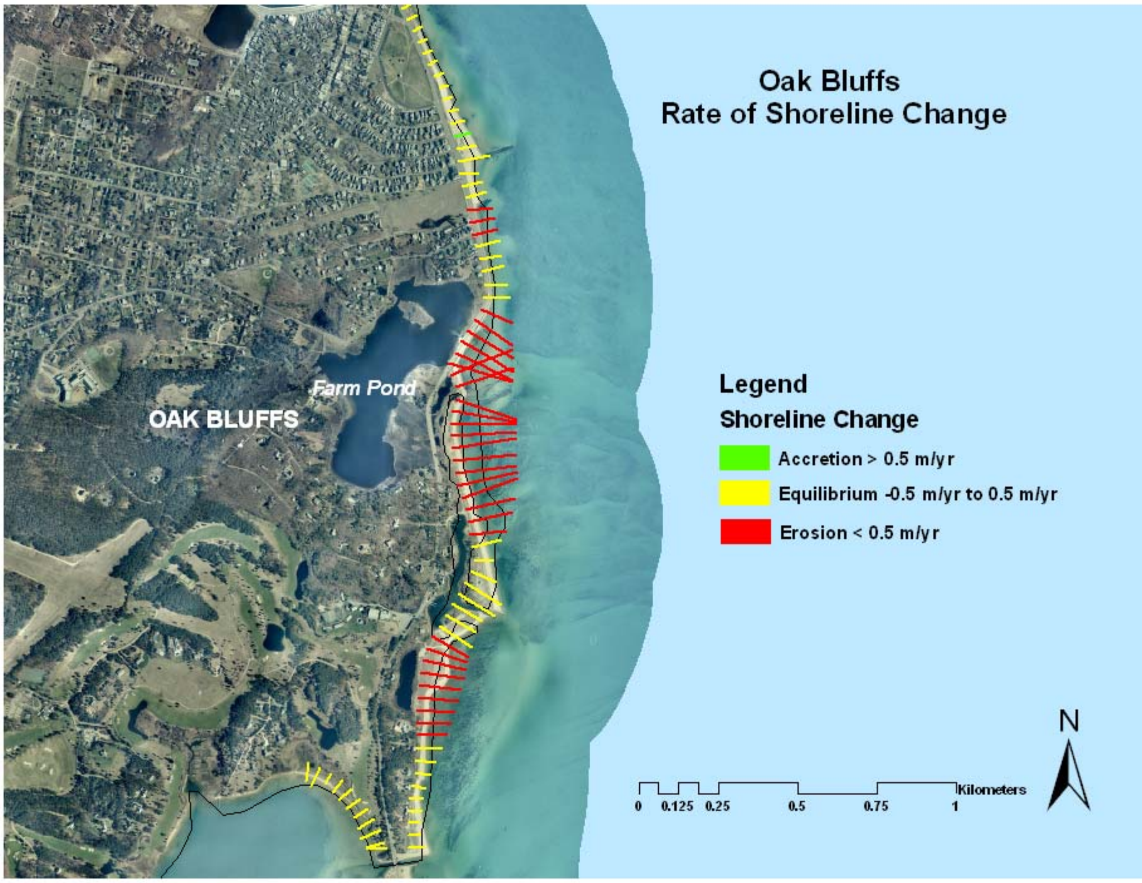

Figure 51. Significant erosion east of Farm Pond in Oak Bluffs.

Figure 52. Accretion on Joseph Sylvia State Beach, Oak Bluffs and Edgartown.

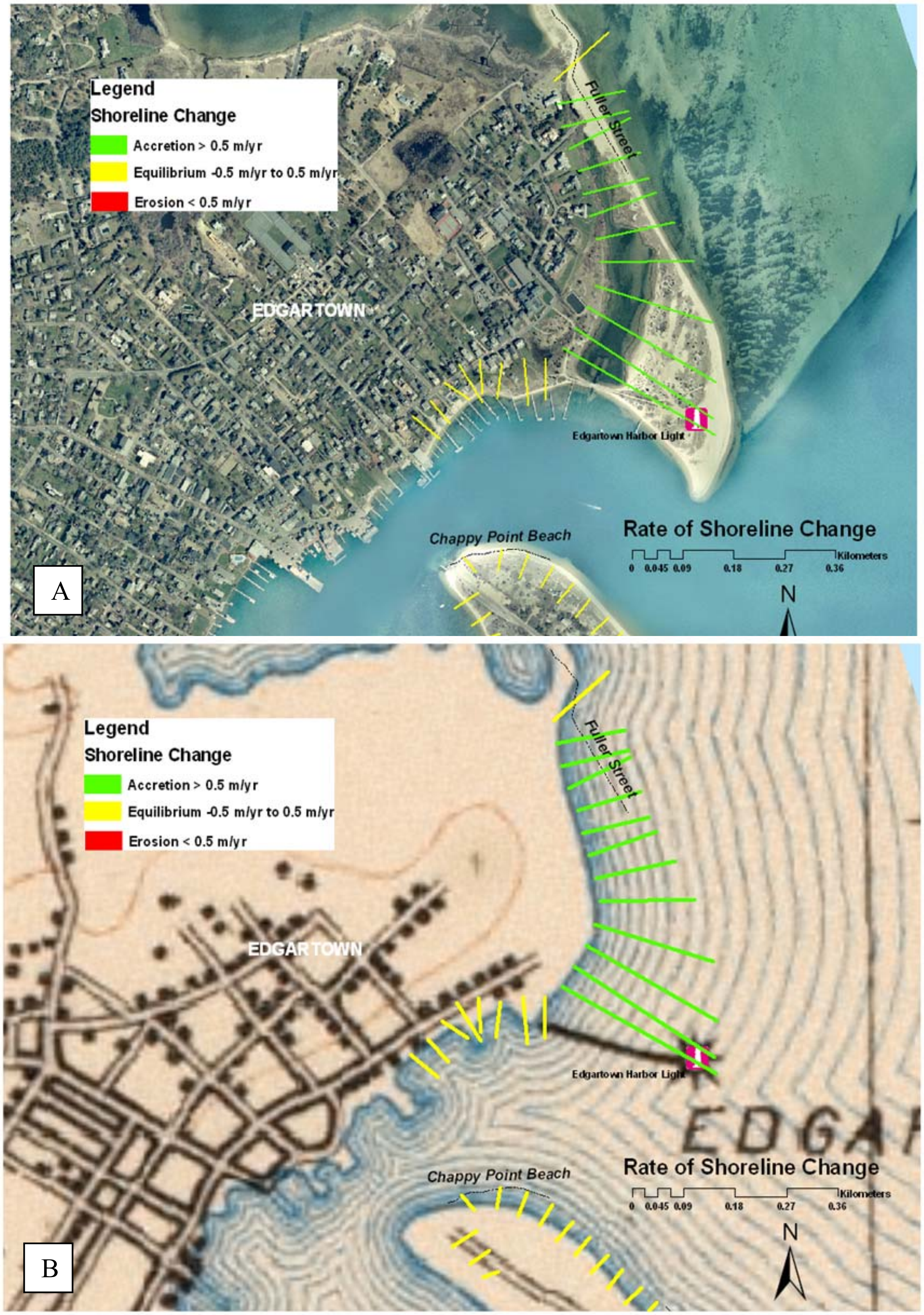

Figure 53. Shoreline changes at the entrance of Edgartown Harbor (A) 2001; (B) 1890s.

Based on shoreline linear regression rates of change, 89% of the transects (432) within the NE site are in equilibrium, with a rate of change of -0.09 m/yr (-3.5 in/yr) (data not shown), 7% (34) of the transects are eroding at -0.94 m/yr (-37 in/yr) (data not shown), and only 4% (21) of the transects are accreting, at a rate of 0.89 m/yr (35 in/yr) (Figure 48; data not shown). For all four time periods, the NE study site had a total erosion of -6.25 km (3.89 miles) of shoreline, with a mean transect loss of -12.84 m (-42.13 ft) (Table 13). This translates to 0.2249 km^2 (0.086 $miles^2$) of land lost.

$$\left(\frac{-6.25\ km}{487}\right) = -0.01284\ km * 17.3\ km = -0.222\ km^2$$

$$\left(\frac{-3.89\ miles}{487}\right) = -0.008\ miles * 10.75\ miles = -0.086\ miles^2$$

NW Historic Erosion. Of the 487 transects in the NW study site, data was available for 72% (352) in ERA01 (1845-1888), 99.5% (485) in ERA02 (1888-1955; however, 117 [24%] of those are from 1897), 64% (310) in ERA03 (1955-1979; although there are 2 transects that have data that range from 1888-1979), and 100% (487) in ERA04 (1955-1994; with 36% from 1955-1994 and 64% from 1979-1994) (Table 9).

As above, to test for a normal distribution of the shoreline rate of change, I converted the LR rate to a z-score, with $\mu = 0$, and $\sigma = 1$. Using the Anderson-Darling test, $A^2 = 10.37$, with a p-value < 0.005. The 95% confidence interval (CI) for the mean is -0.119571 to -0.073899 (Figure 54). The chosen α was 0.05, and the null hypothesis was, therefore, rejected in favor of the alternate hypothesis, i.e., that the linear regression rate of shoreline change data for the NW site are not normally distributed.

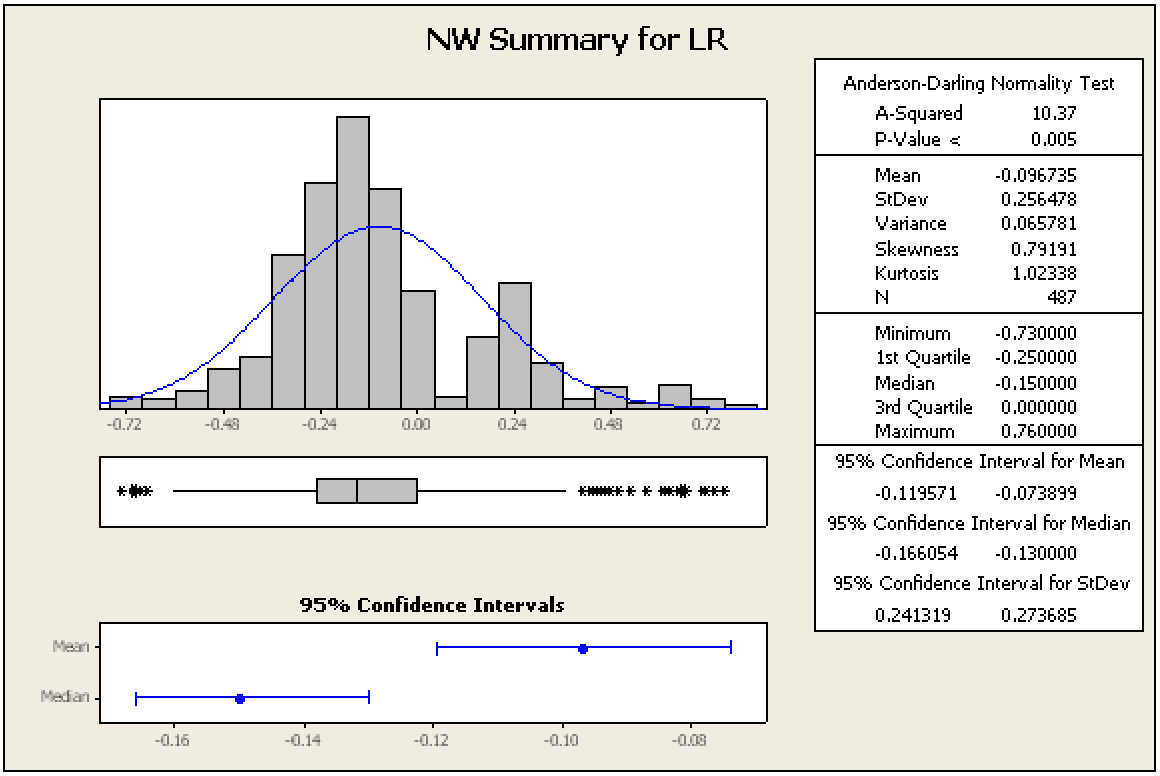

Figure 54. NW site summary statistics for linear regression rates.

The NW study site has one area of accretion located at Lobsterville Beach in Aquinnah **(Figure 55A)** and one side that is eroding, northeast of Cape Higgon, near Paint Mill Brook in Chilmark **(Figure 55B).**

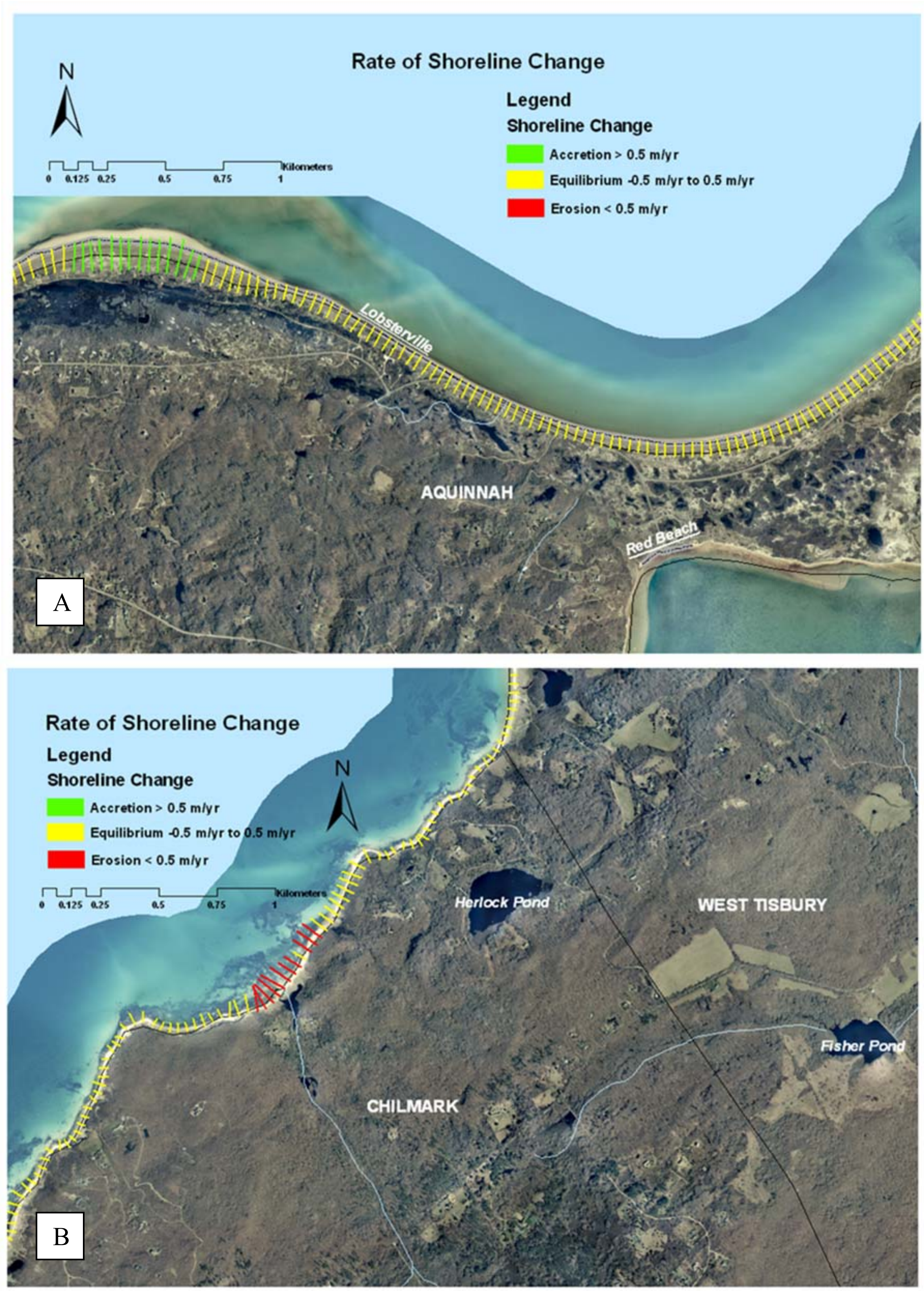

Figure 55. Accretion (A) and Erosion (B) at the NW study site.

Linear regression analysis of the data indicated that the rate of shoreline change for the NW study site is -0.1 m/yr (-4 in/yr) (Table 14), with a standard deviation of 0.256478 (Figure 54). Chilmark had the highest shoreline erosion rate at -0.24 m/yr (-9 in/yr), followed by West Tisbury with -0.17 m/yr (-7 in/yr). Aquinnah was the only town showing shoreline accretion (0.21 m/yr [8 in/yr]) (Table 14).

Location	ERA01 m/yr	ERA02 m/yr	ERA03 m/yr	ERA04 m/yr	ERA01-04 m/yr	LR m/yr	ERA01-04 mean Dist.
NW	-0.03	-0.04	0.19	-0.58	-0.11	-0.10	-16.62
Chilmark	-0.09	-0.16	0.28	-1.45	-0.36	-0.24	-46.05
Aquinnah	0.02	0.18	0.24	0.38	0.21	0.17	24.74
W. Tisbury	0.01	-0.09	0.00	-0.31	-0.10	-0.17	-17.60

Table 14. NW site linear regression rates of shoreline change.

Based on shoreline linear regression rates of change, 94% (458) (Figure 48) of the NW transects are in equilibrium, with a rate of change of -0.1 m/yr (4 in/yr) (data not shown). Three percent of the transects (15) are eroding at a rate of -0.62 m/yr (-24 in/yr) (data not shown), and another 3% (14) are accreting at a rate of 0.66 m/yr (26 in/yr) (data not shown). Overall, the NW study site eroded during ERA01, ERA02, and ERA04. NW ERA03 was the only time period manifesting accretion, at any site (Figure 49). Total erosion for the NW shoreline was -8.09 km (-5.03 miles), with a mean transect loss of -16.62 m (-54.53 ft). This translates to 0.33 km^2 or 0.123 $miles^2$ of land lost calculated by the following:

$$\left(\frac{-8.09\ km}{487}\right) = -0.01662\ km * 19.855\ km = -0.33\ km^2$$

$$\left(\frac{-5.03\ miles}{487}\right) = -0.01\ miles * 12.34\ miles = -0.1234\ miles^2$$

Summary of the Study Sites. The south side of Martha's Vineyard (location of SS site) is in its most natural state, and the most protected by conservation organizations compared to the other sites, yet it had the most erosion. The -1.71 m/yr rate of shoreline change for the south side was higher than that of both the NW and NE sites (Table 15). Overall, the SS site lost 2.6 km^2 (1.04 miles^2) of land.

Study Site	Historical Erosion m/yr
SS	-1.71
NE	-0.11
NW	-0.10

Table 15. Summary of historical shoreline rate of change for each study site, from mid-1800's to 1994.

The NE study site lost only 0.2249 km^2 (0.086 miles^2) of land and, for the most part, appears to be in equilibrium, with a shoreline change rate of -0.11 m/yr (Table 15). The NE study site has the most coastline jetties and groins of the three sites, suggesting that they may play a role in this modest rate of change. However, the NW study site has very few jetties and groins compared to the NE, but, for the most part, also appears to be in equilibrium, with a rate of -0.11 m/yr (Table 15). The NW lost slightly more land area (0.33 km^2 [0.123 miles^2]) than the NE.

The SS study site has 90% of its transects eroding whereas the NE has 7% and the NW has 3% (Figure 48). The NW and NE sites have large percentages of their transects that are in equilibrium (94% and 89%, respectively), while the SS only has 8.5%. The NE has the highest accretion, albeit very minor, at 4%, while the NW has 3%, and the SS has 1.5%.

The highest rate of shoreline erosion (-1.51 m/yr) occurred at the SS site during ERA03 (Table 15). During that same time frame, the NW had the highest accretion rate (0.19 m/yr) of the entire study period. By ERA04, all transects were eroding with a mean shoreline change of -1.21 m/yr for the SS, -0.43 m/yr for the NE, and -0.58 m/yr for the NW. Finally, the SS site has had the most consistent shoreline erosion patterns since ERA02, yet its rate of erosion decreased by 20% during ERA04.

Sea Level Change

Historical and Projected Sea Level Changes in the Proximity of Martha's Vineyard

Data from several monitoring stations located near Martha's Vineyard was used to derive rates of sea level rise (SLR) relevant to the island's coastlines. The scatterplot shown in Figure 56 uses 1930 to 2003 land-based data from the PSMSL (Permanent Service for Mean Sea Level) (2006) and depicts a steady rise of sea levels in Woods Hole (WH) (1930-2003), Nantucket (ACK) (1965-2003), Buzzards Bay (BB) (1956-1976), and at the entrance to the Cape Cod Canal (CC) (1956-1975).

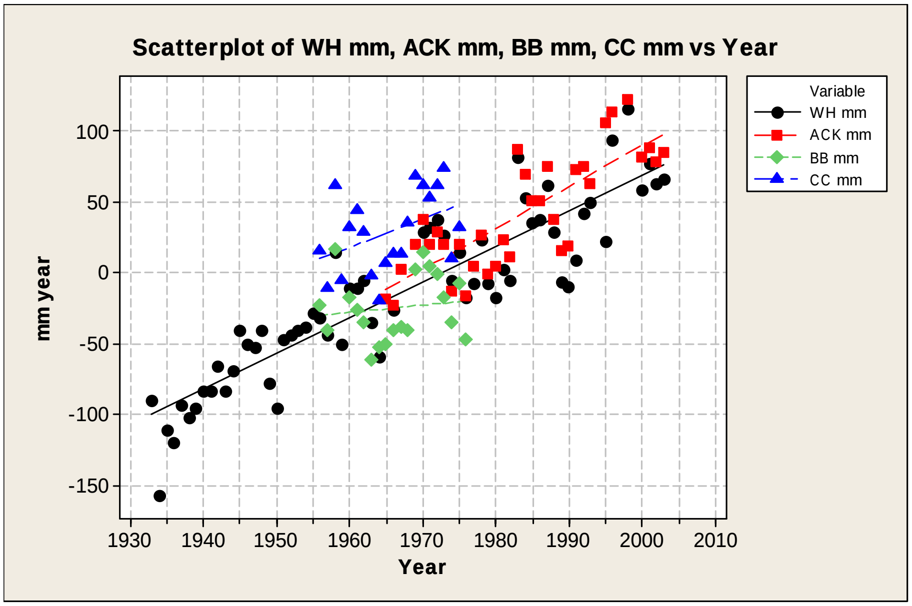

Figure 56. Scatterplot of sea level rise from 1930-2003 (Woods Hole [WH], Nantucket [ACK], Buzzards Bay [BB], and the Cape Cod Canal [CC]).

Using linear trend analysis of the 1933 to 2003 data for Woods Hole (with no data for 1965, and 1967-1969), the fitted trend yields a rate of sea level rise of 2.56 mm/yr (0.1 in/yr) (Figure 57A). Linear regression analysis showed a rate of 2.51 mm/yr (0.099 in/yr) (Figure 57B); R^2 adj is 80.6%, p-value is 0.0. These rates are relatively close to that reported by NOAA for the 1932 to 1999 time frame (NOAA, 2005d). NOAA's measurements yielded a monthly mean sea level trend of 2.59 mm/yr (0.85 ft/century), with a standard error of 0.12 mm/yr. Interestingly, linear regression analysis of the Woods Hole data from 1933 to 1964 indicates a higher than expected SLR of 3.24 mm/yr (0.13 in/yr) (Figure 58A), and a lower than expected trend, from 1966 to 2003 (no data for 1965), of 2.078 mm/yr (0.08 in/yr) (Figure 58B).

Linear trend analysis of the Nantucket data from 1965 to 2003 (1968 data missing) yielded a rate of sea level rise of 3.08 mm/yr (0.12 in/yr) (Figure 59A). Linear regression analysis of the data yielded a rate of 2.90 mm/yr (Figure 59B) (0.11 in/yr, R^2 adj is 63.7%, p-value is 0.0). Both values are relatively close to the Nantucket mean sea level trend reported by NOAA (3 mm/yr; 0.98 ft/century; standard error = 0.32 mm/yr), based on monthly data from 1965 to 1999 (NOAA, 2005d).

My results for Woods Hole and Nantucket were slightly lower than NOAA's, an observation consistent with the fact that when I looked at SLR rates from 1965 to 2003, sea levels were not rising as quickly as compared to 1933 to 1964. From 1965-2003, Woods Hole experienced a rise of 30 mm (1.18 in) and the waters around Nantucket rose 41 mm (1.6 in) (PSMSL, 2006).

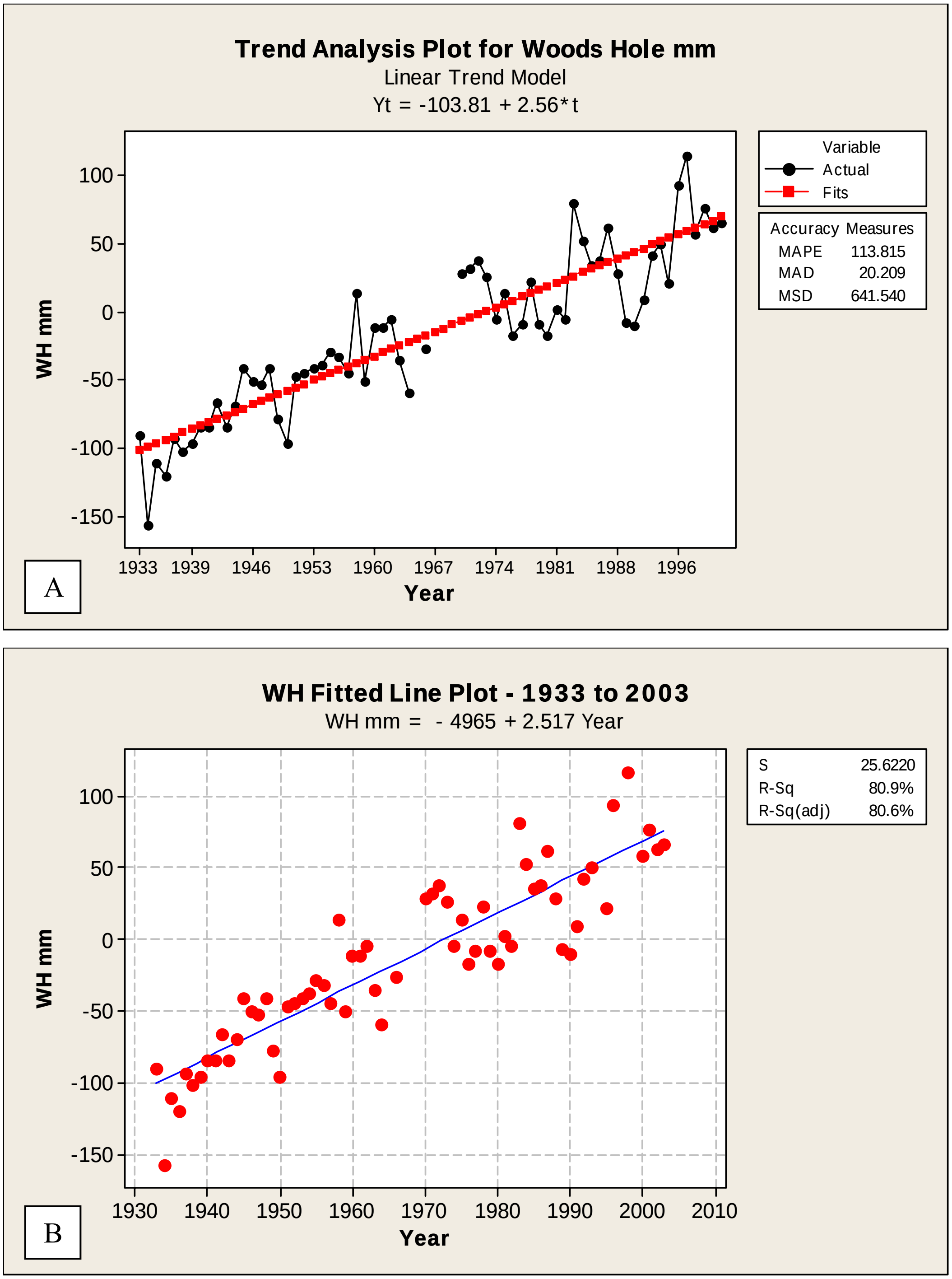

Figure 57. Sea level trend analysis plot (A) and regression analysis (B) near Woods Hole (1933-2003).

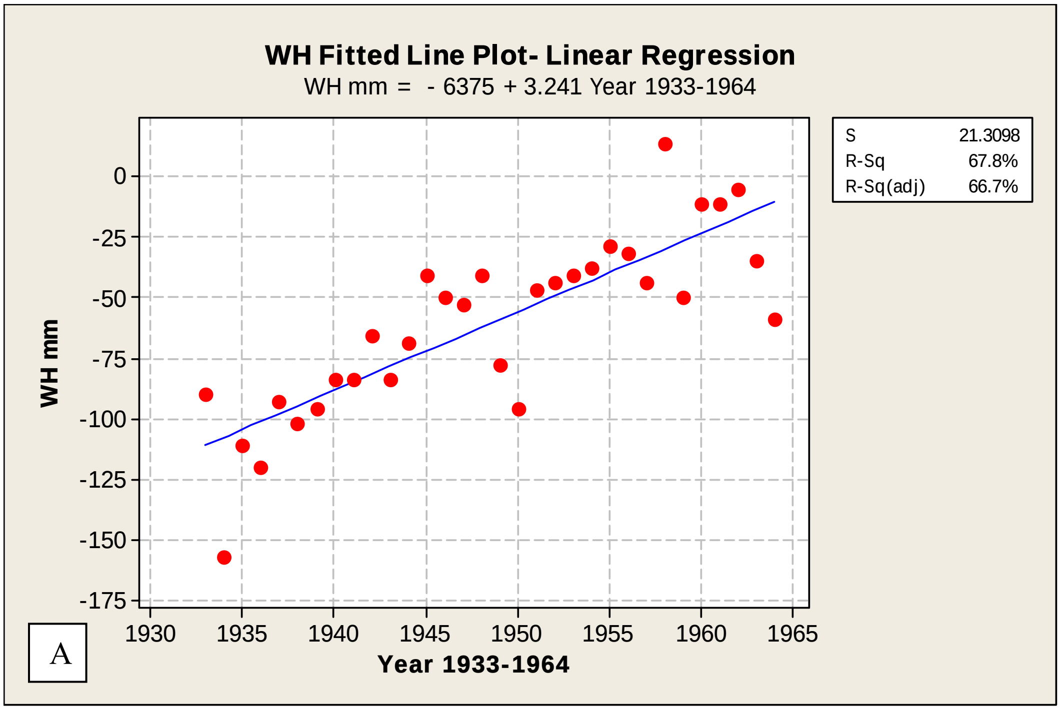

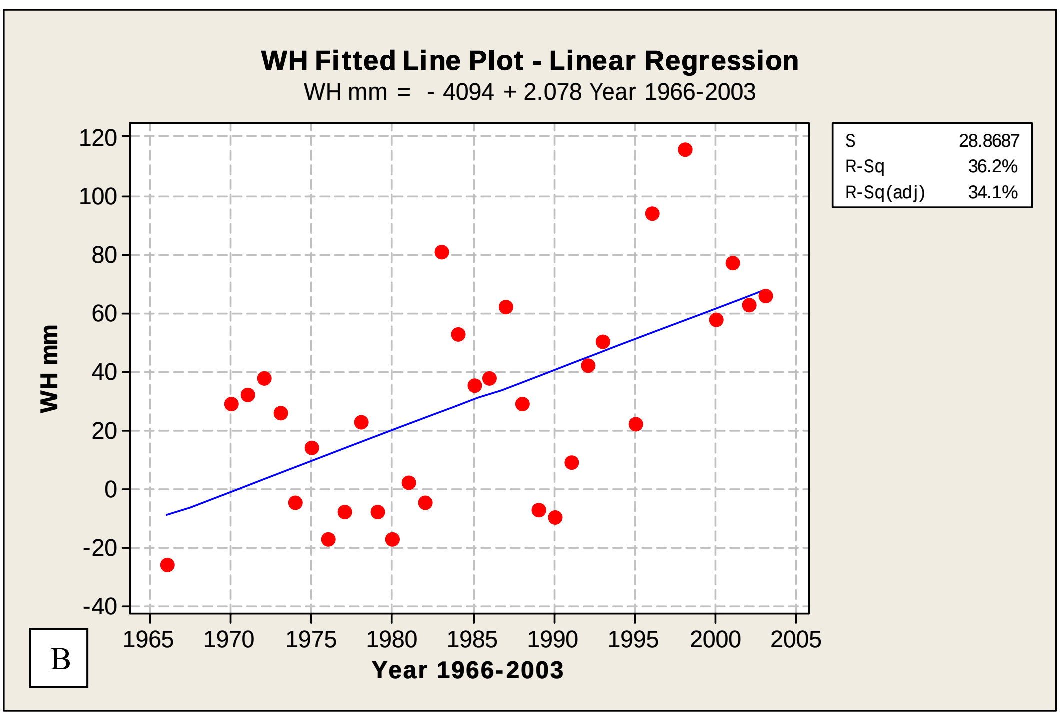

Figure 58. Rate of sea level rise from 1933-1964 (A) and from 1966-2003 (B) near Woods Hole.

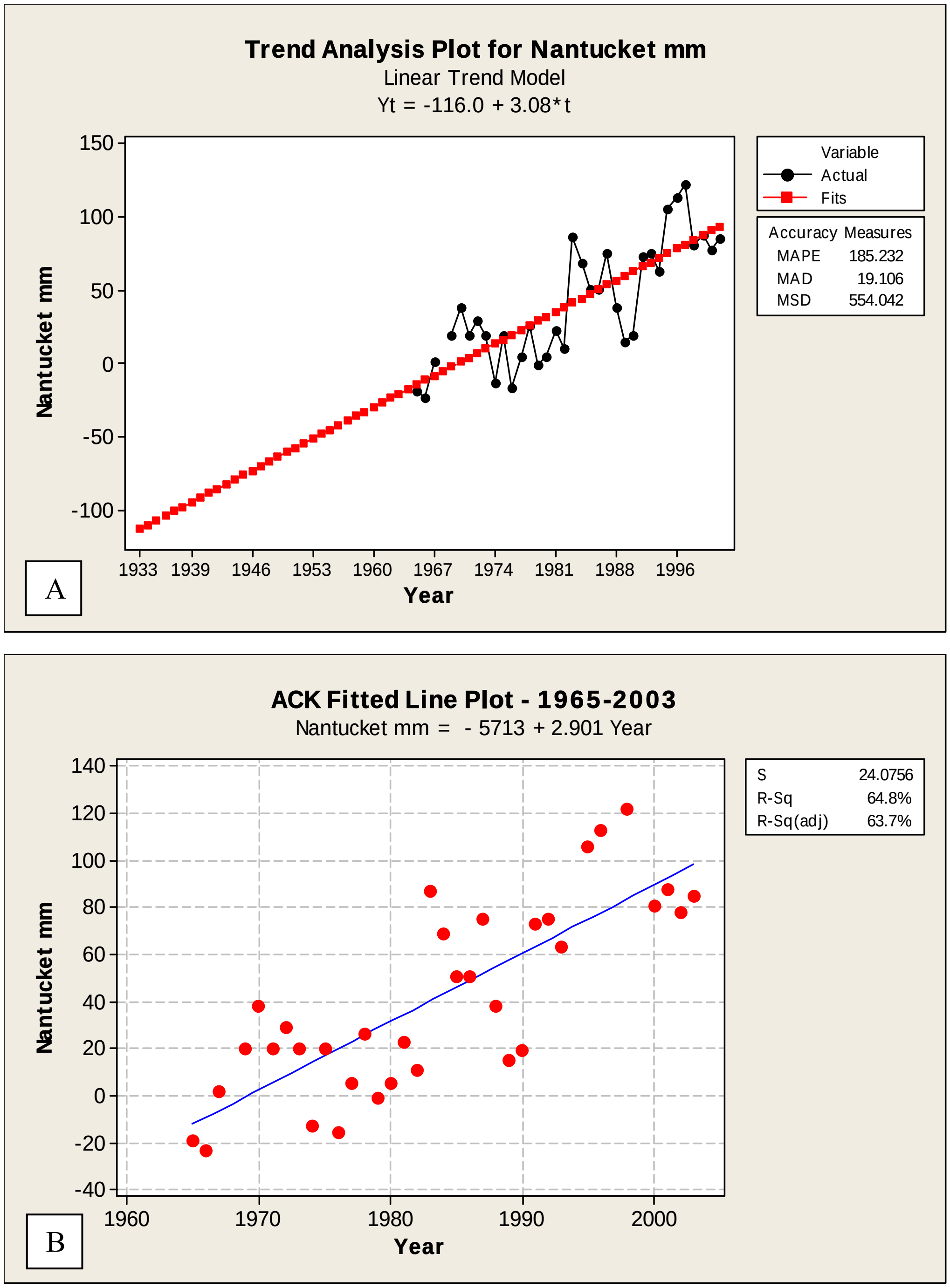

Figure 59. Trend analysis of the rate of sea level rise (A) and linear regression (B) near Nantucket from 1965-2003.

Linear and exponential trend analyses of these historical sea level data were then used to derive three scenarios of future SLR near Martha's Vineyard. A fourth scenario was derived from IPCC 2006 data. The first scenario (MV Linear) was based on the results from the waters near Nantucket (0.003 m/yr; 0.01 ft/yr). This scenario provides an extremely conservative estimate because it assumes that, for the next 100 years, the rate of sea level rise mimics the last 100 years, with no significant increase in global temperatures, nor any compensatory effects of eustatic and/or steric components to alter the ocean levels. While these may be unrealistic assumptions, the calculation does provide a baseline from which to begin an analysis. The results from this method indicate that the seas around MV will rise by another 0.3 m (1 ft) in 100 years Table 16, Figure 60).

The second scenario starts with the MV Linear results and applies an exponential growth curve model ($Yt = \beta_0 * \beta_1^t * e_t$) or ($Y_t = 0.00 * (2.804t)$) to estimate the rate of sea level rise (A Exponential) (Table 16, Figure 60). The results in this scenario (0.58 m by 2100) closely approximate that of the third scenario, namely the IPCC projections (0.59 m; 1.94 ft by 2100 (Table 16, Figure 61). The fourth scenario used the same exponential growth curve ($Yt = \beta_0 * \beta_1^t * e_t$) or ($Y_t = 0.00*(3.78**t)$) (B exponential) inherent to the IPCC projections and indicated that seas will rise by 1.14 m (3.74 ft) by 2100, a value almost twofold higher than the original IPCC projections (Table 16, Figure 61).

Having obtained evidence that segments of the Martha's Vineyard coastline are eroding, and that the island's coastal waters are rising, I then sought to evaluate the geophysical parameters that might influence the effects of SLR on erosion. The next sections address these parameters.

YEAR	#1 - MV LINEAR	#2 - A EXPONENTIAL	#3 - IPCC PROJECTIONS	#4 - B EXPONENTIAL
2000	0.003	0.01	0.003	0.00876
2025	0.075	0.027	0.075	0.03
2050	0.15	0.074	0.2	0.01
2075	0.225	0.21	0.375	0.34
2100	0.3	0.58	0.59	1.14

Table 16. Historical and projected sea level rise in meters.

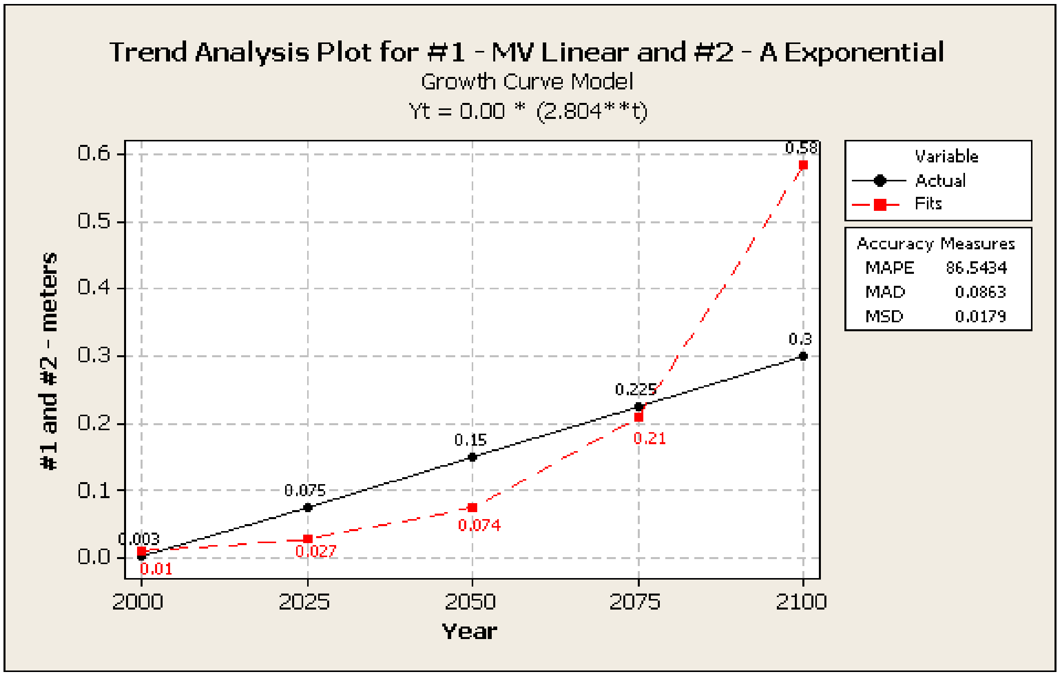

Figure 60. Trend analysis plot for scenarios #1 and #2.

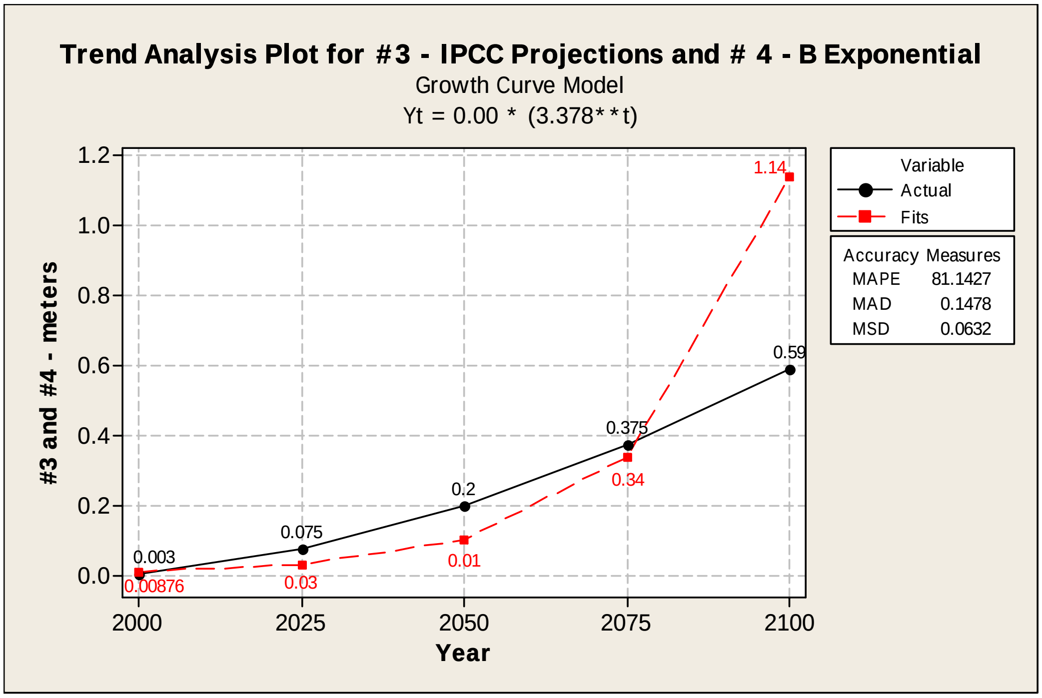

Figure 61. Trend analysis plot for scenarios #3 and #4.

Depth of Closure (for Bruun's Rule)

Figure 62 shows an estimated depth of closure for Martha's Vineyard, the -20 m (-66 ft) contour line. The average distance to this contour line from the SS site is approximately 4 km (2.5 miles). From the NE site, the distance to the contour line is 10 km (6 miles), and from the NW site it drops off quickly within 1 km (0.62 miles). Using Pythagorean's Theorem, the slope on the SS site is 0.005 (0.5%) and the angle is 0.286°; the NE site's slope is 0.002 (0.2%) and the angle is 0.11°; and the NW site's slope is 0.02 (2%), with an angle of 1.15°. The NW site is thus the steepest of the three study sites.

As the distance increases from the -20 m contour line, the slope and angle remains low, even when the -300 m depth range is reached at 150 km from the SS study site (Figure 63); this translates into a slope of 0.002 (0.2%) with an angle of 0.11°.

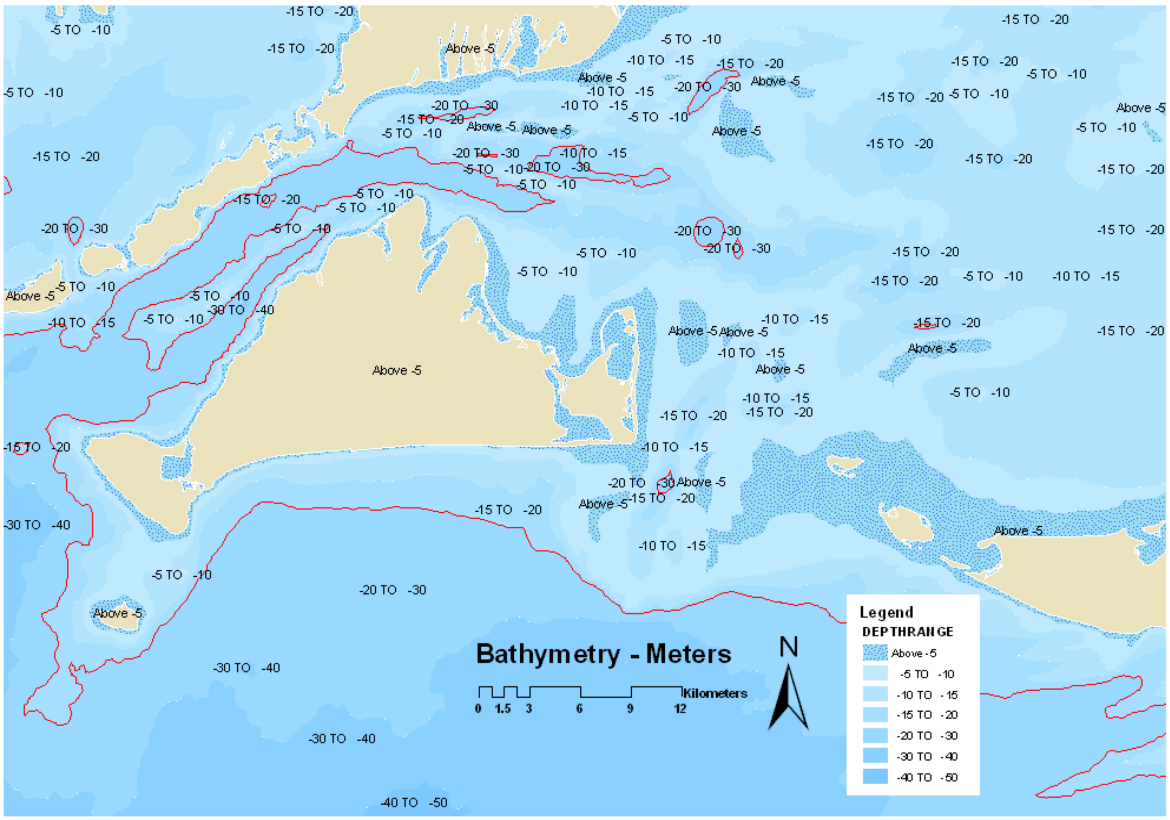

Figure 62. Bathymetry and estimated depth of closure for Martha's Vineyard.

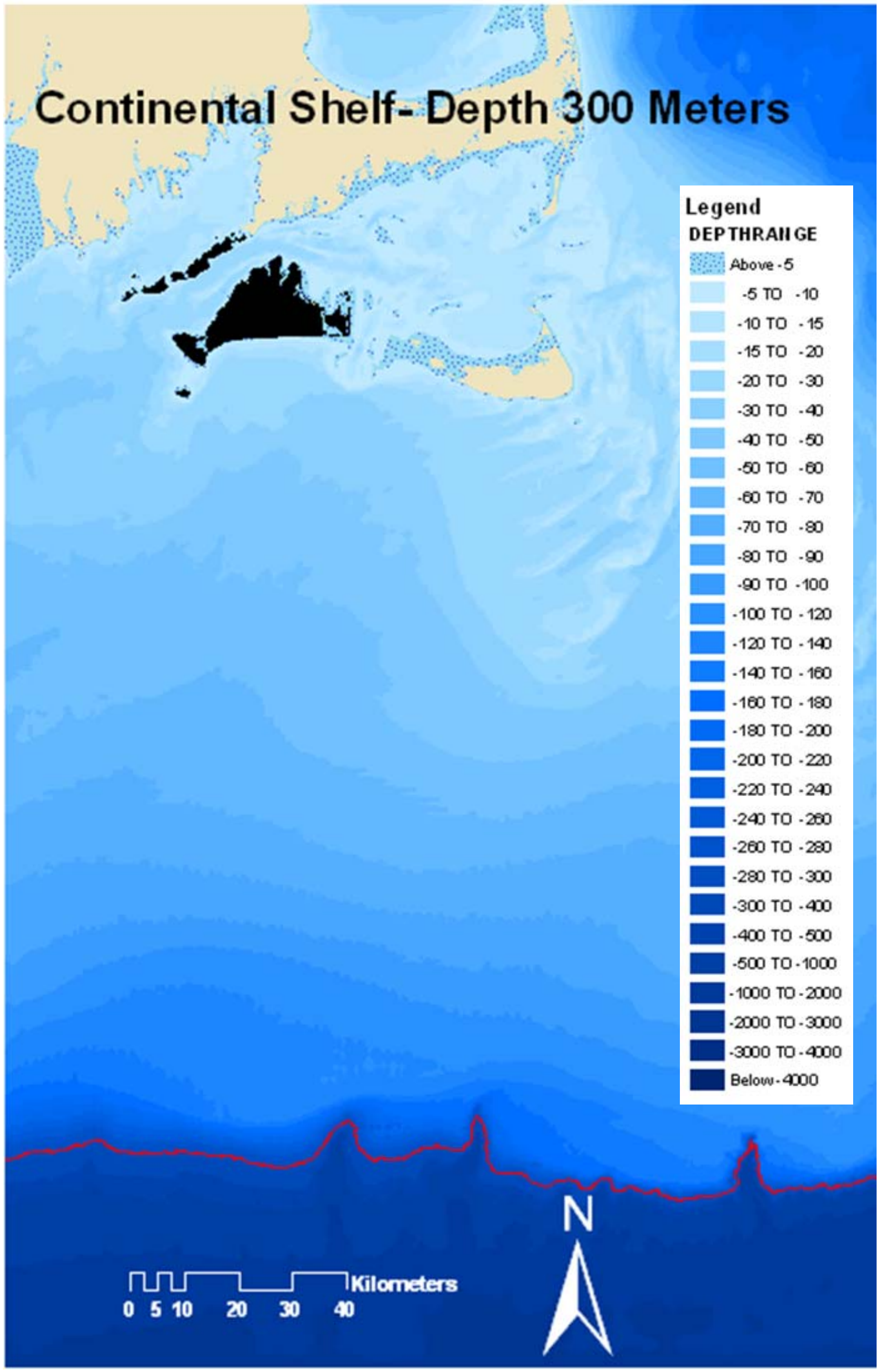

Figure 63. Continental shelf off the coast of Martha's Vineyard.

Coastal Retreat Based on the Bruun Rule

Bruun's shoreline recession model solves for short-term erosion along coastlines based on an equilibrium profile (Bruun, 1962). While there is some debate in the scientific community about its usefulness, it is nevertheless used as a reference for study of erosion patterns. Bruun's model is useful in situations where coastlines are relatively sandy and easily erodible, as opposed to rocky shorelines. Application of the rule assumes that the shoreline profile is in equilibrium and that there is sufficient wave energy to erode, transport, and redistribute sediments over the profile. The original model does not include longshore drift. Based on these standard criteria, Martha's Vineyard is an appropriate location to test Bruun's model, except for one item. The NE and NW study sites do not face the open ocean and the continental shelf. Rather, these two study sites respectively face the Elizabeth Island chain and Cape Cod.

Using Bruun's methodology as a basis for determining coastal retreat on sandy shorelines, my results indicate that the SS study site does not fit the predicted ratio for the rate of erosion vs. SLR, while the data for the NE and NW study sites are within close proximity of the ratio. For the SS site, the ratio is ~ 1:567, meaning that for every meter (3.28 ft) of SLR, the shoreline would theoretically retreat by 567 m (1860 ft) (Table 17). This result exceeds Bruun's ratio more than fivefold. The ratio for the shoreline of the NE site is 1:40, suggesting that this shoreline would retreat by ~ 40 m (131 ft) for every meter of SLR. These results parallel those of the NW study site which yield a ratio of 1:37, i.e., a shoreline retreat of ~ 37 m (121 ft) for each meter of SLR. The latter data indicate that the NE and NW study sites are eroding less than the Bruun model predicts.

Study Site	Historical Erosion/yr (m)	Historial SLR/yr (m)	Bruun's Ratio
SS	-1.71	0.003	1:566.66
NE	-0.1052	0.0026	1:40.46
NW	-0.0967	0.0026	1:37.2

Table 17. Results for each study site based upon Bruun's ratio.

To project shoreline retreat through 2100, I incorporated the ratios derived from the three study sites on Martha's Vineyard. Based upon SLR projections from the Results section "Historical and Projected Sea Level Changes in the Proximity of Martha's Vineyard," three scenarios were considered for the 100 year period: 1) SLR maintains a linear trend near MV at 0.003 m/yr on the south side and 0.0026 on the NE and NW sides; 2) SLR will proceed at IPCC projected rates near MV, beginning at 0.003 m/yr and ending at 0.59 m/yr; and 3) SLR will proceed exponentially near MV, at a rate derived from the IPCC projections. This set of scenarios eliminates scenario #2 used earlier from Table 16.

Using the first scenario, the amount of shoreline retreat at the SS site would range from 42.5 m in 25 years to 170 m in 100 years (139.44 ft to 577.74 ft). The NE site would retreat significantly less, with ranges from 2.63 m in 25 years to 10.52 m in 100 years (8.63 ft to 34.51 ft), and the NW site would approximate the NE study site, from 2.42 m to 9.67 m (7.94 ft to 31.73 ft) (Table 18).

Using the second scenario, the SS study site would retreat approximately 42.5 m in 25 years (similar to the linear trend model) then increase to 334.33 m by 100 years (139.44 ft to 1096.88 ft) (Table 18). The NE study site would experience 3.03 m to 23.87 m (9.94 ft to 78.31 ft) of shoreline retreat and the NW site would experience 2.79 m to 21.95 m (9.15 ft to 72.01 ft) of retreat in the same time periods.

Scenario #1	25 years	50 years	75 years	100 years
SS	42.5	84.99	127.5	170
NE	2.63	5.26	7.89	10.52
NW	2.42	4.84	7.25	9.67

Scenario #2	25 years	50 years	75 years	100 years
SS	42.5	113.33	212.5	334.33
NE	3.03	8.09	15.17	23.87
NW	2.79	7.44	13.95	21.95

Scenario #3	25 years	50 years	75 years	100 years
SS	17.00	5.67	192.66	645.99
NE	1.21	0.40	13.76	46.12
NW	1.12	0.37	12.65	42.41

Table 18. Projected shoreline erosion based upon three scenarios for sea level rise.

In the third scenario, sea levels could increase by approximately 1.14 m (4 ft) in 100 years and the last 25 years of the century would witness the most significant shoreline retreat (Table 18). By 2100, estimates indicate that the SS site would retreat by approximately 646 m (2119.42 ft), the NE by 46 m (150.92 ft), and the NW by 42 m (137.80 ft).

Overall, the projections for shoreline retreat on Martha's Vineyard suggest that the second scenario would promote approximately twice the current rate of erosion, and that the third scenario would cause the shorelines to recede approximately fourfold further than they would at the current rate.

GIS Layers for Candidate Predictor Variables

Soil Taxonomy, Texture, and Ternary Diagram

Coastal erosion studies historically have focused on sandy beaches, barrier beaches, marshes, and rocky shorelines. Martha's Vineyard has all these features. An understanding of soil types and their composition thus lays the foundation for further detailed analysis of the erosion process on Martha's Vineyard.

Using the modeling tools in ESRI® ArcGIS® v9.2, I supplemented the USDA tabular data with the following categories: soil taxonomy; soil texture; types of highly erodible land by water; and hydrologic groupings. This section summarizes the results obtained for the soils present on all of MV, including soil taxonomy, texture, and a ternary diagram based on Shepard's model. Soil specifics for each study site are described in the section entitled "Soil and Percent of Sand at Study Sites."

There are 60 classifications of soil on Martha's Vineyard, including the miscellaneous categories: beaches, urban land, pits, sand and gravel, and water (which, in turn, is subcharacterized into water [fresh], water ocean, and water saline). The remaining 54 soils, condensed into 18 major soil classifications, belong to five taxonomic groups: Entisols, Histols, Inceptisols, Spodosols, and Utisols (Fletcher & Roffinoli, 1986) (Table 19). (A complete description of each type of soil is presented in Appendix B.

Entisols are relatively young soils that comprise the most extensive soil worldwide, covering 19% of the earth's ice-free surface (Palm *et al.*, 2007). These soils make up 17.1% of the surface in temperate biomes and they are also prevalent in the desert biome, in tropical savannas, and Mediterranean biomes (Palm *et al.*, 2007). Entisols occur in areas where erosion or deposition rates are faster than the rate of soil development, such as dunes, steep slopes, and flood plains (USDA, 2007a). Their parent material is sandy eolian material, a fine sand with a particle size ~ 0.1-0.25 mm. Sixty-five percent of the soils on the Vineyard are Entisol, and these are located throughout the island, but predominately along its northeastern portion (Figure 64). On average, the percentages of sand, silt, and clay in Entisols, are 57.5, 22.2, and 3.7, respectively. This soil can be found on the Vineyard at any slope, ranging from sea level to slopes as high as 25%. Entisols types include the following:

- Carver, Loamy Coarse Sand
- Eastchop, Loamy Sand
- Klej, Loamy Coarse Sand
- Udipsamments, no classification

Inceptisols are the second most extensive soils worldwide and are also considered to be relatively young (Palm *et al.*, 2007). They make up about 16% of the world's ice-free land surface, and 18.7% of the soils in temperature biomes (Palm *et al.*, 2007). This type of soil is prevalent in boreal forests, temperate coniferous forests, temperate mixed forests, montane grasslands, and Mediterranean and tropical/subtropical coniferous forests (Palm *et al.*, 2007). The parent material is composed of glacial till (Table 20). Inceptisols comprise 27% of the soils on MV (Table 19) where they are frequently found at slopes between 0-3%, but can range as high as 15%. Most of Martha'a Vineyard Inceptisols are located in the outwash plains and the end moraines on the southwestern tip of the island (Figure 64). In these areas the average percentage of sand is 63.6%, silt, 24.6%, and clay, 10%. Inceptisol soils include:

- Katama, sandy loam

- Nantucket, Sandy Loam
- Pompton, Sandy Loam
- Ridgebury Variant, Fine Loamy Sand
- Riverhead, Sandy Loam

Entisols and Inceptisols are two of the "youngest" soil orders in the world, due in part to natural erosion and sedimentation processes (Palm *et al.*, 2007). Many of these soils are located on alluvial plains, such as those present on Martha's Vineyard, and may be more susceptible to droughts, floods, and river erosion (Palm *et al.*, 2007).

Histosols, commonly known as bogs, peats, or mucks, have a high content of organic matter (USDA, 2007a), and low bulk density, and are predominantly found in boreal regions of Canada, Finland, and Russia (Palm et al., 2007). Histosols result from decomposed plant remains that accumulate faster than they decay in water, forest litter, or moss (USDA, 2007a). When drained and exposed to air, Histosols may subside because of microbial decomposition (USDA, 2007a). Approximately 1% of the world's ice-free surface contains Histosols (Palm *et al.*, 2007; USDA, 2007a). Histosols comprise three percent of the soils on the Vineyard (Table 19), where they are found at slopes between 0-1%, near bodies of water (Figure 64). Histosols include:

- Freetown and Swansea, mucks
- Pawcatuck and Matunuck, mucky peats

Spodosols, also known as podzols, make up approximately 4% of the world's ice-free surface, and are typically found in sandy soils of northern temperate regions, such as northeastern North America and Scandinavia, and usually under coniferous forests (Palm *et al.*, 2007; USDA, 2007a). Their parent material consists of basal till (Table 20), and cover only 1% of Martha's Vineyard (Table 19). This type of soil has the highest percentage of sand (80.2%) and, on MV, it is primarily located on the southwestern tip, and at the tips of the south coastal ponds (Figure 65). Spodosols include:

- Berryland, Loamy Sand

Utisols are acidic and have low nutrient capital (Palm *et al.*, 2007). These soils are common throughout the humid and sub-humid tropics as well as in non-glaciated temperate regions, such as the southeastern U.S. and southeastern China (Palm *et al.*, 2007; USDA, 2007a). The parent material of Utisols includes fluvial and/or marine sediments (Table 20). Utisols make up 4.6% of the soils in temperature biomes (Palm *et al.*, 2007) and 4% of the soils on MV (Table 19). These soils are principally located on the western edge of the Vineyard, as part of the end moraines (Figure 64). Utisols include the following soil:

- Chilmark, Sandy Loam

SOIL TAXONOMY	SOIL m^2	ACRES	PCT AREA	% Sand	% Silt	% Clay
ENTISOLS	145,562,081	35,969	65%	57.5	22.2	3.7
HISTOSOLS	7,350,946	1,816	3%	0	0	1.5
INCEPTISOLS	59,468,540	14,695	27%	63.6	24.6	10
SPODOSOLS	2,683,608	663	1%	80.2	16.8	3
UTISOLS	9,077,472	2,243	4%	66.5	29.5	4
TOTALS	224,142,647	55,387	100%			

Table 19. Summary table of soil taxonomic classifications on Martha's Vineyard.

Soil Taxonomy	Parent Material	Soil	Texture	% Sand	% Silt	% Clay	% slope
Entisols	Sandy Eolian Material	Carver	Loamy Coarse Sand	79	18	3	0-3% to 15-25%
		Eastchop	Loamy Sand	80.5	17	2.5	3-8% to 15-25%
		Klej	Loamy Coarse Sand	83.8	9.2	7	0-3%
		Plymouth*	Sandy Loam	67.3	29.7	3	
		Whitman*	Silt Loam	34.2	59.3	6.5	
		Udipsamments		0	0	0	3-15%
Histosols	Organic Material	Freetown & Swansea	Mucks	0	0	3	0-1%
		Pawcatuck & Matunuck	Mucky Peats	0	0	0	0-1%
Inceptisols	Glacial Till	Haven*	Fine Sandy Loam	62.7	25.8	11.5	
		Katama	Sandy Loam	69.1	23.9	7	0-3%
		Moshup*	Loam	44.3	40.7	15	
		Nantucket	Sandy Loam	66.1	29.4	4.5	3-8% to 8-15%
		Pompton	Sandy Loam	67.4	19.6	13	0-3%
		Ridgebury Variant	Fine Loamy Sand	63.9	21.1	15	0-3%
		Riverhead	Sandy Loam	69.6	23.9	6.5	0-3%
		Tisbury*	Very Fine Sandy Loam	65.5	27	7.5	
Spodosol	Basal Till	Berryland	Loamy Sand	80.2	16.8	3	0-2%
Utisols	Fluvial or Marine Sediments	Chilmark	Sandy Loam	66.5	29.5	4	3-8%
*not at transects				55.6	21.7	6.2	

Table 20. Soil taxonomy on Martha's Vineyard.

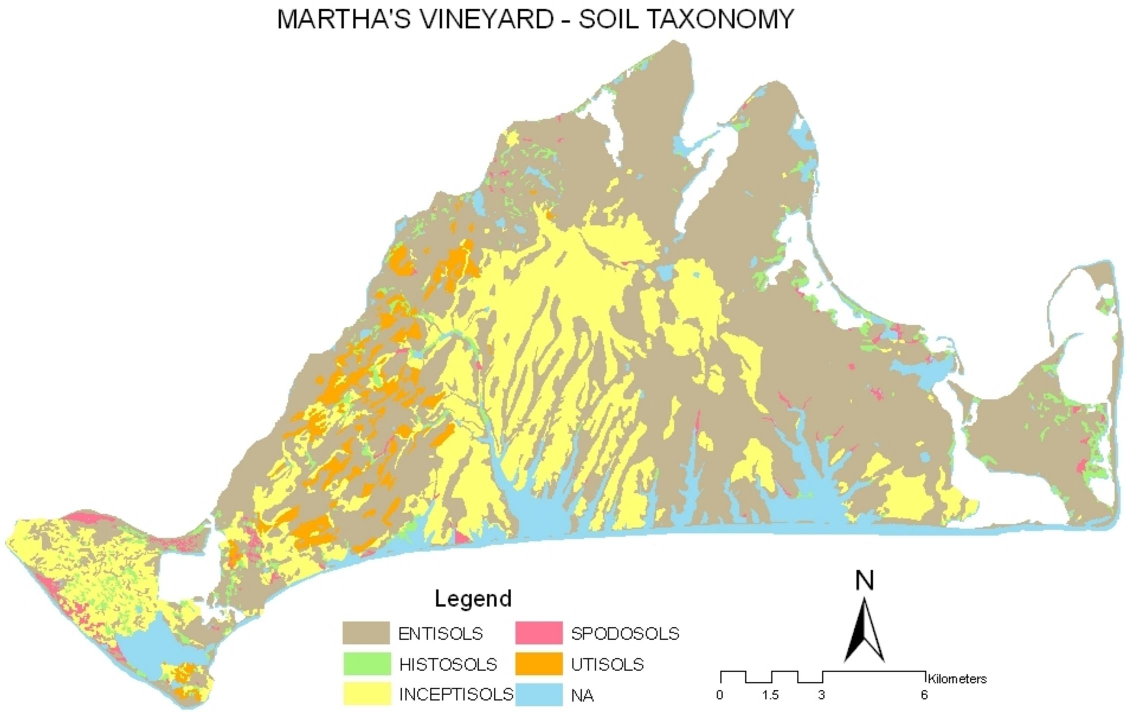

Figure 64. Soil taxonomy map of Martha's Vineyard.

To classify sediments, Shepard (1954) divided a ternary diagram into three main classes by the percentage of sand, silt, and clay. The USDA's modified version of this diagram includes the following 12 categories: clay, silty clay, silty clay loam, silt loam, silt, loam, sandy loam, loamy sand, sand, sandy clay loam, sandy clay, and clay loam (USDA, 2007a). Figure 65 presents the application of this diagram to the soils of Martha's Vineyard.

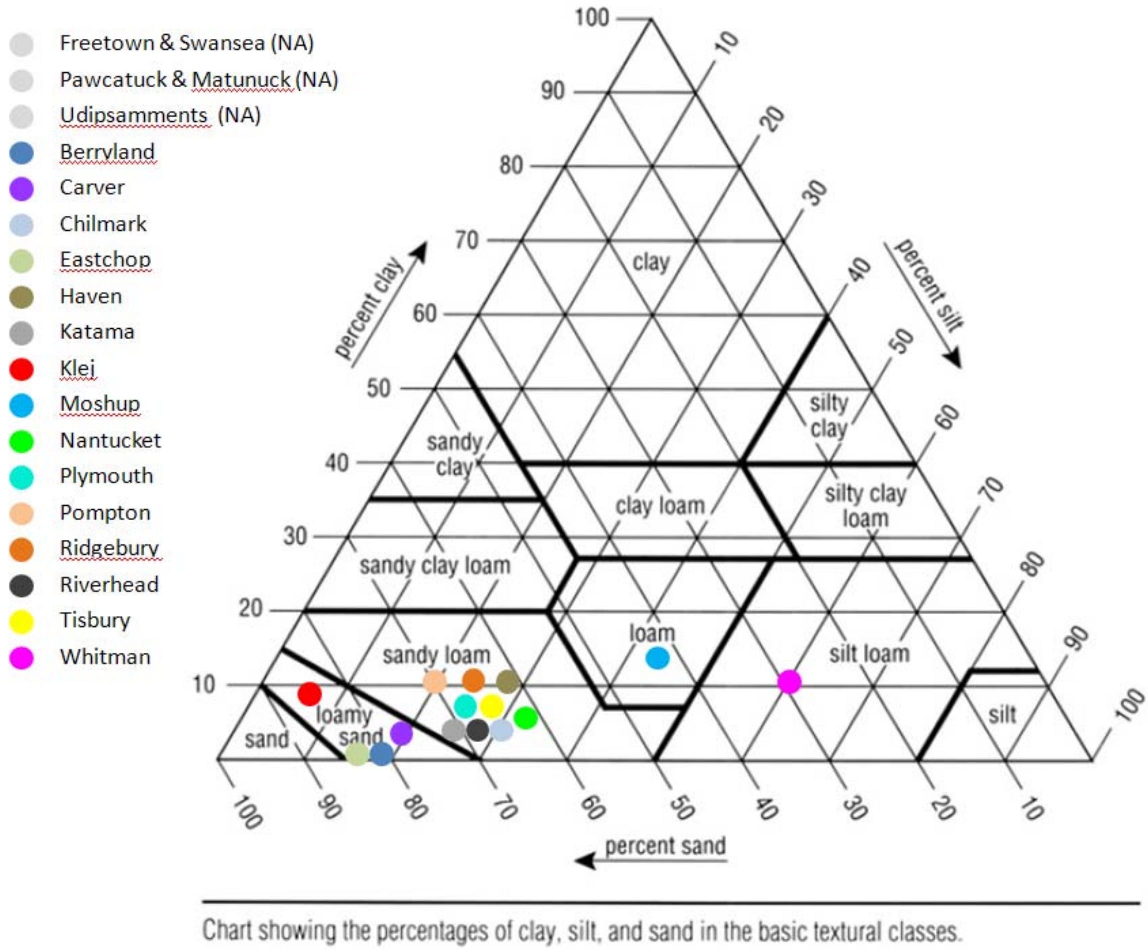

Figure 65. Ternary diagram showing the percentages of clay, silt, and sand on Martha's Vineyard.

Of the 18 condensed soil types, three do not apply to the ternary diagram (Figure 66): Udipsamments, Freetown and Swansea, and Pawcatuck and Matunuck. The latter are also minor components of Udipsamments (USDA, 2007b). Udipsamments are found in very deep and excessively drained areas, typically on coastal sand dunes (Fletcher & Roffinoli, 1986; USDA, 2007b), including those of Martha's Vineyard. When mapped using ESRI® ArcGIS®, all the Udipsamments are located directly on the MV coastline, at various beach systems. Freetown and Swansea soils are located in bogs and their parent material consists of highly-decomposed herbaceous material (USDA, 2007b). Pawcatuck and Matunuck soils are considered mucky peats (USDA, 2007b) and these soils on the Vineyard are located in marshes. These soils are classified as hydric because they are frequently ponded for long, or very long durations, and the water table is very high (0.15 m or 0.5 ft) (USDA, 2007b).

The remaining 15 soils are presented on the soil texture triangle, Figure 65, based on Shepard's texture soil classifications. From these data, it is evident that the most prevalent soil texture on Martha's Vineyard is sandy loam, followed by loamy sand, silt loam, loam, and sand.

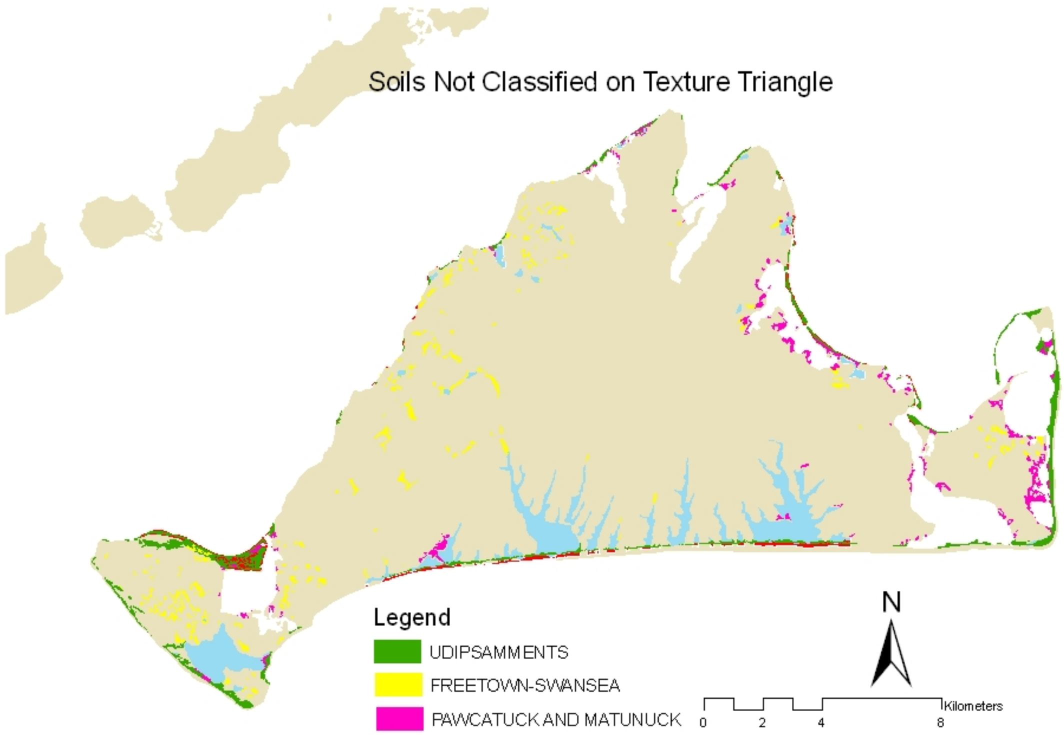

Figure 66. Map of soils not classified on ternary diagram.

Geophysical Features Within 800 m of the Martha's Vineyard Shoreline

To focus my analyses further, I chose to obtain high resolution GIS data for that segment of Martha's Vineyard most likely to be directly affected by erosion in the next 100 years. Since my most aggressive estimates for MV coastal erosion during that time frame (see below) indicate that all changes will occur well within 800 m (approximately 0.5 miles) of the shoreline I have arbitrarily set that distance as a boundary for further consideration.

Geology. The geologic categories on Martha's Vineyard are depicted in Figure 67. The geologic structure adjacent to the coastline of the SS study site consists primarily of beach deposits. These are backed on the western edge of the study site by 3.6 km (2.2 miles) of Martha's Vineyard Moraine Deposits, an area thought to be early Wisconsinan in age (Oldale, 1992), i.e., between 35,000 and 11,150 years old (Fullerton & Bush, 2004). The Gay Head moraine deposits, thought to of Illinoian age (Oldale, 1992), i.e., between 310,000 and 128,000 years old (Fullerton & Bush, 2004), comprise the eastern edge of the SS study site. The remainder of this site consists primarily of Martha's Vineyard moraine outwash, scattered with coastal ponds. This outwash is overlain by stratified drift, thought to derive from the early Wisconsinan age (Oldale, 1992).

The geologic composition of the NE study site consists of a mixture of Martha's Vineyard moraine outwash and moraine deposits, beach deposits, and a few coastal ponds. Unlike the SS site, the NE study side coastline is interspersed between these three variables, not just beach and sand deposits.

The most southwestern tip of the NW study site is composed of beach deposits, followed by Gay Head moraine deposits and the Martha's Vineyard moraine deposits.

Southwest of Menemsha Pond, the primary geologic material is beach deposits. Beyond Menemsha Harbor, most of the coastline is composed of Martha's Vineyard moraine. Heading northeast, the coastline is dotted with pockets of beach deposits just north of Peaked Hill, south of Cape Higgon and Cedar Tree Neck, and ending with beach deposits at Lambert's Cove. On the NW side, the Martha's Vineyard moraine deposits are backed by the Gay Head moraine deposits.

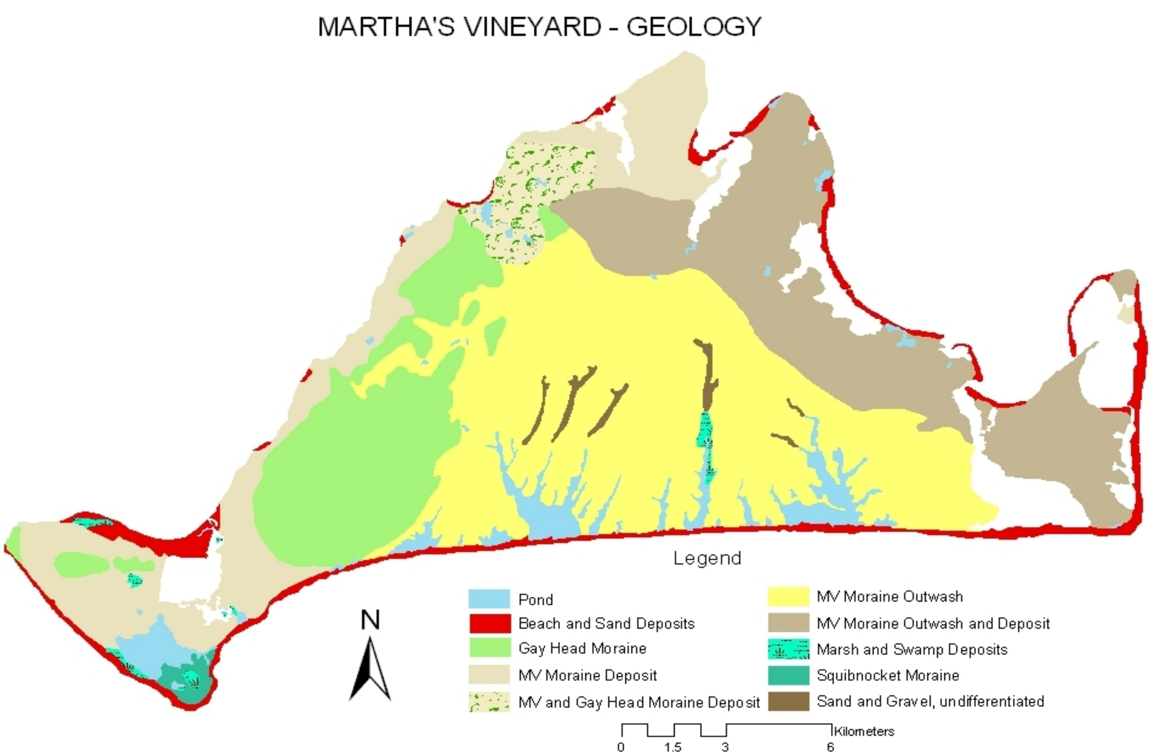

Figure 67. Map of geologic characteristics on Martha's Vineyard.

Surficial Geology. The three principal categories of surficial geology on Martha's Vineyard include: 1) sand and gravel deposits; 2) till; and 3) end moraines. While these categories are similar to those used to define the island's geology, they are more superficial in that they only define the surface materials that overlie the geology (Figure 68).

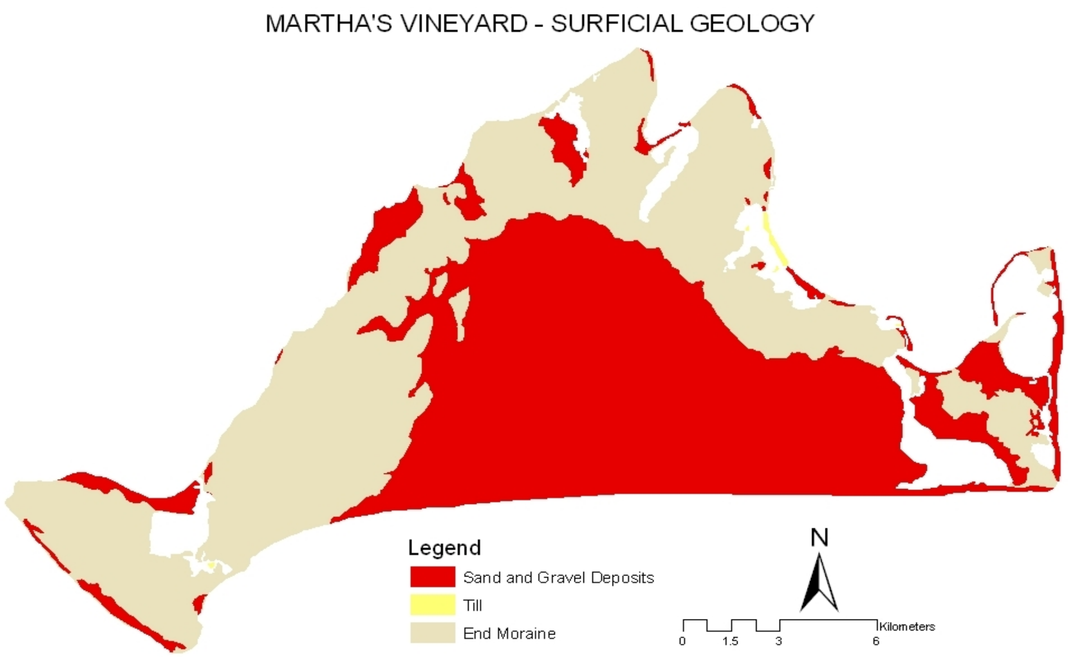

Figure 68. Map of surficial geology on Martha's Vineyard.

Table 21 and Table 22 identify the surficial geology attributes within each study site. At the SS site, 50.45% of the surficial geology is comprised of end moraines that are in close proximity to the MV and Gay Head moraine deposits. An additional 49.54% of the SS site is composed of sand and gravel deposits, with only 0.01% classified as till. Surficial geology of the NE study site is similar to its geology classifications, with the major difference located along the barrier beaches between Oak Bluffs and Edgartown. The Oak Bluffs side is classified as till (0.14%), whereas the Edgartown side is classified as sand and gravel deposits. The NE area consists of 50.07% sand and gravel deposits and 49.79% end moraines. The surficial geology of the NW side is similar to its geological classifications, with a major exception near Cedar Tree Neck. This sand and gravel classification is significantly larger than the geological classification of beach deposits. Overall, 95.15% of the NW consists of end moraines and only 4.85% is considered sand and gravel deposits.

SURFICIAL GEOLOGY	SS %	NE %	NW %
END MORAINES	50.45%	50.07%	95.15%
SAND AND GRAVEL DEPOSITS	49.54%	49.79%	4.85%
TILL	0.01%	0.14%	0.00%
TOTALS	**100.00%**	**100.00%**	**100.00%**

Table 21. Percentage of surficial geology attributes by study sites.

SS Surficial Geology Attributes	Area in Acres	Percent of Area
End Moraines	27,471.10	50.45
Sand and Gravel Deposits	26,972.00	49.54
Till	6.9	0.01
TOTALS	**54,450.00**	**100**

NE Surficial Geology Attributes	Area in Acres	Percent of Area
Sand and Gravel Deposits	29,063.30	50.07
End Moraines	28,906.00	49.79
Till	81.2	0.14
TOTALS	**58,050.50**	**100**

NW Surficial Geology Attributes	Area in Acres	Percent of Area
End Moraine	27,471.10	95.15
Sand and Gravel Deposits	1,399.80	4.85
TOTALS	**28,870.90**	**100**

Table 22. Percentage of surficial geology areas by study sites.

Soil and Percent of Sand at the Study Sites

SS Site. Overall, Martha's Vineyard soil types comprise 55.6% sand, 21.7% silt, and 6.2% clay (Table 20). At the SS site, the average percentages are 54.36% sand, 18.84% silt, and 5.74% clay (Table 23). The highest proportion of sand is on the western side of the SS site, where it ranges from 80% to 100% (Figure 69). The percentage of sand on the central and eastern portions of the SS site range from the mid 60s to 79%. Right along the coastline, the barrier beaches are entirely comprised of sand, with an area of 2,429,059 m² (600 acres).

SS Soil Summary	SS m^2	SS Soil Pct	% Sand	% Silt	% Clay
BEACHES	1,445,784	3.62%	100.00	0.00	0.00
BERRYLAND	295,095	0.74%	80.20	16.80	3.00
CARVER	20,104,428	50.32%	79.00	18.00	3.00
CHILMARK	629,741	1.58%	66.50	29.50	4.00
EASTCHOP	4,770,423	11.94%	80.50	17.00	2.50
FREETOWN AND SWANSEA	123,097	0.31%	0.00	0.00	3.00
HAVEN	1,691,757	4.23%	62.70	22.50	11.50
KATAMA	2,387,437	5.98%	69.10	23.90	7.00
KLEJ	976,614	2.44%	83.80	9.20	7.00
MOSHUP	298,950	0.75%	44.30	40.70	15.00
NANTUCKET	926,027	2.32%	66.10	29.40	4.50
PAWCATUCK AND MATUNUCK	335,691	0.84%	0.00	0.00	0.00
PITS, SAND AND GRAVEL	22,584	0.06%	0.00	0.00	0.00
POMPTON	741,078	1.85%	67.40	19.60	13.00
RIDGEBURY VARIANT	45,051	0.11%	63.90	21.10	15.00
RIVERHEAD	3,395,799	8.50%	69.60	23.90	6.50
TISBURY	448,429	1.12%	65.50	27.00	7.50
UDIPSAMMENTS	1,277,926	3.20%	0.00	0.00	0.00
WHITMAN VARIANT	37,801	0.09%	34.20	59.30	6.50
TOTALS	**39,953,712**	**100.00%**	**54.36**	**18.84**	**5.74**

Table 23. SS study site soil summary and percent of sand, silt, and clay.

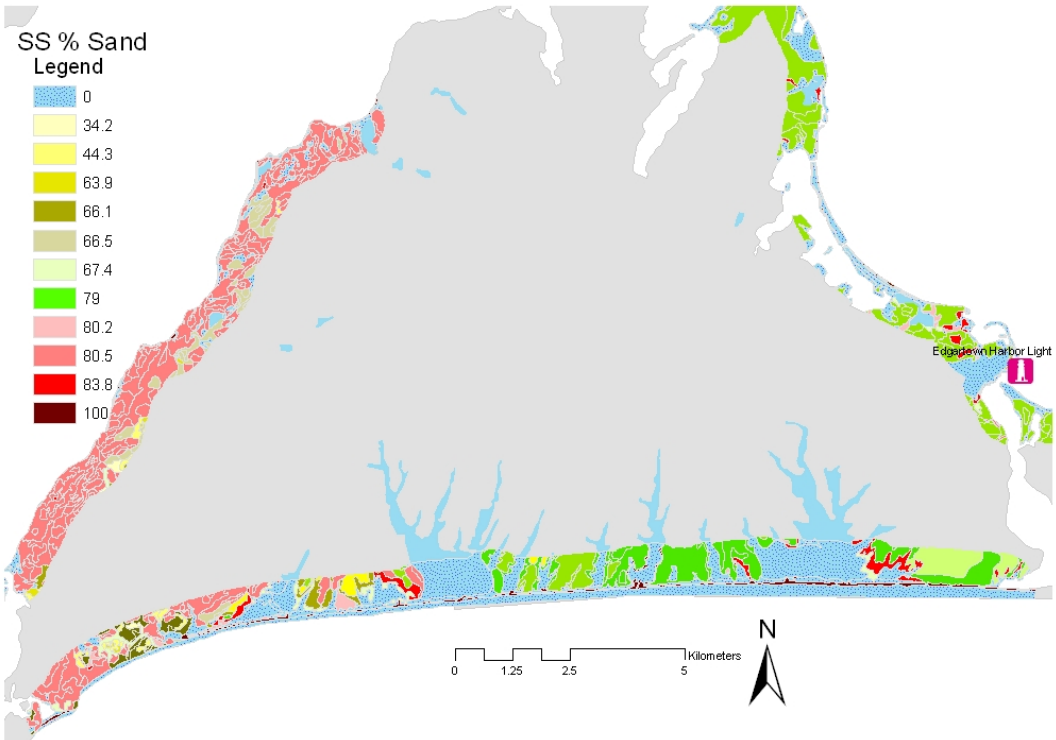

Figure 69. Percentage of sand at the study sites.

The largest percentage of soil type within 800 m (0.5 miles) of the SS coastline is Carver, an Entisol, with 50.32% (20,104,428 m^2; 4,968 acres) of the total area of 39,953,712 m^2 (9,873 acres) (Table 23). It should be noted that I left out the category of water in these results (the total area of land plus water is 58,984,046 m^2/14,575 acres, data not shown). Most of the Carver soils are located in the central and eastern portions of the SS study site (Figure 70). The composition of Carver soil is loamy, coarse sand, consisting of approximately 79% sand, 18% silt, and 3% clay (Table 20). The parent material is derived from coarse sand eolian deposits, and it is underlain by fluvial deposits (Turenne, 2007). This type of soil is very deep, excessively drained, and is primarily in broad areas on outwash plains (Turenne, 2007). The soils form in thick layers of coarse and very coarse sand that contain less than 20 percent rock fragments, most of which are fine gravel (Soil Survey Division, 2002). It is predominantly found at slopes ranging from 0-15%, but it can range as high as 25-45% (Soil Survey Division, 2002). Carver soils are typically found in woodlands, croplands, and in residential developments. The common trees on this soil are pitch pine, scrub oak, scarlet oak, black oak, and white oak (Fletcher & Roffinoli, 1986).

On the far western end of the SS study, the soil is predominantly Eastchop, a loamy sand, with a small amount of Chilmark soil adjacent to it (Figure 70). Eastchop soils are considered to be sandy loam. The barrier beaches along the SS are classified as Udipsamments and Beaches. Beaches cannot be an "official" soil because they don't support plant life. Beach soils are commonly found adjacent to the ocean and are continually washed and rewashed by waves. The sand on the beaches is generally gravelly and cobbly (Fletcher & Roffinoli, 1986). Udipsamments along the shore were created from sandy eolian material, generally found on sand dunes along the coast (Fletcher & Roffinoli, 1986). These soils are excessively drained and have little to no vegetation (Fletcher & Roffinoli, 1986). What vegetation does grow includes a cover of grasses, such as beachgrass, poison ivy, beach plum, and bayberry (Fletcher & Roffinoli, 1986). Trees are difficult to establish and grow in this soil, particularly along the coastline (Fletcher & Roffinoli, 1986).

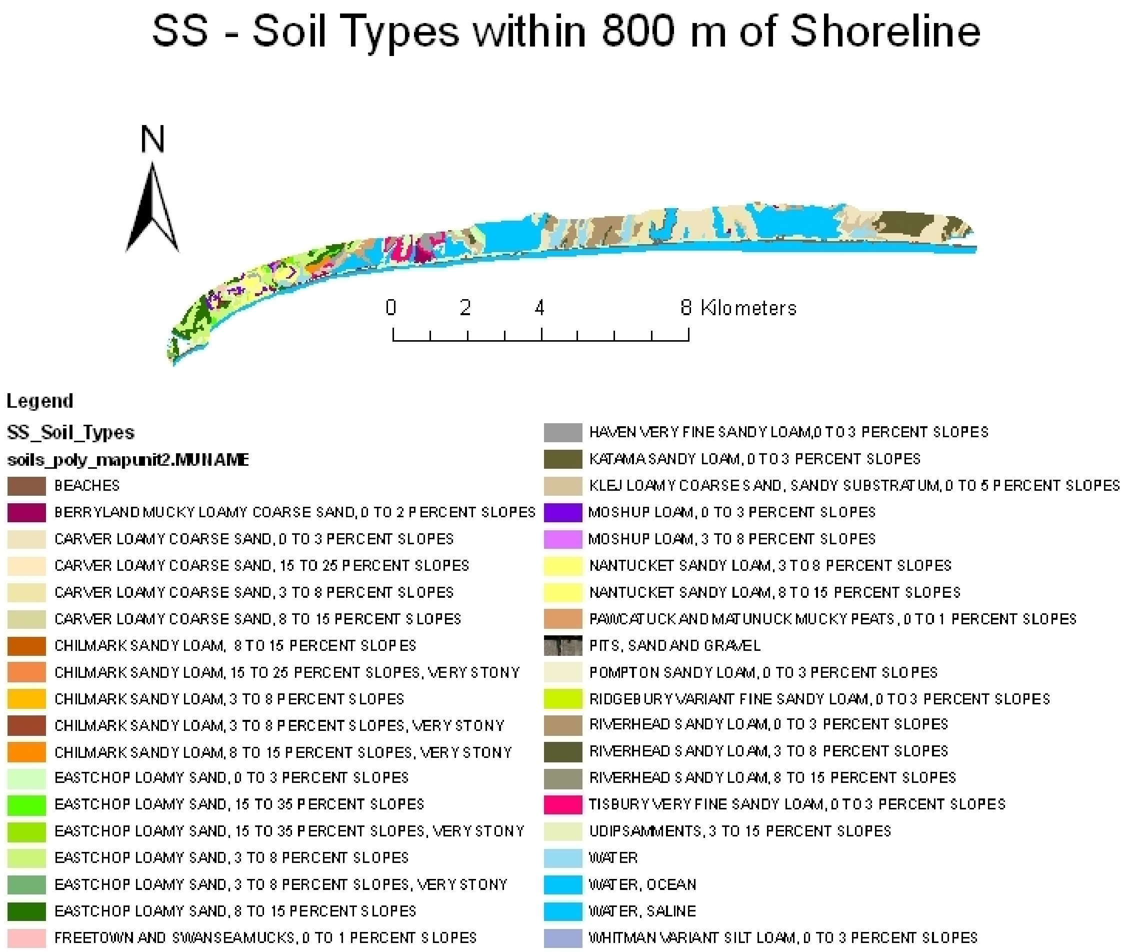

Figure 70. SS study site soil types within 800 m of shoreline.

Nonbedrock escarpment is defined by the USDA (1998) as “a relatively continuous and steep slope or cliff, which was produced by erosion or faulting, that breaks the general continuity of more gently sloping land surfaces. Exposed earthy material is nonsoil or very shallow soil.” The only location that has nonbedrock escarpment (ESO) is located at the far western end of the SS site, and it is approximately 3 km (1.86 miles) long. This segment includes Nashaquitsa Cliffs and a portion of Lucy Vincent Beach (Figure 71).

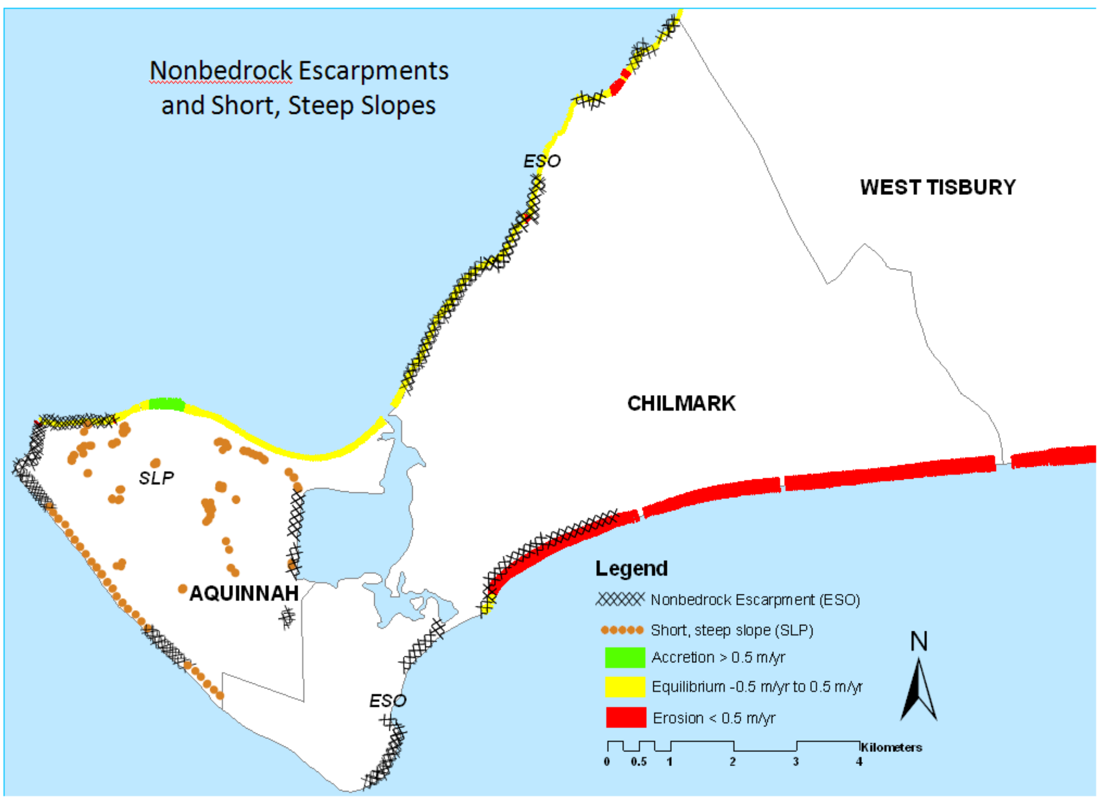

Figure 71. Map of nonbedrock escarpment locations in Chilmark and Aquinnah.

NE Site. At the NE site the average percentages of sand, silt, and clay are 50.67%, 10.01%, and 3.23%, respectively (Table 20). From East Chop Light to Edgartown Light, the percentage of sand in the soil ranges from around 79% to 0% in areas that are either urban land or organic matter (Figure 72). On Chappaquiddick Island, the most eastern location of the NE study site, the percentage of sand is mostly in the low 80% range. The composition of the soil on the NE study site is very similar to that of the SS site. Slightly more than 80% of the soils are classified as Carver and cover 25,768,580 m^2 (6,368 acres) (Table 24). The remaining soil classifications on the NE side include: Beaches, Berryland, Eastchop, Freetown and Swansea, Katama, Klej, Pawcatuck and Matunuck, Pompton, Udipsamments, and urban land (the latter is not on the south side). Total land acreage, without water, on the NE side is 31,936,752 m^2 (7,892 acres); with the inclusion of water, it is 50,636,365 m^2 (12,513 acres) (data not shown).

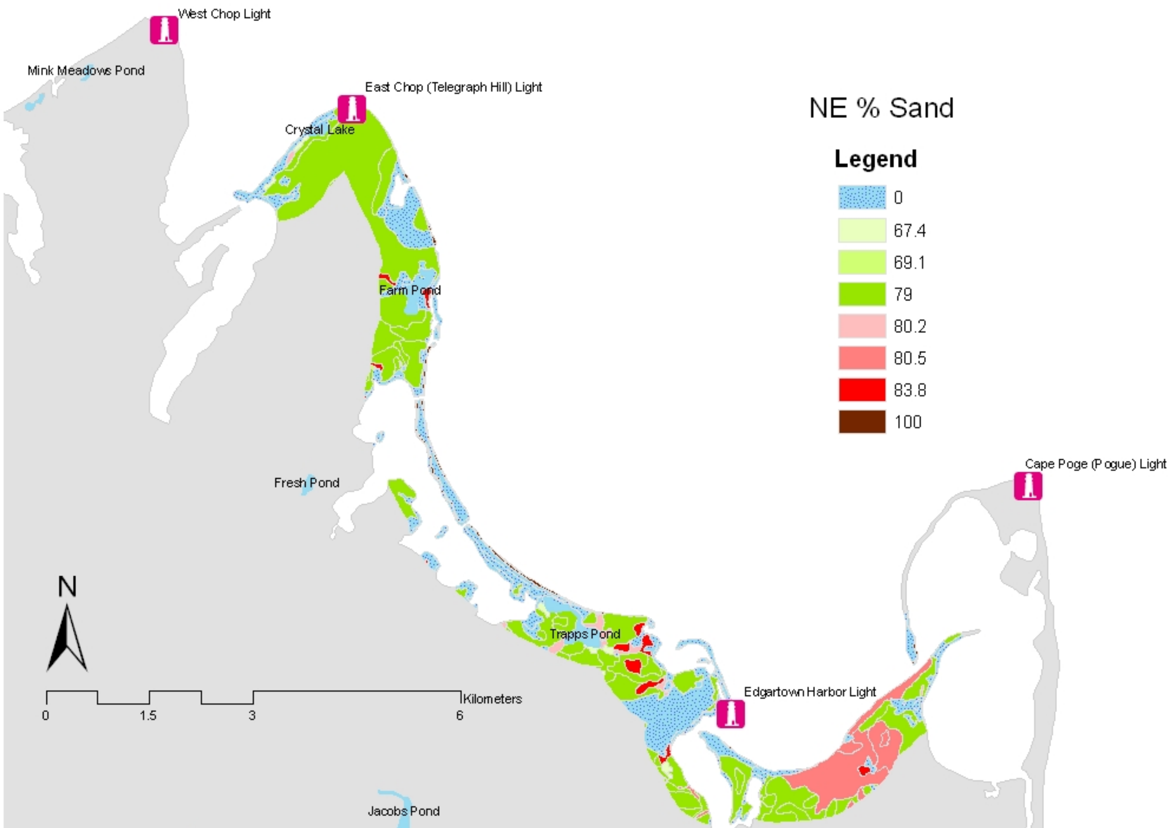

Figure 72. Percentage of sand at the NE study site.

NE Soil Summary	NE m^2	NE Soil Pct	% Sand	% Silt	% Clay
BEACHES	307,848	0.96%	100.00	0.00	0.00
BERRYLAND	172,360	0.54%	80.20	16.80	3.00
CARVER	25,768,580	80.69%	79.00	18.00	3.00
EASTCHOP	1,423,092	4.46%	66.50	29.50	4.00
FREETOWN AND SWANSEA	187,863	0.59%	80.50	17.00	2.50
KATAMA	10,483	0.03%	0.00	0.00	3.00
KLEJ	340,769	1.07%	83.80	9.20	7.00
PAWCATUCK AND MATUNUCK	981,102	3.07%	0.00	0.00	0.00
POMPTON	138,111	0.43%	67.40	19.60	13.00
UDIPSAMMENTS	1,129,656	3.54%	0.00	0.00	0.00
URBAN LAND	1,476,888	4.62%	0.00	0.00	0.00
TOTALS	**31,936,752**	**100.00%**	**50.67**	**10.01**	**3.23**

Table 24. NE study site soil summary and percent of sand, silt, and clay.

Soils within the NE study site consist primarily of Carver Coarse Sand (81%) and Pawcatuck and Matunuck Mucky Peats (37%) (Table 24). The remaining soil types in this area are Klej Loamy Coarse Sand – Sandy Substratum (1%), Udipsamments (7%), East Chop Loamy Sand (6%), Beaches (6%), Pompton Sandy Loam (6%), Berryland Mucky Loamy Coarse Sand (5%), Freetown and Swansea Mucks (4%), Urban Land (3%), and Katama Sandy Loam (0.7%). More than half (58.74%) of this soil is excessively drained, highly permeable, and with low water capacity, while 32.17% of the soil is poorly drained. These soils are found around bodies of water, such as streams, swamps, ponds, and shore areas. The beach areas, including some sand dunes, have no plant cover, and are inundated twice daily by tides. Urban areas are covered by buildings, structures, and/or asphalt.

The NE study site has numerous barrier beaches, with elevations from sea level to 4 m (13.12 ft). Edgartown has 15 barrier beaches, but only 7 are included in the study site for a total of 394,837 m^2 (98 acres). Oak Bluffs has 11 barrier beaches, but only 9 are included in the study site for a total of 419,553 m^2 (104 acres). Tisbury has 1, but it is not included in the study site. The NE site encompasses two main barrier beaches, Joseph Sylvia State Beach (Oak Bluffs), a 3.2 km (2 mile) beach, and Bend in the Road Beach (Edgartown). Overall, the NE site includes 1,213,168 m^2 (300 acres) of barrier beaches (Figure 73).

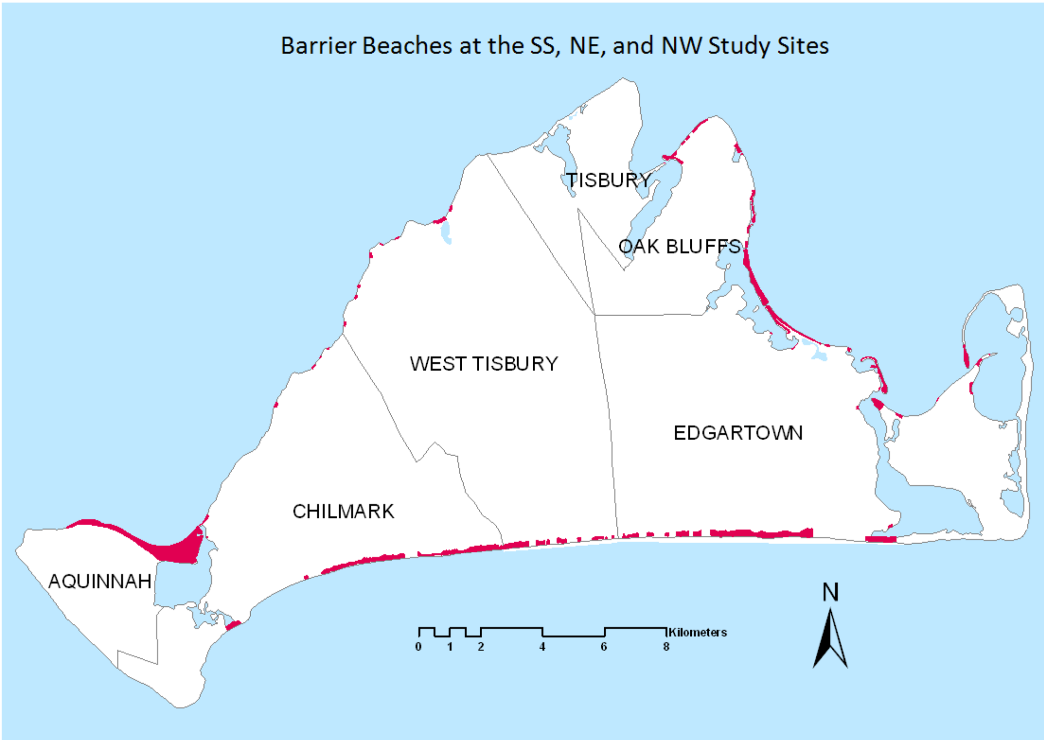

Figure 73. Barrier beaches at the SS, NE, and NW study sites.

The soil within 800 km of the coastline in Oak Bluffs is predominantly Carver and it has approximately 318 m^2 (0.079 acres) of urban land to the south of Oak Bluffs Harbor. Soils adjacent to the shore from Oak Bluffs to Edgartown are classified mostly as Beaches and Udipsamments. Edgartown has approximately 874 m^2 (0.22 acres) of urban land within the 800 m (0.5 miles) boundary. Berryland soils are located in the vicinity of ponds that contain saline water. Eastchop soils are located in areas of Chappaquiddick Island that are fronted by nonbedrock escarpment. Nonbedrock escarpment (ESO) is located at both ends of the NE study site (Figure 75). The first, southwest of East Chop Lighthouse, is slightly more than 1 km (0.62 miles) long, as shown in (Figure 75 and Figure 76). The latter figure is representative of the coastline along Oak Bluffs, including East Chop Lighthouse. The second area is on Chappaquiddick Island, to the east of Edgartown Harbor, the length of the latter escarpment is approximately 3 km (1.86 miles).

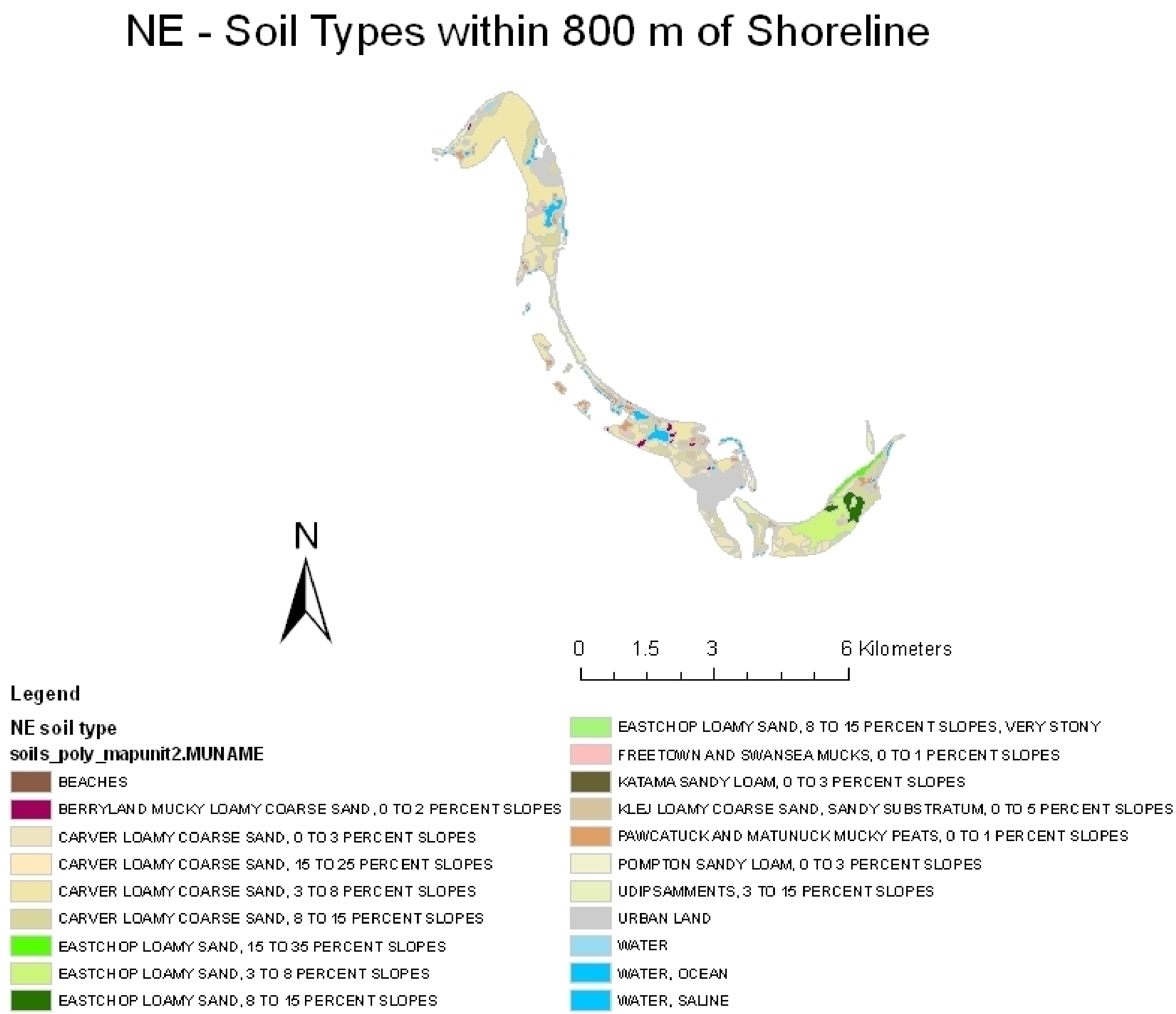

Figure 74. NE study site soil types within 800 m of shoreline.

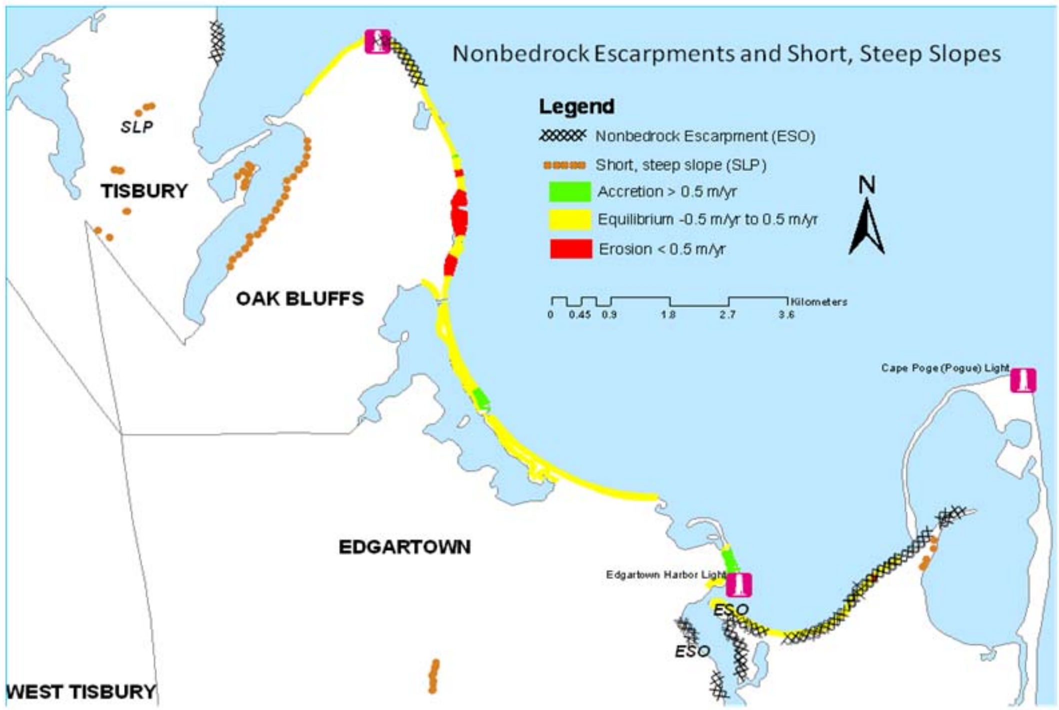

Figure 75. NE study site nonbedrock escarpment and short, steep slopes.

Figure 76. Nonbedrock escarpment and short, steep slopes in Oak Bluffs.

NW Site. Within 800 m (0.5 miles) of the coastline at the NW site the average percentages of sand, silt, and clay are, respectively, 54.71%, 18.61%, and 5.46% (Table 25). Including water in the area calculations, the NW site encompasses 27,029,689 m^2 (6,679 acres) (data not shown). Omitting water from the soil classification leaves 23,394,160 m^2 (5,781 acres) for this site. Approximately 50% of the NE site soil is composed of Eastchop, an Entisol, with most of it northeast of Menemsha Harbor (Figure 77). Eastchop soil is primarily loamy sand, composed of approximately 80% sand, 17% silt, and 3% clay, with some very stony areas. The Eastchop series consists of very deep excessively drained soils, formed in sandy glacial outwash with varying amounts of eolian influence (Turenne, 2007). The surface layer is very dark brown loamy sand about 12.7 cm (5 inches) thick. The slope of the soil ranges from 3-8% to 15-25%, and in some areas can be as high as 35%. Eastchop soils are found at nearly level to steep surfaces, on moraines and outwash plains, small hills, knolls, and ridges in the western part of Martha's Vineyard. Permeability is rapid or very rapid (Soil Survey Division, 2002).

NW Soil Summary	NW m^2	NW Soil Pct	% Sand	% Silt	% Clay
BEACHES	681,590	2.91%	100.00	0.00	0.00
BERRYLAND	520,105	2.22%	80.20	16.80	3.00
CARVER	38,432	0.16%	79.00	18.00	3.00
CHILMARK	1,777,507	7.60%	66.50	29.50	4.00
EASTCHOP	11,856,949	50.68%	80.50	17.00	2.50
FREETOWN AND SWANSEA	721,906	3.09%	0.00	0.00	3.00
KLEJ	13,631	0.06%	83.80	9.20	7.00
MOSHUP	568,234	2.43%	44.30	40.70	15.00
NANTUCKET	4,458,008	19.06%	66.10	29.40	4.50
PAWCATUCK AND MATUNUCK	149,547	0.64%	0.00	0.00	0.00
POMPTON	36,449	0.16%	67.40	19.60	13.00
RIDGEBURY VARIANT	431,533	1.84%	63.90	21.10	15.00
UDIPSAMMENTS	1,641,383	7.02%	0.00	0.00	0.00
WHITMAN VARIANT	498,886	2.13%	34.20	59.30	6.50
TOTALS	**23,394,160**	**100.00%**	**54.71**	**18.61**	**5.46**

Table 25. **NW study site soil summary and percent of sand, silt, and clay.**

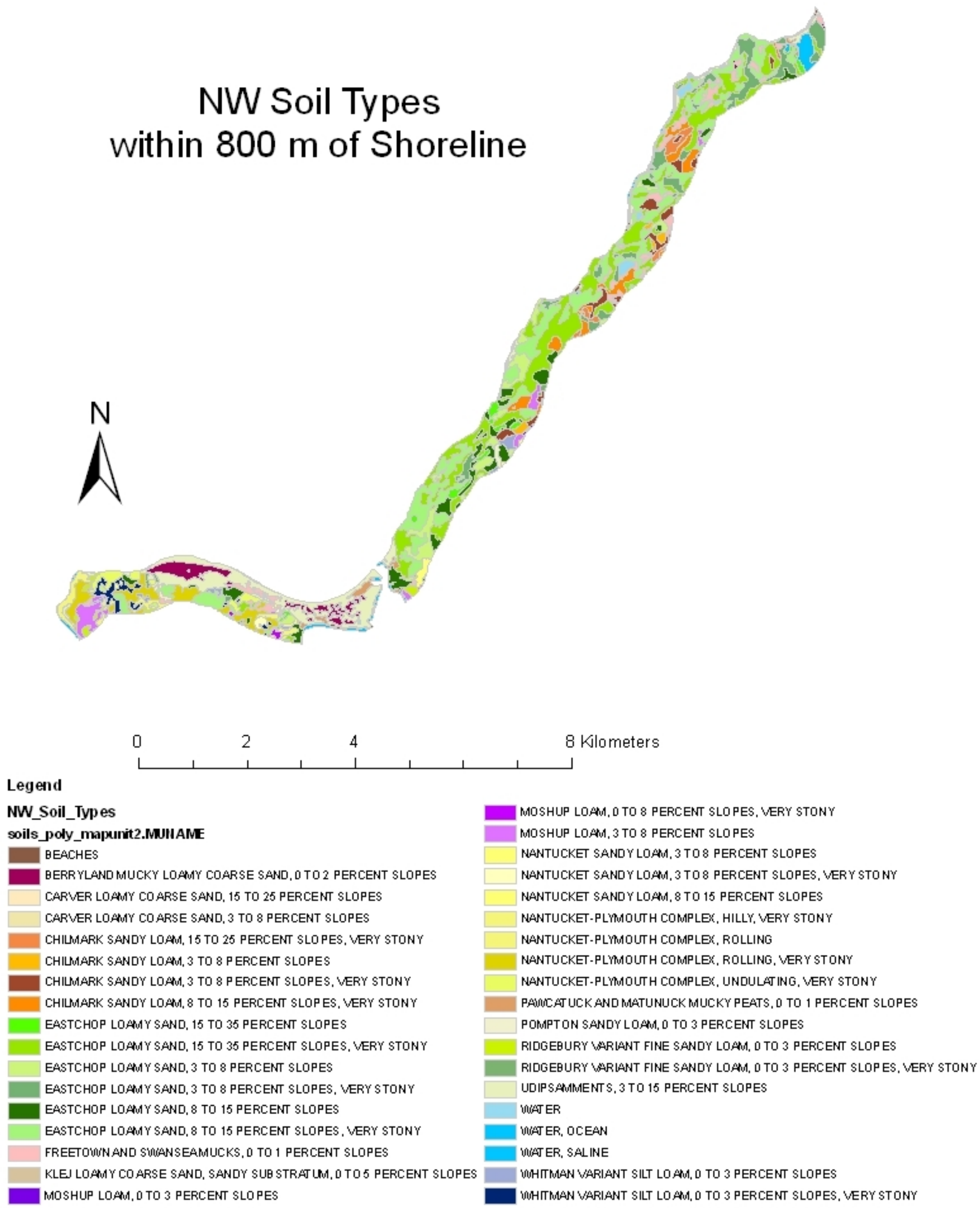

Figure 77. NW study site soil types within 800 m of shoreline.

Because most of the Eastchop soil is in woodlands, most often the surface is covered with a layer of loose, undecomposed and decomposed leaves and twigs approximately 7.62 cm (3 inches) thick (Fletcher & Roffinoli, 1986). Eastchop soils are located in croplands, and areas that are used as pasture, and a few are used as homesites (Fletcher & Roffinoli, 1986). The common trees on this soil are pitch pine, scrub oak, scarlet oak, black oak, and white oak (Fletcher & Roffinoli, 1986). Northeast of Menemsha Harbor, the soils are predominantly Eastchop, while southwest of the harbor the soils consist mostly of Udipsamments, Nantucket, and Berryland (Figure 77).

West, southwest of Menemsha Harbor, Udipsamments and Nantucket soils are widespread, and significantly interspersed with Berryland (Figure 77). The majority of the soils that are part of the barrier beach in this area (1,397,832 m^2 or 345 acres) are Udipsamments and Berryland.

The overall length (7 km; 4.35 miles) of nonbedrock escarpment on the NW site exceeds that of any similar stretches at the NE and SS study sites. Just east of Gay Head Cliffs, the ESO is approximately 1 km (0.62 miles) long (Figure 71). Northeast of Menemsha Harbor it is approximately 4 km (2.49 miles) long, and the remaining portion of the study site includes 2 km (1.24 miles) of interspersed ESO. The NW study site is also the only sit that has a narrow soil slope area that is at least two slope classes steeper than the slope class of the surrounding map unit (USDA, 1998). Finally, there are several beaches within 800 m (0.5 miles) of the NW coastline. These include: Lobsterville, Red Beach (which is on Menemsha Pond), Menemsha Beach, and Great Rock Bight.

Slope

The three study sites all differ with respect to the percentage of their overall areas within 800 m of the shoreline that manifest specific slopes (Table 26). The SS site has the least amount of slope, mostly ranging from no slope to 3%; the NE side is mostly at sea level or 3-8% slope; and the NW side has the most slope, ranging from 8-25%. For details on the approximate areas covered by each slope class, see Appendix B).

SLOPE	SS %	NE %	NW %
0 = NO SLOPE	34.75%	40.45%	15.98%
A = 0-3%	48.04%	7.09%	8.81%
B = 3-8%	10.86%	44.06%	16.43%
C = 8-15%	5.22%	7.74%	38.11%
D =15-25%	1.13%	0.66%	20.67%
TOTALS	**100.00%**	**100.00%**	**100.00%**

Table 26. Percentage of slope by study sites.

SS Site. The SS study site is relatively flat in that 35% of its area has no slope and 48% has a slope of 0-3% (Table 26). Most of this relatively flat land is centrally and easterly located in the SS site (Figure 78) and has an overall length of 18 km. Eleven percent of the SS site has a slope of 3-8%. Approximately 5% has a slope of 8-15%, including a segment that encompasses most of the barrier beaches (Figure 73). The average elevation of these beaches is approximately 4 m (data not shown). Only 1% of the SS site has a slope of 15-25%, with the steepest portion on the western side in Aquinnah, near the Gay Head cliffs. There is one section on the eastern side of the study site that has a slope of 15-25%; it is located on the western shore of Jobs Neck Pond. Set back from the active coastline, the edges of the coastal ponds increase in slope to 3-8%.

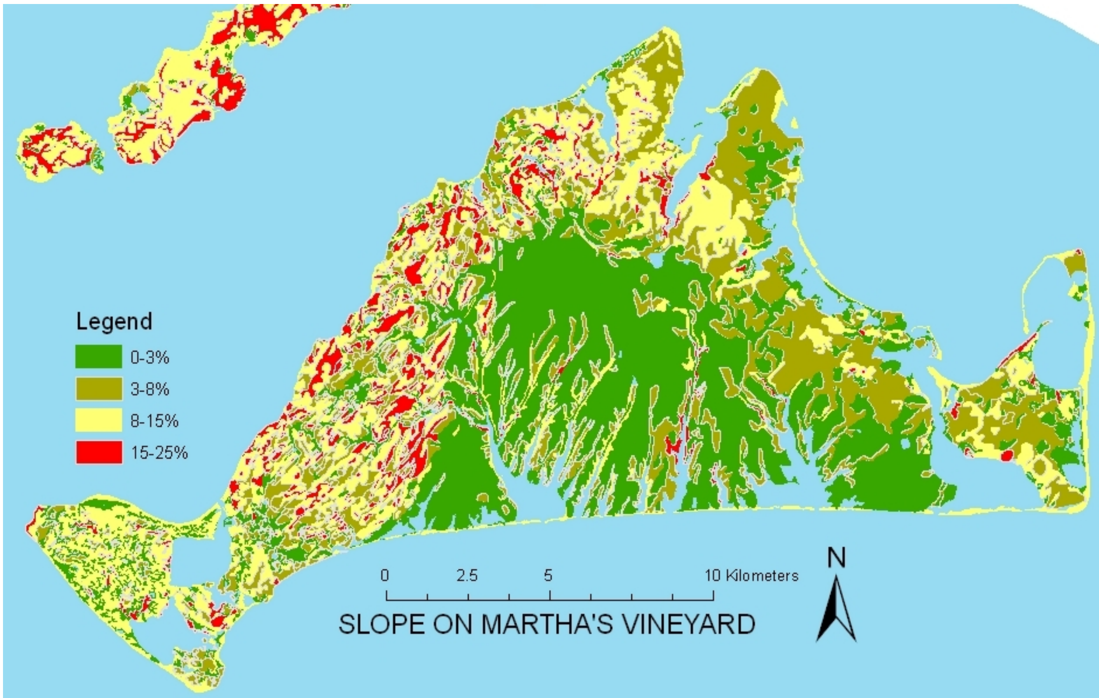

Figure 78. Map of slope on Martha's Vineyard.

NE Site. Almost 40% of the NE study site has a slope of 3-8% (Table 26). The remaining land in the NE site includes a substantial area that is nearly flat to a 3% slope (23%), an area with no slope (18%), a segment with a relatively steep slope of 8-15% (17%), and a small portion (2%) with a slope of 15-25%. The shorelines on either side of the East Chop lighthouse have a slope of 8-15% up to the entrance of Oak Bluffs Harbor (Figure 78). The shoreline elevation from East Chop Light to Oak Bluffs Harbor is relatively steep, ranging from sea level to ~ 14 m within ~ 15 m and is mostly armored by large boulders (Figure 76). Within ~ 480 m of Oak Bluffs Harbor, the elevation drops to ~ 2 m when it becomes a barrier beach (Figure 73). From Oak Bluffs Harbor, to Edgartown Harbor, and across the entrance of Edgartown Harbor, to Chappy Beach, the slope ranges from relatively flat to 8-15% as well. Again, once the entrance of Edgartown Harbor is reached, the elevation ranges from sea level to 4 m slightly inland. On Chappaquiddick Island, the most eastern portion of the NE site has a slope of 15-25%.

NW Site. As a result of its end moraine the NW study site has more of a slope than the SS and NE sites. Approximately 38% of this study site has a slope of 8-15%; 20% has a slope of 12-25%, 16% has a slope of 3-8%, 16 % has no slope, and 9% has a minor slope of 0-3% (Table 26, Figure 73).

Highly Erodible Land

Almost half of the SS study site is classified as not highly erodible; 40% of the NE study site is labeled not applicable and 56% of the NW site is classified as highly erodible land (Table 27, Figure 79). All these classifications were obtained from the USDA and NRCS, except for the erodible category, which I added for the beach classification. The beaches are the smallest percentage of HEL at every study site. NA primarily consists of urban land and water, whether it is fresh, ocean, or saline. For details on the approximate areas covered by each erodible class, see Appendix B.

HEL Characteristics	SS %	NE %	NW %
ERODIBLE	2.45%	0.61%	2.52%
HIGHLY ERODIBLE LAND	9.01%	17.19%	55.57%
NA	32.30%	39.85%	13.45%
NOT HIGHLY ERODIBLE LAND	48.04%	18.90%	8.86%
POTENTIALLY HIGHLY ERODIBLE LAND	8.20%	23.45%	19.60%
TOTALS	**100.00%**	**100.00%**	**100.00%**

Table 27. Percentage of land by erodible characteristics for each study site.

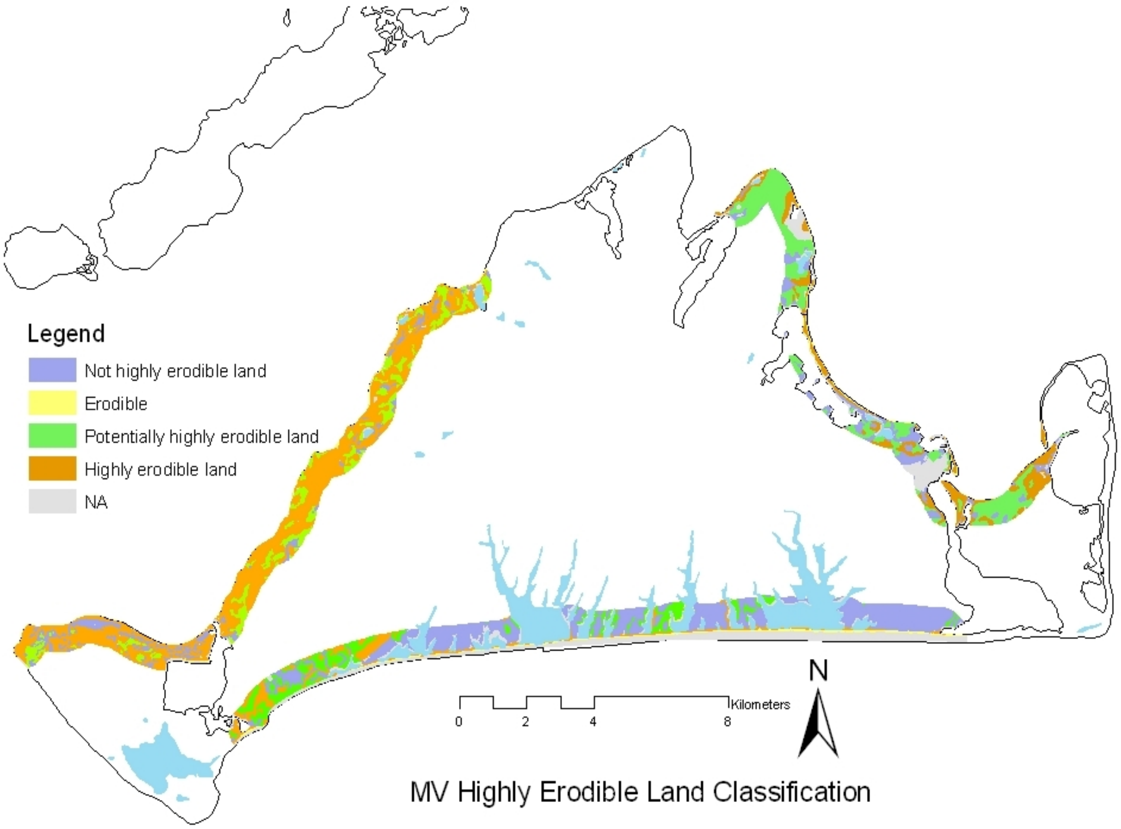

Figure 79. Map of erodible land classifications for the study sites.

Wetlands

SS Site. Wetlands abutting the SS site coastline are barrier beach systems and coastal beaches, behind which are barrier beach-coastal dunes and coastal dunes, respectively (Figure 80). This pattern varies only in Chilmark, at the base of Wequobsque Cliffs, and it is classified as coastal bank bluffs or sea cliffs. The area parallel to the coast is classified as a coastal beach. Rocky intertidal shorelines exist on the point and, scattered throughout the 800 m (0.5 mile) SS study site, are salt marshes (in most cases around the coastal ponds), shrub swamps, and an occasional tidal flat.

Wetlands on the SS site comprise 18,978,138 m² (4,689.6 acres) (Table 28), or approximately one-third of the total study site (~58,984,065 m² or 14,575 acres). If the "open water" category is removed from the analysis, then the barrier beach system comprises 32.55% of the site, the largest attribute at all three sites (Table 29). Salt marshes and barrier beach-coastal dune systems follow at 21.58% and 17.73%, respectively. These three attributes comprise close to 72% of the wetland category on the SS site.

SS WETLAND DESCRIPTION	ACRES	% OF WETLANDS
BARRIER BEACH-COASTAL DUNE	172.21	3.67
BARRIER BEACH SYSTEM	316.16	6.74
COASTAL BANK BLUFF OR SEA CLIFF	22.65	0.48
COASTAL BEACH	99.47	2.12
COASTAL DUNE	64.72	1.38
OPEN WATER	3,718.30	79.29
ROCKY INTERTIDAL SHORE	3.10	0.07
SALT MARSH	209.53	4.47
SHRUB SWAMP	78.37	1.67
TIDAL FLAT	5.09	0.11
TOTALS	4,689.60	100

Table 28. Wetland classifications by acreage and percentage on the SS study site.

WETLAND DESCRIPTION	SS %	NE %	NW %
BARRIER BEACH-COASTAL DUNE	17.73%	18.35%	14.73%
BARRIER BEACH SYSTEM	**32.55%**	25.50%	**26.54%**
COASTAL BANK BLUFF OR SEA CLIFF	2.33%	2.80%	6.77%
COASTAL BEACH	10.24%	6.37%	12.05%
COASTAL DUNE	6.66%	1.66%	2.09%
ROCKY INTERTIDAL SHORE	0.32%	0.22%	8.27%
SALT MARSH	21.58%	**37.12%**	0.18%
SHRUB SWAMP	8.07%	6.77%	22.41%
TIDAL FLAT	0.52%	1.21%	6.96%
TOTALS	**100.00%**	**100.00%**	**100.00%**

Table 29. Wetland classifications by percentage for SS, NE, and NW study sites.

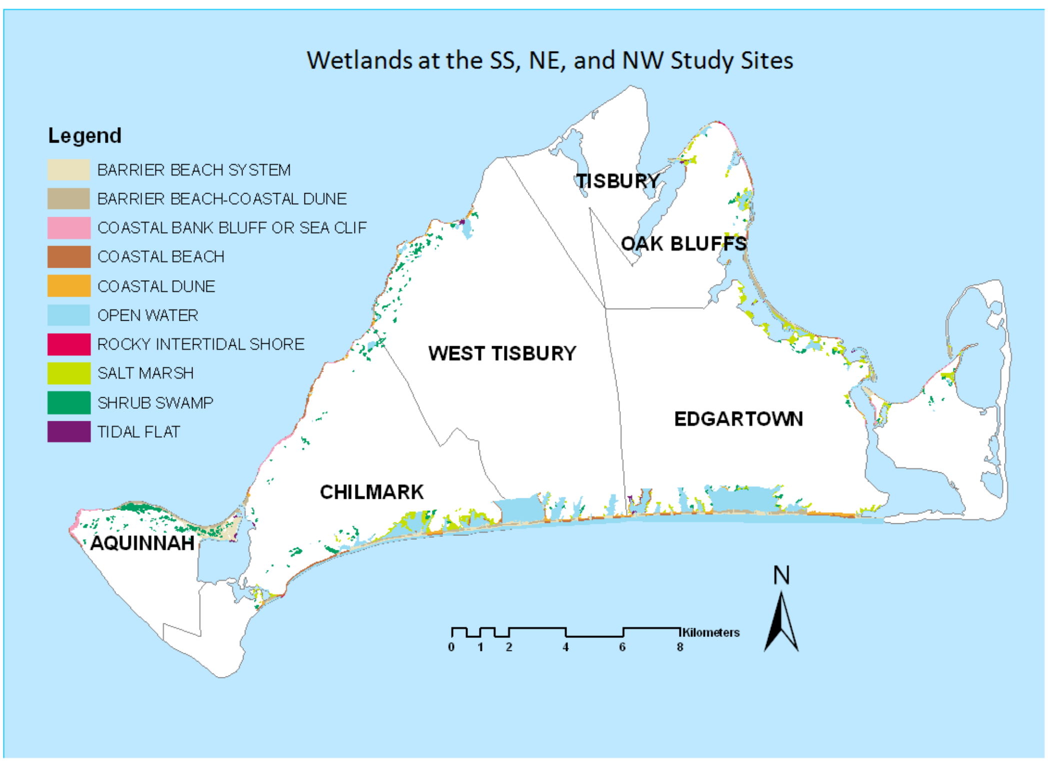

Figure 80. Map of the wetlands at the SS, NE, and NW study sites.

NE Site. The dominant SS pattern is not prevalent at the NE study site, except at a few locations that coincide with the Massachusetts Barrier Beach Data Layer (Figure 80). The NE study site has several sea cliffs parallel to the coastline that are located to the southeast of East Chop Light. These extend to the Highlands area and then resume after the entrance to Oak Bluffs Harbor and continue until the vicinity of Farm Pond in Oak Bluffs. More sea cliffs are located near North Neck/Cape Poge. While the percentage of cliff area is only 2.8% of the wetland category (Table 29), approximately 35% of the shoreline consists of these cliffs. (Sea cliffs encompass approximately 6 km (3.73 miles) out of 17.3 km (10.75 miles) of shoreline (i.e., 35% of the total shoreline). As expected, the barrier beach fronting Sengekontacket Pond is classified as barrier beach system and barrier beach-coastal dunes. There are numerous salt marshes bordering the NE site's coastal ponds, including: Lagoon, Sengekontacket, Trapp, and Eel, as well Cape Poge Bay. Slightly more than 37% of the NE wetlands consist of salt marshes, followed by barrier beach systems (25.5%), and barrier beach-coastal dunes (18.35%) (Table 29). The total area of wetlands in the NE site is 19,319,693 m² (4774 acres), encompassing approximately 38% of the site (Table 30).

NE WETLAND DESCRIPTION	ACRES	% OF WETLANDS
BARRIER BEACH-COASTAL DUNE	119.79	2.51
BARRIER BEACH SYSTEM	166.45	3.49
COASTAL BANK BLUFF OR SEA CLIFF	18.28	0.38
COASTAL BEACH	41.59	0.87
COASTAL DUNE	10.82	0.23
OPEN WATER	4,121.00	86.32
ROCKY INTERTIDAL SHORE	1.41	0.03
SALT MARSH	242.31	5.08
SHRUB SWAMP	44.20	0.93
TIDAL FLAT	7.87	0.16
TOTALS	4,773.71	100

Table 30. Wetland classifications by acreage and percentage on the NE study site.

NW Site. Barrier beach systems, shrub swamps, barrier beach-coastal dunes, and coastal beaches are the dominant wetland categories on the NW study site (Table 31). This study site has the largest percentage of sea cliffs, rocky intertidal shores, tidal flats, and shrub swamps, compared to the SS and NE study sites. Most of the shrub swamps are located southwest of Menemsha Pond. Compared to the SS and NE sites, salt marshes are close to non-existent (Figure 80). The coastal bank bluffs or sea cliffs consume approximately 30% of the NW shoreline (5.9 km/21 km), even though the percentage of cliffs is small (6.8%).

NW WETLAND DESCRIPTION	ACRES	% OF WETLANDS
BARRIER BEACH-COASTAL DUNE	122.99	7.90
BARRIER BEACH SYSTEM	221.59	14.23
COASTAL BANK BLUFF OR SEA CLIFF	56.56	3.63
COASTAL BEACH	100.58	6.46
COASTAL DUNE	17.43	1.12
MARSH	69.01	4.43
OPEN WATER	722.50	46.35
ROCKY INTERTIDAL SHORE	1.51	0.10
SHRUB SWAMP	187.15	12.05
TIDAL FLAT	58.11	3.73
TOTALS	1,557.42	100

Table 31. Wetland classifications by acreage and percentage on the NE study site.

Land Use

The following land use results are reported two different ways. The first is a summary of land use descriptions condensed into five categories: beach, developed land, salt marsh, upland, and water (Table 32). These results comprise the data used in further analyses. The second summary is derived from the 1997 LUS21 codes from MassGIS. No analysis was done with these categories and the data are reported here for informational purposes only (Table 33).

LUS DESCRIPTION	SS % LUS	NE % LUS	NW % LUS
BEACH	1.55%	0.96%	1.13%
DEVELOPED LAND	0.66%	8.15%	0.07%
SALT MARSH	0.63%	2.97%	0.49%
UPLAND	**88.39%**	**86.97%**	**98.08%**
WATER	8.76%	0.95%	0.22%
TOTALS	**100.00%**	**100.00%**	**100.00%**

Table 32. Summary percentage of land use characteristics for each study sites.

LUS DESCRIPTION	SS %	NE %	NW %
COMMERCIAL	0.67	0.67	0.21
CROPLAND	3.37	0.00	0.00
FOREST	5.39	8.75	4.58
LOW DENSITY RESIDENTIAL	47.45	45.16	62.08
MED. DENSITY RESIDENTIAL	1.35	6.06	0.63
HIGH DENSITY RES.	0.00	1.68	0.00
MULTI-FAMILY RESIDENTIAL	0.34	0.00	0.00
INDUSTRIAL	0.34	0.00	0.00
OPEN LAND	17.51	12.79	11.25
PARTICIPATION RECREATION	2.36	4.71	0.42
PASTURE	6.40	0.67	7.92
SALT MARSH	4.04	9.76	3.13
TRANSPORTATION	0.34	0.00	0.00
URBAN OPEN	1.01	1.68	1.04
WASTE DISPOSAL	0.34	0.00	0.00
WATER	0.00	2.69	2.71
WATER BASED RECREATION	1.68	4.71	4.17
WETLAND	0.00	0.67	1.88
WOODY PERENNIAL	7.41	0.00	0.00
TOTALS	**100.00**	**100.00**	**100.00**

Table 33. Land use classified by MassGIS and the percent of area for each study site.

At all three study sites, the upland land use category encompassed the largest percentage of land area (SS = 88.39%, NE = 86.97%, and NW = 98.08%) (Table 32). Uplands primarily include any non-developed land areas, from low density residential areas to forests. Water is the next largest land use class on the SS site, comprising 8.76%. Slightly more than 8% of the NE has developed land, the largest percentage of the three study sites. This result is particularly surprising in light of the presence of the more populated towns of Oak Bluffs and Edgartown in the NE site (Figure 81).

Using the categories supplied by MassGIS low density residential comprised the highest percentage of area at all three study sites (SS = 47.45%; NE = 45.16%; and NW = 62.08%; these lots are larger than 2,023 m²/0.5 acres) (Table 33). Open land is the next largest for all the sites, with the SS site at 17.51%, the NE site at 12.79%; and the NW site at 11.25%. Open land includes abandoned agriculture; power lines; and areas of no vegetation.

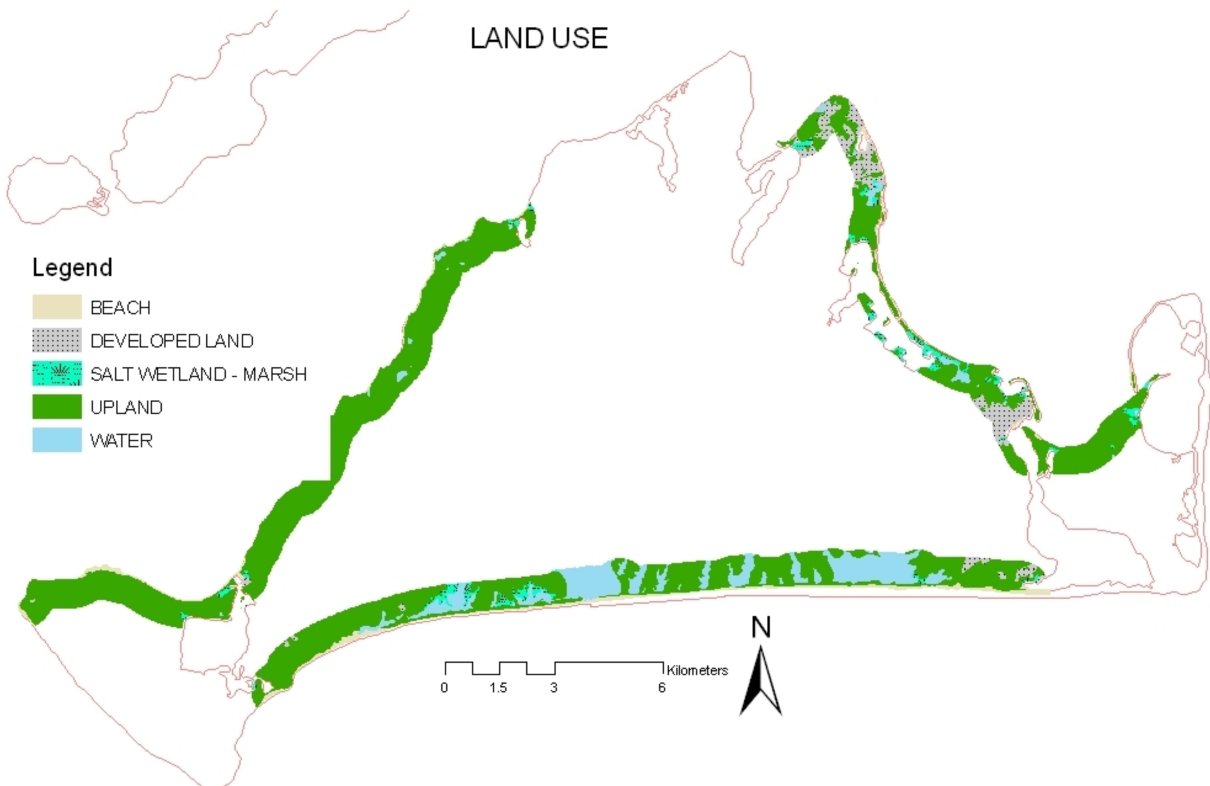

Figure 81. Land use characteristics at SS, NE, and NW study sites.

Compound Direction

SS Site. Compass directions indicate the directions faced by the transects along the study sites. The majority (77%) of the transects on the SS site faced directly south (Table 34). The remaining variation occurs at the far western edge of the study site, where 19% faced southeast, along with the remaining directions (Figure 82).

SS DIRECTION	NUMBER	SS %
E	5	1
ESE	3	1
S	376	77
SE	12	2
SSE	91	19
TOTALS	**487**	**100**

Table 34. SS study site percentage of compass directions for transects.

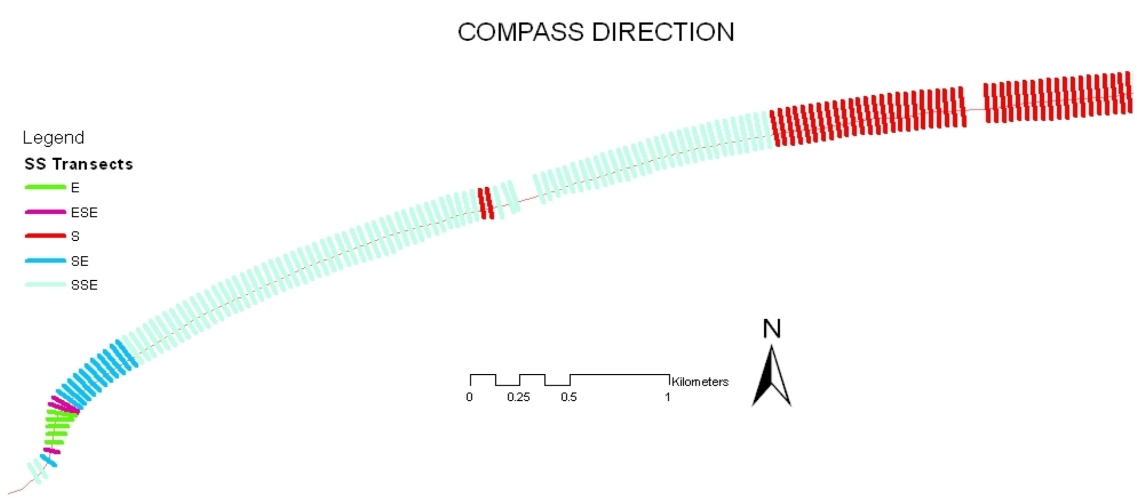

Figure 82. Map of SS transect compass directions.

NE Site. Because of the complexity of the NE shorelines, near Sengekontacket Pond, there are a wider range of compass directions (Figure 83). Overall, the most prevalent direction at the NE site is east northeast at 22%, followed by north northeast at 12%, and northwest at 11% (Table 35, Figure 83, Figure 84).

NW Site. The patterns on the NW site are not as unidirectional as the SS site, nor as varied as the NE site. The dominant direction on this side is north, with WNW at 31%, NW at 18%, N at 15%, NNW at 14%, and NNE at 12% (Table 35). The northeasterly transects are primarily located around Menemsha Bight, and the remaining are east of Cape Higgon, Cedar Tree Neck, and Lambert Cove (Figure 85, Figure 86).

NE DIRECTION	NUMBER	NE %
E	40	8
ENE	106	22
ESE	22	4
N	32	7
NE	37	8
NNE	59	12
NNW	19	4
NW	52	11
S	7	1
SE	5	1
SSE	2	0
SSW	11	2
SW	28	6
W	13	3
WNW	14	3
WSW	40	8
TOTALS	**487**	**100**

NW DIRECTION	NUMBER	NW %
ENE	2	0
N	74	15
NE	6	1
NNE	56	12
NNW	69	14
NW	90	18
W	38	8
WNW	149	31
WSW	3	1
TOTALS	**487**	**100**

Table 35. NE and NW study sites percentage of compass directions for transects.

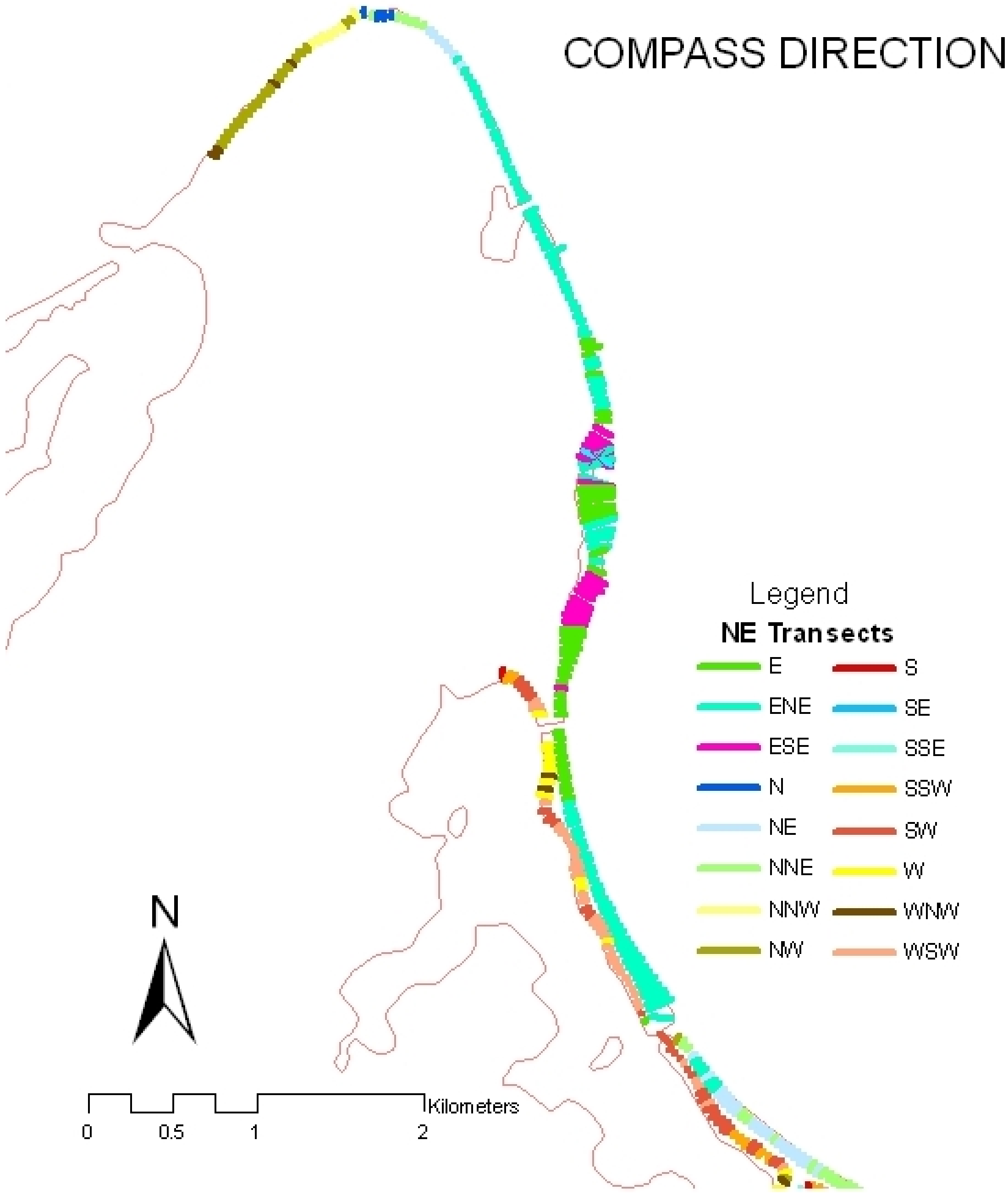

Figure 83. Map of the northern NE study site compass direction transects.

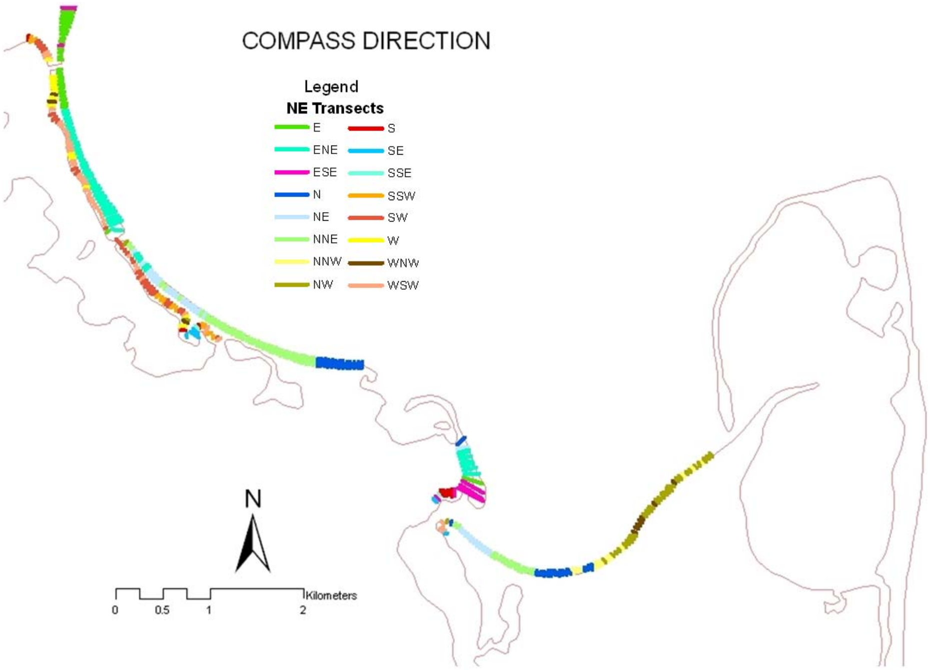

Figure 84. Map of the southern NE study site compass direction transects.

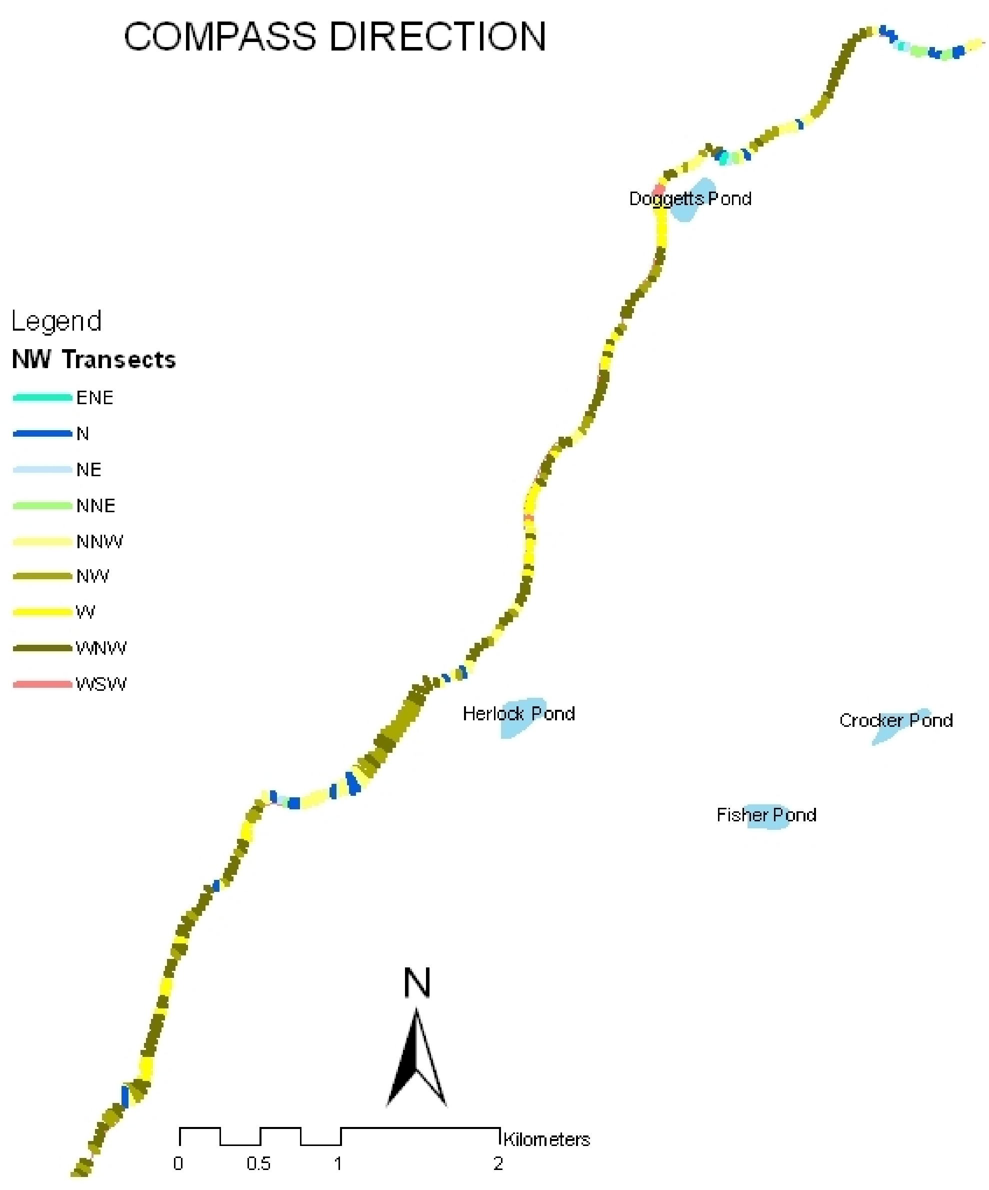

Figure 85. Map of the northern NW study site compass direction transects.

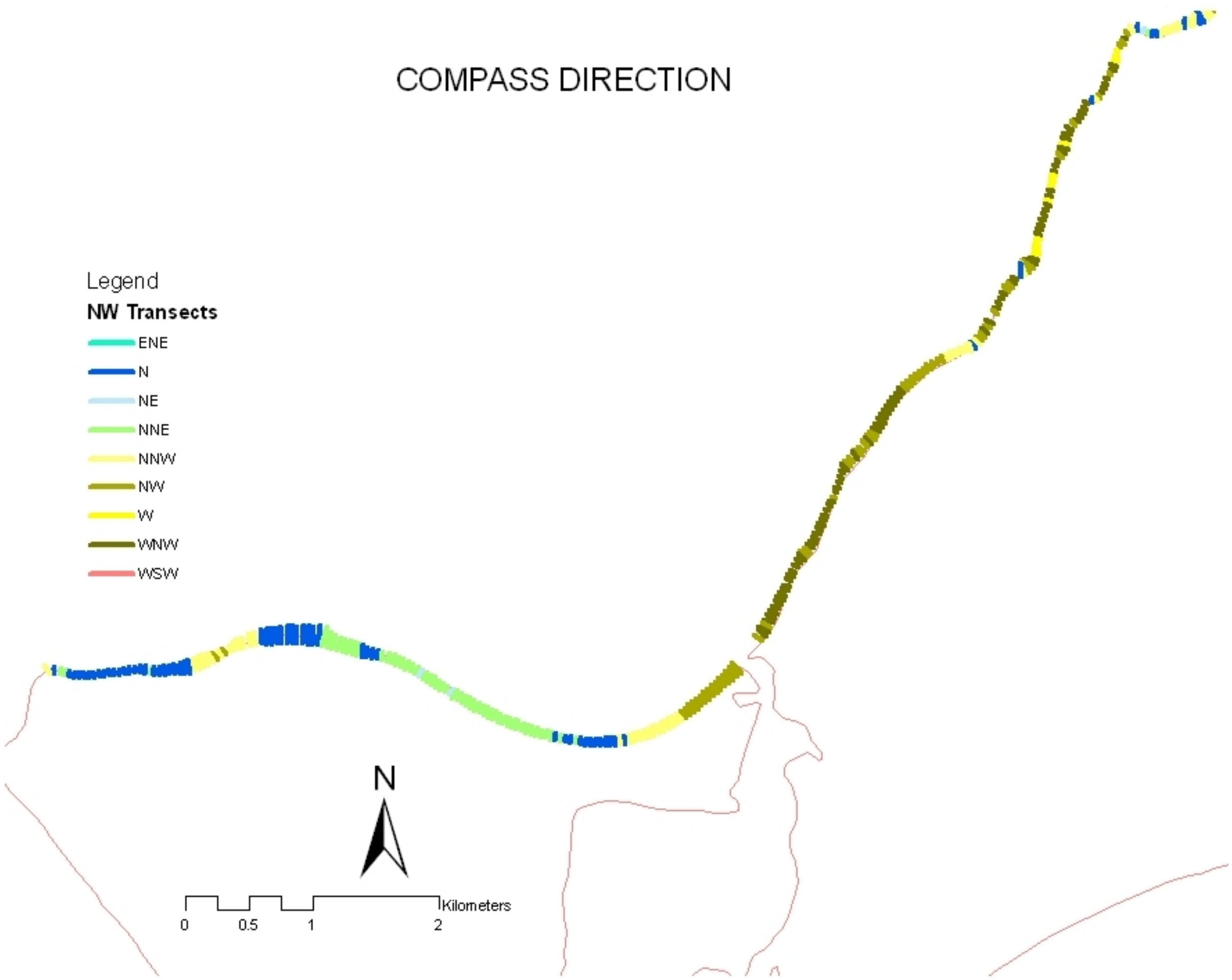

Figure 86. Map of the southern NW study site compass direction transects.

<u>Wind and Waves</u>.

Wind and wave information was consolidated from the Coastal Hydraulics Laboratory, Wave Information Studies (WIS), WIS Model #074, a site located southwest of Aquinnah at longitude -71.00024 and latitude 41.24976 (Figure 30). Data from this WIS model was collected every hour for 19 years (1980-1999), for a total of 175,294 occurrences (see Appendix A (Appendix 1 - Appendix 4) for details by month and direction).

The following analyses of this data accurately reflect the wind and wave environment for the SS study site of Martha's Vineyard. A reasonable assumption being made is that it also approximates the general wind and wave climate at the NW site, but, most likely, is somewhat inaccurate for the NE site. Vineyard Sound and Nantucket Sound do not have buoys or WIS models that record the relevant data. Therefore, no information was available for the NE study site. Hence, the following results should only be considered a very general approximation of the wind and wave climate for MV.

Wind. During the summer months (April through September), the highest mean wind speed (6.46 m/sec) was recorded in April and the lowest (4.39 m/sec) in July (Figure 87). By September, the wind speed begins to increase to a mean of 5.81 m/sec. The summer prevailing winds are from the SW and SSW, with a mean wind speed of 5.09 m/sec and 5.46 m/sec, respectively (Table 36). The highest mean wind speeds during the summer months are from the NNE and NE at 6.04 and 6.09 m/sec, despite the fact that this is not the prevailing direction.

A steady increase in wind speed occurs during the winter months (October through March). This increase is already apparent in October (7.08 m/sec), peaks in December and January (9.11 and 9.18 m/sec, respectively), and tapers off by March

(7.942 m/sec) (Figure 87). The prevailing and strongest winds during the winter months are from the W, WNW, and NW with speeds averaging 9.04, 9.56, and 9.73 m/sec, respectively (Table 36).

For all months, wind speeds between 4-5.99 m/sec occur 24% of the time, winds 6-7.99 m/sec occur 23.5% of the time, and winds 2-3.99 occur 18% of the time (Figure 89). Winds greater than 16 m/sec occur less than 2% of the time. Overall, 10% of the time the winds are from the SW and 10% from the NW (Figure 88A, B). Further, the winds for both seasons have remained constant, from 1980-1999 (Figure 90).

For additional wind speed data by percent of occurrence and compass direction, by month see Appendix A (Appendix 1 - Appendix 4).

Dir	Summer Mean wsp m/sec	Winter Mean wsp m/sec	WINTER % Direction	SUMMER % Direction
N	5.93	8.39	0.64	0.46
NNE	6.04	8.75	0.42	0.34
NE	6.09	8.53	0.39	0.42
ENE	5.03	7.68	0.25	0.31
E	4.93	7.39	0.26	0.36
ESE	4.61	6.94	0.2	0.31
SE	4.41	6.95	0.27	0.37
SSE	4.52	6.99	0.25	0.39
S	4.90	7.13	0.39	0.73
SSW	**5.46**	7.39	0.44	**0.87**
SW	**5.09**	7.79	0.66	**1.07**
WSW	4.68	7.89	0.53	0.64
W	4.96	**9.04**	**0.87**	0.64
WNW	5.45	**9.56**	**0.95**	0.52
NW	5.83	**9.73**	**1.11**	0.56
NNW	5.53	8.61	0.69	0.38

Table 36. Mean summer and winter wsp (m/sec) and percent of direction.

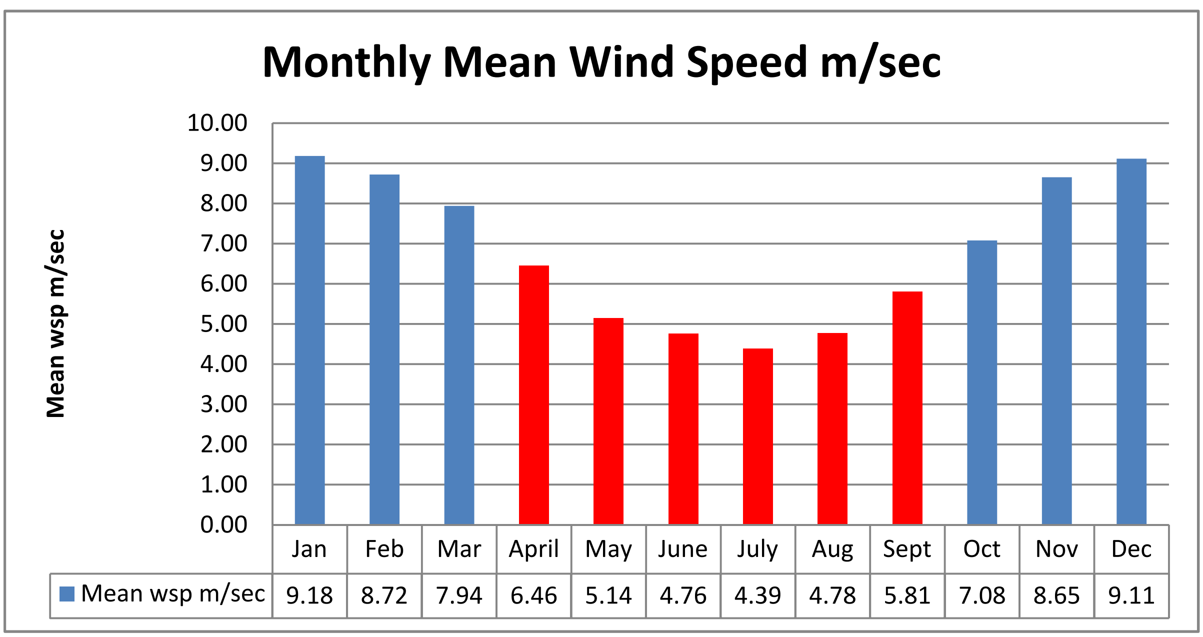

Figure 87. Histogram of monthly mean wind speed m/sec.

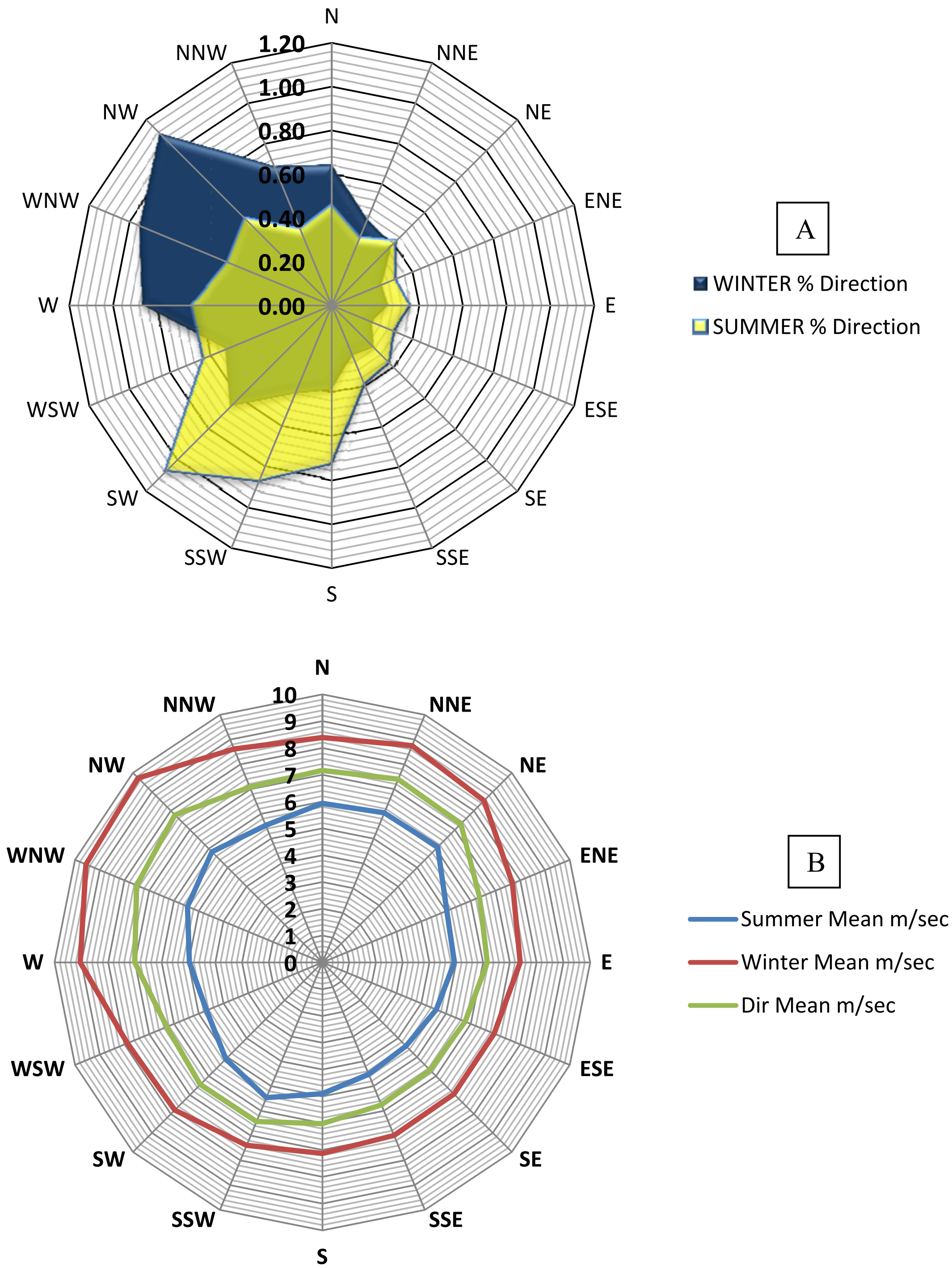

Figure 88. Compass rose indicating percent of winter and summer wind direction (A), and compass rose with summer, winter and mean directional wind speed m/sec (B).

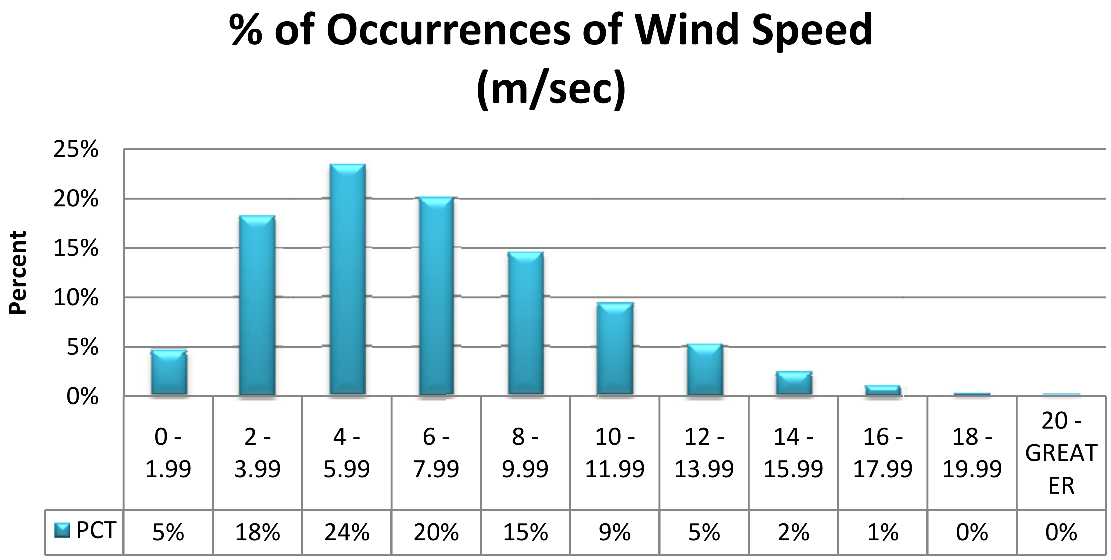

	0 - 1.99	2 - 3.99	4 - 5.99	6 - 7.99	8 - 9.99	10 - 11.99	12 - 13.99	14 - 15.99	16 - 17.99	18 - 19.99	20 - GREATER
PCT	5%	18%	24%	20%	15%	9%	5%	2%	1%	0%	0%

Figure 89. Percent of wind speed (m/sec) for all months.

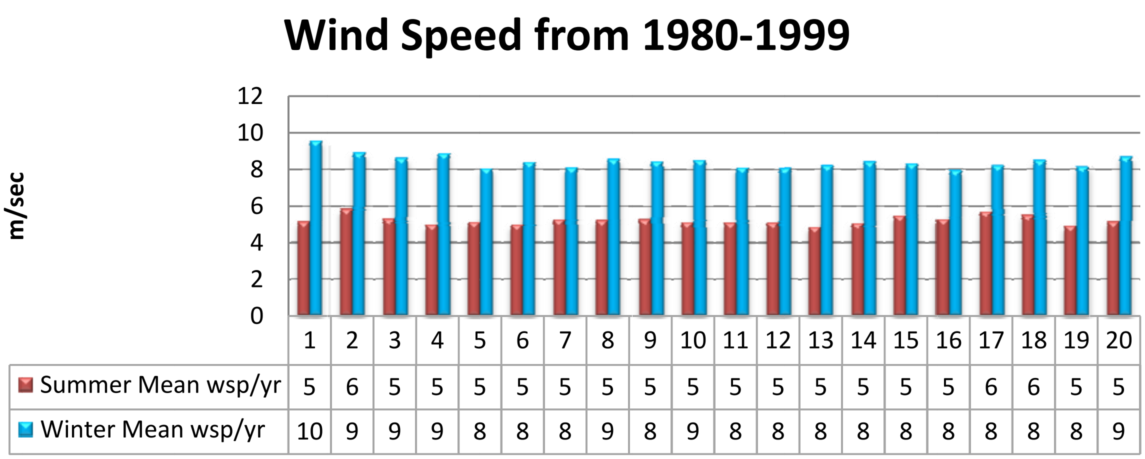

	1	2	3	4	5	6	7	8	9	10	11	12	13	14	15	16	17	18	19	20
Summer Mean wsp/yr	5	6	5	5	5	5	5	5	5	5	5	5	5	5	5	5	6	6	5	5
Winter Mean wsp/yr	10	9	9	9	8	8	8	9	8	9	8	8	8	8	8	8	8	8	8	9

Figure 90. Histogram of mean wind speed data per year from 1980 to 1999, by summer and winter seasons.

Waves. During the summer months of April through September, the primary wave direction is from the SSW (Table 37). The winter months, October through March, have a comparable mean wave direction from the SSW and the SW (Table 38, Figure 91). Waves coming from the N are essentially non-existent during July, but are most prevalent in October (Table 38, Figure 92). Easterly wave movement occurs during the months of March and September; southerly waves occur during July and August, and wave direction from the W occurs in January. Overall, 22% of the time the waves are from the SSW, 15% of the time they are from the S, and 10% of the time they are from SW (Table 38, Figure 93). Wave height was not analyzed for this study.

Wave Dir	Winter % Mean Wave Direction	Summer % Mean Wave Direction	Jan-Mar % Mean Wave Direction	Apr-June % Mean Wave Direction	July-Sept % Mean Wave Direction	Oct-Dec % Mean Wave Direction
N	0.26	0.1	0.24	0.12	0.07	0.27
NNE	0.2	0.08	0.18	0.11	0.05	0.22
NE	0.16	0.09	0.14	0.11	0.06	0.17
ENE	0.17	0.11	0.16	0.12	0.1	0.18
E	0.26	0.2	0.27	0.21	0.19	0.25
ESE	0.34	0.39	0.32	0.42	0.35	0.36
SE	0.38	0.63	0.35	0.61	0.66	0.41
SSE	0.41	0.76	0.38	0.67	0.84	0.44
S	0.73	1.7	0.76	1.53	1.87	0.69
SSW	**1.11**	**2.62**	**1.23**	**2.57**	**2.66**	**0.99**
SW	**1.01**	0.74	0.95	0.74	0.74	1.07
WSW	1	0.35	0.96	0.42	0.27	1.04
W	0.97	0.26	0.94	0.31	0.2	1
WNW	0.6	0.15	0.61	0.15	0.14	0.59
NW	0.41	0.11	0.41	0.1	0.12	0.41
NNW	0.31	0.1	0.33	0.11	0.08	0.29

Table 37. Percent of mean wave direction by seasons, 1980-1999.

DEGREE CENTER	WAVE DIRECTION	JAN	FEB	MAR	APR	MAY	JUN	JUL	AUG	SEP	OCT	NOV	DEC	CASES	PCT
0	N	0.27	0.24	0.22	0.19	0.12	0.06	0.01	0.05	0.15	0.33	0.25	0.23	3694	2.1
-22.5	NNE	0.18	0.17	0.18	0.12	0.13	0.07	0.01	0.04	0.11	0.3	0.15	0.22	2959	1.7
-45	NE	0.15	0.14	0.13	0.13	0.14	0.07	0.01	0.04	0.12	0.21	0.14	0.16	2550	1.5
-67.5	ENE	0.15	0.18	0.14	0.12	0.16	0.07	0.01	0.09	0.19	0.21	0.19	0.14	2911	1.7
-90	E	0.26	0.23	0.32	0.22	0.25	0.15	0.05	0.18	0.34	0.29	0.23	0.23	4836	2.8
-112.5	ESE	0.31	0.32	0.33	0.38	0.59	0.3	0.13	0.37	0.55	0.47	0.33	0.28	7656	4.4
-135	SE	0.28	0.33	0.43	0.51	0.71	0.6	0.34	0.85	0.78	0.6	0.37	0.27	10651	6.1
-157.5	SSE	0.32	0.31	0.52	0.58	0.88	0.55	0.56	0.95	1.02	0.65	0.38	0.28	12293	7
-180	S	0.64	0.65	1	1.33	1.51	1.76	2.14	2.13	1.33	0.88	0.68	0.5	25514	14.6
-202.5	SSW	1.14	1.02	1.52	2.1	2.52	3.09	3.95	2.44	1.59	1.06	0.99	0.93	39217	22.4
-225	SW	1.01	0.87	0.96	0.84	0.58	0.8	0.77	0.68	0.78	1.01	1.06	1.14	18394	10.5
-247.5	WSW	1.27	0.83	0.79	0.63	0.32	0.32	0.21	0.21	0.38	0.68	1.12	1.33	14174	8.1
-270	W	1.12	0.91	0.8	0.45	0.28	0.21	0.13	0.18	0.29	0.77	0.96	1.27	12913	7.4
-292.5	WNW	0.68	0.66	0.48	0.26	0.12	0.08	0.1	0.09	0.24	0.46	0.64	0.68	7880	4.5
-315	NW	0.38	0.46	0.38	0.18	0.07	0.06	0.06	0.11	0.2	0.33	0.42	0.48	5446	3.1
-337.5	NNW	0.31	0.38	0.29	0.17	0.1	0.05	0.02	0.08	0.15	0.25	0.29	0.34	4206	2.4

Table 38. Percent of wave direction by month, 1980-1999.

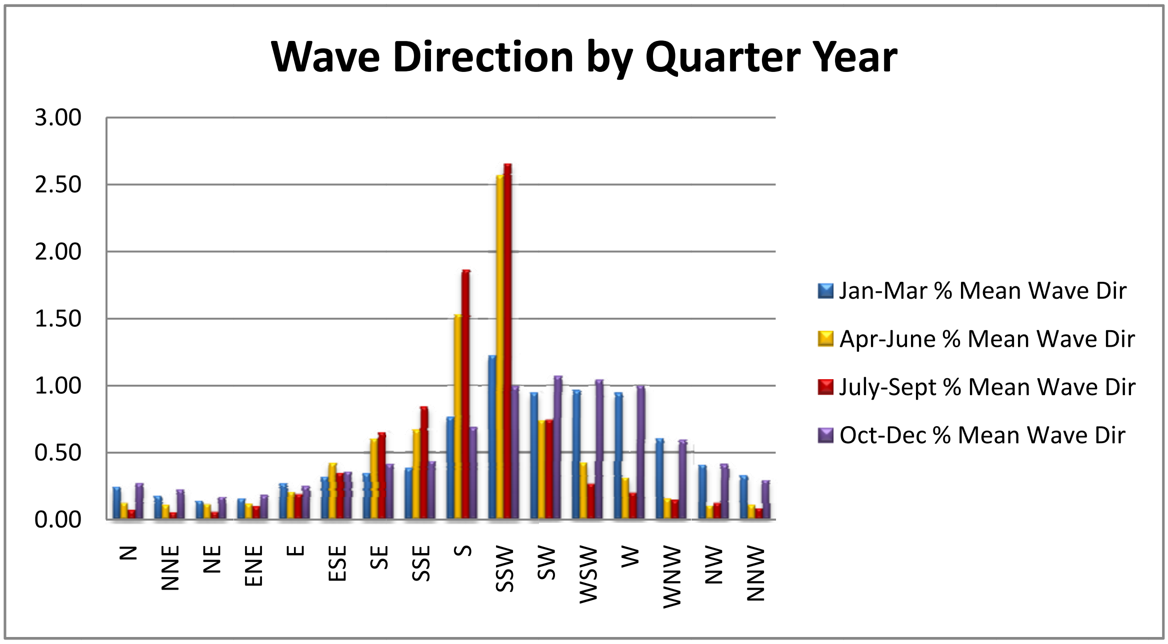

Figure 91. Wave direction by quarter for years 1980-1999.

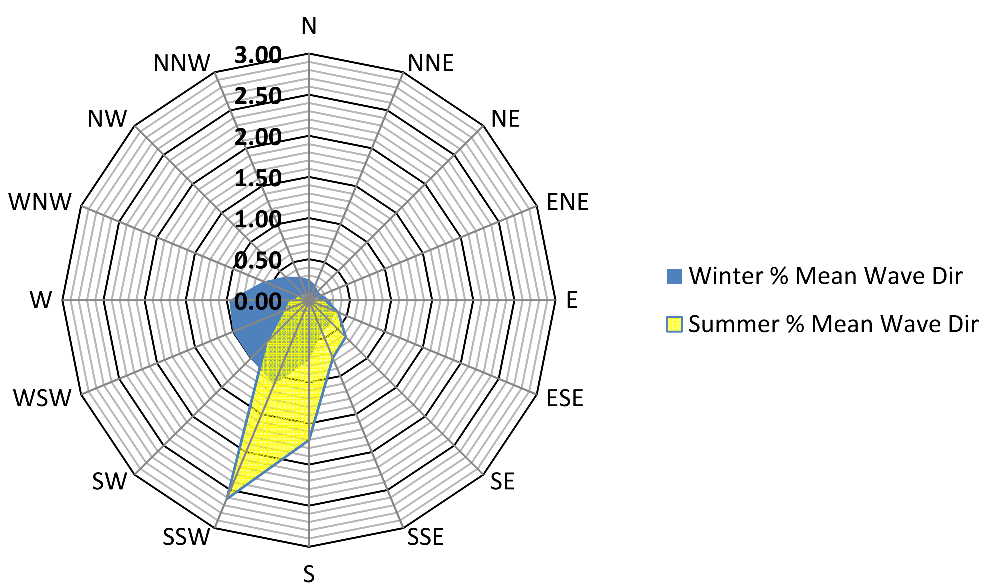

Figure 92. Summer and winter percent of mean wave direction (1980-1999).

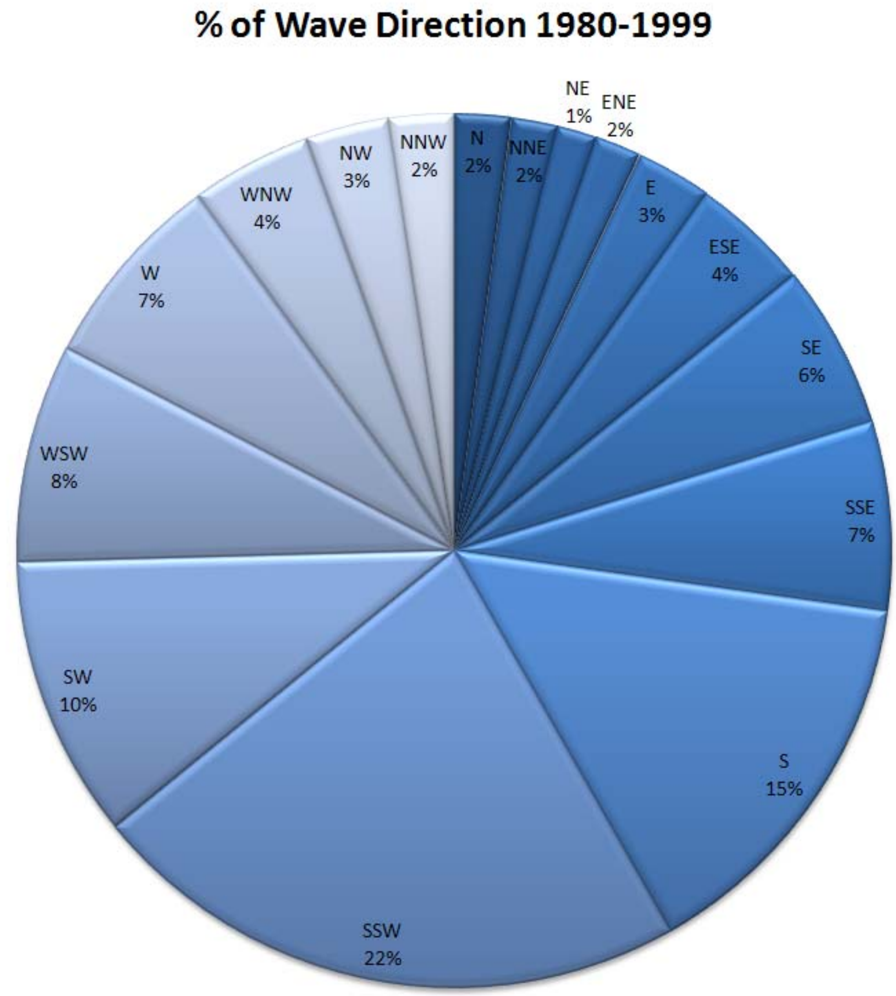

Figure 93. Pie chart of the percentage of wave direction vs. time.

Spatial Analysis of Shoreline Erosion

Spatial Autocorrelation (Moran's *I* Index and Z-score)

To determine if there were any patterns to coastal erosion, or accretion, at the study sites, I used ESRI® ArcGIS® v9.2 to determine if there were any positive or negative spatially autocorrelated patterns. I calculated the average distance between neighboring transects, first using 5 nearest neighbors, then 400. By testing both extremes of distance, a more accurate depiction of spatial autocorrelation for each study site should surface.

Results for 5 neighbors show that the average distance for the SS site was 120 m, 111 m for the NE site, and 115 m for NW site. The average distances between 400 neighbors are 12,284 m for the SS site, 7,557 m for the NE site, and 10,081 m for the NW site.

Once the average distance in meters for 5 and 400 neighbors was determined, the spatial pattern was calculated using Moran's *I* Index. My hypothesis was that there would be a positive spatial correlation between closer neighbors than those farther away, based on regional variable theory. Results indicate that at all spatial scales, for all study sites, there are positive spatial autocorrelations.

Table 39 shows the results of this analysis by Moran *I* Index, z-score, variance, and significance level for each study site, by average distance to neighbors. While each result shows a significant positive spatial autocorrelation, the Moran *I* Index reflects slightly more dispersion as the distance increases from ~115 m to ~10,000 m. Z-scores in every site are far beyond the typical standard deviations (±2.54), thereby indicating essentially no probability of randomness of erosion patterns at any site. The null hypothesis can be rejected for all sites. This analysis indicates that there are patterns of erosion, equilibrium, and/or accretion at each study site (Table 39).

SS Spatial Autocorrelation Results	SS Neighbors, Avg Distance (5, 120 m)	SS Neighbors, Avg Distance (400, 12284 m)
Moran's I Index	0.79	0.34
Z-score	25.66	34.3
Variance	0.0000963	0.000102
Significance Level	0.01	0.01

NE Spatial Autocorrelation Results	NE Neighbors, Avg Distance (5, 111 m)	NE Neighbors, Avg Distance (400, 7557 m)
Moran's I Index	0.75	0.27
Z-score	24.06	32.75
Variance	0.0000985	0.000069
Significance Level	0.01	0.01

NW Spatial Autocorrelation Results	NW Neighbors, Avg Distance (5, 115 m)	NW Neighbors, Avg Distance (400, 10081 m)
Moran's I Index	0.92	0.53
Z-score	28.25	54.89
Variance	0.001062	0.000094
Significance Level	0.01	0.01

Table 39. Spatial autocorrelation results for the SS, NE, and NW study sites.

Fractal Dimension Analysis

Fractal dimensions are used in geomorphology as a means of descriptive parameterization of patterns and landscape topography (Baas, 2002). In this thesis, fractal dimension analysis was used to describe the shoreline change patterns at each study site, not the actual position or length of the shoreline, as Mandelbrot (1967) did in his classic work. The historical linear regression rates for each transect were used as a means to identify whether shorelines were gradually changing over a significantly long time frame, or whether the stresses of rising seas were causing the shorelines to change more rapidly.

To view the variability of the study site shoreline patterns, based on trend analysis, see Figure 94, Figure 95, and Figure 96. The linear regression sample points were fitted to a surface by using a least squares polynomial regression. These three-dimensional plots clearly indicate an irregular pattern of shoreline change rates for all the study sites. These observations, and the results from fractal analysis, suggest that the coastal study sites have not reached a self organizing pattern, possibly due to recent changes in sea level.

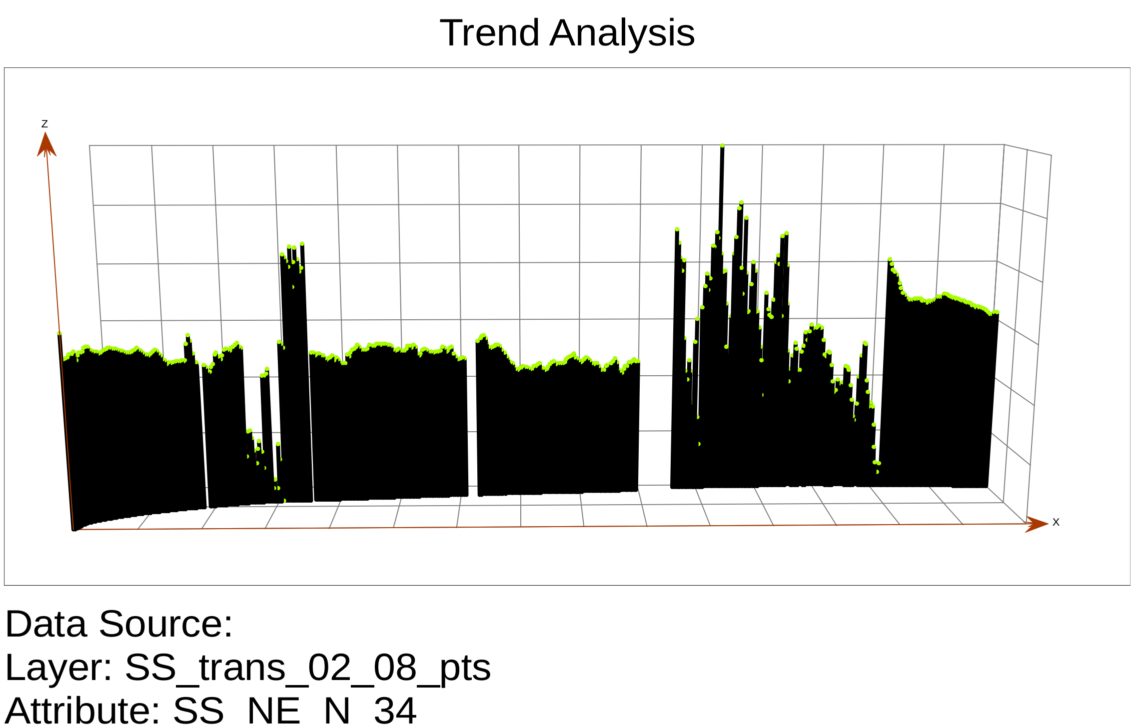

Figure 94. SS site trend analysis of shoreline change behavior based on historical linear regression rates.

Trend Analysis

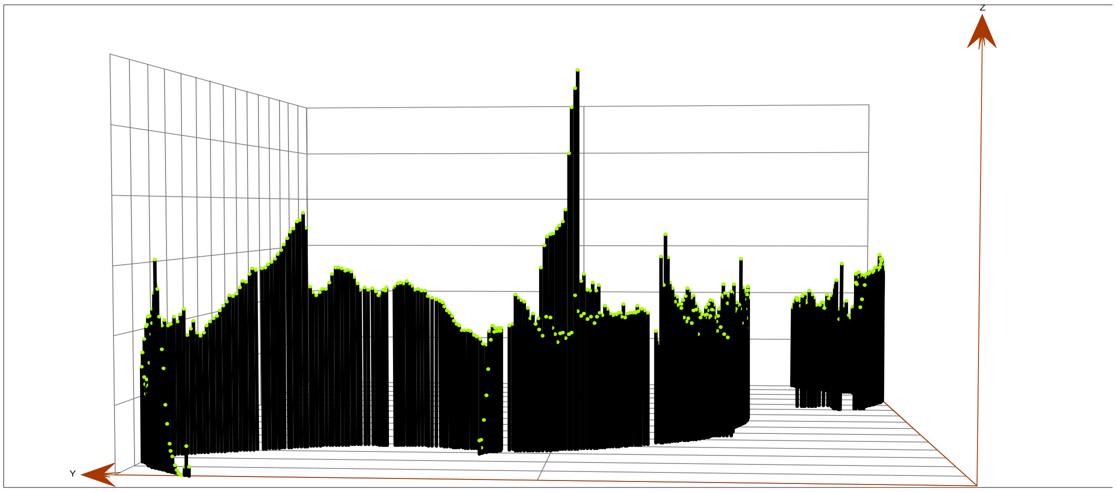

Data Source:
Layer: NE_Trans_02_08_pts
Attribute: SS NE N 34

Figure 95. NE site trend analysis of shoreline change behavior based on historical linear regression rates.

Trend Analysis

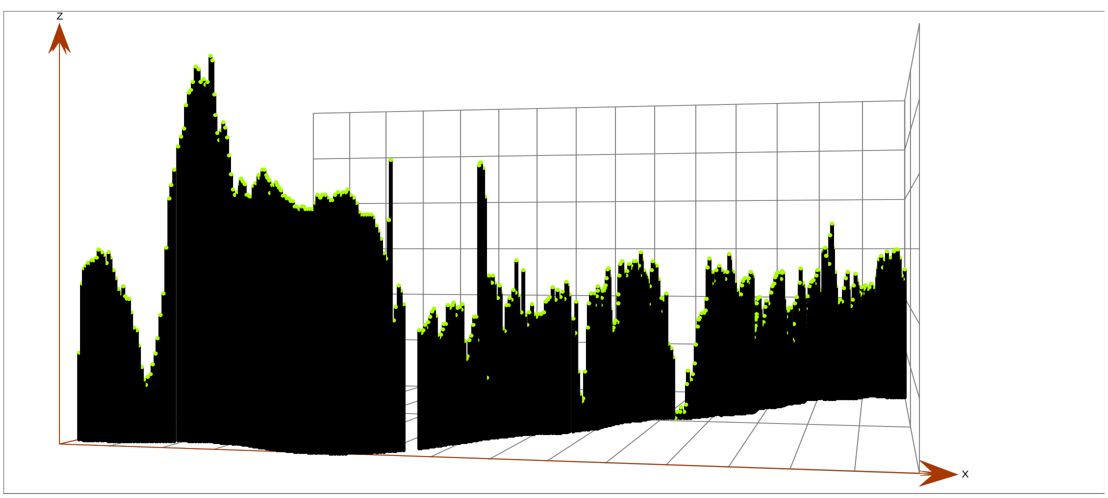

Data Source:
Layer: NW_Trans_02_08_pts
Attribute: SS NE N 34

Figure 96. NW site trend analysis of shoreline change behavior based on historical linear regression rates.

SS Fractal Dimension Analysis. The prediction kriging model had a mean of -0.0005966, a root-mean-square of 0.3857, an average standard error of 0.3829, a mean standardized of -0.0007156, and a root-mean-square standardized of 1.008. The predicted plot, shown in Figure 97, indicates a good kriging model because the points are fitted closely to the blue line. With autocorrelation, the blue line should be closer to the 1:1, black dashed, line (Johnston *et al.*, 2003).

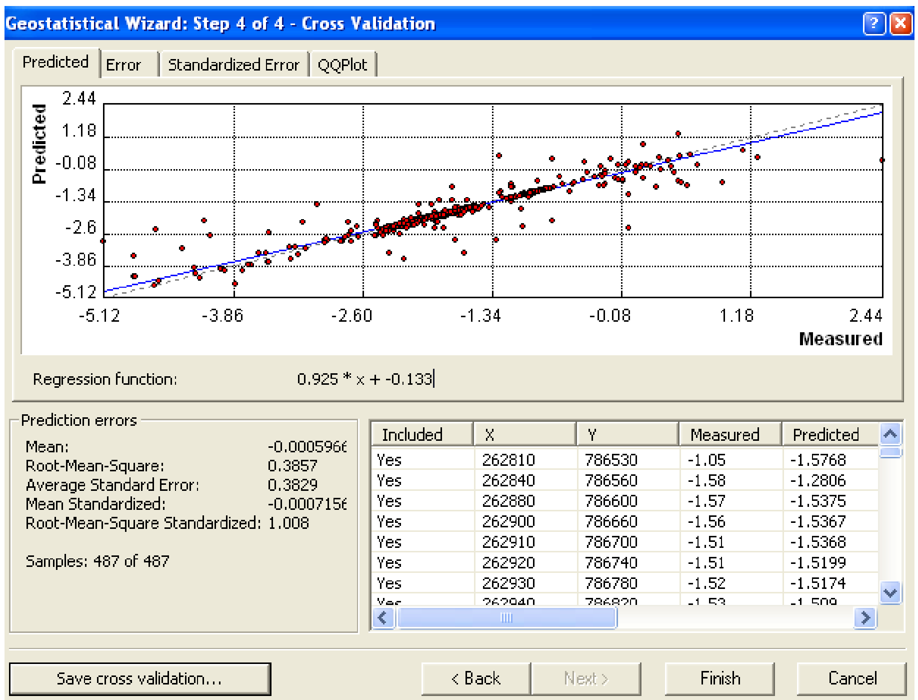

Figure 97. Cross validation predicted errors from the SS site point data based on historical linear regression results.

Based on the semivariogram, the range is 503 m (~0.5 km). This is also where the model levels out (Figure 98), indicating that, along the 21 km of shoreline, there is an autocorrelation of erosion rates within 0.5 km of each transect, but no autocorrelation beyond that. The nugget size for this analysis is 0.038, indicative of small measurement errors. The partial sill is 0.758, the sill is 0.796, the root-mean-square is 0.386, the average standard error is 0.383, and RMS Standardized is 1.008.

At 50 m (164 ft), one can expect to see a 0.15 m/yr (0.6 in/yr) change in shoreline, at 150 m (492 ft) a 0.37 m/yr change, and, at 300 m (984 ft), a 0.64 m/yr change (Figure 99). Beginning at 500 m (1640 ft) and beyond, one can expect to see a 0.8 m/yr variation in shoreline change. The regression rate for these data is 0.00158, derived from the slope of the semivariogram, with a p-value of 0 and an R^2 of 96.6%. Like the spatial autocorrelation analysis in the previous section, these results validate a strong correlation of shoreline change patterns within 0.5 km of each transect.

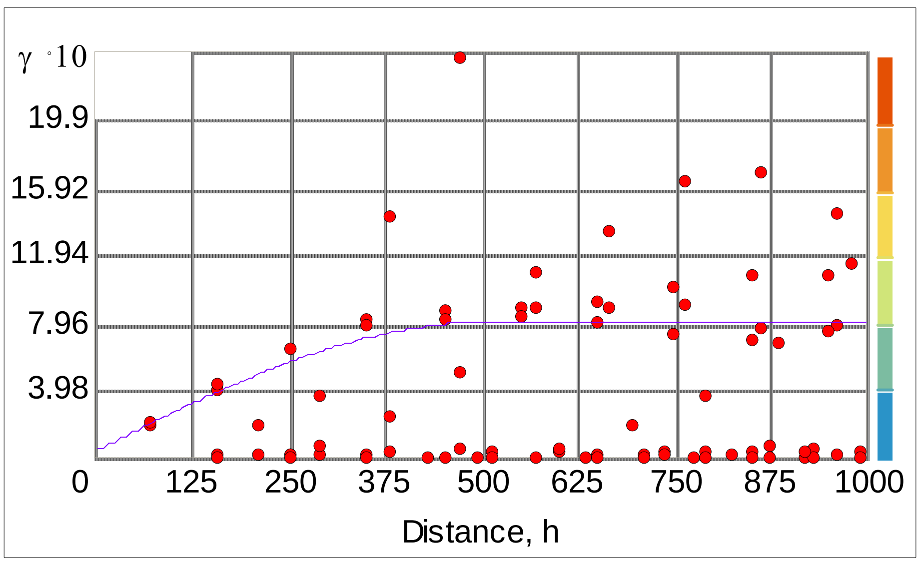

Figure 98. SS study site semivariogram for point data based upon the linear regression rate for 487 transects.

To further understand this shoreline pattern, fractal analysis results indicate a fractal dimension of D = 1.99. The formula to calculate this was: *D = (4-m)/2, D = (4-0.00158)/2, D = (3.99842)/2, D = 1.99)*, where *m* equals the slope of the semivariogram, derived from least squares linear regression. A high D value, such as this, implies that short range effects dominate the patterns of coastal erosion on the south side of Martha's Vineyard, rather than a coastline exhibiting long range stable effects

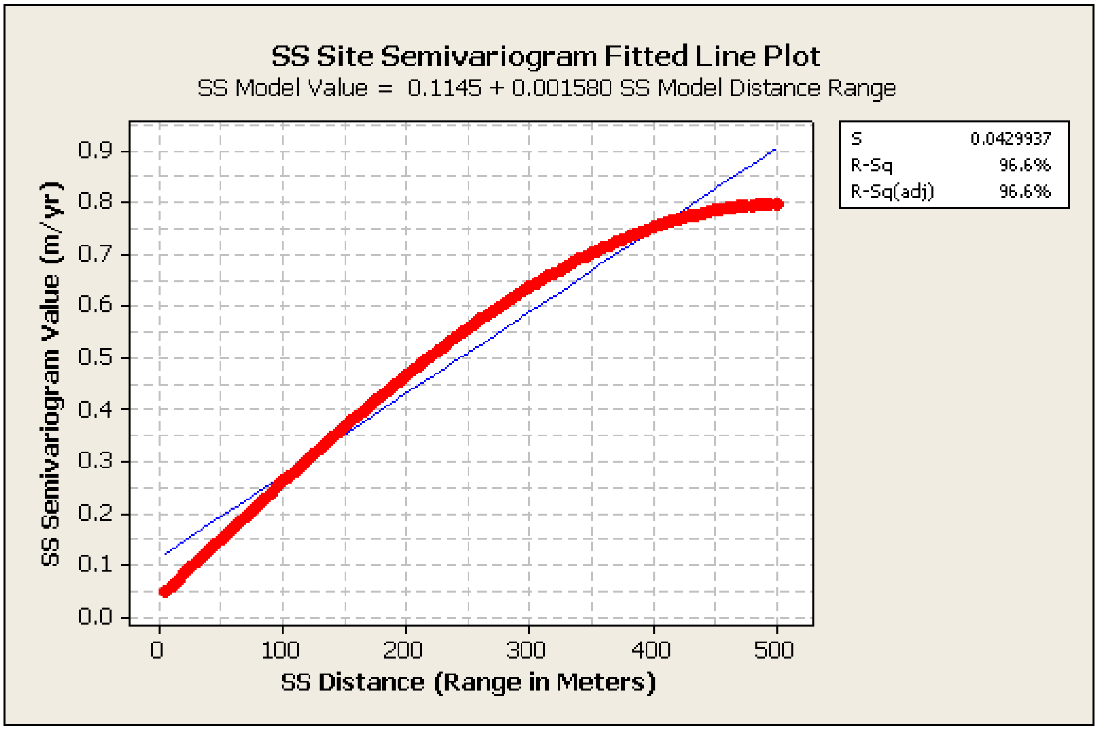

Figure 99. SS study site semivariogram fitted line plot - shoreline change m/yr vs distance in meters.

(Burrough, 1981).

<u>NE Site Fractal Dimension Analysis</u>. Kriging results from the NE study site indicate a prediction mean of -0.001438, a root-mean-square of 0.08457, an average standard error of 0.09971, a mean standardized of -0.0007005, and a root-mean-square standardized of 0.7962. The predicted plot, shown in (Figure 100), indicates an excellent kriging model, with autocorrelation, because the points are fitted very closely to the blue line.

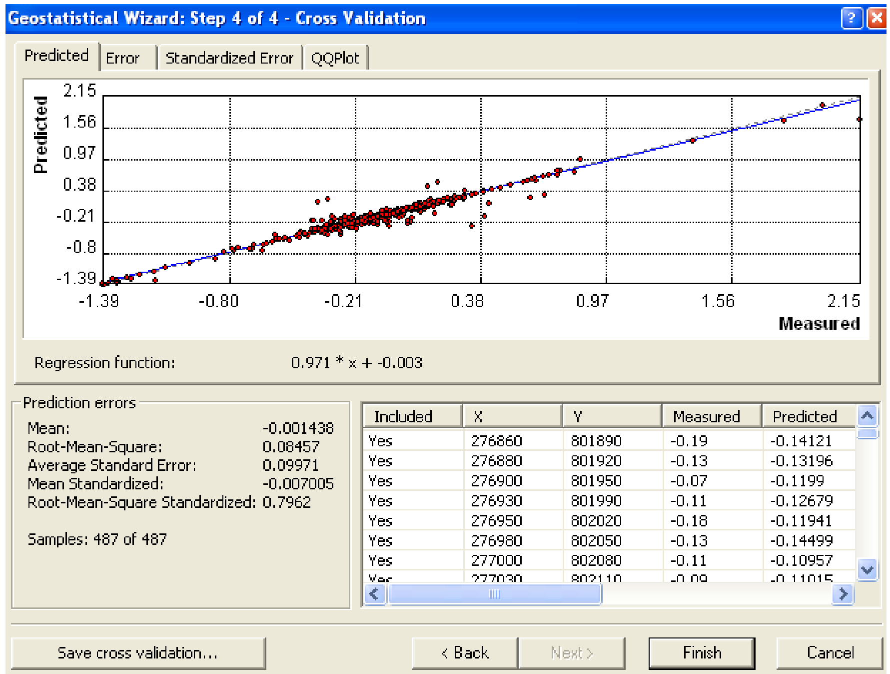

Figure 100. Cross validation predicted errors from the NE site point data based on historical linear regression results.

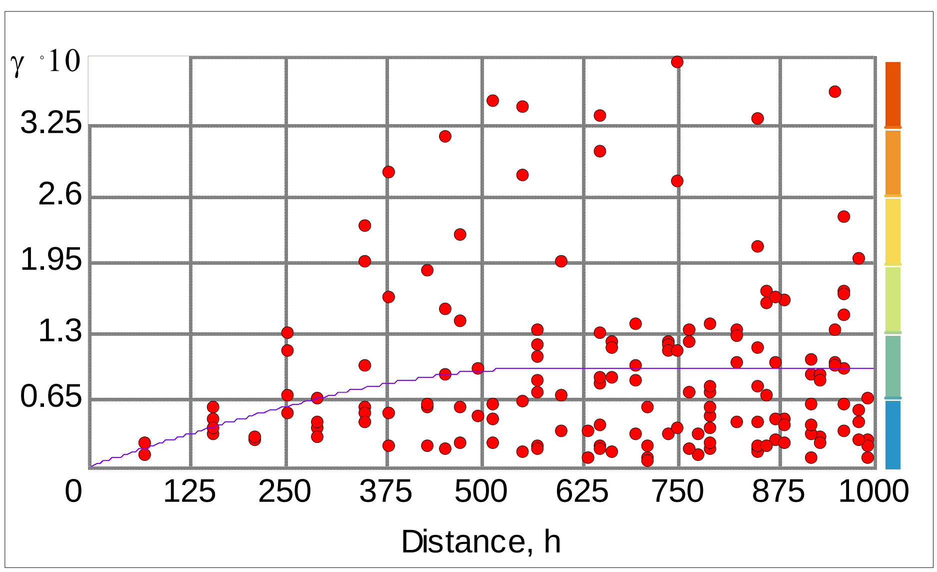

Figure 101. NE study site semivariogram for point data based upon the linear regression rate for 487 transects.

Based on the semivariogram, the range for the NE site is 577 m (0.577 km). This is also where the model levels out (Figure 101), indicating that, along the 17.3 km of shoreline, there is an autocorrelation of shoreline change rates within 0.577 km of each transect, but no autocorrelation beyond that point. The nugget size here is 0, indicative of no measurement errors. The partial sill and sill are 0.09346, the root-mean-square is 0.386, the average standard error is 0.383, and the root-mean-square standardized is 1.008 (Figure 100).

At 50 m (164 ft), one can expect to see a 0.012 m/yr (0.5 in/yr) change in shoreline. At 150 m (492 ft), a 0.04 m/yr change, and at 300 m (984 ft), a 0.067 m/yr change (Figure 102). Beginning at 575 m (1886 ft) and beyond, one can expect to see a 0.09 m/yr variation in shoreline change. The regression rate is 0.00169, derived from the slope of the semivariogram, with a p-value of 0 and an R^2 of 96.6%. Like the spatial autocorrelation analysis in the previous section, these results validate a strong correlation of shoreline change patterns within 0.5 km of each transect.

To further understand this shoreline pattern, fractal analysis results indicate a fractal dimension of D = 1.99. The formula to calculate this was: $D = (4-m)/2$, $D = (4-0.00169)/2$, $D = (3.99831)/2$, $D = 1.99$), where m equals the slope of the semivariogram, derived from least squares linear regression. A high D value, such as this, implies that short range effects dominate the patterns of coastal erosion on the northeast side of Martha's Vineyard, rather than a coastline exhibiting long range stable effects (Burrough, 1981).

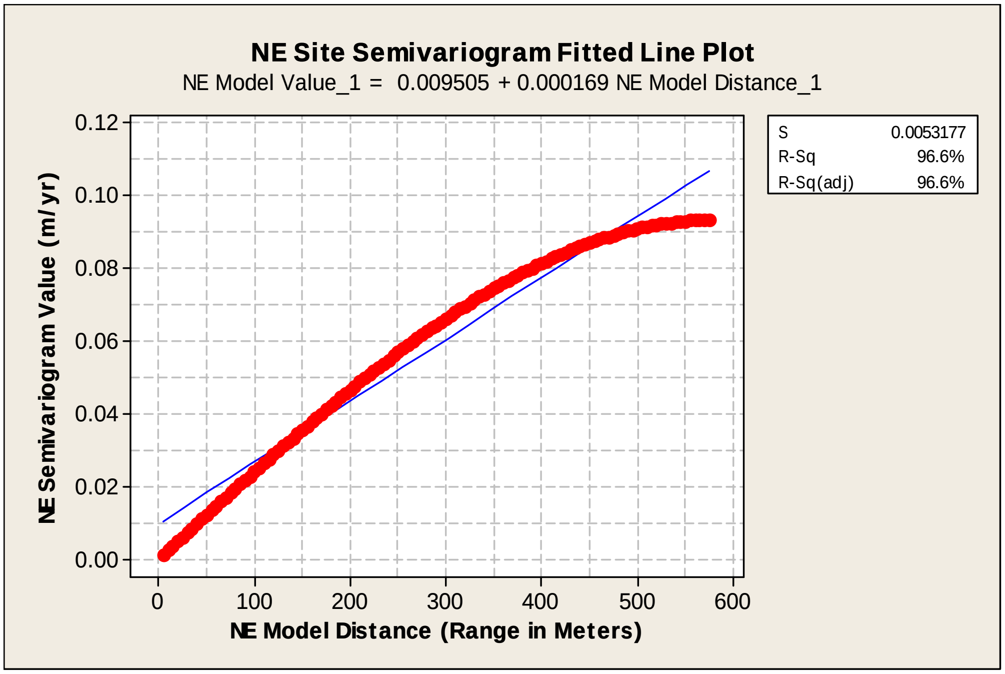

Figure 102. NE study site semivariogram for point data based upon the linear regression rate for 487 transects.

NW Site Fractal Dimension Analysis. Kriging results from the NW study site indicate a prediction mean of -0.0006977, a root-mean-square of 0.0583, an average standard error of 0.05, a mean standardized of -0.006853, and a root-mean-square standardized of 1.13. The predicted plot, shown in Figure 103, indicates an excellent kriging model, with autocorrelation, because the points are fitted very closely to the blue line.

Based on the semivariogram, the model levels out at approximately 1075 m (~1 km) (Figure 104), suggesting that, along the 19.85 km shoreline, there is an autocorrelation of shoreline change rates within 1 km of each transect, but none beyond that point. The nugget size here is 0, indicative of no measurement errors, and the partial sill and sill are 0.046352. Results from linear regression of the slope from the semivariogram show a p-value of 0 and an R^2 of 96.6%, which means that one can expect to see a variable shoreline change within 1 km of each of the transects. Beyond that, distance, the range shows no autocorrelation.

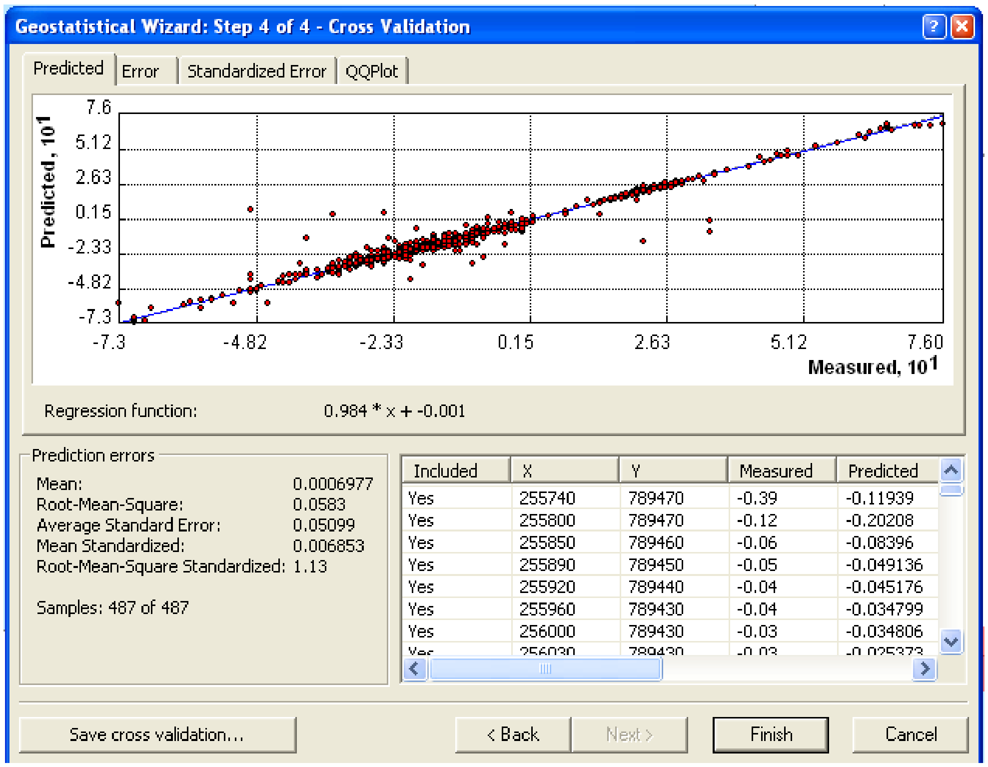

Figure 103. Cross validation predicted errors from the NW site point data based on historical linear regression results.

Compared to the other two locations, the NW study site has the least variation within 50 m. At this distance, one could only expect to see a shoreline change rate of 0.004 m/yr (0.16 in/yr); at 510 m, the rate of shoreline change that can be expected is 0.03 m/yr. When it reaches its sill, the range is 1065 m and the rate increases slightly to 0.046 m/yr.

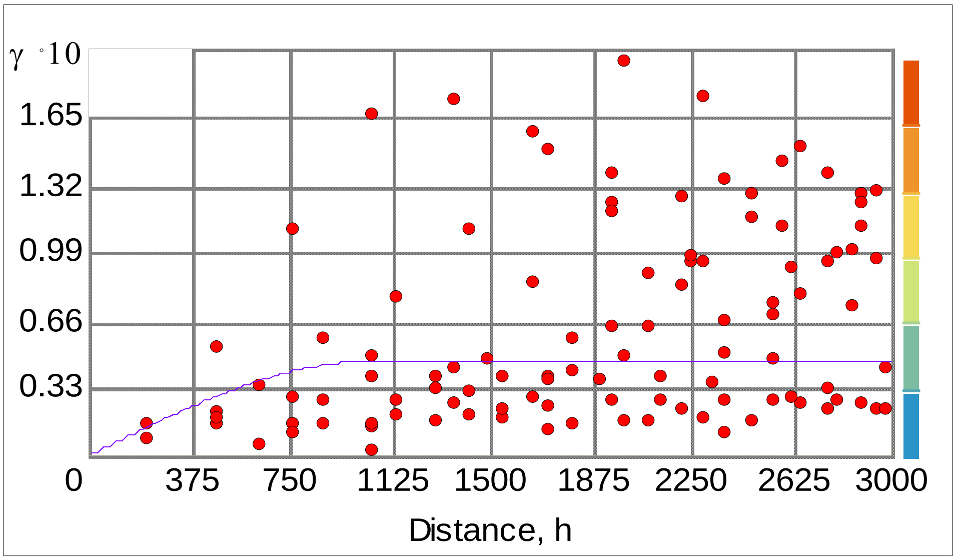

Figure 104. NW study site semivariogram for point data based upon the linear regression rate for 487 transects.

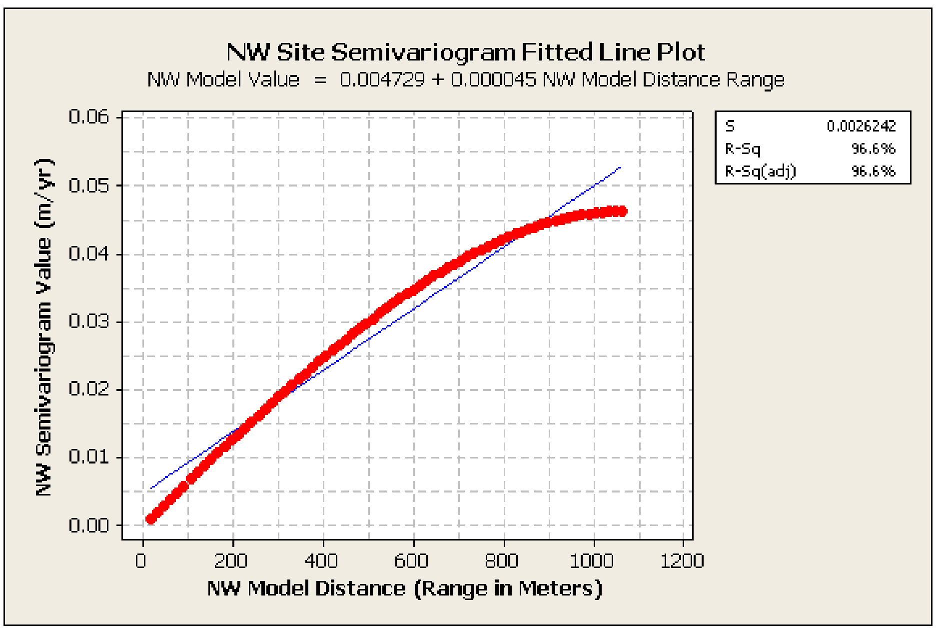

Figure 105. NW study site semivariogram for point data based upon the linear regression rate for 487 transects.

For the NW study site, results indicate a fractal dimension of D = 1.99. The formula to calculate this was: $D = (4-m)/2$, $D = (4-0.000045)/2$, $D = (3.999955)/2$, $D = 1.99$), where m equals the slope of the semivariogram, derived from least squares linear regression. Like the other two study sites, a high D value, such as this, suggests that short range effects still dominate the patterns of coastal erosion on the northwest side, even though the rate of change is small.

Applying the ordinary prediction kriging model to all the study sites, results show that the south side of MV is at the greatest risk for erosion, with only two minor areas indicating equilibrium (Figure 106). The NE study site has one hot spot along the coast, just south of Oak Bluffs Harbor and north of Sengekontacket Pond. Accretion occurs just north of the mouth of Sengekontacket Pond and near Fuller Street Beach, at the entrance of Edgartown Harbor. One hot spot on the northwest side of the Vineyard is located northeast of Cape Higgon, while the Lobsterville Beach location indicates accretion.

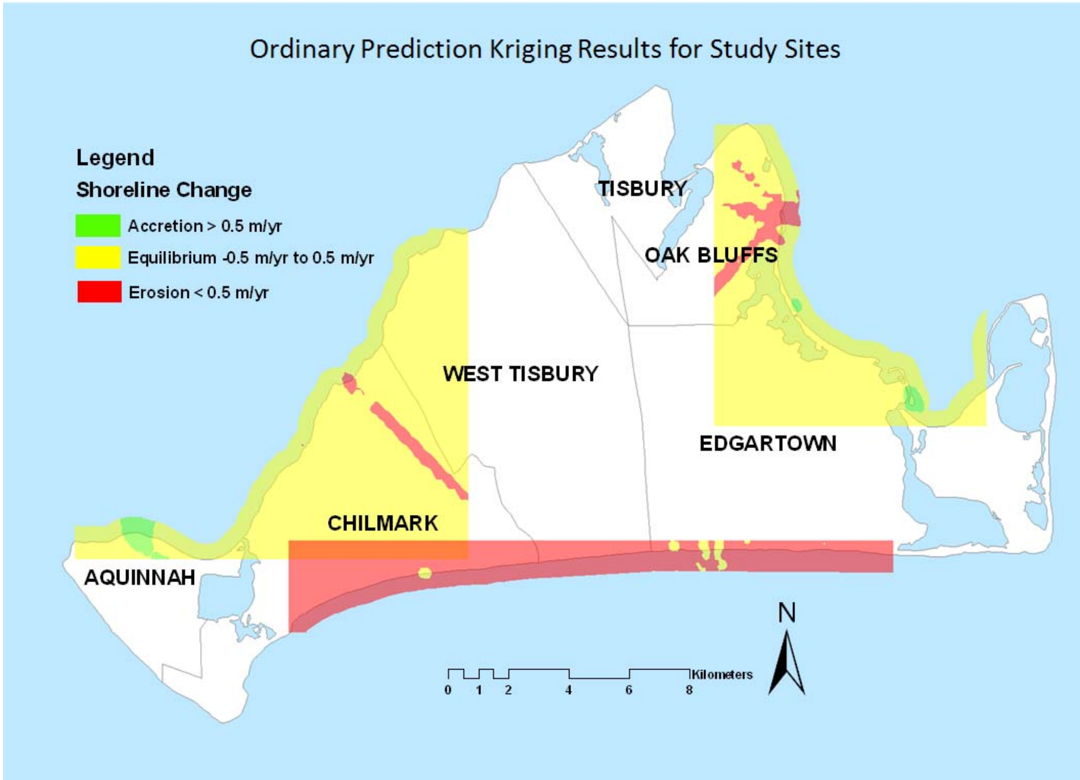

Figure 106. Map of SS, NE, and NW study site ordinary prediction kriging results based on historical shoreline changes.

Predicting Erosion from GIS Layers

Linear, Quadratic, Cubic, and Multiple Linear Regression

A linear regression analysis was performed on every attribute within each variable for the purpose of investigating the relationship between the response variable (historical rate of shoreline change - LR) and the predictor variable (the percentage of a transect that intersects with the attribute). The α-level used throughout this analysis is 0.05. For this section, the adjusted R^2 is reported, even though it is more conservative than R^2, because it adjusts for the number of explanatory terms in the model, the degrees of freedom. Detailed results for all the study sites, by variables and attributes, are located at the end of each study site (Table 40, Table 41, Table 42).

SS Regression Results

Geology. There are four geology attributes within the SS study site: Beach Deposits, Moraine Deposits, Moraine Outwash, and Pond. Transects that contained "Moraine Outwash" had the highest rate of erosion (-1.01 m/yr) and "Moraine Deposits" had the highest rate of accretion (2.87 m/yr). Multiple regression for all these attributes resulted in a p-value of 0 and an R^2 adjusted of 18.8%.

Surficial Geology. There are 2 surficial geology attributes associated with the SS site: End Moraine and Sand Deposits. Sand Deposits had the highest rate of erosion with a linear regression rate of -0.859 m/yr and transects that contained End Moraines accreted at 0.859 m/yr. Multiple regression for this variable resulted in a p-value of 0 and an R^2 adjusted rate of 10.6%.

Soil. There are 13 types of soil contained within the transects at the SS study site (Table 40). Three types of soils had high rates of erosion based on linear regression, namely: Riverhead, at -13 m/yr (its p-value [0.612] was not significant); Katama, at -11.9 m/yr; and Pawcatuck and Matunuck, at -9.68 m/yr. Three soils showed accretion: Nantucket, at 2.05 m/yr; Eastchop, at 1.74 m/yr; and Chilmark, at 1.62 m/yr (p-value [0.699] was not significant). The Beaches attribute showed the highest R^2 adjusted value of 24.3%, using a quadratic regression model. Including all soils along the SS, the p-value was 0 and the R^2 adjusted value is 40.7%.

Average Percentage of Sand. The linear regression rate of change is -0.742 m/yr, a p-value of 0, and an R^2 adjusted value of 2.8%. By using a cubic regression model the R^2 adjusted value increased to 6% and the p-value is 0.

Soil and Average Percentage of Sand. Using multiple regression to combine all the soil attributes and the average percentage of sand within the soil, the results indicate that the p-value is 0, and the R^2 adjusted value is 43.8%. This variable has the highest adjusted R^2 value for all the variables along the SS study site.

Slope. There are 5 attributes within this variable, ranging from no slope to 15-25% slope. Attributes that show accretion using linear regression included: "3-8% slope," with the highest rate of accretion at 2.03 m/yr, followed by "15-25% slope," with 1.34 m/yr (this has a non-significant p-value = 0.316) and "no slope," at 0.323 m/yr with a p-value of 0.04. Slopes that demonstrated erosion are "0-3%" (p-value = 0) and "8-15%," with -0.839 m/yr (p-value = 0.089). Using multiple regression for this variable, the results indicate that the adjusted R^2 is 9.6% and the p-value = 0. Every attribute within this variable displayed quadratic tendencies.

Average Slope. The linear regression rate for average slope is 0.00531 m/yr, with a p-value of 0.834, which is not significant, and an adjusted R^2 value of 0%. Using a quadratic model, the p-value became more significant at 0.001 and the adjusted R^2 improved to 2.3%

Slope and Average Slope. Multiple regression for all the features with the Slope variable and the "Average Slope" result in a p-value of 0 and an adjusted R^2 of 15.6%.

Erodible Soil Features. There are 5 attributes within the Erodible Soil Feature Variable, which include: Not Highly Erodible, Potentially Highly Erodible, Erodible, Highly Erodible, and NA (not applicable). The classification that had the highest rate of erosion is "Erodible Land" at -2.96 m/yr, with a p-value = 0 and an adjusted R^2 = 11.3%. Using a quadratic model, this attribute resulted in a p-value = 0 and an adjusted R^2 of 24.3%. "Potentially Highly Erodible Land" had the highest accretion at 2.03 m/yr, a p-value = 0, and an adjusted R^2 of 6.9%. By using a quadratic model, the adjusted R^2 increased slightly to 7.9%, and the p-value remained at 0. Overall, the p-value is 0 and the adjusted R^2 is 40.2% using multiple regression.

Wetland. There are 9 attributes within the Wetland variable. Two of them demonstrate cubic tendencies (Barrier Beach and Dune and Salt Marsh), two demonstrate quadratic tendencies (Barrier Beach and Open Water), while the remaining attributes are linear (Table 40). The transects that intersected Salt Marsh had the highest rate of erosion (-3.041 m/yr) and the highest accretion (9.075 m/yr) occurred when transects intersected with Shrub Swamps, but the p-value was not significant at 0.131 and the adjusted R^2 is 0.3%. Combining all the Wetland attributes, using multiple regression, the p-value is 0 and the adjusted R^2 is 29.2%.

Land Use. There are five attributes within Land Use: Beach, Upland, Water, Cropland, Marsh, and Developed Land. The highest accretion occurred in areas classified as Water (1.03 m/yr, p-value = 0, adjusted R^2 = 10.5%) and Marsh (0.934 m/yr, p-value = 0.232, adjusted R^2 = 0.1% [not significant]). The highest erosion resulted in areas classified as Cropland (-2 m/yr), but this value had a p-value of 0.419 and an adjusted R^2 of 0.1%. Multiple regression results indicate that Land Use explains 13.3% of the variation with a p-value of 0.

Compass Direction. Transects within the SS study site face five directions: E, ESE, S, SE, and SSE. Transects facing E and ESE have the highest rate of accretion. The former has a shoreline rate of change of 1.18 m/yr, p-value of 0.006, and an adjusted R^2 of 1.3%, which is not very significant. The latter, ESE, has a rate of change of 1.08 m/yr, p-value of 0.05, and an adjusted R^2 of 0.6%, again not very significant. Only the transects with a southerly exposure (S) indicate erosion at -0.698 m/yr, with a p-value of 0, and adjusted R^2 of 9.2%. Multiple regression for the SS transects result in a p-value of 0 and an adjusted R^2 of 9.6%. This does not account for much of the variation in shoreline patterns.

Winter and Summer Wind Speed by Percentage of Direction. Winter wind speed times the percent of direction has the highest rate of erosion at -5.523 m/yr, p-value of 0, and adjusted R^2 of 8.9%. During the summer months, erosion continues, but at a lesser rate of -3.219 m/yr, p-value of 0, and adjusted R^2, which is slightly higher than the winter months of 9.4%.

Winter and Summer Wave by Percentage of Direction. Winter wave action by the percent of direction has the highest rate of erosion for all variables, -16.5 m/yr, p-value of 0, and an adjusted R^2 of only 7.2%. Waves during the summer months continue to erode the shoreline at a rate of -6.047 m/yr, p-value of 0, and an adjusted R^2 value of 9.9%.

Winter Wind Speed and Winter Waves by Percentage of Direction. Winter winds and winter waves have the highest rate of erosion within their variables. By using multiple regression for these two variables, the p-value is 0, and the adjusted R^2 value is 9.8% (not shown). This does not account for much of the variation of shoreline change even though, combined, their rate of erosion is quite high.

SS Attribute/Variable	LR	P-value	R^2 adj	x2 p-value	x2 R^2 adj	x3 p-value	x3 R^2 adj
GEO BEACH DEPOSITS	-0.13	0.45	0.001				
GEO MORAINE DEPOSITS	2.87	0.002	1.7				
GEO MORAINE OUTWASH	-1.01	0	4.5				
GEO POND	1.34	0	6.4	0	13.9		
Geology (all features)		**0**	**18.8**				
SG END MORAINE	0.86	0	10.6				
SG SAND DEPOSITS	-0.86	0	10.6				
Surficial Geology (all features)		**0**	**10.6**				
BEACHES	-2.96	0	11.3	0	24.3		
BERRYLAND	0.69	0.841	0				
CARVER	-0.84	0	3.7				
CHILMARK	1.62	0.699	0				
EASTCHOP	1.74	0	3.9				
KATAMA	-11.90	0	2.7				
KLEJ	-1.06	0.168	0.2				
NANTUCKET	2.05	0	5.8				
PAWCATUCK AND MATUNUCK	-9.68	0.002	1.7				
POMPTON	0.62	0.44	0				
RIVERHEAD	-13.00	0.612	0				
UDIPSAMMENTS	-1.93	0	5.1				
WATER	0.76	0	4.8	0	16.4		
Avg % Sand	**-0.74**	**0**	**2.8**	**0**	**3.6**	**0**	**6**
Soil (all features, not avg % sand)		**0**	**40.7**				
Soil (all features, including avg % sand)		**0**	**43.8**				

SS Attribute/Variable	LR	P-value	R^2 adj	x2 p-value	x2 R^2 adj	x3 p-value	x3 R^2 adj
NO SLOPE	0.32	0.04	0.7	0	3.3		
0-3% SLOPE	-0.84	0	4.2	0	4.7		
3-8% SLOPE	2.03	0	6.9	0	7.9		
8-15% SLOPE	-0.53	0.089	0.4	0	5.6		
15-25% SLOPE	1.34	0.316	0				
Avg Slope	**0.01**	**0.834**	**0**	**0.001**	**2.3**		
Slope (all features, not avg slope)		**0**	**9.6**				
Slope (all features, including avg slope)		**0**	**15.6**				
NOT HIGHLY ERODIBLE LAND	-0.84	0	4.2	0	4.7		
POTENTIALLY HIGHLY ERODIBLE LAND	2.03	0	6.9	0	7.9		
ERODIBLE	-2.96	0	11.3	0	7.9		
HIGHLY ERODIBLE LAND	-0.44	0.153	0.2	0	7.9		
NA	0.76	0	4.8	0	7.9		
Erodible Soil Features		**0**	**40.2**				
WETLAND BARRIER BEACH	-0.67	0.059	0.5	0.001	2.3		
WETLAND BARRIER BEACH - DUNE	-0.05	0.901	0	0.556	0	0.003	2.3
WETLAND COASTAL BLUFF	0.95	0.336	0				
WETLAND COASTAL BEACH	1.79	0	6.8				
WETLAND COASTAL DUNE	2.08	0	7.8				
WETLAND ROCKY INTERTIDAL SHORE	0.68	0.478	0				
WETLAND SALT MARSH	-3.04	0.006	1.3	0.106	0.5	0	3.6
WETLAND TIDAL FLATS							
WETLAND SHRUB SWAMP	9.08	0.131	0.3				
WETLAND OPEN WATER	-1.08	0	6.8	0	9.7		
Wetland (all features)		**0**	**29.2**				
LUS BEACH	-0.24	0.089	0.4	0	8.5		
LUS UPLAND	-0.93	0	7.2	0	8.6		
LUS WATER	1.03	0	10.5				
LUS CROPLAND	-2.00	0.419	0				
LUS MARSH	0.93	0.232	0.1				
LUS (all Land Use features)		**0**	**13.3**				

SS Attribute/Variable	LR	P-value	R^2 adj	x2 p-value	x2 R^2 adj	x3 p-value	x3 R^2 adj
E	1.18	0.006	1.3				
ESE	1.08	0.05	0.6				
S	-0.70	0	9.2				
SE	0.89	0.001	1.9				
All SS Directions Combined	**-0.02**	**0**	**9.6**				
Winter Wind Speed x % Direction	**-5.52**	**0**	**8.9**				
Summer Wind Speed x % Direction	**-3.22**	**0**	**9.4**				
Winter Wave % Direction	-16.50	0	7.2				
Summer Wave % Direction	-6.05	0	9.9				

Table 40. SS site regression results for every attribute and variable.

NE Regression Results

Geology. Of the three attributes within the Geology variable for the NE site, Beach Deposits is the only one that had minor accretion at 0.0993 m/yr (p-value = 0; adjusted R^2 = 1.2%). Using a cubic model improves the adjusted R^2 to 13.9%. The Pond attribute eroded the most at -0.381 m/yr with a p-value of 0.257 m/yr and an adjusted R^2 of 0.1%, while using the cubic regression model the p-value lowers to 0.014 and the adjusted R^2 rises to 1.6% (still not very significant). Moraine Outwash has a shoreline change rate of -0.101 m/yr, p-value is 0.011, and an adjusted R^2 = 1.1%. Fitting the data to a cubic model, the p-value changes to 0 and the adjusted R^2 increases to 19.5%. Results from multiple regression analysis on all the geology attributes indicate a p-value of 0 and an adjusted R^2 of 28% (Table 41).

Surficial Geology. Of the three attributes within this variable, only End Moraine was associated with erosion (-0.2515 m/yr, p-value = 0, adjusted R^2 = 9.1%). Applying a cubic regression model, increases the adjusted R^2 to 15.8%. Sand Deposits had modest accretion at 0.1196 m/yr (p-value = 0.001, adjusted R^2 = 2.2%). Sand Deposits data fits better with a cubic model as well, resulting in a p-value of 0 and an adjusted R^2 of 10.7%. Till/Bedrock's data fits better with a quadratic model resulting in p-value of 0 and an adjusted R^2 of 8.6%. The linear regression model for Till/Bedrock indicated slight accretion at 0.1376 m/yr, with a p-value of 0.002 and an adjusted R^2 of 1.8%. The multiple regression results for all attributes within Surficial Geology show a p-value of 0 and an adjusted R^2 of 15.6% (Table 41).

Soil. Eight types of soils at the NE study site intersect with the transects (Table 41). The soil that displayed the most erosion is Berryland (-1.286 m/yr), but the p-value (0.354) was not significant and its adjusted R^2 = 0%. The attribute with the highest erosion and the highest adjusted R^2 of 26.8%, using a cubic model, was Water; with a linear rate of erosion of -0.8617 m/yr, p-value of 0, and an adjusted R^2 of 23.5%. Udipsamments had modest accretion at 0.4362 m/yr, with a p-value of 0, and an adjusted R^2 of 17.4%. Multiple regression analysis for all the soils results in a p-value of 0 and an adjusted R^2 of 42.04%. This variable has the second highest adjusted R^2 for the NE study site.

Average Percentage of Sand. The linear regression rate of shoreline change relative to the average percentage of sand was insignificant. The LR is -0.164 m/yr, with a p-value of 0.002, and an adjusted R^2 of 1.7%. Using a cubic regression model, the p-value became 0 and the adjusted R^2 rose to 3.1% (Table 41).

Soil and Average Percentage of Sand. Combining all the soil attributes and the percent of sand within the soil the p-value is 0 and the adjusted R^2 is 38.7%, i.e., not as high as the results from Soil only (Table 41). The percentage of sand within the soil variable does not account for much of the variation in shoreline change.

Slope. There are five attributes within this variable, ranging from no slope to 15-25% slope (Table 41). Land that was classified as No Slope had the most erosion at -0.3154 m/yr (p-value = 0; adjusted R^2 = 6.8%. Fitting the data to a quadratic model improved the fit slightly (p-value = 0; adjusted R^2 = 8.5%). Multiple regression including all slopes resulted in a p-value of 0 and an adjusted R^2 of 18.6%.

Average Slope. The linear regression rate of average slope, at the NE study site, is 0.01277 (p-value = 0, adjusted R^2 = 2.4%). The average slope data fit a cubic model better (p-value = 0; adjusted R^2 = 13.9%) (Table 41).

Slope and Average Slope. Multiple regression was used to combine all the attributes with slope and Average Slope, resulting in a p-value of 0 and an adjusted R^2 of 18.3% (Table 41).

Erodible Soil Features. Of the five attributes within this variable, the category NA (not applicable) results in the most erosion (rate of change of -0.5991 m/yr; p-value = 0; adjusted R^2 = 15.6%) (Table 41). Highly Erodible Land's (HEL) rate of shoreline change is actually accreting at 0.284 m/yr (p-value = 0; R^2 = 7.9%). Fitting the data for HEL to a cubic model, the adjusted R^2 rose to 10.7%.

Wetland. There are ten attributes of wetland categories within this variable (Table 41). Two attributes with significant data are Barrier Beach/Dune and Open Water. Barrier Beach/Dune indicates modest accretion at 0.478 m/yr (p-value = 0; adjusted R^2 = 13.3%). Fitting this data to a quadratic model, the p-value remains at 0 and the adjusted R^2 increases slightly to 14.3%. The next attribute classified as Open Water has -0.7723 m/yr of erosion (p-value = 0; adjusted R^2 = 31.5%). Again, fitting this data to a quadratic regression model, the adjusted R^2 increased slightly to 32.3%. Five of the attributes within the category of Wetlands fit a cubic model, but did not increase the R^2 values significantly. Only two of the attributes fit a linear model and three of the attributes fit a quadratic model. Multiple regression results in a p-value of 0 and an adjusted R^2 of 47.6%; this variable has the highest proportion of variance on the northeast side.

Land Use. There are four attributes with the NE LUS variable (Table 41). The only feature that has erosion is Beach, at -0.207 m/yr with the data fitting a cubic model, a p-value of 0, and an adjusted R^2 of 13.3%. All the other attributes exhibited accretion. The one that was the least significant was Marsh, while Upland accreted at 0.1143 m/yr, with a cubic p-value of 0, and an adjusted R^2 of 19.9%. Developed land basically showed little change of shoreline with accretion at 0.09154 m/yr, a cubic p-value of 0, and an adjusted R^2 of 17.6%. Multiple regression for this variable results in a p-value of 0 and an adjusted R^2 of 35.8%.

Compass Direction. There are 16 different compass directions at the NE study site, the most at any study site (Table 41). The only attribute that has any significance is E (east), eroding at the rate of -0.2904 m/yr, with a p-value of 0, and an adjusted R^2 of 4.3%. Multiple regression for this variable results in a p-value of 0 and an adjusted R^2 of 7.3%.

Winter and Summer Wind Speed by Percentage of Direction. Neither the winter or summer wind speed by the percentage of direction is significant (Table 41). Both seasons indicate slight erosion, both p-values are above 0.05, and both adjusted R^2 values are 0%.

Winter and Summer Wave by Percentage of Direction. Wave direction by the percentage of direction is not significant for the summer and/or winter (Table 41). Erosion is very minor for the winter months; the quadratic p-value is 0.053 with an adjusted R^2 of 0.8%. Summer month values are similar, with a p-value of 0.029 and adjusted R^2 of 1%.

Winter Wind Speed and Winter Waves by Percentage of Direction. Historically, northeasterly wind and waves cause the most shoreline damage, but using multiple regression on the NE study site, the p-value is 0.343 and an adjusted R^2 of 0. These results are not significant (Table 41).

NE Attribute/Variable	LR	P-value	R^2 adj	x2 p-value	x2 R^2 adj	x3 p-value	x3 R^2 adj
GEO BEACH DEPOSITS	0.10	0.008	1.2	0	5.5	0	13.9
GEO MORAINE OUTWASH	-0.10	0.011	1.1	0	10.9	0	19.5
GEO POND	-0.38	0.257	0.1	0.029	1	0.014	1.6
Geology (all features)		**0**	**28**				
SG END MORAINE	-0.25	0	9.1	0	13.3	0	15.8
SG SAND DEPOSITS	0.12	0.001	2.2	0	8.1	0	10.7
SG TILL / BEDROCK	0.14	0.002	1.8	0	8.6		
Surfical Geology (all features)		**0**	**15.6**				
BEACHES	0.09	0.182	0.2				
BERRYLAND	-1.29	0.354	0				
CARVER	-0.11	0.067	0.5				
EASTCHOP	-0.27	0	3.3				
PAWCATUCK AND MATUNUCK	-0.01	0.896	0				
UDIPSAMMENTS	0.44	0	17.4				
WATER	-0.86	0	23.5	0	26.8		
URBAN	0.07	0.538	0				
Avg % Sand	**-0.16**	**0.002**	**1.7**	**0.004**	**1.9**	**0**	**3.1**
Soil (all features, not avg % sand)		**0**	**42.04**				
Soil (all features, including avg % sand)		**0**	**38.7**				

NE Attribute/Variable	LR	P-value	R^2 adj	x2 p-value	x2 R^2 adj	x3 p-value	x3 R^2 adj
NO SLOPE	-0.32	0	6.8	0	8.5		
0-3% SLOPE	-0.02	0.847	0				
3-8% SLOPE	-0.14	0.022	0.9				
8-15% SLOPE	0.40	0	14.8				
15-25% SLOPE	-0.27	0	2.3				
Avg Slope	**0.01**	**0**	**2.4**	**0**	**12.6**	**0**	**13.9**
Slope (all features, not avg slope)		**0**	**18.6**				
Slope (all features, including avg slope)		**0**	**18.3**				
NOT HIGHLY ERODIBLE LAND	-0.02	0.847	0				
POTENTIALLY HIGHLY ERODIBLE LAND	-0.14	0.9	0.9				
ERODIBLE	0.09	0.182	0.2				
HIGHLY ERODIBLE LAND	0.28	0	7.9	0	8.4	0	10.7
NA	-0.60	0	15.6				
Erodible Soil Features		**0**	**20.3**				
WETLAND BARRIER BEACH	0.13	0.0029	0.8	0.005	1.8		
WETLAND BARRIER BEACH - DUNE	0.48	0	13.3	0	14.3		
WETLAND COASTAL BLUFF	-0.09	0.3	0	0	2.8	0	3.8
WETLAND COASTAL BEACH	0.03	0.67	0	0	2.8	0	3
WETLAND COASTAL DUNE	0.54	0	3	0	3.6	0	8
WETLAND ROCKY TERTIDAL SHORE	-0.36	0.241	0.1	0.112	0.5	0.001	2.8
WETLAND SALT MARSH	0.10	0.362	0	0.322	0.1	0.013	1.6
WETLAND TIDAL FLATS	-5.42	0.006	1.3				
WETLAND SHRUB SWAMP	-1.41	0.492	0				
WETLAND OPEN WATER	-0.77	0	31.5	0	32.3		
Wetland (all features)		**0**	**47.6**				
LUS BEACH	-0.21	0	4.2	0	10.7	0	13.3
LUS UPLAND	0.11	0.002	1.7	0	11.8	0	19.9
LUS MARSH	-0.02	0.802	0	0.464	0		
LUS DEVELOPED LAND	0.09	0.114	0.3	0	13.5	0	17.6
LUS (Land Use all features)		**0**	**35.8**				

NE Attribute/Variable	LR	P-value	R^2 adj	x2 p-value	x2 R^2 adj	x3 p-value	x3 R^2 adj
E	-0.29	0	4.3				
ESE	-0.02	0.75	0				
S	0.14	0.341	0				
SE	0.03	0.853	0				
SSE	0.05	0.866	0				
N	0.01	0.845	0				
ENE	0.11	0.006	1.3				
NE	0.20	0.002	1.8				
NNE	0.10	0.07	0.5				
NNW	-0.09	0.31	0				
NW	-0.15	0.005	1.4				
SSW	-0.01	0.902	0				
SW	0.00	0.965	0				
W	-0.01	0.898	0				
WNW	-0.16	0.117	0.3				
WSW	0.00	0.957	0				
All NE Directions Combined		**0**	**7.3**				
Winter Wind Speed x % Direction	**-0.31**	**0.343**	**0**				
Summer Wind Speed x % Direction	**-0.20**	**0.287**	**0**				
Winter Wave % Direction	**-1.00**	**0.35**	**0**	**0.053**	**0.8**		
Summer Wave % Direction	**-0.47**	**0.17**	**0.2**	**0.029**	**1**		

Table 41. NE site regression results for every attribute and variable.

NW Regression Results

Geology. There are four attributes within the Geology variable on the NW site (Table 42). The highest rate of accretion occurred in areas categorized as Marsh, at 0.5043 m/yr, cubic p-value of 0, and an adjusted R^2 of 8.1%. However, Beach Deposits, with slightly less accretion at 0.3391 m/yr, were clearly more significant, having a quadratic regression p-value of 0 and an adjusted R^2 of 42.1%. Moraine Deposits was the only attribute that showed any erosion (-0.156 m/yr), a linear regression p-value of 0, and an adjusted R^2 of 7.9%. The multiple regression p-value is 0 and an adjusted R^2 of 46% for all the Geology attributes on the NW site.

Surficial Geology. There are only two attributes within this variable - End Moraine and Sand Deposits (Table 42). End Moraine has a linear regression rate of -0.1782 m/yr (p-value = 0; adjusted R^2 =10.9%). The Sand Deposits attribute accreted at 0.2651 m/yr (p-value = 0; adjusted R^2 = 25.6%). Multiple regression for Surficial Geology results in a p-value of 0 and an adjusted R^2 of 25.5%.

Soil. There are seven different types of soils within the transect area (Table 42). Water has the highest adjusted R^2, 68.4%, and a p-value of 0, when a cubic regression model is used. The linear regression rate shows erosion at -0.7104 m/yr, a p-value of 0, and an adjusted R^2 of 61.7%. Multiple regression with all the soil attributes results in a p-value of 0 and an adjusted R^2 of 79.3%.

Average Percentage of Sand. The average percentage of sand in the soils do not account for a significant portion of the variation. Linear regression results suggest that this has no effect at all (0.00547 m/yr; p-value = 0.921; adjusted R^2 = 0%). Fitting the data to a cubic model makes the regression significant (p-value = 0; adjusted R^2 = 6.8%).

Soil and Average Percentage of Sand. Including all soil attributes and percentage of sand, multiple regression results in a p-value of 0, and an adjusted R^2 of 79.9%. This regression has the highest adjusted R^2 value for all variables on the NW study site.

Slope. There are five attributes within this variable, ranging from no slope to 15-25% slope (Table 42). The most significant attribute on the NW study site is the 8-15% Slope attribute, with a quadratic p-value of 0 and an adjusted R^2 of 59.9%. Linear regression for this attribute indicates accretion at 0.6712 m/yr (p-value = 0; adjusted R^2 = 58.6%). The attribute with the second most significance is No Slope, with a cubic regression p-value of 0 and an adjusted R^2 of 53.8%. Linear regression for No Slope shows slight erosion at -0.6776 m/yr (p-value = 0; adjusted R^2 = 49.8%).

Average Slope. The linear regression rate for Average Slope is 0.03452 m/yr (p-value = 0; adjusted R^2 = 25.3%). Fitting the data to a cubic regression model increases the adjusted R^2 to 32.4% (p = 0) (Table 42).

Slope and Average Slope. Including Slope and Average Slope, multiple regression results show a p-value of 0 and an adjusted R^2 value of 63.9% (Table 42).

Erodible Soil Features. The NW study site has four attributes under this variable (Table 42). The two most significant attributes are Highly Erodible Land and NA. Highly Erodible Land has a linear regression rate of shoreline change of 0.6197 m/yr and fitting the data to a cubic model, the p-value is 0 and the adjusted R^2 is 52.4%. The attribute NA has slight erosion at -0.6776 m/yr and this data fits well to a cubic model as well, with a p-value of 0 and an adjusted R^2 of 53.8%. Multiple regression results for the Erodible Soil variable yields a p-value of 0 and an adjusted R^2 of 54.5%.

Wetland. There are eight attributes within the Wetland variable at the NW study site (Table 42). Open Water is most significant, with a linear regression rate of -0.646 m/yr. Its data fits best with a cubic regression model (p = 0; adjusted R^2 = 53.1%). The Barrier Beach/Dune attribute had the highest adjusted R^2 of 64.4%, and a linear regression rate of 0.7106 m/yr, but its p-value (0.7106) is not significant. Multiple regression results for the NW Wetland variable indicate a p-value of 0 and an adjusted R^2 of 77.9%. This category has the second highest R^2 value for the NW study site.

Land Use. There are only three attributes of Land Use at the NW study site that intersect with the transects (Table 42). All three attributes indicate minor accretion, with Beach having the most significant results, followed closely by Upland. The linear regression rate for Beach is 0.1041 m/yr (p = 0; adjusted R^2 value = 2.7%). Using a quadratic model increases the adjusted R^2 significantly to 23% (p = 0). The same scenario applies to the Upland attribute; the linear regression rate is 0.06249 m/yr (p = 0.023; adjusted R^2 = 0.9%). Fitting the data for Upland to a quadratic model, the p-value improves to 0 and the adjusted R^2 rises to 22.9%. The Water attribute is not significant at all. Multiple regression results for all of Land Use results in a p-value of 0 and an adjusted R^2 of 22.7%.

Compass Direction. There are nine different directions the transects face at the NW study site (Table 42). The most significant direction on this side is NNE, with a linear regression rate of 0.3763 m/yr (p = 0; adjusted R^2 = 21.8%). Combining all the Compass Direction attributes, multiple regression results in a p-value of 0 and an adjusted R^2 of 35.7%.

Winter and Summer Wind Speed by Percentage of Direction. Linear regression of Winter Wind Speed by Percentage of Direction results in a shoreline rate change of 1.184 (p = 0; adjusted R^2 = 5.6%; (Table 42). The linear regression rate of Summer Wind Speed by Percentage of Direction is similar to the winter values. The LR is 0.6728 m/yr (p = 0; adjusted R^2 = 5.6%).

Winter and Summer Wave by Percentage of Direction. Winter Wave by Percentage of Direction linear regression results show accretion of 3.601 m/yr (p = 0; adjusted R^2 = 4.9%) (Table 42). Summer Wave by Percentage of Direction accretes at a rate of 1.211 m/yr (p = 0; adjusted R^2 = 5.4%).

Winter Wind Speed and Winter Waves by Percentage of Direction. Using multiple regression to combine Winter Wind Speed and Winter Waves by Percentage of Direction results in a p-value of 0 and an adjusted R^2 value of 5.6% (Table 42).

NW Attribute/Variable	**LR**	**P-value**	**R^2 adj**	**x2 p-value**	**x2 R^2 adj**	**x3 p-value**	**x3 R^2 adj**
GEO BEACH DEPOSITS	0.34	0	36.9	0	42.1		
GEO MORAINE DEPOSITS	-0.16	0	7.9				
GEO POND	0.12	0.465	0				
GEO MARSH	0.50	0	5.9	0	7.5	0	8.1
Geology (all features)		**0**	**46**				
SG END MORAINE	-0.18	0	10.9				
SG SAND DEPOSITS	0.27	0	25.6				
Surfical Geology (all features)		**0**	**25.5**				

NW Attribute/Variable	LR	P-value	R^2 adj	x2 p-value	x2 R^2 adj	x3 p-value	x3 R^2 adj
BEACHES	0.15	0.002	1.8	0	12.1	0	13.6
EASTCHOP	-0.20	0	2.8	0	10.1	0	13
NANTUCKET	-0.14	0.372	0	0.065	0.7		
UDIPSAMMENTS	0.73	0	65.7				
WATER	-0.71	0	61.7	0	65.1	0	68.4
FREETOWN AND SWANSEA	-1.44	0.352	0				
RIDGEBURY	0.19	0.61	0				
Avg % Sand	**0.01**	**0.921**	**0**	**0.003**	**2**	**0**	**6.8**
Soil (all features, not avg % sand)		**0**	**79.3**				
Soil (all features, including avg % sand)		**0**	**79.9**				
NO SLOPE	-0.68	0	49.8	0	52.5	0	53.8
0-3% SLOPE	0.10	0.785	0				
3-8% SLOPE	-0.03	0.766	0	0.163	0.3		
8-15% SLOPE	0.67	0	58.6	0	59.9		
15-25% SLOPE	-0.27	0	3.3	0	7.6		
Avg Slope	**0.03**		**25.3**	**0**	**31.2**	**0**	**32.4**
Slope (all features, not avg slope)		**0**	**64**				
Slope (all features, including avg slope)		**0**	**63.9**				
NOT HIGHLY ERODIBLE LAND	0.10	0.785	0				
POTENTIALLY HIGHLY ERODIBLE LAND	-0.03	0.766	0	0.163	0.3	0.113	0.6
HIGHLY ERODIBLE LAND	0.62	0	45.8	0	50.1	0	52.4
NA	-0.68	0	49.9	0	52.5	0	53.8
Erodible Soil Features		**0**	**54.5**				
WETLAND BARRIER BEACH	0.55	0	17.8	0	31.4		
WETLAND BARRIER BEACH - DUNE	0.71	0.7106	64.4				
WETLAND COASTAL BLUFF	-0.12	0.226	0.1				
WETLAND COASTAL BEACH	-0.28	0	10.6	0	27.6	0	39.3
WETLAND COASTAL DUNE	0.04	0.788	0	0.084	0.6	0.048	1
WETLAND ROCKY INTERTIDAL SHORE	-0.27	0.026	0.8	0.045	0.9	0.055	1.9
WETLAND SALT MARSH	1.37	0.474	0				
WETLAND OPEN WATER	-0.65	0	50.3	0	51.3	0	53.1
Wetland (all features)		**0**	**77.9**				

NW Attribute/Variable	LR	P-value	R^2 adj	x2 p-value	x2 R^2 adj	x3 p-value	x3 R^2 adj
LUS BEACH	0.10	0	2.7	0	23		
LUS UPLAND	-0.06	0.023	0.9	0	22.9		
LUS WATER	0.33	0.572	0				
LUS (Land Use all features)		**0**	**22.7**				
N	0.19	0	6.5				
ENE	0.06	0.754	0				
NE	0.16	0.132	0.3				
NNE	0.38	0	21.8				
NNW	0.00	0.963	0				
NW	-0.13	0	3.6				
W	-0.11	0.014	1				
WNW	-0.17	0	8.9				
WSW	-0.26	0.078	0.4				
All NW Directions Combined		**0**	**35.7**				
Winter Wind Speed x % Direction	**1.18**	**0**	**5.6**				
Summer Wind Speed x % Direction	**0.67**	**0**	**5.6**				
Winter Wave % Direction	**3.60**	**0**	**4.9**				
Summer Wave % Direction	**1.21**	**0**	**5.4**				

Table 42. NW site regression results for every attribute and variable.

Transect Means/Attribute (> 25%)

It was apparent from the previous regression methods that, although many regressions were significant across all sites, and many explained more than 50% of the R^2, no discernible pattern emerged across all sites from any of the variables and/or attributes as to an underlying explanation for the coastal erosion patterns. Using the ordinary least squares linear regression results from each attribute, and retaining the attributes that had a transect mean > 25%, I sought to uncover a pattern.

Using the > 25% rule, out of the 12 attributes listed for the SS site, the only attribute associated with erosion was Land Use Beach, consisting of a mean of 48.47% on the transects. Seven of the attributes consisted of a combination of erosion, equilibrium, and accretion. However, there were no attributes that just displayed accretion (Table 43).

In the NE study site there were 20 attributes that encompassed more than 25% on the transects. Erosion was associated with transects that faced E or ESE, as well as with three other attributes: Water within the Soil category, NA within the Erodible Land variable, and Beach within the Land Use variable (Table 44). Equilibrium was maintained with MV Moraine Outwash within Geology and Coastal Beach within Wetland. Coastal areas that accreted included transects that contained Till/Bedrock within Surficial Geology, compass direction ENE, and Barrier Beach/Dunes within the Wetland variable (Table 44).

Transects with the NW compass direction were the only attribute along the NW study site that experienced erosion. Coastal equilibrium occurred with two attributes, Wetland Coastal Beach and transects that faced WNW. Transects that accreted included:

Wetland Barrier Beach/Dune, transects facing N, Udipsamments soils, and transects that had a slope between 8 and 15% (Table 45).

Again, no clear relationship between erosion and any attribute emerged that was consistent across all sites.

SS Attribute	Erosion Mean	Equilib Mean	Accretion Mean
Geo Beach Deposits	84.38%	56.44%	51.49%
Wetland Water	64.81%	63.36%	89.44%
SG Sand Deposits	83.72%	85.37%	100.00%
South	76.08%	85.37%	100.00%
Soil Water	59.92%	65.63%	89.44%
No Slope	73.25%	68.94%	93.08%
HEL NA	59.92%	65.63%	89.44%
LUS Upland	42.44%	32.86%	
LUS Beach	48.47%		
LUS Water		64.38%	85.18%
Geo Pond		36.10%	48.51%
Erodible		33.10%	36.40%

Table 43. Mean SS site attributes that are > 25% on the transects.

NE Attribute	Erosion Mean	Equilib Mean	Accretion Mean
Geo Beach Deposit	76.04%	66.16%	81.81%
HEL (Highly Erodible Land)	23.27%	44.52%	74.18%
Wetland Open Water	72.37%	28.21%	
SG End Moraines	80.04%	29.04%	
No Slope	67.98%	34.35%	
E	41.18%		
ESE	29.41%		
Soil Water	53.63%		
NA (HEL not categorized)	53.63%		
LUS Beach	71.08%		
Geo MV Moraine Outwash		26.66%	
Wetland Coastal Beach		24.81%	
Soil Udipsamments		34.99%	74.18%
8-15% Slope		38.82%	74.18%
LUS Upland		60.46%	68.88%
Wetland Barrier Beach		41.65%	66.44%
SG Sand Gravel		48.73%	55.80%
SG Till Bedrock			**38.10%**
ENE			**71.43%**
Wetland Barrier Beach Dune			**49.51%**

Table 44. Mean NE site attributes that are > 25% on the transects.

NW Attribute	Erosion Mean	Equilib Mean	Accretion Mean
No Slope	90.16%	65.02%	34.19%
LUS Beach	65.16%	43.79%	69.60%
LUS Upland	34.84%	56.07%	30.40%
HEL NA	90.16%	65.02%	34.19%
Geo Moraine Deposit	80.00%	31.45%	
Wetland Open Water	75.14%	28.47%	
SG End Moraines	100.00%	36.66%	
Soil Water	78.32%	33.73%	
NW	60.00%		
Wetland Coastal Beach		36.61%	
WNW		32.10%	
Geo Beach Deposits		30.36%	100.00%
SG Sand Gravel		43.69%	100.00%
Soil Beaches		31.29%	34.19%
HEL		31.00%	65.81%
Wetland Barrier Beach Dune			**73.80%**
N			**78.57%**
Soil Udipsamments			**65.81%**
Slope 8-15%			**65.81%**

Table 45. Mean NW site attributes that are > 25% on the transects.

Akaike Information Criterion (AIC)

The Akaike Information Criterion (AIC) method was used to select the "best" regression model of one or more attributes that most likely influenced shoreline erosion patterns on Martha's Vineyard. This method measures the goodness of fit of an estimated statistical model.

I used AIC in three different ways for each study site to rank: 1) the ten major variables (Geology, Surficial Geology, Soil, Average % of Sand, Slope, Erodible Land, Wetland, Land Use, Compass Direction, and Winter Wind and Winter Waves) based upon multiple regression results from the section "Linear, Quadratic, Cubic, and Multiple Linear Regression"; 2) the individual attributes that had more than 25% of the attribute along the transect (including Average Slope, Summer Wind, and Summer Waves); and 3) combinations of attributes.

AIC results are provided for the ten major variables and the individual attributes greater than 25%. However, by combining various attributes within each study site, it quickly became apparent that the probability of finding the right combination was low because the SS has 55 attributes, the NE has 60 attributes, and the NW has 48 attributes (these attributes include Average Percent of Sand, Average Percent of Slope, Winter Wind, and Winter Waves, that were not included in the section "Transect Means/Attribute >25%"). The linear regression results for Summer Wind and Summer Waves were not significant for any of the three study sites and were, therefore, eliminated as a major variable from this study.

SS Site. Results for the ten major variables for the SS site (Table 46) ranked Erodible Land first, followed by Soil, and Wetland.

NE Site. On the NE site (Table 46) Wetland was ranked first, followed by soil (as in the SS), and then Land Use. The bottom three ranked variables are the same as the SS site, but ranked slightly differently. Compass Direction was ranked eighth, and Average Percent of Sand was ranked ninth.

NW Site. The NW study site was slightly different (Table 46). The first ranked variable was Soil, followed by Wetland, and then Slope. Coming in eighth was Land Use, then Average Percent of Sand, and Winter Wind and Waves.

For more AIC details, see Appendix A (Appendix 7- Appendix 14).

SS Model - Major Variables	p-value	R sq (adj)	AIC Rank
LR vs Erodible	0	40.2	1
LR vs Soil	0	40.7	2
LR vs Wetland	0	24.6	3
LR vs Slope	0	21.1	4
LR vs Geology	0	18.8	5
LR vs LUS	0	13.3	6
LR vs Surficial Geology	0	10.6	7
LR vs Compass Direction	0	9.8	8
LR vs Winter Wind and Waves	0	8.9	9
LR vs Avg % Sand	0	6	10

NE Model - Major Variables	p-value	R sq (adj)	AIC Rank
LR vs Wetland	0	47.60	1
LR vs Soil	0	38.30	2
LR vs Land Use	0	35.80	3
LR vs Geology	0	28.00	4
LR vs Erodible	0	20.30	5
LR vs Slope	0	18.60	6
LR vs Surficial Geology	0	15.60	7
LR vs Compass Direction	0	7.30	8
LR vs Avg % Sand	0	3.10	9
LR vs Winter Wind & Waves	0.343	0.00	10

NW Model - Major Variables	p-value	R sq (adj)	AIC Rank
LR vs Soil	0	79.3	1
LR vs Wetland	0	77.9	2
LR vs Slope	0	64.0	3
LR vs Erodible	0	54.5	4
LR vs Geology	0	46.0	5
LR vs Compass Direction	0	35.7	6
LR vs Surficial Geology	0	25.5	7
LR vs Land Use	0	22.7	8
LR vs Avg % Sand	0	6.8	9
LR vs Winter Wind & Waves	0	5.6	10

Table 46. SS, NE, and NW sites Akaike Information Criterion major variables results.

Table 47 shows the results of the SS AIC ranked regressions for individual attributes that encompass more than 25% of the transect. On the SS site, the quadratic version of Erodible was ranked first, followed by the quadratic version of Soil Water, and the quadratic version of Geo Pond. The categories of Summer Wind and Wave are ranked higher than Winter Wind and Wave.

SS Attributes > 25% on transects	p-value	R sq (adj)	AIC Rank
Erodible (x, x2)	0	28.2	1
Soil Water(x, x2)	0	16.4	2
Geo Pond (x, x2)	0	13.9	3
SG Sand Deposits	0	10.6	4
LUS Water	0	10.5	5
LR vs Summer Wave % Direction	0	9.9	6
LR vs Summer Wind and Wave	0	9.9	7
LR vs Summer Windspeed & Direction	0	9.4	8
South	0	9.2	9
Avg % Sand (x, x2, x3)	0	9.1	10
LR vs Winter Windspeed & Direction	0	8.9	11
LR vs Winter Wind and Wave	0	8.9	12
LUS Upland (x, x2)	0	8.6	13
LUS Beach (x, x2)	0	8.5	14
LR vs Winter Wave % Direction	0	7.2	15
HEL NA (x, x2)	0	5	16
Wetland Water	0	3.4	17
No Slope (x, x2)	0	3.3	18
Avg Slope (x. x2)	0.001	2.3	19
Geo Beach Deposits	0.45	0	20

Table 47. SS site Akaike Information Criterion attributes results.

Table 48 shows the results of the NE site AIC ranked regressions for individual attributes, that encompass more than 25% of the transect. The quadratic version of Wetland Open Water ranked number one, followed by the quadratic version of Soil Water, and the cubic version of Land Use Upland. Compass direction ESE was the least influential attribute followed by Winter Wind Speed and Direction, then Summer Wind Speed and Direction.

NE Attributes > 25% on Transects	p-value	R-sq (adj)	AIC Rank
Wetland Open Water (x, x2)	0	32.3	1
Soil Water (x, x2)	0	26.8	2
LUS Upland (x, x2, x3)	0	19.9	3
Geo Moraine Outwash (x, x2, x3)	0	19.5	4
Soil Udipsamments	0	17.4	5
HEL NA	0	15.6	6
SG End Moraines (x, x2, x3)	0	15.8	7
8-15% Slope	0	14.8	8
Wetland Barrier Beach Dune (x, x2)	0	14.3	9
Geo Beach Deposits (x, x2, x3)	0	13.9	10
Avg Slope (x, x2, x3)	0	13.9	11
LUS Beach (x, x2, x3)	0	13.8	12
SG Sand Deposits (x, x2, x3)	0	10.7	13
HEL (Highly Erodible Land) (x, x2, x3)	0	10.7	14
SG Till & Bedrock (x, x2)	0	8.6	15
No Slope (x, x2)	0	8.5	16
E	0	4.3	17
Avg Sand (x, x2, x3)	0	3.1	18
Wetland Coastal Beach (x, x2, x3)	0	3	19
Wetland Barrier Beach (x, x2)	0	1.8	20
ENE	0.006	1.3	21
Summer Wave % Direction (x, x2)	0.029	1	22
Winter Wave % Direction (x, x2)	0.053	0.8	23
Summer Wind Speed & Direction	0.287	0	24
Winter Wind Speed & Direction	0.343	0	25
ESE	0.75	0	26

Table 48. NE site Akaike Information Criterion attributes results.

Table 49 shows the results of the NW AIC ranked regressions for individual attributes that encompass more than 25% of the transect. The cubic version of Soil Water was ranked number one, followed by Soil Udipsamments, and Wetland Barrier Beach/Dune. Factors that were not significant on the NW site included the transects with a compass direction facing the NW, followed by Winter Wave Percent of Direction, and Summer Wave Percent of Direction.

NW Attributes > 25% on Transects	p-value	R-sq (adj)	AIC Rank
Soil Water (x, x2, x3)	0	68.4	1
Soil Udipsamments	0	65.7	2
Wetland Barrier Beach - Dune	0	64.4	3
8-15% Slope (x, x2)	0	59.9	4
HEL NA (x, x2, x3)	0	53.8	5.5
No Slope (x, x2, x3)	0	53.8	5.5
Wetland Open Water (x, x2, x3)	0	53.1	7
Highly Erodible Land (x, x2, x3)	0	52.4	8
Geo Beach Deposits (x, x2)	0	42.1	9
Wetland Coastal Beach (x, x2, x3)	0	39.3	10
Avg Slope (x, x2, x3)	0	25.3	11
SG Sand Deposits	0	25.6	12
LUS Beach (x, x2)	0	23	13
LUS Upland	0	22.9	14
Soil Beaches (x, x2, x3)	0	13.6	15
SG End Moraine	0	10.9	16
WNW	0	8.9	17
Geo Moraine Deposits	0	7.1	18
N	0	6.5	19
Avg % Sand (x, x2, x3)	0	6.8	20
Winter Wind Speed & Direction	0	5.6	21
Summer Wind Speed & Direction	0	5.6	22
Summer Wave % Direction	0	5.4	23
Winter Wave % Direction	0	4.9	24
NW	0	3.6	25

Table 49. NW site Akaike Information Criterion attributes results.

Principal Component Analysis (PCA)

Every attribute within the raster was reclassified based upon the linear regression rate of shoreline change (see Chapter 3 and Appendix A (Tables: Appendix 5 and Appendix 6) for reclassifications for each attribute). These ratings ranged from 1 to 5 based upon the following criteria (see below):

- 1 = significant accretion (> 1 m/yr)
- 2 = accretion (0.05 to 1 m/yr)
- 3 = equilibrium (0.5 to -0.5 m/yr)
- 4 = erosion (-0.5 to -1 m/yr)
- 5 = significant erosion (> - 1 m/yr).

I used ArcGIS® v9.2 to derive correlation matrices (CMs) for the three study sites based upon the criteria described above. A CM provides the Pearson correlation coefficient for relationships between variables. A strong positive linear relationship yields a positive number, close to +1.0, and a strong negative linear relationship is close to -1.0. Numbers that are mid-range and close to zero have weak linear relationships, or may actually be nonlinear. The correlation matrix has a main diagonal of 1, indicating that the correlation between an attribute and itself is always perfect. A value of -1.0 is a perfect negative (inverse) correlation; 0.0 indicates no correlation; and +1.0 is a perfect positive correlation.

The CMs were based on eight variables, i.e., Geology, Surficial Geology, Wetland, Soil, Slope, Sand, Erodible Land (HEL), and Land Use, and their calculation yielded 28 unique correlations. Winter Waves and Winter Wind were eliminated from the analyses because the CM results were all zeroes (data not shown). Compass Direction was removed in the next series of analyses because the communality results were less than 1% (data not shown).

PCA Scree Plots were used to judge the relative magnitude of eigenvalues. These plots compare the eigenvalue associated with a principal component to the number of the component. Finally, PCA Loading Plots were used to display the loadings for the second component (y-axis) versus the loadings for the first component (x-axis)(lines are drawn from each loading to the (0,0) point). CM eigenvalues, loadings, and scree plots were all derived by analyzing the CMs in *Minitab 15*^{TM}.

PCA Results for the SS Site

Correlation Matrix. For the SS site, the strongest positive correlation is between Erodible Land (HEL) and Slope (SLP), with a value of 0.751 (Table 50). There is a moderate positive correlation between geology and surficial geology, surficial geology and slope, surficial geology and sand, and erodible land and land use. There is a moderate negative correlation between surficial geology and land use, and soil and erodible land. There are only minor correlations between wetlands and the other variables, as well as sand and other variables.

PCA Interpretations. The *more significant* eigenvector value loadings in PC1 include soil (SOIL 0.414), erodible land (HEL -0.469), and land use (LUS -0.469) (first column in Table 50), represented by this component. These results suggest that there is an inverse relationship between soil types and classification of erodible land and/or land usage. *Significant* positive correlations include wetland (WET 0.314) and sand (SAND 0.399).

There are two *very significant* vector (loading) values in PC2: surficial geology (SG 0.553) and slope (SLP 0.504), which this principal component characterizes. There are two additional factors that are *significant*: geology (GEO 0.371) and erodible land (HEL 0.304) (Table 50). The remaining loadings suggest no significance.

The third principal component, PC3, has two *very significant* eigenvectors: geology (GEO -0.688) and wetland (WET 0.528). Slope (SLP 0.394) is also considered *significant* in this analysis (Table 50).

The highest loading in the entire eigenvector matrix is in PC6, for surficial geology (SG -0.763) (Table 50). However, most of the variance is already accounted for by PC3. Therefore, this data is not considered meaningful. Geology is the highest component loading within the first three principal components, and it is the second highest out of all eight of the components.

Figure 107 plots the first two principal components based on the loadings of each variable, accounting for 68.7% of the variance in the entire dataset. Land use (LUS) and sand have an inverse relationship, as well as erodible land (HEL), wetland, and soil. The surface plot (Figure 107) combines the first three components and indicates a significant influence between erodible land, land use, and soil on PC1, surficial geology and slope on PC2, and geology and wetlands on PC3.

The first three principal components, PC1, PC2, and PC3, account for 84.20% of the variation (Table 50). PC1 accounts for 42.10% of the variation, PC2 for 26.60%, and PC3 accounts for 15.54% of the variance. A large percentage of the variation is explained within these three components; consequently, the remaining principal components are discarded in the analysis. The scree plot (Figure 107) demonstrates that the highest eigenvalue is located on principal component 1 and steadily (Table 50) decreases as the component number increases. After component 3, the eigenvalues rate of change declines, validating the percentage of variance accounted for within the first three components. A common rule of thumb in analyzing PCA using correlation matrices is to discard any components with eigenvalues less than 1, indicating that a component is worth less than a single variable (Kaiser, 1960; SAS, 2008).

Communality. Communality results, based on the first three components, indicate that the variable geology (GEO) shares 61.28% of the variance of the first three principal components, followed by slope (SLP) at 46.40%, wetland (WET) at 39.48%, and surficial geology (SG) at 38.09%. The least important factor on the south side is soil (SOIL) at 24.19% (Table 50).

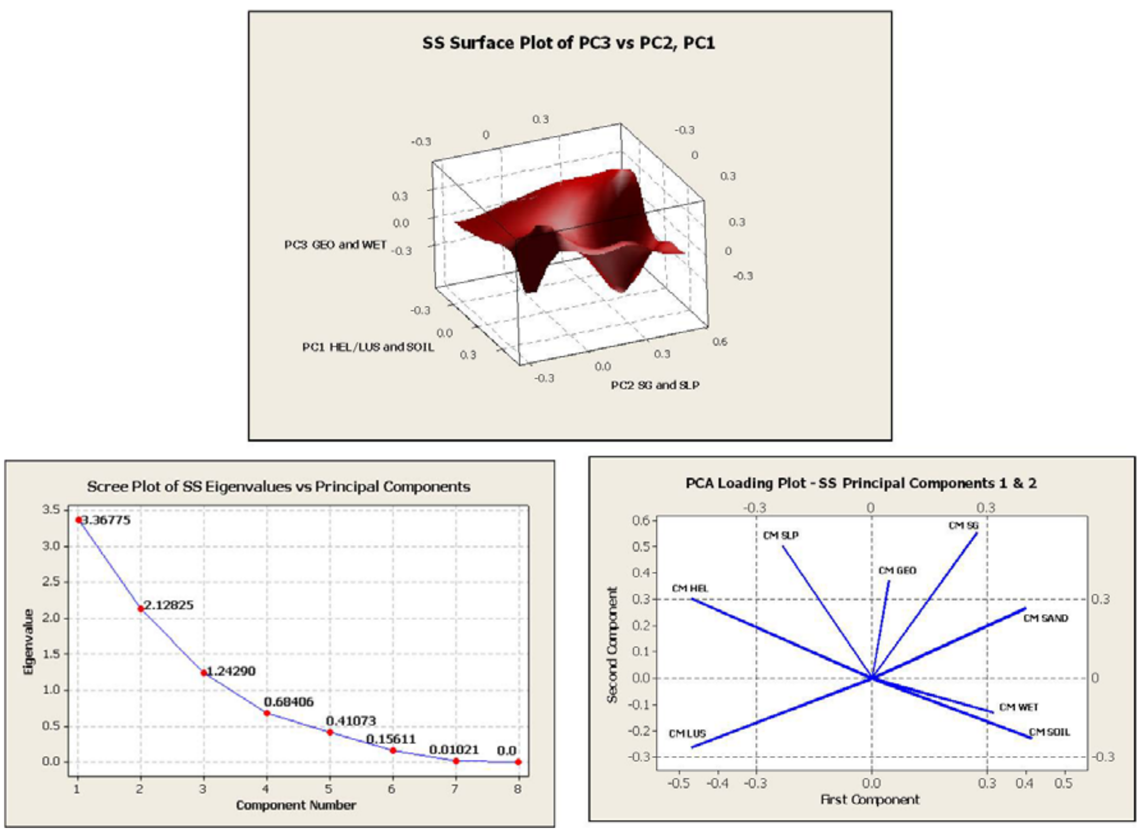

Figure 107. PCA surface, scree, and loading plots of the SS study site.

SS Variable	GEO	SG	WET	SOIL	SLP	SAND	HEL	LUS
GEOLOGY	1							
SURFICIAL GEOLOGY	0.3684	1						
WETLAND	-0.1429	0.112	1					
SOIL	-0.0239	0.0804	0.0627	1				
SLOPE	0.075	0.3839	0.0334	-0.0933	1			
SAND	0.0819	0.4776	0.1907	0.2264	0.2924	1		
ERODIBLE LAND	0.1201	0.1058	-0.1617	-0.3762	0.751	-0.1401	1	
LAND USE	-0.1328	-0.3019	-0.2532	-0.2535	0.0056	-0.2185	0.3372	1

SS Variable	PC1	PC2	PC3	PC4	PC5	PC6	PC7	PC8	1-3 COMMUNALITY
GEOLOGY	0.043	0.371	-0.688	-0.362	-0.053	0.365	-0.256	0.233	**61.28%**
SURFICIAL GEOLOGY	0.271	0.553	-0.04	-0.016	0.147	-0.763	-0.034	0.118	**38.09%**
WETLAND	0.314	-0.132	0.528	-0.64	-0.07	0.055	-0.224	0.37	**39.48%**
SOIL	0.414	-0.228	-0.136	0.506	-0.525	-0.047	-0.171	0.441	24.19%
SLOPE	-0.234	0.504	0.394	0.223	-0.311	0.187	-0.553	-0.22	**46.40%**
SAND	0.399	0.268	0.203	0.359	0.582	0.456	0.113	0.2	27.22%
ERODIBLE LAND	-0.469	0.304	0.17	0.018	-0.234	0.062	0.531	0.564	34.13%
LAND USE	-0.469	-0.263	-0.046	0.152	0.453	-0.18	-0.503	0.441	29.12%
SS Eigenvalues	3.37	2.13	1.24	0.68	0.41	0.16	0.01	0	
% Variance	42.10%	26.60%	15.54%	8.55%	5.13%	1.95%	0.13%	0.00%	
Cumulative	42.10%	68.70%	84.20%	92.80%	97.90%	99.90%	100.00%	100.00%	

Table 50. SS site correlation matrix and principal component analysis, significant components highlighted.

PCA Results for the NE Site

Correlation Matrix. The NE study site suggests that there are no linear correlations (0) for 25 of the 28 variables (Table 51). This does not, however, mean that there is no correlation. Correlation coefficients only measure linear relationships; therefore, a meaningful nonlinear relationship can exist even if the correlation coefficient is 0 (Minitab 15™, 2006). A very significant positive correlation exists between wetland and soil. There is a significant negative correlation between sand and soil (-0.3763) and a very minor negative correlation between sand and wetland (-0.0806). That said, it should be noted that the NE correlation matrix data are derived from calculations in which the values between many of the data layers are the same. Theoretically, no relationship is shown because there is no variance, thereby no correlation exists. A further analysis of the data layers will be done in future studies.

PCA Interpretations. The scree plot indicates a quick decline from PC1 to PC2, but levels off until PC6, where it begins to decline rapidly (Figure 108). Within the first four principal components, 73.2% of the variables were accounted for and the remaining four components (PC5, PC6, PC7, and PC8) were not analyzed because they only accounted for approximately 27% of the variance (Table 51). PC1 accounts for 30.35% of the variance, followed by 14.29% each for PC2, PC3, and PC4.

Among the first four components there are several *very significant* principal components: PC1 is characterized by soil (-0.629) and wetland (-0.579); PC2 by slope (0.733) and geology (-0.586); PC3 by erodible land (-0.645) and surficial geology (0.689); and PC4 by erodible land (0.587) and geology (-0.515) (Table 51). Eigenvalues defined as *more significant* are found in PC1 sand (0.483) and in PC4 surficial geology (0.463). There is one *significant* component on PC2: land use (-0.396).

PC1 indicates an inverse relationship between sand and soil/wetland, PC2 between slope and geology/surficial geology, PC3 between erodible land and surficial geology, and, on PC4, between erodible land and geology, and between surfical geology and land use (Table 51). Figure 108 plots the first two principal components, and plots the first three components.

Communality. Communality was calculated based on the first four principal components and the results indicate that surficial geology accounts for 79.18% of these components, followed by erodible land for 76.79%, geology for 68.93%, and slope for 56.57%. The variables that are the least accounted for are land use at 22.27% and sand at 23.33% (Table 51).

NE Variable	SOIL	SAND	SLP	HEL	GEO	SG	LUS	WET
SOIL	1							
SAND	-0.3763	1						
SLOPE	0	0	1					
ERODIBLE LAND	0	0	0	1				
GEOLOGY	0	0	0	0	1			
SURFICIAL GEOLOGY	0	0	0	0	0	1		
LAND USE	0	0	0	0	0	0	1	
WETLAND	0.5992	-0.0806	0	0	0	0	0	1

NE Variable	PC1	PC2	PC3	PC4	PC5	PC6	PC7	PC8	1-4 Communality	1-5 Communality
SOIL	-0.629	0	0	0	0	0.006	-0.577	0.521	39.56%	39.56%
SAND	0.483	0	0	0	0	0.7	-0.047	0.524	23.33%	23.33%
SLOPE	0.085	0.733	0.04	-0.14	-0.492	-0.271	0.174	0.299	**56.57%**	**80.78%**
ERODIBLE LAND	0.085	0.007	-0.645	0.587	0.198	-0.271	0.174	0.299	**76.79%**	**80.71%**
GEOLOGY	0.085	-0.586	-0.271	-0.515	-0.343	-0.271	0.174	0.299	**68.93%**	**80.69%**
SURFICAL GEOLOGY	0.085	-0.309	0.689	0.463	-0.128	-0.271	0.174	0.299	**79.18%**	**80.82%**
LAND USE	0.085	0.154	0.187	-0.396	0.765	-0.271	0.174	0.299	22.27%	**80.80%**
WETLAND	-0.579	0	0	0	0	0.38	0.716	0.091	33.52%	33.52%
Eigenvalues	2.43	1.14	1.14	1.14	1.14	0.88	0.12	0.00		
% Variance	30.35%	14.29%	14.29%	14.29%	14.29%	11.05%	1.45%	0.00%		
Cumulative	30.35%	44.60%	58.90%	73.20%	87.50%	98.50%	100.00%	100.00%		

Table 51. NE site correlation matrix and principal component analysis, significant components highlighted.

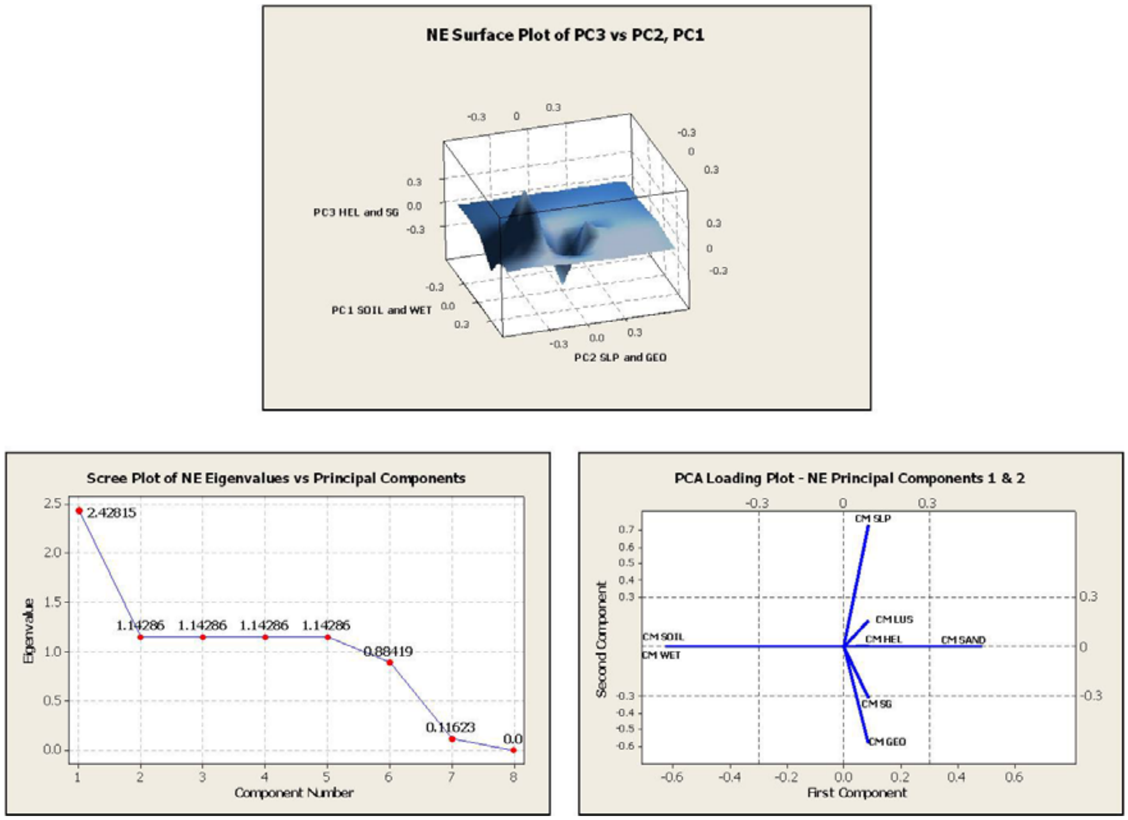

Figure 108. PCA surface, scree, and loading plots of the NE study site.

PCA Results for the NW Site

Correlation Matrix. The strongest positive correlation on the NW site is between Slope (SLP) and Erodible Land (HEL), with a value of 0.666, followed by Soil and Slope (0.5196), Soil and HEL (0.5063), Wetland and Soil (0.4403), Wetland and Slope (0.3337), and Wetland and HEL (0.3324) (Table 52). There is only one moderately negatively correlated variable, i.e., HEL and Sand (-0.3215). Eighteen of the 28 unique correlations indicate no correlation (0) and, comparable to the NE site, these may indicate a nonlinear relationship. It should be noted that the NW correlation matrix data are derived from calculations in which the values between many of the data layers are the same. Theoretically, no relationship is shown because there is no variance, thereby no correlation exists. A further analysis of the data layers will be done in future studies.

PCA Interpretations. The first three principal components account for 74.80% of the variance, such that PC1 accounts for 45.20%, PC2 is 15.30%, and PC3 is 14.29% (Table 52). The scree plot (Figure 109) shows a rapid drop from PC1 to PC2, with a leveling off from PC2 to PC4, and then a slow decline in eigenvalues from there. Subsequent analysis focused on the first three principal components.

The only variable that is considered *significan*t on PC1 is wetland (-0.386), while slope (-0.48), erodible land (-0.486), and soil (-0.456) are considered *more significant* (Table 52). The only variable on PC2 that has any value that is *very significant* is sand (-0.757). Surficial geology (-0.757) is *very significant* on PC3, followed by geology (0.4852), considered more significant, and land use (0.363) as *significant*.

A plot of the first two components (Figure 109) suggests that there is an overall inverse relationship between erodible land/slope/wetland/soil and geology/surficial geology/land use/sand. Interestingly, Figure 109 plots the first three components and it manifested a nearly flat surface. Included in this figure are the symbols and project lines for each variable. Overall, the numbers appear flat, somewhere around -0.1 and -0.2.

Communality. The most significant component on the NW site is surficial geology, which shares 78.10% of the variance with the first three principal components, followed by sand, which shares 64.76%, and then geology, at 32.11% (Table 52). Wetlands, at 18.94%, shares the smallest amount of varaiance with the first three PCs in this analysis.

NW Variable	SAND	SLP	HEL	SOIL	GEO	SG	LUS	WET
Sand	1							
Slope	-0.043	1						
HEL	-0.3215	0.666	1					
Soil	0.1064	0.5196	0.5063	1				
Geology	0	0	0	0	1			
Surficial Geology	0	0	0	0	0	1		
LUS	0	0	0	0	0	0	1	
Wetland	-0.0061	0.3337	0.3324	0.4403	0	0	0	1

NW Variable	PC1	PC2	PC3	PC4	PC5	PC6	PC7	PC8	1-3 Communality	1-4 Communality
SAND	0.273	-0.757	0	0	-0.216	-0.094	-0.032	-0.544	64.76%	64.76%
SLOPE	-0.48	0.038	0	0	-0.407	-0.383	-0.675	-0.027	23.18%	23.18%
ERODIBLE LAND	-0.486	0.265	0	0	-0.221	-0.119	0.584	-0.538	30.64%	30.64%
SOIL	-0.456	-0.257	0	0	-0.106	0.838	-0.103	0.032	27.40%	27.40%
GEOLOGY	0.184	0.288	0.452	-0.68	0.062	0.18	-0.24	-0.35	32.11%	78.35%
SURFICIAL GEOLOGY	0.184	0.288	-0.815	-0.052	0.062	0.18	-0.24	-0.35	78.10%	78.37%
LAND USE	0.184	0.288	0.363	0.732	0.062	0.18	-0.24	-0.35	24.86%	78.44%
WETLAND	0.386	0.201	0	0	0.846	0.174	0.14	0.212	18.94%	18.94%
Eigenvalues	3.61	1.22	1.14	1.14	0.56	0.23	0.09	0.00		
% Variance	45.18%	15.30%	14.29%	14.29%	7.05%	2.82%	1.07%	0.00%		
Cumulative	45.20%	60.50%	74.80%	89.10%	96.10%	98.90%	100.00%	100.00%		

Table 52. NW site correlation matrix and principal component analysis, significant components highlighted.

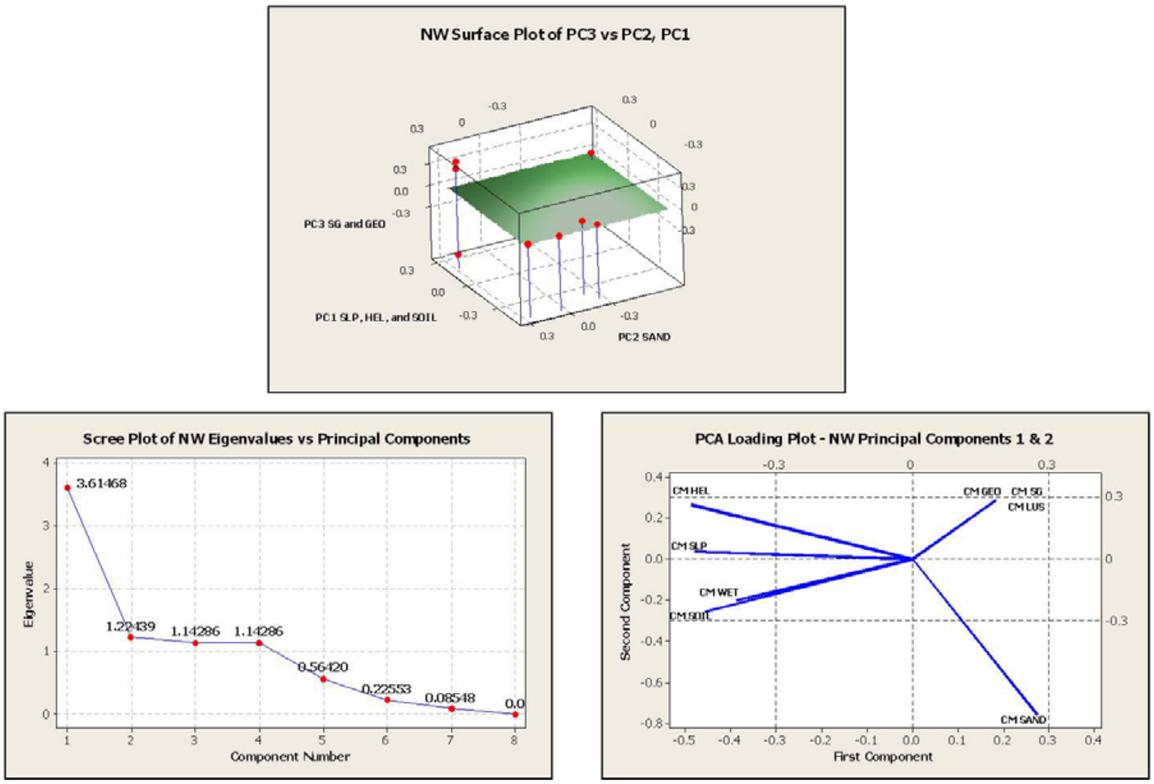

Figure 109. PCA surface, scree, and loading plots of the NW study site.

PCA analyses of MV identify two significant variables: geology and surficial geology. The criterion to determine the number of components to retain for analysis was set between 70-80% of the cumulative percent of the variance (SAS, 2008). Using this criterion, by retaining the first three principal components on the SS and the NW site, ~84% and 89% of the variation was accounted for, respectively. Four principal components were retained on the NE site accounting for ~73% of the variation with the components. Table 53 summarize the significant (> 0.30 or < -0.30), more significant (> 0.40 or < -0.40), and very significant components (> 0.50 or < -0.50) (Hair *et al.*, 1987) for each study site. Applying communality to the SS study site, the variable, geology shares 61.28% of the variance of the first three principal components, followed by slope at 46.40%, wetland at 39.48%, and surficial geology at 38.09% (Table 54). Geology's significance was picked up in a third principal component. Through univariate regression analysis and multiple regression analysis, the significance of this component remained hidden. These results adequately portray the south side of Martha's Vineyard. Glacial outwash plains are easily erodible and are known to be unstable as long the drift material remains easily accessible for fluvial erosion and transportation (Ballantyne, 2002a; Church & Ryder, 1972). Applying communality to the NE study site, the variable surficial geology shares 79.18% of the variance of the first four principal components, followed by erodible land at 76.79%, geology at 68.93%, and slope at 56.57% (Table 54). For the NW site, similar analyses indicate that the variable surficial geology shares 78.1% of the variance of the first four principal components, followed by sand at 64.76%, geology at 32.11%, and erodible land at 30.64%. As with geology's significance on the

SS site, the appearance of geology and surficial geology as the third principal component of the NW site was dependent on the use of PCA communality (Table 54).

SS PC1	LOADING	SS PC2	LOADING2	SS PC3	LOADING3		
HEL	-0.469	SG	0.553	GEO	-0.688		
LUS	-0.469	SLP	0.504	WET	0.528		
SOIL	0.414	GEO	0.371	SLP	0.394		
SAND	0.399	HEL	0.304				
WET	0.314						
NE PC1	**LOADING**	**NE PC2**	**LOADING2**	**NE PC3**	**LOADING3**	**NE PC4**	**LOADING4**
SOIL	-0.629	SLP	0.733	SG	0.689	HEL	0.587
WET	-0.579	GEO	-0.586	HEL	-0.645	GEO	-0.515
SAND	0.483	SG	0.553			SG	0.463
						LUS	-0.396
NW PC1	**LOADING**	**NW PC2**	**LOADING2**	**NW PC3**	**LOADING3**		
HEL	-0.486	SAND	-0.757	SG	-0.815		
SLP	-0.48			GEO	0.452		
SOIL	-0.456			LUS	0.363		
WET	-0.386						

Table 53. Summary of significant principal components for each study site.

STUDY SITE	VARIABLE	COMMUNALITY
SS COMMUNALITY	GEOLOGY	61.28%
	SLOPE	46.40%
	WETLAND	39.48%
	SURFICAL GEOLOGY	38.09%
NE COMMUNALITY	SURFICAL GEOLOGY	79.18%
	ERODIBLE LAND	76.79%
	GEOLOGY	68.93%
	SLOPE	56.57%
NW COMMUNALITY	SURFICIAL GEOLOGY	78.10%
	SAND	64.76%
	GEOLOGY	32.11%
	ERODIBLE LAND	30.64%

Table 54. Summary of communality results for each study site.

The communality results from the PCA, summarized in Table 55 below, thus uncovered two variables that were significant for all three study sites: geology and surficial geology. Given the paraglacial nature of Martha's Vineyard, these results were not surprising, but only through PCA did these variables become meaningful. Sand was also a significant factor explaining shoreline change for the NW study site, an observation consistent with a substantial body of earlier research on coastal erosion that focused on sandy shores. The importance of slopes on the SS and NE sites was consistent with their comparability, especially as compared to the steeper terrain of the NW site. The importance of wetlands to erosion on the SS site was consistent with its proximity to numerous coastal ponds and surrounding wetlands whereas the highly erodible land variable that emerged for the NE and NW sites was not readily interpretable since no commonalties seemed to apply.

GEO	SG	SLOPE	HEL	WET	SAND
SS	SS	SS	NE	SS	NW
NE	NE	NE	NW		
NW	NW				

Table 55. Summary of communality results by variable.

Once again, it should be noted that the NE and NW correlation matrix data are derived from calculations in which the values between many of the data layers are the same. A further analysis of the data layers will be done in future studies.

Geomorphological Risk Assessment

The EPA defines risk "to be the chance of harmful effects to human health or to ecological systems resulting from exposure to an environmental stressor" (EPA, 2008). Here, the environmental stressor is an increase in sea level around Martha's Vineyard and the risk under consideration is the risk of erosion. The evaluation of this risk that follows is based on the historical and statistical analyses of the three study sites described in earlier sections of this thesis.

The risk assessment per se was derived from the calculated mean for each raster, based upon the retained principal components for each study site (SS and NW sites: three principal components; NE site: four components). To identify the specific areas at risk from coastal erosion, I first considered the 100-year historical data on erosion patterns, as manifested by the linear regression rates for each attribute and for each study site. The numbers 1 through 5 were used to simplify the analysis. A rating of “1” indicates a low risk of shoreline erosion because shorelines were accreting more than 1 m/yr; a “2” was considered a low to medium risk because shorelines were accreting at the rate of 0.05 to 1 m/yr; “3” suggests a medium risk, with the shorelines fluctuating between accretion and erosion at 0.5 to -0.5 m/yr; Medium to high risk, a “4”, was assigned to shorelines eroding at the rate of -0.5 to -1 m/yr; and a high risk of “5” was used to indicate shoreline erosion greater than -1 m/yr. Note that the risk ratings are identical to the reclassification methods used in the PCA analysis.

The individual risk assessments for each variable and for each study site are summarized below. The mean from each raster cell is represented as the geomorphological risk assessment, including wetlands and eliminating wetlands. The culmination of this analysis yielded three types of interpolated maps of Martha’s Vineyard that: 1) predict, by IDW and kriging, respectively, which areas on the island have the potential to be vulnerable to coastal erosion; and 2) identify the prediction kriging standard errors associated with the predicted values.

Risk Assessment for the SS Site. The risk assessment values range from 1 to 5 for *Soil, Sand, Wetland,* and *HEL* (Table 56). *Slope* ranges from 1 to 4, *Geology* 1 to 3, *Land Use* and *Surficial Geology* from 2 to 4. The variable *Sand* has the highest mean of 4.24, with a standard deviation of 1.27, followed by *Wetland* with a mean of 3.8, and *Soil* with a mean of 3.75. As an individual variable, *Geology* has the least influence on this side with a mean of 2.09. Table 56 and Figure 110 show the results for each of these variables. However, as shown in the previous section, once PCA was performed, the variable *Geology* accounted for 61% of the first three components, thereby becoming the leading factor (Table 50). (These results strongly imply that the result from one variable does not adequately portray the interaction between multiple variables.)

SS Layer	MIN	MAX	MEAN	STD
Soil	1	5	3.75	1.37
Sand	1	5	4.24	1.27
Wetland	1	5	3.80	0.78
HEL	1	5	2.87	1.21
Slope	1	4	3.08	0.92
Geo	1	3	2.09	0.54
LUS	2	4	3.30	0.91
SG	2	4	3.61	0.79

Table 56. SS site risk assessment by major variables.

The results from computing the mean risk assessment for the SS study site indicate that the areas that are at the highest risk of erosion are predominantly located immediately adjacent to the coastline, including areas identified as coastal ponds (Figure 111). A significant portion of the SS site is also at medium to high risk of erosion based on the combination of all the variables. Figure 111 illustrates the mean with and without wetlands in the calculations.

The SS site IDW prediction map results are shown in Figure 112 and Figure 119. Clearly, most of the coastal south side is at risk of erosion, ranging from mean values of 2.9 - 3.8 for equilibrium, 3.8 – 4.2 for medium to high risk, and 4.2 to 5 for high risk. Two areas that are potentially not at risk are located near Stonewall Beach, on the western end of the study site, and between West Tisbury and Edgartown.

Kriging results on the south side of the Vineyard suggest erosion around Nashaquitsa Cliffs, Stone Wall Beach, and Ocean at Chilmark Pond Preserve. Inland areas around Nashaquitsa Pond have a low risk of eroding (Figure 120). Heading east, the barrier beaches indicate a high risk of erosion. The eastern edges of Tisbury Great Pond are at a high to medium high risk when compared to the western edges of the pond (that have a medium, to medium-high risk). Jobs Neck Ponds are located in a high risk area, as are points within Jacobs Pond in Edgartown. The western side of Norton Point Beach, near Atlantic Drive, is at high risk. The study site areas are well within the 0.4-0.47 prediction standard error (Figure 121).

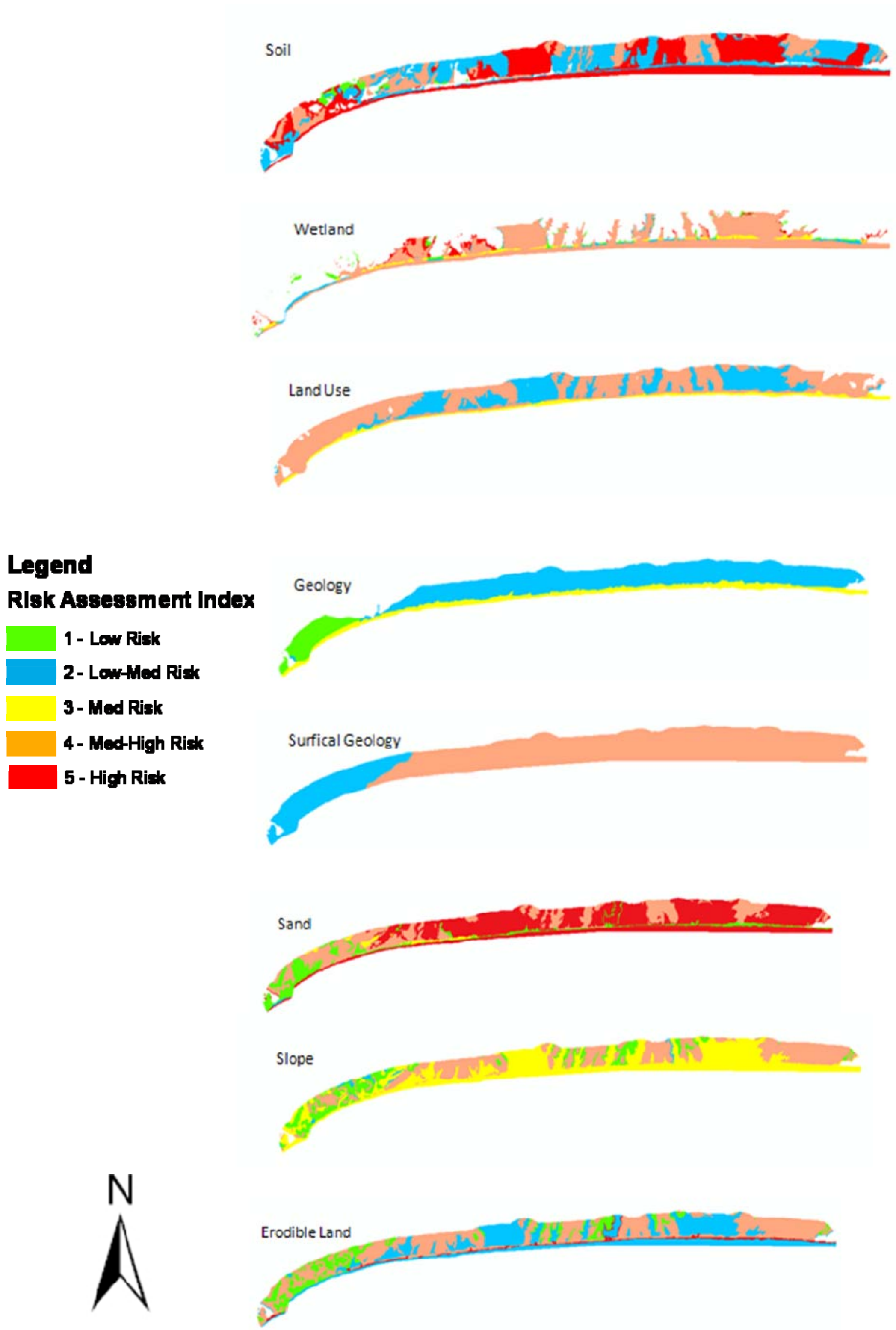

Figure 110. SS site mean risk assessment for each major variables.

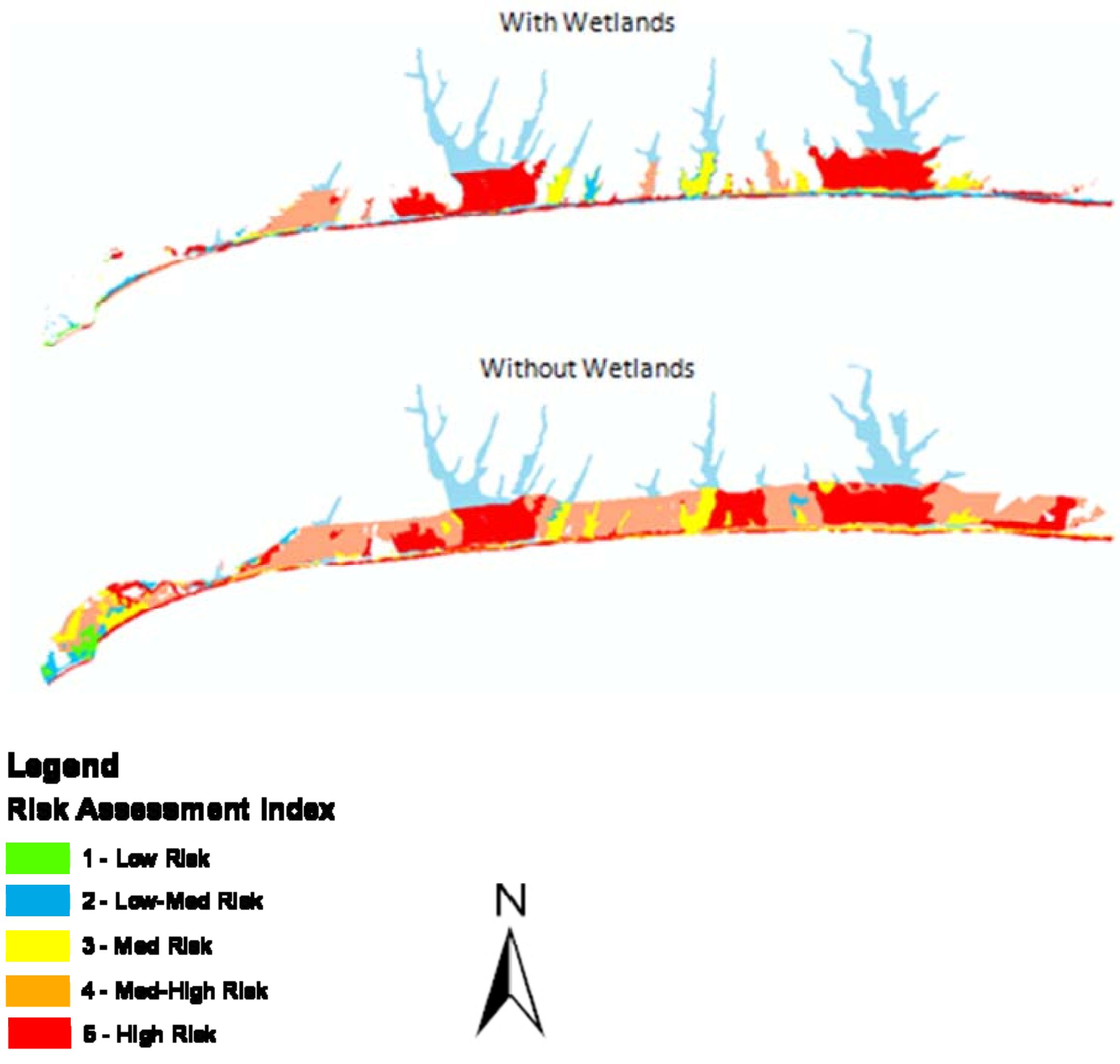

Figure 111. Mean risk assessment results for the SS study site, with and without wetlands in the analysis.

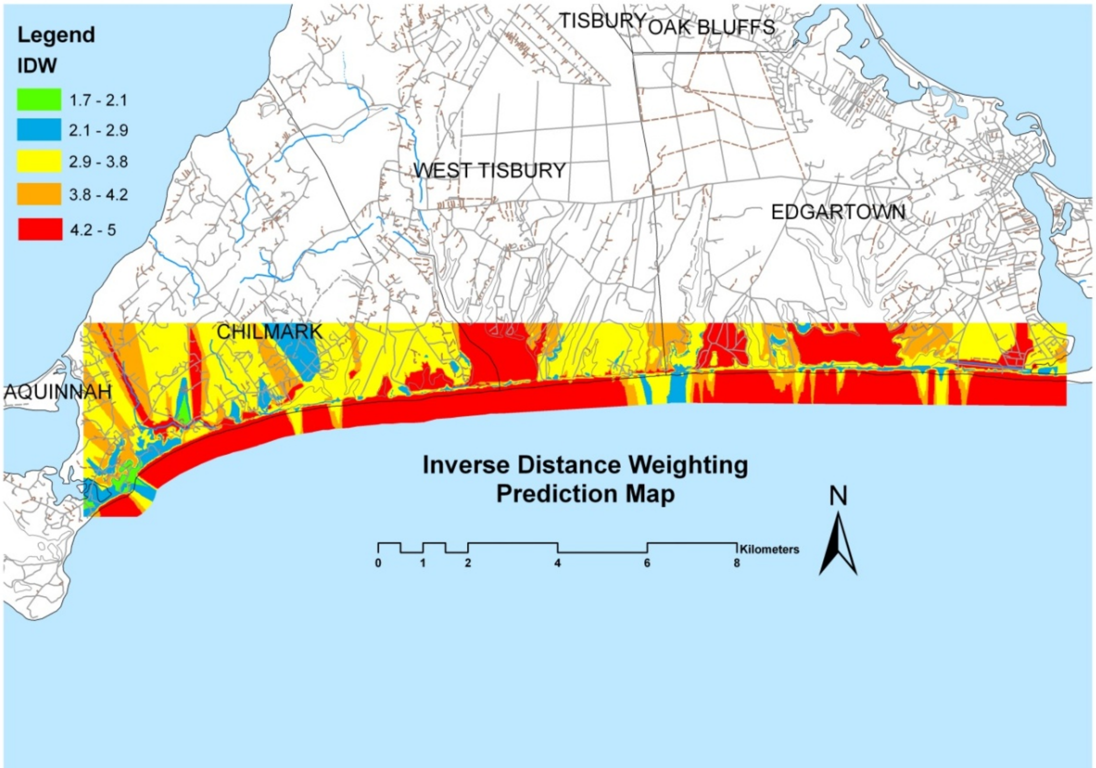

Figure 112. Inverse Distance Weighting (IDW) for the SS site based upon risk assessment.

Risk Assessment for the NE Site. At this site, the risk assessment values range from 1 to 5 for only one variable, *Sand*, with a mean of 3.19, with the highest standard deviation of 1.55 (Table 57). While this variable appears to have the most risk associated with erosion (Figure 113), the *Wetlands* variable has the highest mean at 3.44, and a standard deviation of 0.51. *Soil* has a range between 3 and 5, with a mean of 3.11. *Slope, HEL, Slope, Surficial Geology, Geology*, and *Land Use* were all rated a 3, and clearly had a mean of 3, with no standard deviation, indicating that these factors are relatively stable on the NE side. PCA results shown earlier suggest that *Surficial Geology* has the strongest influence on coastal erosion (79% communality), followed by *HEL* (erodible land, 77%), then *Geology* (69%), and *Slope* (57%) (Table 51). (Note that these patterns are not apparent if each layer is analyzed individually).

NE LAYER	MIN	MAX	MEAN	STD
SAND	1	5	3.19	1.55
WET	3	5	3.44	0.51
SOIL	3	5	3.11	0.32
SLP	3	3	3.00	0.00
HEL	3	3	3.00	0.00
SG	3	3	3.00	0.00
GEO	3	3	3.00	0.00
LUS	3	3	3.00	0.00

Table 57. NE site risk assessment by major variables.

The results from computing the mean risk assessment for the NE study site indicate that calculations which include Wetlands project a medium risk of erosion, primarily bordering the coastal areas (Figure 114). If Wetlands are excluded from the mean, then the NE side is overall at low risk for significant coastal erosion.

Applying IDW, most of the NE side is ranked low to medium risk (Figure 115, Figure 119). The entrances to Oak Bluffs Harbor and Edgartown Harbor are at low risk of being eroded (Figure 120). Locations around North Neck Road (on Chappaquidick), Golf

Club Road (in Edgartown), and near Farm Pond Rod are at medium risk of erosion Figure 120). The prediction kriging map for the NE clearly shows that the downtown area of Oak Bluffs is at low risk and that the bluffs on either side of it are at low to medium risk, much like the IDW analysis (Figure 115, Figure 119). The study site areas are well within the 0.4-0.47 prediction standard error (Figure 121).

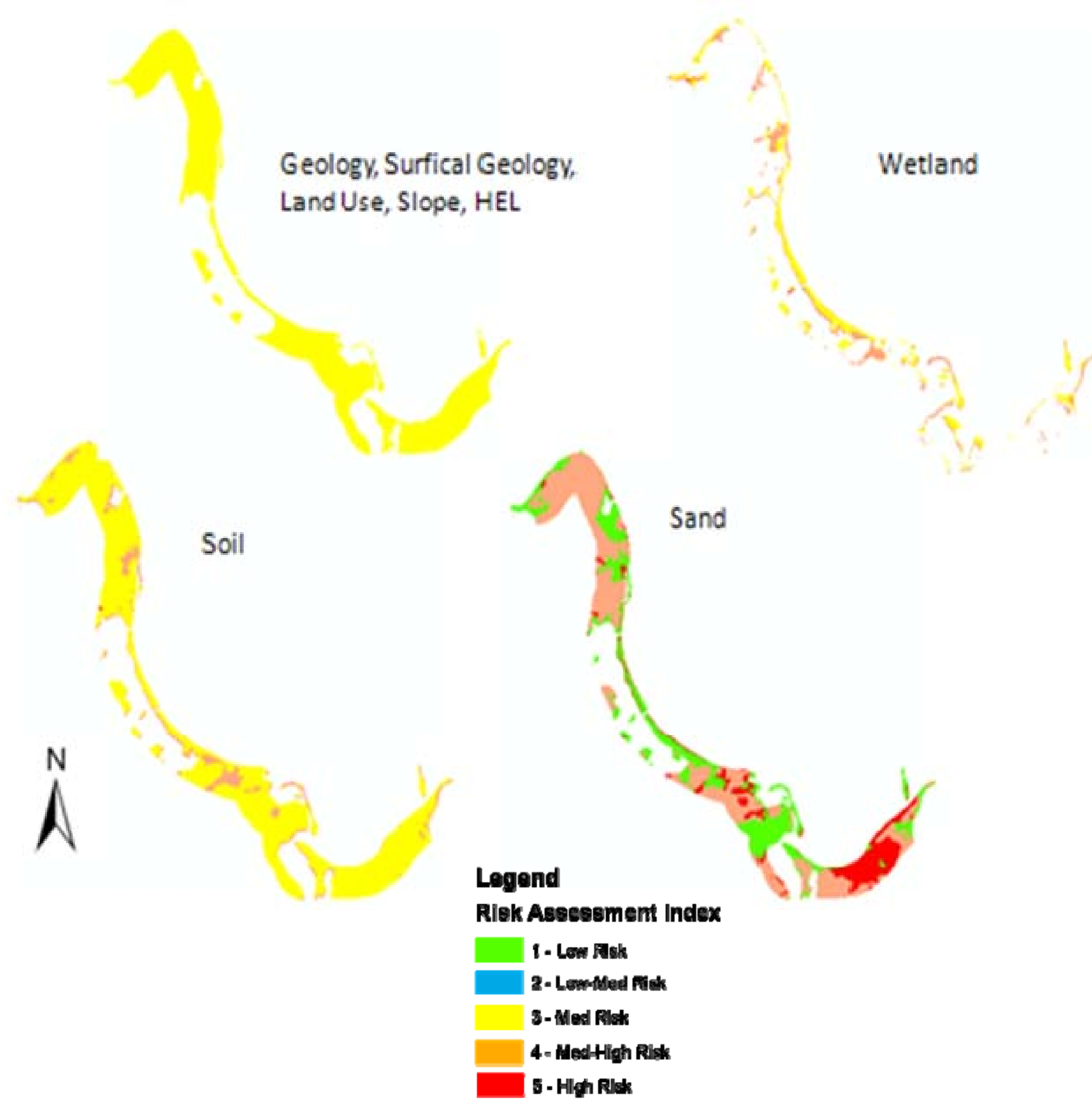

Figure 113. NE site mean risk assessment for each major variables.

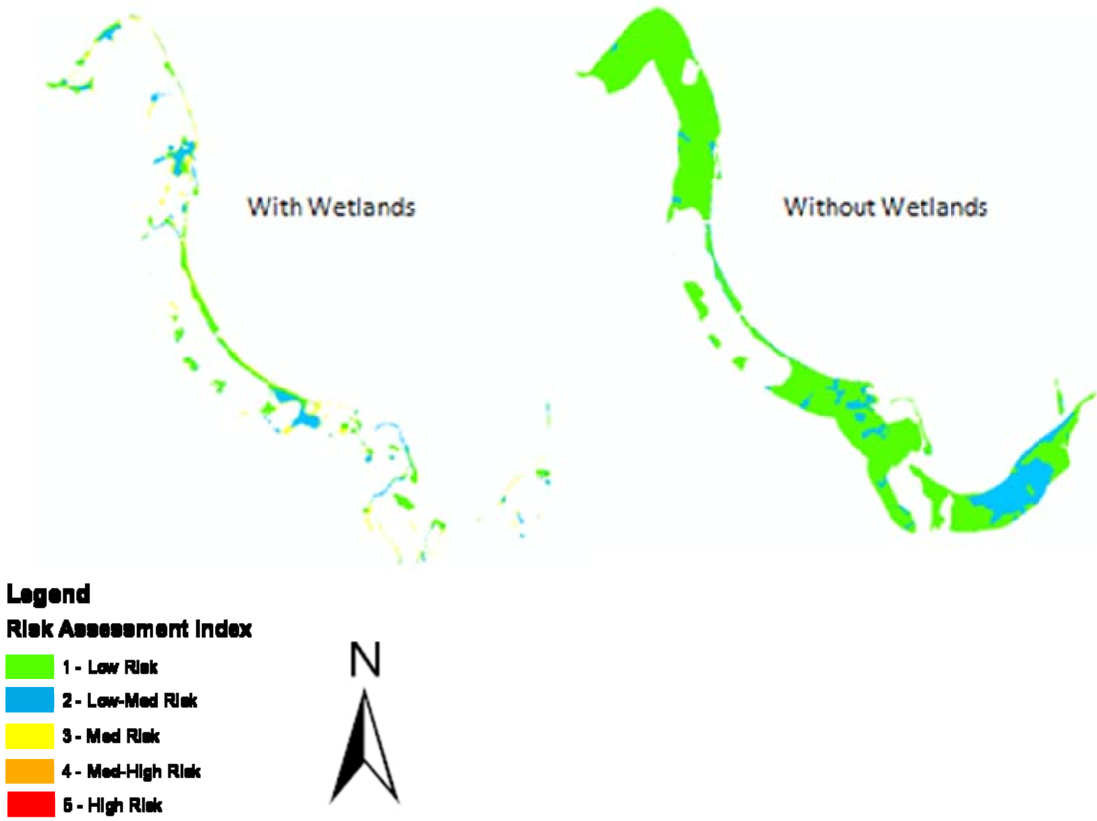

Figure 114. Mean risk assessment results for the NE study site, with and without wetlands in the analysis.

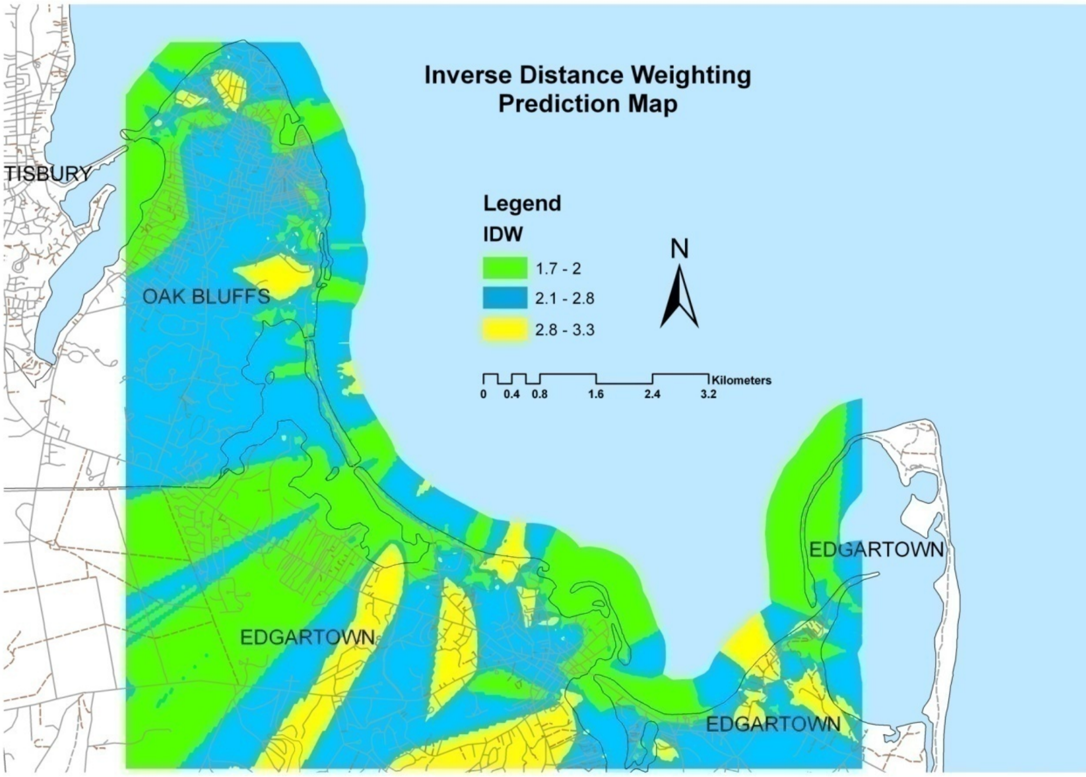

Figure 115. Inverse Distance Weighting (IDW) for the NE site based upon risk assessment.

Risk Assessment for the NW Site. The risk assessment values range from 1 to 5 for only the *Sand* layer, which has the highest mean of 3.99, and the highest standard deviation of 1.52 (Table 58, Figure 116). Half of the variables have a range from 2 to 4, including *Slope, HEL, Soil*, and *Wetlands*. *Geology, Surfical Geology*, and *Land Use* all have a mean of 3 and a zero variance. On the NW site, the PCA results indicate that *Surfical Geology* (78%) has the most influence, followed by *Sand* (65%), and *Geology* (32%) (Table 52) *Sand* is the only variable that is somewhat correlated with the PCA results.

The mean values for the retained variables suggest that the land southwest of Menemsha Harbor, Menemsha Bight, is at low to medium risk of erosion (Figure 117), with or without wetlands included in the calculations. Areas northeast of the harbor are more likely to erode, once wetlands were factored in to the equation, and are considered a medium risk. Coastal areas in close proximity to Cape Higgon are at medium to high risk, as well as beach areas near Forest Road, Cedar Tree Neck, and James Pond in West Tisbury.

NW LAYER	MIN	MAX	MEAN	STD
SAND	1	5	3.99	1.52
SLOPE	2	4	2.64	0.57
HEL	2	4	2.37	0.55
SOIL	2	4	2.97	0.45
WET	2	4	2.94	0.71
GEO	3	3	3.00	0.00
SG	3	3	3.00	0.00
LUS	3	3	3.00	0.00

Table 58. NW site risk assessment by major variables.

However, once IDW was applied, the medium to high risk areas transformed into lesser risk assessments, suggesting that the NW side is relatively stable with a medium to low risk of coastal erosion based upon the variables (Figure 118, Figure 119).

Kriging, however, fined tuned the IDW results (Figure 120) and identified a small location near Cape Higgon that rose back to medium to high risk. Just south of Cape Higgon, before Great Rock Bight, the area is at low to low-medium risk of erosion. The Prospect Hill area, in Chilmark, is at medium risk, and it diminishes as one approaches Menemsha Harbor from the north. The land surrounding Menemsha Bight is at low risk, as well as the Lobsterville area. Coastal areas on the north side of Aquinnah, near Oxcart Road, are at low risk. There is a medium risk of erosion near Driftwood Lane in Aquinnah, in between Lobsterville Road and Oxcart Road. The prediction standard error for the NW study sites is between 0.4 and 0.47 (Figure 121).

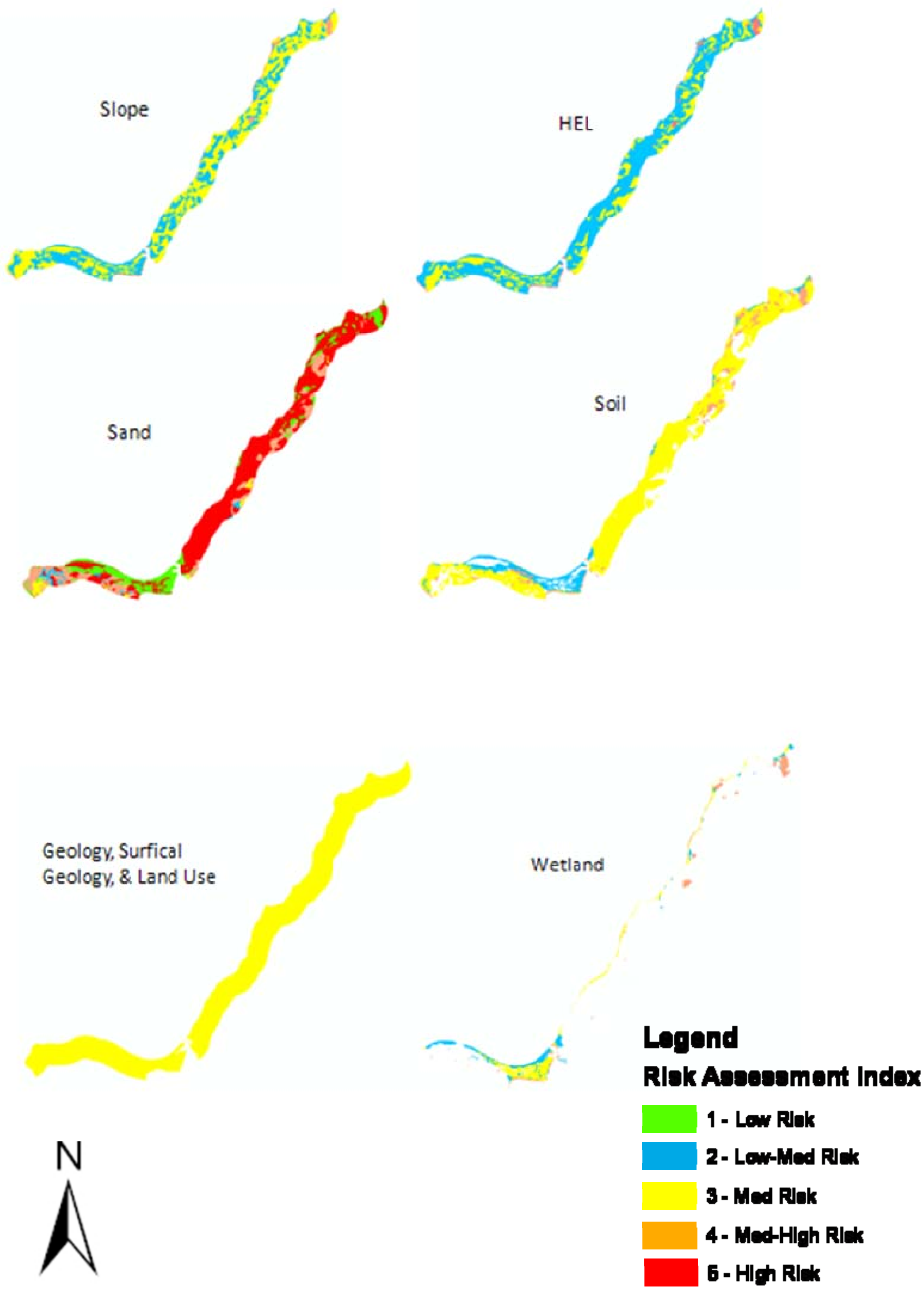

Figure 116. NW site mean risk assessment for each major variables.

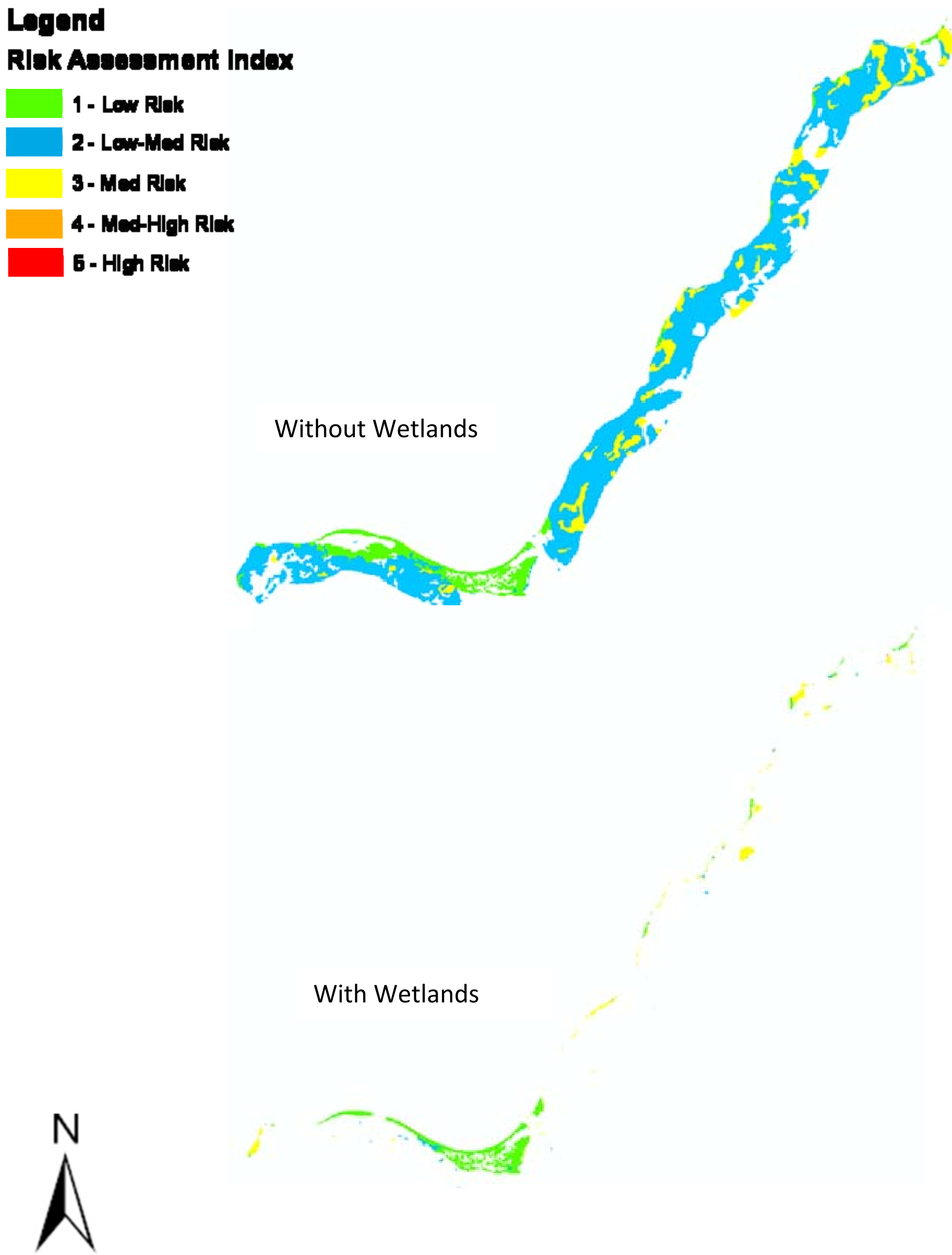

Figure 117. Risk assessment results for the NW study site, with and without wetlands in the analysis.

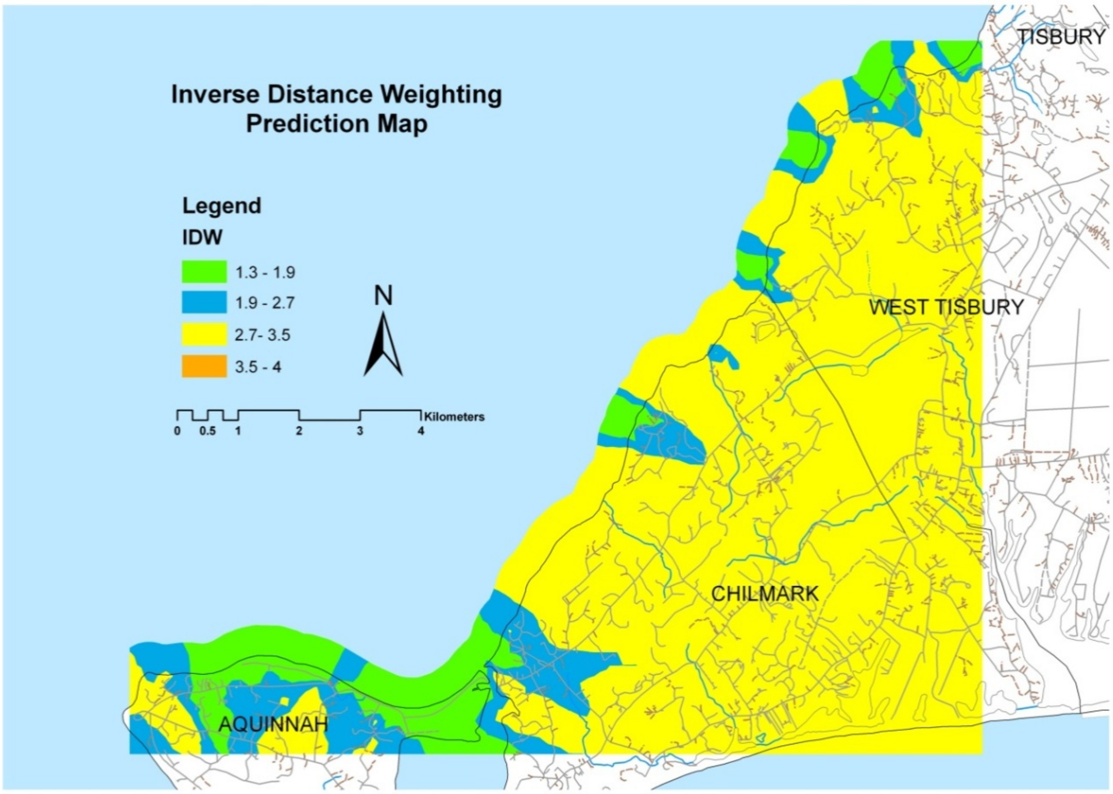

Figure 118. Inverse Distance Weighting (IDW) for the NW site based upon risk assessment.

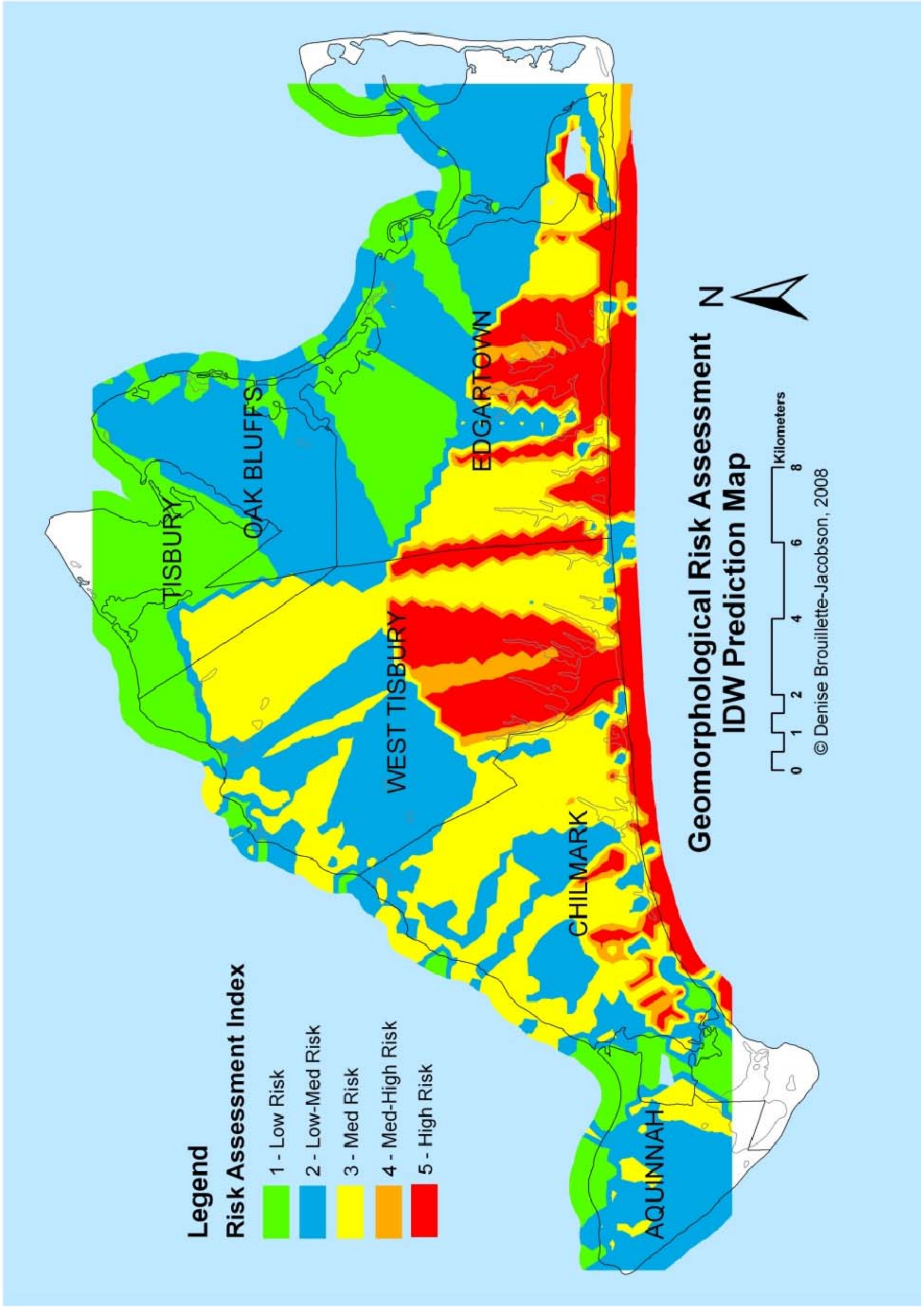

Figure 119. IDW Risk assessment for Martha's Vineyard .

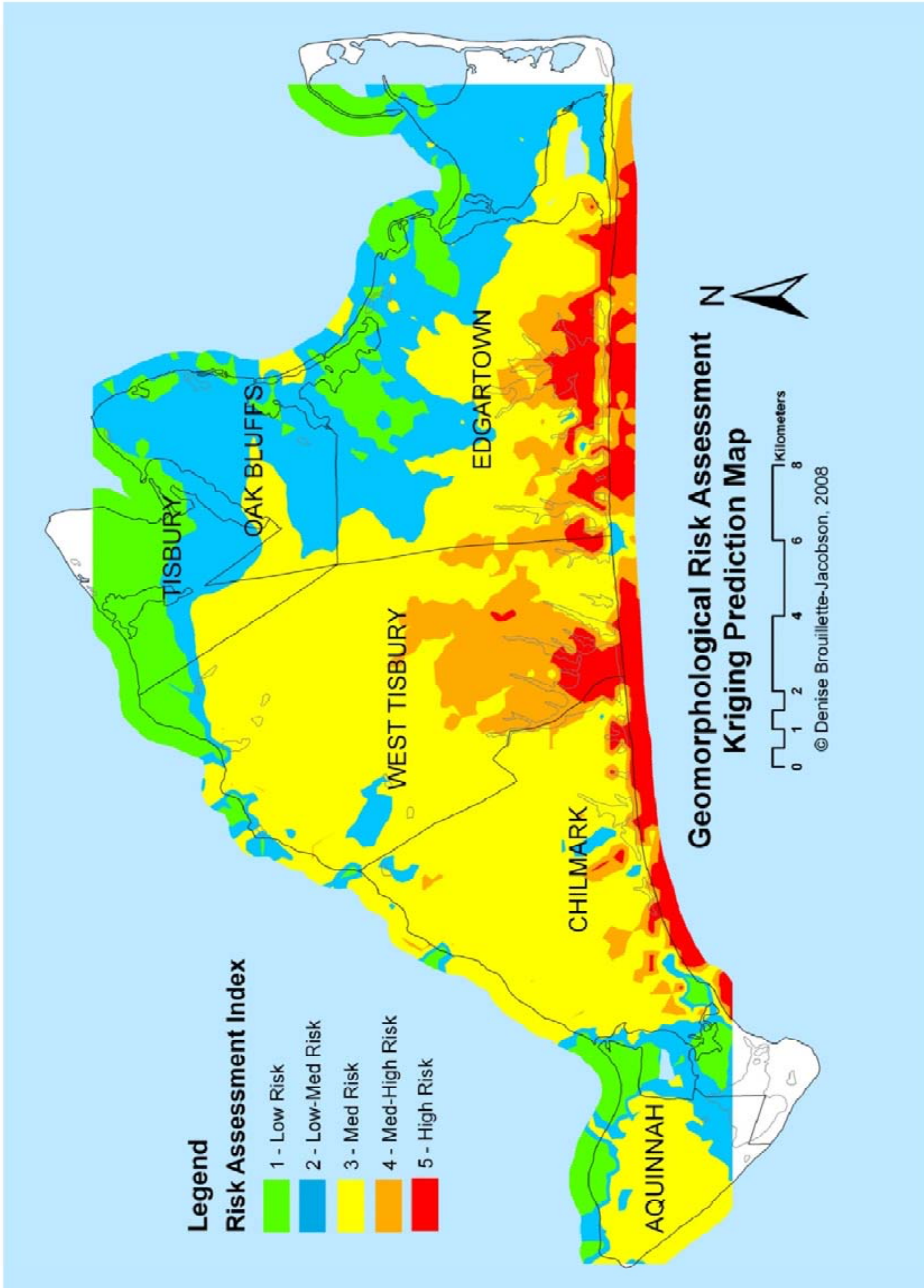

Figure 120. Kriging predictions for geomorphological risk assessment for Martha's Vineyard .

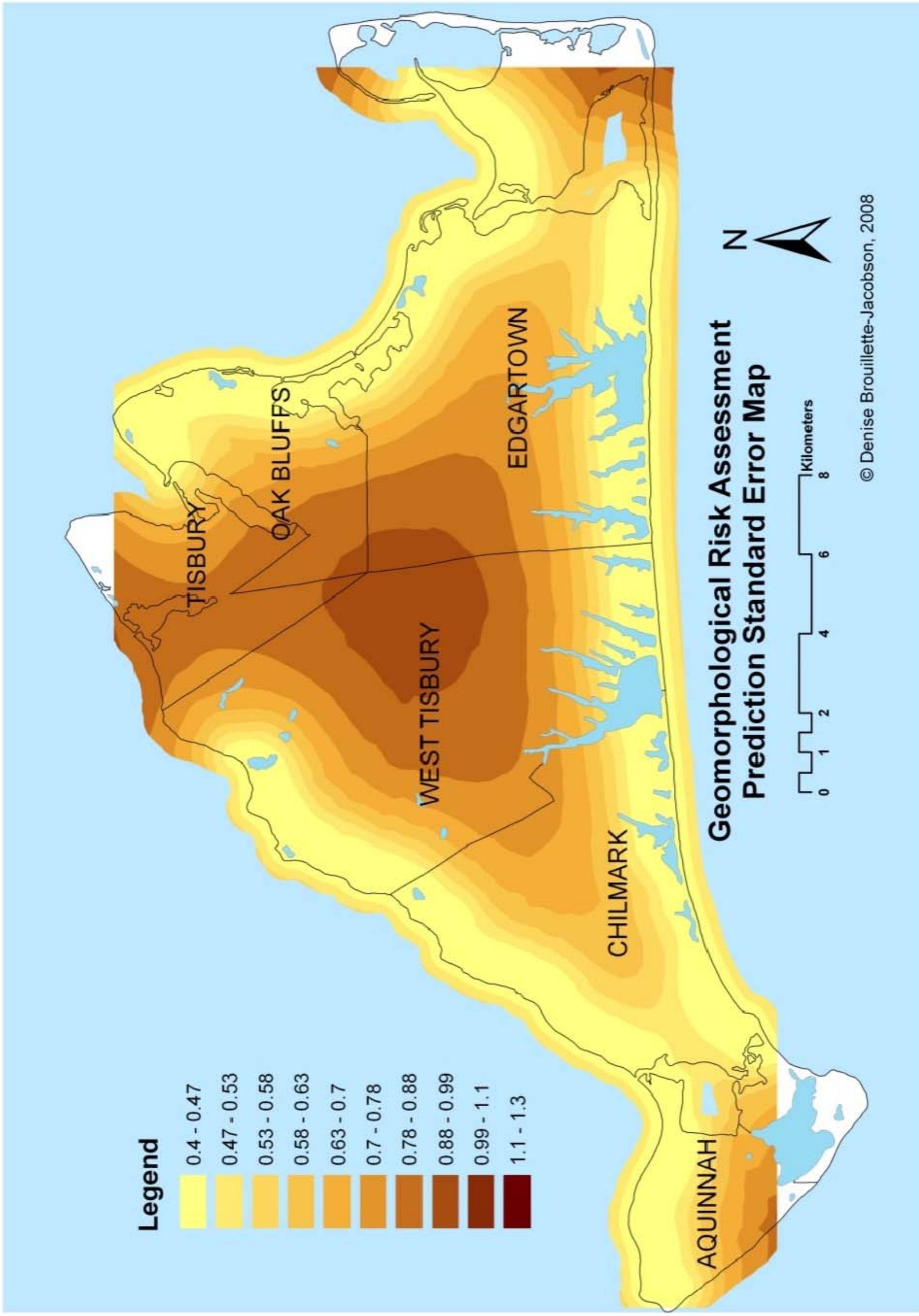

Figure 121. Kriging prediction standard error map based upon geomorphological risk assessment for Martha's Vineyard.

CHAPTER 5

DISCUSSION

In this thesis I have evaluated the vulnerability of the small island of Martha's Vineyard to coastal erosion. As a paraglacial island, MV is still reworking its glacial sediments and may take tens of thousands of years to become non-glaciated. The highly unstable geologic structure of the south side of the Vineyard enables it to erode at a much faster rate than that predicted by the Bruun rule (Table 17) and statistics show that the low-lying coastal areas on the south side will lose a significant portion of its land as the sea continues to rise (Table 18, Figure 120). Accordingly, an understanding of the factors influencing this enhanced rate of erosion merited detailed consideration and comprised a major focus of this thesis. My analyses of these factors, as well as additional considerations of Martha's Vineyard *per se* are discussed below.

Sea level rise in the vicinity of Martha's Vineyard. Although there is ample evidence for ongoing sea level rise at numerous sites around the world, I first sought to determine whether sea levels were rising in the vicinity of Martha's Vineyard. Data were obtained for Buzzard's Bay, the Cape Cod Canal, Woods Hole, and Nantucket, and all manifested ongoing sea level rise during most, but not all time periods (Figure 56). Given the proximity of Nantucket and Wood's Hole to Martha's Vineyard, I focused on the data from those two sites. From 1933 to 2003, trend analyses indicated that sea level was rising at 2.56 mm/yr in Woods Hole (Figure 57A). Similar analyses for Nantucket, from 1965 to 2003, indicated a rate of 3.08 mm/year (Figure 59A). Differences in these sea levels may be due to glacial isostatic adjustments along the coastline. Linear regression rates for Woods Hole, from 1933 to 1964, indicated a rise of 3.24 mm/yr (0.13 in/yr)

(Figure 58A); however, from 1966 to 2003, the Woods Hole rate declined to 2.08 mm/yr (0.08 in/yr), (Figure 58B) suggesting that the seas may not be rising as quickly during this period. During the same time, linear regression analysis for Nantucket yielded a rate of 2.9 mm/yr (Figure 59B). Thus, while there was some uncertainty as to precise rates, it was evident that sea levels in the vicinity of Martha's Vineyard are rising.

Even if global temperatures had stabilized in the year 2000, models show that sea levels are likely to continue to rise unabated with proportionately much greater increases compared to temperature increases (Meehl *et al.*, 2005). These models project that sea levels could rise by an additional 320% due to thermal expansion by the end of the 21st century (Meehl *et al.*, 2005). Accordingly, I sought to derive estimates for the rate of sea level rise for the coastline of Martha's Vineyard for the next 100 years. The 2007 IPCC report projected a range of sea level rise from to 0.18 m to 0.59 m by the year 2100 (IPCC WGI, 2007). Since seas rose by approximately 0.3 meters near Martha's Vineyard over the last 70 years, the lower end of the IPCC projection (0.18 m) seemed unrealistic for the study area. Hence, I estimated that the range of sea level rise around Martha's Vineyard by the year 2100 would be from 0.3 m to 0.58 m and may reach as high as 1.14 m.

My rationale for these estimates was as follows: The IPCC acknowledges that seas have been rising at the rate of approximately 0.003 m/yr, particularly in the northwest Atlantic region (IPCC WGI, 2007). In order for MV seas to reach the IPCC's projection of 0.59 m by the year 2100, the rates of sea level rise would have to increase exponentially (Figure 60). Taking into account the possibility of such exponential increases in rates, and the acknowledgments of researchers on the IPCC panel that their projections are too modest (Kerr, 2006a; Peltier, 2007), I considered it not unreasonable to expect sea levels to rise by as much as 1.14 m by 2100 (Figure 61).

Erosion of the Martha's Vineyard coastline. An analysis of the effects of sea level rise on coastal erosion obviously required evidence that the Martha's Vineyard coast was eroding. Shoreline change maps created by the Massachusetts Coastal Zone Management and Thieler *et al*., (2001) indicated that, from 1851 to 1994, 74% of the MV shoreline maintained an equilibrium that ranged from 0.5 m/yr to -0.5 m/yr, 24% of the island eroded with rates faster than -0.5 m/yr, and 2% accreted with rates faster than 0.5 m/yr. Excluding the equilibrium factor, 85% of the island eroded with a shoreline rate of change less than zero, 14% accreted with a rate greater than zero, and only 1% had a mean shoreline change rate of zero (Results Chapter, MV ERA01-04 Cumulative Data).

A closer look at the individual study sites showed that the south side of Martha's Vineyard had the highest linear rate of shoreline change per year (-1.71 m/yr) (Table 15), with 90% of the shoreline eroded and 2.6 km^2 of land lost to the sea. Note that the linear regression analyses have a resolution of ± 0.12 m/yr and individual shoreline positions are generally accurate to within ±8.5 m (Thieler *et al.*, 2001).

The two other study sites eroded as well, but significantly less. Seven percent of the transects indicated erosion on the NE site (Figure 48), and had a mean linear regression rate of -0.11 m/yr (Table 15). Most of the significant erosion occurred during the last time period (1978 to 1994), at a rate of -0.43 m/yr (Table 13). Four percent of the NE site transects indicated accretion (> 0.5 m/yr) and the remaining 89% had a shoreline change rate between -0.5 m/yr to 0.5 m/yr (Figure 48). Oak Bluffs saw most of the erosion at -0.19 m/yr, while Edgartown had an erosion rate of -0.01 m/yr (Table 13). The NE site lost approximately 0.22 km^2 of land.

Ninety-four percent of the NW study site manifested a relatively stable shoreline, with rates between -0.5 m/yr and 0.5 m/yr (Figure 48). Three percent of the transects accreted, and 3% of them eroded. The mean linear regression rate of change for the NW site was -0.1 m/yr (Table 14, Table 15), leading to a loss of approximately 0.33 km^2 of shoreline.

Factors affecting erosion: testing for the applicability of Bruun's rule. Alternate coastal erosion models notwithstanding, the primary and most widely accepted model is Bruun's and it serves as the baseline from which many other models are derived. Hence, Bruun's methodology (1962) was applied to all three study sites, with the expectation that the ratio of sea level rise to erosion rates would fall between 50 to 100 times the rate of increase of sea level rise. Even extending the rule for erosion to approximately 100 to 150 times that of sea level change (Douglas *et al.*, 2001; Leatherman *et al.*, 2000b; Zhang *et al.*, 2004) these ratios did not apply to the south coast of the Vineyard.

Of the three study sites, the SS site is the only coastline that fits the criteria set forth by Bruun and others. This open-ocean coastline is relatively sandy and easily erodible, with sufficient wave energy to erode, transport, and redistribute the sediments over the profile. The other two sites have similar characteristics, but do not face the open ocean, potentially making their results ambiguous with respect to Bruun's rule.

Using a rate of sea level rise of 0.003 m/yr, the Bruun ratio for the SS study site was calculated to be 1:567 (Table 17), a value markedly different from Bruun's predicted ratio. Using this as a standard ratio for the south side of Martha's Vineyard, sea level rise at 0.003 m/yr and a steady linear rate of erosion of -1.71 m/yr would erode the SS coastline by 42.5 m in 25 years, 85 m in 50 years, 127.5 m in 75 years, and 170 m by 2100 (Scenario #1) (Table 18). Following the IPCC's modest sea level projections (Scenario #2), based on a sea level increase of 0.59 m, the south side could experience shoreline loss of 334 m, and maybe even as much as 646 m based upon an increase of sea level by 1.14 m (Scenario #3) (Table 18).

The NE and NW study site results were significantly lower, and resembled the lower end of Bruun's rule, i.e., ratios of 1:40 and 1:37, respectively (Table 18). For both of these sites the sea level rise rate was 0.0026 m/yr. Using the second scenario, the NE study site would experience 3.03 m to 23.87 m of shoreline retreat and the NW site would experience 2.79 m to 21.95 m of retreat in the same time periods. In the third scenario, sea levels could increase by approximately 1.14 m in 100 years and the last 25 years of the century would witness the most significant shoreline retreat. By 2100, estimates indicate that the NE shoreline would erode by 46 m and the NW by 42 m (Table 18).

Addressing erosion one attribute at a time. Clearly, sea levels are rising and Martha's Vineyard is eroding at a much faster rate on the south side of the island than at the other two study sites with predominantly northeastern and northwestern exposure. The northwest coast takes the brunt of winter winds and the northeastern side of the Vineyard has direct exposure to Northeasters, but both of these study sites appear to be on the low end of the coastal erosion spectrum for this island. In fact, the NE and NW areas are manifesting accretion in some spots. Any number of environmental conditions could factor into these results, including the length of fetch, sediment supply, longshore transport, or simply manmade stone walls and jetties.

To better understand the erosion patterns for each study site, a multistep process was initiated, attribute by attribute, variable by variable, and multiple variables by the linear regression rate of historical erosion. Several variables (i.e., geology, surficial geology, wetland, land use, soils, percent of sand, slope, erodible land, wind, waves, and compass direction) were chosen as relevant aspects to be considered simultaneously when evaluating shoreline erosion. Initially, these variables were analyzed separately, and then reintegrated, based upon their importance in coastal erosion. Surprisingly, wind, waves, and compass direction results were not significant as separate entities. These variables may inherently be factored into the existing erosion results for the geophysical variables, as is the rise in sea level, and they were, therefore, eliminated from the final analysis.

Single variables vs. erosion. Bruun's methodology addressed sandy shores, slopes, and depth of closure, based on the equilibrium profile theory (Bruun, 1962). Refinements to Bruun's model, as mentioned previously, consider sandy beaches as a major variable in erosion (Douglas *et al.*, 2001; Leatherman *et al.*, 2000b; Zhang *et al.*, 2004). Other variables considered previously to be important in erosion include sediment transport (Jaffe *et al.*, 1997), wave and tidal energy (FitzGerald *et al.*, 2000), wave height, wave period, wave direction, water levels, and sediment size (Dolan, 1966). Further, storms, storm tides, duration of storms, storm surge, wave energy, wave-induced set up, sediment supply related to storms, cross-shore processes, and local tides have been examined individually and in a variety of combinations to determine the significance in shoreline recession (Austin *et al.*, 2000; Bryan *et al.*, 2001; Buynevich & Evans, 2003; Fein, 2007; FitzGerald *et al.*, 2002; Forbes *et al.*, 2004; Hill *et al.*, 2004; Keim *et al.*, 2004; McNinch, 2004; Miller & Dean, 2004; Ogden, 1974; Plum Vineyard, 2007; Seccombe, 2007; Sigelman, 2007; The Trustees of Reservations, 2007; Uchupi *et al.*, 2005; USGS, 2005; Zhang *et al.*, 2001). In addition, Phillips and Williams completed a foreshore analysis using regression models of the mean high water mark versus the mean beach level to determine whether the beach gained or lost material (Phillips & Williams, 2007).

All these models have their own merits by limiting the number of variables under investigation. By understanding the coastline's response to storms, sediment supply, and wetlands, as a few examples, a much larger and more complex picture of shoreline dynamics emerges. I concluded that it is essential to understand and model as many variables as possible, first individually, and then to use multivariate analysis in order to unmask any underlying phenomena.

Analyses of single attributes at the SS site. On the SS study site, individual attributes that had significant p-values and high R^2 values included "beaches" in the soil variable ($p = 0$, $R^2 = 24.3\%$, quadratic regression) and "erodible land" ($p = 0$, $R^2 = 24.3\%$, quadratic regression) (Table 40). These attributes are correlated because "beaches" in the soil variable is classified as "erodible land." "Beaches" comprises 3.6% of the soil and "erodible land" comprises 2.45% within the SS site. Transects that were comprised of "beaches" within the soil variable range from transects that do not contain it to approximately 40% of the transects with this attribute. The majority of the transects that contain "beaches" and "erodible land" have a shoreline change rate between -1 m/yr and -3 m/yr. The greater the percentage on the transects, the less erosion occurs, although it is slight. “Beaches” are adjacent to much of the coastline and around Oyster Pond. An argument could be made that “beaches” should be considered a sandy shore and it was the most significant attribute on the south side study site, albeit with a relatively low R^2 value.

By evaluating shoreline change on transects that had more than 25% of an attribute, the only attribute that was unique to erosion was “beach” under the land use variable (Table 43). Results from linear quadratic regression analysis indicated a p-value of 0 and an R^2 of 8.5% (Table 40).

Meanwhile, “winter wave direction” had the highest linear regression rate of -16.5 m/yr, a p-value of 0, and an R^2 of 7.2%, followed by “summer wave direction,” with a linear regression rate of -6 m/yr, a p-value of 0, R^2 of 9.9% (Table 40). The latter data suggest that waves play a prominent role in erosion, but do not explain their relationship with the historical linear regression rate.

Analyses of single attributes at the NE Site. The NE study sites features a different set of attributes that were significant. Within the wetlands variable, the “open water” attribute explains most variance for this study site ($p = 0$, $R^2 = 32.3\%$, quadratic regression) **(**Table 41). This attribute accounts for ~86% of the wetlands variable at this study site (Table 30). Wetlands “open water” is defined as a generic map unit for any permanent, open body of water (pond, lake, reservoir, etc.) that does not support rooted plants (USDA, 2007a). Most of the transects that intersect “open water” range from 80% to none at all. The bulk of the transects appear to have a shoreline change margin of 0 ± 0.5 m/yr. However, as the percentage of “open water” increases on the transects, erosion increases as well. By 80% on the transect, the rate of change is between -1 m/yr and -1.5 m/yr.

The next highest attribute is "water," within the soil variable ($p = 0$, $R^2 = 26.8\%$, quadratic regression) (Table 41). "Water" within the soil category includes fresh water, saline, and/or ocean. Most of this soil "water" includes a few of the coastal ponds, such as Crystal Lake, Oak Bluffs Harbor, Farm Pond, Sengekontacket Pond, and Trapps Pond.

Wind speeds and wave directions, for both summer and winter, were insignificant because p-values were greater than 0.5 and the R^2 values were close to zero (Table 41). The wind and wave results are not surprising because this data was derived from a buoy southwest of Aquinnah, which is on the opposite side of the island. No buoy data was available for the waters off the northeast coast of Martha's Vineyard.

Interpreting these results suggests that the "water" categories within the wetlands and soil variables were once land based, but have since been inundated by water.

Examining the mean of the NE site transects that had more than 25% of an attribute suggested that transects facing E and ESE experienced erosion, as well land that is not classified in the erodible land variable (NA), and within the land use variable "beach" transects (Table 44). This simple method picked up the attribute soil "water," but no wetland "open water." The erosion mean for the transects that encompassed wetland "open water" was ~72%, but slightly more than 28% of the transects fell within the equilibrium rank.

Drawing any conclusions from these univariate analyses would be difficult, if not impossible, even though sixty attributes were evaluated.

Analyses of single attributes at the NW Site. Unlike the SS and NE study sites, the NW site had several attributes of significance. Two attributes were related to geology and surficial geology. The first was “beach deposits” within the geology variable ($p = 0$, $R^2 = 42.1\%$ quadratic) and the other was “sand and gravel deposits” ($p = 0$, $R^2 = 25.6$ linear) within the surficial geology variable (Table 42). Geology “beach deposits” are primarily located southwest of Menemsha Harbor, near Menemsha Bight/Lobsterville Beach and in small pockets near Cape Higgon, Cedar Tree Neck, and Lambert Cove. Results indicate that there was a wide variability of ranges with transects that had 100% “beach deposits,” ranging from accretion ~0.8 m/yr to -0.5 m/yr. Most of the transects either had this attribute or they didn’t have it, with very few in between.

The surficial geology attribute of “sand deposits” is on the coastal side of Menemsha Bight, similar to geology “beach deposits, but “sand and gravel deposits” on the northwestern coast of this study site overlay the “Martha’s Vineyard moraine.” This attribute is similar to geology’s “beach deposit” in that most of the transects either had this attribute or they didn’t, with very few in between. The values ranged from ~0.8 m/yr to -0.5 m/yr.

There were two attributes within the soil variable that were significant, the first was “Udipsamments” ($p = 0$, $R^2 = 65.7\%$) (Table 42), as the percentage of this soil increases on the transects, there is more accretion. Within the study site, Udipsamments are primarily located on the sand dunes at the entrance to Menemsha Harbor and to the southwest side of Menemsha Pond, along Lobsterville Beach. Only 7% of the soils within the NW site are classified as such, when “water” was removed from the variable (Table 25). Typically there is little vegetation on these dunes, or if there is some, there is beachgrass, poison ivy, beach plum, and bayberry that are fragile and can be easily destroyed (Turenne, 2007). Linear regression results show accretion for Udipsamments at the rate of 0.7 m/yr (2 ft/yr). There are a few isolated locations on the northwest side of this study site with Udipsamments' soil that indicated erosion (Figure 77).

A significant portion of the "water" attribute ($p = 0$, $R^2 = 68.4\%$, cubic regression) Table 14, Table 42**)** for soils is located along the northeast coast of this site and adjacent to Menemsha Pond. The fitted line plot shows that as the percentage of "water" increases on the transect, more erosion occurs. Half of the soil at this site was Eastchop and only minor results were found ($p = 0$, $R^2 = 13$, cubic regression).

There were two attributes within the variable slope "no slope" ($p = 0$, $R^2 = 53.8\%$, cubic regression) and "8-15% slope" ($p = 0$, $R^2 = 59.9\%$ quadratic regression) (Table 14). Areas with "no slope" are classified by MassGIS as water or urban land (MassGIS, 2008). This attribute is located along the shoreline of Menemsha Pond, south of Cape Higgon, and south of Cedar Tree Neck. As the percentage of "no slope" increases on the transects, the rate of shoreline erosion increases. The slope along the Lobsterville Beach shoreline is classified as "8-15%" with the remaining attribute scattered throughout the rest of the study site. Quadratic regression suggest that as the percentage of "8-15%" slope increase on the transects, the rate of shoreline accretion increases.

Two attributes within the highly erodible land variable had significant results, "Highly erodible land" ($p = 0$, $R^2 = 52.4\%$, cubic), and "HEL NA" ($p = 0$, $R^2 = 53.8\%$, cubic) (Table 14, Table 42). "Highly erodible land" results indicated that as the percentage of this attribute increased on the transect, accretion occurred after the attribute increased to ~40% on the transect. Slightly more than 55% of this attribute comprises the erodible land variable. The attribute “NA” for erodible land was not classified by the USDA as having any erodible properties; therefore, I labeled it as such. As this non-classified attribute increased on the transects, more erosion occurred.

Three attributes within the wetlands variable were significant: “barrier beach” ($p = 0$, $R^2 = 43.0\%$, cubic regression), “coastal beach” ($p = 0$, $R^2 = 39.3\%$ cubic), and “open water” ($p = 0$, $R^2 = 53.1$ cubic regression) (Table 14, Table 42). When “barrier beach” occupied between 20-40% of the transect, accretion occurred, from 0.1 m/yr to 0.8 m/yr. As the amount of this attribute increased on the transect, more erosion occurred around the 80% mark, ~ -0.2 m/yr, and increasing to 0.2 m/yr as the percentage on the transect reached 100%. While a cubic regression model fit the data on “coastal beach” the best, most of the transects had values between -0.1 m/yr and -0.3 m/yr. Transects that only had 20% of “coastal beach” showed more erosion than all the others. As “open water” increased on the transect, they indicated more erosion. The range within this attribute was from -0.1 m/yr to -0.8 m/yr. The “open water” attribute comprise 79% of the variable, wetland.

The “upland” attribute with land use was significant ($p = 0$, $R^2 = 22.9\%$, quadratic regression) (Table 14, Table 42). “Upland” contains other attributes that were combined to simplify the analysis, and these are pasture, forest, open land, participation recreation, residential > ½ acre lots, and urban open land. Whether the transects had no “upland” or 100% “upland” the values were similar, between no shoreline change at all, to -0.7 m/yr. The variation occurs when the percentage of the transects range from 20% to 60% which suggests accretion at the transects, and on some as much as 0.8 m/yr. Approximately 98% of this attribute accounts for land use on the NW study site.

Transect compass direction for the "NNE" was significant on the NW side ($p = 0$, $R^2 = 21.8\%$), resulting in accretion with a linear regression rate of 0.38 m/yr (Table 14). There were 56 of these transects, accounting for 12% of all the transects at the NW site. Transects with this compass direction ranged in values from 0.8 m/yr to -0.1 m/yr. WNW compass directions account for 31% of the direction on this side ($p = 0$, $R^2 = 8.9$).

"Wind speed by the percentage of direction" for both summer and winter had significant p-values but very low R^2 values ($p = 0$, $R^2 = 5.6\%$) (Table 14, Table 42). "Winter wave" and "summer wave" had low p-values as well as low R^2 values ($p = 0$, $R^2 = 4.9$, $p = 0$, $R^2 = 5.4\%$, respectively). All of these climate attributes resulted in accretion along the NW study site; the most significant was "winter wave by percent of direction" of 3.6 m/yr and "winter wind speed by percent of direction" at 1.18 m/yr.

Interpretations based on all these univariate statistics suggest that the attributes that contained water (soil, slope, wetlands) eroded more as the percentage of each attribute increased on the transect. This implies that the land has eroded and is now in the water. Accretion occurred when the transects faced NNE, there was Udipsamments, and as the slope increased to 8-15%. Geology "beach deposits" and surficial geology "sand and gravel deposits" fluctuated between the shoreline eroding or accreting, appearing unstable. In the wetlands variable, as the percentage of "barrier beach" increased on the transect, more erosion occurred.

Examining the transects that had more than 25% of an attribute, the only attribute that only showed erosion was compass direction NW (Table 45). Attributes that only indicated equilibrium were wetland "coastal beach" and compass direction WNW. There were four attributes that experienced accretion and they are wetland "barrier beach dune," compass direction N, soil “Udipsamments,” and slope “8-15%.” This method picked up soil “Udipsamments” and slope “8-15%” as well as the regression analysis, but all the other attributes experienced a mix of shoreline change rates.

Single variable summary. In an attempt to pick the “best” model to explain shoreline erosion on MV, I used the Akaike Information Criterion (AIC) based on individual variables and attributes; results indicated that the variables “Soil” and “Wetland” were ranked in the top 3 for all study sites. However, according to the Akaike weights (Appendix A - Appendix 7), “Erodible Land” on the SS had a 56% probability of being the correct model, while “Soil” had a 44% probability, and “Wetland” had less than 1.85E-25 of being correct. As an attribute, “Erodible” had a 100% probability of being the correct model based on quadratic regression results Appendix 10).

On the NE study site, the variable “Wetland” had a 100% probability of being the correct model (Appendix A - Appendix 8) and “Wetland Open Water” had a 100% probability as well, based on quadratic regression results Appendix 11). The NW study site AIC results indicated that the variable “Soil” had a 100% probability of being the correct model (Appendix A - Appendix 9) and that the attribute “Soil Water” had a 100% probability (Appendix A - Appendix 13).

Another pattern that emerged for all three sites was that winter wind and waves, compass direction, and the average percentage of sand for each transect consistently scored near the bottom of the top ten variables.

An argument could be made that sandy shores indeed played a significant factor in shoreline change on the SS and NW study sites. Regression analyses indicated that the SS site had soil “beaches” and “erodible land” that equally displayed similar erosion factors as the sea level rose, albeit erosion rates decreased slightly as the percentage increased. On the NW study site, both of the attributes within the variable geology and surficial geology are sandy. Udipsamments are sandy, found on sand dunes, and wetlands "barrier beach" is considered sandy. In spite of this, Bruun's rule still didn't work for either of the two "sandy" sides. The most unusual result, for all the sites, was the lack of significance from wind, waves, and compass direction as an outcome of linear regression analysis. One possibility is that these variables may inherently be factored into the existing erosion results for each of the attributes, as is the rise in sea level; therefore, they were eliminated from the final analysis.

Collectively, the univariate analyses and AIC revealed no clear, significant patterns for coastal erosion, accretion, or even stability for all three study sites. Ruling out winter winds and waves, compass direction, and the percentage of sand within the sites was informational; it did not reveal what was significant.

Multiple factors vs. erosion: the application of PCA. PCA methods have occasionally been used in coastal erosion research. For example, an in-depth study of multiple variables by Phillips (1986) took into account fetch, orientation, tidal range, depth contours, elevation above mean low water and high water, shoreline width, sandy deposits, peat outcrops, vegetation, slope, and grain size. By using a spatial analytic approach to geomorphological problems, alongshore patterns of shoreline erosion in Delaware Bay were revealed. The results of this study indicated that major factors affecting shoreline erosion are erosive energy through planform morphology and resistance. These factors were determined by the relative amounts of each type of sediment, their juxtaposition, and the vertical shoreline morphology.

The PCA studies of Fenster *et al*. (1993) suggested that vegetation patterns were the primary factor influencing long-term shoreline erosion rates on Assateague Island National Seashore, in Maryland. Roman and Nordstrom (1988), using the same model system, developed the concept of critical erosion rates to model vegetation dynamics on sediment-starved barrier islands, also using PCA. In 1984, Fisher *et al*. (1984) used PCA to partition the topographic variance of beach profiles into a few major definable and uncorrelated modes of variation of the Outer Banks in North Carolina. The effect of topographic organization of the shore zone and dune stabilization was analyzed for two beach profile data sets. Dune stabilization caused the narrowing of the active beach width and steepening of the beach profile over a period of 40 years, while the eigenvectors remained essentially intact (Fisher *et al.*, 1984).

Kunte and Wagle (1994) used PCA to compare erosion patterns of sandy tracts and rocky cliffs and promontories in Goa, India. Coastlines in South China were analyzed with PCA as part of an investigation of 34 typical arc-shaped coastline configurations and their geomorphic development. Wave power and size of the opening of the bays were decisive factors in those shoreline changes (Zhijun & Chunchu, 2004). Miller and Dean (2007a; 2007b) used PCA analysis to identify and characterize the shoreline variability at three sites, one of which (Duck, North Carolina) is compatible with the geomorphology of Martha's Vineyard. Their results suggest that, in some cases, structures that are perpendicular to the shore have a significant impact on the adjacent shoreline, and that seasonal variations in the local wave climate do not play the primary role in controlling shoreline morphology.

While the three study sites on Martha's Vineyard were picked for their unique geomorphology, the environmental conditions to which they are exposed are quite similar. This thesis could have focused on just the south side of the Vineyard, or just the entrance to Edgartown Harbor, as examples. What would have been reported for the south side would imply that the whole island of MV would vanish in no time. Or, if just the northeastern side of the island was studied, one could argue that the Vineyard is quite stable and even accreting in some locations. By focusing on a narrow window, the "big picture" is often overlooked. One of the goals of this thesis was to examine coastal erosion on Martha's Vineyard, not by one, two, or three variables/attributes, but to use as many variables as realistically possible. By looking at the Vineyard as a system, I uncovered variables that did not appear to be significant at all through univariate statistics.

As noted in Chapter 4, the NE and NW correlation matrix data are derived from calculations in which there are no differences in the values of many of the data layers, a result suggesting that further analysis of the data layers is warranted. However, the analysis for the SS study site had enough variation between the data layers to suggest that the PCA and communality results adequately portray the south side of Martha's Vineyard.

Unlike previously published coastal PCA studies, the SS study site analysis revealed that the geologic foundation shared 61.28% of the variance and surficial geology shared 38.09% (Table 54). The slope of the low lying outwash plains shared 46.40% of the variance and wetlands accounted for 39.48%. Seventy-nine percent of the wetland variable on the SS site consisted of the attribute "Open Water," and was mostly related to the retreating shorelines. The SS site PCA results are thus consistent with the geomorphology of the Vineyard.

Risk assessment: the identification of specific MV areas that may be particularly vulnerable to coastal erosion in the next 100 years. Martha's Vineyard has a yearly population of slightly more than 15,000 (U.S. Census Bureau, 2008), but hosts over 75,000 tourists during the summer months, and at least 25,000, daily visitors (MVC, 2004, 2006). With visitors and second-home owners comprising "the driving force of the island's economic base" (MVC, 2006), long term coastal planning is critical to the social stability of the island. While not the focus of this thesis, it was a driving factor behind studying coastal erosion patterns on the island. At some future point in the history of Martha's Vineyard, most of the island, if not all, will succumb to the forces of the ocean. However, before that time, an understanding of erosion and accretion propensities could have a practical outcome, namely insights as to which regions of MV might be at risk within the next 100 yrs.

Accordingly, a risk assessment was derived from the calculated mean for each raster, this analysis showed that the south side of Martha's Vineyard was at a high risk for significant future erosion. Within the SS study site, the areas at the highest risk of erosion are predominantly located immediately adjacent to the coastline, including areas identified as coastal ponds (Figure 121). While it may be premature to base public policy on these results, independent validation of this result could serve as an impetus for reevaluation of MV's public planning with respect to the location of homes, wells, and key components of the island's infrastructure. Ultimately, a coastal island may never reach a sustainable level in perpetuity because of all the natural and manmade forces acting upon it. The best that can be hoped for is that, with long-term planning, the inhabitants of Martha's Vineyard will safely retreat from the island, rather than attempt to guard themselves against the forces of the ocean.

Technical difficulties. There were a few technical difficulties that surfaced in the analyses of all the study sites in this investigation. One problem concerned transects that were mostly in the water, e.g., those shown in Figure 122. Since these transects were analyzed with respect to their geophysical composition, "water" was the primary attribute for many of the variables. In a future study, new transects should be cast to include more land area within a study site. While the current data was excellent for studying shorelines and the rate of erosion, the "land" properties may not have been accurately described.

A second problem pertained to lack of appropriate wind and wave data that directly influenced the shorelines of the NE and NW study sites because buoy data was not available for these locations (Figure 30). Because of this, the NE study site results may not accurately reflect the influence of wind and waves on the shoreline.

Finally, as mentioned several times in this thesis, the PCA results for the NE and NW study sites (Table 51 and Table 52) were derived from calculations in which there were no differences in the values between the raster data layers. This may have distorted the results because of a lack of variance between the many data layers. Using raw data, rather than normalized data, may alter the final results, an approach that should be considered in a subsequent study.

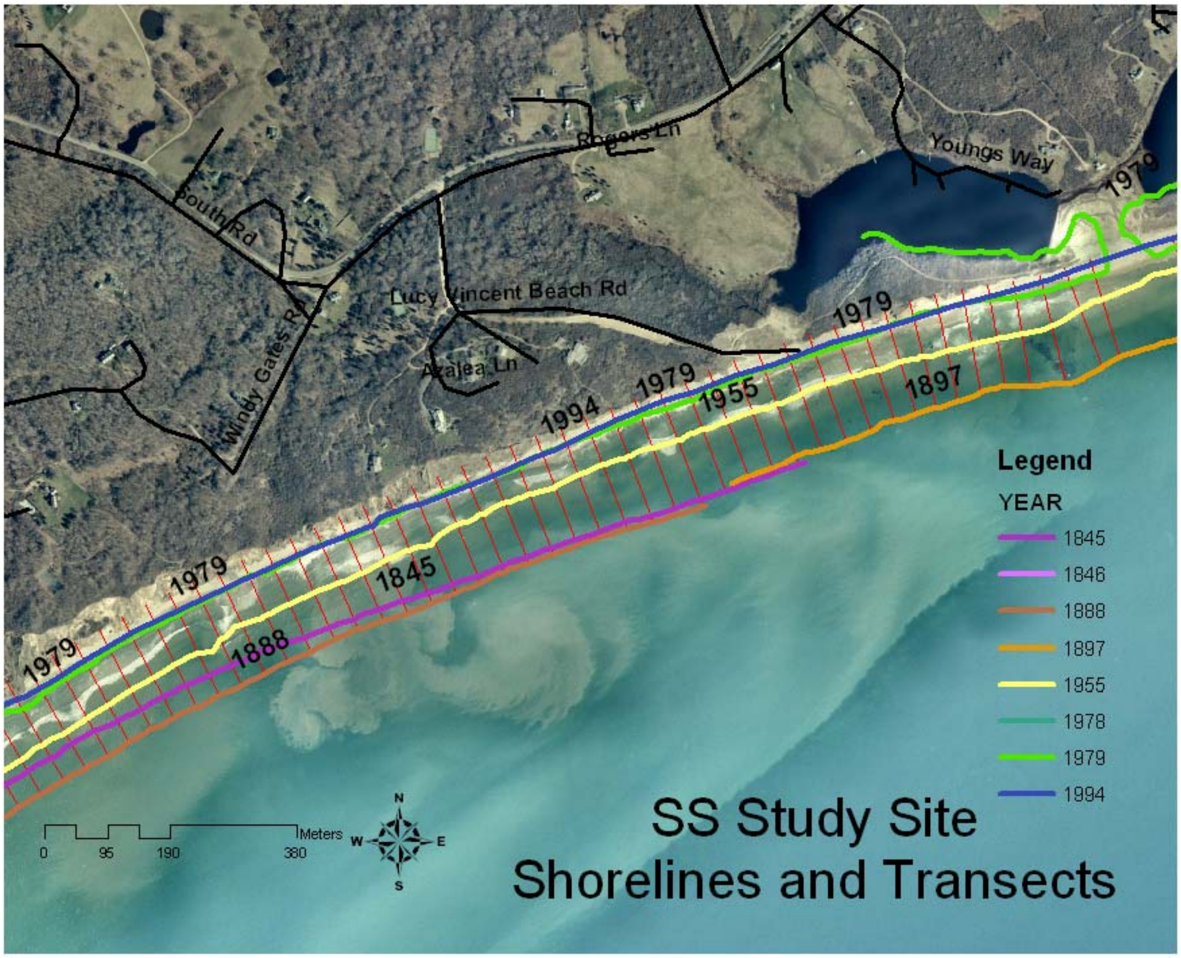

Figure 122. Example of technical difficulties with transects in the water.

Conclusions and perspectives. To understand the fundamental processes driving coastal erosion on the paraglacial island of Martha's Vineyard, mathematical models and spatial data analysis were employed to discover the underlying processes driving the evolution of a natural system. This was a multistep process, based on historical shoreline data that spanned 149 years, sea level data from Woods Hole and Nantucket that respectively covered 71 and 38 years, and wind and wave conditions consolidated from 19 years of historical data from a buoy off the southwestern coast of the Vineyard. Data on shoreline erosion from almost 1500 transects were assessed with respect to geology, surficial geology, wetland, land use, soils, percent of sand, slope, erodible land, wind, waves, and compass direction. The culmination of these analyses led me to five key conclusions, namely that: 1) the three sites manifested different rates of erosion and accretion, from a loss of approximately 0.1 m/yr at the NE and NW sites to over 1.7 m/yr at the SS site; 2) the NE and NW sites fit the ratio predicted by Bruun for the rate of erosion vs. SLR, but the SS site exceeded that ratio more than fivefold; 3) the shoreline erosion patterns for all three sites are dominated by short-range effects, not long-range stable effects; 4) geological components play key roles in erosion on MV, a possibility consistent with the island's paraglacial nature; and 5) the south side of MV is the segment of the coastline that is particularly vulnerable to significant erosion over the next 100 years.

These conclusions were not evident from simple statistical analyses. Rather, they emerged from more complex analyses, including fractal dimension analysis, multivariate statistics, and spatial data analysis. The complexity of the analysis undoubtedly was a function of the complexity of the problem. As noted by Carter and Woodroffe (1997), multiple factors besides sea level positions contribute to the progressive change in coastal landscapes and all of these factors need to be considered when studying the coastal environment because they work together as a system. To limit analyses to only one or two variables may not fully unravel the interactions between all of them.

This study was initiated with a set of specific hypotheses addressing MV erosion from the perspective of Bruun's Rule (Bruun, 1962). More specifically, I postulated that the south side of Martha's Vineyard, being typical of many of the sandy east coast barrier beaches that have been studied in the past, would erode at 50-100 times the rate of sea level rise. The corresponding null hypothesis, that the south side would not erode at the same ratio as the Bruun Rule, was borne out. Likewise, I postulated that erosion on the northeast side of Martha's Vineyard would also follow a rate 50-100 times the rate of sea level rise, but that it would erode at a faster rate than the south side and the northwest side because it is exposed to Northeasters and has substantial coastal armoring and jetties that should exacerbate erosion. The null hypothesis was that the NE site would not experience a faster rate of erosion than the Bruun Rule, but would experience significant erosion due to the effects of Northeasters. Again, the null hypothesis was favored, although the NE site's erosion was limited to specific sub-sites. Finally, I postulated that the northwest side of Martha's Vineyard would also erode at 50-100 times the rate of sea level rise, and that its comparative protection from storms relative to the south and northeast sides would render it less susceptible to erosion. Here, too, the null hypothesis, that the NW side should be relatively stable, maintaining an equilibrium, was also borne out.

A sediment budget, or transport analysis, was not included in this thesis, but it is a variable worth considering in a future study because it may be a contributing factor to the high erosion rates along the south coast of the Vineyard. River inputs of sediment are virtually non-existent on Martha's Vineyard, thereby increasing the importance of sea level rise to release additional sediments further inland. In theory, when these sediments slide into the sea, an equilibrium profile should be re-established. Longshore sediment movement to the vicinity of Martha's Vineyard originates from the coastal waters of Connecticut and Rhode Island and moves northeast, splitting its path when it reaches the waters near Aquinnah. The shorelines of the SS site are fed with this sediment while some of it continues to move northeasterly (van Gaalen, 2004). How much of this sediment feeds the south coast is unclear, but the main source of surficial sediments in this area are primarily derived from the reworking of Holocene glacial debris (Poag, 1978; Townsend *et al.*, 2004). Ballantyne (2002b) suggests that, on paraglacial coasts, where the main source of sediment is composed of reworked in situ glacigenic deposits, additional sediment supplies may be prolonged by rising sea levels.

The swash zone for coastal Martha's Vineyard may be another important variable that needs to be considered in the future because the effects of infiltration and exfiltration are generally used to explain why beaches with a low water table tend to accrete and beaches with a high water table tend to erode (Horn, 2006). Finally, storm predictions indicate that the number of storms will increase by 5% and that storm tracks will be nearer to the coastal areas of the North Atlantic and will propagate approximately 10% faster (Perrie *et al.*, 2006). Although wind and wave analyses indicated that these components were not significant factors in shoreline change at any of the study sites, this may change as the number and intensity of storms increases over the next 100 years, bringing with them their strong coastal impacts (DGS, 1998; MA CZM, 2002; USGS, 2005; Zhang *et al.*, 2000).

APPENDIX A: SUPPLEMENTAL FIGURES AND TABLES

Appendix Page

1. Wind data from WIS Station #74, 1980-1999. Wind direction and wind speed (m/sec) by month. (derived from USACE, 2008). 357

2. Wind speed (m/sec) chart by percent of occurrence by month from 1980-1999 (derived from USACE, 2008). 358

3. Wave data from WIS Station #74, 1980-1999. Wave direction by percent of time (derived from USACE, 2008). 359

4. Wave Rose from WIS Station #74, 1980-1999, from http://frf.usace.army.mil/cgi-bin/wis/atl/atl_main.html. 360

5. Geology, Surficial Geology, Soil, and Slope - Reclassification/Risk Assessment Index of Attributes, based on linear regression rates for each attribute derived from the percentage of the attribute on the transects. 361

6. Erodible Land, Wetlands, Land Use and Compass Direction – Reclassification/ Risk Assessment Index of Attributes , based on linear regression rates for each attribute derived from the percentage of the attribute on the transects. 362

7. AIC results for the SS study site based on the variables (values derived from multiple linear regression). 363

8. AIC results for the NE study site based on the variables (values derived from multiple linear regression). 364

9. AIC results for the NW study site based on the variables (values derived from multiple linear regression). 365

10. AIC results for the SS study site based on the attributes that had more than 25% of the attribute within the transects (x, x^2 = quadratic regression, x,x^2, x^3 = cubic linear regression). 366

11. AIC results for the NE (part 1) study site based on the attributes that had more than 25% of the attribute within the transects (x, x^2 = quadratic regression, x,x^2, x^3 = cubic linear regression). 367

12. AIC results for the NE (part 2) study site based on the attributes that had more than 25% of the attribute within the transects (x, x^2 = quadratic regression, x,x^2, x^3 = cubic linear regression). 368

13. AIC results for the NW (part 1) study site based on the attributes that had more than 25% of the attribute within the transects (x, x^2 = quadratic regression, x,x^2, x^3 = cubic linear regression). 369

14. AIC results for the NW (part 2) study site based on the attributes that had more than 25% of the attribute within the transects (x, x^2 = quadratic regression, x,x^2, x^3 = cubic linear regression). 370

15. Aerial photo of the coastal ponds along the SS study site, photo provided by marthasvineyardhill.com. 371

16. Norton Point Breach, April 2007. (A) The falling tide flows through the breach of out Katama Bay. (B) An aerial view looking east toward Wasque Point. Photos provided by Ralph Stewart, The Martha's Vineyard Times, 2008. 371

1980-1999 ATL WIS STATION: 74 LAT: 41.25 N, LON: -71.00 W, WIND AND WAVE PERCENT OCCURRENCES OF MEAN DIRECTION BY MONTH (USACE, 2008)

WIND DIRECTION	JAN	FEB	MAR	APR	MAY	JUN	JUL	AUG	SEP	OCT	NOV	DEC	CASES	PCT
N	0.61	0.68	0.71	0.58	0.45	0.35	0.3	0.51	0.56	0.63	0.62	0.6	11568	6.60%
NNE	0.41	0.43	0.43	0.37	0.42	0.28	0.18	0.37	0.39	0.53	0.32	0.42	7971	4.55%
NE	0.37	0.39	0.39	0.44	0.56	0.32	0.23	0.43	0.52	0.48	0.38	0.33	8490	4.84%
ENE	0.24	0.2	0.35	0.28	0.38	0.23	0.24	0.32	0.43	0.23	0.23	0.23	5862	3.34%
E	0.24	0.25	0.29	0.37	0.41	0.31	0.27	0.33	0.46	0.33	0.21	0.24	6504	3.71%
ESE	0.17	0.21	0.19	0.37	0.34	0.28	0.26	0.29	0.31	0.23	0.22	0.17	5296	3.02%
SE	0.22	0.25	0.28	0.36	0.47	0.35	0.33	0.42	0.3	0.38	0.31	0.2	6768	3.86%
SSE	0.22	0.17	0.33	0.35	0.45	0.39	0.44	0.38	0.33	0.3	0.28	0.19	6694	3.82%
S	0.34	0.23	0.43	0.62	0.68	0.74	0.95	0.77	0.61	0.6	0.42	0.32	11775	6.72%
SSW	0.4	0.36	0.52	0.67	0.76	0.97	1.11	0.95	0.78	0.56	0.44	0.37	13830	7.89%
SW	0.55	0.59	0.61	0.65	0.85	1.25	1.44	1.29	0.96	0.81	0.72	0.67	18207	**10.39%**
WSW	0.46	0.42	0.44	0.52	0.58	0.71	0.8	0.68	0.52	0.56	0.66	0.62	12197	6.96%
W	1.05	0.75	0.75	0.73	0.72	0.7	0.71	0.52	0.47	0.77	0.88	1	15873	9.06%
WNW	1.18	0.83	0.92	0.68	0.53	0.51	0.5	0.46	0.42	0.73	0.92	1.12	15436	8.81%
NW	1.28	1.17	1.1	0.75	0.54	0.5	0.48	0.45	0.66	0.84	1.03	1.25	17606	**10.04%**
NNW	0.74	0.79	0.75	0.48	0.36	0.33	0.27	0.32	0.5	0.53	0.56	0.75	11217	6.40%
TOTALS													175294	100.00%

WSP (m/sec)	JAN	FEB	MAR	APR	MAY	JUN	JUL	AUG	SEP	OCT	NOV	DEC	CASES	PCT
0 - 1.99	0.05	0.06	0.18	0.43	0.94	0.81	0.87	0.71	0.41	0.17	0.06	0.02	8270	4.72%
2 - 3.99	0.48	0.62	1.04	1.59	2.24	2.54	3	2.73	1.82	1.18	0.53	0.53	32068	18.29%
4 - 5.99	1.18	1.21	1.57	1.95	2.42	2.58	2.9	2.69	2.38	2.07	1.36	1.24	41240	23.53%
6 - 7.99	1.69	1.56	1.78	1.82	1.59	1.47	1.25	1.56	1.97	1.99	1.73	1.68	35202	20.08%
8 - 9.99	1.69	1.57	1.49	1.25	0.81	0.58	0.36	0.58	1.01	1.63	1.87	1.74	25571	14.59%
10 - 11.99	1.47	1.25	1.24	0.67	0.34	0.21	0.09	0.17	0.42	0.82	1.25	1.51	16556	9.44%
12 13.99	0.97	0.79	0.7	0.35	0.15	0.03	0.01	0.04	0.15	0.38	0.79	0.92	9231	5.27%
14 - 15.99	0.65	0.45	0.26	0.09	0	0	0.01	0	0.03	0.15	0.41	0.43	4341	2.48%
16 - 17.99	0.21	0.17	0.17	0.04	0	0	0	0	0.02	0.07	0.17	0.24	1907	1.09%
18 - 19.99	0.06	0.05	0.06	0.02	0	0	0	0	0.01	0.01	0.04	0.11	641	0.37%
20 GREATER	0.02	0.02	0.01	0.01	0	0	0	0	0	0.01	0.02	0.06	267	0.15%
TOTALS													175294	100.00%

Appendix 1. Wind data from WIS Station #74, 1980-1999. Wind direction and wind speed (m/sec) by month. (derived from USACE, 2008).

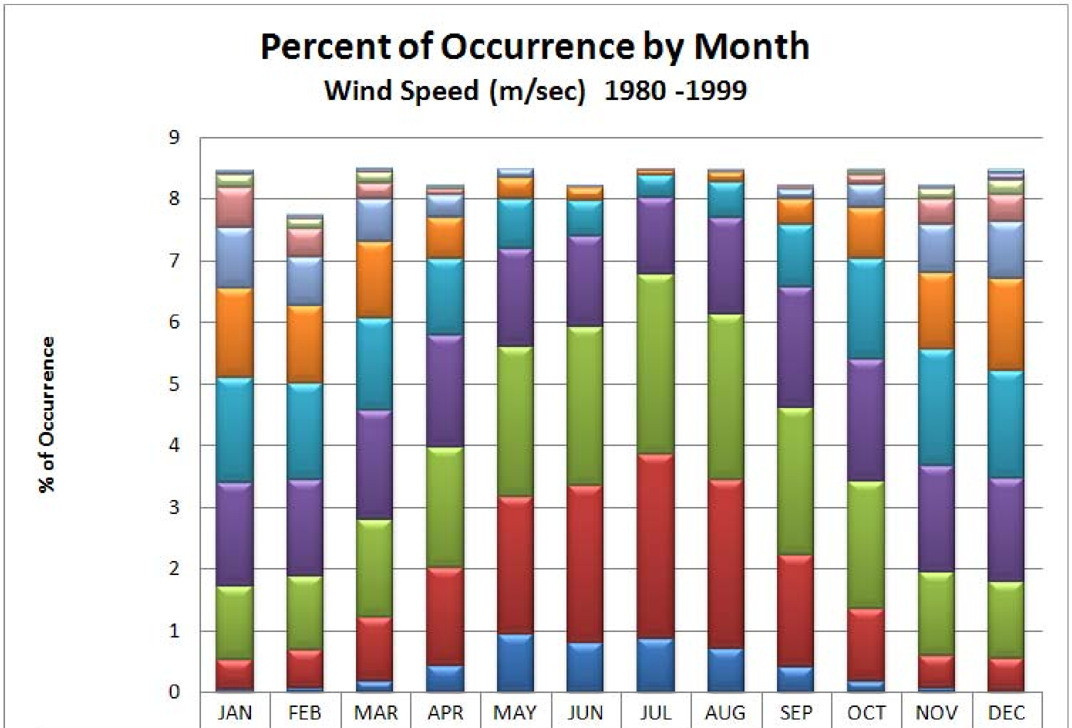

	JAN	FEB	MAR	APR	MAY	JUN	JUL	AUG	SEP	OCT	NOV	DEC
20 - GREATER	0.02	0.02	0.01	0.01	0	0	0	0	0	0.01	0.02	0.06
18 - 19.99	0.06	0.05	0.06	0.02	0	0	0	0	0.01	0.01	0.04	0.11
16 - 17.99	0.21	0.17	0.17	0.04	0	0	0	0	0.02	0.07	0.17	0.24
14 - 15.99	0.65	0.45	0.26	0.09	0	0	0.01	0	0.03	0.15	0.41	0.43
12 - 13.99	0.97	0.79	0.7	0.35	0.15	0.03	0.01	0.04	0.15	0.38	0.79	0.92
10 - 11.99	1.47	1.25	1.24	0.67	0.34	0.21	0.09	0.17	0.42	0.82	1.25	1.51
8 - 9.99	1.69	1.57	1.49	1.25	0.81	0.58	0.36	0.58	1.01	1.63	1.87	1.74
6 - 7.99	1.69	1.56	1.78	1.82	1.59	1.47	1.25	1.56	1.97	1.99	1.73	1.68
4 - 5.99	1.18	1.21	1.57	1.95	2.42	2.58	2.9	2.69	2.38	2.07	1.36	1.24
2 - 3.99	0.48	0.62	1.04	1.59	2.24	2.54	3	2.73	1.82	1.18	0.53	0.53
0 - 1.99	0.05	0.06	0.18	0.43	0.94	0.81	0.87	0.71	0.41	0.17	0.06	0.02

Appendix 2. Wind speed (m/sec) chart by percent of occurrence by month from 1980-1999 (derived from USACE, 2008).

WAVE DIRECTION	JAN	FEB	MAR	APR	MAY	JUN	JUL	AUG	SEP	OCT	NOV	DEC	CASES	PCT
N	0.27	0.24	0.22	0.19	0.12	0.06	0.01	0.05	0.15	0.33	0.25	0.23	3694	2.11%
NNE	0.18	0.17	0.18	0.12	0.13	0.07	0.01	0.04	0.11	0.3	0.15	0.22	2959	1.69%
NE	0.15	0.14	0.13	0.13	0.14	0.07	0.01	0.04	0.12	0.21	0.14	0.16	2550	1.45%
ENE	0.15	0.18	0.14	0.12	0.16	0.07	0.01	0.09	0.19	0.21	0.19	0.14	2911	1.66%
E	0.26	0.23	0.32	0.22	0.25	0.15	0.05	0.18	0.34	0.29	0.23	0.23	4836	2.76%
ESE	0.31	0.32	0.33	0.38	0.59	0.3	0.13	0.37	0.55	0.47	0.33	0.28	7656	4.37%
SE	0.28	0.33	0.43	0.51	0.71	0.6	0.34	0.85	0.78	0.6	0.37	0.27	10651	6.08%
SSE	0.32	0.31	0.52	0.58	0.88	0.55	0.56	0.95	1.02	0.65	0.38	0.28	12293	7.01%
S	0.64	0.65	1	1.33	1.51	1.76	2.14	2.13	1.33	0.88	0.68	0.5	25514	14.55%
SSW	1.14	1.02	1.52	2.1	2.52	3.09	3.95	2.44	1.59	1.06	0.99	0.93	39217	22.37%
SW	1.01	0.87	0.96	0.84	0.58	0.8	0.77	0.68	0.78	1.01	1.06	1.14	18394	10.49%
WSW	1.27	0.83	0.79	0.63	0.32	0.32	0.21	0.21	0.38	0.68	1.12	1.33	14174	8.09%
W	1.12	0.91	0.8	0.45	0.28	0.21	0.13	0.18	0.29	0.77	0.96	1.27	12913	7.37%
WNW	0.68	0.66	0.48	0.26	0.12	0.08	0.1	0.09	0.24	0.46	0.64	0.68	7880	4.50%
NW	0.38	0.46	0.38	0.18	0.07	0.06	0.06	0.11	0.2	0.33	0.42	0.48	5446	3.11%
NNW	0.31	0.38	0.29	0.17	0.1	0.05	0.02	0.08	0.15	0.25	0.29	0.34	4206	2.40%
TOTALS													**175294**	**100.00%**

Appendix 3. Wave data from WIS Station #74, 1980-1999. Wave direction by percent of time (derived from USACE, 2008).

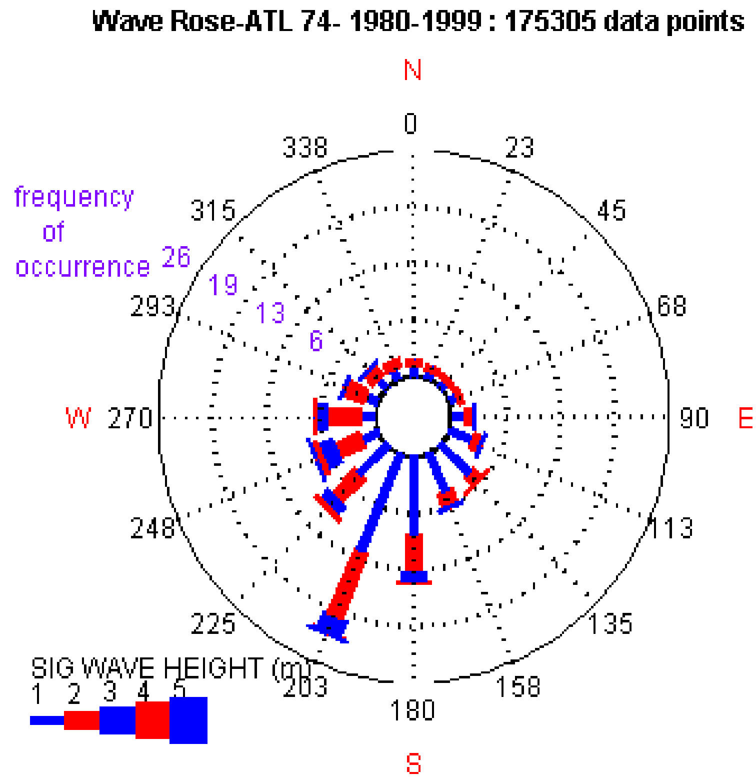

Appendix 4. Wave Rose from WIS Station #74, 1980-1999, from http://frf.usace.army.mil/cgi-bin/wis/atl/atl_main.html.

FEATURE/ATTRIBUTES	SS RISK	NE RISK	NW RISK
GEO BEACH DEPOSITS	3	3	3
GEO MORAINE DEPOSITS	1	-	3
GEO MORAINE OUTWASH	2	3	-
GEO POND	2	3	3
GEO MARSH	-	-	3
SG END MORAINE	2	3	3
SG SAND DEPOSITS	4	3	3
SG TILL / BEDROCK	-	3	-
BEACHES	5	3	3
BERRYLAND	2	4	-
CARVER	4	3	-
CHILMARK	2		-
EASTCHOP	2	3	3
KATAMA	5	-	-
KLEJ	4	-	-
NANTUCKET	1	-	3
PAWCATUCK AND MATUNUCK	5	3	-
POMPTON	2	-	-
RIVERHEAD	5	-	-
UDIPSAMMENTS	4	3	2
WATER	2	4	4
URBAN	-	3	
FREETOWN AND SWANSEA	-	-	4
RIDGEBURY	-	-	3
AVG % SAND	4	3	3
NO SLOPE	3	3	4
0-3% SLOPE	4	3	3
3-8% SLOPE	1	3	3
8-15% SLOPE	3	3	2
15-25% SLOPE	2	3	3
AVG SLOPE	3	3	3

Appendix 5. Geology, Surficial Geology, Soil, and Slope - Reclassification/Risk Assessment Index of Attributes, based on linear regression rates for each attribute derived from the percentage of the attribute on the transects.

FEATURE/ATTRIBUTES	SS RISK	NE RISK	NW RISK
POTENTIALLY HIGHLY ERODIBLE LAND	1	3	3
ERODIBLE	5	3	-
HIGHLY ERODIBLE LAND	4	3	2
HEL NA	2	3	4
WETLAND BARRIER BEACH	4	3	3
WETLAND BARRIER BEACH - DUNE	3	3	2
WETLAND COASTAL BLUFF	2	3	3
WETLAND COASTAL BEACH	2	3	3
WETLAND COASTAL DUNE	1	3	3
WETLAND ROCKY INTERTIDAL SHORE	2	3	3
WETLAND SALT MARSH	5	3	2
WETLAND TIDAL FLATS		5	-
WETLAND SHRUB SWAMP	1	4	-
WETLAND OPEN WATER	4	4	4
LUS BEACH	3	3	3
LUS UPLAND	4	3	3
LUS WATER	2	-	3
LUS CROPLAND	5	-	-
LUS MARSH	2	3	-
LUS DEVELOPED LAND	-	3	-
E	2	3	-
ESE	2	3	-
S	4	3	-
SE	2	3	-
SSE	3	3	-
N	-	3	3
ENE	-	3	3
NE	-	3	3
NNE	-	3	3
NNW	-	3	3
NW	-	3	3
SSW	-	3	-
SW	-	3	-
W	-	3	3
WNW	-	3	3
WSW	-	3	3

Appendix 6. Erodible Land, Wetlands, Land Use and Compass Direction – Reclassification/Risk Assessment Index of Attributes , based on linear regression rates for each attribute derived from the percentage of the attribute on the transects.

SS Model - Variables	p-value	R-sq (adj)	Number of Data Points	Number of Parameters Fitted	K	Regression Sum of Squares (SSE)	AIC	Rank	Delta	exp(-delta/2)	Akaike Weights
LR vs Erodible	0.0000	40.2	487	10	11	260.71	-282.31	1	0	1.00E+00	5.58E-01
LR vs Soil	0.0000	40.7	487	15	16	255.65	-281.85	2	0.47	7.91E-01	4.42E-01
LR vs Wetland	0.0000	24.6	487	10	11	328.61	-169.58	3	112.73	3.31E-25	1.85E-25
LR vs Slope	0.0000	21.1	487	9	10	344.22	-148.98	4	133.33	1.12E-29	6.23E-30
LR vs Geology	0.0000	18.8	487	5	6	357.38	-138.71	5	143.61	6.55E-32	3.65E-32
LR vs LUS	0.0000	13.3	487	8	9	379.15	-103.91	6	178.40	1.82E-39	1.02E-39
LR vs Surficial Geology	0.0000	10.6	487	2	3	395.96	-94.79	7	187.53	1.90E-41	1.06E-41
LR vs Compass Direction	0.0000	9.8	487	5	6	397.10	-87.39	8	194.93	4.70E-43	2.62E-43
LR vs Winter Wind and Waves	0.0000	8.9	487	2	3	403.35	-85.79	9	196.53	2.11E-43	1.18E-43
LR vs Avg % Sand	0.0000	6	487	4	5	414.45	-68.56	10	213.75	3.84E-47	2.14E-47
Weight Sum											**1.00**

Appendix 7. AIC results for the SS study site based on the variables (values derived from multiple linear regression).

NE Model - Variables	p-value	R-sq (adj)	Number of Data Points	Number of Parameters Fitted	K	SSE	AIC	Rank	Delta	exp(-delta/2)	Akaike Weights
LR vs Wetland	0.0000	47.60	487	23	24	34.73	-1237.99	1	0.00	1.00E+00	1.00E+00
LR vs Soil	0.0000	38.30	487	10	11	42.04	-1170.98	2	67.01	2.81E-15	2.81E-15
LR vs Land Use	0.0000	35.80	487	12	13	43.57	-1149.62	3	88.37	6.45E-20	6.45E-20
LR vs Geology	0.0000	28.00	487	10	11	49.07	-1095.70	4	142.29	1.27E-31	1.27E-31
LR vs Erodible	0.0000	20.30	487	8	9	54.51	-1048.45	5	189.54	6.95E-42	6.95E-42
LR vs Slope	0.0000	18.60	487	7	8	55.82	-1038.89	6	199.10	5.84E-44	5.84E-44
LR vs Surficial Geology	0.0000	15.60	487	7	8	57.90	-1021.08	7	216.91	7.91E-48	7.91E-48
LR vs Compass Direction	0.0000	7.30	487	16	17	62.39	-966.74	8	271.25	1.26E-59	1.26E-59
LR vs Avg % Sand	0.0000	3.10	487	4	5	66.83	-957.25	9	280.74	1.09E-61	1.09E-61
LR vs Winter Wind & Waves	0.3430	0.00	487	3	4	69.29	-941.62	10	296.37	4.41E-65	4.41E-65
Weight Sum											**1.00**

Appendix 8. AIC results for the NE study site based on the variables (values derived from multiple linear regression).

NW Model - Major Variables	p-value	R-sq (adj)	Number of Data Points	Number of Parameters Fitted	K	Regression Sum of Squares (SSE)	AIC	Rank	Delta	exp(-delta/2)	Akaike Weights
LR vs Soil	0.0000	79.3	487	14	15	6.43	-2077.44	1	0.00	1.00E+00	1.00E+00
LR vs Wetland	0.0000	77.9	487	17	18	6.85	-2040.90	2	36.54	1.16E-08	1.16E-08
LR vs Slope	0.0000	64.0	487	11	12	11.30	-1808.98	3	268.46	5.06E-59	5.06E-59
LR vs Erodible	0.0000	54.5	487	10	11	14.29	-1696.42	4	381.02	1.83E-83	1.83E-83
LR vs Geology	0.0000	46.0	487	8	9	17.01	-1615.67	5	461.77	5.34E-101	5.34E-101
LR vs Compass Direction	0.0000	35.7	487	9	10	20.21	-1529.68	6	547.77	1.13E-119	1.13E-119
LR vs Surficial Geology	0.0000	25.5	487	3	4	23.73	-1463.44	7	614.01	4.68E-134	4.68E-134
LR vs Land Use	0.0000	22.7	487	5	6	24.47	-1444.61	8	632.83	3.83E-138	3.83E-138
LR vs Avg % Sand	0.0000	6.8	487	4	5	29.61	-1353.63	9	723.82	6.69E-158	6.69E-158
LR vs Winter Wind & Waves	0.0000	5.6	487	2	3	30.11	-1349.57	10	727.87	8.81E-159	8.81E-159
Weight Sum											**1.00**

Appendix 9. AIC results for the NW study site based on the variables (values derived from multiple linear regression).

SS Attributes > 25% on transects	p-value	R sq (adj)	Number of Data Points	Number of Parameters Fitted	K	SSE	AIC	AIC Rank	Delta	exp(-delta/2)	Akaike Weights
Erodible (x, x2)	0	28.2	487	3	4	126.32	-649.18	1	0.00	1.00E+00	1.00E+00
Soil Water(x, x2)	0	16.4	487	3	4	369.40	-126.60	2	522.57	3.35E-114	3.35E-114
Geo Pond (x, x2)	0	13.9	487	3	4	380.59	-112.06	3	537.11	2.33E-117	2.33E-117
SG Sand and Gravel Deposits	0	10.6	487	2	3	395.96	-94.79	4	554.39	4.13E-121	4.13E-121
LUS Water	0	10.5	487	2	3	396.60	-94.00	5	555.18	2.79E-121	2.79E-121
LR vs Summer Wave % Direction	0	9.9	487	2	3	398.97	-91.10	6	558.08	6.54E-122	6.54E-122
LR vs Summer Wind and Wave	0	9.9	487	3	4	398.18	-90.06	7	559.12	3.88E-122	3.88E-122
LR vs Summer Windspeed & Direction	0	9.4	487	2	3	401.38	-88.17	8	561.01	1.51E-122	1.51E-122
South	0	9.2	487	2	3	402.09	-87.31	9	561.87	9.82E-123	9.82E-123
Avg % Sand (x, x2, x3)	0	9.1	487	4	5	399.22	-86.79	10	562.38	7.59E-123	7.59E-123
LR vs Winter Windspeed & Direction	0	8.9	487	2	3	403.35	-85.79	11	563.39	4.58E-123	4.58E-123
LR vs Winter Wind and Wave	0	8.9	487	3	4	402.89	-84.34	12	564.84	2.22E-123	2.22E-123
LUS Upland (x, x2)	0	8.6	487	3	4	403.80	-83.24	13	565.94	1.28E-123	1.28E-123
LUS Beach (x, x2)	0	8.5	487	3	4	404.38	-82.54	14	566.63	9.06E-124	9.06E-124
LR vs Winter Wave % Direction	0	7.2	487	2	3	411.01	-76.62	15	572.56	4.68E-125	4.68E-125
HEL NA (x, x2)	0	5	487	3	4	419.87	-64.23	16	584.95	9.55E-128	9.55E-128
Wetland Water	0	3.4	487	2	3	427.72	-57.21	17	591.96	2.87E-129	2.87E-129
No Slope (x, x2)	0	3.3	487	3	4	427.29	-55.70	18	593.47	1.34E-129	1.34E-129
Avg Slope (x. x2)	0.001	2.3	487	3	4	431.75	-50.64	19	598.53	1.07E-130	1.07E-130
Geo Beach Deposits	0.45	0	487	2	3	443.33	-39.75	20	609.42	4.63E-133	4.63E-133

Appendix 10. AIC results for the SS study site based on the attributes that had more than 25% of the attribute within the transects (x, x^2 = quadratic regression, x, x^2, x^3 = cubic linear regression).

NE Attributes > 25% on Transects	p-value	R-sq (adj)	Number of Data Points	Number of Parameters Fitted	K	Regression Sum of Squares (SSE)	AIC	Rank	Delta	exp(-delta/2)	Akaike Weights
Wetland Open Water (x, x2)	0.0000	32.3	487	3	4	46.78	-1132.97	1	0.00	1.00E+00	1.00E+00
Soil Water (x, x2)	0.0000	26.8	487	3	4	50.63	-1094.42	2	38.56	4.24E-09	4.24E-09
LUS Upland (x, x2, x3)	0.0000	19.9	487	4	5	55.27	-1049.71	3	83.26	8.33E-19	8.33E-19
Geo Moraine Outwash (x, x2, x3)	0.0000	19.5	487	4	5	55.52	-1047.55	4	85.42	2.82E-19	2.82E-19
Soil Udipsamments	0.0000	17.4	487	2	3	57.25	-1036.63	5	96.35	1.20E-21	1.20E-21
HEL NA	0.0000	15.6	487	2	3	58.48	-1026.19	6	106.78	6.51E-24	6.51E-24
SG End Moraines (x, x2, x3)	0.0000	15.8	487	4	5	58.12	-1025.25	7	107.72	4.06E-24	4.06E-24
8-15% Slope	0.0000	14.8	487	2	3	59.00	-1021.96	8	111.01	7.83E-25	7.83E-25
Wetland Barrier Beach Dune (x, x2)	0.0000	14.3	487	3	4	59.28	-1017.63	9	115.34	9.01E-26	9.01E-26
Geo Beach Deposits (x, x2, x3)	0.0000	13.9	487	3	4	59.42	-1016.49	10	116.48	5.09E-26	5.09E-26
Avg Slope (x, x2, x3)	0.0000	13.9	487	4	5	59.39	-1014.71	11	118.26	2.09E-26	2.09E-26
LUS Beach (x, x2, x3)	0.0000	13.8	487	4	5	59.82	-1011.23	12	121.75	3.66E-27	3.66E-27
SG Sand & Gravel Deposits (x, x2, x3)	0.0000	10.7	487	4	5	61.64	-996.62	13	136.35	2.46E-30	2.46E-30
HEL (Highly Erodible Land) (x, x2, x3)	0.0000	10.7	487	4	5	61.64	-996.58	14	136.39	2.42E-30	2.42E-30
SG Till & Bedrock (x, x2)	0.0000	8.6	487	3	4	63.19	-986.54	15	146.43	1.60E-32	1.60E-32
No Slope (x, x2)	0.0000	8.5	487	3	4	63.25	-986.06	16	146.91	1.26E-32	1.26E-32
East	0.0000	4.3	487	2	3	66.32	-964.94	17	168.03	3.26E-37	3.26E-37
Avg Sand (x, x2, x3)	0.0000	3.1	487	4	5	66.83	-957.25	18	175.73	6.94E-39	6.94E-39

Appendix 11. AIC results for the NE (part 1) study site based on the attributes that had more than 25% of the attribute within the transects (x, x^2 = quadratic regression, x, x^2, x^3 = cubic linear regression).

NE Attributes > 25% on Transects	p-value	R-sq (adj)	Number of Data Points	Number of Parameters Fitted	K	Regression Sum of Squares (SSE)	AIC	Rank	Delta	exp(-delta/2)	Akaike Weights
Wetland Coastal Beach (x, x2, x3)	0	3	487	4	5	66.89	-956.81	19	176.16	5.59E-39	5.59E-39
Wetland Barrier Beach (x, x2)	0	1.8	487	3	4	67.91	-951.41	20	181.56	3.76E-40	3.76E-40
East North East	0.006	1.3	487	2	3	68.35	-950.27	21	182.7	2.13E-40	2.13E-40
Summer Wave % Direction (x, x2)	0.029	1	487	3	4	68.41	-947.86	22	185.11	6.37E-41	6.37E-41
Winter Wave % Direction (x, x2)	0.053	0.8	487	3	4	68.58	-946.63	23	186.34	3.44E-41	3.44E-41
Summer Wind Speed & Direction	0.287	0	487	2	3	69.26	-943.86	24	189.12	8.59E-42	8.59E-42
Winter Wind Speed & Direction	0.343	0	487	2	3	69.29	-943.62	25	189.35	7.64E-42	7.64E-42
East South East	0.75	0	487	2	3	69.41	-942.8	26	190.17	5.07E-42	5.07E-42

Appendix 12. AIC results for the NE (part 2) study site based on the attributes that had more than 25% of the attribute within the transects (x, x^2 = quadratic regression, x, x^2, x^3 = cubic linear regression).

NW Attributes > 25% on Transects	p-value	R-sq (adj)	Number of Data Points	Number of Parameters Fitted	K	RSS (SSE)	AIC	Rank	Delta	exp(-delta/2)	Akaike Weights
Soil Water (x, x2, x3)	0.0000	68.4	487	4	5	10.03	-1880.80	1	0.00	1.00E+00	1.00E+00
Soil Udipsamments	0.0000	65.7	487	2	3	10.94	-1842.56	2	38.24	4.97E-09	4.97E-09
Wetland Barrier Beach - Dune	0.0000	64.4	487	2	3	11.37	-1823.92	3	56.88	4.46E-13	4.46E-13
8-15% Slope (x, x2)	0.0000	59.9	487	3	4	12.78	-1764.79	4	116.01	6.43E-26	6.43E-26
HEL NA (x, x2, x3)	0.0000	53.8	487	4	5	14.69	-1695.17	5.5	185.63	4.90E-41	4.90E-41
No Slope (x, x2, x3)	0.0000	53.8	487	4	5	14.69	-1695.17	5.5	185.63	4.90E-41	4.90E-41
Wetland Open Water (x, x2, x3)	0.0000	53.1	487	4	5	14.89	-1688.32	7	192.48	1.60E-42	1.60E-42
Highly Erodible Land (x, x2, x3)	0.0000	52.4	487	4	5	15.12	-1681.01	8	199.79	4.13E-44	4.13E-44
Geo Beach Deposits (x, x2)	0.0000	42.1	487	3	4	18.44	-1586.27	9	294.53	1.11E-64	1.11E-64
Wetland Coastal Beach (x, x2, x3)	0.0000	39.3	487	4	5	19.28	-1562.60	10	318.20	8.03E-70	8.03E-70
Avg Slope (x, x2, x3)	0.0000	25.3	487	4	5	21.47	-1510.17	11	370.63	3.30E-81	3.30E-81
SG Sand Deposits	0.0000	25.6	487	2	3	23.74	-1465.26	12	415.54	5.85E-91	5.85E-91
LUS Beach (x, x2)	0.0000	23.0	487	3	4	24.50	-1447.84	13	432.96	9.64E-95	9.64E-95
LUS Upland	0.0000	22.9	487	3	4	24.54	-1447.10	14	433.69	6.68E-95	6.68E-95
Soil Beaches (x, x2, x3)	0.0000	13.6	487	4	5	27.45	-1390.52	15	490.28	3.45E-107	3.45E-107
SG End Moraine	0.0000	10.9	487	2	3	28.43	-1377.40	16	503.40	4.87E-110	4.87E-110
West Northwest	0.0000	8.9	487	2	3	29.05	-1366.98	17	513.82	2.66E-112	2.66E-112
Geo Moraine Deposits	0.0000	7.1	487	2	3	29.40	-1361.18	18	519.62	1.47E-113	1.47E-113

Appendix 13. AIC results for the NW (part 1) study site based on the attributes that had more than 25% of the attribute within the transects (x, x^2 = quadratic regression, x, x^2, x^3 = cubic linear regression).

NW Attributes > 25% on Transects	p-value	R-sq (adj)	Number of Data Points	Number of Parameters Fitted	K	Regression Sum of Squares (SSE)	AIC	Rank	Delta	exp(-delta/2)	Akaike Weights
North	0.0000	6.5	487	2	3	29.83	-1354.00	19	526.80	4.05E-115	4.05E-115
Avg % Sand (x, x2, x3)	0.0000	6.8	487	4	5	29.61	-1353.63	20	527.17	3.36E-115	3.36E-115
Winter Wind Speed & Direction	0.0000	5.6	487	2	3	30.11	-1349.57	21	531.23	4.42E-116	4.42E-116
Summer Wind Speed & Direction	0.0000	5.6	487	2	3	30.11	-1349.45	22	531.35	4.16E-116	4.16E-116
Summer Wave % Direction	0.0000	5.4	487	2	3	30.17	-1348.55	23	532.25	2.65E-116	2.65E-116
Winter Wave % Direction	0.0000	4.9	487	2	3	30.34	-1345.85	24	534.95	6.88E-117	6.88E-117
Northwest	0.0000	3.6	487	2	3	30.76	-1339.17	25	541.63	2.44E-118	2.44E-118

Appendix 14. AIC results for the NW (part 2) study site based on the attributes that had more than 25% of the attribute within the transects (x, x^2 = quadratic regression, x, x^2, x^3 = cubic linear regression).

Appendix 16. Aerial photo of the coastal ponds along the SS study site, photo provided by marthasvineyardhill.com.

Appendix 15. Norton Point Breach, April 2007. (A) The falling tide flows through the breach of out Katama Bay. (B) An aerial view looking east toward Wasque Point. Photos provided by Ralph Stewart, The Martha's Vineyard Times, 2008.

APPENDIX B: VARIABLE AND ATTRIBUTE DESCRIPTIONS

Feature	Description
GEOLOGY BEACH DEPOSITS	**Beach deposits.**—Beach deposits mark the present or former shorelines of the sea or lakes. These deposits are low ridges of sorted material and are commonly sandy, gravelly, cobbly, or stony. Deposits on the beaches of former glacial lakes are usually included with glacial drift (Soil Survey Division Staff, 1993), Chp 3. **Beach** - (a) A gently sloping zone of unconsolidated material, typically with a slightly concave profile, extending landward from the low-water line to the place where there is a definite change in material or physiographic form (such as a cliff) or to the line of permanent vegetation (usually the effective limit of the highest storm waves); a shore of a body of water, formed and washed by waves or tides, usually covered by sand or gravel; (b) the relatively thick and temporary accumulation of loose water-borne material (usually well-sorted sand and pebbles) accompanied by mud, cobbles, boulders, and smoothed rock and shell fragments, that is in active transit along, or deposited on, the shore zone between the limits of low water and high water (Soil Survey Division Staff, 1993), Chp 3.
GEOLOGY MORAINE DEPOSITS	**Moraine** [glacial geology] - (a) [material] A mound, ridge, or other topographically distinct accumulation of unsorted, unstratified glacial drift, predominantly till, deposited primarily by the direct action of glacier ice, in a variety of landforms. (b) [landform] A general term for a landform composed mainly of till that has been deposited by a glacier; a kame moraine is a type of moraine similar in exterior form to other types of moraines but composed mainly of stratified outwash materials. Types of moraine include: disintegration, end, ground, kame, lateral, recessional, and terminal (Soil Survey Division Staff, 1993), Chp 3.
GEOLOGY MORAINE OUTWASH	When glacial ice melts, its runoff may form a series of rivers or braided streams. Theses rivers carry rock fragments from the end of the

	glacial conveyor belt, spreading layers of sand and gravel over a broad areas, and forming an outwash plain. (Skehan, 2001). **Outwash** [glacial geology] - Stratified and sorted sediments (chiefly sand and gravel) removed or "washed out" from a glacier by melt-water streams and deposited in front of or beyond the end moraine or the margin of a glacier. The coarser material is deposited nearer to the ice. Compare - pitted outwash, drift, esker, kame, till (Soil Survey Division Staff, 1993), Chp 3.
GEOLOGY POND	**Pond** - (a) A natural body of standing fresh water occupying a small surface depression, usually smaller than a lake and larger than a pool. (b) A small artificial body of water, used as a source of water. Compare - salt pond (Soil Survey Division Staff, 1993), Chp 3. **Salt Pond** - A large or small body of salt water in a marsh or swamp along the seacoast (Soil Survey Division Staff, 1993), Chp 3.
GEOLOGY MARSH	**Marsh** - Periodically wet or continually flooded areas with the surface not deeply submerged. Covered dominantly with sedges, cattails, rushes, or other hydrophytic plants. Compare - salt marsh, swamp, bog, fen (Soil Survey Division Staff, 1993), Chp 3. **Salt Marsh** - Flat, poorly drained area that is subject to periodic or occasional overflow by salt water, containing water that is brackish to strongly saline, and usually covered with a thick mat of grassy halophytic plants; e.g., a coastal marsh periodically flooded by the sea, or an inland marsh, (or salina) in an arid region and subject to intermittent overflow by salty water. Compare - tidal marsh, mud flat (Soil Survey Division Staff, 1993), Chp 3.
SURFICIAL GEOLOGY END MORAINE	**Terminal moraines** mark the farthest position of an ice sheet from its source of snow. An end moraine is any other moraine that grows at the toe of a glacier but is not the farthest one from the center of snow accumulation. Most moraines are end moraines (Skehan, 2001.)

	A ridge-like accumulation that is being or was produced at the outer margin of an actively flowing glacier at any given time; a moraine that has been deposited at the outer or lower end of a valley glacier (Soil Survey Division Staff, 1993), Chp 3. **Moraine** [glacial geology] - (a) [material] A mound, ridge, or other topographically distinct accumulation of unsorted, unstratified glacial drift, predominantly till, deposited primarily by the direct action of glacier ice, in a variety of landforms. (b) [landform] A general term for a landform composed mainly of till that has been deposited by a glacier; a kame moraine is a type of moraine similar in exterior form to other types of moraines but composed mainly of stratified outwash materials. Types of moraine include: disintegration, end, ground, kame, lateral, recessional, and terminal (Soil Survey Division Staff, 1993), Chp 3.
SURFICIAL GEOLOGY SAND DEPOSITS	**Glacial Beach Deposits.**—These consist of rock fragments and sand. They mark the beach lines of former glacial lakes. Depending on the character of the original drift, beach deposits may be sandy, gravelly, cobbly, or stony (Soil Survey Division Staff, 1993)
SURFICIAL GEOLOGY TILL / BEDROCK	Stratified deposits of sand and gravel deposited by melt-water streams flowing from the glacial ice. Proglacial outwash was deposited away from the glacial ice and tends to have small coarse fragments. http://nesoil.com/gis/join.htm **Till** [glacial] - Dominantly unsorted and unstratified drift, generally unconsolidated and deposited directly by a glacier without subsequent reworking by meltwater, and consisting of a heterogeneous mixture of clay, silt, sand, gravel, stones, and boulders; rock fragments of various lithologies are imbedded within a finer matrix that can range from clay to sandy loam. Compare - ablation till, basal till, flowtill, lodgment till, drift, moraine (Soil Survey Division Staff, 1993), Chp 3. The unsorted glacial debris that comprises till is

	depositd directly by a glacier; it is not reworhed by meltwater. Till consists of a mixture of clay, silt, sand, gravel, and boulders of various sizes and shaped, compacted by the weight of overlying ice. A thin mantle of till, generally about 15 feet thick, covers a large part of Massachusetts (Skehan, 2001) The till of MV contains rock fragments from bedrock to the northwest in Massachusetts and Rhode Island (Skehan, 2001). This is that part of the glacial drift deposited directly by the ice with little or no transportation by water. It is generally an unstratified, heterogeneous mixture of clay, silt, sand, gravel, and sometimes boulders. Some of the mixture settled out as the ice melted with very little washing by water, and some was overridden by the glacier and is compacted and unsorted. Till may be found in ground moraines, terminal moraines, medial moraines, and lateral moraines. In many places it is important to differentiate between the tills of the several glaciations. Commonly, the tills underlie one another and may be separated by other deposits or old, weathered surfaces. Many deposits of glacial till were later eroded by the wave action in glacial lakes. The upper part of such wave-cut till may have a high percentage of rock fragments(Soil Survey Division Staff, 1993). Glacial till ranges widely in texture, chemical composition, and the degree of weathering that followed its deposition. Much till is calcareous, but an important part is noncalcareous because no carbonate rocks contributed to the material or because subsequent leaching and chemical weathering have removed the carbonates (Soil Survey Division Staff, 1993).
WETLAND BARRIER BEACH	Includes: Barrier Beach System, Barrier Beach-Coastal Beach, Barrier Beach-Coastal Dune, Barrier Beach-Open Water **Barrier Beach** – A low-lying strip of land generally consisting of coastal beaches and coastal dunes extending roughly parallel to the

	trend of the coast. It is separated from the mainland by a narrow body of fresh, brackish or saline water or a marsh system. A barrier beach may be joined to the mainland at one or both ends (310 CMR 10.29) (MA DEP, 2007).
WETLAND COASTAL BEACH	Includes: Coastal Bank Bluff or Sea Cliff, Coastal Beach, Coastal Dune **Coastal bank** means the seaward face or side of any elevated landform, other than a coastal dune, which lies at the landward edge of a coastal beach, land subject to tidal action (310 CMR 10.30) (MA DEP, 2007). Coastal banks can be inferred to be associated with lowlands subject to tidal action or subject to coastal storm flowage. Coastal banks, therefore, can occur around non-tidal ponds, lakes and streams provided that these elevated landforms confine water associated with coastal storm events, up to the 100-year storm elevation or storm of record. **Coastal Beach** means unconsolidated sediment subject to wave, tidal and coastal storm actions which forms the gently sloping shore of a body of salt water and includes tidal flats. Coastal beaches extend from the mean low water landward to the dune line, coastal bankline or the seaward edge of existing man-made structures, when these structures replace on of the above lines, whichever is closest to the ocean (310 CMR 10.27) (MA DEP, 2007). **Coastal Dune** – Any natural hill, mound or ridge of sediment landward of a coastal beach deposited by wind action or storm overwash (310 CMR 10.28) (MA DEP, 2007).
WETLAND MARSH	Includes: Salt Marsh, Shallow Marsh Meadow or Fen, Shrub Swamp, Deep Marsh **Salt Marsh** means a coastal wetland that extends landward up to the highest tide line, that is, the highest spring tide of the year, and is characterized by plants that are well adapted to or prefer living in saline soils. Dominant plants within salt marshes are salt meadowcord

	grass (*Spartina patens*) and/or saltmarsh cord grass (*Spartina alterniflora*). A salt marsh may contain tidal creeks, ditches, and pools (310 CMR 10.32) (MA DEP, 2007). **Marsh** - Periodically wet or continually flooded areas with the surface not deeply submerged. Covered dominantly with sedges, cattails, rushes, or other hydrophytic plants. Compare - salt marsh, swamp, bog, fen. (Soil Survey Division Staff, 1993)
WETLAND ROCKY INTERTIDAL SHORE	Rocky Intertidal Shore means naturally occurring rocky areas, such as bedrock or boulder-strewn areas between the mean high water line and the mean low water line (310 CMR 10.31) (MA DEP, 2007).
WETLAND UPLAND	Non-wetland areas - As of the March 2006 update, ARC_CODE 99 no longer exists, as all OQ index tile boundaries have been removed and all features edge-matched and dissolved based on attributes, and attribute discrepancies have been resolved. ARC_CODE 88 defines the edge of the layer except for ocean areas. **Upland** [geomorphology] - An informal, general term for (a) the higher ground of a region, in contrast with a lowlying, adjacent land such as a valley or plain. (b) Land at a higher elevation than the flood plain or low stream terrace; land above the footslope zone of the hillslope continuum. Compare - lowland. (Soil Survey Division Staff, 1993)
WETLAND WATER	Open Water. **Water** [soil survey] - A generic map unit for any permanent, open body of water (pond, lake, reservoir, etc.) that does not support rooted plants. (Soil Survey Division Staff, 1993)
WETLAND TIDAL FLAT	Tidal Flat means any nearly level part of a coastal beach which usually extends from the mean low water line landward to the more steeply sloping face of the coastal beach or which may be separated from the beach by land under the ocean. (310 CMR 10.27) **Tidal Flat** - An extensive, nearly horizontal, barren or sparsely vegetated tract of land that

	is alternately covered and uncovered by the tide, and consists of unconsolidated sediment (mostly clays, silts and/or sands and organic materials). Compare – tidal marsh**,** wind-tidal flat. (Soil Survey Division Staff, 1993)
N	350°-10° (mean = 0°)
NNE	11°-34° (mean = 11.5°)
NE	35°-55° (mean = 45°)
ENE	56°-79° (mean = 67.5°)
E	80°-100° (mean = 90°)
ESE	101°-124° (mean = 112.5°)
SE	125°-145° (mean = 135°)
SSE	146°-169° (mean = 157.5°)
S	170°-190° (mean = 180°)
SSW	191°-214° (mean = 202.5°)
SW	215°-235° (mean = 225°)
WSW	236°-259° (mean = 247.5°)
W	260°-280° (mean = 270°)
WNW	281°-304° (mean = 292.5°)
NW	305°-325° (mean = 315°)
NNW	326°-349° (mean = 337.5°)
SOIL BEACHES	This unit is dominantly nearly level, but some areas adjacent to the ocean are gently sloping and is continually washed and rewashed by waves. The areas of this unit typically are long and narrow and are 50 to 300 feet wide. The beach map unit is not vegetated and generally consists of fine to coarse sand with layers of gravelly and cobbly sand. Some areas have a gravelly or cobbly surface. The area nearest the water is gently sloping and is inundated twice daily by tides. The entire beach is generally flooded by spring tides and storm events. Included with this map unit in mapping are small areas of Hooksan, Ipswich, Pawcatuck, and Matunuck soils. Also included are areas of unvegetated dune sand. Vegetation does not grow in these areas because of inundation by salt water and frequent reworking of the sand by wave action. Beaches are mainly used for recreation and are unsuited for most other uses.(Fletcher & Roffinoli, 1986)
SOIL BERRYLAND	**Spodosols**, sandy, siliceous, mesic Typic

	Haplaquods, loamy sand, 0-2% slopes. Berryland soil is very deep, nearly level, and very poorly drained. This soil formed in glacial fluvial and lacustrine deposits on outwash plains and deltas in depressions, at the base of swales, and in low areas adjacent to ponds and streams (Turenne, 2007). It is classified in hydrologic group D (Turenne, 2007). Parent Material: Sandy eolian deposits and/or fluviomarine sediments Slope: 0 to 2 percent(Soil Survey Division, 2002) Typically the surface layer is black loamy sand about 5 inches thick. Very deep, nearly level, very poorly drained soil formed in glacial fluvial and lacustrine deposits. Berryland soils are on outwash plains and deltas in depressions, at the base of swales, and in low areas adjacent to ponds and streams. Typically the surface layer is black loamy sand about 5 inches thick. The common trees on this soil are red maple and tupelo.
SOIL CARVER	**Entisols**, Siliceous, mesic Typic Udipsamments, loamy coarse sand, slope ranges from 0-3% to 15-25%. Very deep, excessively drained soils formed in thick deposits of coarse and very coarse sands. Carver soils are in broad areas on outwash plains, terraces and deltas. Hydrologic group A.(Turenne, 2007) Parent Material: Coarse sand eolian deposits underlain by fluvial deposits.(Turenne, 2007) Carver soils are level to steep soils on pitted and dissected outwash plains and moraines. Slopes are dominantly 0 to 15 percent but range to 45 percent. The soils formed in thick layers of coarse and very coarse sand that contain less than 20 percent rock fragments, most of which are fine gravel.(Soil Survey Division, 2002) The surface layer is dark grayish brown loamy coarse sand about 3 inches thick. Very deep, excessively drained soils formed in thick deposits of coarse and very coarse sands.

	Carver soils are in broad areas on outwash plains, terraces and deltas. Most areas of this soil are in woodland. Some areas are in cropland; and some are in residential development. The common trees on this soil are pitch pine, scrub oak, scarlet oak, black oak, and white oak.
SOIL CHILMARK	**Utisols**, Fine-loamy, mixed, mesic Typic Hapludults, sandy loam, very stony, 3-8% slope. The Chilmark series consists of very deep, well drained soils formed in a loamy or sandy aeolian mantle and the underlying fine or moderately fine coastal plain sediments. They are gently sloping to moderately steep soils on moraines. Slope ranges from 3 to 25 percent.(Soil Survey Division, 2002) Chilmark soils are gently sloping to moderately steep soils on landscapes that are very close to the bases of terminal moraines and on gently sloping or undulating lower parts of the moraines. Slope ranges from 3 to 25 percent. The soils formed in a loamy or sandy aeolian mantle and the underlying ice-thrusted fine or moderately fine coastal plain sediments dominated by poorly mixed tertiary clays. (Soil Survey Division, 2002) Hydrologic group C.(Soil Survey Staff, 2007) This soil is very deep, gently sloping, and well drained. It is on broad areas, hills, knolls, and ridges in the western part of Martha's Vineyard. The common trees on this soil are white oak, eastern white pine, and scarlet oak.
SOIL EASTCHOP	**Entisols**, Siliceous, mesic Typic Udipsamments, loamy sand and in some areas very stony, slope ranges from 3-8% to 15-25%. The Eastchop series consists of very deep, excessively drained soils formed in sandy glacial outwash. They are nearly level to steep soils on moraines and outwash plains. Slope ranges from 0 to 35 percent. Permeability is rapid or very rapid.(Soil Survey Division, 2002) hydrologic group A (Soil Survey Staff, 2007). Typically, the surface is covered with a layer of

	loose, undecomposed and decomposed leaves and twigs 3 inches thick. The surface layer is very dark brown loamy sand about 5 inches thick. This soil is very deep, nearly level, and excessively drained. It is on broad areas on outwash plains, small hills, knolls, and ridges in the western part of Martha's Vineyard. Most areas of this soil are in woodland. Some areas are in cropland, and some areas are used as pasture, and a few are used as homesites. The common trees on this soil are pitch pine, scrub oak, scarlet oak, black oak, and white oak.
SOIL FREETOWN AND SWANSEA	**Histosols**, Dysic, mesic Typic Medisaprists, muck, 0-1% slope. Very deep, nearly level, very poorly drained organic soil formed in more than 51 inches of highly decomposed organic material. Freetown soils are in depressions, kettle holes, along streams and rivers or on flat, level areas of uplands or outwash plains. Hydrologic group D(Turenne, 2007) Parent Material: Freetown soils formed in greater than 51 inches of organic material.(Turenne, 2007) Parent material: Highly-decomposed herbaceous organic material – found in bogs (USDA, 2007b) The Freetown series consists of very deep, very poorly drained organic soils formed in more than 51 inches of highly decomposed organic material. They are in depressions or on level areas on uplands and outwash plains. Slope ranges from 0 to 1 percent.(Soil Survey Division, 2002) Freetown soils are in bogs that range from small enclosed depressions to bogs of several hundred acres in size. These bogs are on lake plains, outwash plains, till plains and moraines.(Soil Survey Division, 2002) The Swansea series consists of very poorly drained organic soils. They formed in 16 to 51 inches of highly decomposed organic material over sandy mineral. These soils are in

	depressions or on flat level areas on uplands and outwash plains. Permeability is moderate or moderately rapid in the organic material and very rapid in the substratum. Swansea soils are in bogs that range from small enclosed depressions to bogs of several hundred acres in size. They are on outwash plains, till plains and moraines.(Soil Survey Division, 2002) Typically, the Freetown soils consist of layers of dark reddish brown and black muck to a depth of 60 inches or more. The Swansea soils have a surface layer of dark reddish brown muck about 19 inches thick. These soils are very deep, level, and very poorly drained. They are in depressions and areas adjacent to streams and bodies of open water. Included are areas that were formerly cranberry bogs. They have a surface layer of coarse sand 5 to 12 inches thick over the muck. Some areas have water ponded on the surface most of the year. Most areas of these soils are wooded or have shrubby vegetation. The common trees on this unit are red maple, tupelo, and Atlantic white-cedar.
SOIL KATAMA	**Inceptisols**, Sandy, mixed, mesic Typic Haplumbrepts, sandy loam, 0-3% slopes. Hydrologic group B (Soil Survey Staff, 2007) The Katama series consists of very deep, well drained soils formed in a loamy mantle and underlying sandy deposits. They are level to gently sloping soils on outwash plains. Slope ranges from 0 to 8 percent. Permeability is moderately rapid in the upper part of the solum and moderately rapid or rapid in the lower part and in the substratum.(Soil Survey Division, 2002) Katama soils are on broad nearly level to gently sloping outwash plains. They are adjacent to the ocean and 10 to 20 feet above sea level. Slope commonly is 0 to 3 percent, but ranges to 8 percent. The soils developed in sandy outwash that in many places has been reworked by wind. The climate is oceanic and dense sea fogs are very common.(Soil Survey Division, 2002)

	Typically, the surface layer is very dark grayish brown sandy loam 6 inches thick, it is very deep, nearly level, and well drained. It is found in broad areas in the southeastern corner of the town of Edgartown. Many areas of this soil are in cropland. A few areas are used as homesites, and some areas are in native vegetation. Strong winds and salt spray severely hinder tree growth.
SOIL KLEJ	**Entisols**, Mesic, coated Aquic Quartzipsamments, loamy coarse sand, sandy substratum, 0-3% slopes Parent Material: Sandy fluvio-marine sediments(Soil Survey Division, 2002) Hydrologic group B (Soil Survey Staff, 2007) This soil is very deep, nearly level to gently sloping, and moderately well drained. It is in depressions and in low areas adjacent to bodies of open water. Typically, the surface is covered with a 3-inch-thick layer undecomposed and decomposed leaves and twigs. The surface layer is light brownish gray loamy coarse sand about 4 inches thick. Most areas of this soil are in woodland and some areas are in cropland. The common trees on this soil are white oak, black oak, scarlet oak, and red maple.
SOIL NANTUCKET	**Inceptisols**, Coarse-loamy, mixed, mesic Typic Dystrochrepts, undulating, very stony, and sandy loam, 3-8% to 8-15% slope. The Nantucket series consists of very deep, well drained soils formed in dense glacial till. They are moderately deep to dense till. They are gently sloping to strongly sloping soils on or near terminal moraines. Permeability is moderately rapid in the solum and moderately slow or slow in the substratum. Slope ranges from 3 to 15 percent. Nantucket soils are gently sloping or strongly sloping soils on terminal moraines or ground moraines in close proximity to terminal moraines. Slope is 3 to 15 percent. The soils formed in loamy glacial till or till mixed or folded with Pleistocene Age silts and clays. (Soil Survey Division, 2002)

	Hydrologic group C (Soil Survey Staff, 2007)
SOIL PAWCATUCK AND MATUNUCK	**Histosols**, Euic, mesic Typic Sulfihemists, mucky peats, 0-1% slopes Hydrologic group D (Soil Survey Staff, 2007) The Pawcatuck series consists of very deep, very poorly drained soils formed in organic deposits over sandy mineral material. They are in tidal marches subject to inundation by salt water twice daily. Slope ranges from 0 to 1 percent. Permeability is moderate to rapid in the organic layers and very rapid in the underlying mineral sediments. Pawcatuck soils are level soils in tidal marshes. They are subject to tidal flooding twice daily except in areas protected by dikes and tide gates. Pawcatuck soils developed in partially decomposed organic material from salt tolerant herbaceous plants over sandy sediments.(Soil Survey Division, 2002) The Matunuck series consists of very deep, very poorly drained soils formed in thick sand deposits. They are in tidal marshes subject to inundation by salt water twice daily. Matunuck soils are level soils in tidal marshes along the Atlantic Ocean. They are subject to tidal flooding twice daily except, in areas protected by dikes and tide gates. Matunuck soils formed in thick sand deposits with organic surfaces.(Soil Survey Division, 2002) This unit consists of very deep, level, very poorly drained soils in tidal areas subject to daily inundation. The soils are adjacent to shore areas and brackish ponds. Typically, the Pawcatuck soils have a surface layer of very dark grayish brown mucky peat about 10 inches thick. The next layer is black mucky peat about 9 inches thick. The Matunuck soils have a surface layer of very dark grayish brown mucky peat about 10 inches thick. Most areas of this unit are in salt-tolerant grasses. The daily tidal flooding limits the unit for most uses other than as wetland wildlife habitat.

SOIL POMPTON	**Inceptisols**, Coarse-loamy, mixed, mesic Aquic Dystrochrepts, sandy loam, 0-3% slopes Hydrologic group B (Soil Survey Staff, 2007) The Pompton series consists of deep moderately well drained and somewhat poorly drained soils formed in water-sorted sediments. They are on outwash plains and terraces in waterways and low positions. Slope ranges from 0 to 8 percent. Pompton soils are nearly level to sloping soils on broad outwash plains deltaic deposits and in slightly concave drainageways that dissect outwash terraces. The soils developed in water sorted sandy and gravelly materials dominated by granitic gneiss with lesser amounts of many other kinds of materials. (Soil Survey Division, 2002) This soil is very deep, nearly level, and somewhat poorly drained. It is in closed depressions, at the base of swales, in low areas which border ponds and swamps, and in drainageways. Typically, the surface layer is very dark grayish brown sandy loam about 10 inches thick. Most areas of this soil are in woodland. Some areas have a shrubby vegetation. The common trees on this soil are red maple, tupelo, and white oak.
SOIL RIDGEBURY	**Inceptisols**, Fine, mixed, acid, mesic Typic Haplaquepts, sandy loam, 0-3% slopes Very deep, level, somewhat poorly and poorly drained soil formed in compact glacial till derived mainly from granite, gneiss and schist. Ridgebury soils are on upland depressions and drainageways. Hydrologic group C (Soil Survey Staff, 2007; Turenne, 2007) Parent Material: Dense till.(Turenne, 2007) The Ridgebury series consists of very deep, somewhat poorly and poorly drained soils formed in till derived mainly from granite, gneiss and schist. They are commonly shallow to a densic contact. They are nearly level to

	gently sloping soils in low areas in uplands. Slope ranges from 0 to 15 percent. The soils formed in loamy till derived mainly from granite, gneiss and schist.(Soil Survey Division, 2002) Very deep, level, somewhat poorly and poorly drained soil formed in compact glacial till derived mainly from granite, gneiss and schist. Ridgebury soils are on upland depressions and drainageways in the western part of Martha's Vineyard. Most areas of this soil are in woodland and some areas are used for pasture. The common trees on this soil are red maple and tupelo.
SOIL RIVERHEAD	**Inceptisols**, Coarse-loamy, mixed, mesic Typic Dystrochrepts, sandy loam, 0-3% slopes. (USDA, 2007a) The Riverhead series consists of very deep, well drained soils formed in glacial outwash deposits derived primarily from granitic materials. They are on outwash plains, valley trains, beaches, and water-sorted moraines. Slope ranges from 0 to 50 percent slopes. Riverhead soils are nearly level to steep soils on outwash plains, valley trains, beaches, and water-sorted moraines. The soils developed in 20 to 40 inches of water-sorted sandy loam or fine sandy loam relatively low in gravel content over stratified gravel and sand. (Soil Survey Division, 2002) Hydrologic group B (Soil Survey Staff, 2007) This soil is very deep, nearly level, and well drained. It is in large, broad areas on outwash plains in the central and southern parts of Martha's Vineyard. Typically, the surface layer is dark grayish brown sandy loam about 4 inches thick. The subsoil is 20 inches thick. The upper 12 inches of the subsoil is yellowish brown sandy loam, and the lower 8 inches is yellowish brown loamy sand. Most areas of this soil are in woodland. Many areas are in grassland, and some areas are in cropland. A few areas are used as homesites. The common trees on this soil are white oak, eastern white

	pine, scarlet oak, black oak, and red pine. (Fletcher & Roffinoli, 1986)
SOIL UDIPSAMMENTS	**Entisols**, Siliceous, mesic Udipsamments, rolling, 3-15% slopes (USDA, 2007a) These soils are very deep and excessively drained. They are on sand dunes along the coast. Slopes are complex and generally range from 3 to 15 percent. The areas generally are long and narrow or are irregular in shape, and they range from 4 to 500 acres. (Fletcher & Roffinoli, 1986) Hydrologic group A (Soil Survey Staff, 2007) Udipsamments are pale brown sand to a depth of 60 inches or more. These soils are very deep and excessively drained. They are on sand dunes along the coast. Included are areas of recently deposited sand on which there is little or no vegetation. Most areas of these soils have a cover of grasses and shrubs. Most of the vegetation is fragile and easily destroyed by foot or vehicular traffic. Trees are difficult to establish and grow slowly. The common plants on these soils are beachgrass, poison ivy, beach plum, and bayberry. (Turenne, 2007)
SOIL URBAN	This unit consists of nearly level to moderately steep areas where urban works and structures such as buildings, industrial areas, and other paved areas cover at least 85 percent of the surface. Included with this unit in mapping are many small areas where the original soil material has been disturbed by construction and areas where fill has been added. Also included are small areas of undisturbed soils.
SOIL WATER	Includes fresh water, saline, and ocean.
NOT HIGHLY ERODIBLE LAND	The erodible classifications are based on an evaluation of water erosion hazard of the components within the map unit and is distributed in the Soil Survey Geographic (SSURGO) database (USDA, 2007c). All the soil components of a single class have

	the same classification.
POTENTIALLY HIGHLY ERODIBLE LAND	The soil components have multiple classifications.
ERODIBLE	Beaches did not have any classifications by the USDA. This category was defined for beaches only.
HIGHLY ERODIBLE LAND	All the soil components of a single class apply.
NA	If no soil components had a classification by the USDA, other the beaches, this description was used.
NO SLOPE	Water or urban land.
0-3% SLOPE	**Slope** - (also called slope gradient or gradient) The inclination of the land surface from the horizontal. Percent slope is the vertical distance divided by the horizontal distance, then multiplied by 100. SW (Soil Survey Division Staff, 1993)
3-8% SLOPE	See above.
8-15% SLOPE	See above.
15-25% SLOPE	See above.
LUS BEACH	**Water Based Recreation**: This category describes water-based recreation facilities such as developed freshwater and saltware sandy beach areas, plus associated parking lots.
LUS UPLAND	Includes: Pasture, Forest, Open Land, Participation Recreation, Residential > ½ acre lots, Urban Open. **Pasture:** Land is generally used for grazing of animals and for the growing of grasses for hay. It is often hilly, may have poor drainage or stoniness, lack high soil fertility, and the field boundaries may be less defined than cropland. There may be scattered trees or shrubs in the field. This is land that is probably not suitable for tillage. Associated facilities include barns and other outbuildings. **Forest:** Trees are classified as forests when the tree canopy covers at least 50% of the space when viewed from above on an aerial image. **Open Land:** Open lands include vacant land, idle agriculture, rock outcrops, and barren areas. Land is classified as vacant if it is

	abandoned land that isn't being used for any other land use and does not have enough vegetation to be classified as Forest or Successional. It may include structures which can indicate that the land was previously used for one of the urban categories. Idle agriculture is pasture, cropland and other agricultural lands that have not been active for a few years. Often, early successional vegetation is seen growing in around the edges and there is no evidence of any land or vegetation management. Sandy areas have very little visible vegetation. These are generally patches of sand in shrub-scrub areas that indicate highly permeable soils with very little organic material. Rock outcrops are areas of rock with very sparse visible vegetation, usually found in steep areas with a lot of topographic relief, usually cliffs. Barren areas are areas that are very sparsely vegetated and may be a combination of rock and sand but are characterized by little or no vegetation and a visible rock or sandy surface. Powerlines and pipeline corridors are separately classified. **Participation Recreation:** This category describes recreation facilities used by the public for active recreation and includes ballfields, tennis courts, basketball courts, ski areas, playgrounds, and bike paths plus associated parking lots. Golf courses are broken out into their own category (#26 below.) Developed recreation facilities will be labeled as such, even when associated with institutional land uses such as schools, as will recreation facilities at state parks. **Residential**: Lot sizes are visually determined by comparing the houses in an area to the surrounding houses, observing the spacing between the houses and the relative amount of yard space between them. **Urban Open**: Urban Open are areas that are in the process of being developed from one land use to another. Since these are transitional lands, it is not always apparent what the new land use will be so they are classified as this

	category. Typically, these areas are being developed for residential, commercial or industrial use. Comparison to older imagery shows that it was previously another land use or land cover category.
LUS WATER	This category includes open water, such as lakes, ponds, lagoons, bays or rivers wide enough to be mapped as a polygon instead of a line. This includes any open water feature on the land side of the ocean coastline. Retention basins will be included in this category if they have standing water in them. This category is included in the DEP Wetlands layer, but will be independently classified and areas that differ from the DEP layer will be flagged for review by DEP.
LUS CROPLAND	Cropland is generally tilled land used to grow row crops. There is usually evidence of intense land management. The land is often flat, well drained and the field boundaries are generally very well defined. This category also includes turf farms that grow sod. Unused tillable land that is usually mowed annually to maintain its agricultural value is included in this category. Associated facilities include barns and other outbuildings.
LUS MARSH	Includes: Saltwater wetland, and non-forested freshwater wetland. **Non-forested freshwater wetland:** These areas include seasonally flooded basins or flats, bogs, shrub swamps, wet meadows, shallow marshes, deep marshes, or small beaver ponds. **Saltwater wetland:** These wet areas include all tidal salt marshes (generally flooded twice daily), irregularly flooded salt meadows, or ditched salt meadows.
LUS DEVELOPED LAND	Includes: Residential (Multifamily, < ¼ acre lots, ¼- ½ acre lots), Commercial **Residential**: All residential categories are based on the size of the maintained lot and include the house and the yard area except for Multi-Unit Residential. Lot sizes are visually determined by comparing the houses in an area to the surrounding houses, observing the

	spacing between the houses and the relative amount of yard space between them. Other land cover types (such as Forest, Wetland or Water), even though they may be on a residential property, are usually mapped separately if they exceed the minimum mapping unit. Exceptions to this rule will depend on the geometry and the degree of isolation of the non-residential polygon. Duplexes (usually with 2 front doors/pathways and sometimes 2 driveways) will be classified as Multi-Unit Residential. Building sizes of residences (except for some duplexes and multi-unit complexes) are significantly smaller than almost all commercial and industrial buildings. **Commercial:** Large commercial facilities (such as malls, shopping centers and larger strip commercial areas) are typically well landscaped with parking strategically arranged around the building in multiple areas and are used for the distribution or merchandising of goods and services such as stores, hotels, motels, restaurants, theaters, shopping centers, offices, parking garages or gas stations. There are often a few loading docks associated with some of these facilities. These land uses are often found in residential areas or grouped with other commercial facilities. Parking areas are included. Smaller commercial facilities (such as neighborhood stores or smaller strip commercial areas) often look similar to residential areas but are sometimes distinguishable by their larger parking areas (compared to residential parking) often behind the building down a driveway with spaces for 5 or 10 vehicles or if in a dense residential area, they may actually be commercial at the ground level and apartments above. Also included in this category are office parks, medical offices and lawn and garden centers that do not produce or grow the product. Commercial buildings are almost always larger than residential structures.

BIBLIOGRAPHY

(1996) Coastal Zone Management Act of 1972, as amended through P.L. 104-150, The Coastal Zone Protection Act of 1996.

(CZMA, 1996) Coastal Zone Management Act of 1972, as amended through P.L. 104-150, The Coastal Zone Protection Act of 1996.

Abdalati, W., Konrad Steffen (2001) Greenland ice sheet melt extent: 1979–1999. *Journal of Geophysical Research*, **106**, 33,983–33,988.

Abdalati, W., Krabill, W., Frederick, E., Manizade, S., Martin, C., Sonntag, J., Swift, R., Thomas, R., Wright, W., & Yungel, J. (2001) Outlet glacier and margin elevation changes: Near-coastal thinning of the Greenland Ice Sheet. *Journal of Geophysical Research*, **106**, 33,729–33,742.

Adger, W.N., Hughes, T.P., Folke, C., Carpenter, S.R., & Rockstrom, J. (2005) Social-Ecological Resilience to Coastal Disasters. *Science*, **309**, 1036-1039.

Akaike, H. (1974) A new look at the statistical model identification. *IEEE Transactions on Automatic Control*, **19**, 716-723.

Alley, R.B., Clark, P.U., Huybrechts, P., & Joughin, I. (2005) Ice-Sheet and Sea-Level Changes. *Science*, **310**, 456-460.

AMS (2006) 27^{th} Conference on Hurricanes and Tropical Meterology. American Meterological Society (AMS), Boston, MA, Monterey, California.

Anderson, D.R., Burnham, K.P., & Thompson, W.L. (2000) Null Hypothesis Testing: Problems, Prevalence, and an Alternative. *The Journal of Wildlife Management*, **64**, 912-923.

Anderson, S.P. (2007) Biogeochemistry of Glacial Landscape Systems. *Annual Review of Earth and Planetary Sciences*, **35**, 375-399.

Anderson, T.W. & Darling, D.A. (1952) Asymptotic Theory of Certain "Goodness of Fit" Criteria Based on Stochastic Processes. *The Annals of Mathematical Statistics*, **23**, 193-212.

Anderson, T.W. & Darling, D.A. (1954) A Test of Goodness of Fit. *Journal of the American Statistical Association*, **49**, 765-769.

Ansley, J.E. (2000) The Teacher-Friendly Guide to the Geology of the Northeastern US, Vol. 2008. The Palentological Research Institution, affliated with Cornell University, Ithaca, NY.

Augustin, L., Barbante, C., Barnes, P.R.F., Barnola, J.M., Bigler, M., Castellano, E., Cattani, O., Chappellaz, J., Dahl-Jensen, D., Delmonte, B., Dreyfus, G., Durand, G., Falourd, S., Fischer, H., Flückiger, J., Hansson, M.E., Huybrechts, P., Jugie, G., Johnsen, S.J., Jouzel, J., Kaufmann, P., Kipfstuhl, J., Lambert, F., Lipenkov, V.Y., Littot, G.C., Longinelli, A., Maggi, R.L., Masson-Delmotte, V., Miller, H., Mulvaney, R., Oerlemans, J., Oerter, H., Orombelli, G., Parrenin, F., Peel, D.A., Petit, J.-R., Raynaud, D., Ritz, C., Ruth, U., Schwander, J., Siegenthaler, U., Souchez, R., Stauffer, B., Steffensen, J.P., Stenni, B., Stocker, T.F., Tabacco, I.E., Udisti, R., Wal, R.S.W.v.d., Broeke, M.v.d., Weiss, J., Wilhelms, F., Winther, J.-G., Wolff, E.W., & Zucchelli, M. (2004) Eight glacial cycles from an Antarctic ice core. *Nature*, **429**, 623-628.

Austin, T., Edson, J., McGillis, W., von Alt, C., Purcell, M., Petitt, R., McElroy, M., Ware, J., & Stokey, R. (2000) The Martha's Vineyard Coastal Observatory: a long term facility for monitoring air-sea processes. In OCEANS 2000 MTS/IEEE, Vol. 3, pp. 1937-1941, Providence, Rhode Island.

Baas, A.C.W. (2002) Chaos, fractals and self-organization in coastal geomorphology: simulating dune landscapes in vegetated environments. *Geomorphology*, **48**, 309-328.

Balco, G., Stone, J.O.H., Porter, S.C., & Caffee, M.W. (2002) Cosmogenic-nuclide ages for New England coastal moraines, Martha's Vineyard and Cape Cod, Massachusetts, USA. *Quaternary Science Reviews*, **21**, 2127-2135.

Ballantyne, C.K. (2002a) A general model of paraglacial landscape response. *The Holocene*, **12**, 371-376.

Ballantyne, C.K. (2002b) Paraglacial geomorphology. *Quaternary Science Reviews*, **21**, 1935-2017.

Banks, C.E. (1911) *The history of Martha's Vineyard, Dukes County, Massachusetts (Volume 3)* Dukes County Historical Society, Edgartown, MA.

Barnola, J.M., Raynaud, D., Korotkevich, Y.S., & Lorius, C. (1987) Vostok ice core provides 160,000-year record of atmospheric CO2. *Nature*, **329**, 408-414.

Bascom, W. (1964) *Waves and Beaches, the Dynamics of the Ocean Surface*, First edn. Anchor Books, Doubleday & Company, Inc., Garden City, NY.

Bashkirtsev, V.S. & Mashnich, G.P. (2003) Will we face global warming in the nearest future? *Geomagnetism and Aeronomy*, **43**, 124-127.

Beatley, T., Brower, D.J., & Schwab, A.K. (2002) *An Introduction to Coastal Zone Management*, Second edn. Island Press, Washington, Covelo, London.

Benchley, P. & Gradwohl, J. (1995) Threats to the health of the oceans. In Ocean Planet: Writings and Images of the Sea. Smithsonian Institute.

Benn, D.I. & Evans, D.J.A. (1998) *Glaciers and Glaciation* A Hodder Arnold Publication.

Berger, A.L. (1978) Long-term variations of daily insolation and Quaternary climatic change. *Journal of Atmospheric Science*, **35**, 2362-2367.

Bernd-Cohen, T. & Gordon, M. (1999) State Coastal Program Effectiveness in Protecting Natural Beaches, Dunes, Bluffs, and Rock Shores. *Coastal Management*, **27**, 187-217.

Bertness, M.D. (1998) *The Ecology of Atlantic Shorelines*, First edn. Sinauer Associates, Inc., Sunderland, MA.

Berz, G. (1993). Views of the Insurance Industry. Institute for Environmental Studies, University of Vrije.

Blake, E.S., Rappaport, E.N., Jarrell, J.D., & Landsea, C.W. (2005). The Deadliest, Costliest, and Most Intense United States Tropical Cyclones from 1851 to 2004 (and other frequently requested hurricane facts), NOAA Technical Memorandum NWA TPC-4. Tropical Prediction Center, National Hurricane Center, Miami, Florida.

Bouws, E., Janninie, D., & Kouen, G.J. (1996) The increasing wave height in the North Atlantic Ocean. *Bulletin of the American Meterological Society*, **77**, 2275-2277.

Brett, C.E. & Caudill, F.R. (2004) Tectonic Setting. President and Fellows of Harvard College, Department of Invertebrate Palenontology, Museum of Comparative Zoology, Harvard University.

Briguglio, L. (2004) Small Island Developing States and their Economic Vulnerabilities. In International Workshop on 'Vulnerability and Resilence of Small States'. The Global Development Research Center Programme, Partner of UN Ocean Atlas, The Ocean Project, GIN Global Island Network, World Ocean Network, University Gozo Centre, Malta.

Broccoli, A.J. & Manabe, S. (1990) Can existing climate change models be used to study anthropogenic changes in tropical cyclone climate? *Geophysical Research Letters*, **17**, 1917-1920.

Broecker, W.S. (2003) Does the Trigger for Abrupt Climate Change Reside in the Ocean or in the Atmosphere? *Science*, **300**, 1519-1522.

Broecker, W.S. (2004) Future Global Warming Scenarios. *Science*, **304**, 388b.

Brown University (2006) Coastal Studies. In Geological Sciences at Brown University, Providence, Rhode Island.

Bruce, J.P., Burton, I., & Egener, I.D.M. (1999). Disaster Mitigation and Preparedness in a Changing Climate: A Synthesis Paper Prepared for Emergency Preparedness Canada, Environment Canada, and the Insurance Bureau of Canada. Minister of Public Works and Government, Ottawa, Canada.

Bruun, P. (1962) Sea-Level Rise as a Cause of Shore Erosion, Proceedings Paper 3065. In Journal of the Waterways and Harbors Division, Vol. WW1, pp. 117-130. American Society of Civil Engineers.

Bryan, B., Harvey, N., Belperio, T., & Bourman, B. (2001) Distributed process modeling for regional assessment of coastal vulnerability to sea-level rise. *Environmental Modeling and Assessment*, **6**, 57-65.

Buonaccorsi, J. (2008) Use of Polynomial Models and Strong Multicollinearity (ed D. Brouillette-Jacobson), Amherst, MA.

Burnham, K.P. & Anderson, D.R. (1998) *Model selection and inference: a practical information-theoretic approach.* Springer-Verlag, New York.

Burrough, P.A. (1981) Fractal dimensions of landscapes and other environmental data. *Nature*, **294**, 240-242.

Burrough, P.A. (2002). Fractals and Geostatistical Methods in Landscape Studies. In *Fractals in Geography* (eds N. Siu-Ngan Lam & L. De Cola), pp. 87-121. The Blackburn Press, Caldwell, N.J.

Buynevich, I.V. & Evans, R. (2003) Extending the Documentary Records of Shoreline Change for Martha's Vineyard and Nantucket. Woods Hole Oceanographic Institution, Coastal Ocean Institute and Rinehart Coastal Research Center, Woods Hole, Massachusetts.

Caldwell, J.M. (1949) Beach Erosion. *The Scientific Monthly*, **69**, 229-235.

Carter, R.W.G. (1991) Near-future sea level impacts on coastal dune landscapes. *Landscape Ecology (Historical Archive)*, **6**, 29-39.

Carter, R.W.G. & Orford, J.D. (1993) The morphodynamics of coarse clastic beaches and barriers: a short and long-term perspective. *Journal of Coastal Research*, **Special Issue 15**, 158-179.

Carter, R.W.G. & Woodroffe, C.D. (1997). Coastal evolution: an introduction. In *Coastal Evolution: Late Quaternary shoreline morphodynamics* (eds R.W.G. Carter & C.D. Woodroffe), pp. 1-31. Cambridge University Press, Cambridge, U.K.

Casey, T.L. (1911) Subsidence of Atlantic Shoreline. *Science*, **34**, 80-81.

Cazenave, A. & Nerem, R.S. (2003) Present-Day Sea Level Rise: Observations and Causes. *Geophysical Research Abstracts*, **5**.

Chang, G.C. & Dickey, T.D. (2001) Sediment resuspension over a continental shelf during Hurricanes Edouard and Hortense. *Journal of Geophysical Research*, **106**, 9517-9531.

Changnon, S.A., Changnon, D., Fosse, E.R., Hoganson, T., Roth Sr., R.J., & Totsch, J. (1997) Effects of Recent Weather Extremes on the Insurance Industry: Major Implications for the Atmospheric Sciences. *American Meterological Society*, **78**, 425-435.

Church, J.A. (2007) OCEANS: A Change in Circulation? *Science*, **317**, 908-909.

Church, M. & Ryder, J.M. (1972) Paraglacial Sedimentation: A Consideration of Fluvial Processes Conditioned by Glaciation. *Geological Society of America Bulletin*, **83**, 3059-3072.

Cicin-Sain, B. & Knecht, R.W. (1999). Coastal Tourism and Recreation: The Driver of Coastal Development. Center for the Study of Marine Policy, University of Delaware and NOAA, National Ocean Service.

Clark, P.U., Pisias, N.G., Stocker, T.F., & Weaver, A.J. (2002) The role of the thermohaline circulation in abrupt climate change. *Nature*, **415**, 863-869.

Coastal Landform (2008a) Encyclopεαdia Britannica. from Encyclopædia Britannica Online.

Coastal Landform (2008b) Encylopαεdia Britannica Online, Vol. 2008.

Cohen, J.E., Small, C., Mellinger, A., Gallup, J., Sachs;, J., Vitousek, P.M., & Mooney;, H.A. (1997) Estimates of Coastal Populations. *Science*, **278**, 1209c-1213.

Cross, V.A. (2004) Digitial Cape Cod and the Islands Geologic Map. This is part of the following larger work: Hallett, B.W., Paskevich, V.F., Poppe, L.J., Brand, S.G., and Blackwood, D.S. (2004). *A Pictorial Survey of the Bedrock Beneath Western Cape Cod, Massachusetts: Open-File Report 03-001*, U.S. Geological Survey, Coastal and Marine Geology Program, Woods Hole Science Center, Woods Hole, MA. The source map is from R.N. Oldale and R.A. Barlow, 1986. Geological Map of Cape Cod and the Islands, Massachusetts 1986. Miscellaneous Investigation Series, Map I-1763., Woods Hole, Massachusetts.

Crosset, K.M., Culliton, T.J., Wiley, P.C., & Goodspeed, T.R. (2004). Population Trends Along the Coastal United States: 1980-2008. U.S. Department of Commerce, National Oceanic and Atmospheric Administration, National Ocean Service.

Crowell, M. & Leatherman, S.P. (1999) Coastal Erosion Mapping and Management. *Journal of Coastal Research*, pp.196.

Culliton, T.J. (1998). Population: Distribution, Density, and Growth. National Oceanic and Atmospheric Administration, Silver Spring, MD.

Cunningham, S.A., Kanzow, T., Rayner, D., Baringer, M.O., Johns, W.E., Marotzke, J., Longworth, H.R., Grant, E.M., Hirschi, J.J.-M., Beal, L.M., Meinen, C.S., & Bryden, H.L. (2007) Temporal Variability of the Atlantic Meridional Overturning Circulation at 26.5^0 N. *Science*, **317**, 935-938.

Dalrymple, R.A. (1997) Depth of Closure. Center for Applied Coastal Research, Ocean Engineering Laboratory, University of Delaware, Newark, DE.

Dao, H. (1998). Calculated for Earthwatch by Hy DAO. Department of Geography, University of Geneva, using ArcWorld (1:3,000,000) with horizontal distances corrected for latitude.

Denny, M.W. (1987) Life in the Maelstrom: The biomechanics of wave-swept rocky shores. *Trends in Ecology & Evolution*, **2**, 61-66.

Denny, M.W. (1988) *The Biology and Mechanics of the Wave-Swept Environment* Princeton University Press, Princeton, NJ.

DGS (1998) Storms of 1998, What is a Northeaster? Why are Northeasters Damaging Storms? In Open File Report No. 40 Summary Report, The Coastal Storms of January 27-29 and February 4-6, 1998, Delaware and Maryland. Delaware Geological Survey, University of Delaware, Newark, DE.

Dickey, T.D. & A.J. Williams III (2001) Interdisciplinary ocean process studies on the New England shelf. *Journal of Geophysical Research*, **106**, 9427-9434.

Dodge, S.D. (1935) A Study of Population Regions in New England on a New Basis. *Annals of the Association of American Geographers*, **25**, 197-210.

DOE (2006) Coastal Zone Management Act and related legislation, DOE Environmental Policy & Guidance. Department of Energy, U.S., Washington, D.C.

Dolan, R. (1966) Beach Changes on the Outer Banks of North Carolina. *Annals of the Association of American Geographers*, **56**, 699-711.

Douglas, B.C., Kearney, M.S., & Leatherman, S.P. (2001) *Sea Level Rise: History and Consequences*, First edn. Academic Press.

Douglass, S.L. (2002) Saving America's Beaches: The Causes of and Solutions to Beach Erosion. In Advanced Series on Ocean Engineering, Vol. 19. World Scientific, New Jersey.

Dowdeswell (2006) The Greenland Ice Sheet and Global Sea-Level Rise. *Science*, **311**, 963-964.

Dowsett, H.J., Thompson, R., Barron, J., Cronin, T., Fleming, F., Ishman, R., Poore, D., Willard, D., & Holtz, T. (1994) Joint investigationsof the Middle Pliocene climate. *Global and Planetary Change*, **9**, 169-195.

Edwards, R.J., van de Plassche, O., Gehrels, W.R., & Wright, A.J. (2004) Assessing sea-level data from Connecticut, USA, using a foraminiferal transfer function for tide level. *Marine Micropaleontology*, **51**, 239-255.

Ellis, M.Y. (1978) *Coastal Mapping Handbook* Department of the Interior, U.S. Geological Survey and U.S. Department of Commerce, National Ocean Service and Office of Coastal Zone Management, U.S. Government Printing Office, Washington, D.C.

El-Raey, M., Dewidar, K., & El-Hattab, M. (1999) Adaptation to the Impacts of Sea Level Rise in Egypt. *Mitigation and Adaptation Strategies for Global Change*, **4**, 343-361.

Emanuel, K. (2005) Increasing destructiveness of tropical cyclones over the past 30 years. *Nature*, **436**, 686-688.

Emanuel, K. (2006) Environmental Influences on Tropical Cyclone Variability and Trends. In Proceedings of 27th Conference on Hurricanes and Tropical Meterology. American Meterological Society (AMS), Boston, MA, Monterey, California.

Emanuel, K.A. (1987) The dependence of hurricane intensity on climate. *Nature*, **326**, 483-485.

Emery, K.O. & Uchupi, E. (1972) *Western North Atlantic Ocean: topography, rocks, structure, water, life, and sediments,* American Association of Petroleum Geologists, Tulsa, Oklahoma.

EPA (1997) Climate Change and Massachusetts, EPA 230-F-97-008u. United States Environmental Protection Agency, Office of Policy, Planning and Evaluation.

EPA (2005) Wet Weather Flow Research, Glossary, Terms and Acronyms. United States Environmental Protection Agency, Washington, D.C.

EPA (2006) Emissions. United States Environmental Protection Agency, Washington, D.C.

EPA (2008) Risk Assessment Portal, Vol. 2008. U.S. Environmental Protection Agency, Washington, D.C.

ESRI® (2006) ESRI®: GIS and Mapping Software, Redlands, California.

Fairchild, H.L. (1926) Pleistocene Features of Southern New England. *Science*, **63**, 260-262.

Fein, I. (2007) Spring Gale Roars Through Island; Norton Point Beach is Breached, Vol. 2007. Vineyard Gazette Online, Edgartown, MA.

Fenster, M., Dolan, R., & Elder, J. (1993) New Method for Predicting Shoreline Positions from Historical Data. *Journal of Coastal Research*, **9**, 147-171.

Field, J.C., Boesch, D.F., Scavia, D., Buddemeier, R., Burkett, V.R., Cayan, D., Fogarty, M., Harwell, M., Howarth, R., Mason, C., Pietrafesa, L.J., Reed, D., Royer, T., Sallenger, A., Spranger, M., & G.Titus, J. (2001). Potential Consequences of Climate Variability and Change on Coastal Areas and Marine Resources, Chapter 16. US Climate Change Science Program/US Global Change Research Program, Washington, D.C.

Finkl, C. (1996) Potential Impacts of a Federal Policy Promoting "No New Beach Replenishment Activities" on U.S. Shorelines: Iterations from SE Florida. *Proceedings of the 1996 National Conference on Beach Preservation Technology*, 281-296.

Finkl, C.W. (2004) Coastal Classification: Systematic Approaches to Consider in the Development of a Comprehensive Scheme. *Journal of Coastal Research*, **20**, 166-213.

Fisher, N., Dolan, R., & Hayden, B.P. (1984) Variations in Large-Scale Beach Amplitude Along the Coast. *Journal of Sedimentary Research*, **54**, 73-85.

FitzGerald, D.M., Buynevich, I.V., Davis, R.A., & Fenster, M.S. (2002) New England tidal inlets with special reference to riverine-associated inlet systems. *Geomorphology*, **48**, 179-208.

FitzGerald, D.M., Buynevich, I.V., Fenster, M.S., & McKinlay, P.A. (2000) Sand dynamics at the mouth of a rock-bound, tide-dominated estuary. *Sedimentary Geology*, **131**, 25-49.

FitzGerald, D.M., Rosen, P.S., & van Heteren, S. (1994). New England Barriers. In *Geology of Holocene Barrier Island Systems* (ed Edited by R.A. Davis Jr.), pp. 305-394. Springer-Verlag, Berlin.

Fitzgerald, D.M. & Van Heteren, S. (1999) Classification of paraglacial barrier systems: coastal New England, USA. *Sedimentology*, **46**, 1083-1108.

Flanagan, S.M., Nielsen, M.G., Robinson, K.W., & Cole, J.F. (1999). Water-Quality Assessment of the New England Coastal Basins in Maine, Massachusetts, New Hampshire, and Rhode Island: Environmental Settings and Implications for Water Quality and Aquatic Biota. U.S. Department of the Interior, U.S. Geological Survey, Pembroke, New Hampshire.

Fletcher, P.C. & Roffinoli, R.J. (1986). Soil Survey of Dukes County, Massachusetts. U.S. Department of Agriculture Soil Conservation Service, Washington, D.C.

Forbes, D.L., Orford, J.D., Carter, R.W.G., Shaw, J., & Jennings, S.C. (1995) Morphodynamic evolution, self-organisation, and instability of coarse-clastic barriers on paraglacial coasts. *Marine Geology, Large-Scale Coastal Behavior*, **126**, 63-85.

Forbes, D.L., Parkes, G.S., Manson, G.K., & Ketch, L.A. (2004) Storms and shoreline retreat in the southern Gulf of St. Lawrence. *Marine Geology*, **210**, 169-204.

Forbes, D.L. & Syvitski, J.P.M. (1997). Paraglacial Coasts. In *Coastal Evolution: Late Quaternary Shoreline Morphodynamics* (eds R.W.G. Carter & C.D. Woodroffe), pp. 373-424. University Press, Cambridge, U.K.

Forbes, D.L. & Taylor, R.B. (1987). Coarse-grained beach sedimentation under paraglacial conditions, Canadian Atlantic coast. In *Glaciated Coasts* (ed Editors D.M. FitzGerald and P.S. Rosen), pp. 51-86. Academic Press, San Diego.

Foster, D.R., Hall, B., Barry, S., Clayden, S., & Parshall, T. (2002) Cultural, environmental and historical controls of vegetation patterns and the modern conservation setting on the island of Martha's Vineyard, USA. *J Biogeography*, **29**, 1381-1400.

Fullerton, D.S. & Bush, C.A. (2004) Glacial Limits, Vol. 2008. U.S. Geological Survey, The National Atlas of the United States.

Fullerton, D.S., Bush, C.A., & Pennell, J.N. (2004) Map of Surficial Deposits and Materials in the Eastern and Central United States (East of 102 Degrees West Longitude), Version 1.0, Vol. 2008. U.S. Geological Survey Geologic Investigations Series I-2789, U.S. Department of the Interior, U.S Geological Survey (USGS), Denver, Colorado.

Garson, D.G. (2008) Factor Analysis. North Carolina State University.

Gehrels, W.R., Belknap, D.F., Black, S., & Newnham, R.M. (2002) Rapid sea-level rise in the Gulf of Maine, USA, since AD 1800. *Holocene*, **12**, 383-390.

Gehrels, W.R., Kirby, J.R., Prokoph, A., Newnham, R.M., Achterberg, E.P., Evans, H., Black, S., & Scott, D.B. (2005) Onset of recent rapid sea-level rise in the western Atlantic Ocean. *Quaternary Science Reviews*, **24**, 2083-2100.

Geng, Q. & Sugi, M. (2001) Variability of the North Atlantic Cyclone Activity in Winter Analyzed from NCEP–NCAR Reanalysis Data. *Journal of Climate*, **14**, 3863-3873.

Giese, G. (1997). Potential Impacts of Sea-Level Rise in Massachusetts. New England Regional Climate Change Impacts Workshop Summary Report, September 3-5, 1997, Woods Hole Oceanographic Institution.

Giese, G.S., Aubrey, D.G., & Zeeb, P. (1987). Passive Retreat of Massachusetts Coastal Upland Due to Relative Sea-Level Rise.

Giles, J. (2005) Climate sceptics place bets on world cooling down. *Nature*, **436**, 897.

Gookin, W.F. (1949) Who was Bartholomew Gosnold? *The William and Mary Quarterly, 3rd Ser.*, **6**, 398-415.

Gray, W.M. (2006) Global Warming and Hurricanes. In Proceedings of 27th Conference on Hurricanes and Tropical Meterology. American Meterological Society (AMS), Boston, MA, Monterey, California.

Haarsma, R.J., Mitchell, J.F.B., & Senior, C.A. (1993) Tropical disturbances in GCM. *Climate Dynamics*, **8**, 247-257.

Hair, J.F., Anderson, R.E., & Tatham, R.L. (1987) *Multivariate data analysis with readings*, Second edn. Macmillan Publishing Company, New York, NY.

Hansen, J. (2007) Global Warming: The Threat to the Planet (2007 Leo Szilard Lecture). American Physical Society, Jacksonville, Florida.

Hansen, J., Sato, M., Kharecha, P., Russell, G., Lea, D.W., & Siddall, M. (2007) Climate change and trace gases. *Phil. Trans. R. Soc. Lond. A, The Royal Society*, **365**, 1925-1954.

Hardin, G. (1968) The Tragedy of the Commons. *Science*, **162**, 1243-1248.

Hebert, P.J., Jarrell, J.D., & Mayfield, M. (1996). The Deadliest, Costliest, and Most Intense United States Hurricanes of the Century (and Other Frequently Requested Hurricane Facts). National Hurricane Center, Coral Gables, Florida.

Hill, H.W., Kelley, J.T., Belknap, D.F., & Dickson, S.M. (2004) The effects of storms and storm-generated currents on sand beaches in Southern Maine, USA. *Marine Geology, Storms and their significance in coastal morpho-sedimentary dynamics*, **210**, 149-168.

Hoel, M.L. (1986) *Land's Edge: A Natural History of Barrier Beaches from Maine to North Carolina*, First edn. The Little Book Publishing Company, Newbury, Massachusetts.

Horn, D.P. (2006) Measurements and modelling of beach groundwater flow in the swash-zone: a review. *Continental Shelf Research, Swash-Zone Processes*, **26**, 622-652.

Houghton, R. (2004) Global Carbon Cycle. Woods Hole Research Center, Woods Hole, MA.

Houston, J.R. (1996). The Economic Value of Beaches. Florida Shore & Beach Preservation Association.

Hoyos, C.D., Agudelo, P.A., Webster, P.J., & Curry, J.A. (2006) Deconvolution of the Factors Contributing to the Increase in Global Hurricane Intensity. *Science*, **312**, 94-97.

Imbrie, J., Boyle, E., Clemens, S., Duffy, A., Howard, W., Kukla, G., Kutzbach, J., Martinson, D., McIntyre, A., Mix, A., Molfino, B., Morley, J., Peterson, L., Pisias, N., Prell, W., Raymo, M., Sackleton, N., & Toggweiler, J. (1992) On the structure and origin of major glaciation cycles. 1. Linear responses to Milankovitch forcing. *Paleoceanography*, **7**, 701-738.

Institute for Geophysics (2005) Atmosphere and Ocean Dynamics, Vol. 2005. University of Texas, Austin, Texas.

IPCC (2001a). Climate Change 2001: Impacts, Adaptation, and Vulnerability. Prepared under the guidance of Working Group II Co-chairmen Osvaldo Canziani (Argentina) and James McCarthy (US). Cambridge University Press, Cambridge, United Kingdom and New York, NY, USA.

IPCC (2001b). Climate Change 2001: Third Assessment Report (TAR). World Meteorological Organization and United Nations Environment Programme, Geneva, Switzerland.

IPCC (2002). Climate Change and Biodiversity. World Meteorological Organization and United Nations Environment Programme, Geneva, Switzerland.

IPCC (2006) Intergovernmental Panel on Climate Change (IPCC). World Meteorological Organization and United Nations Environment Programme, Geneva, Switzerland.

IPCC (2007) Climate Change 2007. In Intergovernmental Panel on Climate Change (IPCC). World Meteorological Organization and United Nations Environment Programme, Geneva, Switzerland.

IPCC WGI (2007). Climate Change 2007: The Physical Science Basis. Contribution of Working Group I to the Fourth Assessment Report of the Intergovernmental Panel on Climate Change (IPCC). Cambridge University Press, Cambridge, United Kingdom and New York, NY, USA.

Jaffe, B.E., List, J.H., & Sallenger Jr., A.H. (1997). Massive sediment bypassing on the lower shoreface offshore of a wide tidal inlet. In *Marine Geology*, Vol. 136, pp. 131-149. Cat Island Pass, Louisiana.

Johannessen, O.M., Khvorostovsky, K., Miles, M.W., & Bobylev, L.P. (2005) Recent Ice-Sheet Growth in the Interior of Greenland. *Sciencexpress Report*.

Johnson, D.W. (1910) The Supposed Recent Subsidence of the Massachusetts and New Jersey Coasts. *Science*, **32**, 721-723.

Johnson, D.W. (1925) *The New England-Acadian Shoreline* Wiley, New York.

Johnson, D.W. & Stolfus, M.A. (1924) The Submerged Coastal Plain and Oldland of New England. *Science*, **59**, 291-293.

Johnston, K., Ver Hoef, J.M., Krivoruchko, K., & Lucas, N. (2003). ArcGIS® 9, Using ArcGIS Geostatistical Analyst®. ESRI®, Redlands, California.

Jones, S.R. & Mangun, W.R. (2001) Beach nourishment and public policy after Hurricane Floyd: where do we go from here? *Ocean & Coastal Management*, **44**, 207-220.

Kaiser, H.F. (1960) The application of electronic computers to factor analysis. *Educational and Psychological Measurement*, **20**, 141-151.

Kana, T.W. (1995) A mesoscale sediment budget for Long Island, New York. *Marine Geology, Large-Scale Coastal Behavior*, **126**, 87-110.

Kanzow, T., Cunningham, S.A., Rayner, D., Hirschi, J.J.-M., Johns, W.E., Baringer, M.O., Bryden, H.L., Beal, L.M., Meinen, C.S., & Marotzke, J. (2007) Observed Flow Compensation Associated with the MOC at 26.5^0 N in the Atlantic. *Science*, **317**, 938-941.

Karl, T.R. & Trenberth, K.E. (2003) Modern Global Climate Change. *Science*, **302**, 1719-1723.

Kates, R.W., Clark, W.C., Corell, R., Hall, J.M., Jaeger, C.C., Lowe, I., McCarthy, J.J., Schellnhuber, H.J., Bolin, B., Dickson, N.M., Faucheux, S., Gallopin, G.C., Grubler, A., Huntley, B., Jager, J., Jodha, N.S., Kasperson, R.E., Mabogunje, A., Matson, P., Mooney, H., Moore III, B., O'Riordan, T., & Svedlin, U. (2001) Environment and Science: Sustainability Science. *Science*, **292**, 641-642.

Keeling, C.D. & Whorf, T.P. (2004). Atmospheric CO2 records from sites in the SIO air sampling network. Carbon Dioxide Information Analysis Center, Oak Ridge National Laboratory, U.S. Department of Energy, Oak Ridge, Tenn.

Keim, B.D., Muller, R.A., & Stone, G.W. (2004) Spatial and temporal variability of coastal storms in the North Atlantic Basin. *Marine Geology*, **210**, 7-15.

Kennedy, D. & Hanson, B. (2006) Ice and History. *Science*, **311**, 1673.

Kent, M., Newnham, R., & Essex, S. (2002) Tourism and sustainable water supply in Mallorca: a geographical analysis. *Applied Geography*, **22**, 351-374.

Kerr, R.A. (2005) Greenhouse Warming: Climate Modelers See Scorching Future as a Real Possibility. *Science*, **307**, 497a.

Kerr, R.A. (2006a) Climate Change: A Worrying Trend of Less Ice, Higher Seas. *Science*, **311**, 1698-1701.

Kerr, R.A. (2006b) Climatology: A Tempestuous Birth for Hurricane Climatology. *Science*, **312**, 676-678.

Kintisch, E. (2005) Climate Change: Global Warming Skeptic Argues U.S. Position in Suit. *Science*, **308**, 482.

Klein, Y.L., Osleeb, J.P., & Viola, M.R. (2004) Tourism-Generated Earnings in the Coastal Zone: A Regional Analysis. *Journal of Coastal Research*, **20**, 1080–1088.

Kocin, P.J. & Uccellini, L.W. (2004) A Snowfall Impact Derived from Northeast Storm Snowfall Distributions. *Bulletin of the American Meterological Society*, **85**, 177-194.

Kunte, P.D. & Wagle, B.G. (1994) Analysis of space-borne data for coastal zone information extraction of Goa coast, India. *Ocean & Coastal Management*, **22**, 187-200.

Lambeck, K., Esat, T.M., & Potter, E.-K. (2002) Links between climate and sea levels for the past three million years. *Nature*, **419**, 199-206.

Leatherman, S.P., Douglas, B.C., & Crowell, M. (1998) Considerations for shoreline position prediction. *Journal of Coastal Research*, **14**, 1025.

Leatherman, S.P., Zhang, K., & Douglas, B.C. (2000b) Sea Level Rise Shown to Drive Coastal Erosion: A Reply. *EOS Transactions*, **81**, 437-441.

Lorius, C., Jouzel, J., Ritz, C., Merlivat, L., Barkov, N.I., Korotkevich, Y.S., & Kotlyakov, V.M. (1985) A 150,000-year climatic record from Antarctic ice. *Nature*, **316**, 591-596.

MA CZM (2001) Massachusetts Historic Shoreline Change Project. Massachusetts Office of Coastal Zone Management, Boston, Masschusetts.

MA CZM (2002). Massachusetts Coastal Zone Management Plan. The Massachusetts Office of Coastal Zone Management, Commonwealth of Massachusetts, Executive Office of Environmental Affairs, National Oceanic and Atmospheric Administration, Boston, MA.

MA CZM (2006a) Governor Romney's Charge to the Massachusetts Coastal Hazards Commission. Massachusetts Office of Coastal Zone Management, Boston, MA.

MA CZM (2006b) Massachusetts Office of Coastal Zone Management. Commonwealth of Massachusetts.

MA DEP (2007) 310 CMR 10.00: The Wetlands Protection Act Regulations, October 2007. In Wetlands, Vol. 2008, Boston, MA.

Mandelbrot, B.B. (1967) How long is the coast of Britain? Statistical self-similarity and fractional dimension. *Science*, **156**, 636-638.

Mann, K.H. (2000) *Ecology of Coastal Waters, With Implications for Management*, Second edn. Blackwell Science, Malden, Massachusetts.

Marlowe, H. (1999). Assessing the Economic Benefits of America's Coastal Regions. National Oceanic and Atmospheric Administration, Silver Spring, MD.

Marotzke, J. (2000) Abrupt climate change and thermohaline circulation: Mechanisms and predictability. *PNAS*, **97**, 1347-1350.

Marsh, O.C. (1898) The Jurassic Formation of the Atlantic Coast-Supplement. *Science*, **8**, 145-154.

Martha's Vineyard Land Bank Commission (2008) Martha's Vineyard Land Bank Properties, Vol. 2008. Martha's Vineyard Land Bank Commission, Edgartown, Massachusetts.

Mass.Gov (2003) Island of Martha's Vineyard Watershed. In Preserving Massachusetts' Water Resources, Vol. 2005. Executive Office of Environmental Affairs, Boston, Massachusetts.

Massachusetts Ocean Management Task Force (2004). The Massachusetts Ocean Management Task Force Technical Report. Massachusetts Office of Coastal Zone Management, Boston, Ma.

MassGIS (2008) Massachusetts Geographic Information System, Office of Geographic and Environmental Information (MassGIS). Commonwealth of Massachusetts, Executive Office of Energy and Environmental Affairs, Boston, MA.

Matheron, G. (1971) *The Theory of Regionalized Variables and its Applications* E´cole national supe´rieure des mines.

Mayewski, P.A., Keim, B., Zielinski, G.A., Wake, C., Carpenter, K., Cox, J., Souney, J., Sanborn, P., & Rodgers, M. (1998). New England's Changing Climate, Weather, and Air Quality. Climate Change Research Center, Institute for the Study of Earth, Oceans, and Space, University of New Hampshire, Durham, NH.

McCoy, J., Johnston, K., Kopp, S., Borup, B., Willison, J., & Payne, B. (2002). ArcGIS® 9, Using ArcGIS Spatial Analyst®. ESRI®, Redland, California.

McGarigal, K., Cushman, S., & Stafford, S. (2000) *Multivariate Statistics for Wildlife and Ecology Research* Springer-Verlag, New York.

McNinch, J.E. (2004) Geologic control in the nearshore: shore-oblique sandbars and shoreline erosional hotspots, Mid-Atlantic Bight, USA. *Marine Geology*, **211**, 121-141.

Meehl, G.A., Washington, W.M., Collins, W.D., Arblaster, J.M., Hu, A., Buja, L.E., Strand, W.G., & Teng, H. (2005) How Much More Global Warming and Sea Level Rise? *Science*, **307**, 1769-1772.

Meier, M.F. & Wahr, J.M. (2002) Sea level is rising: Do we know why? *PNAS*, **99**, 6524-6526.

Mendenhall, W., Beaver, R.J., & Beaver, B.M. (2003) *Introduction to Probability and Statistics*, Eleventh edn. Brooks/Cole, Thompson Learning Inc.

Michener, W.K., Blood, E.R., Bildstein, K.L., Brinson, M.M., & Gardner, L.R. (1997) Climate Change, Hurricanes and Tropical Storms, and Rising Sea Level in Coastal Wetlands. *Ecological Applications*, **7**, 770-801.

Miller, J.K. & Dean, R.G. (2004) A simple new shoreline change model. *Coastal Engineering*, **51**, 531-556.

Miller, J.K. & Dean, R.G. (2007a) Shoreline variability via empirical orthogonal function analysis: Part I temporal and spatial characteristics. *Coastal Engineering*, **54**, 111-131.

Miller, J.K. & Dean, R.G. (2007b) Shoreline variability via empirical orthogonal function analysis: Part II relationship to nearshore conditions. *Coastal Engineering*, **54**, 133-150.

Minitab 15™ (2006) Statistical Software. Minitab Inc., State College, PA.

Mitchell, J.F.B., Manabe, S., Tokioka, T., & Meleshko, V. (1990). Equilibrium climate change. In *Climate Change: the IPCC scientific assessment* (eds J.T. Houghton, G.J. Jenkins & J.J. Ephraums), pp. 131-172. Cambridge University Press, Cambridge, England.

Mockus, V., Werner, J., Woodward, D.E., Nielsen, R., Dobos, R., Hjelmflt, A., & Hoeft, C.C. (2007). Chapter 7: Hydrologic Soil Groups. United States Department of Agriculture, Natural Resources Conservation Service.

Mood, F. (1933) Why the "Vineyard". *The New England Quarterly*, **6**, 131-136.

Moran, P.A.P. (1948) The Interpretation of Statistical Maps. *Journal of Royal Statistical Society. Series B (Methodological)*, **10**, 243-251.

Morang, A. & Parson, L. (2002). Coastal Terminology and Geologic Environments, Chapter 1. In *Coastal Engineering Manual - Part IV* (ed A. Morang), pp. 54. U.S. Army Corps of Engineers, Coastal & Hydraulics Laboratory, Washington, D.C.

Morang, A. & Parson, L.E. (2006). Coastal Terminology and Geologic Environments, Part IV, Chapter 1. In *Coastal Engineering Manual*, pp. 54. U.S. Army Corps of Engineers, Coastal & Hydraulics Laboratory, Washington, D.C.

Munk, W. (2003) Ocean Science: Ocean Freshening, Sea Level Rising. *Science*, **300**, 2041-2043.

Musgrave, G.W. (1955). How much of the rain enters the soil? In *Water: U.S. Department of Agriculture. Yearbook.*, pp. 151-159, Washington, D.C.

MV Landbank Commission Martha's Vineyard Landbank Commission, Enjoying the Properties, Edgartown, Massachusetts.

MV Times (2008) New breach occurs in Norton Point Beach. In The Martha's Vineyard Times.

MVC (2004) Martha's Vineyard Commission, Vol. 2005, Oak Bluffs, MA.

MVC (2005). Martha's Vineyard Indicators Project: Measures of Sustainability. Martha's Vineyard Commission (MVC), Oak Bluffs, MA.

MVC (2006) Economic Profile of Martha's Vineyard. Martha's Vineyard Commission (MVC), Oak Bluffs, MA.

NAP (1999) *The Impacts of Natural Disasters: A Framework for Loss Estimation* National Academy Press, Commission on Geosciences, Environment and Resources, Committee on Assessing the Coasts of Natural Disasters, National Research Council.

NECC (2003) Global Warming in New England States (ed T. Dutzik). New England Climate Coalition.

NERA (2002). NERA Foundation Document. New England Regional Assessment, Institute for the Study of Earth, Oceans, and Space. Morse Hall, University of New Hampshire, Durham, New Hampshire.

Nicholls, R.J. (2004) Coastal flooding and wetland loss in the 21st century: changes under the SRES climate and socio-economic scenarios. *Global Environmental Change, Climate Change*, **14**, 69-86.

Nicholls, R.J., Birkemeier, W.A., & Lee, G.-h. (1998) Evaluation of depth of closure using data from Duck, NC, USA. *Marine Geology*, **148**, 179-201.

NOAA (1998) Climatic Wind Data for the United States. National Climatic Data Center, National Oceanographic Atmospheric Administration, Ashville, North Carolina.

NOAA (2003a) Beach Nourishment - Barrier Islands: Formation and Evolution. National Oceanic Atmospheric and Administration, U.S. Department of Commerce, Silver Spring, Maryland.

NOAA (2003b) Beach Nourishment - Coastal Geology, Coastal Ecology, Human Dimension, Engineering. In A Guide for Local Government Officials. National

Oceanic Atmospheric and Administration, U.S. Department of Commerce, Silver Spring, Maryland.

NOAA (2003c) Geologic Regimes of the Atlantic and Gulf Coasts. National Oceanic Atmospheric and Administration, U.S. Department of Commerce, Silver Spring, Maryland.

NOAA (2003d) Woods Hole, MA, Station ID:8447930. In Tides & Currents. U.S. Department of Commerce, National Oceanic and Atmospheric Administration, National Ocean Service, Silver Spring, Maryland.

NOAA (2004). An Ocean Blueprint for the 21st Century. Final Report. National Oceanic and Atmospheric Administration, U.S. Department of Commerce, Washington, D.C.

NOAA (2005a). Population Trends Along the Coastal United States: 1980-2008. National Oceanic Atmospheric and Administration, U.S. Department of Commerce, Washington, D.C.

NOAA (2005b). Population Trends Along the Coastal United States: 1980-2008. National Oceanic Atmospheric and Administration, U.S. Department of Commerce.

NOAA (2005c) The Saffir-Simpson Hurricane Scale. National Oceanic and Atmospheric Administration/National Weather Service, National Hurricane Center, Tropical Prediction Center, Miami, Florida.

NOAA (2005d) Tides & Currents, Woods Hole, MA. National Oceanic Atmospheric and Administration, U.S. Department of Commerce, Silver Spring, Maryland.

NOAA (2006a) Climate of 2005 - Annual Climate Review - U.S. Summary. In National Climatic Data Center. National Oceanic and Atmospheric Administration, U.S. Department of Commerce, Silver Spring, Maryland.

NOAA (2006b) Global Warming. National Oceanic Atmospheric and Administration, U.S. Department of Commerce, Silver Spring, Maryland.

NOAA (2006c) NOAA Uses New Post-Storm Rating System for Big Northeast Snowstorms: Winter Storms Ranked Like Tornado F-Scale. National Oceanic Atmospheric Administration (NOAA), U.S. Department of Commerce, NOAA's National Centers for Environmental Prediction, and National Climatic Data Center, Silver Spring, Maryland.

NOAA (2006d) The Northeast Snowfall Impact Scale (NESIS). National Oceanographic Atmospheric Administration (NOAA), U.S. Department of Commerce, Silver Spring, Maryland.

NOAA (2006e) Station Information for Nantucket Island, MA, Vol. 2007. National Oceanographic Atmospheric Administration, National Ocean Service Center for Operational Oceanographic, Products and Services (CO-OPS), 1305 East-West Highway, Silver Spring, Maryland, 20910.

NOAA (2006f) U.S. Climate at a Glance. National Oceanic Atmospheric and Administration, National Climatic Data Center, U.S. Department of Commerce, Silver Spring, Maryland.

NOAA (2007a) Annual Temperature/Precipitation Massachusetts. National Oceanic Atmospheric and Administration, National Climatic Data Center, U.S. Department of Commerce, Silver Springs, Maryland.

NOAA (2007b) Tidal Current Predictions State Selection 2007 (Massachusetts), Vol. 2008. National Ocean Service (NOS), U.S. Department of Commerce, National Oceanic and Atmospheric Administration (NOAA), Silver Spring, Maryland.

NRC (2001) *Climate Change Science: An Analysis of Some Key Questions* National Academy Press, Washington, D.C.

O'Brien, G. (1995) *A Guide to Nature on Cape Cod and the Islands* Parnassus Imprints, Hyannis, MA.

Ogden, I., J. Gordon (1974) Shoreline changes along the southeastern coast of Martha's Vineyard, Massachusetts for the past 200 years. *Quaternary Research*, **4**, 496-508.

Oldale, R.N. (1992) *Cape Cod and the Islands: The Geologic Story*, First edn. Parnassus Imprints, East Orleans, Massachusetts.

Oldale, R.N. (1993/1994) Geologic Origins of Stellwagen Bank. Stellwagen Bank National Marine Sanctuary, reprinted with permission from The Cape Naturalist.

Oldale, R.N. & Barlow, R.A. (1986). Geologic Map of Cape Cod and the Islands, Massachusetts. U.S. Geological Survey (USGS), Woods Hole Science Center, MA.

Oliver, M., Webster, R., & Gerrard, J. (1989) Geostatistics in Physical Geography. Part I: Theory. *Transactions of the Institute of British Geographers*, **14**, 259-269.

Orford, J.D., Forbes, D.L., & Jennings, S.C. (2002) Organisational controls, typologies and time scales of paraglacial gravel-dominated coastal systems. *Geomorphology*, **48**, 51-85.

Orians, G.H. (1986) *An ecological and evolutionary approach to landscape aesthetics* Allen & Unwin, London.

Palm, C., Sanchez, P., Ahamed, S., & Awiti, A. (2007) Soils: A Contemporary Perspective. *Annual Review of Environment and Resources*, **32**, 99-129.

Parris, T.M. & Kates, R.W. (2003) CHARACTERIZING AND MEASURING SUSTAINABLE DEVELOPMENT. *Annual Review of Environment and Resources*, **28**, 559-586.

PBS (2000-2001) World Resources: People and Ecosystems - The Fraying Web of Life. In Earth on Edge: Coastal Ecosystems (ed B. Moyers). World Resources Institute and PBS.

Peltier, W.R. (1999) Global sea level rise and glacial isostatic adjustment. *Global and Planetary Change*, **20**, 93-123.

Peltier, W.R. (2002) Global glacial isostatic adjustment: palaeogeodetic and space-geodetic tests of the ICE-4G (VM2) model. *Journal of Quaternary Science*, **17**, 491-510.

Peltier, W.R. (2007) Will oceans surge 59 centimetres this century - or 25 metres? Department of Physics, University of Toronto.

Perrie, W., Jiang, J., & Zhenxia, L. (2006) The Impact of Climate Change on Northwest Atlantic Extratropical Hurricanes and Winter Storms. In Proceedings of 27th Conference on Hurricanes and Tropical Meterology. American Meterological Society (AMS), Boston, MA, Monterey, California.

Pethick, J.S. (1984) *An Introduction to Coastal Geomorphology* John Wiley & Sons.

Petit, J.R., Jouzel, J., Raynaud, D., Barkov, N.I., Barnola, J.-M., Basile, I., Bender, M., Chappellaz, J., Davis, M., Delaygue, G., Delmotte, M., Kotlyakov, V.M., Legrand, M., Lipenkov, V.Y., Lorius, C., PEpin, L., Ritz, C., Saltzman, E., & Stievenard, M. (1999) Climate and atmospheric history of the past 420,000 years from the Vostok ice core, Antarctica. *Nature*, **399**, 429-436.

Philander, S.G. (2000) *Is the Temperature Rising? The Uncertain Science of Global Warming* Princeton University Press.

Phillips, J.D. (1986) Spatial Analysis of Shoreline Erosion, Delaware Bay, New Jersey. *Annals of the Association of American Geographers*, **76**, 50-62.

Phillips, M.R. & Williams, A.T. (2007) Depth of Closure and Shoreline Indicators: Empirical Formulae for Beach Management. *Journal of Coastal Research*, **23**, 487-500.

Pielke, R.A., Jr. (1997). Trends in Hurricane Impacts in the United States. Environmental and Societal Impacts Group, National Center for Atmospheric Research, Boulder, Colorado.

Pirazzoli, P.A. (1997). Tectonic Shorelines. In *in Coastal Evolution: Late Quaternary Shoreline Morphodynamics* (eds Editors, R.W.G. Carter & C.D. Woodroffe), pp. 517. Cambridge University Press, Cambridge, United Kingdom.

Plum Vineyard (2007) Chappy Breaks Up with Martha's Vineyard. Plum TV Inc., Martha's Vineyard.

Poag, C.W. (1978) Stratigraphy of the Atlantic Continental Shelf and Slope of the United States. *Annual Review of Earth and Planetary Sciences*, **6**, 251-280.

Priscu, J.C., Adams, E.E., Lyons, W.B., Voytek, M.A., Mogk, D.W., Brown, R.L., McKay, C.P., Takacs, C.D., Welch, K.A., Wolf, C.F., Kirshtein, J.D., & Avci, R. (1999) Geomicrobiology of Subglacial Ice Above Lake Vostok, Antarctica. *Science*, **286**, 2141-2144.

PSMSL (2006) Permanent Service for Mean Sea Level, Vol. 2007. Proudman Oceanographic Laboratory, Liverpool, United Kingdom.

Rahmstorf, S., Cazenave, A., Church, J.A., Hansen, J.E., Keeling, R.F., Parker, D.E., & Somerville, R.C.J. (2007) Recent Climate Observations Compared to Projections. *Science*, **316**, 709.

Redfield, A.C. (1967) Postglacial Change in Sea Level in the Western North Atlantic Ocean. *Science*, **157**, 687-692.

Rico, R. & Rico, A. (1998) Billingsgate Island Light, Lighthouse Page.

Rignot, E. & Kanagaratnam, P. (2006) Changes in the Velocity Structure of the Greenland Ice Sheet. *Science*, **311**, 986-990.

Rindfuss, R.R., Walsh, S.J., Turner, B.L., II, Fox, J., & Mishra, V. (2004) Developing a science of land change: Challenges and methodological issues. *PNAS*, **101**, 13976-13981.

Robbins, R. (1994) Vernacular American Landscape: Methodists, Camp Meetings, and Social Respectability. *Religion and American Culture*, **4**, 165-191.

Robinson Jr., G.R. & Kapo, K.E. (2003) Generalized lithology and lithogeochemical character of near-surface bedrock in the New England region. In U.S. Geological Survey Open-File Report, 03-225. U.S. Geological Survey, Reston, VA.

Rohling, E.J., Fenton, M., Jorissen, F.J., Bertrand, P., Ganssen, G., & Caulet, J.P. (1998) Magnitudes of sea-level lowstands of the past 500,000 years. *Nature*, **394**, 162-165.

Roman, C.T. & Nordstrom, K.F. (1988) The effect of erosion rate on vegetation patterns of an east coast barrier island. *Estuarine, Coastal and Shelf Science*, **26**, 233-242.

Sanford, S. (1915) The Rise of Sea Level Shown by Coastal Dunes. *Science*, 348-349.

SAS (2008) Principal Component Analysis, Chapter 1. SAS Institute Inc.

Saunders, M.A. (2006) Increasing Atlantic Hurricane Activity in Prospect from Global Warming. In Proceedings of 27th Conference on Hurricanes and Tropical Meterology. American Meterological Society (AMS), Boston, MA, Monterey, California.

Schlee, J., Behrendt, J.C., Grow, J.A., Robb, J.M., Mattick, R., Taylor, P.T., & Lawson, B.J. (1976) Regional geologic framework off northeastern United States. *AAPG Bulletin*, **60**, 926-951.

Scott, D. (2003) Climate change and tourism and the mountain regions of North America. In Climate Change and Tourism, Proceedings of the first International Conference on Climate Change and Tourism. World Tourism Organisation, Madrid, Djerba, Tunisia.

Scott, D., McBoyle, G., & Mills, B. (2003) Climate change and the skiing industry in Southern Ontario (Canada): exploring the importance of snowmaking as a technical adaptation. *Climate Research*, **23**, 171-181.

Scripps Institution of Oceanography (2005) Charles David Keeling: Climate Science Pioneer 1928-2005, Vol. 2005. Scripps Institution of Oceanography, University of California, San Diego.

Sea Grant Woods Hole (2003) New Shoreline Change Data Reveal Massachusetts is Eroding. In Marine Extension Bulletin. Woods Hole Oceanographic Institution Sea Grant Program, Cape Cod Cooperative Extension, Woods Hole, MA.

Seccombe, M. (2007) County Seeks Disaster Funds Following Breach at Katama, County Manager Joins Rush for State, Federal Money, and Takes Heat for It, Vol. 2007. Vineyard Gazette Online, Edgartown, MA.

Shepard, F.P. (1954) Nomenclature based on sand-silt-clay ratios. *Journal of Sedimentary Petrology*, **24**, 151-158.

Shepard, F.P. & Wanless, H.R. (1971) *Our Changing Coastline* McGraw-Hill, New York.

Sheriff's Meadow Foundation (2005) Cedar Tree Neck Sanctuary, Vol. 2008. Sheriff's Meadow Foundation, A Vineyard Land Trust, Vineyard Haven, Massachusetts.

Shlyakhter, A. & Wilson, R. (1997). Integrated Risk Analysis of Global Climate Change. In *Fundamentals of Risk Analysis and Risk Management* (ed V. Molak), pp. 472. Lewis Publishers, a CRC Press Company, Boca Raton, Florida.

Sigelman, N. (2007) County manager would heal Norton Point breach. The Martha's Vineyard Times, Vineyard Haven.

Sigman, D.M. & Boyle, E.A. (2000) Glacial/interglacial variations in atmospheric carbon dioxide. *Nature*, **407**, 859-869.

Simmonds, I. & Keay, K. (2002) Surface fluxes of momentum and mechanical energy over the North Pacific and North Atlantic Oceans. *Meteorol. Atmos. Phys.*, **80**, 1-18.

Smith, H.J. (2004) Climate Science: All Rise. *Science*, **304**, 1877d-.

Smith, H.T.U. (1954) Coastal Dunes. In Proceedings of the Coastal Geography Conference. Office of Naval Research, Department of the Navy, Washington, D.C.

Soil Survey Division (2002) Official Soil Series Descriptions, View by Name, Vol. 2008. USDA-NRCS Soil Survey Division, U.S. Department of Agriculture (USDA), Natural Resources Conservation Service (NRCS).

Soil Survey Division Staff (1993) *Soil Survey Manual* Soil Conservation Service, U.S. Department of Agriculture, Natural Resources Conservation Service, Handbook 18.

Soil Survey Staff (1999). Soil Taxonomy: A Basic System of Soil Classification for Making and Interpreting Soil Surveys, Second Edition, Agriculture Handbook, Number 436. United States Department of Agriculture and Natural Resources Conservation Service.

Soil Survey Staff (2006). Keys to Soil Taxonomy, Tenth Edition. United States Department of Agriculture and Natural Resources Conservation Service.

Soil Survey Staff (2007) U.S. General Soil Map (STATSGO2), Vol. 2008. United States Department of Agriculture and Natural Resources Conservation Service.

Souza, A.J., Dickey, T.D., & Chang, G.C. (2001) Modeling water column structure and suspended particulate matter on the Middle Atlantic continental shelf during the passages of Hurricanes Edouard and Hortense. *Journal of Marine Research*, **59**, 1021-1045.

SPARC (2006) Climate Change and Disaster Losses: Understanding and Attributing Trends and Projections. In Workshop on Climate Change and Disaster Losses (eds P. Hoppe & R.A. Pielke, Jr.), pp. pp. 270. Science Policy Assessment and Research on Climate (SPARC), U.S. National Science Foundation, GKSS Institute for Coastal Research, and Tyndall Centre for Climate Change Research, Hohenkammer, Germany.

Stainforth, D.A., Aina, T., Christensen, C., Collins, M., Faull, N., Frame, D.J., Kettleborough, J.A., Knight, S., Martin, A., Murphy, J.M., Piani, C., Sexton, D., Smith, L.A., Spicer, R.A., Thorpe, A.J., & Allen, M.R. (2005) Uncertainty in predictions of the climate response to rising levels of greenhouse gases. *Nature*, **433**, 403-406.

Steffen, K., S.V. Nghiem, R. Huff, G. Neumann (2004) The melt anomaly of 2002 on the Greenland Ice Sheet from active and passive microwave satellite observations. *Geophysical Research Letters*, **31**.

Stronge, W.D. (2001). The Economic Value of our Beaches and Coastal Properties, Florida Shore & Beach Preservation Association.

Sykes, L.R. (1978) Intraplate Seismicity, Reactivation of Preexisting Zones of Weakness Alkaline Magmatism, and Other Tectonism Postdating Continental Fragmentation. *Reviews of Geophysics and Space Physics*, **16**, 621.

Tarbuck, E.J. & Lutgens, F.K. (2000) *Earth Science*, Ninth edn. Prentice Hall, Upper Saddle River, New Jersey.

The Heinz Center (2000) Evaluation of Erosion Hazards. In A Collaborative Project of The H. John Heinz III Center for Science, Economics and the Environment, Vol. 2005. Prepared for the Federal Emergency Management Agency, Contract EMW-97-CO-0375.

The Maury Project (1998) Visit to an Ocean Planet. In Seawater Mixing and Sinking. American Meterological Society, NASA Jet Propulsion Laboratory, California Institute of Technology.

The Trustees of Reservations (2006a) Coastal Salt Ponds and Their Watersheds, West Tisbury, Vol. 2006. The Trustees of Reservations, Martha's Vineyard, Massachusetts.

The Trustees of Reservations (2006b) Long Point Wildlife Refuge, Martha's Vineyard, Massachusetts.

The Trustees of Reservations (2007) Norton Point Beach, Martha's Vineyard.

Thieler, E.R. & Hammar-Klose, E.S. (1999). National Assessment of Coastal Vulnerability to Sea-Level Rise: Preliminary Results for the U.S. Atlantic Coast, U.S. Geological Survey Open-File Report 99-593. U.S. Geological Survey, Woods Hole Field Center, Woods Hole, Massachusetts.

Thieler, E.R., O'Connell, J.F., & Schupp, C.A. (2001). Massachusetts Historic Shoreline Change Project: 1800s to 1994, Technical Report. U.S. Geological Survey and Woods Hole Oceanographic Institution, Woods Hole, MA.

Tobler, W. (1970) A Computer Movie Simulating Urban Growth in the Detroit Region. *Economic Geography*, **46**, 234-240.

Townsend, C.W. (1911) Coastal Subsidence in Massachusetts. *Science*, **33**, 64.

Townsend, D.W., Thomas, A.C., Mayer, L.M., Thomas, M.A., & Quinlan, J.A. (2004). Oceanography of the Northwest Atlantic Continental Shelf, Chapter 5. In *The Sea: The Global Coastal Ocean: Interdisciplinary Regional Studies and Synthees* (eds A.R. Robinson & K.H. Brink), pp. 1-57. Harvard University Press.

Townsend, I. & Pethick, J. (2002) Estuarine flooding and managed retreat. *Phil. Trans. R. Soc. Lond. A, The Royal Society*, **360**, 1477-1495.

Trochim, W.M. (2006) The Research Methods Knowledge Base:Correlation, 2nd Edition., Vol. 2008.

Tuan, Y.-F. (1990) *Topophilia: A Study of Environmental Perception, Attitudes, and Values* Columbia University Press Morningside Edition, New York.

Turenne, J. (2007) Soil Survey Data For New England States, Warwick, Rhode Island.

Twichell, D.C., Butman, B., & Lewis, R.S. (1987). Shallow structure, surficial geology and processes currently shaping the bank. In *in Georges Bank* (ed R.H. Backus), pp. 31-38. MIT Press, Cambridge, MA.

U.S. Census Bureau (2008), Vol. Accessed in 2005 and 2006, 2007, 2008. U.S. Department of Commerce.

U.S. FWS (1991a) Northeast Coastal Areas Study, Significant Coastal Habitats, Martha's Vineyard Coastal Sandplain and Beach Complex. U.S. Fish & Wildlife Service, National Conservation Training Center, Conservation Library, Shepherdstown, West Virginia.

U.S. FWS (1991b) Northeast Coastal Areas Study: Significant Coastal Habitats of Southern New England and Portions of Long Island, New York. In National Conservation Training Center, Vol. 2005. U.S. Fish & Wildlife Service, U.S. Department of the Interior, Washington, D.C.

Uchupi, E., Graham Giese, Neal Driscoll, & Aubrey, D.G. (2005) Postglacial Geomorphic Evolution of a Segment of Cape Cod Bay and Adjacent Cape Cod, Massachusetts, U.S.A. *Journal of Coastal Research*, **21**, 1085-1106.

Uchupi, E. & Mulligan, A.E. (2006) Late Pleistocene stratigraphy of Upper Cape Cod and Nantucket Sound, Massachusetts. *Marine Geology*, **227**, 93-118.

UCS (2006) Global Warming. Union of Concerned Scientists, Cambridge, MA.

UN (1998) Characteristics of the Coast: Major Problems and Issues, United Nations Year of the Oceans, Chapter Two. In 1998 United Nations Year of the Oceans. United Nations.

UN (2003). Oceans and Coastal Areas: Emerging Issues.

UNEP (1992). Rio Declaration on Environment and Development. United Nations Environment Programme.

UNEP (2000) Potential Impacts of Climate Change. United National Environment Programme, Nairobi, Kenya.

United States (2008) Atlantic Coastal Plain, Encyclopedia Britannica Online.

Upham, W. (1879) The Formation of Cape Cod (Continued). *The American Naturalist*, **13**, 552-565.

US Commission on Ocean Policy (2004). Living on the Edge: Economic Growth and Resource Conservation Along the Coast: Chapter 9 -Managing Coasts and their Watersheds. U.S. Commission on Ocean Policy, Washington, D.C.

USACE (1995) Engineering and Design - Coastal Geology, Vol. CECW-EG, Engineer Manual: EM 1110-2-1810, pp. 297. Department of the Army, U.S. Army Corps of Engineers (USACE), Washington, D.C.

USDA (1998) National Soil Survey Handbook (NSSH Amendment 4) [online], Vol. 2008. U.S. Department of Agriculture (USDA), Natural Resources Conservation Service (NRCS).

USDA (2007a) National Soil Survey Handbook (NSSH) Title 430-VI [Online], Vol. 2008. U.S. Department of Agriculture (USDA), Natural Resources Conservation Service (NRCS).

USDA (2007b) Soil Data Mart: MA007 - Dukes County, Massachusetts, Vol. 2008. U.S. Department of Agriculture (USDA), Natural Resources Conservation Service (NRCS).

USDA (2007c) Soil Survey Geographic (SSURGO) database for Dukes County, Massachusetts. U.S. Department of Agriculture (USDA), Natural Resources Conservation Service (NRCS), Fort Worth, Texas.

USGS (2004) Massachusetts Islands Drainage Basin. United States Geologic Survey.

USGS (2005) Hurricane and Extreme Storm Impact Studies - Hurricanes, El-Niño, & Northeasters - An Introduction. U.S. Department of the Interior, U.S. Geological Survey, Center for Coastal & Watershed Studies.

USGS (2007) Islands Drainage Basin - Bedrock Geology, Vol. 2008. U.S. Department of the Interior, U.S. Geological Survey.

van Gaalen, J.F. (2004) Longshore Sediment Transport From Northern Maine To Tampa Bay, Florida: A Comparison Of Longshore Field Studies To Relative Potential Sediment Transport Rates Derived From Wave Information Study Hindcast Data. Master of Science, College of Marine Science, University of South Florida.

Velicogna, I. & Wahr, J. (2006) Measurements of Time-Variable Gravity Show Mass Loss in Antarctica. *Science**xpress***, 1-4.

Vellinga, M. & Wood, R.A. (2002) Global Climatic Impacts of a Collapse of the Atlantic Thermohaline Circulation. *Climatic Change*, **54**, 251-267.

Wampanoag Tribe of Gay Head (2006) Aquinnah. Aquinnah Cultural Center, Aquinnah, MA.

Wang, G. & Schimel, D. (2003) Climate Change, Climate Modes, and Climate Impacts. *Annual Review of Environment and Resources*, **28**, 1-28.

Wang, X.L., Swail, V.R., & Zwiers, F.W. (2006) Climatology and changes of extratropical storm tracks and cyclone activity: Comparison of ERA-40 with NCEP/NCAR Reanalysis for 1958-2001. *Journal of Climate*, **19**, 3145-3166.

Warner, S.B.J. (1999) Today's Boston; A History. *The Massachusetts Historical Review*, **1**, pp. 13.

WCED (1987). Our Common Future, also known as The Brundtland Report. World Commission on Environment and Development (WCED), Norway.

Weart, S. (2003). The Carbon Dioxide Greenhouse Effect. In *The Discovery of Global Warming*. Harvard University Press, Cambridge, MA.

Webster, P.J., Holland, G.J., Curry, J.A., & Chang, H.-R. (2005) Changes in Tropical Cyclone Number, Duration, and Intensity in a Warming Environment. *Science*, **309**, 1844-1846.

Webster, R. & Oliver, M.A. (2001) *Geostatistics for Environmental Scientists* John Wiley & Sons, Ltd., West Sussex, England.

WHOI (2006). Warmer than a Hot Tub: Atlantic Ocean Temperatures Much Higher in the Past - Study Suggests Climate Models Underestimate Future Warming. Woods Hole Oceanographic Institute, Woods Hole, MA.

Wilson, E.O. (1984) *Biophillia*, Tenth edn. Harvard University Press, Cambridge, MA and London, England.

WRI (2001). Pilot Analysis of Global Ecosystems: Coastal Ecosystems. World Resources Institute, Washington, D.C.

YOTO (1998) Year of the Ocean, Perspectives on Marine Environment Quality Today. In Year of the Ocean. United Nations, National Oceanic and Atmospheric Administration.

Zhang, K., Douglas, B.C., & Leatherman, S.P. (2000) Twentieth-Century Storm Activity along the U.S. East Coast. *Journal of Climate*, **13**, 1748 (14p, 5 charts, 2 diagrams, 13 graphs, 1 map).

Zhang, K., Douglas, B.C., & Leatherman, S.P. (2001) Beach erosion potential for severe nor'easters. *Journal of Coastal Research*, **17**, 309-321.

Zhang, K., Douglas, B.C., & Leatherman, S.P. (2004) Global Warming and Coastal Erosion. *Climatic Change*, **64**, 41-58.

Zhijun, D. & Chunchu, L. (2004) Coastline configuration and geomorphologic development mode of arc-shaped coast in South China. *Geomorphological Evolution*, **14**, 473-480.

Zoback, M.D. & Zoback, M.L. (1981) State of Stress and Intraplate Earthquakes in the United States. *Science*, **213**, 96-104.